Nuclear Dynamics

Lecture Notes

Agnieszka Sorensen

Facility for Rare Isotope Beams
Michigan State University

Spring 2026

Contents

The content of these lectures is based on *numerous* sources. Among those most often recurring are textbooks by Hans Paetz gen. Schieck [1], Charles J. Joachain [2], Albert Messiah [3], Daphne Jackson [4], Ian Thompson & Filomena Nunes [5], Carlos Bertulani & Paweł Danielewicz [6], George Satchler [7], and Kenneth Krane [8]. I also used sources from the *Course of Theoretical Physics* by Lev D. Landau & Evgeny M. Lifshitz [9, 10] as well as my memories of lectures by Profs. Jan Sobczyk and Krzysztof Redlich from University of Wrocław. Other sources include lecture notes by R. G. Littlejohn from University of California, Berkeley.

Generative AI models `ChatGPT` and `Claude` were used to polish some of the derivations. In all instances, the model output was extensively scrutinized before it was used – *never* simply copied – to write the lecture notes. Whenever it was possible to identify published source material explaining the same concepts, that material was given both preference and deference.

While I endeavor to identify specific sources at the end of each lecture, these acknowledgments are likely to be far from perfect. If there are any omissions or mistakes, both in the content and in the references, I will be happy to learn about them and apply corrections. The readers looking for more information are encouraged to perform a broad search, and especially to look toward older texts which tend to provide both detailed derivations and ample discussion of the physical meaning behind the formulas.

Lecture 1

Nuclear reactions

Prerequisites: none.
Guiding question: ***What are nuclear reactions, and why do we care?***

1.1 How it started, how it's going

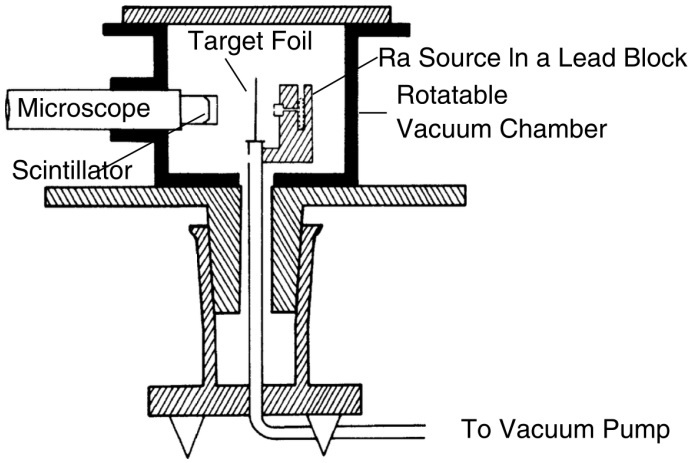

Figure 1.1: The setup of the Rutherford, Geiger, and Marsden experiment for scattering of α particles from a gold foil. Figure from Ref. [1].

Modern nuclear physics began with α-particle scattering experiments, carried out in 1909 by Hans Geiger and Ernest Marsden under the direction of Ernest Rutherford. The setup for the experiments is shown in Fig. 1.1. In these experiments, α-particles (now known to be helium-4 nuclei) were scattered from a thin gold foil. The experimental setup (see Fig. 1.1) consisted of a radioactive source of α particles – a sample of radium which decayed through the $^{226}\mathrm{Ra} \rightarrow {}^{222}\mathrm{Rn}+\alpha$ reaction[1] – placed inside a lead block with a small hole serving as a collimator. The resulting beam of α-particles was directed at the gold foil, and scattered α-particles were detected using a zinc sulfide fluorescent screen. Individual scattering events were observed visually as brief flashes of light (scintillations), which were counted by eye at different scattering angles.

[1]This is a simplification. The decay chain of radium-226 consists of $^{226}\mathrm{Ra} \rightarrow {}^{222}\mathrm{Rn} + \alpha$, $^{222}\mathrm{Rn} \rightarrow {}^{218}\mathrm{Po} + \alpha$, $^{218}\mathrm{Po} \rightarrow {}^{214}\mathrm{Pb}+\alpha$, $^{214}\mathrm{Pb} \rightarrow {}^{214}\mathrm{Bi}+\beta^- \rightarrow {}^{214}\mathrm{Po}+\beta^- \rightarrow {}^{210}\mathrm{Pb}+\alpha$, and $^{210}\mathrm{Pb} \rightarrow {}^{210}\mathrm{Bi}+\beta^- \rightarrow {}^{210}\mathrm{Po}+\beta^- \rightarrow {}^{206}\mathrm{Pb}+\alpha$.

The experiment which started it all is a perfect illustration of how we learn about nuclear systems through nuclear reactions:

1. *We take two entities, at least one of which is a nucleus.* In Rutherford's case, these entities were helium and gold nuclei, but one can also consider, *e.g.*, collisions of electrons with nuclear targets, as done at the Jefferson Lab (JLab) or at the future Electron–Ion Collider (EIC).

2. *We shoot one of them against the other.* In Rutherford's case, "shooting" was merely collimating a radioactive source, but in modern setups it often involves extremely complex procedures for accelerating and directing the beams.

3. *We detect the reaction products to study the interactions governing the reaction.* For Rutherford, this was done by counting flashes on a scintillating screen, while modern experiments rely on sophisticated detectors.

While the basic experimental idea is the same as in 1909, modern nuclear experiments differ a lot by technological progress, which determines what studies are possible.

Instead of just relying on natural radioactivity, we can prepare projectiles and target of various species. At the Facility for Rare Isotope Beams (FRIB), the projectile itself is typically produced in a prior nuclear reaction: A primary beam induces fragmentation or fission, the resulting reaction products are separated by magnetic rigidity[2], and selected rare isotopes are delivered as secondary beams to reaction targets. Such experiments are not possible without state-of-the-art accelerator and beam-transport techniques to control the identity, energy, and phase space of the projectile.

To access various energies of the interactions, we can use accelerators: from linear accelerators (LINACs), to cyclotrons, to colliders such as the Relativistic Heavy Ion Collider (RHIC) at the Brookhaven National Laboratory (BNL) and the Large Hadron Collider (LHC) at CERN, which operate with two counter-propagating beams of protons and/or nuclei, enabling access to ultrarelativistic reaction energies.

Sophisticated detectors such as Time Projection Chambers (TPCs) can reveal not only where the particles emerging from the interaction go, but also what is their energy, momentum, charge, *etc.* In facilities operating with stable beams, the detectors are often what determines the available statistics and, therefore, viable measurements: for example, in heavy-ion collision experiments the STAR detector at RHIC can record 10^3 events per second, the HADES detector at GSI, Germany, can record 10^4 events per second, and the future CBM detector at the Facility for Antiproton and Ion Research (FAIR), Germany, will be able to handle 10^7 events per second[3].

As the energy and/or precision of experiments increases, so does the complexity of extracting the sought after information from the experiment[4]. To extract characteristics of a particular process, one needs to understand what other processes can contribute to and confound the observables. For example, extractions of the density- and isospin-dependence of the nuclear equation of state (EOS) are influenced by assumptions on the used optical potential (*i.e.*, momentum-dependence of the interaction). Considerations of background were already present in Rutherford's case: before performing the experiment with the gold foil, Geiger and Marsden performed one *without it* to count how many scatterings occur due to scattering of the α-particles off of the air molecules and the apparatus itself: collimators, screens, *etc.*

[2]Magnetic rigidity is defined as $B\rho = p/q$, where p is the momentum and q the charge of a particle. In a magnetic field B, particles with a given p/q follow a path with a specific radius ρ. At rare-isotope facilities, this property is exploited to separate reaction products by species.

[3]Interestingly, at such high rates of events one of the key questions to address is the storage of the resulting ginormous volumes of data. At CBM, this will involve real-time selection of recorded data.

[4]Another way to think about this is that if something is easy to measure, it already has been measured.

1.2 Why should one study nuclear reactions?

The question is deliberately a bit subversive. Rutherford's experiments have revealed the structure of the atom, a result that fundamentally reshaped physics. However, Rutherford and his collaborators did not know this outcome in advance. In hindsight, the importance of those experiments appears obvious, but it was not so at the time. To some extent, this illustrates a broader principle: progress in fundamental science often comes from exploring open questions, *both* big and small, and one can never be certain where the next "big" discovery may lie. In the context of nuclear reactions, such open questions remain abundant.

Beyond this philosophical motivation, there are also concrete scientific reasons to study nuclear reactions. Nuclear reactions provide direct information about the forces between nucleons. While these forces ultimately arise from a known fundamental theory, quantum chromodynamics (QCD), the nonperturbative nature of QCD at low energies makes first-principles predictions of nuclear interactions practically impossible. As a result, nuclear reaction experiments – which need to be described with nuclear reactions theory – are a perfect test bed for models of nuclear interactions.

Apart from probing the nuclear interactions, reaction observables are used to infer detailed information about nuclear structure. Examples include single-particle energies and occupancies, collective excitations, or deformation. In many cases, reactions provide access to structural information that cannot be obtained from spectroscopy alone, particularly for unstable or short-lived nuclei.

Furthermore, chains of nuclear reactions are key to understanding astrophysical phenomena. They determine the synthesis of the elements and the composition of stars, the pathways of energy generation in stars, and the evolution of stellar systems. Understanding these processes requires reliable reaction rates, often under extreme conditions which are inaccessible in the laboratory.

At sufficiently high energies, nuclear collisions access regimes where the substructure of nucleons becomes relevant and descriptions in terms of quarks and gluons are more appropriate. Properties of such systems are probed within ultrarelativistic heavy-ion collisions: nuclear reactions taken to an extreme which allow one to explore questions about chiral symmetry restoration, deconfinement, and phases of QCD matter.

1.3 Notation

Before we discuss how nuclear dynamics – *i.e.*, the subject of this class – can affect the outcomes of experiments, we need to establish basic notation which we will use to talk about the reactions.

Let us consider a projectile "a", a target "A", and a reaction between them which produces two products "b" and "B":

$$\mathrm{a} + \mathrm{A} \rightarrow \mathrm{b} + \mathrm{B} \ . \tag{1.1}$$

Together, b and B are called an *exit channel* of the reaction. Since reactions between a and A can proceed through different mechanisms and produce different products b and B, there may be multiple distinct exit channels. Conversely, a given exit channel may be populated from different *entrance channels* corresponding to different choices of projectiles, targets, or initial quantum numbers.

A common alternative way of writing Eq. (1.1) is

$$\mathrm{A(a,b)B} \ , \tag{1.2}$$

which makes explicit which particle serves as the target and which as the projectile. This notation arose historically in the context of direct reactions, where a and b are typically light particles and A

and B are comparatively heavy nuclei. In such cases, the recoil nucleus B often carries low kinetic energy and may not be detected (it may even not leave the target), while experimental observables are dominated by the light ejectile b. By construction, in such reactions the primary interest lies in the properties of the projectile-like particles, which carry direct information about the reaction mechanism and nuclear structure, while the information about the residual nucleus B is mainly used to ensure conservation laws are satisfied.

1.4 Classification

1.4.1 Channels

The reaction may be *elastic*, which means that the interaction does not change the identity of the projectile and target (including not inducing excited states in the reacting nuclei), *i.e.*,

$$\mathrm{a} + \mathrm{A} \rightarrow \mathrm{a} + \mathrm{A} \quad \text{or} \quad \mathrm{A(a,a)A} \ . \tag{1.3}$$

where we write the same reaction in the two notations introduced above. This is the case for Rutherford scattering of α particles off of gold nuclei. A modern example of how can one utilize such a reaction is a recent experiment performed at RIKEN (Japan), which measures proton elastic scattering from the neutron-rich ^{132}Sn at 200 MeV/nucleon with the aim to deduce the neutron skin thickness of ^{132}Sn and, through that, constrain the isospin-dependence of the EOS [11].

An *inelastic channel* means that the projectile and target maintain their identities but at least one of them is excited into a higher internal state,

$$\mathrm{a} + \mathrm{A} \rightarrow \mathrm{a}' + \mathrm{A}' \quad \text{or} \quad \mathrm{A(a,a')A'} \ . \tag{1.4}$$

In denoting inelastic reactions, a superscript * is used to denote an excited state. For example, in the scattering of neutrons off oxygen-16 we write

$$^{16}\mathrm{O} + \mathrm{n} \rightarrow {}^{16}\mathrm{O}^* + \mathrm{n} \quad \text{or} \quad {}^{16}\mathrm{O(n,n)}{}^{16}\mathrm{O}^* \ . \tag{1.5}$$

Another example is Coulomb (*i.e.*, purely electromagnetic) excitation in scattering of protons on lead,

$$^{208}\mathrm{Pb} + \mathrm{p} \rightarrow {}^{208}\mathrm{Pb}^* + \mathrm{p} \rightarrow {}^{208}\mathrm{Pb} + \mathrm{p} + \gamma \quad \text{or} \quad {}^{208}\mathrm{Pb(p,p}\gamma){}^{208}\mathrm{Pb} \ , \tag{1.6}$$

where the reaction excites the Exciting the 3^-_1 octupole state at 2.615 MeV. Elastic and inelastic together are often called *scattering channels*.

Finally, the name *reaction channels* denotes modes of interaction where the projectile and/or the target change identity. For example, the first ever nuclear reaction studied in the laboratory was

$$^{14}\mathrm{N} + \alpha \rightarrow {}^{17}\mathrm{O} + \mathrm{p} \ , \tag{1.7}$$

discovered by Rutherford in 1919. Fig. 1.2 shows a cloud chamber photograph of this reaction, obtained by Patrick Blackett in 1925[5].

It's important to note that not everyone may follow the above definitions, and in particular the low- and high-energy nuclear physics communities may use them differently. For example, in the field of heavy-ion collisions, scattering is called "inelastic" whenever it is not elastic, including reactions leading to particle production.

[5] Blackett won the 1948 Nobel prize for his work with cloud chambers.

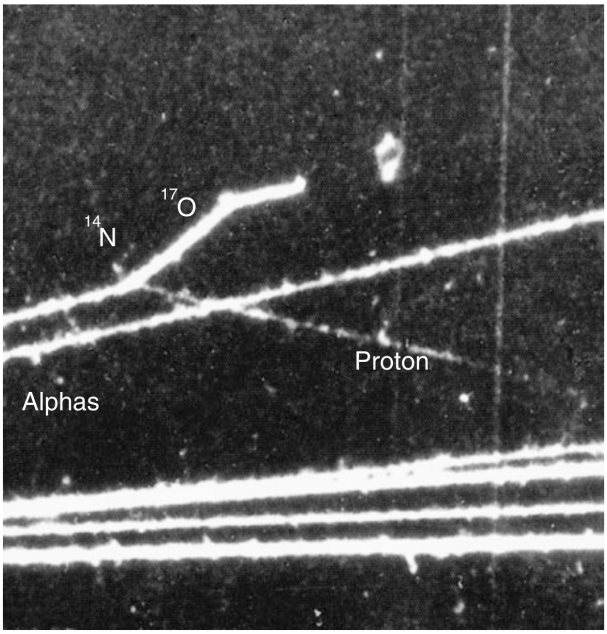

Figure 1.2: A cloud chamber photograph of the first nuclear transmutation reaction obtained in the laboratory. While the original experiment was performed by Rutherford in 1919, the photograph was obtained by Blackett in 1925. The photograph shows ionization tracks due to the incoming α particles (semi-thick tracks), of which one strikes the target: a ^{14}N nucleus. The reaction leads to an outgoing heavy particle (thick track) and a light particle (thin track), identified as a proton. Conservation of charge implies that the heavy particle is a ^{17}O nucleus. The photograph also shows subsequent Coulomb ("Rutherford") scattering of ^{17}O on another ^{14}N nucleus. Figure from Ref. [1].

1.4.2 Reaction channels

Since there are numerous possibilities for different reactions due to various underlying mechanisms, reaction channels are further divided into certain classes of reactions:

- *Transfer reactions* are those in which one or more nucleons are transferred between the projectile and target during the collisions. They can be further divided into *stripping reactions*, such as when the target nucleus strips a neutron off of an incident deuteron, A(d,p)B, and *pick-up reactions*, such as when an incident proton picks up a neutron from the target nucleus to become a deuteron, A(p,d)B.
- A *knock-out reaction* removes one (or more) nucleons from the projectile (or the target), typically at high energy, without transferring it to the target (or the projectile). As an example, we can have ^{48}Ca(p, pn)^{47}Ca.
- *Break-up reactions* include a target or projectile breaking up, *e.g.*,

$$\mathrm{A(a, b + c)A} \ . \tag{1.8}$$

  A good example is the deuteron breakup,

$$\mathrm{d + A \rightarrow p + n + A} \ , \tag{1.9}$$

  which is interesting because the deuteron is extremely weakly bound so that breakup occurs readily over a wide range of collision energies.

- In *fusion reactions*, the projectile is fully absorbed by the target or, more generally, the projectile and target merge (at least temporarily). As a result, fusion always involves a formation of a single composite nucleus (even if only as an intermediate step.) For example, the current element with the highest atomic number ever produced is the oganesson with $Z = 118$, produced in 2002 through a heavy-ion fusion reaction

$$^{249}\mathrm{Cf} + {}^{48}\mathrm{Ca} \to {}^{297}\mathrm{Og}^* \to {}^{294}\mathrm{Og} + 3n \quad \text{or} \quad {}^{249}\mathrm{Cf}({}^{48}\mathrm{Ca}, 3\mathrm{n})^{294}\mathrm{Og} \ . \tag{1.10}$$

  Currently, scientists at the Lawrence Berkeley National Laboratory (LBNL) are pursuing creating the element with $Z = 120$ (unbinilium) through

$$^{249}\mathrm{Cf} + {}^{50}\mathrm{Ti} \to {}^{299}\mathrm{Ubn}^* \to {}^{299-x}\mathrm{Ubn} + x\mathrm{n} \quad \text{or} \quad {}^{249}\mathrm{Cf}({}^{50}\mathrm{Ti}, x\mathrm{n})^{299-x}\mathrm{Ubn} \ . \tag{1.11}$$

  Another interesting example, involving lighter nuclei, is the well-known *triple-alpha process*

$$^{8}\mathrm{Be} + \alpha \to {}^{12}\mathrm{C}^* \ , \tag{1.12}$$

  in which Helium-4 and Berylium-8 nuclei form an excited *unbound* state of ^{12}C: a $^{12}\mathrm{C}^*$ *resonance*[6]. This resonance can then decay either into 3 alpha particles,

$$^{12}\mathrm{C}^* \to 3\alpha \ , \tag{1.13}$$

  or stabilizes (*i.e.*, transforms into a bound, ground state of ^{12}C) via electromagnetic decay,

$$^{12}\mathrm{C}^* \to {}^{12}\mathrm{C} + \gamma \quad \text{or} \quad {}^{12}\mathrm{C}^* \to {}^{12}\mathrm{C} + e^+ + e^- \ . \tag{1.14}$$

  Crucially, the probability of the resonant reaction channel for ^{12}C production is much higher (by orders of magnitude) than the probability for 3 alpha particles to form a stable, non-resonant ^{12}C state. Because of that, this reaction provides a crucial contribution to the overall production of carbon-12 in stellar media. The $^{12}\mathrm{C}^*$ resonance is called the *Hoyle resonance* after Fred Hoyle, who predicted it in 1954 [13] after concluding that the existence of such a resonance is the only way to explain the measured quantities of ^{12}C in the Universe. Note that whether a fusion reaction is exo- or endothermic depends on the mass numbers of the interacting nuclei. In particular, fusion reactions involving nuclei with mass numbers beyond that of iron require providing the energy from an external source, see Fig. 1.3.
- *Charge-exchange reactions* change the charge but not mass of the interacting nuclei, *e.g.*

$$(\mathrm{p},\ \mathrm{n}) \quad \text{or} \quad ({}^3\mathrm{He}, \mathrm{t}) \ . \tag{1.15}$$

  Exchanging a proton and a neutron flips the isospin projection while leaving total number of nucleons unchanged. Because the strong interaction is approximately isospin symmetric, many gross nuclear properties are preserved, allowing charge-exchange reactions to selectively probe the isospin dependence of nuclear forces.

[6] Resonances are quasi-bound nuclear states which correspond to sharp peaks (*i.e.*, enhanced reaction probabilities) in the energy dependence of the reaction – hence the name. These peaks cannot be reproduced by simple potential scattering calculations alone. The possibility that states above threshold (*i.e.*, with positive energies excluding formation of a bound state) can *temporarily* behave like a bound state was first shown by George Gamow in his 1928 theory of α decay [12]. Then in 1936, Gregory Breit and Eugene Wigner connected peaks in reaction spectra to finite lifetimes of such intermediate states formed from the reactants.

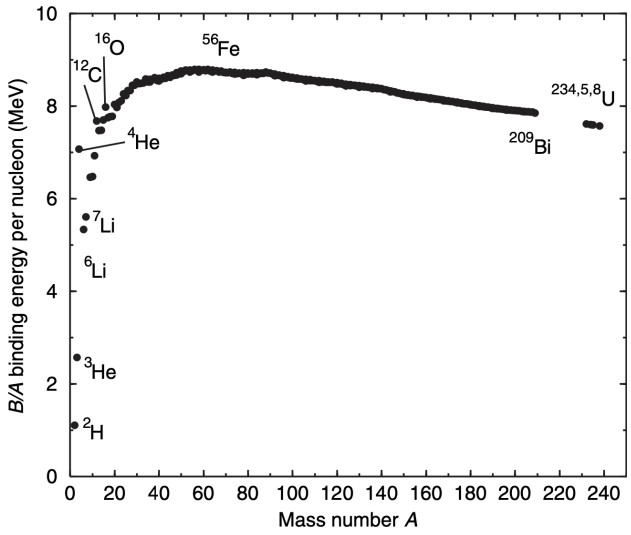

Figure 1.3: Binding energies per nucleon for all naturally occurring long-lived isotopes of A nucleons. Figure from Ref. [5].

- *Capture reactions* are those in which the projectile is absorbed, forming a compound nucleus that subsequently de-excites by γ emission. An example is the radiative neutron capture,

$$^{1}\mathrm{H}(\mathrm{n},\gamma)d\ , \tag{1.16}$$

  which is the dominant mechanism for deuteron formation at low energies. Note that by the above definition, the triple-alpha process, Eq. (1.12), could also be classified as a capture instead of as a fusion reaction[7]. Typically, however, the term "capture" is used when a light projectile is absorbed by a much heavier target, while fusion is more commonly used when two nuclei of comparable masses merge. Moreover, fusion can involve various decay modes, for example particle evaporation, while capture specifically refers to reactions where the compound nucleus de-excites by emitting gamma rays.
- In *fission reactions*, a heavy nucleus splits into two (or more) fragments. An example is the reaction

$$^{235}\mathrm{U} + \mathrm{n} \rightarrow {}^{236}\mathrm{U}^{*} \rightarrow {}^{95}\mathrm{Zr} + {}^{139}\mathrm{Cs} + 2\mathrm{n}\ , \tag{1.17}$$

  which illustrates the asymmetric fragment production and prompt neutron emission.

In-class Activity 1a: Reaction channels of d + ^{238}U

The same projectile and target can undergo reactions of various types. For example, collisions of a deuteron with a ^{238}U nucleus can lead (among others!) to

$$\mathrm{d} + {}^{238}\mathrm{U} \rightarrow {}^{240}\mathrm{Np} + \gamma \tag{1.18}$$
$$\rightarrow {}^{239}\mathrm{Np} + \mathrm{n} \tag{1.19}$$
$$\rightarrow {}^{239}\mathrm{U} + \mathrm{p} \tag{1.20}$$
$$\rightarrow {}^{237}\mathrm{U} + \mathrm{t} \tag{1.21}$$

Which class of reaction channels does each of these belong to?

[7] This shows that classifications such as these usually don't form a complete and orthogonal set.

Solution

The first reaction is an example of a capture reaction, while the following three are examples of a transfer reaction, where the first two are stripping reactions and the last is a pick-up reaction.

1.4.3 Kinds of reactions

An orthogonal way to classify nuclear reactions is to consider the properties of reaction mechanisms:

- *Direct reactions* are characterized by a short interaction time (they are "fast") and involve only few degrees of freedom, *e.g.*, only a few nucleons on the surface of the nucleus or only the nucleus as one entity. Thus, the interaction is "direct" in the sense that the few relevant degrees of freedom interact between each other while the rest of the system provides a more or less static background. These can include elastic, inelastic, transfer, knockout, and break-up reactions. In these fast reactions, the directions of the final nuclei are strongly correlated with the direction of the initial nuclei.
- *Resonant reactions* are characterized by prominent peaks in reaction rates. These peaks correspond to metastable configurations of nucleons, and they may occur in elastic scattering (for example, when the nuclear attractive force combines with the centrifugal barrier to keep the colliding nuclei together[8]) or from more complicated multi-step processes. There are also strongly collective resonances, known as the *giant resonances*, in which the nucleus undergoes a motion as a whole: for example, in giant dipole resonances all the neutrons oscillate against all the protons, while in giant monopole resonances the whole nucleus undergoes radial oscillations, rendering the nucleus alternately larger and smaller; the latter, also known as "breathing mode" oscillations, can be used for extracting the incompressibility of nuclear matter at saturation.
- *Compound-nucleus reactions*, in which the reacting nuclei form a long-lived but ultimately unstable nucleus[9] are characterized by very long interaction times so that the outcome of the reaction does not depend on the kinematic details of the entrance channel (*i.e.*, the compound nucleus decays isotropically). These can include neutron capture at low energy, fusion–evaporation, as well as many many (n,γ) and (p,α) reactions.

1.4.4 Heavy-ion collisions

A category of its own is needed for *heavy-ion collisions*, which within the low-energy nuclear physics community are also sometimes called *central reactions*[10]. In these experiments, two heavy nuclei collide at energies which lead to their complete disintegration. The resulting systems are characterized by many-body, non-perturbative dynamics and, depending on the energy, can probe phenomena such as interactions in dense nuclear medium (*i.e.*, systems composed of densely packed nucleons)

[8] The term "centrifugal barrier" reflects a kinematic constraint due to conservation of angular momentum in a two-body system. If two bodies approach each other with nonzero sideways (transverse) separation (*i.e.*, the collision is not head on), the system has nonzero angular momentum. As the transverse separation between the bodies decreases due to an attractive potential, conservation of angular momentum requires an increase in their angular velocity, which can only happen at the cost of their radial, or "inward", kinetic energy (*i.e.*, the energy of moving closer together). At a certain point the radial ("inward") component of the relative velocity vanishes, corresponding to a minimum separation, after which the distance between the particles increases again. This turning point, together with the attractive interaction, can lead to a temporary trapping of the two bodies: an intermediate state that is neither bound nor immediately separating.

[9] Therefore, they may also be thought of as a type of resonant reactions.

[10] Note, however, that this term is *not* recognized by most members of the heavy-ion community.

or, at ultrarelativistic energies, quark-gluon plasma. We will cover these experiments in some detail toward the end of the class.

1.5 How we describe all that

As one may expect, the many reaction types require different formalisms. Elastic and inelastic scattering can be described by using *partial-wave analysis*, *optical models*, and *coupled-channel methods*. Direct reactions, such as transfer reactions, can often be described as "one-step processes" within the *distorted wave Born approximation (DWBA)* or, if a one-, two-, or higher-order step approach is not applicable, by means of coupled-channels methods. Resonant reactions are often well-captured within the *Breit-Wigner approach* or, for multi-step processes, coupled channels approaches. Compound nucleus reactions can be understood within *Bohr's independence hypothesis* or, in more complicated cases, *Hauser–Feshbach theory*. We will discuss all these in the following lectures.

Modeling heavy-ion collisions is done by simulating the many-body dynamical evolution of the colliding systems. Depending on the energy range, the simulations are based on *microscopic transport* approaches, such as those rooted in the Boltzmann-Uehling-Uhlenbeck (BUU) equation, or on *relativistic viscous hydrodynamics*– approaches very different from those constituting the bulk of this class. Still, nuclear reaction theory enters these simulations in the form of fundamental input on nucleon-nucleon and, at high energies, hadron-hadron scattering. Since the processes in question cover a considerable energy range, the description is usually achieved by means of a well-informed parametrization. For example, low- to intermediate-energy elementary elastic collisions are described by approaches based on partial wave analysis and resonance production captured within the Breit-Wigner description. At very high collision energies, descriptions of interactions by means of hadron-hadron collisions give way to string-based particle production models.

1.6 Basic constraints

1.6.1 Energy and momentum

In any reaction, *e.g.* for a hypothetical reaction A(a,b)B, the total energy must be conserved,

$$E_A + E_a = E_b + E_B \ . \tag{1.22}$$

This must be true at all times, including far away from the interaction region or, equivalently, long before and long after the reaction. At those times, no potentials should contribute to the energy, so that we can write explicitly[11]

$$\sqrt{m_A^2 + \boldsymbol{p}_A^2} + \sqrt{m_a^2 + \boldsymbol{p}_a^2} = \sqrt{m_b^2 + \boldsymbol{p}_b^2} + \sqrt{m_B^2 + \boldsymbol{p}_B^2} \ . \tag{1.23}$$

While conservation of momentum requires that $\boldsymbol{p}_A + \boldsymbol{p}_a = \boldsymbol{p}_b + \boldsymbol{p}_B$, in general $\boldsymbol{p}_B \neq \boldsymbol{p}_A$ and $\boldsymbol{p}_b \neq \boldsymbol{p}_a$ even if the reaction is elastic so that the labels a, b and A, B refer to the same species. Consequently, the total kinetic energy before and after reaction can change. Remembering that the relativistic kinetic energy K is defined as

$$E = m + K \ , \tag{1.24}$$

[11] Here and whenever possible, I will use natural units in which $c = \hbar = k_B = 1$. Consequently, the unit for energy, mass, and momentum is the same: eV (or MeV, or GeV – whichever is most useful at a given moment).

where m is the rest mass, we can rewrite Eq. (1.23) as

$$(m_A + m_a) - (m_b + m_B) = (K_b + K_B) - (K_A + K_a) \ . \tag{1.25}$$

Because masses (or, equivalently, identities) of target, projectile, and reaction products are known for a particular reaction, it is useful to define the *Q-value of the reaction*,

$$Q = (m_A + m_a) - (m_b + m_B) \ . \tag{1.26}$$

As evident from Eq. (1.25), the Q-value is equal to the difference between the final and the initial total kinetic energy. If $Q < 0$, it means that producing the reaction products b and B required using up some of the initial kinetic energy; we call such a reaction *endothermic*. If $Q > 0$, it means that producing b and B released some additional energy into the system; we call such a reaction *exothermic*.

Note that the above definition may be somewhat confusing in the case where an excited state is created. For example, in the case of a reaction

$$\mathrm{a} + \mathrm{A} \rightarrow \mathrm{b} + \mathrm{B}^* \tag{1.27}$$

we should use either

$$Q = (m_A + m_a) - (m_b + m_B) - E_B^* \tag{1.28}$$

or

$$Q = (m_A + m_a) - (m_b + m_B^*) \ , \tag{1.29}$$

where m_B is the ground state mass, E_B^* is the excitation energy, and m_B^* is the excited state mass.

1.6.2 Conserved charges

In any reaction, baryon number is strictly conserved[12]. The same is true about charge. Note that in both cases, reactions that produce a particle and an antiparticle at the same time are still allowed as the *net* baryon number and *net* charge are zero. However, such reactions require a lot of energy to be transformed into mass – *e.g.*, about 2 GeV in case of a proton and antiproton pair – and thus are not relevant for low-energy nuclear reactions. One should naturally remember that while charge must be conserved, it can be transferred. For example, charged pion production through a reaction

$$\mathrm{p} + \mathrm{p} \rightarrow \mathrm{p} + \mathrm{n} + \pi \tag{1.30}$$

is perfectly allowed and, in fact, forms a crucial element of heavy-ion collision experiments at FRIB.

1.6.3 Total angular momentum and parity

Total angular momentum $\boldsymbol{J}$ is always conserved. For a given nucleus A, its *intrinsic angular momentum* is a vector sum of its orbital angular momentum and spin, $\boldsymbol{J}_A = \boldsymbol{L}_A + \boldsymbol{S}_A$ (here, "intrinsic" refers to the *internal* total angular momentum of nucleus A, as distinct from the orbital angular momentum of the reaction system). Then for a given reaction $A(a,b)B$ we have

$$\boldsymbol{J}_A + \boldsymbol{J}_a + \boldsymbol{l}_i = \boldsymbol{J}_b + \boldsymbol{J}_B + \boldsymbol{l}_f \ , \tag{1.31}$$

[12] Current best estimates place the limit on proton's lifetime at around 10^{34} years.

where $\boldsymbol{l}_i$ and $\boldsymbol{l}_f$ refer to the initial and final orbital angular momenta of the relative motion between the collision partners, respectively.

Considerations of angular momentum can be powerful. For example, in the reaction

$$^{10}\mathrm{B} + {}^{4}\mathrm{He} \rightarrow {}^{1}\mathrm{H} + {}^{13}\mathrm{C} \tag{1.32}$$

it is known that ^{10}B has $J(^{10}\mathrm{B}) = 3$ in the ground state, while the α-particle has zero angular momentum, $J(^{4}\mathrm{He}) = 0$. At low reaction energies, the relative motion of the reactants will be dominated by contributions from the s-wave[13] which carries $l_i = 0$. Therefore, the total initial total angular momentum of the system is $J_i = 3$. The final products of the reaction have equal intrinsic angular momenta of $J(^{1}\mathrm{H}) = J(^{13}\mathrm{C}) = \frac{1}{2}$, so that their sum can be either 0 or 1. Depending on the relative sign of contributions from $J(^{1}\mathrm{H}) + J(^{13}\mathrm{C})$ and l_f, the possible values of l_f are then constrained to 2, 3, or 4.

Strong interaction also always conserves parity, which allows one to further constrain the possible outcomes of a reaction. For example, in the above example, ^{10}B, ^{4}He, and the proton have all even parities, while ^{13}C has odd parity. For two-body channels, the total parity is given by

$$\pi_{\mathrm{total}} = \pi_1 \pi_2 (-1)^l \ . \tag{1.33}$$

Thus, given $l_i = 0$, the total initial parity is positive. For the same to be true in the final state, we need $(+)(-)(-1)^{l_f} = 1$, which can only be true for odd l_f. Together with the constraint on l_f based on the conservation of total angular momentum, we deduce that we must have $l_f = 3$.

Lecture sources: This lecture is mainly based on sec. 1.4 in gen. Schieck [1], chapters 1 and 2 in Thompson & Nunes [5], and chapter 1 in Bertulani & Danielewicz [6].

[13] We will discuss the decomposition of the relative motion into partial waves (*i.e.,* angular momentum eigenstates) in Lectures 7– 9.

Lecture 2

Cross sections and frames of reference

Prerequisites: none.
Guiding question: ***What do we actually want to measure?***

2.1 Classical scattering cross section

Given an experimental setup where a reaction takes place at a given location, we can imagine putting a detector at some position relative to that location and counting the number of times a given particle is detected. This number will depend on the details of a particular experiment: it can be expected to be proportional to the physical size of the detector (a detector area covering a larger fraction of the total solid angle will generally register a larger number of events), the time over which the observation is made, and the rate at which a given reaction occurs. While the latter contains the underlying physics (for example, if a given reaction does not produce deuterons, the rate of deuteron production is exactly zero), it also depends on the current of projectiles in the incident beam (increasing both the density and the velocity of the beam increases the number of projectiles that reach the target in unit time) as well as the density and thickness of the target, which are characteristics of a specific experimental setup. Naturally, we would like to extract information that does not depend on the experimental setup.

2.1.1 Total scattering cross section

Let us first consider a simplified scenario: we have a rectangular target of area A_0, thickness d, and the density of scattering centers n_{targ}[1]. We imagine the projectiles to be point particles, spread over a beam of area $A < A_0$ with density n_{proj}, and the scattering centers to be thin hard disks of area ("cross section") σ whose surface is orthogonal to the beam direction (see Fig. 2.1). We consider the problem to be purely mechanistic, so that if a scattering occurs, the scattering particle simply recoils backward[2]. In the limiting case of only one projectile in the beam and only one scattering center in the target, the probability that a scattering event will occur is intuitively

$$P = \frac{\sigma}{A} \,. \tag{2.1}$$

[1]Here, a "target" means a sample of the material that we want to scatter off of, like the thin gold foil from Rutherford's experiments (in which case the scattering centers are gold nuclei).

[2]In other words, there is no interaction at a distance and the only interaction is with the surface of a scattering center, which is perpendicular to the beam.

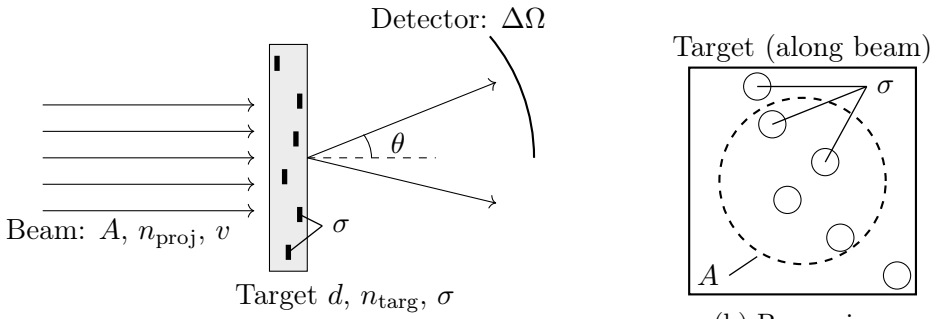

(a) Side view.

(b) Beam view.

Figure 2.1: Geometric picture underlying the definition of the scattering cross section.

If there are many scattering centers, that probability increases. In the setup described above, the total number of scattering centers within the beam area is $N_{\text{targ}} = n_{\text{targ}} A d$, so that now the probability of a scattering event is[3]

$$P = N_{\text{targ}} \frac{\sigma}{A} \ . \tag{2.2}$$

Given a beam of more than one projectile, how many scattering events ΔN will occur within a time Δt? If there are N_{proj} projectiles reaching the target within that time, then on average

$$\Delta N = N_{\text{proj}} N_{\text{targ}} \frac{\sigma}{A} \ . \tag{2.3}$$

For the beam as specified above, the number of projectiles reaching the target within time Δt is

$$N_{\text{proj}} = n_{\text{proj}} A (v \Delta t) = j A \Delta t \ , \tag{2.4}$$

where v is the velocity of projectiles within the beam and we identified $n_{\text{proj}} v$ as the incident particle current density j, *i.e.*, a measure of how many particles cross a surface perpendicular to v per unit time and per unit area[4]. Now, then, ΔN is given by[5]

$$\Delta N = j \Delta t N_{\text{targ}} \sigma \ . \tag{2.5}$$

Clearly, the only quantity in the above equation which corresponds to the microscopic dynamics of the scattering reaction is the size of the scattering center σ, as everything else can change depending on the experiment. For microscopic studies it is also the only one unknown: we can count the number of events ΔN over time Δt, prepare the projectile beam to have a current density j, and prepare a target sample with N_{targ} scattering centers (even on a microscopic level, the number density of, *e.g.*, gold can be easily established). Therefore, it makes sense to rewrite the above equation as

$$\sigma = \frac{\frac{\Delta N}{\Delta t}}{j N_{\text{targ}}} \ , \tag{2.6}$$

where $\Delta N / \Delta t$ is referred to as *event rate*[6]. In this context, σ is called the *scattering cross section*.

[3] Note that to maintain a reasonable definition of the probability, we assume that the density n_{targ} and/or the thickness d are small enough so that $P \leq 1$. This is true if we assume the target to be sufficiently "dilute", which is good enough for our current consideration whose sole aim is to provide an intuitive understanding.

[4] We note that some textbooks refer to j (or J, depending on the notation) as "flux". That is misleading: in physics, flux is the rate at which something passes through a surface. If that "something" is particles, then the unit of flux is 1/[time]. This would not lead to a correct unit for σ, which should be [length]^2.

[5] Note that here we make an assumption that all particles specified by N_{proj} fully traverse the target during Δt, thus making the use of N_{targ} for the number of scattering centers justified. This is the case if $\Delta t \gg d/v$.

[6] Confusingly, many textbooks denote $\Delta N / \Delta t$ as N. There is a subset of people who simply like chaos (see footnote 4).

2.1.2 Differential scattering cross section

Now we can introduce some nuance into this picture. First, scattering may not be occurring between point particles and hard disks, but instead between two point particles (in which case one *needs* to introduce interactions at a distance), two extended objects (like molecules or nuclei), *etc.* In particular, if we consider the special case of scattering between billiard-ball–like entities, it becomes apparent that we may count not only how many scattering events there are overall, but also how many scatterings there are in which particles fly out at a specific angle, $\Delta N(\Omega)$, where Ω denotes the solid-angle coordinates $\Omega = (\theta, \phi)$. Note that since there are infinitely many points on the unit sphere and a finite number of particles that can scatter, the probability to detect a particle within an infinitesimal solid angle $d\Omega$ around Ω vanishes as $d\Omega \to 0$, so that the probability to detect a particle at a specific angle Ω is zero. In other words, it is only meaningful to consider the probability of detecting particles within a finite solid-angle element $\Delta\Omega$ around Ω. Naturally, the larger $\Delta\Omega$ is, the bigger should be the number of registered particles, so that we can conclude that the dependence on $\Delta\Omega$ is a property of the experimental setup (*e.g.*, corresponding to the solid angle extent of the detector) and not of the underlying physical process. Therefore, in defining the *differential cross section* we want to divide this factor out,

$$\frac{d\sigma(\Omega)}{d\Omega} = \frac{\frac{\Delta N(\Omega,\Delta\Omega)}{\Delta t}}{\Delta\Omega j N_{\text{targ}}} , \tag{2.7}$$

where $\Delta N(\Omega, \Delta\Omega)$ now denotes the number of events registered within $\Delta\Omega$, centered around Ω, over time Δt. The angular dependence contains truly nontrivial information: for example, compound nucleus reactions (in which the composite system equilibrates before it decays) typically lead to nearly isotropic angular distributions in the center-of-mass frame[7], reflecting the loss of memory of the entrance channel. In contrast, direct reactions exhibit a strong correlation between the initial and final momenta, resulting in distributions that are *forward-peaked* in the center-of-mass frame[8].

Next, a closer inspection of how particles interact at a microscopic level forces us to leave behind the strict geometric interpretation of the cross section σ, underlying Eqs. (2.1) and (2.2). Indeed, in microscopic problems the size of objects which undergo scattering is generally less important than the range of the interaction between them[9]. Moreover, the concept of a specific area within which the interaction can take place must be thrown out the window once we acknowledge the existence of quantum mechanics. Nevertheless, in experiments we can still measure all the quantities on the right-hand side of Eq. (2.7). In view of this, we just update our idea on what the cross section σ means: instead of taking it as the literal size of the scattering center, we now understand it as an effective area characterizing the likelihood of a given interaction process, determined by the interaction range, strength, and relevant conservation laws[10].

We should now acknowledge another dependency of a cross-section: the energy of the interaction. As a result, one may consider a *double-differential cross section* $\frac{d^2\sigma(\Omega,E)}{d\Omega dE}$. However, often the steep increase in complexity (as well as high experimental statistics needed to resolve both dependencies well) convinces one to instead consider only $\frac{d\sigma(E)}{dE}$ (*i.e.*, the dependence of the cross section on the

[7] We will discuss the center-of-mass frame in the next section.

[8] Note that in discussing angular distributions, it is crucial to specify the reference frame, since transformations between the laboratory and center-of-mass frames can substantially distort angular patterns. We will discuss this soon.

[9] Not to mention that the geometric interpretation becomes really problematic for point-like particles.

[10] Strictly speaking, this reinterpretation has already been implicit above: once the projectiles or targets have finite size (like in the example with billiard balls), the cross section can no longer be identified with a literal geometric area without revisiting the probability argument, Eq. (2.1).

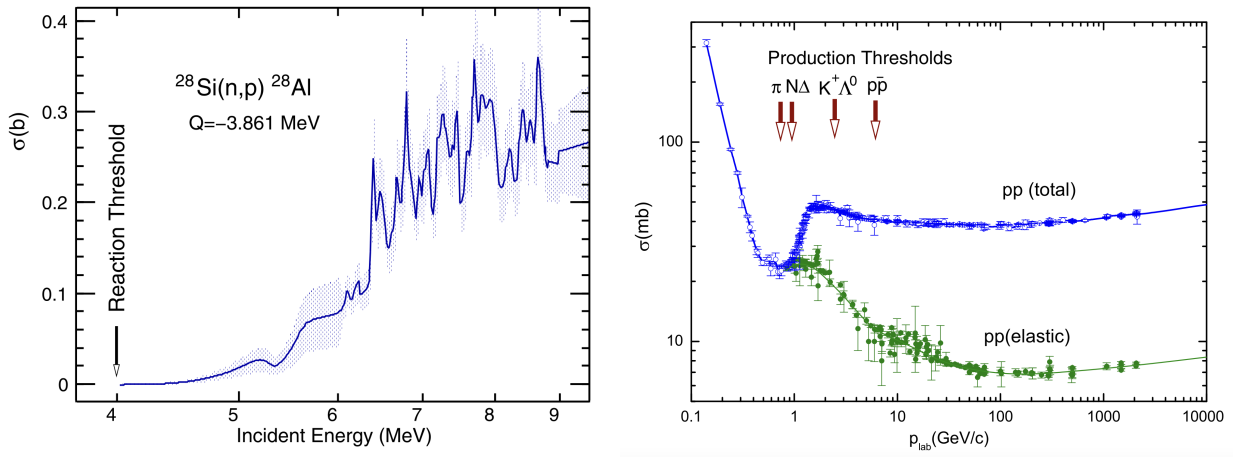

Figure 2.2: *Left panel:* Energy dependence of the cross section for the charge-exchange reaction ^{28}Si(n, p)^{28}Al. Since the reaction has a negative Q-value, one can see the threshold for the reaction. *Right panel:* Energy dependence of the total cross section for p-p scattering. The separation of the elastic and total cross section corresponds to the threshold for pion production. Both figures from Ref. [1].

energy, with the angular dependence integrated out), which reflects the tendency of the projectile and target particles to interact at a given energy. For example, the left panel Fig. 2.2 shows the incident energy dependence of the cross section for the charge-exchange reaction ^{28}Si(n, p)^{28}Al. Note that the reaction has a $Q = -3.861$ MeV < 0, *i.e.*, is endothermic and requires supplying the energy for the reaction. Another example is the energy dependence[11] of the total proton-proton (p-p) cross section, shown in the right panel of Fig. 2.2, where the onset of particle production (π, N, Δ, *etc.*) clearly drives the behavior of the total cross section from $p_{\rm lab} \sim$ 0.8–0.9. GeV and up.

Moreover, $\frac{d\sigma(E)}{dE}$ may simply be more useful than $\frac{d^2\sigma(\Omega,E)}{d\Omega dE}$: for example, to find reaction rates relevant for nuclear reactions in stars (for which the angular dependence is entirely irrelevant), one averages $\frac{d\sigma(E)}{dE}$ over thermal energy distributions. On the other hand, doubly-differential cross sections, when compared with laboratory experiments, can provide more stringent tests for models.

2.1.3 Units

Finally, let us discuss the units. Consistent with its interpretation as an effective area reflecting the probability of scattering, the cross section has units of area. The typical size of a nuclear system is on the order of 10^{-15} m $\equiv$ 1 fm. For heavy nuclei, the nuclear radius is about 7 fm, leading to a "cross-sectional area" on the order of 100 fm^2 $= 10^{-28}$ m^2. Thus it is convenient to define

$$1 \text{ b} = 10^{-28} \text{ m}^2 = 100 \text{ fm}^2 \,, \tag{2.8}$$

where b stands for "barn". The name was apparently coined by Manhattan Project physicists Marshall Holloway and Charles P. Baker in 1942 [14][12] and it is supposed to humorously suggest that a cross section of 10^{-28} m^2 is "as big as a barn." Now, this is true for some processes and not for others. For example, the total proton-proton cross section at momenta on the order of 1–10^3 GeV tends to hover around 40 mb $= 4 \times 10^{-2}$ b (see the right panel in Fig. 2.2), while the proton-pion total cross section peaks at around 200 mb for energies around the $\Delta(1232)$ resonance. On the other hand, typical very low-energy neutron-nucleus cross sections hover around 1–10^2 b.

[11] Or, equivalently, incident momentum dependence.
[12] Reading this short note is highly recommended.

2.2 The center-of-mass frame

Let us consider a reaction $A(a,b)B$ as a two-body problem. We know from experience that an efficient strategy for solving a two-body problem is to reduce it to two one-body problems. This can be done by working in the center-of-mass (CM) frame or, equivalently, introducing relative coordinates. A familiar example is the quantum-mechanical treatment of the hydrogen atom, where transforming to the CM frame reduces the non-trivial portion of the dynamics to that of a single particle moving in an effective potential, greatly simplifying the derivations[13]. In that particular case, the large mass difference between the proton and the electron makes the relative coordinate almost identical to the electron's coordinate with respect to a stationary nucleus, which helps to preserve the intuition.

The same formalism applies equally well to any two-body system, including systems with comparable masses, and it is particularly useful for problems involving scattering of two particles: because the momenta of incoming particles are equal and opposite in the CM frame, many expressions become easier to handle, including simplified conservation laws (*e.g.*, the conservation of momentum is just $\sum_i \boldsymbol{p}_i' = 0$) and fewer kinematic variables to handle (as the problem becomes effectively two- instead of three-dimensional due to symmetry around the axis defined by the incoming particles' momenta), *etc.* For this reason, theoretical treatments of cross sections are almost exclusively done in the CM frame.

The price for this simplification is that (at least at first) the physical interpretation of results may become a bit less transparent: statements about the relative motion of projectile and target do not always translate immediately into an intuitive picture of what is observed experimentally. There are two solutions to this problem: One is to develop the intuition through experience with many examples. If that fails, one can always transform results back to the laboratory frame – or any other physically meaningful frame that seems to offer more insight – where kinematic relations and angular distributions may be easier to interpret. Experience shows that the first approach works: as proof take the fact that it is experimental measurements (measured in the laboratory frame) that often need to be expressed in the CM frame to be compared with theoretical results, and not *vice versa*; clearly, the community considers thinking about the results in the CM frame to be just fine.

2.2.1 Classical mechanics

We now briefly review the classical construction of the center-of-mass reference frame. Let us denote the positions, momenta, and masses of the projectile and target in some frame as $\boldsymbol{r}_p$ and $\boldsymbol{r}_t$, $\boldsymbol{p}_p$ and $\boldsymbol{p}_t$, and m_p and m_t, respectively. When solving a scattering problem, it is convenient to transform the system into a frame where the total momentum $\boldsymbol{P}$ is zero, which simplifies constraints due to momentum conservation. Non-relativistically, if we transform to a frame moving with velocity $\boldsymbol{V}$, the velocities in that frame (denoted with asterisks) are

$$\boldsymbol{v}_p^* = \boldsymbol{v}_p - \boldsymbol{V} \quad \text{and} \quad \boldsymbol{v}_t^* = \boldsymbol{v}_t - \boldsymbol{V} \ . \tag{2.9}$$

Demanding that $\boldsymbol{p}_p^* = -\boldsymbol{p}_t^*$ leads to

$$\boldsymbol{V} = \frac{m_p \boldsymbol{v}_p + m_t \boldsymbol{v}_t}{m_p + m_t} \ . \tag{2.10}$$

Since $\boldsymbol{V} \equiv \frac{d\boldsymbol{R}}{dt}$, it is clear that the coordinate

$$\boldsymbol{R} \equiv \frac{m_p \boldsymbol{r}_p + m_t \boldsymbol{r}_t}{m_p + m_t} \tag{2.11}$$

[13] The trivial part is the motion of the center of mass, described as a free wave.

is at rest in the frame moving with $\boldsymbol{V}$, *i.e.*, its motion in that frame is trivial.

Non-trivial information about the system is contained in a relative coordinate[14]

$$\boldsymbol{r} \equiv \boldsymbol{r}_p - \boldsymbol{r}_t \ . \tag{2.12}$$

Since Newton's second law demands that

$$m_p \frac{d\boldsymbol{v}_p}{dt} = \boldsymbol{F} \quad \text{and} \quad m_t \frac{d\boldsymbol{v}_t}{dt} = -\boldsymbol{F} \ , \tag{2.13}$$

we can write

$$\frac{d^2\boldsymbol{r}}{dt^2} = \frac{d\boldsymbol{v}_p}{dt} - \frac{d\boldsymbol{v}_t}{dt} = \left(\frac{1}{m_p} + \frac{1}{m_t}\right)\boldsymbol{F} = \frac{\boldsymbol{F}}{\mu} \ , \tag{2.14}$$

where we have defined the reduced mass

$$\mu \equiv \frac{m_p m_t}{m_p + m_t} \ . \tag{2.15}$$

Rewriting Eq. (2.14) as

$$\mu \frac{d^2\boldsymbol{r}}{dt^2} = \boldsymbol{F} \tag{2.16}$$

and using the fact that $\boldsymbol{F} = d\boldsymbol{p}/dt$, we immediately obtain that

$$\boldsymbol{p} = \mu \frac{d\boldsymbol{r}}{dt} = \frac{m_p m_t}{m_p + m_t}\left(\boldsymbol{v}_p - \boldsymbol{v}_t\right) = \frac{m_t \boldsymbol{p}_p - m_p \boldsymbol{p}_t}{m_p + m_t} \ . \tag{2.17}$$

Defining $M = m_p + m_t$, we can summarize the new coordinates, now with explicit center-of-mass (CM) and relative (rel) subscripts where appropriate,

$$\begin{cases} \boldsymbol{R}_{\rm CM} = \dfrac{m_p \boldsymbol{r}_p + m_t \boldsymbol{r}_t}{M} \ , & \boldsymbol{r}_{\rm rel} = \boldsymbol{r}_p - \boldsymbol{r}_t \\ \boldsymbol{P}_{\rm CM} = \boldsymbol{p}_p + \boldsymbol{p}_t \ , & \boldsymbol{p}_{\rm rel} = \dfrac{m_t \boldsymbol{p}_p - m_p \boldsymbol{p}_t}{M} \end{cases} \tag{2.18}$$

2.2.2 Reaction thresholds vs. the Q-value

In-class Activity 2a: Reaction thresholds

Consider a reaction A(a,b)B in which $Q < 0$. As this reaction requires supplying energy, it will only be possible for incident energies at or above the threshold for the reaction. Starting from the CM frame, find the threshold (*i.e.*, minimum) laboratory frame kinetic energy of the projectile required for the reaction. Use that result to understand the ^{28}Si(n, p)^{28}Al cross section measurements plotted in the left panel of Fig. 2.2. To get the numerical result, you may use the following values for the masses: $m(^{28}\text{Si}) = 27.977$ amu and $m(\text{n}) = 1.009$ amu.

Hint: At a minimum energy required for the reaction, the products of the reaction are at rest in the CM frame.

[14] For example, think about Coulomb interaction between two particles: the problem only really depends on the distance between the two particles and not on their overall positions.

Solution

We know that in the CM frame,

$$\boldsymbol{p}_a^* = -\boldsymbol{p}_A^* \ , \tag{2.19}$$

and conservation of momentum demands that

$$\boldsymbol{p}_b^* = -\boldsymbol{p}_B^* \ . \tag{2.20}$$

From the conservation of energy we have[a]

$$m_a + \frac{p_a^{*2}}{2m_a} + m_A + \frac{p_A^{*\,2}}{2m_A} = m_b + \frac{p_b^{*2}}{2m_b} + m_B + \frac{p_B^{*\,2}}{2m_B} \ , \tag{2.21}$$

which, using the definition of the Q-value, Eq. (1.26), we can rewrite as

$$Q = -\frac{p_a^{*2}}{2m_a} - \frac{p_A^{*\,2}}{2m_A} + \frac{p_b^{*2}}{2m_b} + \frac{p_B^{*\,2}}{2m_B} \ . \tag{2.22}$$

In the CM frame, the minimum energy required for the reaction to take place corresponds to a situation in which all products of the reaction are at rest, $\boldsymbol{p}_b^* = \boldsymbol{p}_B^* = 0$. Then, using Eq. (2.19), the above equation simplifies to

$$Q = -\frac{p_a^{*2}}{2}\frac{m_a + m_A}{m_a m_A} \ . \tag{2.23}$$

From the equation transforming the velocity from the lab into the CM frame, Eq. (2.9), we see that $\boldsymbol{p_a^*}$ is related to $\boldsymbol{p_a}$ through

$$\boldsymbol{p}_a^* = \boldsymbol{p}_a - m_a \boldsymbol{V} = \boldsymbol{p}_a \left(1 - \frac{m_a}{m_a + m_A}\right) \ , \tag{2.24}$$

where we used the expression for the transformation velocity, Eq. (2.10), in which we put the target velocity at zero. With this, Eq. (2.23) becomes

$$Q = -\frac{p_a^2}{2m_a}\frac{m_A}{m_a + m_A} \ , \tag{2.25}$$

from which we obtain the threshold (minimum) incident kinetic energy needed for the reaction to take place,

$$K_{\rm th} \equiv \left.\frac{p_a^2}{2m_a}\right|_{\rm th} = -Q\frac{m_a + m_A}{m_A} \ . \tag{2.26}$$

In the case of the reaction show in the left-hand panel of Fig. 2.2, using the provided masses of ^{28}Si and the neutron, we get

$$K_{\rm th} = 3.861 \text{ MeV} \times 1.036 = 4 \text{ MeV} \ , \tag{2.27}$$

which agrees with the threshold indicated in the figure.

[a] Remember that in natural units $c = 1$.

The fact that the threshold incident energy in the laboratory frame is larger than the Q-value is often expressed with statements such as "most of the beam energy goes into the center-of-mass motion." This may not be entirely clear upon hearing it for the first time. Fundamentally, the reason behind $K_{\rm th} > -Q$ is momentum conservation: in the laboratory frame, the target is at rest while the projectile is moving, so the entrance channel carries a nonzero total momentum that must be carried by the reaction products. As a result, some kinetic energy is unavoidably tied up in the translational motion and cannot be converted into reaction energy, making the laboratory threshold larger than $-Q$. From the definition, Eq. (2.18), we can see that in this situation the momentum of the center of mass is equal to the initial momentum of the projectile, so the translational motion before and after the reaction is simply the motion of the center of mass.

Finally, a word of caution: Eq. (2.26) differs from a formula computed in, *e.g.*, Bertulani & Danielewicz [6], who quote

$$K_{\rm th} = -Q\frac{m_B + m_b}{m_B + m_b - m_a} \ . \tag{2.28}$$

What is the reason for the difference? It turns out it's... relativity. In our derivation, we mixed classical and relativistic notions about the energy with reckless abandon (using, *e.g.*, expressions like $E = m_a + \frac{p_a^2}{2m_a}$). In this, we acknowledged the possibility that the sum total of masses in the system can change (so that $Q \neq 0$) without also acknowledging that it would affect the definition of the center of mass and, in fact, make it time-dependent. With that, a comparison between the CM frame *after* the reaction and the lab frame *before* the reaction becomes ill-defined. This introduces a small (of order Q/m_A) difference between our expression and that found in Bertulani & Danielewicz, who calculated their expression in the lab frame. Ultimately, *both* results are wrong (although, at the same time, good enough if one only applies them at low energies): the correct expression can be obtained using relativistic kinematics, which is the subject of the next couple of lectures. Therefore, we will revisit this problem soon.

Lecture sources: This lecture is mainly based on chapter 1 in Bertulani & Danielewicz [6]; Section 2.1 also has significant additions based on my memory of Prof. J. Sobczyk's lecture on Elementary Particle Physics (University of Wrocław).

Lecture 3

Relativistic kinematics I

Prerequisites: none.
Guiding question: ***How do space and time reorganize themselves so that the laws of physics remain the same for all inertial observers?***

In this lecture, we explicitly write factors of c to make the derivation more intuitive. However, other than the force of habit which may make $x = ct$ look more natural than $x = t$, nothing prevents one from putting $c = 1$ from the very beginning.

3.1 Inertial reference frames and the principle of relativity

A frame of reference is called *inertial* if, in that frame, a freely moving body (*i.e.*, a body not acted upon by external forces) proceeds with constant velocity. Frames moving at a constant linear velocity relative to one another are inertial. A frame that is accelerating or rotating relative to an inertial frame is not inertial, and describing motion within such a frame requires introducing fictitious forces in order to preserve the usual form of Newton's laws. For example, if we watch a drone onboard a train that begins to accelerate, the freely-moving drone will seemingly begin to accelerate in the opposite direction even though it experiences no force; then, describing its motion within the frame of the train would require introducing fictitious forces simply because if we have $\boldsymbol{a} \neq 0$, then that implies the existence of a force according to $\boldsymbol{F} = m\boldsymbol{a} \neq 0$.

The *principle of relativity* states that all laws of nature take the same form in all inertial systems of reference. This means that the equations expressing the laws of nature must retain their form under transformations of space and time coordinates between inertial frames.

Experiments show that physical influences are not transmitted instantaneously. For example, consider a point charge located a distance Δl from a conducting wire carrying a current. If the current in the wire changes, the resulting change in the electromagnetic field reaches the charge only after some finite time Δt. This finite time reflects the finite propagation speed of electromagnetic field disturbances, equal to $\Delta l/\Delta t$. Experimentally, this speed is found to be c, the speed of light.

As a fundamental property of electromagnetic interactions, c enters the laws of electromagnetism[1]. Then, based on the principle of relativity, such a fundamental constant must enter the laws of physics in the same way in all inertial frames, without singling out any of the possible frames. In particular, the value of c must be the same in all inertial frames[2].

[1] In electrostatic and magnetostatic limits, it is hidden in the constants ε_0 and μ_0 which satisfy $\epsilon_0\mu_0 = c^{-2}$.
[2] Otherwise, an inertial frame could be distinguished by the value of c, contradicting the principle of relativity.

3.2 The Lorentz transformation

Let us consider two inertial frames S and S', where S' moves with respect to S with velocity V; for simplicity, let us assume that V is aligned with the x axis. Let us further assume that at $t = t' = 0$, the origins in both frames coincide.

In the inertial frame S, a free particle satisfies

$$x(t) = x_0 + vt \ , \tag{3.1}$$

i.e., its motion is a straight line in spacetime. If we observe this particle from *another* inertial frame S', its motion again should be that of a free particle moving along a straight line

$$x'(t') = x'_0 + v't' \ . \tag{3.2}$$

Thus, the transformation from S to S' should preserve straight lines, which is satisfied by a linear transformation: any nonlinear transformation would "bend" straight lines into curves[3].

The most general linear transformation between the coordinates in S and S' is given by

$$\begin{cases} t' = At + Bx \\ x' = Ct + Dx \end{cases} \tag{3.3}$$

where A, B, C, and D are all constants that can only depend on V or c. To fix these constants, we consider a number of "special cases." First, we apply the transformation to the position of the origin of the S' frame, which in the S' frame is simply $x' = 0$, while in the S frame it is $x = Vt$. Inserted into the space coordinate transformation, Eq. (3.3), this yields

$$0 = Ct + DVt \qquad \Rightarrow \qquad C = -DV \ , \tag{3.4}$$

so that now we've got

$$\begin{cases} t' = At + Bx \\ x' = D\big(x - Vt\big) \end{cases} \tag{3.5}$$

Next, let us consider a light pulse originating at $t = t' = 0$ from $x = x' = 0$. In S, it satisfies $x = ct$, which plugged into Eq. (3.5) yields

$$\begin{cases} t' = t\big(A + Bc\big) \\ x' = Dt\big(c - V\big) \end{cases} \tag{3.6}$$

Since in S', the light pulse satisfies $x' = ct'$, we can multiply the first of the above equations by c and then demand that its right-hand side is equal to the right-hand side of the second one, yielding

$$c\big(A + Bc\big) = D\big(c - V\big) \ . \tag{3.7}$$

The same logic applies to a light pulse moving in the opposite direction, *i.e.*, with $-c$: in S, it satisfies $x = -ct$, leading to

$$\begin{cases} t' = t\big(A - Bc\big) \\ x' = -Dt\big(c + V\big) \end{cases} \tag{3.8}$$

[3] Another argument for a linear transformation is that space and time are assumed to be homogeneous, *i.e.*, there is no preferred origin in space and no preferred instant in time. This means that the transformation should *not* depend on where or when it takes place, which would not be satisfied with terms of the form x^2, xt, *etc.*

and since we should have $x' = -ct'$, we obtain

$$c\big(A - Bc\big) = D\big(c + V\big) \ . \tag{3.9}$$

Adding both sides of Eqs. (3.7) and (3.9) yields

$$A = D \ , \tag{3.10}$$

while subtraction shows that

$$B = -D\frac{V}{c^2} = -A\frac{V}{c^2} \ . \tag{3.11}$$

Thus we arrive at

$$\begin{cases} t' = A\Big(t - \dfrac{V}{c^2}x\Big) \\ x' = A\Big(x - Vt\Big) \end{cases} \tag{3.12}$$

Finally, we demand that the form of the transformation is exactly the same for the inverse transformation, from S' to S, so that t and x can be expressed in terms of t' and x' as

$$\begin{cases} t = A\Big(t' + \dfrac{V}{c^2}x'\Big) \\ x = A\Big(x' + Vt'\Big) \end{cases} \tag{3.13}$$

where we used the fact that S is moving with velocity $-V$ with respect to S'. We can plug expressions for t' and x', Eq. (3.12), into the above equation, which yields

$$\begin{cases} t = A^2\Big(1 - \dfrac{V^2}{c^2}\Big)t \\ x = A^2\Big(1 - \dfrac{V^2}{c^2}\Big)x \end{cases} \tag{3.14}$$

For this to be true, we need $A^2 = \big(1 - \frac{V^2}{c^2}\big)^{-1}$. It is customary to denote this overall factor by $\gamma = A$, and thus we arrive at

$$\begin{cases} \gamma = \left(1 - \dfrac{V^2}{c^2}\right)^{-1/2} \\ t' = \gamma\Big(t - \dfrac{V}{c^2}x\Big) \\ x' = \gamma\Big(x - Vt\Big) \end{cases} \tag{3.15}$$

The above is known as the *Lorentz transformation*.

To obtain formulae valid in 3D[4], we note that a transformation from S to S' only affects the coordinate components which are parallel to the velocity of the transformation $\boldsymbol{V}$. In other words, for a position vector denoted by $\boldsymbol{x}$, only the $\boldsymbol{x}_{\parallel} \equiv \boldsymbol{x}\cdot\hat{\boldsymbol{V}}$ should be transformed, while $\boldsymbol{x}_{\perp} \equiv \boldsymbol{x} - \boldsymbol{x}\cdot\hat{\boldsymbol{V}}$ should remain untouched. With this insight, we can generalize the above equations to

$$\begin{cases} t' = \gamma\Big(t - \dfrac{\boldsymbol{V}\cdot\boldsymbol{x}}{c^2}\Big) \\ \boldsymbol{x}' = \boldsymbol{x} + (\gamma - 1)\big(\boldsymbol{x}\cdot\hat{\boldsymbol{V}}\big)\hat{\boldsymbol{V}} - \gamma t\boldsymbol{V} \end{cases} \tag{3.16}$$

where the second equation can also be written in the more intuitive form $\boldsymbol{x}' = \boldsymbol{x}_{\perp} + \gamma\big(\boldsymbol{x}\cdot\hat{\boldsymbol{V}} - Vt\big)\hat{\boldsymbol{V}}$, highlighting the decomposition $\boldsymbol{x} = \boldsymbol{x}_{\parallel} + \boldsymbol{x}_{\perp}$ and application of the boost only to $\boldsymbol{x}_{\parallel}$.

[4]Or, to be precise, (1+3)D, as in relativity the time dimension enters on an (almost) equal footing.

3.3 Velocity transformation

Consider a particle in some inertial frame, moving with velocity

$$\boldsymbol{v} = \big(v_x, v_y, v_z\big) = \Big(\frac{dx}{dt}, \frac{dy}{dt}, \frac{dz}{dt}\Big) \ . \tag{3.17}$$

What will its velocity be in a frame moving with velocity V with respect to the original frame? For simplicity, let us assume that V is parallel to the x axis. Then applying the Lorentz transformation, Eq. (3.15), to the infinitesimal displacements dt, dx, dy, and dz yields

$$dt' = \gamma\Big(dt - \frac{V}{c^2}dx\Big) \ , \quad dx' = \gamma\big(dx - Vdt\big) \ , \quad dy' = dy, \quad dz' = dz \ , \tag{3.18}$$

where $\gamma = \big(1 - \frac{V^2}{c^2}\big)^{-1/2}$. This allows us to obtain

$$\begin{cases} v'_x = \dfrac{dx'}{dt'} = \dfrac{dx - Vdt}{dt - \frac{V}{c^2}dx} = \dfrac{v_x - V}{1 - \frac{V}{c^2}v_x} \ , \\ v'_y = \dfrac{dy'}{dt'} = \dfrac{dy}{\gamma\big(dt - \frac{V}{c^2}dx\big)} = \dfrac{v_y}{\gamma\big(1 - \frac{V}{c^2}v_x\big)} \ , \\ v'_z = \dfrac{dz'}{dt'} = \dfrac{dz}{\gamma\big(dt - \frac{V}{c^2}dx\big)} = \dfrac{v_z}{\gamma\big(1 - \frac{V}{c^2}v_x\big)} \ . \end{cases} \tag{3.19}$$

Evidently, the transformation of velocities is nonlinear and, except for the motion purely parallel to the boost direction, it mixes the velocity components: the transformed transverse components depend explicitly on the longitudinal velocity v_x.

By taking $V \to -V$, we obtain the inverse transformations

$$\begin{cases} v_x = \dfrac{v'_x + V}{1 + \frac{V}{c^2}v'_x} \ , \\ v_y = \dfrac{v'_y}{\gamma\big(1 + \frac{V}{c^2}v'_x\big)} \ , \\ v_z = \dfrac{v'_z}{\gamma\big(1 + \frac{V}{c^2}v'_x\big)} \ , \end{cases} \tag{3.20}$$

which provide the velocity of a particle v given its velocity v' in a system moving with V.

We note that the velocity transformation ensures that velocity addition never leads to a velocity larger than c provided that $V \le c$ and v_x, v_y, $v_z \le c$. For simplicity, let us consider a particle moving along the x axis, so that we can solely concentrate on the first expression in Eq. (3.20). We want to show that

$$v = \frac{v' + V}{1 + \frac{V}{c^2}v'} \le c \ . \tag{3.21}$$

Let us then consider

$$c - v = c - \frac{v' + V}{1 + \frac{V}{c^2}v'} = c - \frac{c^2(v' + V)}{c^2 + Vv'} = c\frac{(c^2 + Vv') - (cv' + cV)}{c^2 + Vv'} = c\frac{(c - v')(c - V)}{c^2 + Vv'} \ge 0 \ , \tag{3.22}$$

where the last inequality holds because the terms in the brackets are both positive. Thus, for any $v' \le c$ and $V \le c$, $v \le c$.

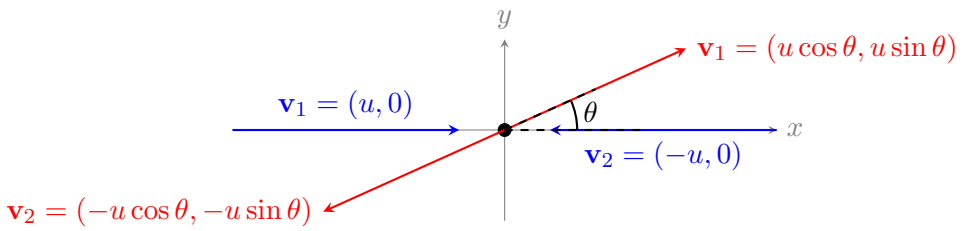

Figure 3.1: Sketch of a scattering event between identical particles.

3.3.1 Classical momentum and the principle of relativity

Let us consider an elastic scattering of identical particles of mass m and velocities $v_{1x} = u$, $v_{2x} = -u$, after which the particles propagate at angles $+\theta$, $-\theta$ with respect to the x axis (see Fig. 3.1). We can check the conservation of momentum, defined as $\boldsymbol{p} = m\boldsymbol{v}$, in two cases: A) in the frame shown in the figure (which is the CM frame), and B) in any other frame.

A) In the original frame we have $p_{1x} = mu$ and $p_{2x} = -mu$ before the scattering and $p_{1x} = mu\cos\theta$, $p_{1y} = mu\sin\theta$, $p_{2x} = -mu\cos\theta$, and $p_{2y} = -mu\sin\theta$ after the scattering. Evidently, $\sum_i p_{i,x} = \sum_i p_{i,y} = 0$ both before and after, so that momentum is conserved.

B) In a frame moving at some velocity V, using the velocity transformation, Eq. (3.19), we have

$$v'_{1x} = \frac{u - V}{1 - \frac{V}{c^2}u} \quad \text{and} \quad v'_{2x} = \frac{-u - V}{1 + \frac{V}{c^2}u} \tag{3.23}$$

before the scattering, so that

$$\sum_i p'_{i,x} = \frac{-2mV\left(1 - \frac{u^2}{c^2}\right)}{1 - \left(\frac{Vu}{c^2}\right)^2} \quad \text{and} \quad \sum_i p'_{i,y} = 0\ . \tag{3.24}$$

After the scattering, we have

$$v'_{1x} = \frac{u\cos\theta - V}{1 - \frac{Vu\cos\theta}{c^2}}\ , \qquad v'_{2x} = \frac{-u\cos\theta - V}{1 + \frac{Vu\cos\theta}{c^2}}\ , \tag{3.25}$$

$$v'_{1y} = \frac{u\sin\theta}{\gamma\left(1 - \frac{Vu\cos\theta}{c^2}\right)}\ , \qquad v'_{2y} = \frac{-u\sin\theta}{\gamma\left(1 + \frac{Vu\cos\theta}{c^2}\right)}\ , \tag{3.26}$$

leading to

$$\sum_i p'_{i,x} = \frac{-2mV\left(1 - \frac{u^2\cos^2\theta}{c^2}\right)}{1 - \left(\frac{Vu\cos\theta}{c^2}\right)^2} \quad \text{and} \quad \sum_i p'_{i,y} = \frac{2mV\frac{u^2}{c^2}\sin\theta\cos\theta}{\gamma\left[1 - \left(\frac{Vu\cos\theta}{c^2}\right)^2\right]}\ , \tag{3.27}$$

which fail to equal Eq. (3.24) for any nontrivial scattering ($\theta \neq 0$) or boost ($V \neq 0$).

The result of the above exercise does *not* mean momentum is not conserved. It means that $\boldsymbol{p} = m\boldsymbol{v}$ is not the correct relativistic momentum. The reason is the non-linearity of velocity transformation, Eq. (3.19): an internal redistribution of velocities that preserves $\sum m\boldsymbol{v}$ in one frame will not, in general, preserve $\sum m\boldsymbol{v}'$ in any other frame, making the conservation of $\sum m\boldsymbol{v}$ frame-dependent and thus contradicting the principle of relativity. Clearly, the classical $\boldsymbol{p} = m\boldsymbol{v}$ must be a non-relativistic limit of some expression which transforms linearly under Lorentz boosts.

3.4 Invariants

3.4.1 Space-time interval

Let us consider a light pulse in 3D. In S, a light pulse emitted from the origin satisfies

$$|\Delta l| = c\Delta t \ , \tag{3.28}$$

where $|\Delta l| = \sqrt{(\Delta x)^2 + (\Delta y)^2 + (\Delta z)^2}$, while in S' it satisfies

$$|\Delta l'| = c\Delta t' \ . \tag{3.29}$$

Both of the above equations can be squared and rewritten as

$$c^2(\Delta t)^2 - (\Delta x)^2 - (\Delta y)^2 - (\Delta z)^2 = 0 \tag{3.30}$$

and

$$c^2(\Delta t')^2 - (\Delta x')^2 - (\Delta y')^2 - (\Delta z')^2 = 0 \ , \tag{3.31}$$

respectively, showing that the quadratic combination $c^2(\Delta t)^2 - (\Delta x)^2 - (\Delta y)^2 - (\Delta z)^2$ is equal zero for light signals in *all* inertial frames. Motivated by this observation, we define the *spacetime interval* Δs between two arbitrary points in spacetime (t_1, x_1, y_1, z_1) and (t_2, x_2, y_2, z_2) as

$$(\Delta s)^2 \equiv c^2(\Delta t)^2 - (\Delta x)^2 - (\Delta y)^2 - (\Delta z)^2 \ . \tag{3.32}$$

In-class Activity 3a: Space-time interval

What is $(\Delta s)^2$ in a reference frame S', which moves with a constant velocity v with respect to the reference frame S? To simplify, consider the problem in (1+1)D (*i.e.*, only t and x axis).

Solution

From the definition of the space-time interval, Eq. (3.32), we have

$$(\Delta s')^2 = c^2(\Delta t')^2 - (\Delta x')^2 \ , \tag{3.33}$$

where $\Delta t' = t'_2 - t'_1$ and $\Delta x' = x'_2 - x'_1$. Applying the Lorentz transformation, Eq. (3.15), term by term to t'_1, t'_2, x'_1, and x'_2 we see that

$$\Delta t' = \gamma\Big(\Delta t - \frac{v}{c^2}\Delta x\Big) \ , \tag{3.34}$$

$$\Delta x' = \gamma\Big(\Delta x - v\Delta t\Big) \ , \tag{3.35}$$

which allows us calculate

$$(\Delta s')^2 = \gamma^2\Big[c^2(\Delta t)^2\Big(1 - \frac{v^2}{c^2}\Big) - (\Delta x)^2\Big(1 - \frac{v^2}{c^2}\Big)\Big] \ . \tag{3.36}$$

Since $\gamma = \Big(1 - \frac{v^2}{c^2}\Big)^{-1/2}$, then $\gamma^2\Big(1 - \frac{v^2}{c^2}\Big) = 1$ and we obtain

$$(\Delta s')^2 = c^2(\Delta t)^2 - (\Delta x)^2 \equiv (\Delta s)^2 \ , \tag{3.37}$$

i.e., the space-time interval Δs is *invariant under the Lorentz transformation.*

Let us take a look at what values Δs^2 can take for separations with a clear physical meaning. We have already seen that $\Delta s = 0$ for two events connected by a light signal, and so we call such space-time intervals *light-like*. If we consider the interval to correspond to the motion of a material object with speed $v < c$, so that $\Delta x = v\Delta t$, then

$$(\Delta s)^2 = c^2(\Delta t)^2 - v^2(\Delta t)^2 > 0 \ . \tag{3.38}$$

Thus, $\Delta s^2 > 0$ for intervals between space-time points that could correspond to the trajectory of a physical object; we call such intervals *time-like* (simply because the term $c^2(\Delta t)^2$ dominates over the $(\Delta x)^2$ term). Conversely, $\Delta s^2 < 0$ for separations which cannot correspond to a physical trajectory; we call such intervals *space-like*. Space-like intervals are between events which cannot be *causally connected*: since no signal traveling at speed $v \leq c$ can connect the events, neither can be the cause of the other.

Finally, we have defined the space-time interval with finite differences, Eq. (3.32), but nothing stops us from taking the limit and considering

$$ds^2 = c^2(dt)^2 - (dx)^2 - (dy)^2 - (dz)^2 \ . \tag{3.39}$$

3.4.2 Proper time

With the space-time invariant defined, Eq. (3.39), we can now consider ds^2 in the frame in which the particle is at rest. The time in that frame is called the *proper time* and denoted with τ, so that

$$(ds')^2 = c^2(d\tau)^2 \ , \tag{3.40}$$

i.e., the value of $d\tau$ is determined by the Lorentz-invariant spacetime interval ds^2,

$$d\tau = \frac{\sqrt{ds^2}}{c} \ , \tag{3.41}$$

and therefore is itself a Lorentz invariant. On the other hand, in an inertial frame in which the particle moves with velocity $\boldsymbol{v} = (v_x, v_y, v_z)$ we have

$$ds^2 = c^2(dt)^2 - (v_x dt)^2 - (v_y dt)^2 - (v_z dt)^2 = (dt)^2\left(c^2 - v^2\right) \ , \tag{3.42}$$

and from the invariance of the space-time interval we get

$$d\tau = dt\sqrt{1 - \frac{v^2}{c^2}} = \frac{dt}{\gamma} \ . \tag{3.43}$$

3.4.3 Proper velocity

The reason for the non-linear behavior of velocities under the Lorenz transformation, Eq. (3.19), is the fact that in $\boldsymbol{v} = \frac{d\boldsymbol{x}}{dt}$ both the numerator and the denominator are subject to a Lorentz boost upon changing the reference frame. If one wants to avoid that, one should define a quantity which simply doesn't have that feature. Indeed, one can define

$$u^i \equiv \frac{dx^i}{d\tau} = \gamma v^i \ , \tag{3.44}$$

where τ is the proper time and in the second equality we used Eq. (3.43). Since the proper time is frame-independent, see Eq. (3.41), one does not transform it upon changing the frame. Then the transformation rule for u^i, called the *proper velocity*[5], is the same as for x^i, Eq. (3.16).

[5]It is not a widely used name, mostly because u^i is part of another object that we will soon introduce and that people tend to refer to instead.

In-class Activity 3b: Transformation properties of u^2

Consider a combination

$$u^2 = \left(c\frac{dt}{d\tau}\right)^2 - \sum_i \left(u^i\right)^2 = \left(c\frac{dt}{d\tau}\right)^2 - \left(\frac{dx}{d\tau}\right)^2 - \left(\frac{dy}{d\tau}\right)^2 - \left(\frac{dz}{d\tau}\right)^2 . \tag{3.45}$$

How does u^2 behave under the Lorentz transformation? Assume that the transformation velocity V is aligned with the x axis.

Solution

With $V \parallel \hat{x}$, we can use Eq. (3.15) to calculate

$$(u')^2 = \left(c\frac{d(t')}{d\tau}\right)^2 - \left(\frac{d(x')}{d\tau}\right)^2 - \left(\frac{dy}{d\tau}\right)^2 - \left(\frac{dz}{d\tau}\right)^2 \tag{3.46}$$

$$= \left(c\gamma\frac{d\left(t - \frac{V}{c^2}x\right)}{d\tau}\right)^2 - \left(\gamma\frac{d\left(x - Vt\right)}{d\tau}\right)^2 - \left(\frac{dy}{d\tau}\right)^2 - \left(\frac{dz}{d\tau}\right)^2 \tag{3.47}$$

$$= c^2\gamma^2\left(\frac{dt}{d\tau} - \frac{V}{c^2}\frac{dx}{d\tau}\right)^2 - \gamma^2\left(\frac{dx}{d\tau} - V\frac{dt}{d\tau}\right)^2 - \left(\frac{dy}{d\tau}\right)^2 - \left(\frac{dz}{d\tau}\right)^2 \tag{3.48}$$

$$= c^2\gamma^2\left[1 - \frac{V^2}{c^2}\right]\left(\frac{dt}{d\tau}\right)^2 - \gamma^2\left[1 - \frac{V^2}{c^2}\right]\left(\frac{dx}{d\tau}\right)^2 - \left(\frac{dy}{d\tau}\right)^2 - \left(\frac{dz}{d\tau}\right)^2 \tag{3.49}$$

$$= c^2\left(\frac{dt}{d\tau}\right)^2 - \left(\frac{dx}{d\tau}\right)^2 - \left(\frac{dy}{d\tau}\right)^2 - \left(\frac{dz}{d\tau}\right)^2 = u^2 , \tag{3.50}$$

where in the last line we used the fact that $\gamma^2 = \left(1 - \frac{V^2}{c^2}\right)^{-1}$, Eq. (3.15). Evidently, u^2 is invariant under the Lorentz transformation.

Lecture sources: This lecture is mainly based on chapter 1 in Landau & Lifshitz's *Classical Theory of Fields* [9],

Lecture 4

Relativistic kinematics II

Prerequisites: Lecture 3
Guiding question: ***How to deal with relativistic problems without losing your mind?***

In this lecture, we explicitly write factors of c to make the derivation more intuitive. However, other than the force of habit which may make $x = ct$ look more natural than $x = t$, nothing prevents one from putting $c = 1$ from the very beginning.

4.1 Four-vectors, the Einstein convention, and invariants

4.1.1 Four-vectors and the metric

By now, we have seen two quantities that are invariant under Lorentz transformations:

1. The space-time interval[1] $ds^2 = c^2(dt)^2 - (dx)^2 - (dy)^2 - (dz)^2$
2. The combination $u^2 = \left(c\frac{dt}{d\tau}\right)^2 - \left(\frac{dx}{d\tau}\right)^2 - \left(\frac{dy}{d\tau}\right)^2 - \left(\frac{dz}{d\tau}\right)^2$

Both expressions are quadratic forms (*i.e.*, linear combinations of squares) which, combined with their invariance with respect to a change of the reference frame, would remind one of the ordinary scalar product of a vector with itself if it were not for the fact that in an ordinary (*i.e.*, Euclidean) scalar product, all terms enter with a plus sign. Evidently, special relativity requires something similar to that, yet different. Let's see where this realization leads.

Inspired by the expression for ds^2, we define the infinitesimal displacement in spacetime as a four-dimensional vector (*four-vector*)

$$dx^\mu = (cdt, dx, dy, dz) \ , \tag{4.1}$$

where the superscript μ indexes the components[2] of dx: the time component $dx^0 = cdt$ and the spatial components $dx^1 = dx$, $dx^2 = dy$, $dx^3 = dz$. Then we *postulate* that the scalar product of dx^μ with itself (*i.e.*, its squared "length") is

$$(dx)^2 = (cdt)^2 - (dx)^2 - (dy)^2 - (dz)^2 \ . \tag{4.2}$$

[1] Here we use its infinitesimal form, but we have already seen that it doesn't really matter; the reason is the linearity of the Lorentz transformation.

[2] There is a minor notation degeneracy between x^μ and $x^1 = x$. Hopefully, it is clear from context which is which.

This behavior of a scalar product can be encoded with a *metric* $g_{\mu\nu}$, which in the operational sense we can think of as a way to keep track of the sign with which the squares of the components of dx^μ enter Eq. (4.2). Specifically, we write

$$(dx)^2 = \sum_\mu \sum_\nu g_{\mu\nu} dx^\mu dx^\nu \ , \tag{4.3}$$

from which we see that to reproduce Eq. (4.2), the metric should have the following properties[3]

$$g^{00} = 1 \ , \quad g^{ii} = -1 \ , \quad g^{\mu\nu} = 0 \ \text{ for } \ \mu \neq \nu \ . \tag{4.4}$$

By now, we have defined dx^μ, Eq. (4.1), as well as the way it forms a scalar product, Eq. (4.3), in such a way that it reproduces the Lorentz invariance of the infinitesimal spacetime interval ds^2. However, since the Lorentz transformation is linear, finite differences transform the same way as infinitesimal ones. Thus, we can generalize from the infinitesimal interval dx^μ, Eq. (4.1), and define the *position four-vector* as

$$x^\mu \equiv (ct, x, y, z) \ , \tag{4.5}$$

From the above discussion we immediately see that

$$x^2 = \sum_\mu \sum_\nu g_{\mu\nu} x^\mu x^\nu \tag{4.6}$$

should be Lorentz invariant. This can be checked by writing the scalar product out and applying the Lorentz transformation, but in the following we will obtain this result formally.

4.1.2 Matrix notation

In the above considerations, elements of the equations such as specific components of $g_{\mu\nu}$ or x^ν are all numbers. However, looking at the double sum appearing in the scalar x^2, Eq. (4.6), one is reminded of matrix and vector multiplication. If we represent x^μ as a column vector

$$x^\mu = \begin{pmatrix} ct \\ x^1 \\ x^2 \\ x^3 \end{pmatrix} \tag{4.7}$$

and the metric as a matrix[4]

$$g_{\mu\nu} = \begin{pmatrix} 1 & 0 & 0 & 0 \\ 0 & -1 & 0 & 0 \\ 0 & 0 & -1 & 0 \\ 0 & 0 & 0 & -1 \end{pmatrix} = \text{diag}(1, -1, -1, -1) \ , \tag{4.8}$$

then the transpose of x^μ is a row vector

$$(x^\mu)^{\mathrm{T}} = \begin{pmatrix} ct, & x^1, & x^2, & x^3 \end{pmatrix} \tag{4.9}$$

and we can get the result of Eq. (4.6), that is the combination $(ct)^2 - x^2 - y^2 - z^2$, by writing

$$x^2 = x^{\mathrm{T}} g x \ . \tag{4.10}$$

[3]Here we follow the standard notation in which Greek indices refer to all spacetime coordinates (time and spatial together), while Roman indices refer to spatial coordinates only.

[4]Note that when writing matrices in this context, we take the *first* index as the row index and the *second* index as the column index. This is because the up or down position of the index marks *transformation properties* with respect to the Lorentz transformation (for example, an object with one up index transforms like a vector). This is why in general $\Lambda^\alpha{}_\beta \neq \Lambda_\beta{}^\alpha \neq \Lambda_\alpha{}^\beta \neq \Lambda^\beta{}_\alpha$.

4.1.3 Lowering and raising indices

Note that

$$x^{\mathrm{T}} g = \left(ct, -x^1, -x^2, -x^3\right) , \tag{4.11}$$

i.e., the action of the metric $g_{\mu\nu}$ on x^ν is to flip the sign of its spatial components. In index notation, this is marked with *lowering the index of* x^μ, so that

$$\sum_\nu g_{\mu\nu} x^\nu \equiv x_\mu , \tag{4.12}$$

where the spatial components of x_μ are equal to the spatial components of x^{mnu} with the opposite sign, $x_i = -x^i$ (the temporal components are the same, $x_0 = x^0$). Thus, one can also write the scalar product, Eq. (4.6), as

$$(x)^2 = \sum_\nu x_\nu x^\nu . \tag{4.13}$$

Since we have an object that lowers an index, Eq. (4.12), we can imagine that we also have an object that raises an index, which we will call $g^{\mu\nu}$:

$$\sum_\nu g^{\mu\nu} x_\nu = x^\mu . \tag{4.14}$$

What is $g^{\mu\nu}$? To establish that, we take a vector x^ν and first lower, then raise its index,

$$\sum_\mu \left(g^{\alpha\mu} \sum_\nu g_{\mu\nu} x^\nu \right) = \sum_\mu g^{\alpha\mu} x_\mu = x^\alpha . \tag{4.15}$$

For this to be true for any arbitrary x^ν, we need

$$\sum_\mu g^{\alpha\mu} g_{\mu\nu} = \delta^\alpha{}_\nu , \tag{4.16}$$

where $\delta^\alpha{}_\nu = \mathrm{diag}(1,1,1,1)$ is the Kronecker delta. Eq. 4.16 means that $g^{\mu\nu}$ is the inverse of $g_{\mu\nu}$. In a flat pseudo-Euclidean space-time, where $g_{\mu\nu}$ is given by Eq. (4.4) (or Eq. (4.8) in the matrix form), the inverse $g^{\mu\nu}$ has exactly the same components as $g_{\mu\nu}$, so that we can write $g^{\mu\nu} = g_{\mu\nu}$.

4.1.4 Co- and contravariant tensors

Objects with indeces down, like x_μ, are called *covariant*, while objects with indeces up, like x^μ, are called *contravariant*. This is because their components transform either like or unlike the components of the basis vectors upon basis transformation.

Consider a 2D example, where we have basis vectors $\hat{\boldsymbol{x}}$ and $\hat{\boldsymbol{y}}$. To *measure* anything, we also need to specify the scale, *i.e.*, the *length* of the basis unit vectors. For example, we can say that $|\hat{\boldsymbol{x}}| = |\hat{\boldsymbol{y}}| = 1$ m. If we now consider a vector which in this basis is represented as $\boldsymbol{v} = (1,1)$, its length is $|\boldsymbol{v}| = \sqrt{2}$ m. Now let us consider a change of basis: let's adopt a new basis in which $|\hat{\boldsymbol{x}}'| = |\hat{\boldsymbol{y}}'| = 1$ cm. Clearly, $|\hat{\boldsymbol{x}}'| = 0.01|\hat{\boldsymbol{x}}|$ and $|\hat{\boldsymbol{y}}'| = 0.01|\hat{\boldsymbol{y}}|$: the length of the basis vectors is reduced. The length of the vector $\boldsymbol{v}$, however, hasn't changed: it's a geometric object which couldn't care less about a specific basis. But its *representation* in the new basis is indeed different: now we have $\boldsymbol{v}' = (100, 100)$ and $|\boldsymbol{v}'| = 100\sqrt{2}$ m. Thus, in terms of the numbers specifying vectors in a given basis, *vectors transform opposite to the transformation of the basis*: they are contravariant.

As already mentioned, covariant objects transform *with* the basis. One of the best examples is the gradient: using the same transformation as above (from meters to centimeters), we can easily see that any infinitesimal distance will transform as $dx' = 100dx$. Thus, $(\frac{d}{dx})' = \frac{1}{100}(\frac{d}{dx})$, *i.e.*, the gradient transforms in the same way as the basis. To visualize this better, imagine that the gradient is applied to a scalar function: if we look at how much the function is changing over some distance and we shorten that distance, then the recorded changes will also be relatively smaller[5]. Because they are covariant, gradients in special relativity are written as $\partial_\mu \equiv \frac{\partial}{\partial x^\mu}$.

Tensors are objects which can have an arbitrary number of indeces denoting components which transform either co- or contravariantly. Four-vectors are *rank-1 tensors*, since they have 1 index which can be either co- or contravariant. The metric $g_{\mu\nu}$ is a *rank-2 tensor*, since it has 2 indices which can be both covariant, both contravariant, or mixed.

4.1.5 Index *vs.* matrix notation

In the following, we will mainly use the index (tensor) notation, but one should feel empowered to switch between the index (tensor) and matrix notation as needed and/or appropriate. The difference between the two is that the index notation is a coordinate-based language for geometric objects (such as vectors and tensors) that keeps track of their type and transformation properties (for example, vectors transform differently than tensors), while matrices are basis-dependent representations of these objects that do not, fundamentally, know about their geometric structure. For example, a vector x^μ is an object in spacetime: you can imagine it as a physical arrow. The properties of this arrow, like length, are fixed $(x)^2 = c^2\tau^2$. Now, the *components* of this arrow are numbers corresponding to a *specific choice of basis* (*e.g.*, in the rest frame or any other frame). Thus, the components alone do not carry a fundamental meaning about what the object is. The way in which we can combine these together (for example, how to take a square of x^μ) is *not* decided by the rules governing the operations on matrices (*i.e.*, linear algebra), but by the properties of the objects (geometry). Thus, under the hood, when we switch to the matrix notation we silently do it in such a way that *it works the way it should*. In that sense, the index (tensor) notation is more fundamental.

4.1.6 Lorentz transformation

Using the four-vector formalism we can write the transformed four-vector $x^{\mu'}$ as

$$x^{\mu'} = \sum_\nu \Lambda^\mu{}_\nu x^\nu \ . \tag{4.17}$$

In the matrix notation, to reproduce the Lorentz transformation from Eq. (3.15), the matrix $\Lambda^\mu{}_\nu$ must be given by

$$\Lambda^\mu{}_\nu = \begin{pmatrix} \gamma & -\gamma\beta & 0 & 0 \\ -\gamma\beta & \gamma & 0 & 0 \\ 0 & 0 & 1 & 0 \\ 0 & 0 & 0 & 1 \end{pmatrix} \tag{4.18}$$

where we define $\beta \equiv \frac{V}{c}$.

[5] Over an interval within which the function behaves approximately linearly – a necessary condition to meaningfully consider a gradient at all.

4.1.7 Einstein convention

Introducing the four-dimensional vector x^μ and the metric $g_{\mu\nu}$ already has led to some systematization of the notation, for example in the form of being able to write the Lorentz transformations, Eq. (3.15), in one equation, Eq. (4.17). Further improvements come from using the *Einstein summation convention*, within which summation over all possible values of repeated indices which are on different levels *is implied*. In other words, whenever the same index appears once upstairs and once downstairs, we sum over it; in the matrix notation, this is just a compact way of writing matrix multiplication[6]. Thus, for example, Eqs. (4.6) and (4.13) can be written as

$$(x^2) = g_{\mu\nu}x^\mu x^\nu = x_\nu x^\nu \ . \tag{4.19}$$

4.1.8 Historical note

The spacetime with a metric $g = \mathrm{diag}(-1, 1, 1, 1)$ is called the *Minkowski spacetime*, and g is called the *Minkowski metric*. They are named after Hermann Minkowski, who in years 1908-1909 recast Einstein's special relativity into the geometric language of four-dimensional spacetime. This reformulation cleaned up the notation and led to new insights, supporting further progress. In particular, it is impossible to imagine *general* relativity without the machinery of spacetimes, metrics, *etc.*

We should note that there is an alternative convention for handling the time and space components in special relativity. While in this text we follow the convention in which the scalar product is

$$x_\mu x^\mu = (x^0)^2 - \boldsymbol{x}^2 \ , \tag{4.20}$$

an alternative way of defining the theory is one in which

$$x_\mu x^\mu = -(x^0)^2 + \boldsymbol{x}^2 \ . \tag{4.21}$$

This is equivalent to defining the Minkowski metric as $g = \mathrm{diag}(-1, 1, 1, 1)$. Mathematically, this difference in sign is perfectly allowable and, if used consistently across the entire theory[7], leads to the same results. One quickly finds that the choice whether to use $g = \mathrm{diag}(1, -1, -1, -1)$ or $g = \mathrm{diag}(-1, 1, 1, 1)$ is extremely field-specific and, moreover, proponents of a given convention are always convinced that *theirs* is the only way to go[8].

4.2 Invariants

Note that while an object with either a superscript or a subscript μ is four-dimensional vector, a combination in which the index μ appears both on the upper and lower level – in which case we say that the index is *contracted* – is a scalar product, *i.e.*, a number. In particular, such a quantity is a *scalar with respect to the Lorentz transformation*, *i.e.*, it is invariant under the Lorentz transformation. We already have seen this in the case of the space-time interval ds^2, which now we can write as $ds^2 = dx_\mu dx^\mu$. Similarly, the scalar product of x^μ with itself is a Lorentz invariant, *i.e.*, it assumes the same value in any frame.

In general, *any* product of the form $A_\mu B^\mu$ is Lorentz invariant (regardless of whether it is meaningful physically or not). This can be (relatively) quickly shown using the matrix representation of the Lorentz transformation, Eq. (4.18). For any pair of Lorentz vectors A^μ, B^μ, we can always

[6] If one carefully follows this convention, a situation in which an index is repeated on the same level, for example as two superscripts, should never arise. If this happens, likely something is wrong with the calculation.

[7] For example, we would have to modify our definition of ds^2 to $ds^2 = -c^2(dt)^2 + (dx)^2 + (dy)^2 + (dx)^2$, *etc.*

[8] I myself believe that using the $\mathrm{diag}(-1, 1, 1, 1)$ metric is next to evil.

consider their Lorentz transformation, $(A')^\mu = \Lambda^\mu{}_\alpha A^\alpha$ and $(B')^\mu = \Lambda^\mu{}_\beta B^\beta$. Then we can always write $(A')_\mu = g_{\mu\nu}(A')^\nu = g_{\mu\nu}\Lambda^\nu{}_\alpha A^\alpha$, and so the scalar product in the new frame is

$$(A')_\mu (B')^\mu = g_{\mu\nu}\Lambda^\nu{}_\alpha \Lambda^\mu{}_\beta A^\alpha B^\beta \ , \tag{4.22}$$

where we recognize that in the index notation all entries in the above equations are numbers so we can move them around as we please (in particular, $g_{\mu\nu}\Lambda^\nu{}_\alpha A^\alpha \Lambda^\mu{}_\beta B^\beta$ is the same as $g_{\mu\nu}\Lambda^\nu{}_\alpha \Lambda^\mu{}_\beta A^\alpha B^\beta$). Now we need to understand what $g_{\mu\nu}\Lambda^\nu{}_\alpha \Lambda^\mu{}_\beta$ means. Making the summations explicit (unnecessary, but perhaps useful), we have (again moving things around as we please)

$$g_{\mu\nu}\Lambda^\nu{}_\alpha \Lambda^\mu{}_\beta = \sum_\mu \sum_\nu \Lambda^\mu{}_\beta g_{\mu\nu}\Lambda^\nu{}_\alpha \ . \tag{4.23}$$

The meaning of $\sum_\nu g_{\mu\nu}\Lambda^\nu{}_\alpha$ is now clear[9]: it's a product of matrix g and matrix Λ, yielding the matrix element $(g\Lambda)_{\mu\alpha}$. But then what is $\sum_\mu \Lambda^\mu{}_\beta (g\Lambda)_{\mu\alpha}$? To make it look like something recognizable, we note that for any matrix A, the transpose is defined through $A^\mu{}_\beta = (A^{\mathrm{T}})_\beta{}^\mu$. This allows us to write

$$\sum_\mu \sum_\nu \Lambda^\mu{}_\beta g_{\mu\nu}\Lambda^\nu{}_\alpha = \sum_\mu (\Lambda^{\mathrm{T}})_\beta{}^\mu (g\Lambda)_{\mu\alpha} \ , \tag{4.24}$$

where we can now see that the second sum corresponds to the product $\Lambda^{\mathrm{T}}(g\Lambda)$. With this identification, we can compute explicitly

$$g\Lambda = \begin{pmatrix} 1 & 0 & 0 & 0 \\ 0 & -1 & 0 & 0 \\ 0 & 0 & -1 & 0 \\ 0 & 0 & 0 & -1 \end{pmatrix} \begin{pmatrix} \gamma & -\gamma\beta & 0 & 0 \\ -\gamma\beta & \gamma & 0 & 0 \\ 0 & 0 & 1 & 0 \\ 0 & 0 & 0 & 1 \end{pmatrix} = \begin{pmatrix} \gamma & -\gamma\beta & 0 & 0 \\ \gamma\beta & -\gamma & 0 & 0 \\ 0 & 0 & -1 & 0 \\ 0 & 0 & 0 & -1 \end{pmatrix} \ , \tag{4.25}$$

and then (since Λ is symmetric, its transpose is the same as Λ)

$$\Lambda^{\mathrm{T}}(g\Lambda) = \begin{pmatrix} \gamma^2(1-\beta^2) & -\gamma^2\beta + \gamma^2\beta & 0 & 0 \\ -\gamma^2\beta + \gamma^2\beta & \gamma^2(\beta^2 - 1) & 0 & 0 \\ 0 & 0 & -1 & 0 \\ 0 & 0 & 0 & -1 \end{pmatrix} = \begin{pmatrix} 1 & 0 & 0 & 0 \\ 0 & -1 & 0 & 0 \\ 0 & 0 & -1 & 0 \\ 0 & 0 & 0 & -1 \end{pmatrix} = g \ . \tag{4.26}$$

Thus, we have shown that Eq. (4.23) reduces to

$$g_{\mu\nu}\Lambda^\nu{}_\alpha \Lambda^\mu{}_\beta = g_{\alpha\beta} \ , \tag{4.27}$$

which, inserted into Eq. (4.22), proves the Lorentz-invariance of the scalar product,

$$(A')_\mu (B')^\mu = A_\mu B^\mu \ . \tag{4.28}$$

Lorentz invariants are extremely powerful in special relativity, as they often allow one to short-circuit computations that would otherwise involve painful application of the Lorentz transformation; we will see examples of this soon. They also allow one to understand better the constraints on various quantities. For example, since $u_\mu u^\mu$ is an invariant, we can in particular calculate it in the rest frame of the particle where $x^\mu = (c\tau, 0, 0, 0)$, immediately leading to $u^2 = u_\mu u^\mu = c^2$. This shows that four-velocity has a fixed spacetime length of c, independent of the particle's motion.

Invariants are the answer to the guiding question of this lecture. Whenever you can, when dealing with relativistic problems, see if using an invariant makes it easier.

[9] Remember that the rule for matrix multiplication is: given a $m \times n$ matrix A and a $n \times p$ matrix B, the product AB is an $m \times p$ matrix with entries given by $(AB)_{ij} = \sum_{k=1}^{n} A_{ik}B_{kj}$.

4.3 Energy and momentum

After all these developments, we can now define the *four-velocity* as

$$u^\mu \equiv \frac{dx^\mu}{d\tau} = \left(c\frac{dt}{d\tau}, \frac{dx}{d\tau}, \frac{dy}{d\tau}, \frac{dz}{d\tau}\right) = \gamma\Big(c, v^1, v^2, v^3\Big) = \gamma\big(c, \boldsymbol{v}\big) \ , \tag{4.29}$$

where we used this occasion to introduce several equivalent notations for four-vectors. As we have already seen in the In-class Activity 3b, $u_\mu u^\mu$ is a Lorentz invariant.

Since we have identified a "velocity-like" quantity which transforms nicely under the Lorentz transformation, we may now attempt to define a *Lorentz-covariant momentum*,

$$p^\nu = mu^\nu = \gamma m\big(c, \boldsymbol{v}\big) \ , \tag{4.30}$$

where $\gamma = \left(1 - \frac{v^2}{c^2}\right)^{-1/2}$, with v being the particle's velocity in the frame in which γ is evaluated. We can immediately tell that we're on the right track as in the non-relativistic limit, where $\gamma \to 1$, the spatial components reproduce the classical expression $\boldsymbol{p} = m\boldsymbol{v}$. Next, let us compute p^2,

$$p^2 = p_\nu p^\nu = \gamma^2 m^2 c^2\left(1 - \frac{v^2}{c^2}\right) = m^2c^2 \ . \tag{4.31}$$

On the other hand, we know that in the particle's rest frame, where $\boldsymbol{v} = 0$, we have

$$p^2 = (p^0)^2 \ . \tag{4.32}$$

Since in that frame the energy of the particle is mc^2, we conclude that the zeroth component of the momentum four-vector is equal $\frac{E}{c}$, so that we can also write

$$p^\mu = \left(\frac{E}{c}, \ \boldsymbol{p}\right) \ . \tag{4.33}$$

This leads to two things: First, we see that the *relativistic energy* is given by

$$E = \gamma mc^2 \ , \tag{4.34}$$

where m is the particle's rest mass. Second, we can formally take the square of Eq. (4.33) and equate it to Eq. (4.31), which leads to

$$\frac{E^2}{c^2} - \boldsymbol{p}^2 = mc^2 \ , \tag{4.35}$$

from which we immediately get

$$E = \sqrt{\boldsymbol{p}^2c^2 + m^2c^4} \ , \tag{4.36}$$

the "canonical" expression for the energy of a free particle in relativistic kinematics. Furthermore, comparing Eqs. (4.30) and (4.34), we can also see that

$$\boldsymbol{v} = \frac{\boldsymbol{p}c^2}{E} \ . \tag{4.37}$$

The same can be obtained by differentiating the energy, Eq. (4.36), with respect to $\boldsymbol{p}$, $\boldsymbol{v} = \frac{\partial E}{\partial \boldsymbol{p}}$ (a sign that Hamilton's equations still apply in special relativity).

Let us stress that the energy in Eq. (4.36) is the *total* energy of a particle that includes its rest mass. The *relativistic kinetic energy* is defined as the part of the total energy that is not mass, *i.e.*,

$$E_{\text{kin}} = E - m = mc^2(\gamma - 1) \ , \tag{4.38}$$

where in the second equality we used Eq. (4.34). We also note that because p^μ is a four-vector, it transforms according to the Lorentz transformation, Eq. (4.18),

$$(p')^\mu = \Lambda^\mu{}_\nu p^\nu \ . \tag{4.39}$$

4.4 The center-of-mass frame

In Newtonian mechanics, the center-of-mass (CM) frame, that is the frame moving along with the coordinate $\boldsymbol{R}_{\rm CM}$, is equivalent with the frame in which the total momentum of the system is equal zero, as we have seen in Section 2.2. However, the definition of a "center of mass" becomes problematic in special relativity, among others because it assumes averaging over the positions of the particles *at the same time*, while the concept of simultaneity is frame-dependent in special relativity. What remains well-defined is the concept of a frame in which all momenta add up to zero. Thus, relativistically, we define the CM frame as that in which

$$\sum_i \boldsymbol{p}'_i = 0 \tag{4.40}$$

is satisfied. Technically, a better name would then be the "center-of-momentum frame", but in practice most people still refer to it as the "center-of-mass frame." To transform, *i.e.*, perform a boost into the CM frame, one needs to compute the CM velocity. Then, to study the kinematics of particles in that frame, one needs to know their relative velocity.

In-class Activity 4a: The center-of-mass frame in special relativity

Let us consider two particles with four-momenta $p_1^\mu = (E_1, \boldsymbol{p}_1)$ and $p_2^\mu = (E_2, \boldsymbol{p}_2)$ in the lab frame. We want to find the velocity of a frame in which $\boldsymbol{p}'_1 + \boldsymbol{p}'_2 = 0$.

Solution

Under a Lorentz boost with an arbitrary velocity $\boldsymbol{v}$, the energy and momentum transform as

$$E' = \gamma(E - \boldsymbol{v}\cdot\boldsymbol{p}) \ , \tag{4.41}$$
$$\boldsymbol{p}' = \boldsymbol{p} + (\gamma-1)(\boldsymbol{p}\cdot\hat{\boldsymbol{v}})\hat{\boldsymbol{v}} - \gamma E\boldsymbol{v} \ , \tag{4.42}$$

where $\hat{\boldsymbol{v}} \equiv \boldsymbol{v}/|\boldsymbol{v}|$. To obtain the CM frame, we want to boost the system to a frame moving with $\boldsymbol{v}$ such that $\boldsymbol{p}'_1 = -\boldsymbol{p}'_2$, *i.e.*,

$$\boldsymbol{p}_1 + (\gamma-1)(\boldsymbol{p}_1\cdot\hat{\boldsymbol{v}})\hat{\boldsymbol{v}} - \gamma E_1\boldsymbol{v} = -\boldsymbol{p}_2 - (\gamma-1)(\boldsymbol{p}_2\cdot\hat{\boldsymbol{v}})\hat{\boldsymbol{v}} + \gamma E_2\boldsymbol{v} \ . \tag{4.43}$$

In the above equation, we can gather similar terms together in the following way,

$$\big(\boldsymbol{p}_1 + \boldsymbol{p}_2\big) + (\gamma-1)\big[(\boldsymbol{p}_1+\boldsymbol{p}_2)\cdot\hat{\boldsymbol{v}}\big]\hat{\boldsymbol{v}} = \gamma\big(E_1+E_2\big)\boldsymbol{v} \ . \tag{4.44}$$

Note that on the right-hand side we have a contribution proportional to $\hat{\boldsymbol{v}}$, while on the left-hand side we have both a contribution pointing in an in-principle random direction (the first term, $\boldsymbol{p}_1+\boldsymbol{p}_2$) and a contribution proportional to $\hat{\boldsymbol{v}}$ (the second term). This equation can only be satisfied in two cases:
1) The $\boldsymbol{p}_1+\boldsymbol{p}_2$ term is zero, from which it follows that $\boldsymbol{v}=0$. This makes sense: we don't need to boost into the CM frame, because *we already are* in the CM frame!
2) The $\boldsymbol{p}_1+\boldsymbol{p}_2$ term is also aligned with $\hat{\boldsymbol{v}}$. In this case, $\big[(\boldsymbol{p}_1+\boldsymbol{p}_2)\cdot\hat{\boldsymbol{v}}\big]\hat{\boldsymbol{v}} = (\boldsymbol{p}_1+\boldsymbol{p}_2)$ and Eq. (4.44) becomes

$$\gamma(\boldsymbol{p}_1+\boldsymbol{p}_2) = \gamma\big(E_1+E_2\big)\boldsymbol{v} \ , \tag{4.45}$$

from which we obtain that the CM velocity is

$$\boldsymbol{v} = \frac{\boldsymbol{p}_1+\boldsymbol{p}_2}{E_1+E_2} \equiv \boldsymbol{v}_{\rm CM} \ . \tag{4.46}$$

In-class Activity 4b: Relative velocity in special relativity

Once we have the CM velocity, we could also like to know the relative velocity between two particles in that frame,

$$\boldsymbol{v}^*_{\rm rel} \equiv \boldsymbol{v}^*_1 - \boldsymbol{v}^*_2 \ , \tag{4.47}$$

where we denote quantities referring to the CM frame with an asterisk. To this end, use the Mandelstam s variable, $s \equiv P_\mu P^\mu$, where P^μ is the total four-momentum of the system.

Solution

Since the particles move in the opposite directions with equal magnitudes of momenta p^*, we can write

$$v^*_{\rm rel} = |\boldsymbol{v}^*_1 - \boldsymbol{v}^*_2| = |\boldsymbol{v}^*_1| + |\boldsymbol{v}^*_2| = \frac{p^*}{E^*_1} + \frac{p^*}{E^*_2} = p^* \frac{E^*_1 + E^*_2}{E^*_1 E^*_2} = p^* \frac{\sqrt{s}}{E^*_1 E^*_2} \ , \tag{4.48}$$

where we have introduced the Mandelstam s variable, defined as $s \equiv P_\mu P^\mu$ with P^μ being the total four-momentum of the system.
The usefulness of s lies in the fact that its value is frame-independent, and in particular we can use s to solve for p^*. In the lab frame, we have

$$s = (p^\mu_1 + p^\mu_2)^2 = \big(E_1 + E_2, \boldsymbol{p}_1 + \boldsymbol{p}_2\big)^2 = (E_1 + E_2)^2 - (\boldsymbol{p}_1 + \boldsymbol{p}_2)^2 \ , \tag{4.49}$$

while in the CM frame we have

$$s = (p^{*,\mu}_1 + p^{*,\mu}_2)^2 = \big(E^*_1 + E^*_2, \boldsymbol{p}^*_1 + \boldsymbol{p}^*_2\big)^2 = \left(\sqrt{m_1^2 + (p^*)^2} + \sqrt{m_2^2 + (p^*)^2}\right)^2 \ , \tag{4.50}$$

since $\boldsymbol{p}^*_1 = -\boldsymbol{p}^*_2$ by definition. Assuming that we can compute the value of s using the quantities known in the lab frame, Eq. (4.50) can be further rewritten to enable solving for p^*,

$$s - m_1^2 - m_2^2 - 2(p^*)^2 = 2\sqrt{m_1^2 + (p^*)^2}\sqrt{m_2^2 + (p^*)^2} \ . \tag{4.51}$$

Squaring of both sides and canceling common terms leads to

$$4s(p^*)^2 = s^2 - 2sm_1^2 - 2sm_2^2 + m_1^4 - 2m_1^2 m_2^2 + m_2^4 \ , \tag{4.52}$$

which can be further rewritten as

$$\begin{aligned} 4s(p^*)^2 &= s^2 - s\big(2m_1^2 + 2m_2^2\big) + \big(m_1^2 - m_2^2\big)^2 && (4.53)\\ &= s^2 - s(m_1 + m_2)^2 - s(m_1 - m_2)^2 + \big[(m_1 + m_2)(m_1 - m_2)\big]^2 && (4.54)\\ &= \big[s - (m_1 + m_2)^2\big]\big[s - (m_1 - m_2)^2\big] \ . && (4.55) \end{aligned}$$

Thus we obtain

$$p^* = \frac{1}{2\sqrt{s}}\sqrt{\big[s - (m_1 + m_2)^2\big]\big[s - (m_1 - m_2)^2\big]} \ , \tag{4.56}$$

and from that, using Eq. (4.48), we arrive at the relative velocity in the CM frame,

$$\boldsymbol{v}_{\rm rel} = \frac{\sqrt{\big[s - (m_1 + m_2)^2\big]\big[s - (m_1 - m_2)^2\big]}}{2E^*_1 E^*_2} \ . \tag{4.57}$$

4.5 When does relativity matter?

Looking at the expressions for relativistic momentum and energy, Eqs. (4.30) and (4.34), we see that we recover the Newtonian expressions as long as $\gamma \approx 1$. How close to 1 is close enough depends on the accuracy we are striving for, which in turn is often set by the sensitivity of a given experiment. For a reasonable measurement, various systematic uncertainties are usually on the order of 5% or 10%. Then, in the zeroth approximation, to apply Newtonian formulae we would also like γ to be within 5% or 10% from 1. What velocities and what kinetic energies per nucleon does this correspond to? Let's plot it!

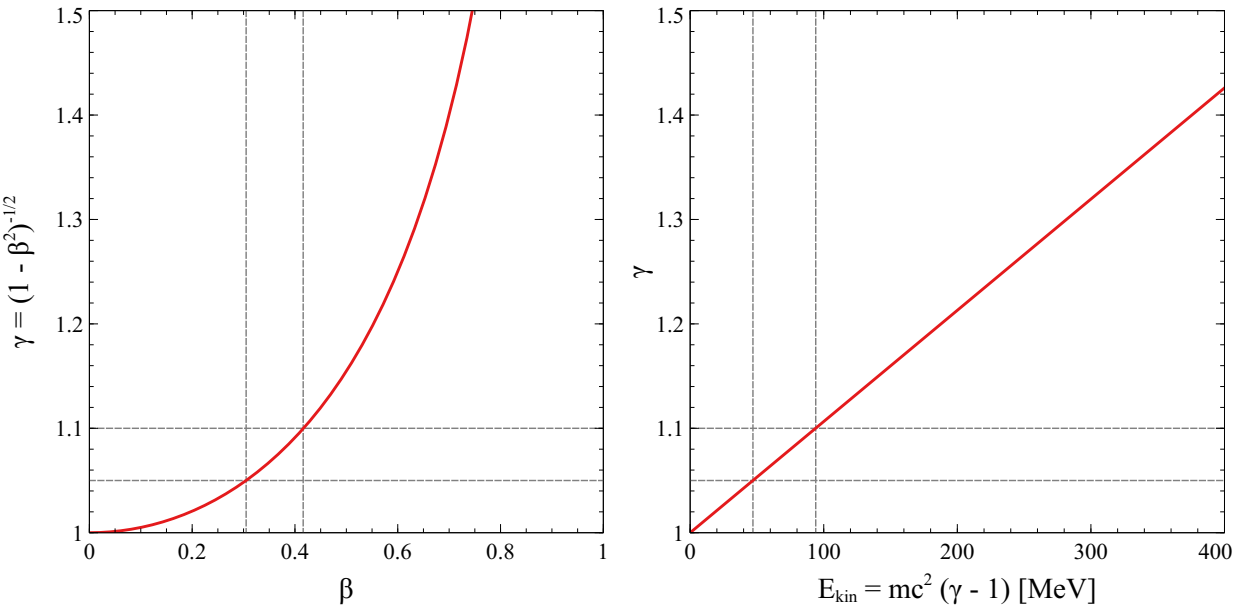

Figure 4.1: The Lorentz γ factor as a function of reduced velocity $\beta = v/c$ (*left panel*) and kinetic energy per nucleon (*right panel.*)

Evidently, the need to use relativistic formulae can be very much within both FRIB ($E_{\text{kin}} \lesssim$ 270 MeV/nucleon) and future FRIB400 energies ($E_{\text{kin}} \lesssim 400$ MeV/nucleon).

Lecture sources: This lecture is mainly based on chapters 1 and 2 in Landau & Lifshitz's *Classical Theory of Fields* [9],

Lecture 5

Classical scattering

Prerequisites: Lecture 2
Guiding question: ***What sets the minimum distance of approach in a collision?***

5.1 Collision geometry and angular momentum

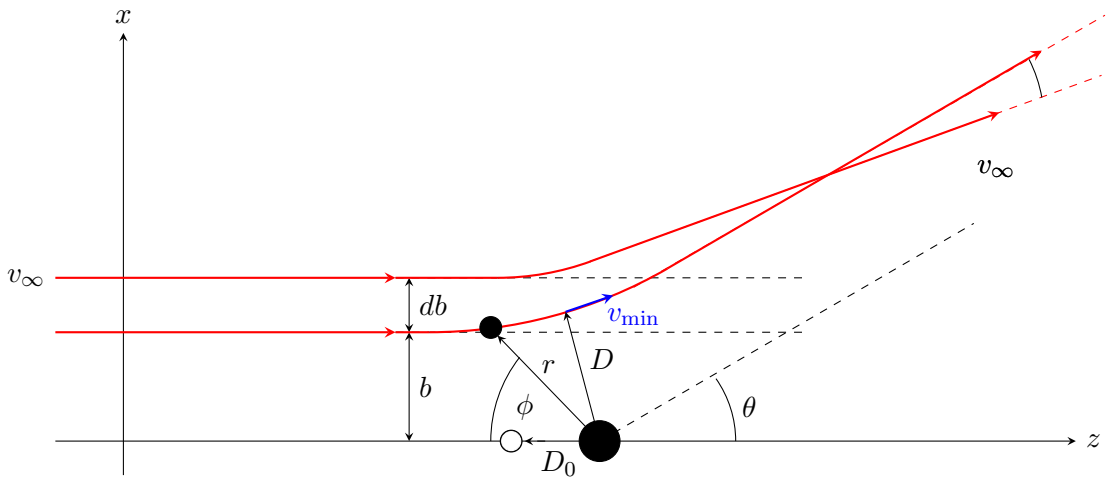

Figure 5.1: Sketch of a classical scattering event.

Let us consider a classical scattering experiment as depicted in Fig. 5.1. Projectiles come in from $z = -\infty$ on trajectories parallel to the z axis. Classically, each scattering event is associated with a definite trajectory. Since there is no randomness to the scattering process, there is a 1-to-1 relationship between the *impact parameter* b, that is the perpendicular distance between a given projectile's initial trajectory and the z axis[1], and the scattering angle θ. Thus, the trajectories can be labeled by their impact parameter b. Since each value of b corresponds to a specific value of the scattering angle θ, we can define the *deflection function* $\theta(b)$. The *distance of closest approach* D is also a function of b, as is the projectile's minimal velocity $v_{\min}$ which occurs at D. In particular, the *smallest distance of closest approach* D_0 corresponds to $b = 0$, *i.e.*, to head-on collisions, in which case $v_{\min} = 0$.

[1]This distance is also equal to the distance of closest approach to the scattering center were the initial projectile trajectory to remain unchanged.

5.1.1 Conservation of angular momentum for central potentials

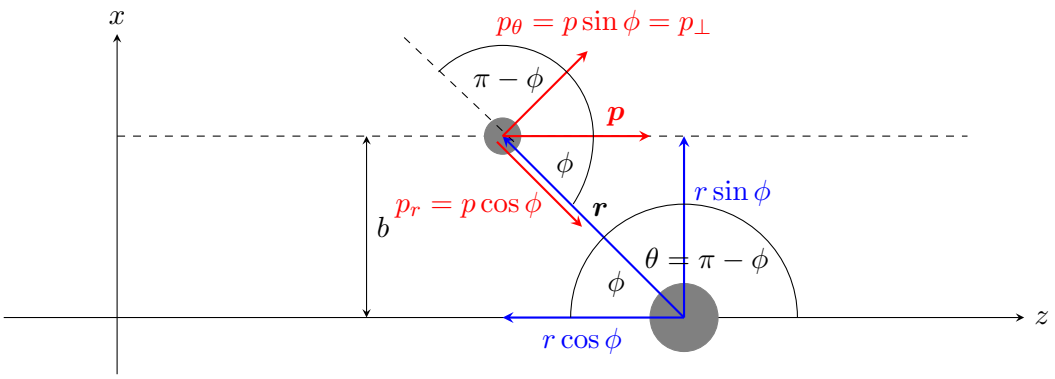

Figure 5.2: Decomposition of the position $\boldsymbol{r}$ and momentum $\boldsymbol{p}$ vectors.

For a purely central (radial) force, Newton's second law gives

$$\frac{d\boldsymbol{p}}{dt} = \boldsymbol{F}(\boldsymbol{r}) = F(r)\hat{\boldsymbol{r}} \ . \tag{5.1}$$

The force is radial in any instant, but the direction of $\hat{\boldsymbol{r}}$ changes as the particle moves. Thus, if we decompose the momentum vector in the *moving* polar basis (see Fig. 5.2),

$$\boldsymbol{p} = p_r\hat{\boldsymbol{r}} + p_\theta\hat{\boldsymbol{\theta}} \ , \tag{5.2}$$

where $\hat{\boldsymbol{r}} = \hat{\boldsymbol{r}}(t)$ and $\hat{\boldsymbol{\theta}} = \hat{\boldsymbol{\theta}}(t)$, then

$$\frac{d\boldsymbol{p}}{dt} = \frac{dp_r}{dt}\hat{\boldsymbol{r}} + p_r\frac{d\hat{\boldsymbol{r}}}{dt} + \frac{dp_\theta}{dt}\hat{\boldsymbol{\theta}} + p_\theta\frac{d\hat{\boldsymbol{\theta}}}{dt} \ . \tag{5.3}$$

The time derivatives of the unit vectors are[2]

$$\frac{d\hat{\boldsymbol{r}}}{dt} = \frac{d\theta}{dt}\hat{\boldsymbol{\theta}} \quad \text{and} \quad \frac{d\hat{\boldsymbol{\theta}}}{dt} = -\frac{d\theta}{dt}\hat{\boldsymbol{r}} \ , \tag{5.4}$$

so that the time derivative of the momentum is

$$\frac{d\boldsymbol{p}}{dt} = \left(\frac{dp_r}{dt} - p_\theta\frac{d\theta}{dt}\right)\hat{\boldsymbol{r}} + \left(p_r\frac{d\theta}{dt} + \frac{dp_\theta}{dt}\right)\hat{\boldsymbol{\theta}} \ . \tag{5.5}$$

Since for a radial force the change in momentum can only occur along the radial direction, Eq. (5.1), it must be that in the above equation the coefficient multiplying $\hat{\boldsymbol{\theta}}$ is zero,

$$\frac{dp_\theta}{dt} + p_r\frac{d\theta}{dt} = 0 \ , \tag{5.6}$$

or equivalently

$$\frac{dp_\theta}{dt} = -p_r\frac{d\theta}{dt} \ . \tag{5.7}$$

[2]This can be derived in the following way: in polar coordinates, we have $\hat{\boldsymbol{r}} = (\cos\theta, \sin\theta)$ and $\hat{\boldsymbol{\theta}} = (-\sin\theta, \cos\theta)$. Then $\frac{d\hat{\boldsymbol{r}}}{dt} = (-\sin\theta, \cos\theta)\frac{d\theta}{dt} = \hat{\boldsymbol{\theta}}\frac{d\theta}{dt}$ and $\frac{d\hat{\boldsymbol{\theta}}}{dt} = (-\cos\theta, -\sin\theta)\frac{d\theta}{dt} = -\hat{\boldsymbol{r}}\frac{d\theta}{dt}$.

Thus we see that even for a purely radial force, p_θ is changing *because the basis is moving*. Furthermore, if we decompose the velocity in the polar coordinates[3],

$$\boldsymbol{v} = \frac{dr}{dt}\hat{\boldsymbol{r}} + r\frac{d\theta}{dt}\hat{\boldsymbol{\theta}} \ , \tag{5.8}$$

we can identify

$$p_r = m\frac{dr}{dt} \quad \text{and} \quad p_\theta = mr\frac{d\theta}{dt} \ . \tag{5.9}$$

With this, we can rewrite Eq. (5.6),

$$mr\frac{d^2\theta}{dt^2} + 2m\frac{dr}{dt}\frac{d\theta}{dt} = 0 \ , \tag{5.10}$$

which is the same as

$$\frac{d}{dt}\left(mr^2\frac{d\theta}{dt}\right) = \frac{d}{dt}\left[r\left(mr\frac{d\theta}{dt}\right)\right] = \frac{d}{dt}\Big[rp_\theta\Big] = \frac{d}{dt}\Big[rp\sin\phi\Big] = \frac{d}{dt}|\boldsymbol{r}\times\boldsymbol{p}| = \frac{d}{dt}|\boldsymbol{L}| = 0. \tag{5.11}$$

Thus the magnitude of the angular momentum is conserved for a purely radial potential $V(r)$.

Moreover, we can also write

$$\frac{d\boldsymbol{L}}{dt} = \frac{d}{dt}\Big(\boldsymbol{r}\times\boldsymbol{p}\Big) = \boldsymbol{r}\times\frac{d\boldsymbol{p}}{dt} = \boldsymbol{r}\times\boldsymbol{F} \ , \tag{5.12}$$

where we used the fact that $\boldsymbol{v}\times\boldsymbol{p} = 0$. Since a radial force satisfies $\boldsymbol{F} \parallel \boldsymbol{r}$, we immediately obtain $d\boldsymbol{L}/dt = 0$, *i.e.*, angular momentum is conserved as a vector.

5.1.2 Angular momentum and kinematics

Crucially, a given impact parameter b corresponds to a specific angular momentum L of the system. Denoting the momentum when the particle is infinitely far way (*i.e.*, outside the influence of the potential) as $\boldsymbol{p}_\infty = m\boldsymbol{v}_\infty$, we see that (using variables as denoted in Fig. 5.1)

$$L = |\boldsymbol{r}\times\boldsymbol{p}_\infty| = |\boldsymbol{r}||\boldsymbol{p}_\infty|\sin(\pi-\phi) = \Big(|\boldsymbol{r}|\sin\phi\Big)|\boldsymbol{p}_\infty| = b|\boldsymbol{p_\infty}| = bm|\boldsymbol{v}_\infty| \ . \tag{5.13}$$

Since L is conserved, the above is true at any point during the evolution.

Alternatively, using the decomposition highlighted in Fig. 5.2, we can write

$$L = |\boldsymbol{r}|\Big(|\boldsymbol{p}_\infty|\sin\phi\Big) = |\boldsymbol{r}|p_\perp \ . \tag{5.14}$$

Since L is conserved, $p_\perp = L/r$ increases as r decreases (due to, *e.g.*, the pull of an attractive central force). Using Eq. (5.14), we can write the total energy in the system as

$$E = \frac{p_r^2}{2m} + \frac{L^2}{2mr^2} + V(r) \ , \tag{5.15}$$

where $L^2/2mr^2$ is referred to as the *centrifugal term*. The radial momentum is then constrained by energy conservation,

$$p_r^2 = 2m\left(E - V(r) - \frac{L^2}{2mr^2}\right) \ , \tag{5.16}$$

[3]This follows immediately from $\boldsymbol{r} = r\hat{\boldsymbol{r}}$, since $\frac{d\boldsymbol{r}}{dt} = \frac{dr}{dt}\hat{\boldsymbol{r}} + r\frac{d\hat{\boldsymbol{r}}}{dt} = \frac{dr}{dt}\hat{\boldsymbol{r}} + r\frac{d\theta}{dt}\hat{\boldsymbol{\theta}}$.

so that p_r decreases whenever $V(r) + \frac{L^2}{2mr^2}$ increases along the trajectory.

Since $L = \text{const}$, the term $L^2/2mr^2$ depends only on r. Moreover, it *looks* like a potential, so much so it is customary to define an *effective potential*

$$V_{\text{eff}}(r) = V(r) + \frac{L^2}{2mr^2} \ , \tag{5.17}$$

so that

$$E = \frac{p_r^2}{2m} + V_{\text{eff}}(r) \ . \tag{5.18}$$

This notation helps one to see that for a repulsive potential, p_r must decrease as r decreases both because $V_{\text{eff}}(r)$ increases and because conservation of angular momentum requires $p_\perp$ to increase. Moreover, even for an attractive interaction, the centrifugal term diverges as r^{-2} as $r \to 0$ and therefore acts as a barrier against close approach for nonzero L. Thus, there is a minimal distance at which the projectile can approach the scattering center provided the attractive potential is not more singular than r^{-2}. Conversely, sufficiently singular attractive potentials can overcome the effects of the centrifugal term, and in that case the particle continues to approach $r = 0$ ("fall to the center"); in practice, the subsequent behavior depends on the short-distance regularization, which can include, *e.g.*, considerations of a finite-size core, absorption, or quantum effects.

For scenarios without a "fall to the center," the distance of closest approach D, also known as the *turning point*, is the point in space where $p_r = 0$. Given Eq. (5.18), D is given by the condition

$$E = V_{\text{eff}}(D) = V(D) + \frac{L^2}{2mD^2} = V(D) + \frac{(mbv_\infty)^2}{2mD^2} \ , \tag{5.19}$$

where we expressed L in terms of the impact parameter b and the incident velocity v_∞, see Eq. (5.13), highlighting the dependence of D on b. This example also highlights why $L^2/(2mD^2)$ is referred to as the *centrifugal barrier*: for fixed E and $V(r)$, increasing L (or, equivalently, b) leads to higher values of D, acting in a manner resembling effects due to a potential barrier[4].

This discussion allows us to answer the question guiding this lecture: the minimum distance of approach in a collision is governed by *all of the following*: the initial energy of the projectile, the interaction between the projectile and target, and the angular momentum of the scattering system.

5.1.3 Forward peaking of cross sections

In Fig. 5.1, we can see that smaller impact parameters correspond to smaller d and larger θ. This can be intuitively understood by considering the impact of a radial potential $V(r)$: the closer the projectile gets to the scattering center, the more it is deflected. One can also understand this by invoking angular momentum: larger impact parameters correspond to larger L, which shifts the turning point to larger radii and kinematically restricts the trajectory to a smaller deflection angle θ.

If the projectile beam has uniform current density j, then the number of particles dN with impact parameters between b and $b + db$ is

$$dN(b) \sim 2\pi b \, db \ . \tag{5.20}$$

Evidently, larger impact parameters correspond to a larger total number of incident particles. Since, for central forces, scattering at a larger impact parameter produces a smaller deflection angle θ, scattering cross sections are naturally peaked at $\theta \approx 0$.

[4]However, one *must* remember that there is no associated force. The effects due to the centrifugal term are kinematic, not dynamic.

5.2 The classical cross section in terms of the impact parameter

Let us consider scattering off a single scattering center. Given the 1-to-1 correspondence between the impact parameter b and the scattering angle θ, the rate of particles scattered between $\theta(b)$ and $\theta(b) + d\theta$ is equal to the rate of incoming particles with impact parameters between b and $b + db$,

$$\frac{dN}{dt} = j\ 2\pi b\ db\ , \tag{5.21}$$

where j is the incoming current density. This is the case simply because all particles at θ must have approached the target at b and no particles are lost in the process. In case of radial potentials, the azimuthal independence of scattering means that the infinitesimal solid angle element $d\Omega = \sin\theta d\theta\ d\phi$ can be integrated out to $2\pi \sin\theta d\theta$. With this, the definition of the differential scattering cross section $\frac{d\sigma(\Omega)}{d\Omega}$, Eq. (2.7), becomes

$$\frac{d\sigma(\Omega)}{d\Omega} = \frac{\frac{dN}{dt}}{d\Omega\ jN_{\text{targ}}} = \frac{b}{\sin\theta}\left|\frac{db}{d\theta}\right|\ , \tag{5.22}$$

where we have used the fact that there is a single scattering center, $N_{\text{targ}} = 1$ and we introduced the absolute value to ensure that the cross section is positive[5]. Since the deflection function $\theta(b)$ determines the scattering completely, so does its inverse[6], $b = b(\theta)$.

In-class Activity 5a: Rutherford scattering

Let us treat scattering of α particles on gold nuclei classically. Assume that the scattering is driven purely by the Coulomb force[a], and that both the projectile and the target can be taken as point particles with respect to that interaction[b]. Moreover, assume that the nucleus is much heavier than the α particle so that $\mu = \frac{m_p m_t}{m_p + m_t} \approx m_p$. To arrive at Rutherford's formula, $\frac{d\sigma}{d\Omega} \propto \sin^{-4}(\theta/2)$, use the following steps:

- Use angular momentum (around the target) to make a connection between velocity at $t = -\infty$ and velocity near the scattering center, the latter expressed in polar coordinates.
- For scattering at an angle θ, what is the v_x component of the α particle's velocity?
- Connect v_x to the Coulomb force by means of the impulse approximation, $\Delta p_x = \int_{-\infty}^{\infty} dt\ F_x$; use angular momentum to eliminate r from your expression.
- Solve for the inverse deflection function $b(\theta)$, then differentiate with respect to θ to obtain the differential scattering cross section.

You will need the half-angle identities,

$$\cos\alpha = 2\cos^2\left(\frac{\alpha}{2}\right) - 1\ , \qquad \sin\alpha = 2\sin\left(\frac{\alpha}{2}\right)\cos\left(\frac{\alpha}{2}\right)\ . \tag{5.23}$$

Solution

The situation is as shown in Fig. 5.1. The Coulomb force between two nuclei of charges Z_1 and Z_2, at distance r, is

$$F_C = \pm\frac{C}{r^2}\ , \tag{5.24}$$

[5] This needs to be done because while db and $d\theta$ are both positive, ensuring that the scattering rate, Eq. (5.21), and the cross section, Eq. (5.22), are also positive, there is no reason to suspect that the rate of change of the impact parameter as a function of the scattering angle, $\frac{db}{d\theta}$, is also always positive.

[6] That is, as long as that inverse is uniquely defined, which is not always guaranteed.

where

$$C = \frac{1}{4\pi\epsilon_0} Z_1 Z_2 e^2 \ . \tag{5.25}$$

The angular momentum of the system (calculated around the target, *i.e.*, around the origin) is

$$L = \mu v_\infty b \ , \tag{5.26}$$

where v_∞ is the speed with which the projectile is approaching the target from infinity and also, by conservation of energy, at which it is moving after the reaction has taken place. Naturally, in the vicinity of the target $v \neq v_\infty$. There, it is convenient to consider the problem in polar coordinates (centered on the target, see Fig. 5.1), in terms of which

$$L \equiv |\boldsymbol{r} \times \boldsymbol{p}| = \mu |\boldsymbol{r} \times \boldsymbol{v}| = \mu r \left| \hat{\boldsymbol{r}} \times \left(\frac{dr}{dt} \hat{\boldsymbol{r}} + r \frac{d\phi}{dt} \hat{\boldsymbol{\phi}} \right) \right| = \mu r^2 \frac{d\phi}{dt} \ . \tag{5.27}$$

For a projectile moving along the z axis, the x-component of the velocity is initially equal zero, $v_{x,0} = 0$. After a scattering into an angle θ, it is $v_{x,\infty} = v_\infty \sin\theta$. This change in v_x can be calculated with the impulse approximation using the x-projection of the acting force,

$$\Delta p_x = \mu \Delta v_x = \mu v_\infty \sin\theta = \int_{-\infty}^{+\infty} dt \ F_x = \int_{-\infty}^{+\infty} dt \ \frac{C}{r^2} \sin\phi \ , \tag{5.28}$$

where we invoked the form of the Coulomb force, Eq. (5.24). Furthermore, we can express r^2 in terms of $d\phi/dt$ by combining Eqs. (5.26) and (5.27), so that

$$\mu \Delta v_x = \mu v_\infty \sin\theta = \int_{-\infty}^{+\infty} dt \ \frac{C}{v_\infty b} \frac{d\phi}{dt} \sin\phi \ . \tag{5.29}$$

Noting that $t = -\infty$ and $t = +\infty$ correspond to $\phi = 0$ and $\phi = \pi - \theta$, respectively[c], we can change the integration variable to $d\phi$ and readily evaluate the integral,

$$\mu v_\infty \sin\theta = \frac{C}{v_\infty b} \int_0^{\pi-\theta} d\phi \ \sin\phi = \frac{C}{v_\infty b} \big(1 + \cos\theta\big) \ . \tag{5.30}$$

Solving for the impact parameter (*i.e.*, for the inverse deflection function), we obtain

$$b(\theta) = \frac{C}{\mu v_\infty^2} \frac{1 + \cos\theta}{\sin\theta} = \frac{C}{\mu v_\infty^2} \cot\left(\frac{\theta}{2}\right) \ , \tag{5.31}$$

where we used the half-angle identities, Eq. (5.23). Finally, we can now calculate

$$\frac{db}{d\theta} = -\frac{C}{2\mu v_\infty^2} \frac{1}{\sin^2\left(\frac{\theta}{2}\right)} \ , \tag{5.32}$$

which can be inserted into the equation for the classical differential cross section, Eq. (5.22), together with the equation for the impact parameter, Eq. (5.31), yielding the differential cross section for Rutherford scattering

$$\frac{d\sigma(\Omega)}{d\Omega} = \left(\frac{C}{2\mu v_\infty^2} \right)^2 \frac{1}{\sin^4\left(\frac{\theta}{2}\right)} \ . \tag{5.33}$$

[a] We will soon see that this is justified.

[b] By Gauss' law, this is valid as long as the projectile and target charge distributions don't overlap at any time.

[c] Here it is useful to remember that the angle θ is defined as the angle between the final momentum and the beam axis. At any random time, it is not true that this is the same angle as the radius r makes with the z axis, $\pi - \phi$. However, one can see that it is true at $t = +\infty$. Indeed, assume that at some time t_0 after the projectile leaves the influence of the potential, it has a position $\boldsymbol{r}_0$ and a velocity $\boldsymbol{v}_\infty$. Then the position at any later time is $\boldsymbol{r} = \boldsymbol{r}_0 + \boldsymbol{v}_\infty(t - t_0)$. The unit vector associated with this position is

$$\frac{\boldsymbol{r}}{|\boldsymbol{r}|} = \frac{\boldsymbol{r}_0 + \boldsymbol{v}_\infty(t-t_0)}{\left|\boldsymbol{r}_0 + \boldsymbol{v}_\infty(t-t_0)\right|} = \frac{\frac{\boldsymbol{r}_0}{|\boldsymbol{v}_\infty|(t-t_0)} + \frac{\boldsymbol{v}_\infty}{|\boldsymbol{v}_\infty|}}{\left|\frac{\boldsymbol{r}_0}{|\boldsymbol{v}_\infty|(t-t_0)} + \frac{\boldsymbol{v}_\infty}{|\boldsymbol{v}_\infty|}\right|} \xrightarrow[t\to\infty]{} \frac{\boldsymbol{v}_\infty}{|\boldsymbol{v}_\infty|} ,$$

where we obtain the final expression by multiplying both the numerator and the denominator by $1/\big(|\boldsymbol{v}_\infty|(t-t_0)\big)$ to expose its behavior in the infinite time limit.

The question to ask now is: What do we learn from this result? To answer it, we need 1) context, and 2) experimental data.

5.3 Rutherford's result *vs.* the Thompson model

In Rutherford's time, one of the leading atomic models was Thompson's "plum pudding" model, in which the positive charge was assumed to be smoothly distributed over the entire atomic volume, with electrons embedded within it. Atomic radii were known to be of order $R \sim 10^{-10}$ m $= 10^5$ fm. It was also known that α particles were heavy, compact objects: the small[7] deflection of α particles in electric and magnetic fields showed that they had a small charge-to-mass ratio, implying a relatively large mass, and experiments showed that they behaved like rigid classical projectiles, implying that they can be treated like point-like particles. Therefore, an expectation for scattering of α particles off a gold foil was established by considering the evolution of a point-like, energetic particle as it traverses an extended (atomic-scale), diffuse cloud of positive charge (*i.e.*, Thompson's atom).

The typical kinetic energy of an α particle emitted from a radioactive source is on the order of 4–6 MeV. Let's compare it with Coulomb repulsion outside of a positively charged sphere of radius R. From Gauss's law, we know that outside a spherically symmetric charge distribution, a test charge experiences the same force as if all the charge were concentrated at the origin. Therefore, the Coulomb potential between the α particle, with charge $Q_\alpha = 2e$, and an "atomic sphere of positive charge"[8], just outside of that sphere, is

$$V_C(R) = \frac{1}{4\pi\epsilon_0}\frac{2Ze^2}{R} , \tag{5.34}$$

where Z is the atomic number of the atom. Using the known conversion factor as published by the Particle Data Group [15],

$$\frac{e^2}{4\pi\epsilon_0} \approx 1.44 \text{ MeV fm} , \tag{5.35}$$

and taking $Z = 79$ (gold nucleus), we obtain

$$V_C(R) = 2.3 \times 10^{-3} \text{ MeV} . \tag{5.36}$$

[7] As compared to that of, *e.g.*, electrons.

[8] Completely neglecting the contribution due to electrons, which *were* supposed to be embedded in it – no comment.

Simply by comparing with the maximum kinetic energy of an α particle coming from a radioactive decay, $E_{\rm kin}^{(\alpha)} \approx 6$ MeV, we see that such a structure would not stop the α projectiles from entering it, nor would it significantly change their energy or direction of motion.

In view of this, we can now consider what influence would traversing the entire extent of a Thompson's atom have on the α projectile. Inside the atom, assuming a uniform distribution of charge, the electric field is again given by the Gauss' law,

$$E(r) = \frac{1}{4\pi\epsilon_0}\frac{Ze}{R^3}r \quad \text{for} \quad r < R \ . \tag{5.37}$$

Unsurprisingly, the α particle would experience the maximal force at $r = R$,

$$F_{\rm max} = \frac{1}{4\pi\epsilon_0}\frac{2Ze^2}{R^2} \ . \tag{5.38}$$

To establish an upper limit of the expected effects, we can make a reasonable assumption that the transverse force $F_\perp$ that the α particle feels while traversing the gold atom satisfies $F_\perp \leq F_{\rm max}$. We can estimate the time it takes to traverse the atom to be

$$\Delta t = \frac{2R}{v} \ , \tag{5.39}$$

where v is the (initial) velocity of the α particle. Therefore, the change in transverse momentum (which is initially zero) satisfies

$$\Delta p_\perp \leq F_{\rm max}\Delta t \approx \frac{1}{4\pi\epsilon_0}\frac{4Ze^2}{Rv} \ . \tag{5.40}$$

For a small deflection, the scattering angle can be approximated as

$$\theta_{\rm max} \approx \frac{\Delta p_\perp}{mv} \approx \frac{1}{4\pi\epsilon_0}\frac{4Ze^2}{Rmv^2} = \frac{1}{4\pi\epsilon_0}\frac{2Ze^2}{RE_{\rm kin}^{(\alpha)}} \ . \tag{5.41}$$

Using the conversion factor from Eq. (5.35), $Z = 79$, and $R = 10^5$ fm, we obtain

$$\theta_{\rm max} \approx 3.792 \times 10^{-4} \approx 0.0217^\circ \ . \tag{5.42}$$

Thus, if the Thompson model of the atom, with the positive charge were spread over a region comparable with the atomic scale, were correct, one would expect the α particles to be negligibly deflected. The observation of large-angle scattering events implied that the positive charge must be concentrated in a region much smaller than the atom, consistent with a point-like target. This led Rutherford to his famous remark that the result was "almost as incredible as if you fired a 15-inch shell at a piece of tissue paper and it came back and hit you."

Not only were Rutherford's measurements incompatible with Thompson's model, but they were also shown to follow the Coulomb scattering formula, Eq. (5.33) and Fig. 5.3, implying that (at the probed energies) the interaction could be described entirely by the point-charge Coulomb force. In particular, no deviations associated with finite charge distributions were observed. This has already pointed toward finding that the positive charge in the atom is concentrated in a small nucleus.

Once one makes that conclusion, a key question to ask is: "how small is it?" Given the apparent point-like behavior of the projectile and target, one can estimate an upper limit on the size of the nucleus by computing the distance of closest approach D. As discussed in Sec. 5.1.2, D corresponds to a minimal velocity $v_{\rm min}$ the projectile has over the evolution, which depends on the impact

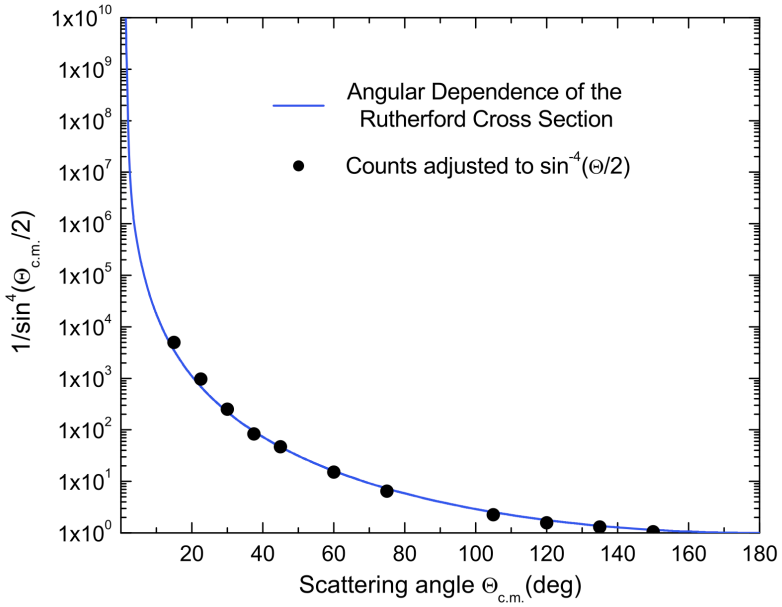

Figure 5.3: Rutherford's data compared with the $\sin^{-4}(\theta/2)$ prediction. Figure from Ref. [1].

parameter. In particular, the smallest possible distance of closest approach D_0 occurs for head-on collisions, in which the projectile momentarily comes to a complete stop before reversing direction. In this case[9], conservation of energy demands that

$$E_{\mathrm{kin},\infty} = \frac{m v_\infty^2}{2} = \frac{C}{D_0} \quad \Rightarrow \quad D_0 = \frac{C}{E_{\mathrm{kin},\infty}} \ . \tag{5.43}$$

Using $E_{\mathrm{kin},\infty} \approx 6$ MeV, $Z_1 = 2$, $Z_2 = 79$, and the conversion factor from Eq. (5.35), we obtain

$$D_0 \approx 40 \text{ fm} \ . \tag{5.44}$$

Today we know that this number is several times larger than the radius of a gold nucleus, $r_{\mathrm{Au}} \approx 7$ fm. Rutherford's experiments showed that while the α projectiles approached the nucleus on distances several orders of magnitude smaller than the atomic radius, the scattering occurred as if the nucleus could be considered a point-like particle, implying that its radius must be smaller than D_0[10] .

5.4 Applicability of the classical description

The question of when a classical description is applicable to an inherently quantum system is subtle, and there is no single criterion. Nevertheless, a necessary condition for a classical description of scattering is that the de Broglie[11] wavelength of the projectile be small compared to the characteristic length scale of the reaction. For α particles emitted from a radioactive source, we have $E_{\mathrm{kin}}^{(\alpha)} \approx 6$ MeV and $m_\alpha \approx 3730$ MeV$/c^2$, and in the non-relativistic regime $p = \sqrt{2 m_\alpha E_{\mathrm{kin}}^{(\alpha)}}$. The de

[9] Note that for head-on collisions, the angular momentum around the target is zero.

[10] The value of D_0 also justifies treating the interaction as purely Coulombic, since the range of the nuclear force is on the order of 1–2 fm.

[11] Pronounced "duh-BROY".

Broglie wavelength is therefore

$$\lambda_{\rm dB} \equiv \frac{h}{p} = \frac{2\pi\hbar}{p} \approx \frac{2\pi\hbar}{\sqrt{2\times 3730\frac{\rm MeV}{c^2}\times 6\ {\rm MeV}}} \approx \frac{2\pi\hbar c}{212\ {\rm MeV}} \approx \frac{2\pi\times 197\ {\rm MeV\ fm}}{212\ {\rm MeV}} \approx 5.8\ {\rm fm}\ . \quad (5.45)$$

where we used the value of $\hbar c$ from the Particle Data Group [15]. In Rutherford scattering at these energies, the relevant classical length scale is set by the distance of closest approach, $D_0 \sim 40$ fm, or by typical impact parameters which are of comparable magnitude. Since $\lambda_{\rm dB} \ll D_0$, the relevant impact parameters satisfy $b \gg \lambda_{\rm dB}$, corresponding to angular momenta $L \sim pb \gg p\lambda_{\rm dB} \sim \hbar$.

There are other criteria, which for example consider the fact that wavefunctions may experience diffraction, rendering classical description invalid. (This has an intuitive analogy in optics where light diffraction on, *e.g.*, a sharp edge invalidates description of wave propagation in terms of well-defined rays.) In scattering problems, diffraction can be induced by strong changes in the scattering potential, for example at the nuclear surface. As a result, one may demand that classical treatment is applied only when the de Broglie wavelength (or, equivalently, the projectile's momentum) does not change substantially due to the potential gradient over one oscillation wavelength,

$$\left|\frac{d\lambda}{dr}\right| \ll 1\ , \quad (5.46)$$

which in turn will be the case if, over one oscillation of the wave, the potential looks essentially constant. This criterion is connected to the Wentzel–Kramers–Brillouin (WKB) semi-classical approximation to the solution of the Schrödinger equation, which assumes that the wavefunction has the form

$$\Psi_{\rm WKB}(x) = A(x)e^{i\int^x dx'\ k(x')} \quad (5.47)$$

with a classical momentum $k(x) = \sqrt{2m\big(E-V(x)\big)}$. In contrast to a plane wave, $\psi(x) = Ae^{ikx}$, whose phase $\Phi = kx$ is linear in x and the wave number $k = \frac{d\Phi}{dx}$ is constant, the phase of $\Psi_{\rm WKB}$ is $\Phi_{\rm WKB} = \int^x dx'\ k(x')$ with a *local* value of $k(x) = \frac{d\Phi_{\rm WKB}}{dx}$. Thus, *locally*, $\psi_{\rm WKB}$ looks like a plane wave. The question is over what ranges in x such a "local plane wave" interpretation is valid. This can be quantified by expanding the phase around some point x_0,

$$\Phi_{\rm WKB}(x) = \Phi(x_0) + k(x_0)(x-x_0) + \frac{1}{2}k'(x_0)(x-x_0)^2 + \dots \quad (5.48)$$

and noting that $\psi_{\rm WKB}$ will locally look like a plane wave over a region $\Delta x = x - x_0$ if the quadratic term is negligible,

$$\big|k'(x_0)\big|(\Delta x)^2 \ll \big|k(x_0)\big|\Delta x \quad \Rightarrow \quad \big|k'(x_0)\big|\Delta x \ll \big|k(x_0)\big|\ . \quad (5.49)$$

Choosing Δx to be on the order of one wavelength, $\Delta x \sim \frac{1}{k(x_0)}$, we arrive at the condition

$$\left|\frac{dk}{dx}\right| \ll k^2\ , \quad (5.50)$$

which is equivalent to the WKB condition in Eq. (5.46). The influence of the potential enters naturally through $k(x) = \sqrt{2\mu\big(E-V(r)\big)}$.

Interestingly, the WKB criterion fails for large angles when applied to Coulomb scattering. Does that mean that Rutherford's formula should fail at large angles? No: the subtle point here is the

assumption for the form of the WKB wavefunction. If that form is not appropriate for the problem at hand, the criterion may well be meaningless, which is the case here. Interestingly, for Coulomb scattering, the quantum problem is in fact fully solvable, and the quantum differential cross section reproduces the Rutherford form up to a constant.

Altogether, establishing whether a classical description works is a tricky business. An important case where a classical approach is likely to fail is scattering of identical particles, where exchange symmetry and the corresponding interference effects may render the classical description invalid[12].

Lecture sources: This lecture is mainly based on chapter 2 in gen. Schieck [1] and chapter 1 Bertulani & Danielewicz [6].

[12] This is not always the case. In particular, in ultrarelativistic collisions the interference effects are often tiny.

Lecture 6

Quantum scattering

Prerequisites: Lecture 2.
Guiding question: ***What does "scattering" mean in quantum mechanics?***

In a scattering experiment, a beam of particles is scattered by a target and the outgoing collision products are recorded by a detector. Since nuclear collisions take place on microscopic scales, both the initial and final states are essentially free particles. As a result, scattering is essentially a process in which the system transitions from one free-particle state to another. The entire information about the properties of the interaction that caused the scattering lays in the momentum (including direction) and energy of the outgoing states – *i.e.*, in the scattering cross section.

6.1 Non-relativistic scattering of two particles in a central potential

Let us consider two particles A, B of masses m_A, m_B, coordinates $\boldsymbol{r}_A$, $\boldsymbol{r}_B$ measured from some fixed origin 0, and momenta $\boldsymbol{p}_A$, $\boldsymbol{p}_B$. We assume that the particles are non-relativistic, carry no spin, and interact through a (real-valued) central potential $V(\boldsymbol{r}_A - \boldsymbol{r}_B)$. The (classical) Hamiltonian of such a system is

$$H = \frac{\boldsymbol{p}_A^2}{2m_A} + \frac{\boldsymbol{p}_B^2}{2m_B} + V(\boldsymbol{r}_A - \boldsymbol{r}_B) \ . \tag{6.1}$$

With $\boldsymbol{p}_A \to i\hat{\boldsymbol{\nabla}}_{\boldsymbol{r}_A}$ and $\boldsymbol{p}_B \to i\hat{\boldsymbol{\nabla}}_{\boldsymbol{r}_B}$[1], we can promote H to the Hamiltonian operator $\hat{\boldsymbol{\mathcal{H}}}$ in the coordinate representation, with which we write down the time-dependent Schrödinger equation for the two-particle system,

$$\hat{\boldsymbol{\mathcal{H}}}\Psi(\boldsymbol{r}_A, \boldsymbol{r}_B, t) = \left[-\frac{\hat{\boldsymbol{\nabla}}^2_{\boldsymbol{r}_A}}{2m_A} - \frac{\hat{\boldsymbol{\nabla}}^2_{\boldsymbol{r}_B}}{2m_B} + V(\boldsymbol{r}_A - \boldsymbol{r}_B) \right] \Psi(\boldsymbol{r}_A, \boldsymbol{r}_B, t) = i\frac{\partial}{\partial t}\Psi(\boldsymbol{r}_A, \boldsymbol{r}_B, t) \ , \tag{6.2}$$

which is a partial differential equation in seven variables. In other words, it's an equation we would rather not be dealing with. The first simplification comes from the fact that the Hamiltonian operator $\hat{\boldsymbol{\mathcal{H}}}$ is time-independent, which means that its eigenvalues and eigenfunctions should be time-independent as well. The only way in which the wavefunction $\Psi(\boldsymbol{r}_A, \boldsymbol{r}_A, t)$ can be a solution of Eq. (6.2) is if it factorizes into a time-dependent and time-independent parts,

$$\Psi(\boldsymbol{r}_A, \boldsymbol{r}_A, t) = \varphi(\boldsymbol{r}_A, \boldsymbol{r}_B) e^{-iE_{\text{tot}}t} \ , \tag{6.3}$$

[1] And, if we wanted to be extremely precise, $V \to V\mathbb{1}$, where $\mathbb{1}$ is the identity operator. In the following, we will not aspire to such levels of precision.

where $\varphi(\boldsymbol{r}_A, \boldsymbol{r}_B)$ are *stationary states* with a well-defined value of the total energy of the system $E_{\rm tot}$. If there are multiple stationary states with $E_{\rm tot}$ then, due to the linearity of the Hamiltonian operator $\hat{\boldsymbol{\mathcal{H}}}$, the most general solution of the Schrödinger equation, Eq. (6.2), is a sum of all solutions of the form as in Eq. (6.3). Inserting Eq. (6.3) into Eq. (6.2) leads to the equation for the time-independent wavefunction $\varphi(\boldsymbol{r}_A, \boldsymbol{r}_B)$,

$$\left[-\frac{\hat{\boldsymbol{\nabla}}^2_{\boldsymbol{r}_A}}{2m_A} - \frac{\hat{\boldsymbol{\nabla}}^2_{\boldsymbol{r}_B}}{2m_B} + V(\boldsymbol{r}_A - \boldsymbol{r}_B)\right]\varphi(\boldsymbol{r}_A, \boldsymbol{r}_B) = E_{\rm tot}\varphi(\boldsymbol{r}_A, \boldsymbol{r}_B)\ , \tag{6.4}$$

which is a partial differential equation in six variables – better, but we need more than that.

Since the potential only depends on the coordinate difference, it is natural to introduce the relative and center-of-mass (CM) coordinates (see Lecture 2),

$$\boldsymbol{r} = \boldsymbol{r}_A - \boldsymbol{r}_B \quad \text{and} \quad \boldsymbol{R} = \frac{m_A\boldsymbol{r}_A + m_B\boldsymbol{r}_B}{m_A + m_B}\ . \tag{6.5}$$

With Eq. (6.5), we can apply the chain rule to compute

$$\boldsymbol{\nabla}_{\boldsymbol{r}_A} = \left(\frac{\partial \boldsymbol{r}}{\partial \boldsymbol{r}_A}\right)\boldsymbol{\nabla}_{\boldsymbol{r}} + \left(\frac{\partial \boldsymbol{R}}{\partial \boldsymbol{r}_A}\right)\boldsymbol{\nabla}_{\boldsymbol{R}} = \boldsymbol{\nabla}_{\boldsymbol{r}} + \frac{m_A}{M}\boldsymbol{\nabla}_{\boldsymbol{R}}\ , \tag{6.6}$$

$$\boldsymbol{\nabla}_{\boldsymbol{r}_B} = \left(\frac{\partial \boldsymbol{r}}{\partial \boldsymbol{r}_B}\right)\boldsymbol{\nabla}_{\boldsymbol{r}} + \left(\frac{\partial \boldsymbol{R}}{\partial \boldsymbol{r}_B}\right)\boldsymbol{\nabla}_{\boldsymbol{R}} = -\boldsymbol{\nabla}_{\boldsymbol{r}} + \frac{m_B}{M}\boldsymbol{\nabla}_{\boldsymbol{R}}\ , \tag{6.7}$$

where $M = m_a + m_B$ is the total mass of the system, and

$$\boldsymbol{\nabla}^2_{\boldsymbol{r}_A} = \boldsymbol{\nabla}^2_{\boldsymbol{r}} + \frac{2m_A}{M}\boldsymbol{\nabla}_{\boldsymbol{r}}\boldsymbol{\nabla}_{\boldsymbol{R}} + \frac{m_A^2}{M^2}\boldsymbol{\nabla}^2_{\boldsymbol{R}}\ , \tag{6.8}$$

$$\boldsymbol{\nabla}^2_{\boldsymbol{r}_B} = \boldsymbol{\nabla}^2_{\boldsymbol{r}} - \frac{2m_B}{M}\boldsymbol{\nabla}_{\boldsymbol{r}}\boldsymbol{\nabla}_{\boldsymbol{R}} + \frac{m_B^2}{M^2}\boldsymbol{\nabla}^2_{\boldsymbol{R}}\ . \tag{6.9}$$

Plugging the above into Eq. (6.4) yields

$$\left[-\frac{\hat{\boldsymbol{\nabla}}^2_{\boldsymbol{R}}}{2M} - \frac{\hat{\boldsymbol{\nabla}}^2_{\boldsymbol{r}}}{2\mu} + V(\boldsymbol{r})\right]\varphi(\boldsymbol{R}, \boldsymbol{r}) = E_{\rm tot}\varphi(\boldsymbol{R}, \boldsymbol{r})\ , \tag{6.10}$$

where $\mu = \frac{m_A m_B}{m_A + m_B}$ is the reduced mass[2]. The advantage resides in the following fact: since the potential V depends only on $\boldsymbol{r}$, the wavefunction $\varphi(\boldsymbol{R}, \boldsymbol{r})$ factorizes into a product of wavefunctions,

$$\varphi(\boldsymbol{R}, \boldsymbol{r}) = \Phi(\boldsymbol{R})\psi(\boldsymbol{r})\ . \tag{6.11}$$

Additionally dividing the total energy into parts associated with the center of mass and relative motion, $E_{\rm tot} = E_{\rm CM} + E$, and inserting the above factorization into the time-independent Schrödinger equation in the CM frame, Eq. (6.10), leads to two equivalent evolution equations:

$$-\frac{\hat{\boldsymbol{\nabla}}^2_{\boldsymbol{R}}}{2M}\Phi(\boldsymbol{R}) = E_{\rm CM}\Phi(\boldsymbol{R})\ , \tag{6.12}$$

$$\left[-\frac{\hat{\boldsymbol{\nabla}}^2_{\boldsymbol{r}}}{2\mu} + V(\boldsymbol{r})\right]\psi(\boldsymbol{r}) = E\psi(\boldsymbol{r})\ . \tag{6.13}$$

[2]Somewhat sloppily, we have also adopted $\varphi(\boldsymbol{r}_A, \boldsymbol{r}_B) \to \varphi(\boldsymbol{R}, \boldsymbol{r})$, while in principle we should have used a new symbol to represent the wavefunction in the CM coordinates. We won't aspire to such levels of semantic precision.

It is evident that Eq. (6.12) describes the evolution of the system's center of mass as that of a free particle with mass M and energy $E_{\rm CM}$, while Eq. (6.13) describes the relative motion in the system in terms of a particle of mass μ subject to a potential $V(\boldsymbol{r})$. Since the solution for a free particle is trivial (and, in any case, we will never use it as in all that follows we will always be concerned with the behavior in the CM frame), now all we have to deal with is Eq. (6.13): a partial differential equation in three variables. This is much better than what we started with!

6.2 Scattering amplitude

In an *elastic scattering* off a potential $V(\boldsymbol{r})$, stationary states must satisfy Eq. (6.13). Since energy is conserved and we know the initial momentum $\boldsymbol{p}_0 = \boldsymbol{k}_0 = m\boldsymbol{v}_0$[3], we are dealing with

$$\left[-\frac{\hat{\boldsymbol{\nabla}}^2_{\boldsymbol{r}}}{2\mu} + V(\boldsymbol{r}) \right] \psi(\boldsymbol{r}) = \frac{k_0^2}{2\mu} \psi(\boldsymbol{r}) \ . \tag{6.14}$$

Introducing $U(\boldsymbol{r}) = 2\mu V(\boldsymbol{r})$ allows us to write the above equation as

$$\left[\hat{\boldsymbol{\nabla}}^2_{\boldsymbol{r}} + k_0^2 - U(\boldsymbol{r}) \right] \psi(\boldsymbol{r}) = 0 \ . \tag{6.15}$$

A stationary solution to Eq. (6.15) is a function describing a 3D wave in the entire space. The form of this function obviously depends on the problem at hand. However, we can make a number of general statements. In particular, we can postulate that asymptotically, the wavefunction should satisfy the boundary condition

$$\psi^{(+)}_{\boldsymbol{k}_0}(\boldsymbol{r}) \xrightarrow[r\to\infty]{} A \left(e^{i\boldsymbol{k}_0\cdot\boldsymbol{r}} + f(\theta,\phi) \frac{e^{ik_0 r}}{r} \right) \ , \tag{6.16}$$

i.e., it should converge to a superposition of a plane wave with a wavevector $\boldsymbol{k}_0$, representing the incoming wave[4], and an outgoing spherical wave $e^{ik_0 r}/r$ with an amplitude depending on θ and ϕ, representing the scattered wave. Since $f(\theta,\phi)$ modulates the behavior of the scattered wave, it is known as the *scattering amplitude*. Let us stress that Eq. (6.16) is not derived from the Schrödinger equation; rather, it is an asymptotic boundary condition appropriate for short-range interactions. For this reason, it is often called an *ansatz* for the scattering wavefunction. Note also that we have restricted the discussion to *elastic scattering*, which in particular means that the incoming and outgoing states describe the same projectile and target with the same internal states – the only thing that changes is the direction of their relative momentum.

6.2.1 Verifying the asymptotic solution

We should verify that the proposed asymptotic solution, Eq. (6.16), indeed solves the Schrödinger equation, Eq. (6.15), *asymptotically*. Since the asymptotic solution represents a free particle, this means that in the limit of $r \to \infty$ we should be able to argue that the potential terms are negligible *compared to other terms in the equation.* To this end, let us write that equation as applied to the asymptotic solution a bit more explicitly,

$$\left(\hat{\boldsymbol{\nabla}}^2_{\boldsymbol{r}} + k_0^2\right) e^{i\boldsymbol{k}_0\cdot\boldsymbol{r}} + \left(\hat{\boldsymbol{\nabla}}^2_{\boldsymbol{r}} + k_0^2\right) f(\theta,\phi)\frac{e^{ik_0 r}}{r} - U(\boldsymbol{r}) e^{i\boldsymbol{k}_0\cdot\boldsymbol{r}} - U(\boldsymbol{r}) f(\theta,\phi)\frac{e^{ik_0 r}}{r} = 0 \ . \tag{6.17}$$

[3]Note that the momentum $\boldsymbol{p}_0$ and wave number vector $\boldsymbol{k}_0$ are only equal in natural units, $\hbar = c = 1$, which we, of course, use here.

[4]Note that for $\boldsymbol{k}_0 = k_0\hat{\boldsymbol{z}}$, $e^{i\boldsymbol{k}\cdot\boldsymbol{r}} = e^{ik_0 z}$.

Since the plane wave solution satisfies $\left(\hat{\boldsymbol{\nabla}}^2_{\boldsymbol{r}} + k_0^2\right) e^{i\boldsymbol{k}_0\cdot\boldsymbol{r}} = 0$ identically[5], we can eliminate that term. To establish whether the terms involving the potential $U(\boldsymbol{r})$ can also be eliminated, thus ensuring that the equation is satisfied[6], we need to compare them with the leading-order behavior of terms involving the scattered wavefunction e^{ikr}/r. In particular, we can see that the term proportional to k_0^2 vanishes as $1/r$. We can thus discard the terms $U(\boldsymbol{r})e^{i\boldsymbol{k}_0\cdot\boldsymbol{r}}$ and $-U(\boldsymbol{r})f(\theta,\phi)e^{ik_0r}/r$ only *if they vanish faster than that.* For $U(\boldsymbol{r})e^{i\boldsymbol{k}_0\cdot\boldsymbol{r}}$, it means that we need to have $U \propto 1/r^{1+\alpha}$ where $\alpha > 0$. In this way, we discover that the asymptotic solution, Eq. (6.15), does *not* work for the Coulomb potential!

6.3 The asymptotic solution and the WKB approximation

To look a this issue more closely, we turn to the Wentzel–Kramers–Brillouin (WKB) semi-classical approximation for the wavefunction, which we already discussed a bit in Lecture 5. To fully motivate the approximation, let us consider a 1D Schrödinger equation[7],

$$-\frac{\hbar^2}{2m}\frac{d^2\psi(x)}{dx^2} + V(x)\psi(x) = E\psi(x) \ , \tag{6.18}$$

which can be also written as

$$\psi''(x) + k^2(x)\psi(x) = 0 \ , \tag{6.19}$$

where we have defined $k(x) = \sqrt{2m\big(E - V(x)\big)}/\hbar$. If the potential were constant, so that $k(x) = k_0$, then the solution would be a plane wave,

$$\psi(x) \sim e^{\pm ik_0x/\hbar} \ . \tag{6.20}$$

Conversely, if one allows the potential to start varying, one can convince themselves that the solution should *locally* look like a plane wave, which can be achieved by allowing the wave number k to vary with x. This suggest a solution of the form

$$\psi_{\mathrm{WKB}}(x) = A(x)e^{\frac{iS(x)}{\hbar}} \ , \tag{6.21}$$

where $S(x)$ is some function of $k(x)$ and we allow the amplitude to vary with x as otherwise, given the varying wave number, the flux would not be conserved. With this, the Schrödinger equation becomes

$$\hbar^2A''(x) + 2i\hbar A'(x)S'(x) + i\hbar A(x)S''(x) - A(x)\big(S'(x)\big)^2 + \hbar^2k^2A(x) = 0 \ . \tag{6.22}$$

[5] This is easy to see by aligning $\boldsymbol{r}$ with a chosen axis, say the z axis as in scattering problems, and applying the Laplacian in Cartesian coordinates.

[6] This would then be the case because of the following: Given the Laplacian operator in spherical coordinates,

$$\hat{\boldsymbol{\nabla}}^2_{\boldsymbol{r}} = \frac{1}{r^2}\frac{\partial}{\partial r}\left(r^2\frac{\partial}{\partial r}\right) + \frac{1}{r^2\sin\theta}\frac{\partial}{\partial\theta}\left(\sin\theta\frac{\partial}{\partial\theta}\right) + \frac{1}{r^2\sin^2\theta}\frac{\partial^2}{\partial\phi^2} = \frac{1}{r^2}\frac{\partial}{\partial r}\left(r^2\frac{\partial}{\partial r}\right) + \frac{1}{r^2}\Delta_\Omega \ ,$$

where we wrote all angular derivatives as Δ_Ω since they do not affect the behavior with r, we would remain with

$$f(\theta,\phi)\frac{1}{r^2}\frac{\partial}{\partial r}\left(r^2\frac{\partial}{\partial r}\right)\frac{e^{ik_0r}}{r} + \frac{e^{ik_0r}}{r^3}\Delta_\Omega f(\theta,\phi) + k_0^2 f(\theta,\phi)\frac{e^{ik_0r}}{r} = 0 \ ,$$

where the first and the last term cancel identically, while the middle term vanishes as $1/r^3$, *i.e.*, is on the order of $\mathcal{O}(r^{-2})$ with respect to the scattered wave.

[7] Since in the following we are going to examine expressions at different orders of $\hbar$, we introduce $\hbar$ back into the equations.

For a semi-classical approximation, we want to look at the leading behavior in $\hbar$ assuming $\hbar \to 0$ (*i.e.*, is negligible compared to other quantities in the equation). For this, we note that the first term in Eq. (6.22) is of order $\hbar^2$, the second term and third term are of order $\hbar^1$, and the fourth and fifth term, given $\hbar k = p$, are of order $\hbar^0$. Thus to the leading (*i.e.*, zeroth) order in $\hbar$ we get

$$\left(\frac{dS(x)}{dx}\right)^2 = \hbar^2 k^2 \qquad \Rightarrow \qquad \frac{dS(x)}{dx} = \pm p(x) \ , \tag{6.23}$$

which is solved by

$$S(x) = \pm \int^x dx' \ p(x') \ . \tag{6.24}$$

Note that Eq. (6.23) is the classical Hamilton-Jacobi equation, *i.e.*, an equation for *Hamilton's principal function* $S(x,t)$[8], also referred to as the *action*, Eq. (6.24), which is the classical action accumulated along the actual trajectory that reaches position x at time t.

Then, looking at terms which are of first order in $\hbar$ in Eq. (6.22), we have

$$2A'(x)S'(x) + A(x)S''(x) = 0 \ , \tag{6.25}$$

which, given the just found form of $S(x)$, Eq. (6.24), becomes

$$\frac{2A'(x)}{A(x)} + \frac{p'(x)}{p(x)} = 0 \tag{6.26}$$

We can integrate the above equation from both sides over x, leading to

$$\int^x dx' \left(\frac{2A'(x')}{A(x')} + \frac{p'(x')}{p(x')}\right) = 2\ln A(x) + \ln p(x) = \ln A^2(x)p(x) = \text{const} \ , \tag{6.27}$$

[8] Formally, Hamilton's principal function $S(\boldsymbol{r},t)$ solves the *time-dependent Hamilton-Jacobi equation*,

$$H(\boldsymbol{r}, \boldsymbol{\nabla} S, t) + \frac{\partial S}{\partial t} = 0 \ .$$

In writing the above equation, we *demand* that S is such that $\frac{\partial S}{\partial t} = -E$ (this just follows from the fact that the Hamiltonian is total energy) and $\boldsymbol{p} = \boldsymbol{\nabla} S$; any system's trajectory is then given by integrating the Hamilton equation, $\frac{d\boldsymbol{r}}{dt} = \frac{\partial H}{\partial \boldsymbol{p}}\big|_{\boldsymbol{p}=\boldsymbol{\nabla} S}$. The point of setting up this formalism is to – instead of solving Newton's equations of motion for the infinitely many possible initial conditions – identify a universal solution which can then be applied to any particular case. The Hamilton-Jacobi equation is formally solved by

$$S(\boldsymbol{r},t) = \int_{t_0}^{t} dt' \ \left(\boldsymbol{p} \cdot \frac{d\boldsymbol{r}}{dt} - H\right) \ ,$$

which you can easily see by performing a variation of S,

$$\delta S = \delta t \Big(\boldsymbol{p} \cdot \frac{d\boldsymbol{r}}{dt} - H\Big) = \boldsymbol{p} \cdot \delta \boldsymbol{r} - H \delta t \ .$$

Since formally we can also write

$$\delta S = \frac{\partial S}{\partial \boldsymbol{r}} \delta \boldsymbol{r} + \frac{\partial S}{\partial t} \delta t \ ,$$

we can immediately identify $\boldsymbol{\nabla} S = \boldsymbol{p}$ and $\partial S/\partial t = -H$, as needed. In the case where the Hamiltonian does not have an explicit time dependence, the solution becomes $S(\boldsymbol{r},t) = W(\boldsymbol{r},t) - Et$, where $W(\boldsymbol{r},t)$, given by

$$W(\boldsymbol{r}) = \int_{\boldsymbol{r}_0}^{\boldsymbol{r}} \boldsymbol{p} \cdot d\boldsymbol{r}' \ ,$$

is often called the *reduced action* and satisfies $H(\boldsymbol{r}, \boldsymbol{\nabla} W) = E$, *i.e.*, W is the spatial action along a classical path.

from which we can immediately see that we need to have

$$A(x) = \frac{A}{\sqrt{p(x)}} \ . \tag{6.28}$$

Altogether then, the semi-classical WKB approximation to the wavefunction is given by[9]

$$\psi_{\rm WKB}(x) = \frac{A}{\sqrt{p(x)}} \exp\left(\frac{i}{\hbar}\int^x dx' \ p(x')\right) \ . \tag{6.29}$$

The WKB approximation allows one to estimate whether the behavior of the potential, from the point where the reaction takes place up to infinity, is compatible with the assumed asymptotic solution. To this end, it is convenient to look at the phase of the WKB wavefunction, which in our problem can be written as[10]

$$\Phi_{\rm WKB}(r) = \int_R^r dr' \ k(r') \ , \tag{6.30}$$

where we explicitly introduced some large reference distance R as the lower limit of the integration. From conservation of energy we know that

$$k(r') = \sqrt{k_0^2 - U(r')} = k_0\sqrt{1 - \frac{U(r')}{k_0^2}} \approx k_0 - \frac{U(r')}{2k_0} \ , \tag{6.31}$$

where we used the fact that far away from the interaction region the potential should be much smaller than the kinetic energy. Then we can compute the change in the phase $\Phi_{\rm WKB}(r)$ due to the influence of $U(r')$,

$$\Delta_U\Phi_{\rm WKB}(r) = -\frac{1}{2k_0}\int_R^r dr' \ U(r') \ . \tag{6.32}$$

The result will obviously depend on the form of $U(r')$. For a Coulomb-like potential, $U(r') = C/r$,

$$\Delta_U\Phi_{\rm WKB}^{\rm (Coul)}(r) = -\frac{C}{2k_0}\int_R^r dr' \ \frac{1}{r} = -\left(\frac{C}{2k_0}\ln r - \frac{C}{2k_0}\ln R\right) \ . \tag{6.33}$$

Evidently, the change in the phase diverges logarithmically with r. This means that for the Coulomb potential, the asymptotic form of the wavefunction must have a contribution like[11]

$$e^{ik_0 r}e^{-i\eta\ln r} \ , \tag{6.34}$$

which is different from the asymptotic form postulated in Eq. (6.16). Once again, we see that our postulated asymptotic solution does not work for Coulomb scattering!

Let us now consider $U(r') = C/r^2$:

$$\Delta\Phi_{\rm WKB}^{\rm (1/r^2)}(r) = -\frac{C}{2k_0}\int_R^r dr' \ \frac{1}{r^2} = \frac{C}{2k_0}\left(\frac{1}{r} - \frac{1}{R}\right) \ , \tag{6.35}$$

[9] Here, we have tacitly only kept the solution which describes a wave moving to the right.

[10] Note that there is a degeneracy between our notation for the phase of the WKB wavefunction and the wavefunction describing the center of mass evolution, however, it should be clear from the context which is which.

[11] Here we neglect the constant factor dependent on R, which can always be absorbed into the overall constant phase of the wavefunction.

which converges to a constant as $r \to \infty$, so that asymptotically the wavefunction has the form

$$e^{ikr} e^{i\Delta\Phi(R)} \ , \tag{6.36}$$

where the influence of the potential only produces a constant phase shift. In this case, then, the asymptotic form from Eq. (6.16) is perfectly justified.

This analysis highlights what it means that the Coulomb interaction is "long-range": it does not satisfy the "standard" asymptotic *ansatz* which assumes that the effects due to the interaction are negligible at infinity. Consequently, including the influence of the Coulomb potential will require modifying the treatment a bit. We will address this in Lecture 10.

6.4 Cross section in quantum mechanics

In Lecture 2, we have defined the differential cross section in Eq. (2.7), repeated here for convenience:

$$\frac{d\sigma(\Omega)}{d\Omega} = \frac{\frac{\Delta N(\Omega,\Delta\Omega)}{\Delta t}}{\Delta\Omega j N_{\text{targ}}} \ . \tag{6.37}$$

Considering a single scattering center, we can rewrite the above as

$$\frac{d\sigma(\Omega)}{d\Omega}\Delta\Omega = \frac{\frac{\Delta N(\Omega,\Delta\Omega)}{\Delta t}}{j_{\text{in}}} \ , \tag{6.38}$$

which gives the number of particles emitted per unit time, per unit projectile (or incident) density current, into the infinitesimal solid angle $\Delta\Omega$ about the direction Ω. To connect this expression to quantities that we can calculate in a quantum-mechanical treatment, first let us see that in general, an outgoing current is given by

$$j_{\text{out}} = n_{\text{out}} \ v = \frac{\Delta N_{\text{out}}}{\Delta V} v = \frac{\Delta N_{\text{out}}}{\Delta V}\frac{\Delta l}{\Delta t} = \frac{\Delta N_{\text{out}}}{\Delta t}\frac{1}{\Delta A} \ , \tag{6.39}$$

so that

$$\frac{\Delta N_{\text{out}}}{\Delta t} = j_{\text{out}}\Delta A \ . \tag{6.40}$$

Using $\Delta A = r^2\Delta\Omega$ and introducing the possibility that the current is not perpendicular to the normal vector of ΔA, we have

$$\frac{\Delta N(\Omega,\Delta\Omega)}{\Delta t} = \boldsymbol{j}_{\text{out}} \cdot \left(\Delta\Omega r^2 \ \hat{\boldsymbol{r}}\right) \ , \tag{6.41}$$

so that Eq. (6.38) becomes (canceling $\Delta\Omega$ on both sides)

$$\frac{d\sigma(\Omega)}{d\Omega} = \frac{r^2 \boldsymbol{j}_{\text{out}} \cdot \hat{\boldsymbol{r}}}{j_{\text{in}}} \ . \tag{6.42}$$

We are now able to state what scattering means in quantum mechanics: it is a redistribution of probability current caused by an interaction. An incoming flux, prepared in a definite direction, is partially depleted and reappears as an outgoing flux into other directions. The interaction is observable only through this change in flux, which is directly reflected in the scattering cross section.

In-class Activity 6a: Probability current in quantum mechanics

How do we obtain a probability current in quantum mechanics?

Solution

We know that that the square of the wavefunction, $|\psi(x)|^2$, is interpreted as a probability density $\rho(x)$, so that $|\psi(x)|^2 dx$ gives the odds that the particle is located within dx from x. Up to a normalization, probability density is equivalent to the concept of ordinary density: if we choose particle at random from the system, it is more likely to be found in a region where the density is high than in a region where it is low. In both cases, we can consider the "conservation of the total number": any change in the number of particles within some arbitrary volume V must be associated with a flux of particles though the surface of this volume,

$$\frac{d}{dt}\int_V d^3r\ \rho(\boldsymbol{r},t) = -\oint_{\partial V} \boldsymbol{j}(\boldsymbol{r},t)\cdot d\boldsymbol{A}\ , \tag{6.43}$$

where $d\boldsymbol{A} = dA\ \hat{\boldsymbol{n}}$. Using the Gauss theorem, $\oint_{\partial V} \boldsymbol{j}(\boldsymbol{r},t)\cdot d\boldsymbol{A} = \int d^3r\ \big(\boldsymbol{\nabla}\cdot\boldsymbol{j}\big)$, we immediately arrive at

$$\int_V d^3r\ \left(\frac{\partial\rho(\boldsymbol{r},t)}{\partial t} + \big(\boldsymbol{\nabla}\cdot\boldsymbol{j}\big)\right) = 0\ , \tag{6.44}$$

which, to be true for any arbitrary volume V, implies the local conservation law,

$$\frac{\partial\rho(\boldsymbol{r},t)}{\partial t} + \big(\boldsymbol{\nabla}\cdot\boldsymbol{j}\big) = 0\ . \tag{6.45}$$

In this context, $\boldsymbol{j}$ is called the *probability current*.
Given the local conservation of probability density, Eq. (6.45), the probability current can be computed using the Schrödinger equation. Indeed, we have

$$\big(\boldsymbol{\nabla}\cdot\boldsymbol{j}\big) = -\frac{\partial\rho(\boldsymbol{r},t)}{\partial t} = -\frac{\partial|\psi(x)|^2}{\partial t} = -\frac{\partial\Big(\psi(x)^*\psi(x)\Big)}{\partial t} = -\left(\frac{\partial\psi^*}{\partial t}\psi + \psi^*\frac{\partial\psi}{\partial t}\right)\ . \tag{6.46}$$

From the Schrödinger equation,

$$\frac{\partial\psi(\boldsymbol{r})}{\partial t} = \frac{i}{2m}\boldsymbol{\nabla}^2\psi(\boldsymbol{r}) - iV(\boldsymbol{r})\psi(\boldsymbol{r})\ , \tag{6.47}$$

and its complex conjugate[a],

$$\frac{\partial\psi^*(\boldsymbol{r})}{\partial t} = -\frac{i}{2m}\boldsymbol{\nabla}^2\psi^*(\boldsymbol{r}) + iV(\boldsymbol{r})\psi^*(\boldsymbol{r})\ , \tag{6.48}$$

we can rewrite the divergence of the current density, Eq. (6.46), as

$$\big(\boldsymbol{\nabla}\cdot\boldsymbol{j}\big) = \frac{i}{2m}\big(\boldsymbol{\nabla}^2\psi^*\big)\psi - \frac{i}{2m}\psi^*\big(\boldsymbol{\nabla}^2\psi\big) = \frac{i}{2m}\boldsymbol{\nabla}\Big[\big(\boldsymbol{\nabla}\psi^*\big)\psi\Big] - \frac{i}{2m}\boldsymbol{\nabla}\big[\psi^*\big(\boldsymbol{\nabla}\psi\big)\big] \tag{6.49}$$

so that we can identify

$$\boldsymbol{j} = \frac{-i}{2m}\Big[\psi^*\big(\boldsymbol{\nabla}\psi\big) - \psi\big(\boldsymbol{\nabla}\psi^*\big)\Big]\ . \tag{6.50}$$

[a] Note that here we assume that the potential V is real.

6.5 Connecting the asymptotic solution to the cross section

With the quantum-mechanical expression for the differential cross section, Eq. (6.42), we are now ready to see how the form of the *ansatz* for the scattering wavefunction, Eq. (6.16), manifest itself in measureable quantities.

To compute $\boldsymbol{j}$ for the asymptotic form of the wavefunction, Eq. (6.16), we first denote

$$\psi^{+}_{\boldsymbol{k}_0} = \psi_{\rm in} + \psi_{\rm sc} \ , \tag{6.51}$$

where we separate the incident and the scattered wave,

$$\psi_{\rm in} = e^{ik_0 z} = A e^{ik_0 r\cos\theta} \quad \text{and} \quad \psi_{\rm sc} = A f(\theta,\phi)\frac{e^{ik_0 r}}{r} \ . \tag{6.52}$$

Then we can write

$$(\psi^{+}_{\boldsymbol{k}_0})^{*}\hat{\boldsymbol{\nabla}}\psi^{+}_{\boldsymbol{k}_0} = \left(\psi^{*}_{\rm in} + \psi^{*}_{\rm sc}\right)\left(\hat{\boldsymbol{\nabla}}\psi_{\rm in} + \hat{\boldsymbol{\nabla}}\psi_{\rm sc}\right) \ . \tag{6.53}$$

Taking the complex conjugate and using the definition of the probability current, Eq. (6.50), we arrive at a general expression

$$\boldsymbol{j} = -\frac{i}{2\mu}\left[\left(\psi^{*}_{\rm in} + \psi^{*}_{\rm sc}\right)\left(\hat{\boldsymbol{\nabla}}\psi_{\rm in} + \hat{\boldsymbol{\nabla}}\psi_{\rm sc}\right) - \left(\psi_{\rm in} + \psi_{\rm sc}\right)\left(\hat{\boldsymbol{\nabla}}\psi^{*}_{\rm in} + \hat{\boldsymbol{\nabla}}\psi^{*}_{\rm sc}\right)\right] \tag{6.54}$$

$$= -\frac{i}{2\mu}\left[\left(\psi^{*}_{\rm in}\hat{\boldsymbol{\nabla}}\psi_{\rm in} - \psi_{\rm in}\hat{\boldsymbol{\nabla}}\psi^{*}_{\rm in}\right) + \left(\psi^{*}_{\rm sc}\hat{\boldsymbol{\nabla}}\psi_{\rm sc} - \psi_{\rm sc}\hat{\boldsymbol{\nabla}}\psi^{*}_{\rm sc}\right) + 2i{\rm Im}\left(\psi^{*}_{\rm sc}\hat{\boldsymbol{\nabla}}\psi_{\rm in} + \psi^{*}_{\rm in}\hat{\boldsymbol{\nabla}}\psi_{\rm sc}\right)\right] \ , \tag{6.55}$$

in which we can identify the incident current,

$$\boldsymbol{j}_{\rm in} \equiv -\frac{i}{2\mu}\left(\psi^{*}_{\rm in}\hat{\boldsymbol{\nabla}}\psi_{\rm in} - \psi_{\rm in}\hat{\boldsymbol{\nabla}}\psi^{*}_{\rm in}\right) \ , \tag{6.56}$$

the scattered current

$$\boldsymbol{j}_{\rm sc} \equiv -\frac{i}{2\mu}\left(\psi^{*}_{\rm sc}\hat{\boldsymbol{\nabla}}\psi_{\rm sc} - \psi_{\rm sc}\hat{\boldsymbol{\nabla}}\psi^{*}_{\rm sc}\right) \ , \tag{6.57}$$

and the current corresponding to the interference between the incident and the scattered wave,

$$\boldsymbol{j}_{\rm int} \equiv \frac{1}{\mu}{\rm Im}\left(\psi^{*}_{\rm sc}\hat{\boldsymbol{\nabla}}\psi_{\rm in} + \psi^{*}_{\rm in}\hat{\boldsymbol{\nabla}}\psi_{\rm sc}\right) \ . \tag{6.58}$$

Let us first calculate $\boldsymbol{j}_{\rm sc}$. In this case, we consider the gradient in spherical coordinates,

$$\hat{\boldsymbol{\nabla}} = \hat{\boldsymbol{r}}\frac{\partial}{\partial r} + \hat{\boldsymbol{\theta}}\frac{1}{r}\frac{\partial}{\partial\theta} + \hat{\boldsymbol{\phi}}\frac{1}{r\sin\theta}\frac{\partial}{\partial\phi} \ . \tag{6.59}$$

Since ultimately we want to obtain $\boldsymbol{j}_{\rm out}\cdot\hat{\boldsymbol{r}}$, we only need to carry out the derivative proportional to $\hat{\boldsymbol{r}}$, as all other terms will vanish in the dot product. Thus we calculate

$$\frac{\partial}{\partial r}\psi_{\rm sc} = A f(\theta,\phi)\frac{e^{ik_0 r}}{r}\left(ik_0 - \frac{1}{r}\right) \ , \tag{6.60}$$

which leads to

$$\psi^{*}_{\rm sc}\frac{\partial}{\partial r}\psi_{\rm sc} = |A|^2\frac{|f(\theta,\phi)|^2}{r^2}\left(ik_0 - \frac{1}{r}\right) \tag{6.61}$$

and, identifying the velocity as $v = \frac{k_0}{\mu}$,

$$\boldsymbol{j}_{\rm sc} \cdot \hat{\boldsymbol{r}} = v|A|^2 \frac{|f(\theta,\phi)|^2}{r^2} \ . \tag{6.62}$$

Next, we look at $\boldsymbol{j}_{\rm in}$. Here, we can use the Cartesian gradient representation, leading to

$$\hat{\boldsymbol{\nabla}}\psi_{\rm in} = \hat{\boldsymbol{z}}\frac{\partial}{\partial z}A^{ik_0 z} = \hat{\boldsymbol{z}}A(ik_0)e^{ik_0 z} \ , \tag{6.63}$$

so that

$$\boldsymbol{j}_{\rm in} = v|A|^2\hat{\boldsymbol{z}} \ . \tag{6.64}$$

In particular, then,

$$\boldsymbol{j}_{\rm in} \cdot \hat{\boldsymbol{r}} = v|A|^2 \cos\theta \ . \tag{6.65}$$

It might seem weird, at a first glance, that the incident current, which corresponds to particles incident along the z direction, has a nonzero contribution at $\theta \neq 0$. This is because of the fundamental mismatch in our thinking: we talk about the incident *beam*, a localized phenomenon with a finite, small extent in the plane transverse to the beam direction, but we model it with a *plane wave*: an object of an infinite extent in the transverse plane. Naturally, this object has a non-zero contribution to $\boldsymbol{j} \cdot \hat{\boldsymbol{r}}$ save for $\theta = \left\{\frac{\pi}{2}, \frac{3\pi}{2}\right\}$.

Finally, let us take a look at $\boldsymbol{j}_{\rm int}$, Eq. (6.58). Considering only the derivatives along r, we obtain

$$\boldsymbol{j}_{\rm int} \cdot \hat{\boldsymbol{r}} \equiv \frac{|A|^2}{\mu}{\rm Im}\left[f^*(\theta,\phi)\frac{e^{-ik_0 r(1-\cos\theta)}}{r}\left(ik_0\cos\theta\right) + f(\theta,\phi)\frac{e^{ik_0 r(1-\cos\theta)}}{r}\left(ik_0 - \frac{1}{r}\right)\right] \ . \tag{6.66}$$

Unlike in the case of $\boldsymbol{j}_{\rm sc} \cdot \hat{\boldsymbol{r}}$ and $\boldsymbol{j}_{\rm in} \cdot \hat{\boldsymbol{r}}$, in $\boldsymbol{j}_{\rm int} \cdot \hat{\boldsymbol{r}}$ there are surviving oscillatory terms of the form

$$e^{\pm ik_0 r(1-\cos\theta)} = \cos\left[k_0 r(1-\cos\theta)\right] \pm \sin\left[k_0 r(1-\cos\theta)\right] \ . \tag{6.67}$$

These terms will oscillate ever more rapidly as $r \to \infty$. This means that even tiny changes in θ lead to strong variation in the cos and sin terms. Since any detector has a finite angular resolution $\Delta\theta$, averaging $\boldsymbol{j}_{\rm int}$ over the detector will sweep through many periods of the sin and cos functions, leading to destructive interference. We may therefore neglect this term altogether[12].

With $\boldsymbol{j}_{\rm int} \cdot \hat{\boldsymbol{r}}$ out of the game and our discussion of what a non-zero flux of $\boldsymbol{j}_{\rm in} \cdot \hat{\boldsymbol{r}}$ at $\theta \neq 0$ means, it is natural that the only contribution to the counts of particles at some angle Ω comes from $\boldsymbol{j}_{\rm sc} \cdot \hat{\boldsymbol{r}}$, computed in Eq. (6.62). Therefore, we identify $\boldsymbol{j}_{\rm out} \cdot \hat{\boldsymbol{r}} = \boldsymbol{j}_{\rm sc} \cdot \hat{\boldsymbol{r}}$. Together with the incident current, Eq. (6.64), the expression for the differential cross section, Eq. (6.42), becomes

$$\frac{d\sigma_{\rm el}(\Omega)}{d\Omega} = |f(\theta,\phi)|^2 \ , \tag{6.68}$$

where the subscript "el" signals the fact that using the general formula for the cross section in terms of incident and outgoing currents, Eq. (6.42), with currents computed based on the *ansatz* for the elastic scattering wavefunction, Eq. (6.16), yields an *elastic* differential scattering cross section.

With this result, we see that the elastic scattering amplitude not only modulates the contribution of the elastically scattered wave into angle Ω: its absolute value is equivalent to the differential

[12] This is not entirely true, since the suppression fails in the forward direction, $\theta \approx 0$, where the phase $k_0 r(1-\cos\theta)$ ceases to change rapidly. We will discuss this in Section 6.7.

elastic scattering cross section in that direction. The importance of $f(\theta, \phi)$ cannot be overstated: it provides a direct link between theoretical calculations and experimental results. Thus most, if not all of the reaction theory, is concerned with computing this quantity.

Finally, the total elastic cross section can now be expressed as

$$\sigma_{\rm el} = \int d\Omega \, \frac{d\sigma_{\rm el}(\Omega)}{d\Omega} = \int d\Omega \, |f(\theta, \phi)|^2 \, . \tag{6.69}$$

Note that, naturally, $f(\theta, \phi)$ is computed at some specific energy (and, similarly, experimental measurements can be done for specific reaction energies). If we make the energy dependence explicit, $f = f(E, \theta, \phi)$, then of course we have

$$\frac{d\sigma_{\rm el}}{d\Omega}(E, \theta, \phi) = |f(E, \theta, \phi)|^2 \quad \text{and} \tag{6.70}$$

and, by extension,

$$\sigma_{\rm el}(E) = \int d\Omega \, \frac{d\sigma_{\rm el}(\Omega)}{d\Omega} = \int d\Omega \, |f(E, \theta, \phi)|^2 \, . \tag{6.71}$$

6.6 Loss of flux

The local conservation law for quantum-mechanical probability, Eq. (6.45), is not always satisfied. Of course, conservation laws prohibit particles from simply disappearing, but one can imagine, for example, a situation in which the identity of a projectile particle changes, reducing the outgoing current in that channel. Such a situation can be modeled, among others, by means of an imaginary potential[13].

In-class Activity 6b: Imaginary potential and loss of flux

Consider a one-dimensional Schrödinger equation

$$i\frac{\partial}{\partial t}\psi(x,t) = \left[-\frac{1}{2m}\frac{d^2}{dx^2} + V(x)\right]\psi(x,t) \, , \tag{6.72}$$

with a purely imaginary, absorptive potential localized in space,

$$V(x) = \begin{cases} 0 \, , & x < 0 \, , \\ -iW \, , & x > 0 \, , \end{cases} \qquad W > 0 \, . \tag{6.73}$$

(a) Show that the continuity equation for $\rho(x,t) = |\psi(x,t)|^2$ becomes

$$\frac{\partial \rho}{\partial t} + \frac{\partial j}{\partial x} = -2W\,|\psi(x,t)|^2 \, . \tag{6.74}$$

(b) For $x > 0$, look for a stationary solution of the form $\psi(x,t) = \psi(x)e^{-iEt}$ with $\psi(x) = e^{ikx}$. Show that k is complex and that the physical branch corresponds to $\mathrm{Im}\, k > 0$.

(c) Compute $j(x)$ for $\psi(x) = e^{ikx}$ and show explicitly that the flux decreases with x for $x > 0$.

[13] Note that such a potential corresponds to a Hamiltonian that is not Hermitian.

Solution

(a) Instead of assuming that the continuity equation has the form given in Eq. (6.45), we use the Schrödinger equation to express $\partial|\psi|^2/\partial t$ as

$$\frac{\partial|\psi|^2}{\partial t} = \frac{\partial\psi^*}{\partial t}\psi + \psi^*\frac{\partial\psi}{\partial t} \tag{6.75}$$

$$= \left(-\frac{i}{2m}\frac{\partial^2}{\partial x^2}\psi^* + iV^*\psi^*\right)\psi + \psi^*\left(\frac{i}{2m}\frac{\partial^2}{\partial x^2}\psi - iV\psi\right) , \tag{6.76}$$

where this time, for obvious reasons, we also take the conjugate of V. Carrying the derivation out similarly as in the In-class Activity 6a, this time we obtain

$$\frac{\partial|\psi|^2}{\partial t} = -\frac{i}{2m}\left(\frac{\partial^2}{\partial x^2}\psi^*\right)\psi + iV^*\psi^*\psi + \frac{i}{2m}\psi^*\left(\frac{\partial^2}{\partial x^2}\psi\right) - iV\psi^*\psi \tag{6.77}$$

$$= -\frac{i}{2m}\left(\frac{\partial}{\partial x}\left[\psi\left(\frac{\partial}{\partial x}\psi^*\right)\right] - \frac{\partial}{\partial x}\left[\psi^*\left(\frac{\partial}{\partial x}\psi\right)\right]\right) + i|\psi|^2\big(V^* - V\big) . \tag{6.78}$$

Identifying

$$j(x) = -\frac{i}{2m}\left[\psi^*\left(\frac{\partial}{\partial x}\psi\right) - \psi\left(\frac{\partial}{\partial x}\psi^*\right)\right] = \frac{1}{m}\mathrm{Im}\left[\psi^*\left(\frac{\partial}{\partial x}\psi\right)\right] \tag{6.79}$$

in full analogy to what we did before, we obtain

$$\frac{\partial|\psi|^2}{\partial t} + \frac{\partial j}{\partial x} = 2\big(\mathrm{Im}\big[V\big]\big)|\psi|^2 . \tag{6.80}$$

For $x \leq 0$, the right-hand side is equal zero and we recover the probability continuity equation, Eq. (6.45), but for $x > 0$, given the explicit form of V, we get

$$\frac{\partial|\psi|^2}{\partial t} + \frac{\partial j}{\partial x} = -2W|\psi|^2 . \tag{6.81}$$

Clearly, in that region there is a *sink of probability*, *i.e.*, the probability "leaks out." This behavior can be interpreted as, for example, *absorption* of incident particles into a nucleus, which naturally comes at the cost of the (probability) density of the incident beam. The fact that the potential has such an influence is directly related to the fact that it is imaginary.

(b) In this case, the time-independent Schrödinger equation is

$$\left[-\frac{1}{2m}\frac{d^2}{dx^2} + V(x)\right]\psi(x) = E\psi(x) . \tag{6.82}$$

Taking the *ansatz* $\psi(x) = e^{ikx}$ leads to

$$\frac{k^2}{2m} - iW = E , \tag{6.83}$$

which immediately leads to a complex wavenumber k,

$$k = \sqrt{2m(E + iW)} . \tag{6.84}$$

(c) Using Eq. (6.79) with the wavefunction *ansatz* and acknowledging that the wavenumber is complex, we obtain

$$j(x) = \frac{1}{m}\mathrm{Im}\left[e^{-ik^*x}ike^{ikx}\right] = \frac{1}{m}\mathrm{Im}\big[ik\big]|\psi(x)|^2 \ . \tag{6.85}$$

Decomposing the wavenumber k into its real and complex parts, $k = k_R + ik_I$, we see that $\mathrm{Im}\big[ik\big] = k_R$ and $|\psi(x)|^2 = e^{-2k_I x}$, yielding

$$j(x) = \frac{k_R}{m}e^{-2k_I x} \ . \tag{6.86}$$

From this form it is evident that the further into the absorptive region ($x > 0$) the projectile goes, the more its probability density current $j(x)$ is suppressed. This is precisely the meaning of "loss of flux": probability current is removed from the channel we are tracking, at a rate governed by the imaginary part of the potential.

6.7 The optical theorem

Let us consider a sphere of a large[14] radius r around the reaction region. If we assume that the scattering is elastic, then the number of particles is conserved and the total flux through the sphere should be zero,

$$r^2 \int d\Omega \ \boldsymbol{j} \cdot \hat{\boldsymbol{r}} = 0 \ , \tag{6.87}$$

where the density current $\boldsymbol{j}$, Eq. (6.55), has incident, scattered, and interference components, so that we can write

$$r^2 \int d\Omega \ \left(\boldsymbol{j}_{\rm in} + \boldsymbol{j}_{\rm sc} + \boldsymbol{j}_{\rm int}\right) \cdot \hat{\boldsymbol{r}} = 0 \ . \tag{6.88}$$

Performing the integration shows that the contribution due to $\boldsymbol{j}_{\rm in}$, Eq. (6.65), is identically zero,

$$r^2 \int d\Omega \ v|A|^2 \cos\theta = 2\pi r^2 v|A|^2 \int_{-1}^{1} d(\cos\theta) \ \cos\theta = 0 \ , \tag{6.89}$$

while the contribution due to the scattered wave flux, Eq. (6.62), has the form

$$r^2 \int d\Omega \ \boldsymbol{j}_{\rm sc} \cdot \hat{\boldsymbol{r}} = r^2 \int d\Omega \ v|A|^2 \frac{|f(\theta,\phi)|^2}{r^2} = v|A|^2 \int d\Omega \ |f(\theta,\phi)|^2 \ . \tag{6.90}$$

As we already argued, the contribution from the interference flux $\boldsymbol{j}_{\rm int} \cdot \hat{\boldsymbol{r}}$, Eq. (6.66), is rapidly oscillating and, therefore, generally integrates to zero over any finite (even if infinitesimal) extent in the solid angle. The exception is the forward direction, $\theta = 0$.

Let us then integrate $\boldsymbol{j}_{\rm int} \cdot \hat{\boldsymbol{r}}$ over an infinitesimal area $dA = r^2 d\Omega$ centered around the z axis with a small opening angle $\delta\theta$, see Fig. 6.1. We can keep only leading-order terms in $1/r$ as well as

[14] That is, large enough that the asymptotic solution is applicable.

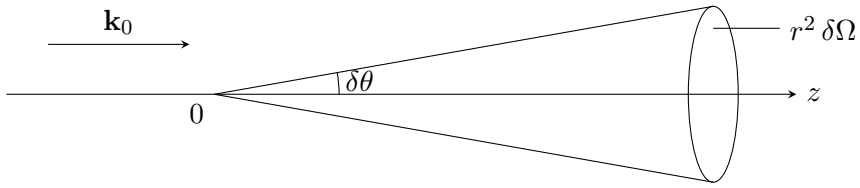

Figure 6.1: Illustration for the derivation of the optical theorem.

put $\theta \approx 0$ in all smoothly-varying (*i.e.*, not rapidly oscillating) terms[15], leading to

$$\int dA\ \boldsymbol{j}_{\rm int}\cdot\hat{\boldsymbol{r}} = \frac{2\pi r^2|A|^2}{\mu}\int_{\cos(\delta\theta)}^{1} d(\cos\theta)\ {\rm Im}\left[\frac{ik_0 f^*(0)}{r}e^{-ik_0 r(1-\cos\theta)} + \frac{ik_0 f(0)}{r}e^{ik_0 r(1-\cos\theta)}\right] \tag{6.91}$$

$$= \frac{2\pi|A|^2}{\mu}{\rm Im}\left[f^*(0)\Big(1-e^{-ik_0 r(1-\cos\delta\theta)}\Big) - f(0)\Big(1-e^{ik_0 r(1-\cos\delta\theta)}\Big)\right] . \tag{6.92}$$

As before, we disregard the oscillatory terms as they will destructively interfere at large r, *i.e.*, in the detector[16], so that overall

$$\int dA\ \boldsymbol{j}_{\rm int}\cdot\hat{\boldsymbol{r}} = \frac{2\pi|A|^2}{\mu}{\rm Im}\Big[f^*(0)-f(0)\Big] = -\frac{4\pi|A|^2}{\mu}{\rm Im}\big[f(0)\big] . \tag{6.93}$$

Together with the contribution due to the scattered density flux, Eq. (6.90), the disappearance of the total flux, Eq. (6.87), leads to

$$v|A|^2\int d\Omega\ |f(\theta,\phi)|^2 - \frac{4\pi|A|^2}{\mu}{\rm Im}\big[f(0)\big] = 0 . \tag{6.94}$$

Since the modulus squared of the scattering amplitude is equivalent to the differential cross section, Eq. (6.68), integrating it over $d\Omega$ yields the total elastic cross section, Eq. (6.69), so that the above equation can be rewritten to yield *the optical theorem*

$$\sigma_{\rm el} = \frac{4\pi}{k_0}{\rm Im}\big[f(0)\big] , \tag{6.95}$$

where we have used $v = k_0/\mu$.

This is a powerful result: the information about the elastic cross section, summing over all possible angles θ, is contained in the scattering amplitude at $\theta = 0$. How is it possible? When you solve the scattering problem, you're looking for the total wavefunction far from the scatterer. This total wavefunction is $\psi^{(+)} = \psi_{\rm in} + \psi_{\rm sc} = e^{ikz} + f(\theta)e^{ikr}/r$. In the forward direction ($\theta = 0$), both terms are present and propagating in the same direction, so they add coherently. Now, conservation of probability demands that if particles are scattered away into other directions (which is what is measured by the total cross-section σ), then the forward beam intensity $|\psi^{(+)}(\theta=0)|^2$ must be depleted compared to the incident intensity $|e^{ikz}|^2$. The only way to reduce $|\psi_{\rm in}+\psi_{\rm sc}|^2$ below $|\psi_{\rm in}|^2$ through addition of $\psi_{\rm sc}$ is if $\psi_{\rm sc}$ interferes destructively with $\psi_{\rm in}$, which requires $\psi_{\rm sc}$ to be imaginary (90° out of phase) when $\psi_{\rm in}$ is real. This destructive interference in the forward direction, encoded in

[15] Note that in the forward direction, the scattering amplitude is additionally independent of ϕ.

[16] For a fixed $\delta\theta > 0$, the phase $\Phi = k_0 r\big(1-\cos\delta\theta\big)$ grows proportionally to r. As $r\to\infty$, the factors $e^{\pm i\Phi}$ oscillate arbitrarily rapidly with respect to any infinitesimal change in r, k_0, or $\delta\theta$. In any realistic situation one effectively averages over a small spread in one of these quantities (due to a finite energy resolution, finite angular acceptance, or considering a wave packet instead of an ideal plane wave), and consequently $\langle e^{\pm i\Phi}\rangle \to 0$.

$\mathrm{Im}[f(0)]$, is what removes flux from the beam, and the optical theorem simply equates this removed flux to the total scattered flux.

Remarkably, the above argument also shows that the optical theorem is applicable to inelastic scattering. This is because $\mathrm{Im}\big[f(0)\big]$ "measures" the loss of flux for *any* reason, whether due to an elastic scattering, inelastic scattering, or a nuclear reaction. Therefore, we can generalize Eq. (6.95) to

$$\sigma_{\mathrm{tot}} = \frac{4\pi}{k_0}\mathrm{Im}\big[f(0)\big] \ , \tag{6.96}$$

where σ_{tot} denotes the *total* cross section.

Lecture sources: This lecture is based mainly on Joachain [2] and Bertulani & Danielewicz [6].

Lecture 7

Partial wave expansion I

Prerequisites: Lectures 2, 5, 6.
Guiding question: ***How does the potential affect the asymptotic wavefunction?***

7.1 Scattering off a spherically symmetric potential

Let us consider the Schrödinger equation for spin-zero particles scattering off of a spin-zero target,

$$\hat{\boldsymbol{\mathcal{H}}}\psi = E\psi \ , \tag{7.1}$$

in which the Hamiltonian contains a spherically-symmetric potential $V = V(r)$. Since the interaction term depends only on the relative position of the projectile and target, we consider the problem in the center-of-mass frame (see Lectures 2 and 6), in which we can write

$$\hat{\boldsymbol{\mathcal{H}}} = -\frac{\hat{\boldsymbol{\nabla}}^2}{2\mu} + V(r) \ , \tag{7.2}$$

where μ is the reduced mass. Since we know that, nonrelativistically, we have $E = \frac{k^2}{2\mu}$, the time-independent Schrödinger equation can be written as

$$\left[\hat{\boldsymbol{\nabla}}^2 + k^2 - U(r)\right]\psi(\boldsymbol{r}) = 0 \ , \tag{7.3}$$

where we again (see Lecture 6) introduced $U(r) = 2\mu V(r)$. Further, the Laplacian can be rewritten in the spherical coordinates (r, θ, ϕ),

$$\hat{\boldsymbol{\nabla}}^2 = \frac{1}{r^2}\frac{\partial}{\partial r}\left(r^2\frac{\partial}{\partial r}\right) + \frac{1}{r^2\sin\theta}\frac{\partial}{\partial\theta}\left(\sin\theta\frac{\partial}{\partial\theta}\right) + \frac{1}{r^2\sin^2\theta}\frac{\partial^2}{\partial\phi^2} \ . \tag{7.4}$$

Solutions to Eq. (7.3) must satisfy specific boundary conditions: First, we would like them to be finite at the origin, making the wavefunction physically admissible at and around the interaction point. Second, they should have the asymptotic behavior of an incoming plane wave and an outgoing spherical wave. This and a number of simplifications induced by the spherical symmetry will allow us to precisely identify how solutions to scattering problems can be built.

7.2 Angular momentum and spherical harmonic solutions

The angular momentum operator is defined as[1]

$$\hat{\boldsymbol{L}} = \hat{\boldsymbol{r}} \times \hat{\boldsymbol{p}} \ . \tag{7.5}$$

Since $\hat{\boldsymbol{p}} = -i\hat{\boldsymbol{\nabla}}$, we can immediately write out explicit expressions for the components of $\hat{\boldsymbol{L}}$,

$$L_x = yp_z - zp_y = -i\left(y\frac{\partial}{\partial z} - z\frac{\partial}{\partial y}\right) = i\left(\sin\phi\frac{\partial}{\partial\theta} + \cot\theta\cos\phi\frac{\partial}{\partial\phi}\right) , \tag{7.6}$$

$$L_y = zp_x - xp_z = -i\left(z\frac{\partial}{\partial x} - x\frac{\partial}{\partial z}\right) = i\left(-\cos\phi\frac{\partial}{\partial\theta} + \cot\theta\sin\phi\frac{\partial}{\partial\phi}\right) , \tag{7.7}$$

$$L_z = xp_y - yp_x = -i\left(x\frac{\partial}{\partial y} - y\frac{\partial}{\partial x}\right) = -i\frac{\partial}{\partial\phi} \ . \tag{7.8}$$

The square of the angular momentum operator is then given by

$$\hat{L}^2 = \hat{L}_x^2 + \hat{L}_y^2 + \hat{L}_z^2 = -\left[\frac{1}{\sin\theta}\frac{\partial}{\partial\theta}\left(\sin\theta\frac{\partial}{\partial\theta}\right) + \frac{1}{\sin^2\theta}\frac{\partial^2}{\partial\phi^2}\right] , \tag{7.9}$$

and, comparing with the Laplacian in spherical coordinates, Eq. (7.4), we can see that we have

$$\hat{\boldsymbol{\nabla}}^2 = \frac{1}{r^2}\frac{\partial}{\partial r}\left(r^2\frac{\partial}{\partial r}\right) - \frac{\hat{L}^2}{r^2} \ . \tag{7.10}$$

The above form[2] as well as the spherical symmetry of the potential inspire us to look for solutions where the radial and angular dependence factorize,

$$\psi(\boldsymbol{r}) = R(r)Y(\theta,\phi) \ . \tag{7.11}$$

With this *ansatz* for $\psi(\boldsymbol{r})$, the Schrödinger equation, Eq. (7.3), becomes

$$Y(\theta,\phi)\frac{1}{r^2}\frac{\partial}{\partial r}\left(r^2\frac{\partial}{\partial r}\right)R(r) - R(r)\frac{\hat{L}^2}{r^2}Y(\theta,\phi) + k^2R(r)Y(\theta,\phi) - U(r)R(r)Y(\theta,\phi) = 0 \ . \tag{7.12}$$

By dividing both sides of the above equation by $R(r)Y(\theta,\phi)$ and rearranging, we arrive at

$$\frac{1}{R(r)}\frac{1}{r^2}\frac{\partial}{\partial r}\left(r^2\frac{\partial}{\partial r}\right)R(r) + k^2 - U(r) = \frac{1}{Y(\theta,\phi)}\frac{\hat{L}^2}{r^2}Y(\theta,\phi) \ . \tag{7.13}$$

Since we managed to get all terms dependent on $R(r)$ on one side and all terms dependent on $Y(\theta,\phi)$ on the other, the only way in which these two sides can be equal (for *any* value of r, θ, and ϕ) is if they are both equal to some constant C. Thus we arrive at two differential equations,

$$\frac{1}{r^2}\frac{\partial}{\partial r}\left(r^2\frac{\partial}{\partial r}\right)R(r) + \Big[k^2 - U(r) - C\Big]R(r) = 0 \ , \tag{7.14}$$

$$\frac{\hat{L}^2}{r^2}Y(\theta,\phi) = CY(\theta,\phi) \ . \tag{7.15}$$

[1] This is an example of the correspondence principle at work.

[2] Note that the Hamiltonian $\hat{\boldsymbol{\mathcal{H}}}$ evidently commutes with $\hat{L}^2$.

Since, by construction, $\hat{L}^2 = \hat{L}_x^2 + \hat{L}_y^2 + \hat{L}_z^2$ commutes with each of the angular momentum components L_x, L_y, L_z, the solutions to Eq. (7.15) must be simultaneous eigenfunctions of $\hat{L}^2$ and one of the angular momentum components[3], which is customarily chosen to be L_z. Such functions are known as the *spherical harmonics* and they satisfy

$$\hat{L}^2 Y_{lm}(\theta,\phi) = l(l+1)Y_{lm}(\theta,\phi) \ , \tag{7.16}$$

$$L_z Y_{lm}(\theta,\phi) = mY_{lm}(\theta,\phi) \ , \tag{7.17}$$

where l and m are the *orbital angular momentum quantum number* and *magnetic quantum number*.

7.3 The radial equation

With the solution to Eq. (7.15) known, we can identify that $C = l(l+1)/r^2$, which transforms the *radial equation*, Eq. (7.14), into

$$\frac{1}{r^2}\frac{\partial}{\partial r}\left(r^2\frac{\partial}{\partial r}\right)R_l(k,r) + \left[k^2 - U(r) - \frac{l(l+1)}{r^2}\right]R_l(k,r) = 0 \ , \tag{7.18}$$

where we put subscript l on the radial function to mark its dependence on the orbital angular momentum quantum number and add an argument k to highlight its dependence on the energy. As we discussed in Lecture 5, the term $\frac{l(l+1)}{r^2}$ is referred to as the centrifugal term. It is convenient to introduce a change of variables with $\rho = rk$, by means of which the above equation becomes

$$\frac{1}{\rho^2}\frac{\partial}{\partial \rho}\left(\rho^2\frac{\partial}{\partial \rho}\right)R_l(k,\rho) + \left[1 - \frac{U(\rho)}{k^2} - \frac{l(l+1)}{\rho^2}\right]R_l(k,\rho) = 0 \ . \tag{7.19}$$

Finally, let us also introduce an alternative radial function,

$$u_l(k,\rho) = \rho R_l(k,\rho) \ , \tag{7.20}$$

which allows us to rewrite the radial equation as

$$\frac{\partial^2}{\partial \rho^2}u_l(k,\rho) + \left[1 - \frac{U(\rho)}{k^2} - \frac{l(l+1)}{\rho^2}\right]u_l(k,\rho) = 0 \ . \tag{7.21}$$

Alternatively, one can also introduce the radial function u_l without introducing the variable ρ, $u_l(k,r) = rR_l(k,r)$, which leads to

$$\frac{\partial^2}{\partial r^2}u_l(k,r) + \left[k^2 - U(r) - \frac{l(l+1)}{r^2}\right]u_l(k,r) = 0 \ . \tag{7.22}$$

Naturally, the solutions to the radial equation depend on the form of $U(r)$ or, equivalently, $U(\rho)$.

7.3.1 Free solutions

When solving a scattering problem, we only need to know the asymptotic solutions (see Section 6.2) where $U \to 0$. By putting $U = 0$ in Eq. (7.19), we obtain the free-particle equation for $R_l(k,\rho)$,

$$\frac{1}{\rho^2}\frac{\partial}{\partial \rho}\left(\rho^2\frac{\partial}{\partial \rho}\right)R_l(k,\rho) = -\left[1 - \frac{l(l+1)}{\rho^2}\right]R_l(k,\rho) \ , \tag{7.23}$$

[3] We recall that since $\left[L_i, L_j\right] = i\epsilon_{ijk}L_k \neq 0$, no function can be an eigenstate of more than one component of L.

and by doing the same with Eq. (7.21), we obtain the free-particle radial equation for $u_l(k,\rho)$,

$$\frac{\partial^2}{\partial\rho^2}u_l(k,\rho) = -\left[1 - \frac{l(l+1)}{\rho^2}\right]u_l(k,\rho) \ . \tag{7.24}$$

Eq. (7.23) is the *spherical Bessel equation*, while Eq. (7.24) is the *Ricatti-Bessel equation*. Naturally, once we know the solution for one of them, we also know the solution for the other through Eq. (7.20).

To gain an intuitive understanding of what these solutions should look like, let us consider the Ricatti-Bessel equation, Eq. (7.24) , in the limit $\rho \to 0$. In this case we can ignore the first term in the square bracket, leading to

$$\frac{\partial^2}{\partial\rho^2}u_l^{(\rho\to 0)}(k,\rho) = \frac{l(l+1)}{\rho^2}u_l^{(\rho\to 0)}(k,\rho) \ , \tag{7.25}$$

which is solved by

$$u_l^{(\rho\to 0)}(k,r) = A(k)\rho^{l+1} + B(k)\rho^{-l} \ . \tag{7.26}$$

In the opposite limit, $r \to \infty$, we get

$$\frac{\partial^2}{\partial\rho^2}u_l^{(\rho\to\infty)}(k,\rho) = -u_l^{(\rho\to\infty)}(k,\rho) \ , \tag{7.27}$$

which admits solutions of the form

$$u_l^{(\rho\to\infty)}(k,\rho) = A(k)\sin(\rho) + B(k)\cos(\rho) \ . \tag{7.28}$$

Thus the exact solutions should have properties which lead to a power-law behavior near the origin and an oscillatory behavior at large ρ, where the degree of the former depends explicitly on the angular momentum quantum number l.

The full solutions to the spherical Bessel equation, Eq. (7.23), are known to be linear combinations of spherical Bessel functions $j_l(\rho)$, which are regular at the origin, and spherical Neumann functions $n_l(\rho)$, which diverge at $\rho = 0$. The spherical Bessel functions $j_\ell(\rho)$ for the lowest three angular momenta are

$$j_0(\rho) = \frac{\sin\rho}{\rho} \ , \qquad j_1(\rho) = \frac{\sin\rho}{\rho^2} - \frac{\cos\rho}{\rho} \ , \qquad j_2(\rho) = \left(\frac{3}{\rho^2} - 1\right)\frac{\sin\rho}{\rho} - \frac{3\cos\rho}{\rho^2} \ , \quad \ldots \tag{7.29}$$

while the first few spherical Neumann functions are

$$n_0(\rho) = -\frac{\cos\rho}{\rho}, \quad n_1(\rho) = -\frac{\cos\rho}{\rho^2} - \frac{\sin\rho}{\rho}, \quad n_2(\rho) = -\left(\frac{3}{\rho^2} - 1\right)\frac{\cos\rho}{\rho} - \frac{3\sin\rho}{\rho^2}, \quad \ldots \ . \tag{7.30}$$

The first few Bessel and Neumann functions are also shown in Fig. 7.1. Then, the solutions to the Ricatti-Bessel equation are the Ricatti-Bessel functions $\hat{\jmath}_l$ and the Ricatti-Neumann functions $\hat{n}_l$, which naturally satisfy

$$\hat{\jmath}_l(\rho) = \rho j_l(\rho) \quad \text{and} \quad \hat{n}_l(\rho) = \rho n_l(\rho) \ . \tag{7.31}$$

Finally, sometimes it is convenient to express the solutions of the radial equations in terms of complex *Haenkel functions*, which are linear combinations of the Bessel and Neumann functions,

$$h_l^{(\pm)}(\rho) = j_l(\rho) \pm i n_l(\rho) \ . \tag{7.32}$$

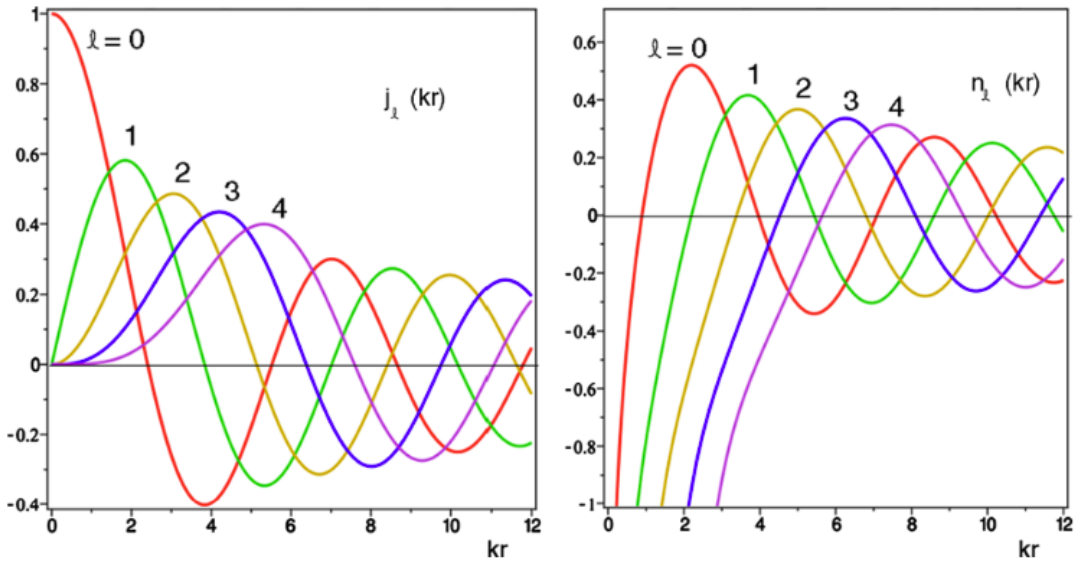

Figure 7.1: The first few Bessel and Neumann functions. Figure from Ref. [1].

The most general solution in any problem is then

$$R_l(r) = \sum_{l=0}^{\infty} \Big[A_l j_l(\rho) + B_l n_l(\rho) \Big] \ , \tag{7.33}$$

or

$$u_l(r) = \sum_{l=0}^{\infty} \Big[a_l \hat{\jmath}_l(\rho) + b_l \hat{n}_l(\rho) \Big] \ , \tag{7.34}$$

or

$$u_l^{(\pm)}(r) = \sum_{l=0}^{\infty} c_l^{(\pm)} h_l^{(\pm)}(\rho) \ , \tag{7.35}$$

where the coefficients A_l, B_l or a_l, b_l or $c_l^{(\pm)}$ are found by demanding that the solution satisfies appropriate boundary conditions. Thus, any solution can be built out of an infinite sum of contributions corresponding to different angular momenta.

It can be shown that the Ricatti functions take the following limits for $\rho \to 0$ and $\rho \to \infty$,

$$\hat{\jmath}_l(\rho \to 0) \sim \frac{\rho^{l+1}}{(2l+1)!!} \ , \qquad \hat{n}_l(\rho \to 0) \sim -\frac{(2l-1)!!}{\rho^l} \ , \tag{7.36}$$

$$\hat{\jmath}_l(\rho \to \infty) \sim \sin\left(\rho - l\frac{\pi}{2}\right) \ , \qquad \hat{n}_l(\rho \to \infty) \sim -\cos\left(\rho - l\frac{\pi}{2}\right) \ . \tag{7.37}$$

It is interesting to consider the phase shift $-l\frac{\pi}{2}$ of the $\rho \to \infty$ limits, that is the fact that compared to the $l = 0$ solution, solutions for $l > 0$ acquire an additional phase offset, proportional to l, which may be thought of as a *radial delay* in the onset of oscillatory behavior. This can be understood directly from the radial equation, Eq. (7.24). Without the centrifugal term $-\frac{l(l+1)}{\rho^2}$, the solution has oscillatory behavior; this is the case at very large ρ where the centrifugal term is suppressed.

Exactly when that oscillatory behavior starts to dominate depends on the value of l: the higher l is, the larger ρ it takes to suppress the centrifugal term. As a result, the shift in onset[4] of the oscillatory behavior is proportional to l, where each unit of l leads to a negative shift of $\pi/2$. This can also be intuitively understood when looking at the explicit form of the solutions, Eqs. (7.29), (7.30), and (7.31): For example, the leading term in the $l = 0$ Ricatti-Bessel function is $\sin\rho$, the leading term in the $l = 1$ Ricatti-Bessel function is $-\cos\rho = \sin(\rho - \frac{\pi}{2})$, the leading term in the $l = 2$ Ricatti-Bessel function is $-\sin(\rho) = \sin(\rho - \pi)$, *etc.*

It is also worth noting that since $\rho = kr$, we can obtain a large ρ either by going to large r or having a projectile with a large momentum[5] k. Thus, for a fixed l, high-momentum waves enter the oscillatory regime at smaller physical radii, while low-momentum waves remain sensitive to the centrifugal term over a larger region.

7.3.2 Angular momentum of free solutions... wait, what?

For a free particle, there is no physically preferred reference point; instead, we can simply choose an arbitrary point in space to serve as the origin. Since we discuss all this in the context of solving for the scattered wavefunction, the chosen "origin" often corresponds to the location of some scattering center; still, if we are *outside the range of the potential*, that point is just as good as any other point for determining the angular momentum of a free wave. Why, then, should the angular momentum of a free wave with respect to an essentially arbitrary point (from the asymptotic point of view) matter *at all*? In particular, why should it determine the solutions?

The key insight is that once an origin is chosen, the decomposition into states with particular values of the angular momentum has a clear geometric interpretation. Angular momentum is defined with respect to that chosen origin and characterizes the transverse structure of the wave rather than its dynamics (for example, if the wavefunction has a finite extent in the transverse plane $R_\perp$, in its expansion as a sum over solutions to the radial equation only terms characterized by l smaller than $l_{\max} \sim kR_\perp$ will contribute). As already highlighted in Lecture 5, the centrifugal term does *not* correspond to some "repulsion" of the particle from the origin[6]. Instead, in the classical limit, it encodes the geometric fact that a straight-line trajectory which misses the origin by a distance b (the impact parameter) does not pass through small r.

This can be seen directly from the definition of the angular momentum, $L = |\boldsymbol{r} \times \boldsymbol{k}|$. Since L is conserved, we may evaluate it at any point along the trajectory. In particular, at the point of closest approach for a free particle where $\angle(\boldsymbol{r}, \boldsymbol{k}) = \pi/2$, one immediately gets $L = bk$. As a result, high-l components correspond to straight lines with a large transverse offset relative to the chosen origin. For such components, the centrifugal term suppresses the wave at small r, see Eqs. (7.23) and (7.24), corresponding exactly to the fact that trajectories with large transverse offset never reach small r. This can also be seen from the limiting behavior of the Ricatti functions, Eq. (7.36). For the regular solution, $\hat{\jmath}_l$, it is evident that the higher the angular momentum quantum number l, the more suppressed is the solution near the origin[7].

[4] Understood as a shift in terms of distance from the origin as measured by ρ.

[5] Note again that in natural units, the momentum p and the wavenumber k are the same thing.

[6] This is important to remember given the fact that not only one often defines the effective potential $U_{\text{eff}}(r) = U(r) + \frac{L^2}{r^2}$ (see Eq. (5.17) and the discussion around it), but some even go as far as calling L^2/r^2 the "centrifugal potential", which is one of the best examples that just because you can do something, it doesn't mean that you should.

[7] We don't discuss the Ricatti-Neumann function $\hat{n}_l$ here since, when considering free particle solutions in a region containing the origin, the requirement that the wavefunction is regular rules out the Ricatti-Neumann functions.

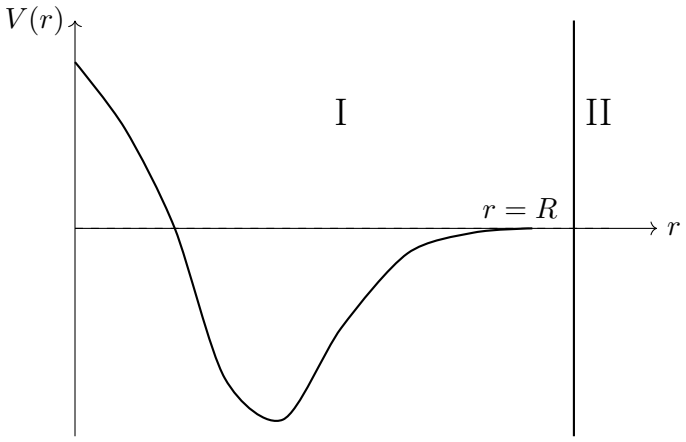

Figure 7.2: Schematic illustration of two regions: where the potential is finite, $r < R$, and where it becomes negligible, $r \geq R$.

7.4 It's all about the phase shifts

Let us now discuss solving the full scattering problem, where we need to acknowledge the existence of two regions in space: a region where the potential is non-zero and a region where it is negligible, which are divided by $r = R$ and marked in Fig. 7.2 with "I" and "II", respectively. Let us assume that, by whatever means, we know the stationary solutions $u_l^{\rm I}$ of the radial Schrödinger equation for non-zero $V(r)$, Eq. (7.21), rewritten here in terms of the spacial radius $r = \rho/k$ and with some terms rearranged,

$$\frac{\partial^2}{\partial r^2} u_l^{\rm I}(k,r) + \left[2\mu\big[E - V(r)\big] - \frac{l(l+1)}{r^2}\right] u_l^{\rm I}(k,r) = 0 \ . \tag{7.38}$$

Then, in region II, we represent the solution as a linear combination of Ricatti functions,

$$u_l^{\rm II}(k,r) = \alpha_l\big[\hat{\jmath}_l(kr) + \beta_l \hat{n}_l(kr)\big] \ . \tag{7.39}$$

To construct a full solution for a given angular momentum quantum number l, one needs to match the functions $u_l^{\rm I}$ and $u_l^{\rm II}$ as well as their first derivatives at the boundary, $r = R$,

$$u_l^{\rm I}(k,R) = \alpha_l\big[\hat{\jmath}_l(kR) + \beta_l \hat{n}_l(kR)\big] \ , \tag{7.40}$$

$$\left.\frac{du_l^{\rm I}(k,R)}{dr}\right|_{r=R} = \alpha_l k\Big[\hat{\jmath}_l'(kR) + \beta_l \hat{n}_l'(kR)\Big] \ . \tag{7.41}$$

Since the two equations need to be satisfied, so is their ratio,

$$\frac{\left.\frac{du_l^{\rm I}(k,R)}{dr}\right|_{r=R}}{u_l^{\rm I}(k,R)} = k\,\frac{\hat{\jmath}_l'(kR) + \beta_l \hat{n}_l'(kR)}{\hat{\jmath}_l(kR) + \beta_l \hat{n}_l(kR)} \ , \tag{7.42}$$

which is convenient to use because it gets rid of the α_l coefficient. Further, we can always multiply both sides by R, which allows us to write the left-hand side as a logarithmic derivative[8]. Defining

$$\mathcal{L}^{\rm I} = \left(\frac{d\ln u_l^{\rm I}(k,r)}{d\ln r}\right)_{r=R} \ , \tag{7.43}$$

[8]Note that we have $\frac{d\ln f(x)}{d\ln x} = \frac{dx}{d\ln x}\frac{d\ln f(x)}{dx} = \frac{x}{f(x)}\frac{df(x)}{dx}$.

we can rewrite Eq. (7.42) as

$$\mathcal{L}^{\mathrm{I}} = kR\,\frac{\hat{\jmath}_l'(kR) + \beta_l \hat{n}_l'(kR)}{\hat{\jmath}_l(kR) + \beta_l \hat{n}_l(kR)}\ . \tag{7.44}$$

Since we assume that we know u_l^{I}, the only unknown in this equation is β_l. Solving for β_l leads to

$$\beta_l = -\frac{kR\hat{\jmath}_l'(kR) - \mathcal{L}^{\mathrm{I}}\hat{\jmath}_l(kR)}{kR\hat{n}_l'(kR) - \mathcal{L}^{\mathrm{I}}\hat{n}_l(kR)}\ . \tag{7.45}$$

This doesn't look extremely exciting unless one looks at the asymptotic limit of the u_l^{II} solution, Eq. (7.39), which we obtain using the asymptotic limits of the Ricatti functions, Eq. (7.37),

$$\lim_{r\to\infty} u_l^{\mathrm{II}}(k,r) = \alpha_l\left[\sin\left(kr - l\frac{\pi}{2}\right) - \beta_l\cos\left(kr - l\frac{\pi}{2}\right)\right]\ . \tag{7.46}$$

Since the arguments of the sine and cosine are the same, we may want to find a way to add the two terms. Given the trigonometric identity $\sin(a+b) = \sin a\cos b + \cos a\sin b$, we notice that defining

$$\beta_l = -\tan\delta_l\ , \tag{7.47}$$

as well as a new overall coefficient α_l' through $\alpha_l = \alpha_l'\cos\delta_l$, we can write

$$\lim_{r\to\infty} u_l^{\mathrm{II}}(k,r) = \alpha_l'\left[\sin\left(kr - l\frac{\pi}{2}\right)\cos\delta_l + \sin\delta_l\cos\left(kr - l\frac{\pi}{2}\right)\right] \tag{7.48}$$

$$= \alpha_l'\left[\sin\left(kr - l\frac{\pi}{2} + \delta_l\right)\right]\ , \tag{7.49}$$

where, by Eqs. (7.45) and (7.47), we have

$$\delta_l = \tan^{-1}\left[\frac{kR\hat{\jmath}_l'(kR) - \mathcal{L}^{\mathrm{I}}\hat{\jmath}_l(kR)}{kR\hat{n}_l'(kR) - \mathcal{L}^{\mathrm{I}}\hat{n}_l(kR)}\right]\ . \tag{7.50}$$

From Eq. (7.49) it is clear that δ_l is a *phase shift*, *i.e.*, a constant shift in the argument of an oscillatory function. Its meaning becomes clear when one considers the case where $V = 0$ everywhere, so that the free particle solution $u_l^{\mathrm{II}}(kr)$, Eq. (7.39), applies in all space. In that case, since we require that the solution is regular at the origin, we need to put $\beta_l = 0$, which is equivalent to $\delta_l = 0$, and asymptotically the solution is just

$$\lim_{r\to\infty} u_l^{\mathrm{II}}(k,r)\Big|_{V=0} = \alpha_l\left[\sin\left(kr - l\frac{\pi}{2}\right)\right]\ . \tag{7.51}$$

Thus, δ_l measures how much the phase of the wavefunction is shifted due to the influence of the potential V. This answers the question guiding this lecture: the effect of the potential on the asymptotic wavefunction is to shift its phase.

This influence of the potential V on δ_l is further evident in the dependence of δ_l on the matching condition, as is easily seen from Eq. (7.50). It cannot be stressed enough that the phase shift δ_l is the *only* effect that the potential $V(r)$ leaves on the final scattered state. In other words, δ_l is *all* we need to know to solve a scattering problem[9].

[9] More precisely, this statement only applies unequivocally to *elastic* scattering from a real potential, in which case the only effect of the interaction is to redistribute the flux in the solid angle. For inelastic scattering and nuclear reactions, this description must be generalized; nevertheless, as you will see in future Lectures, the scattering phase shift remains a central quantity also for these cases.

Finally, because the overall coefficient of the radial solution does not matter for a scattering problem, as we have seen above, there exist many normalizations. For example, in the asymptotic limit one may equally well use $u_l(k,r) \xrightarrow[r\to\infty]{} \sin\left(kr - \frac{1}{2}l\pi + \delta_l\right)$, $u_l(k,r) \xrightarrow[r\to\infty]{} (1/k)\sin\left(kr - \frac{1}{2}l\pi + \delta_l\right)$, or $u_l(k,r) \xrightarrow[r\to\infty]{} (1/k)\left[\sin\left(kr - \frac{1}{2}l\pi\right) + \cos\left(kr - \frac{1}{2}l\pi\right)\tan\delta_l\right]$; the same applies to using non-asymptotic combinations of the Bessel, Neumann, Ricatti, or Haenkel functons. The only requirement here is to be consistent once a normalization has been chosen.

7.5 Sign of the phase shift

To deduce the dependence of the phase shift sign on the potential, it is convenient to look at the Schrödinger equation. Let us look in particular at Eq. (7.21), where for this analysis we can put $l = 0$ without loss of generality,

$$\frac{\partial^2}{\partial\rho^2}u_l(k,\rho) + \left[1 - \frac{U(\rho)}{k^2}\right]u_l(k,\rho) = 0\ . \tag{7.52}$$

If U is attractive, $U < 0$, the effect of the potential is to *increase* the absolute value of the coefficient multiplying $u_l(k,\rho)$. Since this coefficient tells us about how big the second derivative of u_l is, *i.e.*, how fast the wavefunction is oscillating[10], we see that $U < 0$ leads to more rapid oscillations. This means that from 0 out to some arbitrary radius R, u_l will experience more crests than if $U = 0$. That is, if $u_l(U = 0)$ has a crest at r_0, $u_l(U < 0)$ will have the same crest at some $r' < r_0$. This effect can be described by an *advanced* phase, *i.e.*, a *positive* phase shift. Conversely, if U is repulsive, $U > 0$, it implies a *decrease* in the oscillation rate[11] of u_l, so that if $u_l(U = 0)$ has a crest at r_0, $u_l(U > 0)$ will have the same crest at some $r'' > r_0$, which corresponds to a *retarded* phase, *i.e.*, a *negative* phase shift.

7.6 Solutions in the presence of a potential

Above, we assumed that we "somehow" know what $u_l^{\rm I}(k,R)$ and $\left(du_l^{\rm I}(k,r)/dr\right)_{r=R}$ are. In practice, as you can imagine, solving for $u_l^{\rm I}(k,r)$ can be arbitrarily complicated. However, the beautiful thing about being interested only in $u_l^{\rm I}(k,R)$ and $\left(du_l^{\rm I}(k,r)/dr\right)_{r=R}$ is that these quantities are *numbers*. In other words, we don't need access to, for example, analytical properties of $u_l^{\rm I}(k,r)$ or its n-th derivative. Viewed from this perspective, the radial equation, Eq. (7.21), is just an ordinary second-order differential equation: we can integrate it numerically to obtain $u_l^{\rm I}$ and its first derivative at a chosen point R. To do that, it is useful to remember about the following points:

1. Since the matching problem uses the ratio $\left(\frac{du_l^{\rm I}(k,r)}{dr}|_{r=R}\right)/u_l^{\rm I}(k,r)$, the overall normalization of $u_l^{\rm I}(k,R)$ can be arbitrary.

2. The matching radius must lie well outside the range of the potential[12].

3. The solution must be regular at the origin, which forces one to take $u(r = 0) = 0$.

[10] To convince yourself of that, assume that U is a constant: in that case, Eq. (7.52) becomes a harmonic oscillator equation, $\ddot{u} + \omega^2 u = 0$, where ω is the frequency.

[11] This argument assumes $U(\rho)/k^2 < 1$, so that the solution remains oscillatory in the region contributing to the asymptotic phase shift.

[12] One can check this by testing whether increasing the matching radius substantially changes the outcome.

4. The $r = 0$ value of $\frac{du^{\mathrm{I}}(k,r)}{dr}$ can be an arbitrary number, for example 1, since it only affects the overall normalization which is irrelevant.

5. For numerical accuracy *and* stability, the step size ϵ should be small[13].

7.7 Partial wave expansion

We have shown that we can describe the spherical part of the wavefunction ψ with spherical harmonics and the radial part (in regions where the potential vanishes) with Bessel or Neumann functions or their close cousins, the Ricatti and Haenkel functions. Since these functions provide a complete and orthogonal set of functions in the 3D coordinate space, we can describe *any* wavefunction in the region where $U \approx 0$ by *expanding* it in this basis,

$$\psi_{klm}(\boldsymbol{r}) = \sum_{l=0}^{\infty} \sum_{m=-l}^{m=+l} C_{lm}(k) R_l(k,r) Y_{lm}(\theta,\phi) \ . \tag{7.53}$$

This is known as the *partial wave expansion*: the full wave is decomposed into contributions with definite angular momentum, each representing a "partial" spherical-wave component of the total motion. Then, one proceeds by solving the scattering problem for each l separately. The usefulness of this approach lays in two aspects: 1) It provides a well-defined framework to solve a scattering problem, and 2) It is of great benefit especially in cases in which one can argue that only few partial waves significantly contribute. For example, many low-energy considerations are concerned only with the $l = 0$, that is s-wave, contribution.

In the following, we will often consider problems involving plane waves. Notably, a plane wave is not a trivial object. Far from the realistic picture of a single straight trajectory with some transverse offset (giving it a specific angular momentum), a plane wave is a coherent superposition of infinitely many straight-line trajectories with all possible transverse offsets and, thus, no definite impact parameter and no definite angular momentum. However, it is still possible to *expand* a plane wave in terms of partial waves. For a plane wave traveling along the z axis we have

$$e^{i\boldsymbol{kr}} = e^{ikr\cos\theta} = \sum_{l} (2l+1) P_l(\cos\theta) i^l j_l(kr) \ , \tag{7.54}$$

where $P_l(\cos\theta)$ are Legendre polynomials. Thus, the partial-wave expansion reorganizes a plane wave into a sum of contributions which are products of radial and spherical waves of definite angular momentum, each of which may be associated semiclassically with an effective impact parameter $b \sim l/k$. Exact plane-wave propagation along a single direction is recovered after summing over all partial waves.

Lecture sources: This lecture is based mainly on Joachain [2] and Bertulani & Danielewicz [6].

[13] This also can be checked by decreasing the chosen value of ϵ to see whether this substantially changes the result.

Lecture 8

Partial wave expansion II

Prerequisites: Lectures 2, 5, 6, 7.
Guiding question: ***How much information can there be in a phase shift?***

8.1 Cross section

We would like to connect the expressions we got so far within the partial wave analysis (see Lecture 7) with the cross section, which is an experimentally measurable quantity. We begin by rewriting the asymptotic solution with a phase shift due to a potential $V(r)$, Eq. (7.49), as

$$\lim_{r\to\infty} u_l^{\rm II}(k,r) = \alpha_l' \left[\sin\left(kr - l\frac{\pi}{2} + \delta_l\right)\right] \tag{8.1}$$

$$= \frac{\alpha_l'}{2i}\left[e^{ikr}e^{-il\frac{\pi}{2}}e^{i\delta_l} - e^{-ikr}e^{il\frac{\pi}{2}}e^{-i\delta_l}\right] \tag{8.2}$$

$$= \frac{\alpha_l'}{2i}e^{-il\frac{\pi}{2}}e^{-i\delta_l}\left[e^{ikr}e^{2i\delta_l} - (-1)^l e^{-ikr}\right] \tag{8.3}$$

$$= \alpha_l''\left[S_l(k)e^{ikr} - (-1)^l e^{-ikr}\right] , \tag{8.4}$$

where in the second to last step we used the fact that $e^{il\pi} = \cos(l\pi) + i\sin(l\pi) = (-1)^l$, while in the last step we absorbed the constant factor $e^{-il\frac{\pi}{2}}e^{-i\sigma_l}$ into a new coefficient α_l'' as well as defined

$$S_l(k) \equiv e^{2i\delta_l(k)} , \tag{8.5}$$

known as the *S-matrix element*[1]. Using the partial wave expansion, Eq. (7.53), and invoking the azimuthal symmetry in scattering off a radial potential, we then rewrite the asymptotic solution as[2]

$$\psi_{\boldsymbol{k}}^{(+)} = \sum_{l=0}^{\infty} C_l P_l(\cos\theta)\frac{u_l(k,r)}{kr} \xrightarrow[r\to\infty]{} \sum_{l=0}^{\infty} C_l' P_l(\cos\theta)\frac{\left[S_l(k)e^{ikr} - (-1)^l e^{-ikr}\right]}{kr} , \tag{8.6}$$

where we absorbed the coefficient α_l'' into C_l'.

[1] We will address what an S-matrix is in Lecture 14. For now, you can think of $S_l(k)$ as simply a complex number.

[2] Note that from now on, we drop the "0" subscript on the momentum, $\boldsymbol{k}_0 \to \boldsymbol{k}$. Until now, this subscript highlighted the fact that $\boldsymbol{k}$ is the incident momentum and that, due to energy conservation, the same magnitude k characterizes the outgoing wave. However, now the subscript would create a potential for confusion, as many quantities in the following will labeled by $l = 0$ angular momentum quantum number.

We would like to compare the above asymptotic solution, expressed in terms of the scattering matrix elements $S_l(k)$, to the *ansatz* for the asymptotic solution that we postulated in Lecture 6, Eq. (6.16), repeated here for convenience with explicit k-dependence where applicable and acknowledging azimuthal symmetry,

$$\psi_{\boldsymbol{k}}^{(+)}(\boldsymbol{r}) \xrightarrow[r\to\infty]{} A(k)\left(e^{i\boldsymbol{kr}} + f(k,\theta)\frac{e^{ikr}}{r}\right) . \tag{8.7}$$

Using the partial wave expansion of a plane wave, Eq. (7.54), together with the asymptotic limit of the Bessel function[3],

$$\lim_{r\to\infty} j_l(kr) = \frac{\sin\left(kr - l\frac{\pi}{2}\right)}{kr} , \tag{8.8}$$

we can rewrite Eq. (8.7) as

$$\psi_{\boldsymbol{k}}^{(+)}(\boldsymbol{r}) \xrightarrow[r\to\infty]{} A(k)\left(\sum_{l=0}^{\infty}(2l+1)P_l(\cos\theta)i^l\frac{\sin\left(kr - l\frac{\pi}{2}\right)}{kr} + f(k,\theta)\frac{e^{ikr}}{r}\right) . \tag{8.9}$$

To compare the above function with the corresponding expression obtained through the partial wave analysis, Eq. (8.6), we need to express it in terms of incoming and outgoing spherical waves, e^{-ikr} and e^{ikr}, respectively. To this end, we can write

$$\psi_{\boldsymbol{k}}^{(+)}(\boldsymbol{r}) \xrightarrow[r\to\infty]{} A(k)\left[\sum_{l=0}^{\infty}(2l+1)P_l(\cos\theta)i^l\frac{e^{i\left(kr-l\frac{\pi}{2}\right)} - e^{-i\left(kr-l\frac{\pi}{2}\right)}}{2ikr} + f(k,\theta)\frac{e^{ikr}}{r}\right] \tag{8.10}$$

$$= A(k)\left[\sum_{l=0}^{\infty}(2l+1)P_l(\cos\theta)i^l e^{-il\frac{\pi}{2}}\frac{e^{ikr} - (-1)^l e^{-ikr}}{2ikr} + f(k,\theta)\frac{e^{ikr}}{r}\right] \tag{8.11}$$

$$= A(k)\left[\left(\frac{1}{2ik}\sum_{l=0}^{\infty}(2l+1)P_l(\cos\theta) + f(k,\theta)\right)\frac{e^{ikr}}{r} - \sum_{l=0}^{\infty}(2l+1)P_l(\cos\theta)\frac{(-1)^l e^{-ikr}}{2ikr}\right] , \tag{8.12}$$

where we used $i^l = \left(e^{i\frac{\pi}{2}}\right)^l$. For Eqs. (8.6) and (8.12) to represent the same function, the coefficients in front of e^{-ikr} and e^{ikr} must be equal. For e^{-ikr}, this yields

$$C_l' = \frac{A(k)(2l+1)}{2i} , \tag{8.13}$$

which can then be inserted into the equation matching the coefficients of e^{ikr},

$$A(k)\left(\frac{1}{2ik}\sum_{l=0}^{\infty}(2l+1)P_l(\cos\theta) + f(k,\theta)\right) = \sum_{l=0}^{\infty}\frac{A(k)(2l+1)}{2i}P_l(\cos\theta)\frac{S_l(k)}{k} . \tag{8.14}$$

It is then straightforward to solve for the scattering amplitude,

$$f(k,\theta) = \frac{1}{2ik}\sum_{l=0}^{\infty}(2l+1)P_l(\cos\theta)\left[S_l(k) - 1\right] , \tag{8.15}$$

[3]See the relationship between the Bessel and Ricatti-Bessel functions, Eq. (7.31), and the asymptotic limit of the Ricatti-Bessel functions, Eq. (7.37).

which, using the definition of the S-matrix element, Eq. (8.5), can also be rewritten as

$$f(k,\theta) = \frac{1}{2ik}\sum_{l=0}^{\infty}(2l+1)P_l(\cos\theta)\left[e^{2i\delta_l(k)}-1\right] \tag{8.16}$$

$$= \frac{1}{k}\sum_{l=0}^{\infty}(2l+1)P_l(\cos\theta)e^{i\delta_l(k)}\sin\delta_l(k)\ . \tag{8.17}$$

The elastic cross section[4] is then obtained from Eq. (6.68), repeated here for convenience,

$$\frac{d\sigma_{\rm el}(k,\Omega)}{d\Omega} = |f(k,\theta)|^2\ , \tag{8.18}$$

where we made explicit the dependence on the energy (or, equivalently, momentum) of the incident beam. Using the orthogonality of Legendre polynomials,

$$\int d(\cos\theta)\ P_l(\cos\theta)P_{l'}(\cos\theta) = \frac{2}{2l+1}\delta_{l,l'}\ , \tag{8.19}$$

and Eq. (8.15), we can obtain the partial wave expansion of the total elastic cross section,

$$\sigma_{\rm el} = 2\pi\int_{-1}^{1} d(\cos\theta)\ \frac{d\sigma_{\rm el}(k,\Omega)}{d\Omega} = \frac{\pi}{k^2}\sum_{l=0}^{\infty}(2l+1)\left|S_l(k)-1\right|^2 \tag{8.20}$$

$$= \frac{\pi}{k^2}\sum_{l=0}^{\infty}(2l+1)\Big[1+|S_l(k)|^2-2{\rm Re}\big[S_l(k)\big]\Big] = \frac{4\pi}{k^2}\sum_{l=0}^{\infty}(2l+1)\sin^2\delta_l(k)\ , \tag{8.21}$$

where we used the identity $\cos(2x) = 1-2\sin^2 x$. Comparing the expression for the scattering amplitude, Eq. (8.17), at $\theta = 0$ (where we can use $P_l(1) = 1$), and the total elastic cross section in the equation above, we can immediately see that one can write

$$\sigma_{\rm el} = \frac{4\pi}{k}{\rm Im}\big[f(k,0)\big]\ , \tag{8.22}$$

which is the optical theorem we already derived in Eq. (6.95). Note that while previously obtaining the optical theorem required considerable mental gymnastics, here we get it almost for free.

In-class Activity 8a: Hard-sphere scattering

The hard-core nuclear potential can be approximated by an infinitely repulsive square well,

$$V(r) = \begin{cases} +\infty\ , & r<R \quad \text{(region I)} \\ 0\ , & r>R \quad \text{(region II)} \end{cases} \tag{8.23}$$

For such a potential, the wavefunction vanishes for $r < R$, so that its continuity at the boundary requires that $u_l^{\rm II}(k,R) = 0$ (for an infinite potential, no continuity is imposed on the derivative $du_l^{\rm II}/dr$ because the Schrödinger equation is not valid at $r = R$ and therefore cannot be used to derive a matching condition for the derivative[a]). Find the total elastic scattering cross section for scattering off this hard-sphere potential for s-waves (that is, for $l = 0$) in the limit of very low energies.

[4] The derivation of an inelastic cross section within this approach is possible, but it would require introduction of a couple new concepts. We will defer it, therefore, to our discussion of formal scattering theory.

Solution

In region II, we use the asymptotic free solution,

$$\lim_{r\to\infty} u_l^{\rm II}(k,r) = \alpha_l\left[\hat{\jmath}_l(kr) - \tan\delta_l\ \hat{n}_l(kR)\right] \ , \tag{8.24}$$

see Eqs. (7.46) and (7.47). Demanding that $u_l^{\rm II}(k,R)=0$ leads to

$$\tan\delta_l = \frac{\hat{\jmath}_l(kR)}{\hat{n}_l(kR)} \ , \tag{8.25}$$

which for s-waves, given the $l=0$ Bessel and Neumann functions, Eqs. (7.29) and (7.30), is $\tan\delta_0 = -\sin(kR)/\cos(kR) = -\tan(kR)$, from which we immediately obtain

$$\delta_0 = -kR \ . \tag{8.26}$$

Discarding all contributions beyond $l=0$ in the equation connecting the cross section with the phase shifts, Eq. (8.21), we obtain the s-wave elastic cross section,

$$\sigma_{\rm el}^{(0)} = \frac{4\pi}{k^2}\sin^2(kR) \ . \tag{8.27}$$

In the limit of very low energies, we have $k\to 0$ and $\sin kR \approx kR$, yielding $\sigma_{\rm el}^{(0)} \approx 4\pi R^2$.

[a] This can be seen explicitly by considering the Schrödinger equation in 1D. We can always integrate the Schrödinger equation over a small interval around x_0,

$$-\frac{1}{2m}\int_{x_0-\epsilon}^{x_0+\epsilon} dx\ \psi''(x) + \int_{x_0-\epsilon}^{x_0+\epsilon} dx\ V(x)\psi(x) = E\int_{x_0-\epsilon}^{x_0+\epsilon} dx\ \psi(x) \ .$$

In particular, the first term gives $-\frac{1}{2m}\left[\psi'(x_0+\epsilon) - \psi'(x_0-\epsilon)\right]$. If we now take the limit $\epsilon\to 0$, then the right-hand side vanishes for any reasonably bounded (*i.e.*, not diverging) ψ, which leads us to the condition

$$\left[\psi'(x_0^+) - \psi'(x_0^-)\right] = 2m\lim_{\epsilon\to 0}\int_{x_0-\epsilon}^{x_0+\epsilon} dx\ V(x)\psi(x) \ ,$$

where $x_0^\pm = \lim_{\epsilon\to 0}(x_0\pm\epsilon)$. If $V(x)$ is finite, the right-hand side becomes zero in the limit and we obtain the condition for the continuity of the first derivative of the wavefunction, $\psi'(x_0^+) = \psi'(x_0^-)$. If, however, $V(x)$ is infinite, the expression on the right-hand side stops being meaningful (or, equivalently, the Schrödinger equation ceases to be well-defined) and, therefore, the continuity condition cannot be derived.

8.2 Integral representation

There is an alternative to obtaining the phase shifts from matching conditions ar $r=R$, Eq. (7.50). We can take the equation for $u_l(k,\rho)$ in the presence of a potential, Eq. (7.21), and multiply it by the Ricatti-Bessel function $\hat{\jmath}_l(\rho)$,

$$\hat{\jmath}_l(k,\rho)\frac{\partial^2 u_l(k,\rho)}{\partial\rho^2} + \hat{\jmath}_l(k,\rho)\left[1 - \frac{U(\rho)}{k^2} - \frac{l(l+1)}{\rho^2}\right]u_l(k,\rho) = 0 \ , \tag{8.28}$$

and at the same time we can take the Ricatti-Bessel equation, Eq. (7.24), and multiply it by $u_l(k,\rho)$,

$$u_l(k,\rho)\frac{\partial^2 \hat{\jmath}_l(k,\rho)}{\partial\rho^2} + u_l(k,\rho)\left[1 - \frac{l(l+1)}{\rho^2}\right]\hat{\jmath}(k,\rho) = 0 \ , \tag{8.29}$$

where in both equations we now reserve the symbol $u_l(k,\rho)$ for the wavefunction in the presence of a finite potential. Subtracting the second of the above equations from the first, we get

$$\hat{\jmath}_l(k,\rho)\frac{\partial^2 u_l(k,\rho)}{\partial\rho^2} - u_l(k,\rho)\frac{\partial^2 \hat{\jmath}_l(k,\rho)}{\partial\rho^2} = \hat{\jmath}_l(k,\rho)\frac{U(\rho)}{k^2}u_l(k,\rho) \ . \tag{8.30}$$

We then integrate both sides over ρ and apply integration by parts to the left-hand side to obtain

$$\left[\hat{\jmath}_l(k,\rho)\frac{\partial u_l(k,\rho)}{\partial\rho} - u_l(k,\rho)\frac{\partial \hat{\jmath}_l(k,\rho)}{\partial\rho}\right]_0^{+\infty} = \int_0^\infty d\rho\ \hat{\jmath}_l(k,\rho)\frac{U(\rho)}{k^2}u_l(k,\rho) \ . \tag{8.31}$$

Since we demand regularity at the origin, only the contribution from $\rho \to +\infty$ survives on the left-hand side. Thus, the radial function $u_l(k,\rho)$ becomes $u_l(k,\rho) \xrightarrow[r\to\infty]{} \sin\left(\rho - l\frac{\pi}{2} + \delta_l\right)$, Eq. (7.49), while, by Eq. (7.37), $\hat{\jmath}(k,\rho)$ approaches $\hat{\jmath} = \sin\left(\rho - l\frac{\pi}{2}\right)$. Then, using the identity $\sin(a-b) = \sin a\cos b - \cos a\sin b$, Eq. (8.31) becomes an integral equation for the phase shift δ_l,

$$\sin\delta_l = -\int_0^\infty d\rho\ \hat{\jmath}_l(k,\rho)\frac{U(\rho)}{k^2}u_l(k,\rho) \ . \tag{8.32}$$

The advantage of the above equation over the expression derived from the matching condition, Eq. (7.50), lies in the fact that it is amenable to approximations. Indeed, if we consider a weak potential such that $\frac{U(\rho)}{k^2} = \frac{V(\rho)}{E_k} \ll 1$ for any ρ, then we can assume that the radial function $u_l(k,\rho)$ is not much different from the Ricatti-Bessel function $\hat{\jmath}(k,\rho)$, so that we have[5]

$$\sin\delta_l \approx -\int_0^\infty d\rho\ \frac{U(\rho)}{k^2}\hat{\jmath}_l^2(k,\rho) = -\frac{2m}{k}\int_0^\infty dr\ r^2\ V(r) j_l^2(k,r) \ . \tag{8.33}$$

As we will see, this equation is very similar to the Born approximation which we will discuss soon. The above formula also confirms our analysis of the sign of δ_l from Sec. 7.5: an attractive potential gives rise to a positive δ_l, while a repulsive potential yields $\delta_l < 0$.

In-class Activity 8b: Proton-proton $^1S_0$-wave

Figure 8.1 shows the scattering phase shift for $^1S_0$ proton-proton scattering.

(a) What can you say about the proton-proton interaction based on the energy-dependence of the scattering phase shift?

(b) The quantity denoted by ρ or ϕ in the figure accounts for the inelastic channel in proton-proton scattering. What can be happening around 270 MeV?

Solution

(a) The figure shows that the elastic scattering phase shift for proton-proton s-wave scattering is positive for incident kinetic energies below about 250 MeV and negative for higher energies.

[5] If you want to think about this more rigorously, this is the way to do so: In the limit of $U \to 0$, the radial solution must smoothly become the Ricatti-Bessel function $\hat{\jmath}$. Conversely, for a small $U = \epsilon\tilde{U}(\rho)$, we can assume that the solution is equal to $\hat{\jmath}$ plus some perturbation, $u_l = \hat{\jmath} + \epsilon u_l$. Substituting this form into Eq. (8.32), we obtain

$$\sin\delta_l = -\epsilon\int_0^\infty d\rho\ \hat{\jmath}(k,\rho)\frac{\tilde{U}(\rho)}{k^2}u_l(k,\rho) - \epsilon^2\int_0^\infty d\rho\ u_l(k,\rho)\frac{\tilde{U}(\rho)}{k^2}u_l(k,\rho) \ .$$

If $\epsilon \ll 1$, then we only need to keep the first term, which is the same as Eq. (8.33).

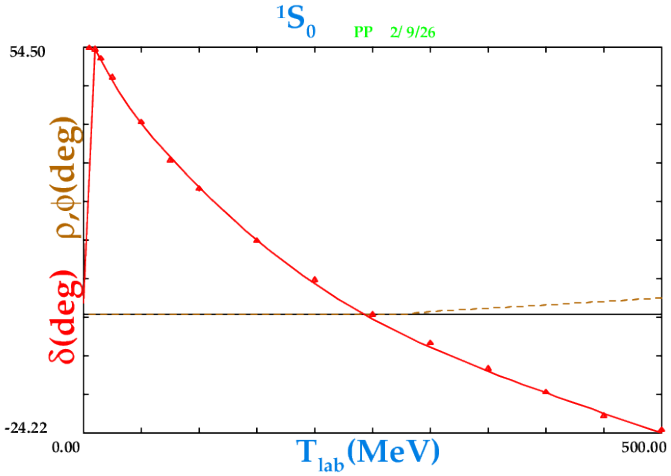

Figure 8.1: The scattering phase shift δ (in degrees) of the $^1S_0$-wave proton-proton scattering as a function of the lab kinetic energy (in MeV). Figure generated using the SAID Partial-Wave Analysis Facility operated by the INS Data Analysis Center, George Washington University [16].

According to Eq. (8.33), this indicates that the effective interaction in the $^1S_0$ channel is predominantly attractive at low energies and repulsive at higher energies. This behavior is consistent with what we know about the nuclear interaction, which exhibits a long-range attraction and a short-range repulsive core. At higher incident energies, the protons probe shorter distances which are increasingly more sensitive to the repulsive part of the interaction.

(b) As we know from Homework 1, Problem 4b, the kinematic threshold for single-pion production in proton-proton collisions, $pp \to pp\pi^0$, is around 290 MeV in the laboratory frame. This onset of a nonzero ρ (or ϕ) in Fig. 8.1 aligns pretty well with that calculation (which does not take into account, *e.g.*, sub-threshold effects, effectively inflating the kinematic threshold), and indeed: the brown dashed line in the figure measures the pion production channel of the proton-proton scattering.

8.3 Scattering length

For small scattering energies, only s-waves contribute appreciably to the scattering. This can be understood from two angles: First, from a classical perspective, the angular momentum l is related to the impact parameter through $l \sim bk$, so that $b \sim l/k$. For small k and any fixed l, we thus obtain a large impact parameter b, and since trajectories with large b barely probe the interaction region, they scatter weakly. In contrast, the $l = 0$ wave is the only one with $b \sim 0$, which means that it efficiently samples the short-range interaction. Second, we remember that the radial equation contains the centrifugal term, $l(l+1)/r^2$. For any $l > 0$, this term produces a "barrier" that prevents low-energy particles from reaching small r. However, since the s-wave ($l = 0$) experiences no centrifugal barrier, it is not suppressed.

From the definition, Eq. (7.50), the s-wave phase shift is given by

$$\tan\delta_0 = \frac{(kR)\hat{j}_0'(kR) - \mathcal{L}^{\rm I}\hat{j}_0(kR)}{(kR)\hat{n}_0'(kR) - \mathcal{L}^{\rm I}\hat{n}_0(kR)} = \frac{(kR)\cos(kR) - \mathcal{L}^{\rm I}\sin(kR)}{(kR)\sin(kR) + \mathcal{L}^{\rm I}\cos(kR)}\,, \tag{8.34}$$

where we substituted explicit forms of the Ricatti functions $\hat{j}_0$, $\hat{j}_0'$, $\hat{n}_0$, and $\hat{n}_0'$ using Eqs. (7.29), (7.30), and (7.31). To the first order in $k \to 0$, we have $\sin(kR) \approx kR$ and $\cos(kR) \approx 1$, so that (denoting the first-order contribution to $\mathcal{L}^{\mathrm{I}}$ as L) we have

$$\tan\delta_0 \approx kR\frac{1-L}{(kR)(kR)+L} \approx kR\left(\frac{1-L}{L}\right) . \tag{8.35}$$

We note that the expression on the right-hand side of the above equation has become very simple: it's basically a product of the wave number and something with a dimension of length. Since k is small, we can take $\tan\delta_0 \approx \delta_0$. Furthermore, we have seen in the In-class Activity 8a that the s-wave phase shift due to the scattering off a hard-sphere of radius R is $\delta_0 = -kR$, Eq. (8.26). With this intuition in mind, we define the *scattering length* as

$$a \equiv -\lim_{k\to 0}\left(\frac{\tan\delta_0}{k}\right) = R\left(\frac{L-1}{L}\right) . \tag{8.36}$$

In this way, we can interpret the scattering length as the radius of an "effective hard sphere" that would produce the same low-energy s-wave shift as the interaction in question. The minus sign is introduced in Eq. (8.36) so that $a > 0$ corresponds to repulsive interactions (like in the case of hard-sphere scattering); consequently, $a < 0$ will correspond to attractive interactions[6]. Then, using the partial wave expansion of the total elastic cross section, Eq. (8.21), we immediately obtain

$$\sigma_{\mathrm{el}}^{(0)} = \frac{4\pi}{k^2}\sin^2\left[\tan^{-1}(-ka)\right] = \frac{4\pi}{k^2}\frac{(ka)^2}{1+(ka)^2} \approx 4\pi a^2 , \tag{8.37}$$

where we have first used the identity $\sin^2(\tan^{-1}x) = x^2/(1+x^2)$ and then the fact that k is small.

The scattering amplitude, Eq. (8.17), in the low-energy limit can be well-approximated by

$$f^{(0)}(k) = \frac{1}{k}e^{i\delta_0(k)}\sin\delta_0(k) , \tag{8.38}$$

which can be rewritten as

$$f^{(0)} = \frac{1}{k}\frac{\sin\delta_0}{e^{-i\delta_0}} = \frac{1}{k}\frac{\sin\delta_0}{\cos\delta_0 - i\sin\delta_0} = \frac{1}{k\cot\delta_0 - ik} , \tag{8.39}$$

where we stopped to explicitly write the k-dependence for clarity. Then, using $\delta_0 = \tan^{-1}(-ka)$, we immediately get

$$f^{(0)} = \frac{1}{-\frac{1}{a} - ik} \approx -a + ia^2k , \tag{8.40}$$

which, together with the optical theorem, Eq. (6.95), once again yields $\sigma_{\mathrm{el}}^{(0)} \approx 4\pi a^2$.

Lecture sources: This lecture is based mainly on Joachain [2] and Bertulani & Danielewicz [6].

[6] In this case, a negative sign somewhat defies a clear-cut interpretation.

Lecture 9

Partial wave expansion III

Prerequisites: Lectures 7, 8.
Guiding question: ***What can phase shifts tell us about the analytic properties of solutions?***

9.1 Resonances

Ordinarily, phase shifts (and, therefore, cross sections) are slowly-varying functions of the incident energy (see, *e.g.*, Fig. 8.1) and of the strength of the potential. However, sometimes a phase shift can change rapidly for a given potential strength or energy range, which dramatically affects the corresponding cross section. When such dramatic behavior occurs, it is called a *resonance*. Often, the reason underlying a resonance is that the scattering system admits formation of a long-lived intermediate state whose energy matches the incoming energy, leading to an amplified response of the system. This response resembles the behavior of a driven oscillator, which resonates when the driving frequency matches its natural mode.

To illustrate how this behavior can arise, let us consider the asymptotic wavefunction written in terms of the S-matrix element, Eq. (8.4), repeated here for convenience,

$$\lim_{r\to\infty} u_l^{\rm II}(k,r) = \alpha_l''\Big[S_l(k)e^{ikr} - (-1)^l e^{-ikr}\Big] \ . \tag{9.1}$$

With this form, the equality of logarithmic derivatives for the l-th partial wave at $r = R$ is[1]

$$\mathcal{L}_l^{\rm I} = R\frac{ik\big[S_l e^{ikR} + (-1)^l e^{-ikR}\big]}{S_l e^{ikR} - (-1)^l e^{-ikR}} = -ikR\frac{(-1)^l + S_l e^{2ikR}}{(-1)^l - S_l e^{2ikR}} \ , \tag{9.2}$$

which we can solve for S_l,

$$S_l = (-1)^l e^{-2ikR}\frac{\mathcal{L}_l^{\rm I} + ikR}{\mathcal{L}_l^{\rm I} - ikR} \ . \tag{9.3}$$

We can always denote

$$A = \mathcal{L}^{\rm I} + ikR = |A|e^{i\phi_A} \quad \text{and} \quad B = \mathcal{L}^{\rm I} - ikR = |B|e^{i\phi_B} \ . \tag{9.4}$$

[1] Note that in principle, we should put a subscript l on the logarithmic derivative $\mathcal{L}$ to stress that it is calculated for a particular partial wave. This would unnecessarily clutter the notation going forward, so we will refrain from doing that. Therefore, one needs to simply remember that the following derivation at all times refers to a specific partial wave l.

Since by its definition, Eq. (8.5), we have $S_l = e^{2i\delta_l}$ and consequently $|S_l| = 1$, it follows by examining Eq. (9.3) that we must have $|A| = |B|$, which can only be the case if $\mathcal{L}^{\rm I}$ is real[2]. In that case we have

$$|A| = |B| = \sqrt{(\mathcal{L}^{\rm I})^2 + (kR)^2} \quad \text{and} \quad \phi_A = \tan^{-1}\left(\frac{{\rm Im}A}{{\rm Re}A}\right) = \tan^{-1}\left(\frac{kR}{\mathcal{L}^{\rm I}}\right) = -\phi_B \ . \tag{9.5}$$

With this, we can rewrite Eq. (9.3) as

$$S_l = e^{i\pi l} e^{-2ikR} e^{2i\phi_A} \ , \tag{9.6}$$

so that the phase shift, which we remember is related to the S_l element through Eq. (8.5), can be written as a sum of three components,

$$\delta_l = l\frac{\pi}{2} + (-kR) + \tan^{-1}\left(\frac{kR}{\mathcal{L}^{\rm I}}\right) \ . \tag{9.7}$$

The combination $\delta_{\rm bg} = l\frac{\pi}{2} + (-kR)$ is the hard-sphere "background phase" associated with choosing the boundary at R and measuring phase relative to outgoing/incoming waves at that point; it is entirely independent of the underlying potential. The third contribution, $\delta_R \equiv \tan^{-1}\left(kR/\mathcal{L}^{\rm I}\right)$, depends on the potential U through $\mathcal{L}^{\rm I}$. From the definition, Eq. (7.43), we have

$$\mathcal{L}^{\rm I} = R\frac{\frac{du_l^{\rm I}(k,r)}{dr}\big|_{r=R}}{u_l^{\rm I}(k,R)} \ . \tag{9.8}$$

The functions $u_l(kR)$ are likely to have some oscillatory properties, in which case so do their derivatives. If this is indeed the case, then, since $k = k(E)$, there exist energies E_R such that the logarithmic derivative is close to zero at the boundary. We can then expand $\mathcal{L}^{\rm I}$ around such an E_R,

$$\mathcal{L}^{\rm I}(E) \approx 0 + (E - E_R)\left(\frac{d\mathcal{L}^{\rm I}}{dE}\right)_{E=E_R} + \mathcal{O}\big((E-E_R)^2\big) \ . \tag{9.9}$$

Denoting[3]

$$a = \left(\frac{d\mathcal{L}^{\rm I}}{dE}\right)_{E=E_R} \ , \tag{9.10}$$

we can then write to the first order in $(E - E_R)$

$$\delta_R \approx \tan^{-1}\left(\frac{kR}{a(E-E_R)}\right) \ . \tag{9.11}$$

Clearly, when $E \to E_R$, the argument of the $\tan^{-1}$ blows up, so that $\delta_R \to \frac{\pi}{2}$. When this happens, the entire phase shift δ_l, Eq. (9.7), is often dominated by the δ_R contribution. If this is the case, then the contribution from the l-th partial wave to the total elastic cross section, given in terms of phase shifts in Eq. (8.21), approaches its maximal possible value of $4\pi(2l+1)/k^2$. In other words,

[2] This is true only for purely elastic scattering. In any other situation, the definition of S_l is generalized to include the possibility that $|S_l| < 1$ and $\mathcal{L}^{\rm I}$ becomes complex. The derivation of resonant behavior for non-elastic processes will be addressed in Lecture 16.

[3] Note: this is *not* the scattering length, which we previously defined using the same letter. There are only so many letters...

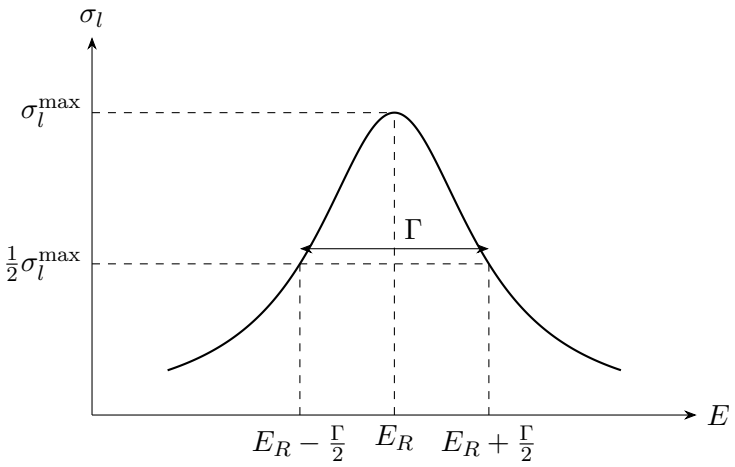

Figure 9.1: Breit-Wigner (Lorentzian) resonance peak centered on E_R, with the full width at half maximum equal Γ.

if a resonance dominates the total phase shift so that $\delta_l \approx \pi/2$ at E_R, the cross section shows a dramatic increase and even saturation around E_R.

We can further rewrite the final result by defining

$$\frac{\Gamma}{2} \equiv -\frac{kR}{a} \ , \tag{9.12}$$

so that the potential-dependent part of the phase shift, Eq. (9.11), becomes

$$\delta_R = -\tan^{-1}\left(\frac{\Gamma/2}{E - E_R}\right) . \tag{9.13}$$

We note that the minus sign comes into Eq. (9.12) because one can rigorously show that $a < 0$ (see Problem 6 in Homework 2). Since Γ is to be understood as a distribution width, we need $\Gamma > 0$. Note also that with this choice, an additional minus sign is also needed in Eq. (9.13). One can verify that this minus sign leads to the correct behavior of δ_R: If one approaches E_R from below, then $E - E_R < 0$ and the overall minus sign ensures that $\delta_R \to +\frac{\pi}{2}$.

With this, assuming that δ_R dwarfs the other two contributions to the total scattering phase shift δ_l and using the fact that $\sin\left(\tan^{-1} x\right) = x/\sqrt{1+x^2}$, the contribution to the cross section due to the l-th partial wave becomes

$$\sigma_l = \frac{4\pi(2l+1)}{k^2}\sin^2\delta_l \approx \frac{4\pi(2l+1)}{k^2}\frac{(\Gamma/2)^2}{(E-E_R)^2 + (\Gamma/2)^2} \ , \tag{9.14}$$

which has the well-known Breit-Wigner form. This form (also known as the Lorentz or Cauchy distribution) allows us to see that Γ plays the role of the full width at half maximum[4], that is, it sets the characteristic energy scale over which the resonance varies. In other words, while E_R provides the location of the peak, Γ gives the range of energies over which this peak extends, see Fig. 9.1.

Once more (see Footnote 1) we note that to be precise, the above derivation should have included subscripts l to stress that the results are obtained for a specific term in the partial wave expansion.

[4]If you're not familiar with these distributions, you can see this by making an explicit check: we have $\delta_R(E = E_R) = \tan^{-1}(\infty) = \pi/2$, while $\delta_R(E = E_R \pm \frac{\Gamma}{2}) = \tan^{-1}(\pm 1) = \pm\pi/4$, *i.e.*, the phase changes by half of its resonant value when E changes by $\pm\Gamma/2$ on either side.

In particular, the energy of the resonance E_R and the resonance width Γ should be understood as referring to a particular partial wave l.

Near the resonance, using Eqs. (9.9), (9.10), and (9.12), we can rewrite the S-matrix element, Eq. (9.3), as

$$S_l \approx (-1)^l e^{-2ikR} \frac{(E - E_R) - i\frac{\Gamma}{2}}{(E - E_R) + i\frac{\Gamma}{2}} \ . \tag{9.15}$$

The denominator vanishes at $E = E_R - i\frac{\Gamma}{2}$. This pole of the S-matrix element conveys important information: recall that for a stationary state the time-dependent amplitude behaves like

$$e^{-iEt} = e^{-iE_R t} e^{-\Gamma t/2} \ . \tag{9.16}$$

This corresponds to an exponential decay with lifetime

$$\tau = \Gamma^{-1} \ . \tag{9.17}$$

This is why "broad resonances" (*i.e.*, those characterized by large values of Γ) have short lifetimes, while the opposite is true for narrow resonances. This also explains why "long-lived intermediate states" lead to an amplified response of the system (that is, pronounced resonances), as we have stated in the beginning of this section: such states correspond to small values of Γ, and the smaller Γ is, the more rapid is the approach of the phase shift to $\pi/2$ – or, equivalently, the divergence of the argument of $\tan^{-1}$ in Eq. (9.13) – as $E \to E_R$.

9.2 Canonical elastic scattering resonance: deep square well

Let us consider a scattering problem with a deep square-well potential,

$$V(r) = \begin{cases} -V_0 & \text{for } r < r_0 \ , \\ 0 & \text{for } r > r_0 \ , \end{cases} \tag{9.18}$$

where $V_0 > 0$. Let us also assume that the potential is deep, $|V_0| \gg E$ and $V_0 \gg l(l+1)/(2\mu r_0^2)$. We will endeavor to calculate the scattering phase shift and discuss its behavior depending on the values of the incident energy and the behavior of the logarithmic derivative $\mathcal{L}^I$ as a function of energy.

To this end, let us denote the region where $r < r_0$ as "region I." The Schrödinger equation for this problem, after the separation of variables, can be reduced to the radial equation, Eq. (7.22),

$$\frac{\partial^2}{\partial r^2} u_l^{\mathrm{I}}(k,r) + \left[k^2 + U_0 - \frac{l(l+1)}{r^2} \right] u_l^{\mathrm{I}}(k,r) = 0 \ , \tag{9.19}$$

where $U_0 \equiv 2\mu V_0$. Denoting $K^2 \equiv k^2 + U_0$, we can also write it as

$$\frac{\partial^2}{\partial r^2} u_l^{\mathrm{I}}(k,r) + \left[K^2 - \frac{l(l+1)}{r^2} \right] u_l^{\mathrm{I}}(k,r) = 0 \ , \tag{9.20}$$

This looks just like a free Ricatti-Bessel equation, Eq. (7.24), and so the solution is the free Ricatti-Bessel function, Eq. (7.31), with $\rho = Kr$,

$$u_l^I(K,r) = A\hat{\jmath}(Kr) \ , \tag{9.21}$$

where we discarded the Ricatti-Neumann function in region I because the solution must be regular at the origin.

For $r > R$, denoted as "region II," the Schrödinger equation describes a free particle and the general solution is

$$u_l^{II}(k,r) = B\Big[\hat{\jmath}_l(kr) - \tan\delta_l \hat{n}(kr)\Big] \ . \tag{9.22}$$

9.2.1 Asymptotic behavior

We will want to match the logarithmic derivative of $u_l^{\rm I}(K,r)$ to the free solution $u_l^{\rm II}(k,r)$ at $r = r_0$. Since $U_0 \gg l(l+1)/r_0^2$, it means that the potential overpowers the angular momentum contribution at $r = r_0$. Consequently, we can approximate the exact solution, Eq. (9.21), by the asymptotic form of the Ricatti-Bessel function[5], Eq. (7.37),

$$u_l^{\rm I}(K,r) \approx \sin\left(Kr - l\frac{\pi}{2}\right) \ . \tag{9.23}$$

Note what this means: near the boundary of the potential well, the solution looks like a *standing wave*. To see this, let us recall that

$$\sin\left(Kr - l\frac{\pi}{2}\right) = \frac{e^{i\left(Kr - l\frac{\pi}{2}\right)} - e^{-i\left(Kr - l\frac{\pi}{2}\right)}}{2i} \ . \tag{9.24}$$

As we have shown in Problem 2, this is a superposition of an outgoing and incoming wave with equal amplitudes. This corresponds to zero net radial flux as well as nodes and antinodes that do not propagate in space. which is the operational definition of a standing wave. Thus, a deep potential well naturally produces an interior wave that is nearly[6] a standing wave, which can be visualized as the boundary reflecting the outgoing flux back into the well[7].

We can now use Eq. (9.23) to compute

$$\mathcal{L}^{\rm I} \approx \frac{r_0}{u_l^{\rm I}(Kr_0)} \frac{du_l^{\rm I}(Kr)}{dr}\bigg|_{r=r_0} = Kr_0 \cot\left(Kr_0 - l\frac{\pi}{2}\right) \ . \tag{9.25}$$

Because $\mathcal{L}^{\rm I}$ is proportional to a cotangent, it can take on wildly different values: it becomes zero whenever the argument satisfies $Kr_0 - l\frac{\pi}{2} \approx \left(n + \frac{1}{2}\right)\pi$, while it diverges for $Kr_0 - l\frac{\pi}{2} \approx n\pi$.

9.2.2 Analysis of $l = 0$ solutions

To analyze the consequences of the matching condition, Eq. (9.25), let us first consider the case for $l = 0$. At $r = r_0$, the logarithmic derivatives must match. Since in region II we can write $u_0^{\rm II}(r) \approx kr + \delta_0$), we immediately get

$$K\cot(Kr_0) = k\cot(kr_0 + \delta_0) \ , \tag{9.26}$$

[5] Another way of seeing why we can do this is noticing that Kr, which enters the argument of the Ricatti-Bessel function, is large at $r = r_0$, which allows us to invoke the asymptotic form of the function.

[6] Only "nearly" because matching to the exterior scattering solution generally introduces a small imbalance between incoming and outgoing amplitudes.

[7] Note that here we don't say *why* the boundary reflects the flux – we just conclude, based on the form of the function, that it does.

which is equivalent to

$$\tan(kr_0 + \delta_0) = \frac{k}{K}\tan(Kr_0) \ , \tag{9.27}$$

so that

$$\delta_0(E) = -kr_0 + \tan^{-1}\left(\frac{k}{K}\tan(Kr_0)\right) \ . \tag{9.28}$$

Given that $K \gg k$, we have $\frac{k}{K} \ll 1$ and *most of the time* we have

$$\delta_0 \approx -kr_0 \quad \text{(modulo } \pi) \ . \tag{9.29}$$

However, it is also possible that energy and distance combine in such a way that $\tan(Kr_0)$ is huge, which is when $Kr_0 \approx \left(n + \frac{1}{2}\right)\pi$, and then

$$\delta_0 \to -kr_0 + \frac{\pi}{2} \quad \text{(modulo } \pi) \ . \tag{9.30}$$

Using the partial wave expansion of the elastic cross section, Eq. (8.21), we can see that the s-wave cross section,

$$\sigma_0 = \frac{4\pi}{k^2}\sin^2\delta_0(k) \ , \tag{9.31}$$

is maximum when $\delta_0(k) \to \frac{\pi}{2}$. This is bound to happen if we have a diverging $\tan(Kr_0)$, even if there might be a slight offset from the value of the energy corresponding to $Kr_0 \approx \left(n + \frac{1}{2}\right)\pi$ since there is also a finite (if small) contribution to the phase shift from $-kr_0$.

9.2.3 Analysis of $l > 0$ solutions

Now let us consider $l \neq 0$. For this case, the scattering phase shift is given by Eq. (7.50), which in our case becomes

$$\delta_l = \tan^{-1}\left[\frac{kr_0\hat{\jmath}_l'(kr_0) - \mathcal{L}^{\rm I}\hat{\jmath}_l(kr_0)}{kr_0\hat{n}_l'(kr_0) - \mathcal{L}^{\rm I}\hat{n}_l(kr_0)}\right] \ . \tag{9.32}$$

For $l > 0$ and $kr_0 \ll 1$ (*i.e.*, for very low energies), the Ricatti-Bessel functions behave as

$$\hat{\jmath}_l(x) \sim \frac{x^{l+1}}{(2l+1)!!} \quad \text{and} \quad \hat{n}_l(x) \sim -\frac{(2l-1)!!}{x^l} \ . \tag{9.33}$$

Assuming the above forms, we see that

$$\tan\delta_l = \left[\frac{kr_0\frac{(l+1)(kr_0)^l}{(2l+1)!!} - \mathcal{L}^{\rm I}\frac{(kr_0)^{l+1}}{(2l+1)!!}}{kr_0 l\frac{(2l-1)!!}{(kr_0)^{l+1}} + \mathcal{L}^{\rm I}\frac{(2l-1)!!}{(kr_0)^l}}\right] = \left[\frac{\frac{(kr_0)^{l+1}}{(2l+1)!!}\Big(l+1-\mathcal{L}^{\rm I}\Big)}{\frac{(2l-1)!!}{(kr_0)^l}\Big(l+\mathcal{L}^{\rm I}\Big)}\right] \propto (kr_0)^{2l+1} \ . \tag{9.34}$$

Since $kr_0 \ll 1$, the right-hand side is small and so we can approximate $\tan\delta_l \approx \delta_l$, which yields

$$\delta_l \propto (kr_0)^{2l+1} \ . \tag{9.35}$$

Once again, we see that higher-order partial waves (*i.e.*, those with large l) are strongly suppressed at low energy. An exception will occur, however, if the denominator in Eq. (9.32) is near zero,

$$kr_0\hat{n}_l'(kr_0) - Kr_0 \cot\left(Kr_0 - l\frac{\pi}{2}\right)\hat{n}_l(kr_0) \approx 0 \ , \tag{9.36}$$

or equivalently

$$kr_0\hat{n}_l'(kr_0) = Kr_0 \cot\left(Kr_0 - l\frac{\pi}{2}\right)\hat{n}_l(kr_0) \ , \tag{9.37}$$

where we inserted the form of the matching logarithmic derivative from Eq. (9.25). Using Eq. (9.33) once again, this leads to

$$\cot\left(Kr_0 - l\frac{\pi}{2}\right) = -\frac{l}{Kr_0} \ . \tag{9.38}$$

Since $Kr_0 \gg 1$, the right-hand side is nearly zero. This gives us a condition for the argument of the cotangent,

$$Kr_0 - l\frac{\pi}{2} = \left(n + \frac{1}{2}\right)\pi \quad \Rightarrow \quad Kr_0 = \left(n + \frac{l+1}{2}\right)\pi \ . \tag{9.39}$$

The above equation is again precisely the condition for the interior solution to be a standing wave with antinodes at the boundary of the potential well[8]. Thus, the scattering phase shift approaches $\pi/2$ whenever the incident energy is such that the solution is a (nearly) standing wave with an antinode at the boundary of the potential well.

9.2.4 How can we have resonances in scattering processes?

This example allows us to build some intuition about resonances: In the solvable case of a deep attractive potential, resonant behavior occurs whenever the combination of the energy (k) and the size of the well (r_0) is such that the internal solution to the scattering problem has an antinode at the boundary. This situation is analogous to a standing wave in an open-ended pipe: the wave reflects strongly but *not perfectly* from the boundary, so that a *nearly* standing pattern forms. Intuitively, a solution that is close to a standing wave tends to remain in the interior region for a relatively long time. The wave repeatedly reflects inside the potential before eventually leaking out. In this sense, resonances correspond to *quasi-bound states*[9].

Why is an occurrence of an antinode at the boundary so important? This can be clearly seen in Fig. 9.2. First, let us note that a large K means that the wavefunction in region I is characterized by a short wavelength, so that it undergoes a full oscillation over a short distance. Conversely, a small k corresponds to a large wavelength, which means that the wavefunction undulates over large distances. Because k is small and the wavefunction in region II varies slowly, the slope of u_l^{II} attains

[8] To see that an antinode occurs at $r = r_0$, insert the resonance condition, Eq. (9.39), into the asymptotic solution, Eq. (9.23).

[9] What is the difference between true bound states and quasi-bound states? The energy of a true bound state is below the continuum threshold ($E < 0$). In that case, the wave function decays exponentially outside the potential, so the particle remains localized indefinitely. A quasi-bound state, on the other hand, has positive energy ($E > 0$) even though it is "bound" by the potential to some region. Because there exist solutions with $E > 0$ outside the potential barrier, the solution can *tunnel* through the barrier to become a scattering state, which allows the probability flux to propagate to infinity. In other words, all states below $E = 0$ are strictly bound because there is nowhere to tunnel to if your energy is negative, $E < 0$. But if $E \geq 0$, there are infinitely many possibilities. You may still have to go through a potential barrier, but that is fine – you can tunnel to freedom.

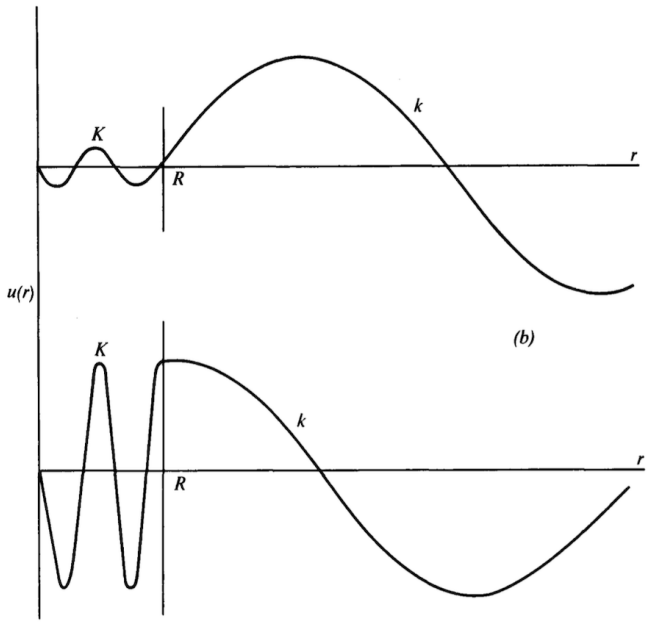

Figure 9.2: Illustration of the relationship between the slope at the boundary and the amplitude of the wavefunction in region I (see text for more details). Figure from Ref. [17].

only moderate values. This has profound consequences since both the value and slope of u_l^{II} at $r = R$ must be matched by u_l^{I}, and a moderate slope combined with a short wavelength in region I mean that for most values of k, u_l^{I} never develops a large amplitude. Since the amplitude of a wavefunction moderates the associated probability density, this means that the relative probability (as compared to outside of that region) of the wavefunction in region I is small. The one exception is when the slope at $r = R$ is near zero: this means that the wavefunctions on both sides are near an extremum (*i.e.*, a maximal amplitude), which allows the wave in region I to have *both* a large oscillation rate and a large magnitude. Now that we have a standing wave with a large amplitude in region I, the total share of probability density corresponding to that state is large – and since being in region I is synonymous with interacting, this directly translates into a large cross section.

In-class Activity 9a: n + α scattering

Figure 9.3 shows the scattering phase shifts extracted from cross section measurements for scattering of neutrons off α particles [18]. What can you say based on these results?

Solution

The results are reported for partial waves labeled in the spectroscopic notation as X_j, where $\mathrm{X} = \{\mathrm{S}, \mathrm{P}, \mathrm{D}, \dots\}$ correspond to $l = \{0, 1, 2, \dots\}$ orbital angular momentum states and j is the magnitude of the total angular momentum $\boldsymbol{j} = \boldsymbol{l} + \boldsymbol{s}$. In the α(n,n)α reaction, the α particle has zero spin, while the neutron carries half-integer spin. Thus, for $l = 1$ there are two possible values of j: $j = 1/2$ and $j = 3/2$, for $l = 2$ we can have $j = 3/2$ and $j = 5/2$, and so forth.
First, the presented data suggests that only the first two partial waves, $l = 0$ and $l = 1$, substantially contribute to the cross section. This is evident if we look at the absolute values of the extracted phase shifts and recall that the contribution to the cross section from a given partial wave is proportional to $\sin^2 \delta_l$, Eq. (8.21). For $\delta_l \ll 1$, we can approximate $\sin \delta_l \approx \delta_l$,

so that we can see that contributions from small δ_l are suppressed as δ_l^2.
We can argue this case more quantitatively. The centrifugal term in the Schrödinger equation is $l(l+1)/(2\mu r^2)$. One can estimate the effects due to the centrifugal barrier by evaluating it at some relevant length scale, which for us is set by the nuclear radius. We can calculate that the reduced mass μ in the n+α system is (using the fact that 1 u $\approx$ 931.5 MeV) $\mu = 745$ MeV, and since the radius of an α particle is on the order of 1.5 fm while the size of the neutron is about 1 fm, let us take $R \sim 3$ fm to be on the safe side (we can hardly expect the nuclei to "touch" at these energies). Then, using the conversion factor $\hbar c = 197$ MeV fm (from the Particle Data Group [15]) so that 1 fm = (1/197) MeV^{-1}, the centrifugal barrier for this system is $V_{\rm cent}^{(l)} \approx l(l+1) \times 2.9$ MeV. With $V_{\rm cent}^{(1)} \approx 5.8$ MeV, $V_{\rm cent}^{(2)} \approx 17.4$ MeV, $V_{\rm cent}^{(3)} \approx 34.8$ MeV, we see that $n + \alpha$ scattering at incident energies ≤ 10 MeV is suppressed for $l \geq 2$.
Next, basing our intuition on the integral equation for the phase shift δ_l in the limit of weak interactions, Eq. 8.33, we can say that the $l = 0$ channel in this reaction is repulsive (since $\delta_0 < 0$), while the $l = 1$ channel is attractive ($\delta_1 > 0$). (One should refrain from making statements about the D channel which exhibits large the error bars.) Does that make sense?

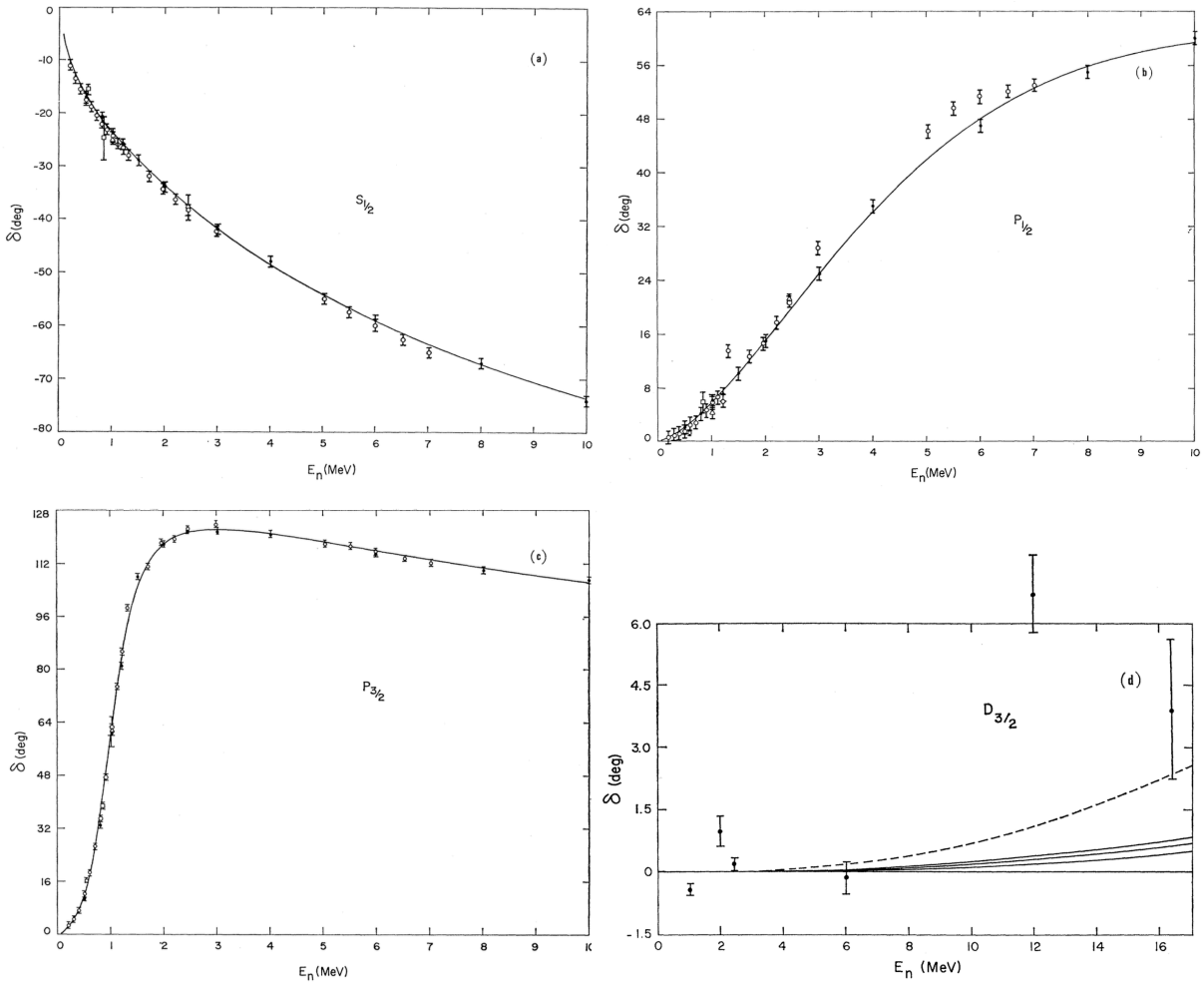

Figure 9.3: Phase shifts for scattering of neutrons off α particles, as extracted by Ref. [18].

In the In-Class Activity 8b we saw that for the s-wave p+p elastic scattering the nuclear interaction is attractive. Why then does the s-wave look repulsive here? The resolution lies in antisymmetrization. When a neutron scatters from the α, the total many-body wavefunction must be antisymmetric under exchange of identical nucleons. The α particle is a composite, closed-shell system in which both protons and neutrons occupy the $0s$ orbital. For an incoming neutron in an s-wave, there is a strong overlap with the occupied $0s$ neutron states inside the α. Antisymmetrization then suppresses the interior amplitude of the scattering wavefunction. This is a consequence of the Pauli principle restricting the allowed Hilbert space which, in an effective single-channel description, manifests itself as a negative phase shift, *i.e.*, an effective repulsion. Finally, the $l = 1, j = 3/2$ ($P_{3/2}$) channel shows a resonance: the scattering phase shift goes through $\pi/2$ as a function of energy, which will produce a peak in the scattering cross section. We can see that the $\delta_{l=1,j=3/2}$ crosses $\pi/2$ around $E_n \approx 1.25$ MeV, and indeed, the n + α scattering cross section shows a peak around that value, see Fig. 9.4.

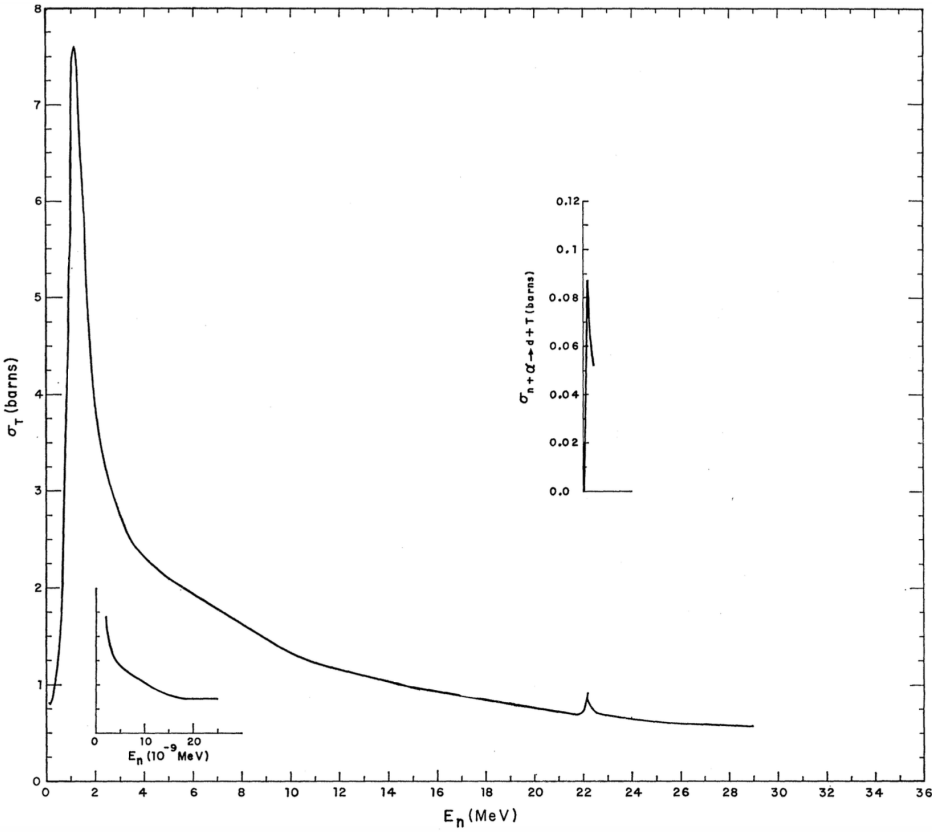

Figure 9.4: Elastic cross section for scattering of neutrons off α particles, as reported by Ref. [18].

9.3 Discussion

From a mathematical perspective, resonances reflect nontrivial features in the analytic structure of the scattering solutions. The rapid variation of the phase shift – and the associated maximum of the cross section – occurs because the logarithmic derivative $\mathcal{L}^{\mathrm{I}}(E)$ passes through zero as a function of energy. Expanding the solutions around that energy leads to a continuation of the solutions to

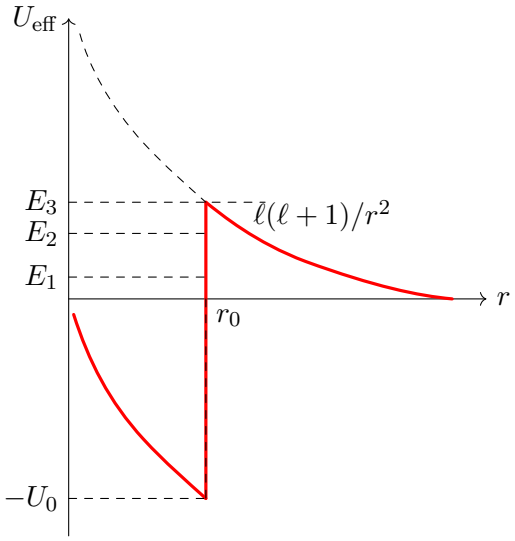

Figure 9.5: A sketch of the condition for shape resonances. The solid line marks the effective potential arising from the combined effects of a deep square well and the centrifugal barrier. States with negative energies (not depicted) are trapped in the potential well indefinitely. Projectiles with energies E_1 and E_2 may tunnel through the centrifugal barrier and then become trapped behind it, but since their energies are positive, they will eventually tunnel out. Projectiles with energies equal or larger than E_3 will not become trapped.

a complex energy, $E = E_\lambda - i\frac{\Gamma}{2}$, where the real part determines the resonance position while the imaginary part sets the width (and, therefore, the lifetime) of the intermediate state.

Intuitively, resonances occur when one of the following happens: either the projectile and target form an intermediate unstable state or the projectile is temporarily trapped by a potential barrier (without forming an intermediate state). The first case is referred to as a *compound nucleus resonances*, while the other type are *shape resonances*. A typical situation for the latter is that of an attractive potential and a centrifugal barrier, where the wave can be temporarily trapped in the potential well, see Fig. 9.5. This type of resonance does not require forming a compound state and describes many low-energy nuclear p-wave resonances, including the above $n + \alpha \to n + \alpha$ reaction.

How do we know that the resonances seen in $n + \alpha$ scattering are not compound-nucleus resonances? The evidence comes from the small number of decay channels and strong partial-wave sensitivity. A compound nucleus can often decay in several ways, including by a γ-ray emission, in addition to disintegrating into the nuclei that formed it. Compound resonances also typically appear in many l-channels, whereas in $n + \alpha$ scattering the resonance occurs only for p-waves. Finally, the observed resonance width, $\Gamma \sim 0.6$ MeV (see Fig. 9.4), is rather large, indicating a short lifetime characteristic of barrier-penetration states rather than long-lived compound nuclei. Compound nucleus formation will be introduced in Lecture 15.

Lecture sources: This lecture is somewhat based on Bertulani & Danielewicz [6], but deviates in how the resonance energy and width are introduced; treatments of Joachain [2] and Messiah [3] were also used.

Lecture 10

Quantum Coulomb scattering

Prerequisites: Lectures 5, 6, 7, 8.
Guiding question: ***How many special functions enter the exact solution of a quantum-mechanical Coulomb problem?***

10.1 Derivation of wavefunctions in the presence of a Coulomb-like potential

You don't need to read this if you are not haunted by the need to know how the solutions to the Coulomb problem arise. If all you need to know is how to use this stuff, consider yourself lucky and go straight to Sec. 10.3.

In a Coulomb-like problem, we are considering the Schrödinger equation

$$\left[-\frac{\nabla^2}{2m}+\frac{V_0}{r}\right]\psi(\boldsymbol{r})=E\psi(\boldsymbol{r})\ , \tag{10.1}$$

or equivalently

$$\left[\nabla^2+2mE-\frac{U_0}{r}\right]\psi(\boldsymbol{r})=0\ , \tag{10.2}$$

where $U_0=2mV_0$ is a constant. We are of course dealing with a spherically-symmetric potential, which is the starting point of Lecture 7. We could then proceed to express everything in spherical coordinates, as we did there. However, Coulomb-like potentials are amenable to another change and separation of variables: that using parabolic coordinates.

The parabolic coordinates are defined as

$$\xi=r+z\ ,\qquad \lambda=r-z\ ,\qquad \phi=\tan^{-1}(y/x)\ , \tag{10.3}$$

where $r=\sqrt{x^2+y^2+z^2}$. One can see that

$$r=\frac{\xi+\lambda}{2}\qquad\text{and}\qquad z=\frac{\xi-\lambda}{2}\ , \tag{10.4}$$

which together with $y=x\tan\phi$ leads to

$$\left(\frac{\xi+\lambda}{2}\right)^2=x^2+x^2\tan^2\phi+\left(\frac{\xi-\lambda}{2}\right)^2\ , \tag{10.5}$$

yielding, when solved for x,

$$x = \sqrt{\xi\lambda}\cos\phi \quad \text{and} \quad y = \sqrt{\xi\lambda}\sin\phi \ . \tag{10.6}$$

Finally, the Laplacian in parabolic coordinates is given by

$$\nabla^2 = \frac{4}{\xi+\lambda}\left[\frac{\partial}{\partial\xi}\left(\xi\frac{\partial}{\partial\xi}\right) + \frac{\partial}{\partial\lambda}\left(\lambda\frac{\partial}{\partial\lambda}\right)\right] + \frac{1}{\xi\lambda}\frac{\partial^2}{\partial\phi^2} \ . \tag{10.7}$$

With this, the Schrödinger equation for a Coulomb-like potential, Eq. (10.2), can be written as

$$\frac{4}{\xi+\lambda}\left[\frac{\partial}{\partial\xi}\left(\xi\frac{\partial}{\partial\xi}\right) + \frac{\partial}{\partial\lambda}\left(\lambda\frac{\partial}{\partial\lambda}\right)\right]\psi(\xi,\lambda) + \left[k^2 - \frac{2U_0}{\xi+\lambda}\right]\psi(\xi,\lambda) = 0 \ , \tag{10.8}$$

where we immediately used the fact that the problem is axially-symmetric, so that the solution does not depend on ϕ. We can then postulate that the solution is given by a product

$$\psi(\xi,\lambda) = f_1(\xi)f_2(\lambda) \ , \tag{10.9}$$

which by plugging into the Schrödinger equation in parabolic coordinates, Eq. (10.8), and multiplying the result by $(\xi+\lambda)/(4f_1f_2)$ leads to

$$\frac{1}{f_1(\xi)}\left[\frac{\partial}{\partial\xi}\left(\xi\frac{\partial}{\partial\xi}\right)\right]f_1(\xi) + \frac{1}{f_2(\lambda)}\left[\frac{\partial}{\partial\lambda}\left(\lambda\frac{\partial}{\partial\lambda}\right)\right]f_2(\lambda) + \left[\frac{k^2}{4}(\xi+\lambda) - \frac{U_0}{2}\right] = 0 \ . \tag{10.10}$$

The above equation can be separated into two equations

$$\frac{\partial}{\partial\xi}\left(\xi\frac{\partial}{\partial\xi}\right)f_1(\xi) + \left[\frac{k^2}{4}\xi - \beta_1\frac{U_0}{2}\right]f_1(\xi) = 0 \ , \tag{10.11}$$

$$\frac{\partial}{\partial\lambda}\left(\lambda\frac{\partial}{\partial\lambda}\right)f_2(\lambda) + \left[\frac{k^2}{4}\lambda - \beta_2\frac{U_0}{2}\right]f_2(\lambda) = 0 \ , \tag{10.12}$$

where $\beta_1 + \beta_2 = 1$.

These equations, by construction, describe the entire Coulomb-like problem. In particular, then, the solutions for $z \ll 0$ should look *somewhat*[1] like incoming plane waves,

$$\psi \propto e^{ikz} \quad \text{for} \quad -\infty < z < 0 \ , \ r \to +\infty \ . \tag{10.13}$$

In parabolic coordinates, such a function looks like

$$\psi \propto e^{ik\frac{\xi-\lambda}{2}} = e^{\frac{1}{2}ik\xi}e^{-\frac{1}{2}ik\lambda} \ , \tag{10.14}$$

so we are clearly looking for

$$f_1(\xi) \propto e^{\frac{1}{2}ik\xi} \quad \text{and} \quad f_2(\lambda) \propto e^{-\frac{1}{2}ik\lambda} \ . \tag{10.15}$$

Indeed, one can easily see that $f_1(\xi) = e^{\frac{1}{2}ik\xi}$ satisfies Eq. (10.11) provided that $\beta_1 = ik/U_0$. This means that $\beta_2 = 1 - ik/U_0$, and Eq. (10.12) takes the form

$$\frac{\partial}{\partial\lambda}\left(\lambda\frac{\partial}{\partial\lambda}\right)f_2(\lambda) + \left[\frac{k^2}{4}\lambda - \frac{U_0}{2} + \frac{ik}{2}\right]f_2(\lambda) = 0 \ . \tag{10.16}$$

[1] We already know this will not be entirely true, see Sec. 6.3.

We can explicitly check that $e^{-\frac{1}{2}ik\lambda}$ does *not* satisfy this equation unless we are dealing with the trivial case $U_0 = 0$. Evidently, we need to postulate a different solution with similar asymptotic properties. This condition is satisfied by

$$f_2(\lambda) = e^{-\frac{1}{2}ik\lambda} w(\lambda) \ , \tag{10.17}$$

where we demand that the function $w(\lambda)$ tends to a constant as $\lambda \to \infty$. Plugging this *ansatz* into Eq. (10.16) yields an equation for $w(\lambda)$,

$$\lambda \frac{\partial^2 w(\lambda)}{\partial \lambda^2} + \big(1 - ik\lambda\big) \frac{\partial w(\lambda)}{\partial \lambda} - \frac{U_0}{2} w(\lambda) = 0 \ . \tag{10.18}$$

Introducing a new variable $\lambda' = ik\lambda$, this equation can be further reduced to

$$\lambda' \frac{\partial^2 w(\lambda')}{\partial \lambda'^2} + \big(1 - \lambda'\big) \frac{\partial w(\lambda')}{\partial \lambda'} - \frac{U_0}{2ik} w(\lambda') = 0 \ , \tag{10.19}$$

in which we recognize[2] the equation for the *confluent hypergeometric function* $F(z)$,

$$z \frac{\partial^2 F(z)}{\partial z^2} + (\gamma - z) \frac{\partial F(z)}{\partial z} - \alpha F(z) = 0 \ , \tag{10.20}$$

with parameters $\alpha = U_0/(2ik)$ and $\gamma = 1$ and variable $z = ik\lambda$. In particular, the solution that is regular at $z = 0$ is the *Kummer function*, defined as a power series

$${}_1F_1(a; b; z) = \sum_{n=0}^{\infty} \frac{(a)_n}{(b)_n} \frac{z^n}{n!} \ , \tag{10.21}$$

where $(a)_n \equiv a(a+1)(a+2)\dots(a+n-1)$. Together with $f_1(\xi)$, we can now write that the Coulomb wavefunction should be given by

$$\psi(\xi, \lambda) \propto e^{\frac{1}{2}ik(\xi - \lambda)} \ {}_1F_1\left(\frac{U_0}{2ik}; 1; ik\lambda\right) \ . \tag{10.22}$$

We want to know the solutions at large r, and from Eq. (10.3) it is evident that large r corresponds to a large λ. This is a moment where we are once again grateful for people who find solutions to awful equations and study their properties so that we can do other, often more absorbing things. In particular, some of these people have shown that for large λ, the confluent hypergeometric function can be expanded as

$${}_1F_1(\alpha; \gamma; z) = \frac{\Gamma[\gamma]}{\Gamma[\gamma - \alpha]} (-z)^{-\alpha} G(\alpha, \alpha - \gamma + 1, -z) + \frac{\Gamma[\gamma]}{\Gamma[\alpha]} e^z z^{\alpha - \gamma} G(\gamma - \alpha, 1 - \alpha, z) \ , \tag{10.23}$$

where

$$G(\alpha, \beta, z) = 1 + \frac{\alpha\beta}{1!\ z} + \frac{\alpha(\alpha+1)\ \beta(\beta+1)}{2!\ z^2} + \dots \tag{10.24}$$

so that

$$G(\alpha, \alpha - \gamma + 1, -z) = 1 - \frac{\alpha(\alpha - \gamma + 1)}{1!\ z} + \frac{\alpha(\alpha+1)\ (\alpha - \gamma + 1)(\alpha - \gamma + 2)}{2!\ z^2} + \dots \tag{10.25}$$

[2] Of course we do...

and

$$G(\gamma-\alpha,1-\alpha,z)=1+\frac{(\gamma-\alpha)(1-\alpha)}{1!\ z}+\frac{(\gamma-\alpha)(\gamma-\alpha+1)\ (1-\alpha)(2-\alpha)}{2!\ z^2}+\dots\ . \tag{10.26}$$

Using $\alpha=U_0/(2ik)$, $\gamma=1$, and $z=ik\lambda$ and discarding terms suppressed by more than η^{-1} yields[3]

$${}_1F_1\left(\frac{U_0}{2ik};1;ik\lambda\right)=\frac{(-ik\lambda)^{-\frac{U_0}{2ik}}}{\Gamma\left[1-\frac{U_0}{2ik}\right]}\left(1-\frac{\left(\frac{U_0}{2ik}\right)^2}{ik\lambda}\right)+\frac{(ik\lambda)^{\frac{U_0}{2ik}}}{\Gamma\left[\frac{U_0}{2ik}\right]}\frac{e^{ik\lambda}}{ik\lambda}\ . \tag{10.27}$$

Further rewriting

$$(-ik\lambda)^{-\frac{U_0}{2ik}}=(-i)^{-\frac{U_0}{2ik}}(k\lambda)^{-\frac{U_0}{2ik}}=\left(e^{-i\frac{\pi}{2}}\right)^{-\frac{U_0}{2ik}}e^{\ln\left[(k\lambda)^{-\frac{U_0}{2ik}}\right]}=e^{\frac{\pi U_0}{4k}}e^{i\frac{U_0}{2k}\ln(k\lambda)} \tag{10.28}$$

and

$$(ik\lambda)^{\frac{U_0}{2ik}}=i^{\frac{U_0}{2ik}}(k\lambda)^{\frac{U_0}{2ik}}=(e^{i\frac{\pi}{2}})^{\frac{U_0}{2ik}}e^{\ln\left[(k\lambda)^{\frac{U_0}{2ik}}\right]}=e^{\frac{\pi U_0}{4k}}e^{-i\frac{U_0}{2k}\ln(k\lambda)} \tag{10.29}$$

as well as using the identity $\Gamma[1+z]=z\Gamma[z]$, we transform Eq. (10.27) into

$${}_1F_1\left(\frac{U_0}{2ik};1;ik\lambda\right)=\frac{e^{\frac{\pi U_0}{4k}}e^{i\frac{U_0}{2k}\ln(k\lambda)}}{\Gamma\left[1-\frac{U_0}{2ik}\right]}\left(1-\frac{\left(\frac{U_0}{2ik}\right)^2}{ik\lambda}\right)-\frac{\frac{U_0}{2k}e^{\frac{\pi U_0}{4k}}e^{-i\frac{U_0}{2k}\ln(k\lambda)}}{\Gamma\left[1+\frac{U_0}{2ik}\right]}\frac{e^{ik\lambda}}{k\lambda}\ . \tag{10.30}$$

Before using this asymptotic form in Eq. (10.22), let us fix the normalization. We are always allowed to choose normalization that makes our life easier. In particular, we propose to use

$$\psi_C(\xi,\lambda)=e^{-\frac{\pi U_0}{4k}}\Gamma\left[1-\frac{U_0}{2ik}\right]e^{\frac{1}{2}ik(\xi-\lambda)}\ {}_1F_1\left(\frac{U_0}{2ik};1;ik\lambda\right)\ . \tag{10.31}$$

Both Eq. (10.22) and the above equation give the exact solution of the Coulomb scattering problem.

10.2 Asymptotic behavior of the Coulomb wavefunctions

We now transform Eq. (10.31) by using the asymptotic form of the Kummer function, Eq. (10.30), recovering the mixed Cartesian-spherical coordinates through relations $\xi-\lambda=2z$ and $\lambda=r-z=r(1-\cos\theta)$, and putting all dependence on the angle θ and Gamma functions that appear in the second term inside a function $f_C(k,\theta)$, which yields

$$\psi_C(\xi,\lambda)\xrightarrow[r\to\infty]{}e^{ikz}\ e^{i\frac{U_0}{2k}\ln[kr(1-\cos\theta)]}\left[1-\frac{\left(\frac{U_0}{2ik}\right)^2}{ikr(1-\cos\theta)}\right]+f_C(k,\theta)\frac{e^{ikr}e^{-i\frac{U_0}{2k}\ln(2kr)}}{r} \tag{10.32}$$

where

$$f_C(k,\theta)=-\frac{\Gamma\left[1-\frac{U_0}{2ik}\right]}{\Gamma\left[1+\frac{U_0}{2ik}\right]}\ \frac{\frac{U_0}{2}e^{-i\frac{U_0}{k}\ln(\sin\frac{\theta}{2})}}{2k^2\sin^2\frac{\theta}{2}}\ . \tag{10.33}$$

[3] Note that $\Gamma[1]=1$.

You may recognize the phase $\sim \ln(2kr)$ from our discussion of the asymptotic scattering solution *ansatz*, Eq. (6.16), in Sec. 6.3, where we saw that a logarithmically diverging phase arises for Coulomb-like potentials, Eq. (6.34).

For application to the Coulomb potential, where $U_0 = 2\mu V_0 = 2\mu Z_1 Z_2 e^2$, we recognize that

$$\frac{U_0}{2k} = \eta \ , \tag{10.34}$$

where η is the Sommerfeld parameter,

$$\eta \equiv \frac{Z_1 Z_2 e^2}{v} \ . \tag{10.35}$$

Thus, we finally obtain the asymptotic Coulomb solution

$$\psi_C(r,z) \xrightarrow[r\to\infty]{} e^{ikz}\ e^{i\eta\ln[k(r-z)]}\left[1+\frac{\eta^2}{ikr(1-\cos\theta)}\right] + f_C(k,\theta)\frac{e^{ikr}e^{-i\eta\ln(2kr)}}{r} \tag{10.36}$$

with

$$f_C(k,\theta) = -\frac{\Gamma[1+i\eta]}{\Gamma[1-i\eta]}\ \frac{\eta e^{-i2\eta\ln(\sin\frac{\theta}{2})}}{2k\sin^2\frac{\theta}{2}} \ , \tag{10.37}$$

which one can also write as

$$f_C(k,\theta) = -e^{2i\sigma_0}\ \frac{\eta e^{-i2\eta\ln(\sin\frac{\theta}{2})}}{2k\sin^2\frac{\theta}{2}} \ , \tag{10.38}$$

where

$$\sigma_0 = \arg\left[\Gamma[1+i\eta]\right] \tag{10.39}$$

is the constant *Coulomb s-wave phase shift*. The first term in Eq. (10.36) represents the incident wave, while the second term is the scattered wave. We can clearly see that the distorting effects due to the Coulomb long-range interaction are present in both.

Interestingly, none of that distortion propagates into the cross section. Given Eq. (10.36), one can now compute the flux of the scattered current $\boldsymbol{j}\cdot\hat{\boldsymbol{r}}$ to obtain the cross section, Eq. (6.42). The additional factors in Eq. (10.36) do lead to additional terms in the scattered currents, however, they are all proportional to r^{-1} and so they vanish asymptotically. As a result, the elastic Coulomb cross section is given by the familiar expression from Eq. (6.68), repeated here for convenience,

$$\frac{d\sigma_C(\Omega)}{d\Omega} = \left|f_C(k,\theta)\right|^2 \ , \tag{10.40}$$

which, using Eq. (10.37), gives

$$\frac{d\sigma_c(\Omega)}{d\Omega} = \frac{\eta^2}{4k^2}\frac{1}{\sin^4(\theta/2)} = \left(\frac{Z_1 Z_2 e^2}{2kv}\right)^2 \frac{1}{\sin^4(\theta/2)} \ , \tag{10.41}$$

which is the same[4] as the classical expression we already obtained in Eq. (5.33).

[4]Note that in natural units, $k = p = \mu v$.

We note that like in the case of resonances, where the behavior of the scattering phase shift was indicative of a pole structure in the energy, the Coulomb phase shift tells us something important about the analytic structure of the problem. Namely, the logarithmic Coulomb phase shift $-\eta \ln(2kr)$ signals the long-range nature of the potential which modifies the asymptotic form of the wavefunction. This has profound and counterintuitive consequences: unlike short-range scattering, there is no asymptotic region where the potential is truly negligible, leading to logarithmic phase corrections that persist to infinity and a differential cross section that diverges at forward angles ($\theta \to 0$), causing the total cross section to diverge due to contributions from arbitrarily large impact parameters. The divergence of the total cross section is an infrared problem analogous to those arising in quantum electrodynamics (QED) from massless photon exchange, requiring careful regularization and redefinition of observables – a theme that recurs throughout quantum field theory (QFT).

10.3 Note about the significance of known exact solutions

Above, we have obtained the full solution of the Coulomb problem, Eq. (10.31), as well as its asymptotic limit, Eq. (10.36).

The fact that the Coulomb problem is solved and solutions are known cannot be stressed enough. The Coulomb functions quoted above solve the problem *everywhere in space*, not only in the asymptotic region. Consequently, there is literally nothing left to be done here: no matching at some $r = R$, no calculation of phase shifts for a particular potential, no free parameters. After the formal machinery is built (*i.e.*, we connect the solutions to the scattering amplitude, scattering phase shifts, and scattering cross sections), that is it – Coulomb scattering becomes plug-and-play. All that will be left to do is to use the formalism we will develop below with the correct values of Z_1 and Z_2.

10.4 Partial wave expansion

Since the pure Coulomb problem can be solved exactly (see above), partial wave expansion is not especially useful in this case, especially as the long-range character of the interaction means that contributions from many partial waves are significant. However, partial wave expansion is crucial for problems which deal with both the Coulomb interaction and a short range potential. Thus, even though we have just solved the Coulomb problem in Sec. 10.1, we now need to come back to the drawing board and do the same in spherical coordinates. The good thing about having gone through the exact solution is that it has exposed us to some of the concepts – *e.g.*, hypergeometric functions – which will make the partial wave expansion more digestible.

For the Coulomb potential, the radial equation, Eq. (7.22), becomes

$$\frac{\partial^2}{\partial r^2} F_l(k,r) + \left[k^2 - \frac{2\eta k}{r} - \frac{l(l+1)}{r^2} \right] F_l(k,r) = 0 \ . \tag{10.42}$$

If the solutions $F_l(k,r)$ are known, then one can expand any function[5] as

$$\psi = \sum_{l=0}^{\infty} C_l P_l(\cos\theta) F_l(k,r) \ . \tag{10.43}$$

We can make a well-informed guess and postulate that $F_l(k,r)$ take the form

$$F_l(k,r) = e^{ikr} (kr)^{l+1} f_l(\alpha r) \ . \tag{10.44}$$

[5]Here we assume that the function does not depend on ϕ, which is appropriate for spherically-symmetric potentials.

Setting $\zeta = \alpha r$, we find that the function $f_l(\zeta)$ satisfies the Kummer-Laplace equation,

$$\zeta \frac{d^2 f_l}{d\zeta^2} + (2l + 2 - \zeta)\frac{df_l}{d\zeta} - (l + 1 + i\gamma) f_l = 0 \tag{10.45}$$

provided that we choose $\alpha = -2ik$. Solutions which are regular at the origin are given by

$$f_l = c_{l1} F_1(l + 1 + i\gamma; 2l + 2; -2ikr) \ , \tag{10.46}$$

from which we immediately obtain the *regular spherical Coulomb functions*,

$$F_l(k, r) = c_l e^{ikr} (kr)^{l+1} {}_1F_1(l + 1 + i\gamma; 2l + 2; -2ikr) \ . \tag{10.47}$$

Asymptotically, $F_l(k, r)$ can be shown to behave as

$$F_l(k, r) \xrightarrow[r\to\infty]{} c_l \frac{e^{\frac{\pi}{2}\eta + i\sigma_l}(2l + 1)!}{2^l \Gamma[l + 1 + i\gamma]} \sin\left(kr - l\frac{\pi}{2} - \eta \ln(2kr) + \sigma_l\right) \ , \tag{10.48}$$

where $\sigma_l = \arg \Gamma[l + 1 + i\eta]$ is the *Coulomb phase shift*. By analogy with the S-matrix element as defined in Eq. (8.5), we define the *Coulomb S-matrix element*

$$S_l^{(C)}(k) \equiv e^{2i\sigma_l} = \frac{\Gamma[l + 1 + i\eta]}{\Gamma[l + 1 - i\eta]} \ . \tag{10.49}$$

Finally, to make our life easier, we can always impose a convenient normalization. In particular, setting

$$c_l = \frac{2^l \left|\Gamma[l + 1 + i\gamma]\right| e^{-\frac{\pi}{2}\eta}}{(2l + 1)!} \tag{10.50}$$

leads to the asymptotic behavior

$$F_l(k, r) \xrightarrow[r\to\infty]{} \sin\left(kr - l\frac{\pi}{2} - \eta \ln(2kr) + \sigma_l\right) \ . \tag{10.51}$$

Since any function can be now expanded in the partial wave expansion, we can do so in particular for the exact Coulomb plane wave, Eq. (10.31),

$$\psi_C = e^{-\frac{\pi U_0}{4k}} \Gamma\left[1 - \frac{U_0}{2ik}\right] e^{\frac{1}{2}ik(\xi - \lambda)} \ {}_1F_1\left(\frac{U_0}{2ik}; 1; ik\lambda\right) = \sum_{l=0}^{\infty} C_l P_l(\cos\theta) \frac{F_l(\eta, r)}{r} \ . \tag{10.52}$$

The coefficients C_l can be found to be $C_l = (2l + 1) i^l e^{i\sigma_l}/k$ (see, *e.g.*, Bertulani & Danielewicz [6]), so that

$$\psi_C = \sum_{l=0}^{\infty} (2l + 1) i^l e^{i\sigma_l} P_l(\cos\theta) \frac{F_l(\eta, r)}{kr} \tag{10.53}$$

and the Coulomb scattering amplitude is given by (see, *e.g.*, Bertulani & Danielewicz [6])

$$f_C(k, \theta) = \frac{1}{2ik} \sum_{l=0}^{\infty} (2l + 1) P_l(\cos\theta) \left[S_l^{(C)}(k) - 1\right] \ . \tag{10.54}$$

10.5 Coulomb and short-range potential

Often, we need to deal with a problem where the potential has both a Coulomb and a short-range nuclear part,

$$V(r) = V_C(r) + V_N(r) \ . \tag{10.55}$$

Then the Schrödinger equation can be put in the form

$$\Big[\nabla^2 + k^2 - \frac{2\eta k}{r}\Big]\psi(\boldsymbol{r}) = U_N(r)\psi(\boldsymbol{r}) \ . \tag{10.56}$$

We already know the solutions ψ_C to the homogeneous equation (where $U_N = 0$). The solution to the inhomogeneous equation will be a sum

$$\psi^{(+)}(\boldsymbol{r}) = \psi_C(\boldsymbol{r}) + \psi_{\rm sc}(\boldsymbol{r}) \ , \tag{10.57}$$

where we adopt an *ansatz*

$$\psi_{\rm sc}(\boldsymbol{r}) = A f_N(k,\theta)\frac{e^{ikr}}{r}e^{-i\eta\ln(2kr)} \ . \tag{10.58}$$

In this way, because the forms of the scattered waves in the pure Coulomb and in the extended problem are the same, we can think of $f_N(k,\theta)$ as a "correction" to the Coulomb scattering amplitude $f_C(k,\theta)$.

Just as before, to find a convenient expression for $f_N(k,\theta)$, we expand $\psi^{(+)}(\boldsymbol{r})$ in terms of partial waves and match coefficients of the incoming and outgoing waves. In this way, we find

$$f_N(k,\theta) = \frac{1}{2ik}\sum_{l=0}^{\infty}(2l+1)P_l(\cos\theta)e^{2i\sigma_l}\big(S_l - 1\big) \ , \tag{10.59}$$

where σ_l is the scattering phase shift due to the Coulomb interaction and $S_l \equiv e^{2i\delta_l}$ is the scattering matrix element connected with the nuclear part of the interaction, where δ_l is the nuclear scattering phase shift. Note that since now the solution is written in terms of the Coulomb functions (as opposed to, *e.g.,* Ricatti functions), the nuclear scattering phase shift δ_l is computed by comparing with an asymptotic Coulomb function (as opposed to, *e.g.*, asymptotic Ricatti-Bessel function).

Finally, since the term $\frac{e^{ikr}}{r}e^{-i\eta\ln(2kr)}$ in $\psi^{(+)}(\boldsymbol{r})$ is now multiplied by the sum

$$f(k,\theta) = f_C(k,\theta) + f_N(k,\theta) \ , \tag{10.60}$$

then, following the same procedures as before, we will obtain the expression for the cross section,

$$\frac{d\sigma(\Omega)}{d\Omega} = \big|f_C(k,\theta) + f_N(k,\theta)\big|^2 = \frac{d\sigma_C}{d\Omega} + \frac{d\sigma_N}{d\Omega} + 2\mathrm{Re}\,\big[f_C^* f_N\big] \ . \tag{10.61}$$

Lecture sources: In this lecture, section 10.1 is based on the treatment in Landau & Lifshitz [10]. Section 10.4 is based on the treatment in Joachain [2]. Section 10.5 is based on Bertulani [6] and Joachain [2].

Lecture 11

Formal scattering theory I

Prerequisites: none.
Guiding question: ***Just how important could a small complex shift be?***

11.1 The inverse of $(E - \hat{H}_0)$

In operator language, the Schrödinger equation can be written as

$$\hat{H}\,|\Psi\rangle = E\,|\Psi\rangle \ , \tag{11.1}$$

where $\hat{H}$ is an operator and $|\Psi\rangle \in \mathcal{H}$ is a vector in Hilbert space[1]. Equivalently, we can also write

$$(E - \hat{H})\,|\Psi\rangle = 0 \ . \tag{11.2}$$

The Hamiltonian operator can be decomposed as

$$\hat{H} = \hat{H}_0 + \hat{V} \ , \tag{11.3}$$

where $\hat{H}_0$ is the free-particle Hamiltonian for which we can also write the Schrödinger equation,

$$(E - \hat{H}_0)\,|\Phi\rangle = 0 \ , \tag{11.4}$$

and $\hat{V}$ is the potential operator[2]. In fact, we can write both the free-particle and interacting Schrödinger equations as

$$(E - \hat{H}_0)\,|\Phi\rangle = 0 \ , \tag{11.5}$$

$$(E - \hat{H}_0)\,|\Psi\rangle = V\,|\Psi\rangle \ . \tag{11.6}$$

Formally, one could attempt to write the solution to Eq. (11.6) as

$$|\Psi\rangle = (E - \hat{H}_0)^{-1} V\,|\Psi\rangle \ , \tag{11.7}$$

[1] In this approach, the wavefunction $\psi(\boldsymbol{r})$ that we've been dealing with so far is a coordinate-space representation of a vector from the Hilbert space. More formally, $\psi(\boldsymbol{r}) = \langle \boldsymbol{r}|\Psi\rangle$, where $|\boldsymbol{r}\rangle$ is a position eigenvector, is a projection of the abstract state $|\psi\rangle$ onto the position eigenbasis.

[2] So far, we have quietly ignored the fact that $\hat{V}$ is an operator because we have been dealing with local potentials in the coordinate basis, whose action on a wavefunction is simply to multiply, *e.g.*, $\hat{V}(\boldsymbol{r})\Psi(\boldsymbol{r}) = V(\boldsymbol{r})\Psi(\boldsymbol{r})$. However, the action of $\hat{V}$ may be more complicated if it is expressed in a different basis or non-local. From now on, we will acknowledge this by marking the potential as an operator.

where $(E-\hat{H}_0)^{-1}$ is the inverse of the operator $(E-\hat{H}_0)$. However, an inverse of a linear operator $\hat{A}$ exists only if $\hat{A}$ is one-to-one, which in particular means that it cannot have any zero eigenvalues. This condition fails for $(E-\hat{H}_0)$, as the free Hamiltonian operator has a continuous spectrum of eigenvalues which is certain to contain any value of E. The solution to this conundrum is to make the variable E *slightly complex* by substituting $E \to E + i\epsilon$. Since $\hat{H}_0$ is self-adjoint[3], its spectrum lies strictly on the real axis. Consequently, while $(E-\hat{H}_0)^{-1}$ is not well defined, the inverse operator[4]

$$\hat{G}_0(E) = \lim_{\epsilon\to 0^+} \big((E+i\epsilon) - \hat{H}_0\big)^{-1} = \lim_{\epsilon\to 0^+} \frac{1}{E - \hat{H}_0 + i\epsilon} \tag{11.8}$$

does exist.

The important point is that the limit in Eq. (11.8) is not obtained by simply putting $\epsilon = 0$: this would yield again the operator $(E-\hat{H}_0)^{-1}$, which continues to be ill-defined when E denotes the spectrum of $\hat{H}_0$ (which it does). Instead, we study the $\epsilon \to 0^+$ limit of $\big((E+i\epsilon) - \hat{H}_0\big)^{-1}$ *when acting on other expressions*, for example inside matrix elements or integrals. Such an "indirect" limit is known as a *limit in a weak sense*, and this is the limit that we can use in this case. In other words, even though the operator $(E-\hat{H}_0)^{-1}$ does not exist, the limit $\lim_{\epsilon\to 0^+} \big((E+i\epsilon) - \hat{H}_0\big)^{-1}$ is well-defined when inserted into various physically relevant expressions[5].

[3] Which means that $\hat{H}_0$ is Hermitian, $\hat{H}_0^\dagger = \hat{H}_0$, and the domains of $\hat{H}_0$ and $\hat{H}_0^\dagger$ are equal.

[4] We note here that writing an inverse operator $\hat{A}^{-1}$ as $1/\hat{A}$ is a slight abuse of notation, as we cannot literally divide by an operator. This notation – which is very often used – is fine as long as we remember what it represents.

[5] A familiar example of an object whose limit is only well-defined when it acts in other expressions is the delta function $\delta(x)$. A function $1/x^2$ is not well-defined for $x = 0$. However, let us consider

$$\delta_\epsilon(x) = \frac{1}{\pi}\frac{\epsilon}{x^2+\epsilon^2} \ .$$

On its own, the limit $\lim_{\epsilon\to 0}\delta_\epsilon(x)$ is not meaningful at $x = 0$. However, let us see what happens if we attempt to integrate $\delta_\epsilon(x)$ over the entire real line (which of course includes $x = 0$),

$$I = \int_{-\infty}^{+\infty} dx\ \delta_\epsilon(x) = \frac{1}{\pi}\int_{-\infty}^{+\infty} dx\ \frac{\epsilon}{x^2+\epsilon^2} = \frac{1}{\pi}\int_{-\infty}^{+\infty} dt\ \frac{1}{(t^2+1)} = \frac{1}{\pi}\big[\tan^{-1} t\big]_{t=-\infty}^{t=+\infty} = \frac{1}{\pi}\Big[\frac{\pi}{2} - \Big(-\frac{\pi}{2}\Big)\Big] = 1 \ ,$$

where in the third equality we substituted $x = \epsilon t$ and then used the fact that $d(\tan^{-1} t)/dt = 1/(1+t^2)$. Clearly, the integral I has a well-defined limit when $\epsilon \to 0$. Now we can also integrate $\delta_\epsilon(x)$ together with a *test function* $f(x)$,

$$I_f = \int_{-\infty}^{+\infty} dx\ f(x)\delta_\epsilon(x) = \frac{1}{\pi}\int_{-\infty}^{+\infty} dt\ f(\epsilon t)\frac{1}{(t^2+1)} \ ,$$

where we again substituted $x = \epsilon t$. Since we anticipate taking $\epsilon \to 0$, we can always expand $f(\epsilon t)$, $f(\epsilon t) \approx f(0) + \epsilon t f'(0) + \mathcal{O}(\epsilon^2)$, which inserted into the I_f integral yields

$$I_f = \frac{f(0)}{\pi}\int_{-\infty}^{+\infty} dt\ \frac{1}{(t^2+1)} + \frac{\epsilon f'(0)}{\pi}\int_{-\infty}^{+\infty} dt\ \frac{t}{(t^2+1)} + \mathcal{O}(\epsilon^2) \ .$$

We already know that the integral in the first term yields π, the integral in the second term is zero because the integrand is odd, and higher order terms are suppressed as $\epsilon \to 0$. Thus

$$\lim_{\epsilon\to 0} I_f = \lim_{\epsilon\to 0}\int_{-\infty}^{+\infty} dx\ f(x)\delta_\epsilon(x) = f(0) \ .$$

This operational behavior defines the meaning of the delta function,

$$\delta(x) = \lim_{\epsilon\to 0}\delta_\epsilon(x) \qquad \text{and} \qquad \int dx\ f(x)\delta(x) = f(0) \ .$$

The delta function is not an ordinary function but a *distribution*: an object defined only through its action under an integral on smooth test functions.

11.2 Lippmann–Schwinger equations

Let us now use the operator formalism to derive a number of useful equations. First, let us subtract the two Schrödinger equations, Eq. (11.5) and Eq. (11.6), by sides,

$$(E - \hat{H}_0)\big(\,|\Psi\rangle - |\Phi\rangle\,\big) = \hat{V}\,|\Psi\rangle \ . \tag{11.9}$$

Multiplying the above equation from the left by $\hat{G}_0(E)$, Eq. (11.8), and moving $|\Phi\rangle$ to the other side yields

$$|\Psi\rangle = |\Phi\rangle + \hat{G}_0(E)\hat{V}\,|\Psi\rangle \ . \tag{11.10}$$

This is a *self-consistent* equation for the eigenvector $|\Psi\rangle$, telling us that $|\Psi\rangle$ is a sum of the free solution $|\Phi\rangle$ and the combined action of the potential $\hat{V}$ and the inverse operator $(E-\hat{H}_0)^{-1}$ on $|\Psi\rangle$.

On the other hand, we can also modify the solution on the right-hand side of Eq. (11.9) by adding and subtracting $|\Phi\rangle$,

$$(E - \hat{H}_0)\big(\,|\Psi\rangle - |\Phi\rangle\,\big) = \hat{V}\big(\,|\Psi\rangle - |\Phi\rangle + |\Phi\rangle\,\big) \ . \tag{11.11}$$

Moving $\hat{V}\big(\,|\Psi\rangle - |\Phi\rangle\,\big)$ to the left-hand side and recognizing that $\hat{H}_0 + \hat{V} = \hat{H}$ then leads to

$$(E - \hat{H})\big(\,|\Psi\rangle - |\Phi\rangle\,\big) = \hat{V}\,|\Phi\rangle \ . \tag{11.12}$$

In full analogy to the operator $\hat{G}_0(E)$, we can now define

$$\hat{G}(E) = \lim_{\epsilon\to 0^+}\big((E+i\epsilon) - \hat{H}\big)^{-1} = \lim_{\epsilon\to 0^+}\frac{1}{E-\hat{H}+i\epsilon} \ , \tag{11.13}$$

which applied to Eq. (11.12) immediately leads to

$$|\Psi\rangle = |\Phi\rangle + \hat{G}(E)\hat{V}\,|\Phi\rangle = \big(1 + \hat{G}(E)\hat{V}\big)\,|\Phi\rangle \ . \tag{11.14}$$

Thus, the full solution of the Schrödinger equation can be written as a sum of the free solution and a combined action of the potential and the inverse operator $(E-\hat{H})^{-1}$ on the free solution $|\Phi\rangle$.

Eqs. (11.10) and (11.14) are known as the *Lippmann–Schwinger equations*. Their usefulness lies in the fact that they allow one to make systematic approximations. Indeed, plugging the entire expression for $|\Psi\rangle$, Eq. (11.10), on the right-hand side of Eq. (11.10) leads to[6]

$$|\Psi\rangle = |\Phi\rangle + \hat{G}_0\hat{V}\Big(\,|\Phi\rangle + \hat{G}_0\hat{V}\,|\Psi\rangle\,\Big) = |\Phi\rangle + \hat{G}_0\hat{V}\,|\Phi\rangle + \hat{G}_0\hat{V}\hat{G}_0\hat{V}\,|\Psi\rangle \ . \tag{11.15}$$

Since we again have $|\Psi\rangle$ on the right-hand side, we can continue doing this. Such an infinite expansion,

$$|\Psi\rangle = |\Phi\rangle + \hat{G}_0\hat{V}\,|\Phi\rangle + \hat{G}_0\hat{V}\hat{G}_0\hat{V}\,|\Phi\rangle + \hat{G}_0\hat{V}\hat{G}_0\hat{V}\hat{G}_0\hat{V}\,|\Phi\rangle + \dots \ , \tag{11.16}$$

is known as the *Born series*, and discarding everything but the first two terms on the right-hand side yields the *1st Born approximation*,

$$|\Psi\rangle \approx |\Phi\rangle + \hat{G}_0\hat{V}\,|\Phi\rangle \ . \tag{11.17}$$

We note that the Born series converges under appropriate conditions, *e.g.*, for a weak $\hat{V}$ or at high energies (which make $\hat{G}_0$ small).

All of this is very pretty, but also rather useless unless we know the form of $\hat{G}_0$ or $\hat{G}$. Since determining $\hat{G}$ for the full Hamiltonian $\hat{H}$ is typically difficult, let us tackle $\hat{G}_0$.

[6] For clarity, here we suppress the argument of $\hat{G}_0$.

11.3 An aside on spectral decomposition

In the following we will use the fact that any self-adjoint operator can be written as a sum of its eigenvalues times projection operators onto its eigenstates. For example, the action of the free Hamiltonian $\hat{H}_0$, whose eigenstates satisfy $\hat{H}_0 |\phi_{\boldsymbol{k}'}\rangle = E_{k'} |\phi_{\boldsymbol{k}'}\rangle$, on a state ψ can be expressed as

$$\hat{H}_0 |\psi\rangle = \left(\int d^3k' \; E_{k'} |\phi_{\boldsymbol{k}'}\rangle \langle\phi_{\boldsymbol{k}'}| \right) |\psi\rangle = \int d^3k' \; E_{k'} \langle\phi_{\boldsymbol{k}'}|\psi\rangle |\phi_{\boldsymbol{k}'}\rangle \; . \tag{11.18}$$

Such an expansion is known as a *spectral decomposition*. To see that Eq. (11.18) is true, recall the completeness relation, that is the fact that the identity operator can be written as[7]

$$\hat{\mathbb{1}} = \int d^3k' \; |\phi_{\boldsymbol{k}'}\rangle \langle\phi_{\boldsymbol{k}'}| \; . \tag{11.19}$$

With this, one can always write[8]

$$\hat{H}_0 |\psi\rangle = \hat{H}_0 \left(\int d^3k' |\phi_{\boldsymbol{k}'}\rangle \langle\phi_{\boldsymbol{k}'}| \right) |\psi\rangle = \int d^3k' \; \hat{H}_0 |\phi_{\boldsymbol{k}'}\rangle \langle\phi_{\boldsymbol{k}'}|\psi\rangle = \int d^3k' \; E_{k'} |\phi_{\boldsymbol{k}'}\rangle \langle\phi_{\boldsymbol{k}}|\psi\rangle \; . \tag{11.20}$$

Moreover, one can show that for any reasonable function f,

$$f(H_0) = \int d^3k' \; f(E_{k'}) |\phi_{\boldsymbol{k}'}\rangle \langle\phi_{\boldsymbol{k}'}| \; . \tag{11.21}$$

In place of a rigorous proof, let us consider the action of $(\hat{H}_0)^2$ on some state $|\psi\rangle$,

$$(\hat{H}_0)^2 |\psi\rangle = \left(\int d^3k' \; E_{k'} |\phi_{\boldsymbol{k}'}\rangle \langle\phi_{\boldsymbol{k}'}| \right) \left(\int d^3k \; E_k |\phi_{\boldsymbol{k}}\rangle \langle\phi_{\boldsymbol{k}}| \right) |\psi\rangle \tag{11.22}$$

$$= \int d^3k' \int d^3k \; E_{k'} E_k |\phi_{\boldsymbol{k}'}\rangle \langle\phi_{\boldsymbol{k}'}|\phi_{\boldsymbol{k}}\rangle \langle\phi_{\boldsymbol{k}}|\psi\rangle = \int d^3k' \; (E_{k'})^2 |\phi_{\boldsymbol{k}'}\rangle \langle\phi_{\boldsymbol{k}'}|\psi\rangle \; , \tag{11.23}$$

where in the third equality we used the orthogonality of the eigenvectors, $\langle\phi_{\boldsymbol{k}'}|\phi_{\boldsymbol{k}}\rangle = \delta^{(3)}(\boldsymbol{k}' - \boldsymbol{k})$. Then we can extend the same logic not only to any power of $\hat{H}_0$, but also any polynomial in $\hat{H}_0$, $f(\hat{H}_0) = \sum_{n=0}^{\infty} a_n \hat{H}_0^n$. Consequently, if a given function $f(\hat{H}_0)$ can be approximated by polynomials on the spectrum of $\hat{H}_0$, then Eq. (11.21) follows by taking an appropriate limit.

[7] This can be seen in the following way: Applying $\int d^3k \; |\phi_{\boldsymbol{k}}\rangle \langle\phi_{\boldsymbol{k}}|$ to an arbitrary state vector $|\psi\rangle$ yields

$$\left(\int d^3k \; |\phi_{\boldsymbol{k}}\rangle \langle\phi_{\boldsymbol{k}}| \right) |\psi\rangle = \int d^3k \; |\phi_{\boldsymbol{k}}\rangle \langle\phi_{\boldsymbol{k}}|\psi\rangle \; ,$$

where $\langle\phi_{\boldsymbol{k}}|\psi\rangle$ are projections of the state $|\psi\rangle$ onto the basis formed by the eigenvectors $|\phi_{\boldsymbol{k}}\rangle$. We can always multiply both sides of the above equation by $\langle\phi_{\boldsymbol{k}'}|$ from the left, yielding

$$\langle\phi_{\boldsymbol{k}'}| \left(\int d^3k \; |\phi_{\boldsymbol{k}}\rangle \langle\phi_{\boldsymbol{k}}| \right) |\psi\rangle = \int d^3k \; \langle\phi_{\boldsymbol{k}'}|\phi_{\boldsymbol{k}}\rangle \langle\phi_{\boldsymbol{k}}|\psi\rangle \; .$$

Since the eigenstates satisfy the orthogonality relation, $\langle\phi_{\boldsymbol{k}'}|\phi_{\boldsymbol{k}}\rangle = \delta^{(3)}(\boldsymbol{k}' - \boldsymbol{k})$, we can rewrite the right-hand side,

$$\langle\phi_{\boldsymbol{k}'}| \left(\int d^3k \; |\phi_{\boldsymbol{k}}\rangle \langle\phi_{\boldsymbol{k}}| \right) |\psi\rangle = \langle\phi_{\boldsymbol{k}'}|\psi\rangle \; .$$

This must be true for any $\langle\phi_{\boldsymbol{k}'}|$, which is only possible if

$$\int d^3k \; |\phi_{\boldsymbol{k}}\rangle \langle\phi_{\boldsymbol{k}}| = \hat{\mathbb{1}} \; .$$

This relation, referred to as *resolution of identity*, is true for any complete set of eigenstates over the Hilbert space.

[8] This is an infinite-dimensional analogue of the fact that a diagonal matrix acts on a vector by multiplying each component by the corresponding eigenvalue. In the basis formed by its own eigenstates, $\hat{H}_0$ is diagonal, components of any vector $|\psi\rangle$ are given by $\langle\phi_{\boldsymbol{k}}|\psi\rangle |\phi_{\boldsymbol{k}'}\rangle$, and the integral replaces the sum because the spectrum of $\hat{H}_0$ is continuous.

11.4 Explicit form of $\hat{G}_0$

We start our quest to compute the $\hat{G}_0$ operator by writing its spectral decomposition[9],

$$\hat{G}_0(E_k) = \left(\int d^3k' \ |\phi_{\boldsymbol{k}'}\rangle \langle \phi_{\boldsymbol{k}'}| \right) \lim_{\epsilon \to 0^+} \left(E_k - \hat{H}_0 + i\epsilon\right)^{-1} \tag{11.24}$$

$$= \lim_{\epsilon \to 0^+} \int d^3k' \ |\phi_{\boldsymbol{k}'}\rangle \langle \phi_{\boldsymbol{k}'}| \left(E_k - E_{k'} + i\epsilon\right)^{-1} \tag{11.25}$$

$$= \lim_{\epsilon \to 0^+} \ 2\mu \int d^3k' \ \frac{|\phi_{\boldsymbol{k}'}\rangle \langle \phi_{\boldsymbol{k}'}|}{k^2 - k'^2 + i\epsilon} \ . \tag{11.26}$$

To proceed, we focus on finding the matrix elements of $\hat{G}_0(E_k)$ in the coordinate basis, given by

$$G_0(E_k; \boldsymbol{r}, \boldsymbol{r}') \equiv \left\langle \boldsymbol{r} \middle| \hat{G}_0(E_k) \middle| \boldsymbol{r}' \right\rangle = \lim_{\epsilon \to 0^+} \ 2\mu \int d^3k' \ \frac{\langle \boldsymbol{r}|\phi_{\boldsymbol{k}'}\rangle \langle \phi_{\boldsymbol{k}'}|\boldsymbol{r}'\rangle}{k^2 - k'^2 + i\epsilon} \tag{11.27}$$

$$= \lim_{\epsilon \to 0^+} \ 2\mu \int d^3k' \ \frac{\phi_{\boldsymbol{k}'}(\boldsymbol{r})\phi^*_{\boldsymbol{k}'}(\boldsymbol{r}')}{k^2 - k'^2 + i\epsilon} \ , \tag{11.28}$$

where in the last step we used the coordinate representation of the eigenvectors, $\langle \boldsymbol{r}|\psi_{\boldsymbol{k}'}\rangle = \psi_{\boldsymbol{k}'}(\boldsymbol{r})$. We know that the normalized free wavefunctions have the form

$$\phi_{\boldsymbol{k}'}(\boldsymbol{r}) = \frac{1}{(2\pi)^{3/2}} e^{i\boldsymbol{k}'\cdot\boldsymbol{r}} \tag{11.29}$$

so that

$$G_0(E_k; \boldsymbol{r}, \boldsymbol{r}') = \lim_{\epsilon \to 0^+} \ \frac{2m}{(2\pi)^3} \int d^3k' \ \frac{e^{i\boldsymbol{k}'\cdot\boldsymbol{r}} e^{-i\boldsymbol{k}'\cdot\boldsymbol{r}'}}{k^2 - k'^2 + i\epsilon} = \lim_{\epsilon \to 0^+} \ \frac{2m}{(2\pi)^3} \int d^3k' \ \frac{e^{i\boldsymbol{k}'\cdot(\boldsymbol{r}-\boldsymbol{r}')}}{k^2 - k'^2 + i\epsilon} \ . \tag{11.30}$$

At this point, we introduce $\boldsymbol{R} \equiv \boldsymbol{r} - \boldsymbol{r}'$, therefore committing to evaluating our integral in spherical coordinates. We align the z direction with $\boldsymbol{R}$ (we can always do that), and thus we have

$$G_0(E_k; \boldsymbol{r}, \boldsymbol{r}') = \lim_{\epsilon \to 0^+} \ \frac{2\mu}{(2\pi)^3} \int_0^\infty dk' \ k'^2 \ \int_{-1}^1 d(\cos\theta_{k'}) \ \int_0^{2\pi} d\phi_{k'} \ \frac{e^{i\boldsymbol{k}'\cdot\boldsymbol{R}}}{k^2 - k'^2 + i\epsilon} \tag{11.31}$$

$$= \lim_{\epsilon \to 0^+} \ \frac{2\mu}{(2\pi)^2} \int_0^\infty dk' \ k'^2 \ \int_{-1}^1 d(\cos\theta_{k'}) \ \frac{e^{ik'R\cos\theta_{k'}}}{k^2 - k'^2 + i\epsilon} \tag{11.32}$$

$$= \lim_{\epsilon \to 0^+} \ \frac{2\mu}{(2\pi)^2} \int_0^\infty dk' \ k'^2 \ \left[\frac{1}{ik'R} \ \frac{e^{ik'Rx}}{k^2 - k'^2 + i\epsilon} \right]_{x=-1}^{x=1} \tag{11.33}$$

$$= \lim_{\epsilon \to 0^+} \ \frac{2i\mu}{(2\pi)^2 R} \left[\int_0^\infty dk' \ k' \ \frac{e^{ik'R}}{k'^2 - k^2 - i\epsilon} - \int_0^\infty dk' \ k' \ \frac{e^{-ik'R}}{k'^2 - k^2 - i\epsilon} \right] \ , \tag{11.34}$$

where we absorbed the minus sign coming from putting the imaginary unit in the numerator by changing the signs of terms in the denominators. In the second integral, we can always make a change of variables $k' \to -k'$, which yields

$$-\int_0^\infty dk' \ k' \ \frac{e^{-ik'R}}{k'^2 - k^2 - i\epsilon} \to -\int_0^{-\infty} dk' \ k' \ \frac{e^{ik'R}}{k'^2 - k^2 - i\epsilon} = \int_{-\infty}^0 dk' \ k' \ \frac{e^{ik'R}}{k'^2 - k^2 - i\epsilon} \ , \tag{11.35}$$

[9] For clarity, here we start putting a momentum label on eigenvectors and eigenvalues, so that, *e.g.*, the energy eigenvectors are now denoted by $|\phi_{\boldsymbol{k}}\rangle$.

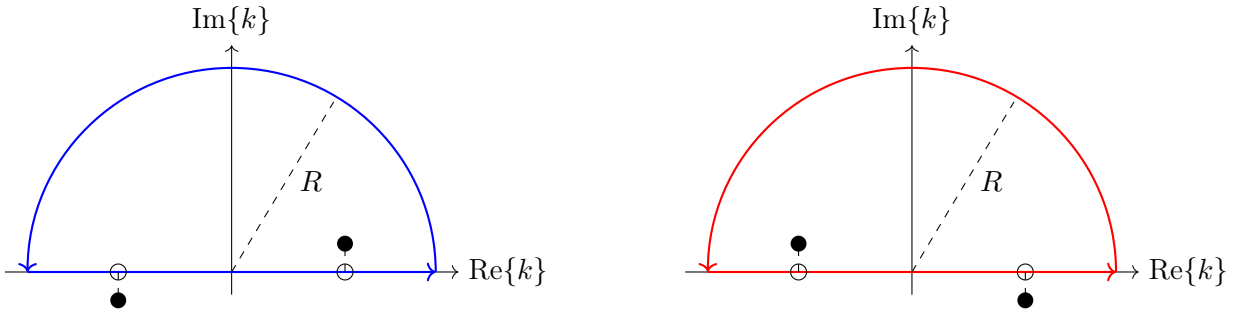

Figure 11.1: Sketch of contour integrations in the complex plane. The integration contours proceed along the entire real axis and then along a semicircle with an infinite radius R. Only pole(s) within the contour contribute to the integral value as given by the residue theorem. The left figure shows the situation where $\hat{G}_0$ is shifted by $+i\epsilon$, while the right figure shows the same for the case where $\hat{G}_0$ is shifted by $-i\epsilon$, affecting which pole is enclosed by the contour.

so that now

$$G_0(E_k;\boldsymbol{r},\boldsymbol{r}') = \lim_{\epsilon\to 0^+} \frac{2i\mu}{(2\pi)^2 R}\int_{-\infty}^{\infty} dk'\; k'\; \frac{e^{ik'R}}{k'^2-k^2-i\epsilon}\;. \tag{11.36}$$

Noting that

$$\frac{1}{2}\left[\frac{1}{k'-(k+i\epsilon)}+\frac{1}{k'+(k+i\epsilon)}\right] = \frac{k'}{k'^2-k^2-2ik\epsilon+\epsilon^2}\;, \tag{11.37}$$

we further rewrite[10]

$$G_0(E_k;\boldsymbol{r},\boldsymbol{r}') = \lim_{\epsilon\to 0^+} \frac{2i\mu}{2(2\pi)^2 R}\int_{-\infty}^{\infty} dk'\;\left[\frac{1}{k'-(k+i\epsilon)}+\frac{1}{k'+(k+i\epsilon)}\right] e^{ik'R}\;. \tag{11.38}$$

At this point we notice the following: if not for the factors of $i\epsilon$, the above integral would be ill defined. Since we are integrating over k' from $-\infty$ to $+\infty$, we would be bound to hit a value of $k'=k$. As it is, even if $k'=k$, the denominators are non-zero because of the factors of $i\epsilon$. This is known as "shifting the poles to the complex plane" – the poles used to be on the real axis, but now they're not. Hurray!

Let's look at this in a bit more detail. For the first term under the integral to hit a pole, we need $k'=k+i\epsilon$. This pole is in the positive complex half-plane (see the left panel in Fig. 11.1). For the other term under the integral to hit a pole, we need $k'=-(k+i\epsilon)$, and this pole is in the negative half-plane. This is more than just a curiosity: since we are already dealing with a complex integrand, we may try to figure out how we could extend the integration to a closed contour in the complex plane so that we could use the residue theorem to calculate the integral. If we succeed in doing that, then the location of the poles will be of key importance for the value of the integral.

To evaluate the integrals, we then take k' to be complex so that $k'=\mathrm{Re}[k']+i\mathrm{Im}[k']$. With this, Eq. (11.38) becomes

$$G_0(E_k;\boldsymbol{r},\boldsymbol{r}') = \lim_{\epsilon\to 0^+} \frac{2i\mu}{2(2\pi)^2 R}\int_{-\infty}^{\infty} dk'\;\left[\frac{1}{k'-(k+i\epsilon)}+\frac{1}{k'+(k+i\epsilon)}\right] e^{i\mathrm{Re}[k']R}e^{-\mathrm{Im}[k']R}\;. \tag{11.39}$$

Consequently, if we extend our integration (which originally was only along the real k' axis) by a semicircle of infinite radius in the upper complex plane (see Fig. 11.1), where $\mathrm{Im}[k']\to+\infty$,

[10] Here, we redefined the ϵ so that $2ik\epsilon\to i\epsilon$, and discarded the ϵ^2 term.

the contribution from that extension will equal exactly zero due to the factor $e^{-\mathrm{Im}[k']R}$. Thus, an integration over such defined closed contour will yield exactly the same result as before, as all contributions beyond the real axis vanish. *However*, since the integration now proceeds along a closed contour, we can use the residue theorem which states that any integration over a closed contour in the complex plane equals the sum of residues of those poles,

$$\oint_{\mathcal{C}} dz\ f(z) = 2\pi i \sum_{\substack{\text{poles } z_i \\ \text{inside } \mathcal{C}}} \mathrm{Res}(f, z_i)\ . \tag{11.40}$$

For a simple pole (*i.e.*, a pole which looks like $1/(x - x_0)$ rather than $1/(x - x_0)^n$ with $n \geq 2$), the residue is "everything multiplying the pole, evaluated at the pole." That is, if we are considering $\frac{f(x)}{x-a}$, the residue is $f(a)$. Note that since only poles inside the contour contribute to the integral, only the first term in Eq. (11.38) will contribute since we closed the contour in the upper half plane. Thus, the contributing pole is equal $k' = k + i\epsilon$ and the integral evaluates to $2\pi i e^{i(k+i\epsilon)R}$, so that

$$G_0(E_k; \boldsymbol{r}, \boldsymbol{r}') = \lim_{\epsilon \to 0^+} \frac{-2\mu}{4\pi R} e^{i(k+i\epsilon)R} = \frac{-2\mu}{4\pi R} e^{ikR}\ , \tag{11.41}$$

where now we were able to take the $\epsilon \to 0^+$ limit without any problems. Recalling that $\boldsymbol{R} \equiv \boldsymbol{r} - \boldsymbol{r}'$, we can further rewrite this as

$$G_0(E_k; \boldsymbol{r}, \boldsymbol{r}') = \frac{-2\mu}{4\pi |\boldsymbol{r} - \boldsymbol{r}'|} e^{ik|\boldsymbol{r}-\boldsymbol{r}'|}\ . \tag{11.42}$$

Thus we reach our goal of evaluating G_0.

Lecture sources: This lecture is mostly based on Bertulani & Danielewicz [6], with a small influence from gen. Schieck [1].

Lecture 12

Formal scattering theory II

Prerequisites: Lectures 6, 11.
Guiding question: ***How do we connect the Lippmann–Schwinger formalism to measurements?***

12.1 Two versions of $\hat{G}_0$

It turns out that the sign in front of $i\epsilon$ in $\hat{G}_0$, which we defined in Eq. (11.8), matters. Indeed, this sign determines which pole is enclosed by the integration contour, see Fig. 11.1: a simple substitution $i\epsilon \to -i\epsilon$ takes us from the pole structure shown in the left panel of that figure to the one shown on the right. Therefore, we now update our definition to include the two possible signs of the $i\epsilon$ term,

$$\hat{G}_0^{(\pm)}(E) \equiv \lim_{\epsilon\to 0^+} \frac{1}{E - \hat{H}_0 \pm i\epsilon} \ . \tag{12.1}$$

Then, carrying this sign throughout the entire calculation of the coordinate-space matrix element of $\hat{G}_0(E)$, performed in Sec. 11.4, yields

$$G_0^{(\pm)}(E_k; \boldsymbol{r}, \boldsymbol{r}') = \frac{-2\mu}{4\pi|\boldsymbol{r} - \boldsymbol{r}'|} e^{\pm ik|\boldsymbol{r}-\boldsymbol{r}'|} \ . \tag{12.2}$$

The two inverse operators $\hat{G}_0^{(\pm)}$ correspond to different states $|\Psi\rangle^{(\pm)}$, which means that we need to also distinguish between two such possible states in the Lippmann–Schwinger equations. Thus we now rewrite these equations as

$$\left|\Psi_{\boldsymbol{k}}^{(\pm)}\right\rangle = |\Phi_{\boldsymbol{k}}\rangle + \hat{G}_0^{(\pm)}(E)\hat{V}\left|\Psi_{\boldsymbol{k}}^{(\pm)}\right\rangle \ , \tag{12.3}$$

$$\left|\Psi_{\boldsymbol{k}}^{(\pm)}\right\rangle = \left(1 + \hat{G}^{(\pm)}(E)\hat{V}\right)|\Phi_{\boldsymbol{k}}\rangle \ . \tag{12.4}$$

Here, $\left|\Psi_{\boldsymbol{k}}^{(\pm)}\right\rangle$ are solutions of the same equation (characterized by some specific $\hat{V}$), with the same energy (characterized by some specific k), but with different boundary conditions. In the following, we will identify what these different boundary conditions are and how we connect the abstract solutions $\left|\Psi_{\boldsymbol{k}}^{(\pm)}\right\rangle$ to the experiment.

12.2 Green's functions

We can take one of the Lippmann–Schwinger equations, say Eq. (12.3), insert two unit operators $\mathbb{1}$ in terms of the coordinate-space eigenvalues, and multiply both sides from the left by $\langle \boldsymbol{r}|$,

$$\left\langle \boldsymbol{r}\middle|\Psi_{\boldsymbol{k}}^{(\pm)}\right\rangle = \langle \boldsymbol{r}|\Phi_{\boldsymbol{k}}\rangle + \langle \boldsymbol{r}|\,\hat{G}_0^{(\pm)}(E)\mathbb{1}V\mathbb{1}\left|\Psi_{\boldsymbol{k}}^{(\pm)}\right\rangle \tag{12.5}$$

$$= \langle \boldsymbol{r}|\Phi_{\boldsymbol{k}}\rangle + \langle \boldsymbol{r}|\,\hat{G}_0^{(\pm)}(E)\left(\int d^3r'\ \left|\boldsymbol{r}'\right\rangle\left\langle \boldsymbol{r}'\right|\right)\hat{V}\left(\int d^3r''\ \left|\boldsymbol{r}''\right\rangle\left\langle \boldsymbol{r}''\right|\right)\left|\Psi_{\boldsymbol{k}}^{(\pm)}\right\rangle \tag{12.6}$$

$$= \langle \boldsymbol{r}|\Phi_{\boldsymbol{k}}\rangle + \int d^3r' \int d^3r''\ \langle \boldsymbol{r}|\,\hat{G}_0^{(\pm)}(E)\left|\boldsymbol{r}'\right\rangle\left\langle \boldsymbol{r}'\right|\hat{V}\left|\boldsymbol{r}''\right\rangle\left\langle \boldsymbol{r}''\middle|\Psi_{\boldsymbol{k}}^{(\pm)}\right\rangle\ . \tag{12.7}$$

Acting with $\langle \boldsymbol{r}|$ from the left on a state vector produces its coordinate-space projection, so that $\left\langle \boldsymbol{r}\middle|\Psi_{\boldsymbol{k}}^{(\pm)}\right\rangle = \Psi_{\boldsymbol{k}}^{(\pm)}(\boldsymbol{r})$ and $\langle \boldsymbol{r}|\Phi_{\boldsymbol{k}}\rangle = \Phi_{\boldsymbol{k}}(\boldsymbol{r})$, while acting with a $\langle \boldsymbol{r}|$ from the left and a $|\boldsymbol{r}'\rangle$ from the right on an operator produces its matrix element between $\boldsymbol{r}'$ and $\boldsymbol{r}$, as in $\langle \boldsymbol{r}|\,\hat{G}_0^{(\pm)}(E)\,|\boldsymbol{r}'\rangle = G_0^{(\pm)}(E_k;\boldsymbol{r},\boldsymbol{r}')$. But then, what is $\langle \boldsymbol{r}'|\,\hat{V}\,|\boldsymbol{r}''\rangle$?

In the coordinate basis, the operation of $\hat{V}$ is equivalent to multiplying by $V(\boldsymbol{r})$, *i.e.,* $\hat{V}\psi(\boldsymbol{r}) = V(\boldsymbol{r})\psi(\boldsymbol{r})$, which makes it easy to forget that $\hat{V}$ is an operator. The action of $\hat{V}$ may be, however, different in other bases. Moreover, the potential can also be non-local, $V(\boldsymbol{r},\boldsymbol{r}')$. In a more precise notation, $V(\boldsymbol{r},\boldsymbol{r}') = \langle \boldsymbol{r}|\,\hat{V}\,|\boldsymbol{r}'\rangle$ is the representation of the potential operator $\hat{V}$ in the coordinate basis. For local potentials, we have $\langle \boldsymbol{r}|\,\hat{V}\,|\boldsymbol{r}'\rangle = V(\boldsymbol{r})\delta^{(3)}(\boldsymbol{r}-\boldsymbol{r}')$. With this, assuming a local potential so that $\langle \boldsymbol{r}'|\,V\,|\boldsymbol{r}''\rangle = V(\boldsymbol{r}')\delta^{(3)}(\boldsymbol{r}'-\boldsymbol{r}'')$, the Lippmann–Schwinger equation in the coordinate basis becomes an integral equation,

$$\Psi_{\boldsymbol{k}}^{(\pm)}(\boldsymbol{r}) = \Phi_{\boldsymbol{k}}(\boldsymbol{r}) + \int d^3r'\ G_0^{(\pm)}(E_k;\boldsymbol{r},\boldsymbol{r}')V(\boldsymbol{r}')\Psi_{\boldsymbol{k}}^{(\pm)}(\boldsymbol{r}')\ . \tag{12.8}$$

Similarly, we can obtain

$$\Psi_{\boldsymbol{k}}^{(\pm)}(\boldsymbol{r}) = \Phi_{\boldsymbol{k}}(\boldsymbol{r}) + \int d^3r'\ G^{(\pm)}(E_k;\boldsymbol{r},\boldsymbol{r}')V(\boldsymbol{r}')\Phi_{\boldsymbol{k}}(\boldsymbol{r}')\ . \tag{12.9}$$

This makes it clear that the operators $\hat{G}_0^{(\pm)}(E)$ are *Green's functions*: mathematical objects which operationally take a localized source, here $V(\boldsymbol{r}')\Psi_{\boldsymbol{k}}^{(\pm)}(\boldsymbol{r}')$ or $V(\boldsymbol{r}')\Phi_{\boldsymbol{k}}(\boldsymbol{r}')$, and determine how it affects the solution $\Psi_{\boldsymbol{k}}^{(\pm)}(\boldsymbol{r})$ at $\boldsymbol{r}$. Then, Eqs. (12.8) and (12.9) integrate over contributions from such sources over the entire space. Further intuition can be gained from expanding the free Lippmann–Schwinger equation, Eq. (12.8), in a Born series,

$$\Psi_{\boldsymbol{k}}^{(\pm)}(\boldsymbol{r}) = \Phi_{\boldsymbol{k}}(\boldsymbol{r}) + \int d^3r'\ G_0^{(\pm)}(E_k;\boldsymbol{r},\boldsymbol{r}')V(\boldsymbol{r}')\Phi_{\boldsymbol{k}}(\boldsymbol{r}') \tag{12.10}$$

$$+ \int d^3r' \int d^3r''\ G_0^{(\pm)}(E_k;\boldsymbol{r},\boldsymbol{r}')V(\boldsymbol{r}')G_0^{(\pm)}(E_k;\boldsymbol{r}',\boldsymbol{r}'')V(\boldsymbol{r}'')\Phi_{\boldsymbol{k}}(\boldsymbol{r}'') + \ldots \tag{12.11}$$

Intuitively, we can then interpret the role of the Green's function $G_0^{(\pm)}$ in, *e.g.*, the second-order term as taking the wave from its scattering at point $\boldsymbol{r}''$ to its next scattering at point $\boldsymbol{r}'$, and then to the measurement point at $\boldsymbol{r}$. This interpretation is sketched in Fig. 12.1, and it is especially appealing as between the scatterings, the propagation is that of a free wave, fitting the nature of G_0. Now, since both the potential and the wave are continuous concepts, the incident wave interacts with the potential (scattering center) at every point in space, and its the combined influence of all these interactions (*i.e.*, integration) that produces the resulting wave $\Psi_{\boldsymbol{k}}^{(\pm)}(\boldsymbol{r})$.

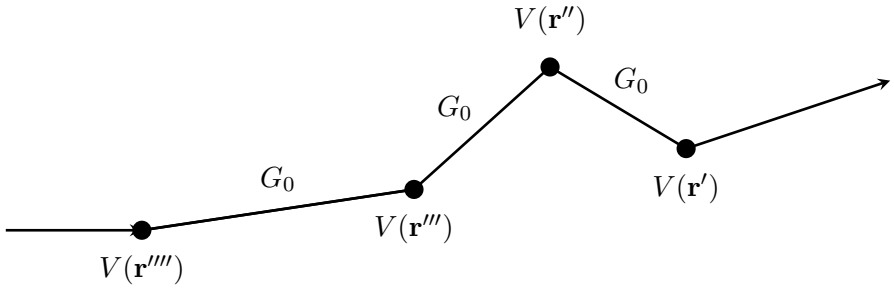

Figure 12.1: Intuitive picture of the propagation of a wave between successive scatterings.

12.2.1 Green's functions are everywhere

The coordinate-space representations of Green's functions we obtained satisfy

$$\left(E_k + \frac{1}{2\mu}\nabla^2_{\boldsymbol{r}}\right) G_0^{(\pm)}(E_k;\boldsymbol{r},\boldsymbol{r}') = \delta^{(3)}(\boldsymbol{r}-\boldsymbol{r}') \ , \tag{12.12}$$

$$\left(E_k + \frac{1}{2\mu}\nabla^2_{\boldsymbol{r}} - V(r)\right) G^{(\pm)}(E_k;\boldsymbol{r},\boldsymbol{r}') = \delta^{(3)}(\boldsymbol{r}-\boldsymbol{r}') \ . \tag{12.13}$$

This much should be clear from the way we defined $\hat{G}_0^{(\pm)}$ and $\hat{G}^{(\pm)}$ as the inverse operators of $\hat{H}_0$ and $\hat{H}$, respectively. However, making this observation allows us to connect the Green functions to intuition we might have from other branches of physics, in particular from electrodynamics. We know that in vacuum, the Maxwell's laws for the electric field $\boldsymbol{E}(\boldsymbol{r})$ are

$$\nabla\cdot\boldsymbol{E}(\boldsymbol{r}) = \frac{\rho(\boldsymbol{r})}{\epsilon_0} \quad \text{and} \quad \nabla\times\boldsymbol{E}(\boldsymbol{r}) = 0 \ . \tag{12.14}$$

The latter implies that the electric field can be written as a gradient of a scalar potential $V(\boldsymbol{r})$, $\boldsymbol{E}(\boldsymbol{r}) = -\nabla V(\boldsymbol{r})$, from which we immediately obtain the Poisson equation,

$$\nabla^2 V(\boldsymbol{r}) = -\frac{\rho(\boldsymbol{r})}{\epsilon_0} \ . \tag{12.15}$$

This equation asks: given the charge distribution $\rho(\boldsymbol{r})$, what is the potential $V(r)$ they produce? We can define a Green's function of the Laplacian operator ∇^2 as

$$\nabla^2 G(\boldsymbol{r},\boldsymbol{r}') = -\delta^{(3)}(\boldsymbol{r}-\boldsymbol{r}') \ , \tag{12.16}$$

i.e., as an inverse of the Laplacian (with a minus sign). With this, we can write the solution as

$$V(\boldsymbol{r}) = \frac{1}{\epsilon_0}\int d^3r' \ G(\boldsymbol{r},\boldsymbol{r}')\rho(\boldsymbol{r}') \ . \tag{12.17}$$

We can convince ourselves that this indeed is the solution by applying the Laplacian to it and checking that it satisfies the Poisson equation, Eq. (12.15). Indeed,

$$\nabla^2 V(\boldsymbol{r}) = \frac{1}{\epsilon_0}\int d^3r' \ \Big(\nabla^2 G(\boldsymbol{r},\boldsymbol{r}')\Big)\rho(\boldsymbol{r}') = -\frac{1}{\epsilon_0}\int d^3r' \ \delta^{(3)}(\boldsymbol{r}-\boldsymbol{r}')\rho(\boldsymbol{r}') = -\frac{\rho(\boldsymbol{r})}{\epsilon_0} \ , \tag{12.18}$$

where in the second equality we invoked Eq. (12.16). Just like in our case, in electrodynamics one can then find the explicit form of the Green's function, $G(\boldsymbol{r},\boldsymbol{r}') = (4\pi|\boldsymbol{r}-\boldsymbol{r}'|)^{-1}$. With this, given the charge distribution $\rho(\boldsymbol{r})$, the potential at any point in space is given by

$$V(\boldsymbol{r}) = \frac{1}{\epsilon_0}\int d^3r' \ \frac{\rho(\boldsymbol{r}')}{4\pi|\boldsymbol{r}-\boldsymbol{r}'|} \ . \tag{12.19}$$

The concept of Green's functions is extremely powerful and thus permeates physics. For example, a relativistic free scalar field $\phi(x)$ obeys the Klein-Gordon equation,

$$\left[\partial_\mu \partial^\mu + m^2\right]\phi(x) = 0 \ . \tag{12.20}$$

The Green function $\Delta_F(x-y)$ for this equation satisfies, by definition,

$$\left[\partial_\mu \partial^\mu + m^2\right]\Delta_F(x-y) = -\delta^{(4)}(x-y) \ . \tag{12.21}$$

One can solve for $\Delta_F(x-y)$ in momentum space,

$$\Delta_F(p) = \frac{i}{p^2 - m^2 + i\epsilon} \ , \tag{12.22}$$

where $p^2 = p_\mu p^\mu$, from which one can obtain its position-space representation by a Fourier transform,

$$\Delta_F(x-y) = \int \frac{d^4p}{(2\pi)^4} \, \frac{ie^{-ip\cdot(x-y)}}{p^2 - m^2 + i\epsilon} \ . \tag{12.23}$$

The Green function Δ_F is more often referred to as a *propagator*, because it describes how disturbances in a quantum field propagate between spacetime points. If one wants to compute any Feynman diagram, it is pretty certain that the calculation will involve integrals over propagators.

12.2.2 Properties of Green's functions and solutions

Given the defining equation for the free Green's function, Eq. (12.1), we can immediately see that

$$\left[\hat{G}_0^{\pm}(E)\right]^\dagger = \lim_{\epsilon\to 0^+}\left[\frac{1}{E - \hat{H}_0 \pm i\epsilon}\right]^{-1} = \lim_{\epsilon\to 0^+}\frac{1}{E - \hat{H}_0 \mp i\epsilon} = \hat{G}_0^{\mp}(E) \ , \tag{12.24}$$

and similarly for the full Green's function,

$$\left[\hat{G}^{\pm}(E)\right]^\dagger = \hat{G}^{\mp}(E) \ . \tag{12.25}$$

Then, taking the Lippmann–Schwinger equation with the full Green's function, Eq. (12.8), we can show that

$$\left[\Psi_{\boldsymbol{k}}^{(\pm)}(\boldsymbol{r})\right]^* = \Phi_{\boldsymbol{k}}^*(\boldsymbol{r}) + \int d^3r' \ \left[G^{(\pm)}(E_k;\boldsymbol{r},\boldsymbol{r}')\right]^\dagger V(\boldsymbol{r}')\Phi_{\boldsymbol{k}}^*(\boldsymbol{r}') \tag{12.26}$$

$$= \Phi_{\boldsymbol{k}}^*(\boldsymbol{r}) + \int d^3r' \ G^{(\mp)}(E_k;\boldsymbol{r},\boldsymbol{r}')V(\boldsymbol{r}')\Phi_{\boldsymbol{k}}^*(\boldsymbol{r}') \tag{12.27}$$

$$= \Phi_{-\boldsymbol{k}}(\boldsymbol{r}) + \int d^3r' \ G^{(\mp)}(E_k;\boldsymbol{r},\boldsymbol{r}')V(\boldsymbol{r}')\Phi_{-\boldsymbol{k}}(\boldsymbol{r}') \ , \tag{12.28}$$

where we used the fact that for the free wavefunction,

$$\Phi_{\boldsymbol{k}}^*(\boldsymbol{r}) = \left(\frac{e^{i\boldsymbol{k}\cdot\boldsymbol{p}}}{(2\pi)^{3/2}}\right)^* = \frac{e^{-i\boldsymbol{k}\cdot\boldsymbol{p}}}{(2\pi)^{3/2}} = \Phi_{-\boldsymbol{k}}(\boldsymbol{r}) \ . \tag{12.29}$$

Looking at the structure of Eq. (12.28), it is evident that we must have

$$\left[\Psi_{\boldsymbol{k}}^{(\pm)}(\boldsymbol{r})\right]^* = \Psi_{-\boldsymbol{k}}^{(\mp)}(\boldsymbol{r}) \ . \tag{12.30}$$

12.3 Scattering amplitude

Let us investigate the states $\left|\Psi_{\boldsymbol{p}}^{(\pm)}\right\rangle$. Starting again from the Lippmann–Schwinger equation, Eq. (12.3), this time inserting only one unit operator $\mathbb{1}$, and multiplying from the left by $\langle \boldsymbol{r}|$ yields

$$\Psi_{\boldsymbol{k}}^{(\pm)}(\boldsymbol{r}) = \Phi_{\boldsymbol{k}}(\boldsymbol{r}) + \langle \boldsymbol{r}|\, \hat{G}_0^{(\pm)}(E)\mathbb{1}\hat{V}\left|\Psi_{\boldsymbol{k}}^{(\pm)}\right\rangle \tag{12.31}$$

$$= \Phi_{\boldsymbol{k}}(\boldsymbol{r}) + \langle \boldsymbol{r}|\, \hat{G}_0^{(\pm)}(E)\left(\int d^3r'\ \left|\boldsymbol{r}'\right\rangle\left\langle \boldsymbol{r}'\right|\right)\hat{V}\left|\Psi_{\boldsymbol{k}}^{(\pm)}\right\rangle \tag{12.32}$$

$$= \Phi_{\boldsymbol{k}}(\boldsymbol{r}) + \int d^3r'\ \langle \boldsymbol{r}|\, \hat{G}_0^{(\pm)}(E)\left|\boldsymbol{r}'\right\rangle\left\langle \boldsymbol{r}'\right|\hat{V}\left|\Psi_{\boldsymbol{k}}^{(\pm)}\right\rangle \tag{12.33}$$

$$= \Phi_{\boldsymbol{k}}(\boldsymbol{r}) - \frac{2\mu}{4\pi}\int d^3r'\ \frac{e^{\pm ik|\boldsymbol{r}-\boldsymbol{r}'|}}{|\boldsymbol{r}-\boldsymbol{r}'|}\left\langle \boldsymbol{r}'\right|\hat{V}\left|\Psi_{\boldsymbol{k}}^{(\pm)}\right\rangle\ , \tag{12.34}$$

where we have used the explicit coordinate-basis form of the free Green's function, Eq. (12.2). Since we want to apply this formalism to scattering problems, we now take the asymptotic limit, $|\boldsymbol{r}| \to \infty$. One can then replace

$$\frac{1}{|\boldsymbol{r}-\boldsymbol{r}'|} \to \frac{1}{r}\ . \tag{12.35}$$

As for the exponential, we first expand and then take the limit[1],

$$\lim_{|\boldsymbol{r}|\to\infty} e^{\pm ik|\boldsymbol{r}-\boldsymbol{r}'|} = \lim_{|\boldsymbol{r}|\to\infty} e^{\pm ik\sqrt{r^2-2\boldsymbol{r}\cdot\boldsymbol{r}'+r'^2}} = \lim_{|\boldsymbol{r}|\to\infty} e^{\pm ikr\sqrt{1-\left(2\frac{\hat{\boldsymbol{r}}\cdot\boldsymbol{r}'}{r}-\left(\frac{r'}{r}\right)^2\right)}} \tag{12.36}$$

$$\approx \lim_{|\boldsymbol{r}|\to\infty} e^{\pm ikr\left(1-\frac{\hat{\boldsymbol{r}}\cdot\boldsymbol{r}'}{r}+\frac{1}{2}\left(\frac{r'}{r}\right)^2\right)} \approx e^{\pm i\left(kr-k\hat{\boldsymbol{r}}\cdot\boldsymbol{r}'\right)} = e^{\pm ikr}e^{\mp i\boldsymbol{k}'\cdot\boldsymbol{r}'}\ , \tag{12.37}$$

where we have defined $\boldsymbol{k}' \equiv k\hat{\boldsymbol{r}}$. With this, Eq. (12.34) becomes

$$\lim_{|\boldsymbol{r}|\to\infty} \Psi_{\boldsymbol{k}}^{(\pm)}(\boldsymbol{r}) = \Phi_{\boldsymbol{k}}(\boldsymbol{r}) + \frac{e^{\pm ikr}}{r}\left(-\frac{2\mu}{4\pi}\int d^3r'\ e^{\mp i\boldsymbol{k}'\cdot\boldsymbol{r}'}\left\langle \boldsymbol{r}'\right|\hat{V}\left|\Psi_{\boldsymbol{k}}^{(\pm)}\right\rangle\right)\ . \tag{12.38}$$

Noticing that the free wavefunction is

$$\phi_{\pm\boldsymbol{k}}(\boldsymbol{r}) = \frac{e^{\pm i\boldsymbol{k}\cdot\boldsymbol{r}}}{(2\pi)^{3/2}}\ , \tag{12.39}$$

we can rewrite Eq. (12.38) as

$$\lim_{|\boldsymbol{r}|\to\infty} \Psi_{\boldsymbol{k}}^{(\pm)}(\boldsymbol{r}) = \frac{e^{i\boldsymbol{k}\cdot\boldsymbol{r}}}{(2\pi)^{3/2}} + \frac{e^{\pm ikr}}{r}\left(-\frac{2\mu}{4\pi}(2\pi)^{3/2}\int d^3r'\ \Phi_{\mp\boldsymbol{k}'}(\boldsymbol{r}')\left\langle \boldsymbol{r}'\right|\hat{V}\left|\Psi_{\boldsymbol{k}}^{(\pm)}\right\rangle\right) \tag{12.40}$$

$$= \frac{1}{(2\pi)^{3/2}}\left[e^{i\boldsymbol{k}\cdot\boldsymbol{r}} + \frac{e^{\pm ikr}}{r}\left(-\frac{2\mu}{4\pi}(2\pi)^3\int d^3r'\ \left\langle \Phi_{\pm\boldsymbol{k}'}\right|\left.\boldsymbol{r}'\right\rangle\left\langle \boldsymbol{r}'\right|\hat{V}\left|\Psi_{\boldsymbol{k}}^{(\pm)}\right\rangle\right)\right]\ , \tag{12.41}$$

where in the second equality we used the fact that

$$\Phi_{\mp\boldsymbol{k}'}(\boldsymbol{r}') = \Phi^*_{\pm\boldsymbol{k}'}(\boldsymbol{r}') = \left\langle \Phi_{\pm\boldsymbol{k}'}\right|\left.\boldsymbol{r}'\right\rangle \tag{12.42}$$

[1]Here, by "taking the limit" we mean "discard terms which are negligible in comparison."

Finally, invoking the resolution of identity in the coordinate basis, we obtain

$$\lim_{|\boldsymbol{r}|\to\infty} \Psi_{\boldsymbol{k}}^{(\pm)}(\boldsymbol{r}) = \frac{1}{(2\pi)^{3/2}}\left[e^{i\boldsymbol{k}\cdot\boldsymbol{r}} + \frac{e^{\pm ikr}}{r}\left(-\frac{2\mu}{4\pi}(2\pi)^3\left\langle \Phi_{\pm\boldsymbol{k}'}\middle|\hat{V}\middle|\Psi_{\boldsymbol{k}}^{(\pm)}\right\rangle\right)\right] . \tag{12.43}$$

In summary, by using the explicit coordinate-basis form of the free Green's function $G_0^{(\pm)}(E)$, Eq. (12.2), in the Lippmann–Schwinger equation, Eq. (12.3), we were able to arrive at the asymptotic expression for the solution of the potential problem. This solution is a sum of a plane wave and a spherical wave multiplied by the matrix element of the potential operator between a plane wave and the solution $\left|\Psi_{\boldsymbol{k}}^{\pm}\right\rangle$. Choosing the + sign in $(\pm)$, we see that $\left|\Psi_{\boldsymbol{k}}^{+}\right\rangle$ describes a solution with an *outgoing* spherical wave, which is the solution adequate for a scattering problem. A direct comparison with the asymptotic ansatz for the scattered wavefunction[2], Eq. (6.16), makes it clear that the scattering amplitude is given by

$$f(\theta,\phi) = -4\mu\pi^2\left\langle \Phi_{\boldsymbol{k}'}\middle|\hat{V}\middle|\Psi_{\boldsymbol{k}}^{(+)}\right\rangle , \tag{12.44}$$

where θ is the observation angle, equal to the angle between the initial ($\boldsymbol{k}$) and final ($\boldsymbol{k}'$) wavevectors. From here, it is straightforward to make a connection with experimental measurements, as the differential cross section is given by $d\sigma/d\Omega = |f(\theta)|^2$, as we derived in Eq. (6.68).

12.4 The importance of the developed formalism

We have now developed a quite advanced theoretical framework.. First, we introduced the inverse operators $\hat{G}_0$ and $\hat{G}$, Eqs. (11.8) and (11.13), in order to arrive at the Lippmann–Schwinger equations, Eqs. (11.10) anc (11.14). Then, we devoted quite some time to compute the explicit form of $\hat{G}_0$ in the coordinate space, Eq. (11.42). In this Lecture, we realized that there are two versions of the inverse operator $\hat{G}_0^{(\pm)}$, Eq. (12.1), corresponding to an outgoing and incoming solution, and finally we used the Lippmann–Schwinger equations together with the explicit form of $\hat{G}_0^{(+)}$, Eq. (12.2), considered in the asymptotic limit of $r \to \infty$, to obtain an expression for the scattering amplitude $f(\theta,\phi)$, Eq. (12.44). What all this effort really worth it?

The answer is a resounding "yes," and to see that, let us recap our history with the scattering amplitude $f(\theta,\phi)$. We first encountered the scattering amplitude in Lecture 6, where it was introduced as the amplitude modulating the contribution of the scattered spherical wave to the asymptotic wavefunction *ansatz*, Eq. (6.16). Then, in Eq. (6.68) we connected the differential cross section to the modulus squared of $f(\theta)$. In Lecture 8, we derived an expression for the scattering amplitude in terms of the S-matrix elements, Eq. (8.15), or equivalently in terms of phase shifts, Eqs. (8.16) and (8.17). Since phase shifts can be computed from matching the solutions of the Schrödinger equation at the boundary separating the region where the potential is nonzero from the region where potential is zero, Eq. (7.50), this constituted the first direct connection between the theory (wavefunctions) and the experiment (the cross section through the modulus of the scattering amplitude). Then, by integrating the radial Schrödinger equation, we obtained the scattering phase shift in terms of an integral over a product of the potential U, the free radial function $\hat{\jmath}_l$, and the full solution in the region with the potential u_l, Eq. (8.32), was the first case of directly

[2]Note that at the time of Lecture 6, we decided not to bother with normalizing the free planes wave by $(2\pi)^{-3/2}$, while within our development of the formal scattering theory in Lectures 11-13 we do use that normalization. As noted already in Lecture 6, an overall normalization constant does not affect the result, which is why we pulled $(2\pi)^{-3/2}$ in front of everything in Eq. (12.43).

connecting $f(\theta,\phi)$ with the form of the potential. In Lecture 10, we computed the exact scattering amplitude for Coulomb scattering, Eq. (10.38), which also directly connected $f(\theta,\phi)$ with the form of the potential (through the Sommerfeld parameter η). Finally, above we considered the asymptotic limit of the free Lippmann–Schwinger equation, Eq. (12.3), to eventually arrive at the scattering amplitude in terms of a matrix element of the potential operator $\hat{V}$, Eq. (12.44).

This is a major result: now, given a potential operator $\hat{V}$ and the full wavefunction $|\Psi\rangle_{\boldsymbol{k}^{(+)}}$, we are able to extract the scattering amplitude $f(\theta,\phi)$. Of course, the knowledge of the full wavefunction is still a high ask. However, using the Born series, Eq. (11.16), we can start from this exact result and make reasonable approximations to make the problem manageable. Thus, we now have at our disposal a *practical* way to calculate the scattering amplitude.

12.5 Momentum transfer, length scales, and scattering angles

Let us now gain insights about the relevant scales in scattering processes.

In-class Activity 12a: Born approximation

As shown in Sec. (11.2), the 1st Born approximation, Eq. (11.17), is obtained by keeping only the first non-trivial term in the Born series, Eq. (11.16). In this case, the expression for the scattering amplitude, Eq. (12.44), reduces to

$$f(\theta,\phi) = -4\mu\pi^2 \left\langle \Phi_{\boldsymbol{k}'} \middle| \hat{V} \middle| \Phi_{\boldsymbol{k}} \right\rangle \ .$$

Assuming a local potential, use the resolution of identity to obtain an expression for $f(\theta)$ in the coordinate basis. Customarily, one introduces $\boldsymbol{q} = \boldsymbol{k}' - \boldsymbol{k}$ in the final expression.

Solution

We take the expression above and insert two resolutions of identity in the coordinate basis,

$$\begin{aligned}
f(\theta,\phi) &= -4\mu\pi^2 \langle \Phi_{\boldsymbol{k}'} | \, \mathbb{1}\hat{V}\mathbb{1} \, | \Phi_{\boldsymbol{k}} \rangle && (12.45)\\
&= -4\mu\pi^2 \langle \Phi_{\boldsymbol{k}'} | \left(\int d^3r' \ |\boldsymbol{r}'\rangle \langle \boldsymbol{r}'| \right) \hat{V} \left(\int d^3r \ |\boldsymbol{r}\rangle \langle \boldsymbol{r}| \right) |\Phi_{\boldsymbol{k}}\rangle && (12.46)\\
&= -4\mu\pi^2 \int d^3r' \int d^3r \ \langle \Phi_{\boldsymbol{k}'} | \boldsymbol{r}' \rangle \langle \boldsymbol{r}' | \hat{V} | \boldsymbol{r} \rangle \langle \boldsymbol{r} | \Phi_{\boldsymbol{k}} \rangle && (12.47)\\
&= -4\mu\pi^2 \frac{1}{(2\pi)^3} \int d^3r' \int d^3r \ e^{-i\boldsymbol{k}'\cdot\boldsymbol{r}'} V(\boldsymbol{r}) \delta^{(3)}(\boldsymbol{r}-\boldsymbol{r}') e^{i\boldsymbol{k}\cdot\boldsymbol{r}} && (12.48)\\
&= -\frac{\mu}{2\pi} \int d^3r \ e^{-i\boldsymbol{q}\cdot\boldsymbol{r}} V(\boldsymbol{r}) = -\frac{\mu}{2\pi} \tilde{V}(\boldsymbol{q}) \ , && (12.49)
\end{aligned}$$

where

$$\tilde{V}(\boldsymbol{q}) \equiv \int d^3r \ e^{-i\boldsymbol{q}\cdot\boldsymbol{r}} V(\boldsymbol{r}) \qquad (12.50)$$

is the Fourier transform[a] of $V(\boldsymbol{r})$ evaluated at the momentum transfer $\boldsymbol{q}$.

[a] Note that we define the Fourier transform without any factors of 2π in front. Other equivalent normalization schemes exist; the key is to be consistent.

In the example above we see that scattering at a given angle probes the potential at a particular momentum transfer $\boldsymbol{q} = \boldsymbol{k} - \boldsymbol{k}'$, *i.e.*, at a particular difference between the initial and final momentum. Since conservation of energy requires $|\boldsymbol{k}| = |\boldsymbol{k}'| = k$, we have

$$q = |\boldsymbol{k} - \boldsymbol{k}'| = \sqrt{2k^2 - 2k^2\cos\theta} = 2k\sin\left(\frac{\theta}{2}\right) , \tag{12.51}$$

where we have used $1 - \cos\theta = 2\sin^2\left(\frac{\theta}{2}\right)$. Thus, large-angle scattering corresponds to large q, while small-angle scattering corresponds to small q.

Moreover, large-angle scattering probes short-distance structure of the potential, whereas small-angle scattering probes long-range structure. This follows directly from the Fourier transform, Eq. (12.50), appearing in the first Born approximation: large $\boldsymbol{q}$ selects short-wavelength (short-distance) components of $V(\boldsymbol{r})$. How so? This is the "work" of the exponential factor in the integrand, $e^{-i\boldsymbol{q}\cdot\boldsymbol{r}} = e^{-iqr\cos\theta}$, which oscillates on a spatial scale of order $1/q$ (since we need $qr \sim 2\pi \sim 1$ for one full oscillation). If q is large, this factor oscillates rapidly as a function of $\boldsymbol{r}$, and those oscillations lead to cancellations when integrated over regions where $V(\boldsymbol{r})$ varies slowly (to visualize this, consider a limiting case where $V(\boldsymbol{r})$ is simply constant over a region where the exponential varies rapidly). The only regions which substantially contribute to the integral are then either those where $V(\boldsymbol{r})$ also varies rapidly (on length scales comparable with or smaller than $1/q$), or at small values of r, $r \lesssim 1/q$, which suppress the rapid oscillations.

Consequently, large values of the transferred momentum q are sensitive to structures in the potential on length scales $r \lesssim 1/q$, which means that large q probes small distances r (note that this is true regardless whether the potential $V(r)$ has some rapidly varying region or not). Conversely, if q is small, then $e^{-i\boldsymbol{q}\cdot\boldsymbol{r}} \approx 1$ throughout the support of the potential, so that the Fourier transform essentially reduces an integral over $V(\boldsymbol{r})$. Such an integral is sensitive to the entire spatial extent of the potential, which is equivalent to saying that small values of q probe long-distance structure.

In-class Activity 12b: Length scales and angles

In Rutherford scattering, we tend to consider only the charge of the nucleus. However, a gold atom in a thin gold foil has all of its electrons intact. In what kinematic regions should we see the effects of the electron cloud?

Solution

From the discussion above, we know that large momentum transfers probe small length scales, while small momentum transfers probe large length-scales. As a result, if we want to probe primarily the effects due to the nuclear charge (a relatively short-distance structure), we must consider large values of q. Conversely, if we want to probe the effects of the atom as a whole (where the electron cloud leads to screening of the nucleus' charge), we must consider small values of q. From the dependence of q on the scattering angle, Eq. (12.51), it's clear that a small momentum transfer can be achieved either by using a projectile with a low momentum k or considering small scattering angles θ. Since in the Rutherford experiment the incident energies of the α particles vary only slightly (between 4 and 6 MeV), it's clear that in this case we can only observe the electron screening effects at very forward scattering angles, $\theta \approx 0$.

The 1st Born approximation is an example linear response (*i.e.*, first-order perturbation theory). Within this approach, the potential acts only once, transferring momentum $\boldsymbol{q}$. The scattering amplitude is then linear in V and, consequently, different Fourier components of the potential do not mix. This is in contrast to higher orders in perturbation theory, where the potential enters the equations

multiple times. In that case, the intermediate propagation between interaction points (corresponding in the Born series, Eq. (11.16), to the presence of $\hat{G}_0(E)$ between two potential operators $\hat{V}$) introduces convolutions in momentum space and mixes different momentum components.

Finally, note that working with the Fourier transform of $V(\boldsymbol{r})$ is natural for scattering experiments, which can only access information about the momenta of the scattering particles. The measured incoming and outgoing momenta determine the momentum transfer $\boldsymbol{q}$ and thus directly probe the momentum-space representation of the potential $\tilde{V}(\boldsymbol{q})$.

Lecture sources: This lecture is mostly based on Bertulani & Danielewicz [6].

Lecture 13

Formal scattering theory III

Prerequisites: Lectures 6, 7, 8, 11, 12.
Guiding question: ***Does the operator formalism let us do something we couldn't do before?***

13.1 The transition matrix

We have seen that the asymptotic expression for the solution of our potential problem, Eq. (12.43), as well as the scattering amplitude, Eq. (12.44), contain a contribution from the matrix element of the potential operator between the final free state with a wavevector pointing along the observation direction, $|\Phi\rangle_{\boldsymbol{k}'}$, and the full scattering state $\left|\Psi_{\boldsymbol{k}}^{\pm}\right\rangle$. Conceptually, the *mixed matrix element* $\left\langle \Phi_{\boldsymbol{k}'}\middle|\hat{V}\middle|\Psi_{\boldsymbol{k}}^{(+)}\right\rangle$ is inconvenient because while the free states are known *a priori*, the full scattering state contains the effect of $\hat{V}$. For practical calculations, it is preferable to express the scattering amplitude in terms of matrix elements taken between initial and final *free states*. While we do not yet know the explicit form of such matrix elements, we can already define them formally.

13.1.1 Definition of the T-matrix and the scattering amplitude

We define the *transition matrix* T, also called the *T-matrix*, by demanding that its elements satisfy

$$T_{\boldsymbol{k}'\boldsymbol{k}} \equiv \left\langle \Phi_{\boldsymbol{k}'}\middle|\hat{T}(E)\middle|\Phi_{\boldsymbol{k}}\right\rangle \equiv \left\langle \Phi_{\boldsymbol{k}'}\middle|\hat{V}\middle|\Psi_{\boldsymbol{k}}^{(+)}\right\rangle \ . \tag{13.1}$$

Note that if $V = 0$, $T_{\boldsymbol{k}'\boldsymbol{k}} = 0$ – *i.e.*, there is no transition.

To obtain an equation for $\hat{T}(E)$, we first note that Eq. (13.1) implies that

$$\hat{T}(E)\,|\Phi_{\boldsymbol{k}}\rangle = \hat{V}\left|\Psi_{\boldsymbol{k}}^{(+)}\right\rangle \ . \tag{13.2}$$

Then we multiply the free Lippmann–Schwinger equation, Eq. (11.10), from the left by $\hat{V}$,

$$\hat{V}\left|\Psi_{\boldsymbol{k}}^{(+)}\right\rangle = \hat{V}\,|\Phi_{\boldsymbol{k}}\rangle + \hat{V}\hat{G}_0^{(+)}(E)\hat{V}\left|\Psi_{\boldsymbol{k}}^{(+)}\right\rangle \ . \tag{13.3}$$

Using Eq. (13.2), we immediately obtain

$$\hat{T}(E)\,|\Phi_{\boldsymbol{k}}\rangle = \hat{V}\,|\Phi_{\boldsymbol{k}}\rangle + \hat{V}\hat{G}_0^{(+)}(E)\hat{T}(E)\,|\Phi_{\boldsymbol{k}}\rangle \ . \tag{13.4}$$

Since the kets are the same in all terms, this is equivalent to the operator equation

$$\hat{T}(E) = \hat{V} + \hat{V}\hat{G}_0^{(+)}(E)\hat{T}(E) \ , \tag{13.5}$$

which is the *free Lippmann–Schwinger equation for the T-matrix*. Similarly, we can take the full Lippmann–Schwinger equation, Eq. (11.14), and also multiply it by $\hat{V}$ from the left, obtaining

$$\hat{V}\left|\Psi_{\boldsymbol{k}}^{(+)}\right\rangle = \hat{V}\left[1 + \hat{G}^{(+)}(E)\hat{V}\right]|\Phi_{\boldsymbol{k}}\rangle \ . \tag{13.6}$$

Using the definition of the $\hat{T}$ operator, Eq. (13.2), on the left-hand side, we get

$$\hat{T}(E)\,|\Phi_{\boldsymbol{k}}\rangle = \hat{V}\left[1 + \hat{G}^{(+)}(E)\hat{V}\right]|\Phi_{\boldsymbol{k}}\rangle \ , \tag{13.7}$$

which also can be cast in the form of the *full Lippmann–Schwinger equation for the $\hat{T}$ operator*,

$$\hat{T}(E) = \hat{V} + \hat{V}\hat{G}^{(+)}(E)\hat{V} \ . \tag{13.8}$$

We note that when we define the T-matrix $\hat{T}(E)$, the parameter E is simply the energy argument of the inverse operator $\hat{G}_0(E)$ or $\hat{G}(E)$ that appears in the Lippmann–Schwinger equations. At this stage, there is no requirement that the energy E coincides with the energies $E = \frac{k^2}{2m}$ and $E' = \frac{k'^2}{2m}$ of the external plane waves. While it may seem odd, it is perfectly allowed to consider matrix elements $\left\langle \Phi_{\boldsymbol{k}'}\middle|\hat{T}(E)\middle|\Phi_{\boldsymbol{k}}\right\rangle$ without imposing any relation between E and the external momenta.

When E is chosen to equal the physical scattering energy E_k, and when the external momenta satisfy the elastic condition $E_{k'} = E_k$, the T-matrix element is said to be *on-shell*[1]. Conversely, if these conditions are not imposed, we say $T(E)$ is *off-shell*.

Defining an operator which does not correspond to a physical state may seem preposterous. However, it *does* make sense, and in fact it is unavoidable in the Lippmann–Schwinger formalism. To see this, consider the free Lippmann–Schwinger equation for the T-matrix, Eq. (13.5). According to this formula and the definition of the T-matrix, Eq. (13.1), the $T_{\boldsymbol{k}',\boldsymbol{k}}$ matrix element is given by

$$\begin{aligned}
T_{\boldsymbol{k}'\boldsymbol{k}} &= \left\langle \Phi_{\boldsymbol{k}'}\middle|\hat{V}\middle|\Phi_{\boldsymbol{k}}\right\rangle + \langle\Phi_{\boldsymbol{k}'}|\,\hat{V}\hat{G}_0^{(+)}(E)\hat{T}(E)\,|\Phi_{\boldsymbol{k}}\rangle && (13.9)\\
&= V_{\boldsymbol{k}'\boldsymbol{k}} + \langle\Phi_{\boldsymbol{k}'}|\,\hat{V}\left(\int d^3q'\ \left|\Phi_{\boldsymbol{q}'}\right\rangle\left\langle\Phi_{\boldsymbol{q}'}\right|\right)\hat{G}_0^{(+)}(E)\left(\int d^3q\ \left|\Phi_{\boldsymbol{q}}\right\rangle\langle\Phi_{\boldsymbol{q}}|\right)\hat{T}(E)\,|\Phi_{\boldsymbol{k}}\rangle && (13.10)\\
&= V_{\boldsymbol{k}'\boldsymbol{k}} + \int d^3q' \int d^3q\ \langle\Phi_{\boldsymbol{k}'}|\,\hat{V}\left|\Phi_{\boldsymbol{q}'}\right\rangle\left\langle\Phi_{\boldsymbol{q}'}\right|\hat{G}_0^{(+)}(E)\,|\Phi_{\boldsymbol{q}}\rangle\,\langle\Phi_{\boldsymbol{q}}|\,\hat{T}(E)\,|\Phi_{\boldsymbol{k}}\rangle && (13.11)\\
&= V_{\boldsymbol{k}'\boldsymbol{k}} + \int d^3q\ V_{\boldsymbol{k}'\boldsymbol{q}}\frac{1}{E - E_q + i\epsilon}T_{\boldsymbol{q}\boldsymbol{k}}(E) \ , && (13.12)
\end{aligned}$$

where we used the fact that $\left\langle\Phi_{\boldsymbol{q}'}\right|\hat{G}_0^{(+)}(E)\,|\Phi_{\boldsymbol{q}}\rangle = \delta^{(3)}(\boldsymbol{q}-\boldsymbol{q}')(E - E_q + i\epsilon)^{-1}$, which can be deduced from the spectral decomposition of $\hat{G}_0(E)$, Eq. (11.26). The on-shell condition is that $E = E_k = E_{k'}$. However, the integral in the above equation is over q, which is entirely unconstrained. We not only allow unphysical momenta in the formalism – we integrate over *infinitely many of them* to get $T_{\boldsymbol{k}\boldsymbol{k}'}$.

The T-matrix element must be on-shell whenever it connects physically observable states. For example, given the definition of the T-matrix element, Eq. (13.1), and the scattering amplitude in terms of the mixed matrix element of $\hat{V}$, Eq. (12.44), we see that the scattering amplitude equals

$$f(\theta,\phi) = -4\mu\pi^2 T_{\boldsymbol{k}'\boldsymbol{k}}\big|_{\text{on-shell}} \ . \tag{13.13}$$

In this expression, because the T-matrix element connects observable states, it *must* be on-shell.

[1]The name reflects the fact that $E = k^2/2m$ defines a shell in momentum space, *i.e.*, a surface pointed to by all momenta whose magnitude equals k. For a physical $E = k^2/2m = k'^2/2m$, the matrix element $T_{\boldsymbol{k}'\boldsymbol{k}}(E)$ is characterized by momenta $\boldsymbol{k}'$ and $\boldsymbol{k}$ on the same shell.

13.1.2 What's the use of a T-matrix?

One may question: why introduce the T-matrix at all? At a first glance, it doesn't contain any information that wasn't already in the Lippmann–Schwinger equation. That's true, but the Lippmann–Schwinger equation solves for the state, while the T-matrix directly gives the scattering amplitude, which is the only part of the state that experiments ever see[2].

In general, it is useful to isolate elements of the theory which correspond to particular types of information. For example, in Lecture 6 we first derived the expression for the scattering cross-section in terms of incoming and outgoing probability currents, Eq. (6.38), and then we used that definition to show that the cross section is equal to the square of the scattering amplitude $f(\theta, \phi)$, Eq. (6.68). The latter equation does not contain any new information *per se*, but it surely helps us organize our understanding of what's happening, not to mention that it saves us having to calculate the incoming and outgoing currents each time[3]. With such perspective, it is useful to have an object like the T-matrix which helps us solidify our understanding of the quantum scattering problem by dividing it into smaller, more manageable, and also more meaningful parts. Moreover, there are situations where working with states becomes nearly impossible but the T-matrix approach still works, including many-body scattering and quantum field theory (QFT). In QFT, the scattered state literally does not exist as a normalizable object, however, the T-matrix remains well-defined.

13.2 The two-potential formula

When deriving the Lippmann–Schwinger equations in Sec. 11.2, we wrote the full Hamiltonian as a sum of the free-particle Hamiltonian and the potential operator,

$$\hat{H} = \hat{H}_0 + \hat{V} \ . \tag{13.14}$$

There are situations in which it may be convenient to separate the potential V into two parts[4],

$$V \to V + U \ . \tag{13.15}$$

An obvious example is given by problems with both Coulomb and nuclear interactions. As another example, many nuclear scattering problems can be treated as "something well known plus something we don't know that well," in which case dividing the potential into two parts may be advantageous if the part that is not known well can be treated as a perturbation about the part that is well understood.

13.2.1 Lippmann–Schwinger equations with distorted waves

Let us write

$$\hat{H} = \hat{H}_0 + \hat{V} + \hat{U} = \hat{H}_1 + \hat{U} \ , \tag{13.16}$$

[2] More precisely, experiments see cross sections, which are obtained by squaring the scattering amplitude.

[3] Likely, what historically happened was that people *were* calculating incoming and outgoing currents each time until somebody noticed a repeating pattern in the result. The Feynman diagrams – arguably a tremendously useful and intuitive abstraction of amplitudes for quantum processes – were introduced in exactly such circumstances.

[4] Here, we choose reusing the symbol V to describe one of the components of the potential over introducing a new variable to avoid clutter in our formulas when we come back to this subject when discussing direct reactions. If it helps, you can think ot this transformation as *adding* a new contribution to the potential U on top of the "old" potential V.

where we have defined

$$\hat{H}_1 \equiv \hat{H}_0 + \hat{V} \ . \tag{13.17}$$

With this, the free Lippmann–Schwinger equation, Eq. (11.10), becomes

$$\left|\Psi_{\boldsymbol{k}}^{(\pm)}\right\rangle = |\Phi_{\boldsymbol{k}}\rangle + \hat{G}_0^{(\pm)}(E)[V+U]\left|\Psi_{\boldsymbol{k}}^{(\pm)}\right\rangle \ , \tag{13.18}$$

while the full Lippmann–Schwinger equation, Eq. (11.14), transforms into

$$\left|\Psi_{\boldsymbol{k}}^{(\pm)}\right\rangle = \left[1 + \hat{\mathcal{G}}^{(\pm)}(E)[V+U]\right]|\Phi_{\boldsymbol{k}}\rangle \ , \tag{13.19}$$

where $\hat{G}_0(E)$ is the free-particle Green's function, Eq. (11.8), just as before, while

$$\hat{\mathcal{G}}^{(\pm)}(E) \equiv \lim_{\epsilon\to 0} \frac{1}{E - [\hat{H}_0 + \hat{V} + \hat{U}] \pm i\epsilon} \ . \tag{13.20}$$

The Hamiltonian $\hat{H}_1$ corresponds to some set of eigenfunctions $\left|\chi_{\boldsymbol{k}}^{(\pm)}\right\rangle$, which satisfy

$$(E - \hat{H}_1)\left|\chi_{\boldsymbol{k}}^{(\pm)}\right\rangle = 0 \ . \tag{13.21}$$

If the eigenfunctions $\left|\chi_{\boldsymbol{k}}^{(\pm)}\right\rangle$ are known, it may be preferable to use them in place of the plane waves in the Lippmann–Schwinger equations. First, setting $U = 0$ and replacing $\hat{H} \to \hat{H}_1$, we can just rewrite the original Lippmann–Schwinger equations in terms of $\left|\chi_{\boldsymbol{k}}^{(\pm)}\right\rangle$,

$$\left|\chi_{\boldsymbol{k}}^{(\pm)}\right\rangle = |\Phi_{\boldsymbol{k}}\rangle + \hat{G}_0^{(\pm)}(E)V\left|\chi_{\boldsymbol{k}}^{(\pm)}\right\rangle \ , \tag{13.22}$$

$$\left|\chi_{\boldsymbol{k}}^{(\pm)}\right\rangle = \left[1 + \hat{G}^{(\pm)}(E)V\right]|\Phi_{\boldsymbol{k}}\rangle \ , \tag{13.23}$$

where $\hat{G}^{(\pm)}$ is the Green's function for $\hat{H}_1$, *i.e.*, the same as the one defined in Eq. (11.13) with $\hat{H} \to \hat{H}_1$. With this, we now come back to the full problem, which is described by

$$(E - \hat{H}_1)\left|\Psi_{\boldsymbol{k}}^{(\pm)}\right\rangle = \hat{U}\left|\Psi_{\boldsymbol{k}}^{(\pm)}\right\rangle \ . \tag{13.24}$$

Repeating the steps in Sec. 11.2 but adjusted by taking $\hat{H}_0 \to \hat{H}_1$, we subtract Eq. (13.21) by sides, leading to

$$(E - \hat{H}_1)\left(\left|\Psi_{\boldsymbol{k}}^{(\pm)}\right\rangle - \left|\chi_{\boldsymbol{k}}^{(\pm)}\right\rangle\right) = \hat{U}\left|\Psi_{\boldsymbol{k}}^{(\pm)}\right\rangle \ . \tag{13.25}$$

Applying $\hat{G}^{(\pm)}(E)$ on both sides then yields

$$\left|\Psi_{\boldsymbol{k}}^{(\pm)}\right\rangle = \left|\chi_{\boldsymbol{k}}^{(\pm)}\right\rangle + \hat{G}^{(\pm)}(E)\hat{U}\left|\Psi_{\boldsymbol{k}}^{(\pm)}\right\rangle \ . \tag{13.26}$$

On the other hand, adding and subtracting $\hat{U}\left|\chi_{\boldsymbol{k}}^{(\pm)}\right\rangle$ on the right-hand side of Eq. (13.25) leads to

$$(E - \hat{H}_1)\left(\left|\Psi_{\boldsymbol{k}}^{(\pm)}\right\rangle - \left|\chi_{\boldsymbol{k}}^{(\pm)}\right\rangle\right) = \hat{U}\left(\left|\Psi_{\boldsymbol{k}}^{(\pm)}\right\rangle - \left|\chi_{\boldsymbol{k}}^{(\pm)}\right\rangle + \left|\chi_{\boldsymbol{k}}^{(\pm)}\right\rangle\right) \ . \tag{13.27}$$

Moving $\hat{U}\Big(\Big|\Psi_{\boldsymbol{k}}^{(\pm)}\Big\rangle - \Big|\chi_{\boldsymbol{k}}^{(\pm)}\Big\rangle\Big)$ to the left side then leads to

$$(E-\hat{H})\Big(\Big|\Psi_{\boldsymbol{k}}^{(\pm)}\Big\rangle - \Big|\chi_{\boldsymbol{k}}^{(\pm)}\Big\rangle\Big) = \hat{U}\Big|\chi_{\boldsymbol{k}}^{(\pm)}\Big\rangle \ , \tag{13.28}$$

to which we can apply $\hat{\mathcal{G}}^{(\pm)}(E)$ on both sides, yielding

$$\Big|\Psi_{\boldsymbol{k}}^{(\pm)}\Big\rangle = \Big[1+\hat{\mathcal{G}}^{(\pm)}(E)\hat{U}\Big]\Big|\chi_{\boldsymbol{k}}^{(\pm)}\Big\rangle \ . \tag{13.29}$$

In this context, the eigenvectors $\Big|\chi_{\boldsymbol{k}}^{(\pm)}\Big\rangle$ are called *distorted waves*, where the name derives from the visual that they are "waves distorted by V." The "updated" Lippmann–Schwinger equations, Eq. (13.26) and (13.29), are then expressed with respect to these distorted waves as opposed to the plane waves, which was the whole point of this exercise.

13.2.2 The T-matrix with distorted waves

If we follow the derivations of Lecture 12 with $\hat{V} \to \hat{\mathcal{V}} = \hat{V} + \hat{U}$, we will naturally get that the scattering amplitude $f(\theta)$ is proportional to the mixed matrix element of $\hat{V}+\hat{U}$,

$$f(\theta) = -\frac{2\mu}{4\pi}(2\pi)^{3/2}\Big\langle \Phi_{\boldsymbol{k}'}\Big|\hat{V}+\hat{U}\Big|\Psi_{\boldsymbol{k}}^{(+)}\Big\rangle \ . \tag{13.30}$$

It would be convenient to express the T-matrix element, defined in Eq. (13.1), with respect to the distorted waves $\Big|\chi_{\boldsymbol{k}}^{(\pm)}\Big\rangle$. Explicitly, we have

$$T_{\boldsymbol{k}'\boldsymbol{k}} \equiv \Big\langle \Phi_{\boldsymbol{k}'}\Big|\hat{V}+\hat{U}\Big|\Psi_{\boldsymbol{k}}^{(+)}\Big\rangle \ . \tag{13.31}$$

Using Eq. (13.22), we can rewrite the free wave as

$$|\Phi_{\boldsymbol{k}'}\rangle = \Big|\chi_{\boldsymbol{k}'}^{(-)}\Big\rangle - \hat{G}_0^{(-)}(E)V\Big|\chi_{\boldsymbol{k}'}^{(-)}\Big\rangle \ . \tag{13.32}$$

Using $(AB)^\dagger = B^\dagger A^\dagger$, $\big(|\psi\rangle\big)^\dagger = \langle\psi|$, and $\big(\hat{G}_0^{(\pm)}(E)\big)^\dagger = \hat{G}_0^{(\mp)}(E)$ (where the latter was shown in Sec. 12.2.2), we can take the Hermitian conjugate of Eq. (13.32),

$$\langle\Phi_{\boldsymbol{k}'}| = \Big\langle\chi_{\boldsymbol{k}'}^{(-)}\Big| - \Big\langle\chi_{\boldsymbol{k}'}^{(-)}\Big|V\hat{G}_0^{(+)}(E) \ , \tag{13.33}$$

where we used the fact that $\hat{V}$ is Hermitian[5]. With this, Eq. (13.31) becomes

$$T_{\boldsymbol{k}'\boldsymbol{k}} = \Big\langle\chi_{\boldsymbol{k}'}^{(-)}\Big|\hat{V}+\hat{U}\Big|\Psi_{\boldsymbol{k}}^{(+)}\Big\rangle - \Big\langle\chi_{\boldsymbol{k}'}^{(-)}\Big|V\hat{G}_0^{(+)}(E)\big[\hat{V}+\hat{U}\big]\Big|\Psi_{\boldsymbol{k}}^{(+)}\Big\rangle \ . \tag{13.34}$$

Using Eq. (13.18), we can see that

$$\hat{G}_0^{(+)}(E)[V+U]\Big|\Psi_{\boldsymbol{k}}^{(+)}\Big\rangle = \Big|\Psi_{\boldsymbol{k}}^{(+)}\Big\rangle - |\Phi_{\boldsymbol{k}}\rangle \ , \tag{13.35}$$

so that we get

$$T_{\boldsymbol{k}'\boldsymbol{k}} = \Big\langle\chi_{\boldsymbol{k}'}^{(-)}\Big|\hat{V}+\hat{U}\Big|\Psi_{\boldsymbol{k}}^{(+)}\Big\rangle - \Big\langle\chi_{\boldsymbol{k}'}^{(-)}\Big|V\Big|\Psi_{\boldsymbol{k}}^{(+)}\Big\rangle + \Big\langle\chi_{\boldsymbol{k}'}^{(-)}\Big|V\Big|\Phi_{\boldsymbol{k}}\Big\rangle \ . \tag{13.36}$$

[5]Note that it has to be, being a component of a Hamiltonian.

Since the middle term cancels with part of the first term, we then obtain

$$T_{\boldsymbol{k}'\boldsymbol{k}} = \left\langle \chi^{(-)}_{\boldsymbol{k}'} \middle| \hat{V} \middle| \Phi_{\boldsymbol{k}} \right\rangle + \left\langle \chi^{(-)}_{\boldsymbol{k}'} \middle| \hat{U} \middle| \Psi^{(+)}_{\boldsymbol{k}} \right\rangle \tag{13.37}$$

$$= \left\langle \Phi_{\boldsymbol{k}'} \middle| \hat{V} \middle| \chi^{(+)}_{\boldsymbol{k}} \right\rangle + \left\langle \chi^{(-)}_{\boldsymbol{k}'} \middle| \hat{U} \middle| \Psi^{(+)}_{\boldsymbol{k}} \right\rangle \ . \tag{13.38}$$

where the second line is an equivalent expression. The above formulae are known as the *two-potential formulae* or the *Gell-Mann–Goldberger relations*.

The *distorted wave Born approximation* (DWBA) then amounts to approximating $\left|\Psi^{(+)}_{\boldsymbol{k}}\right\rangle$ in the second term with $\left|\chi^{(+)}_{\boldsymbol{k}}\right\rangle$, so that

$$T_{\boldsymbol{k}'\boldsymbol{k}} = \left\langle \chi^{(-)}_{\boldsymbol{k}'} \middle| \hat{V} \middle| \Phi_{\boldsymbol{k}} \right\rangle + \left\langle \chi^{(-)}_{\boldsymbol{k}'} \middle| \hat{U} \middle| \chi^{(+)}_{\boldsymbol{k}} \right\rangle \tag{13.39}$$

$$= \left\langle \Phi_{\boldsymbol{k}'} \middle| \hat{V} \middle| \chi^{(+)}_{\boldsymbol{k}} \right\rangle + \left\langle \chi^{(-)}_{\boldsymbol{k}'} \middle| \hat{U} \middle| \chi^{(+)}_{\boldsymbol{k}} \right\rangle \ . \tag{13.40}$$

The approximation is called "Born" because it is of first order in potential U, and "distorted wave" because it uses the distorted waves $\left|\chi^{(+)}_{\boldsymbol{k}}\right\rangle$ instead of plane waves. DWBA is valid as long as $\hat{U}$ is weak compared to $\hat{V}$, so that $\left|\chi^{(+)}_{\boldsymbol{k}}\right\rangle$ is a good approximation of the full solution.

With the two-potential formula, Eq. (13.38), the scattering amplitude, Eq. (12.44), becomes

$$f(\theta) = -4\mu\pi^2 \left[\left\langle \Phi_{\boldsymbol{k}'} \middle| \hat{V} \middle| \chi^{(+)}_{\boldsymbol{k}} \right\rangle + \left\langle \chi^{(-)}_{\boldsymbol{k}'} \middle| \hat{U} \middle| \Psi^{(+)}_{\boldsymbol{k}} \right\rangle \right] . \tag{13.41}$$

Since presumably we know the wavefunctions $\left|\chi^{(+)}_{\boldsymbol{k}}\right\rangle$, it is natural to separate the first term by denoting it as $f_0(\theta)$,

$$f(\theta) = f_0(\theta) - 4\mu\pi^2 \left\langle \chi^{(-)}_{\boldsymbol{k}'} \middle| \hat{U} \middle| \Psi^{(+)}_{\boldsymbol{k}} \right\rangle \Bigg] \ . \tag{13.42}$$

Applying the DWBA then yields

$$f_{\mathrm{DWBA}}(\theta) = f_0(\theta) - 4\mu\pi^2 \left\langle \chi^{(-)}_{\boldsymbol{k}'} \middle| \hat{U} \middle| \chi^{(+)}_{\boldsymbol{k}} \right\rangle \Bigg] \ . \tag{13.43}$$

Inserting two resolutions of identity, together with the assumption that $\hat{U}$ is local, leads to

$$f_{\mathrm{DWBA}}(\theta) = f_0(\theta) - 4\mu\pi^2 \int d^3r \ \left(\chi^{(-)}_{\boldsymbol{k}'}\right)^*(\boldsymbol{r}) U(\boldsymbol{r}) \chi^{(+)}_{\boldsymbol{k}}(\boldsymbol{r}) \ . \tag{13.44}$$

Here we can answer the guiding question of this lecture: while the operator formalism might feel extremely abstract and removed from the experiment, it allows us to cleanly derive practical results which were not available before. The DWBA is an example of such a result – in principle, one *could* derive it without mentioning the word "operator," however, in such a case one would still be using operator methods (for example, a Green's function) without calling them as such.

Lecture sources: This lecture is based on Bertulani & Danielewicz [6].

Lecture 14

Formal scattering theory IV

Prerequisites: Lectures 7, 8, 11, 12, 13.
Guiding question: ***Actually, what is the S-matrix?***

In this lecture, we will formally derive the S-matrix and connect it to both the S-matrix element, introduced in Lecture 8, and the T-matrix, introduced in Lecture 13.

14.1 The evolution operator and the interaction picture

You don't need to read this and the next section if you are not interested in how the S-matrix is constructed. If this is the case, go straight to Sec. 14.2.2. On the other hand, while the derivation requires introducing a couple of concepts which may be new to you, they are rather straightforward and I am confident that you can follow all of the steps below if you have the time and the inclination.

14.1.1 The evolution operator

It will be useful to remind ourselves about the evolution operator $\hat{U}(t, t_0)$, which we define by

$$|\psi(t)\rangle = \hat{U}(t, t_0)\,|\psi(t_0)\rangle \ . \tag{14.1}$$

Applying the Schrödinger equation to $|\psi(t)\rangle$ leads to

$$i\frac{\partial}{\partial t}\hat{U}(t, t_0)\,|\psi(t_0)\rangle = \hat{H}\hat{U}(t, t_0)\,|\psi(t_0)\rangle \ . \tag{14.2}$$

Since $|\psi(t_0)\rangle$ is a fixed state with no time dependence, it simply factors out. Then, since the equation needs to be satisfied for any $|\psi(t_0)\rangle$, we obtain the equation for $\hat{U}$,

$$i\frac{\partial}{\partial t}\hat{U}(t, t_0) = \hat{H}\hat{U}(t, t_0) = (\hat{H}_0 + \hat{V})\hat{U}(t, t_0) \ . \tag{14.3}$$

It is not very surprising that the evolution operator satisfies the same equation as the state, since we defined it to do all the work of propagating states.

14.1.2 The interaction picture

From your quantum mechanics class, you may be familiar with the *Schrödinger picture*: a formulation of quantum mechanics in which the operators are constant in time while the states evolve

according to a given Hamiltonian $\hat{H} = \hat{H}_0 + \hat{V}$: $i\partial_t |\psi(t)\rangle = \hat{H} |\psi(t)\rangle$. You may also be familiar with an alternative, equivalent formulation: the *Heisenberg picture*, in which the states are constant in time while the operators evolve with $\hat{H}$ according to[1] $i\partial \hat{A}_H(t) = \left[\hat{A}_H(t), \hat{H}\right]$, where we put a subscript H on the operator A to stress that it is considered in the Heisenberg picture. There is also a third, mixed option: the *interaction picture*, also known as the *Dirac picture.* In the interaction picture, *both* states and operators evolve: the operators are evolved by $\hat{H}_0$, while the states $|\psi_I(t)\rangle$ are evolved by $\hat{V}$. In other words, if there is no interaction, $|\psi_I(t)\rangle$ are constant.

You may think it's weird that we can choose which object evolves in time. However, remember that neither states nor operators are observable quantities. For all experimentally measurable outcomes, the three above pictures yield the same results. Which one we use is a matter of convenience.

Let us formally introduce the interaction picture. In the Schrödinger picture, we have

$$i\partial_t |\psi(t)\rangle = (\hat{H}_0 + \hat{V}) |\psi(t)\rangle \ . \tag{14.4}$$

If there were no interaction, the solution would be

$$|\psi(t)\rangle = e^{-i\hat{H}_0 t} |\psi(0)\rangle \ . \tag{14.5}$$

If we now want to deal with a state which *does not* change in time when there is no interaction, we can obtain such a state by defining it as

$$|\psi_I(t)\rangle = e^{i\hat{H}_0 t} |\psi(t)\rangle \ . \tag{14.6}$$

If $|\psi(t)\rangle$ only evolves with $\hat{H}_0$, as in Eq. (14.5), then $|\psi_I(t)\rangle$ will equal $|\psi(0)\rangle$, *i.e.*, it will be constant in time – which is exactly what we want.

Let us see what equations those newly defined interaction-picture states $|\psi_I(t)\rangle$ satisfy. Multiplying both sides of Eq. (14.6) by i and then differentiating with respect to time leads to

$$i\partial_t |\psi_I(t)\rangle = -\hat{H}_0 e^{i\hat{H}_0 t} |\psi(t)\rangle + ie^{i\hat{H}_0 t}\partial_t |\psi(t)\rangle \ . \tag{14.7}$$

We can rewrite $\partial_t |\psi(t)\rangle$ on the right-hand side using the Schrödinger equation, Eq. (14.4), obtaining

$$i\partial_t |\psi_I(t)\rangle = e^{i\hat{H}_0 t}\hat{V} |\psi(t)\rangle = e^{i\hat{H}_0 t}\hat{V}e^{-i\hat{H}_0 t} |\psi_I(t)\rangle \ . \tag{14.8}$$

where in the second equality we expressed $|\psi(t)\rangle$ in terms of $|\psi_I(t)\rangle$ using the definition of the interaction-picture state, Eq. (14.6). Defining an operator $\hat{A}$ in the interaction picture as

$$\hat{A}_I(t) \equiv e^{i\hat{H}_0 t}\hat{A}e^{-i\hat{H}_0 t} \ , \tag{14.9}$$

we immediately get

$$i\partial_t |\psi_I(t)\rangle = \hat{V}_I(t) |\psi_I(t)\rangle \ , \tag{14.10}$$

which is again exactly what we want: only the interaction-picture potential $\hat{V}_I$ drives the evolution of $|\psi_I(t)\rangle$.

Finally, we want to find the evolution operator $U_I(t, t_0)$ that evolves the interaction-picture states $|\psi_I(t)\rangle$,

$$|\psi_I(t)\rangle = U_I(t, t_0) |\psi_I(t_0)\rangle \ . \tag{14.11}$$

[1] Things get a little bit more complicated if there is an explicit time dependence in the Hamiltonian, but we will not consider such cases here.

Using the definition of $|\psi_I(t)\rangle$ in terms of the Schrödinger picture state $|\psi(t)\rangle$, Eq. (14.6), leads to

$$e^{i\hat{H}_0 t}\,|\psi(t)\rangle = U_I(t,t_0)e^{i\hat{H}_0 t_0}\,|\psi(t_0)\rangle \ . \tag{14.12}$$

Acting with $e^{-i\hat{H}_0 t}$ from the left and recalling that the Schrödinger picture state evolves with $U(t,t_0)$, Eq. (14.1), immediately leads to

$$U(t,t_0) = e^{-i\hat{H}_0 t}U_I(t,t_0)e^{i\hat{H}_0 t_0} \ , \tag{14.13}$$

which can be inverted to yield

$$U_I(t,t_0) = e^{i\hat{H}_0 t}U(t,t_0)e^{-i\hat{H}_0 t_0} \ . \tag{14.14}$$

On the other hand, inserting the evolution equation for the interaction-picture state, Eq. (14.11), into the interaction-picture Schrödinger equation, Eq. (14.10), we immediately obtain

$$i\partial_t U_I(t,t_0) = \hat{V}_I(t)U_I(t,t_0) \ , \tag{14.15}$$

which, given the initial condition that $U_I(t_0,t_0) = \mathbb{1}$ (which is intuitive given that at $t = t_0$ there is yet nothing for the operator to do), can be formally integrated to

$$U_I(t,t_0) = \mathbb{1} - i\int_{t_0}^{t} dt'\ \hat{V}_I(t')U_I(t',t_0) \ . \tag{14.16}$$

This is a self-consistent equation for which we can establish a well-defined series by repeatedly inserting it in place of $\hat{U}_I(t,t_0)$ on the right-hand side. In this way, we get

$$\hat{U}_I(t,t_0) = \mathbb{1} - i\int_{t_0}^{t} dt'\ \hat{V}_I(t')\left(\mathbb{1} - i\int_{t_0}^{t'} dt''\ \hat{V}_I(t'')\hat{U}_I(t'',t_0)\right) \tag{14.17}$$

$$= \mathbb{1} - i\int_{t_0}^{t} dt'\ \hat{V}_I(t') + i^2\int_{t_0}^{t} dt'\int_{t_0}^{t'} dt''\ \hat{V}_I(t')\hat{V}_I(t'') + \dots \tag{14.18}$$

$$= \mathbb{1} + \sum_{n=1}^{\infty}(-i)^n\int_{t_0}^{t} dt_1\int_{t_0}^{t_1} dt_1\cdots\int_{t_0}^{t_{n-1}} dt_n\ \hat{V}_I(t_1)\hat{V}_I(t_2)\dots\hat{V}_I(t_n) \ , \tag{14.19}$$

i.e., a power series expansion for the interaction-picture time evolution operator $\hat{U}_I(t,t_0)$, known as the *Dyson series*.

14.2 The S-matrix

The *scattering matrix* S, also called the *S-matrix*, is defined by demanding that its elements satisfy

$$S_{\boldsymbol{k}'\boldsymbol{k}} \equiv \lim_{\substack{t_0\to-\infty\\ t\to+\infty}} \left\langle \Phi_{\boldsymbol{k}'}\middle|\hat{U}_I(t,t_0)\middle|\Phi_{\boldsymbol{k}}\right\rangle \ , \tag{14.20}$$

where $\hat{U}_I(t,t_0)$ is the interaction-picture evolution operator. Effectively, this operator answers the (physical!) question: if a particle starts as a free plane wave with momentum $\boldsymbol{k}$, what is the amplitude to find it with a momentum $\boldsymbol{k}'$ in the distant future? Since in scattering experiments we start with a free state and end up with a free state, answering such a question sounds like a great idea. The elements of the S-matrix provide this information since the right-hand side of Eq. (14.20) evolves a state with momentum $\boldsymbol{k}$ from the far past into the distant future and then takes the scalar product of the result with a plane wave of momentum $\boldsymbol{k}'$.

14.2.1 Explicit expression for the S-matrix

This is where the formalism developed in Sec. 14.1 pays off: we can immediately insert the Dyson series, Eq. (14.18), into the S-matrix element definition, Eq. (14.20), which yields

$$S_{\boldsymbol{k}'\boldsymbol{k}} \equiv \lim_{\substack{t_0\to-\infty\\ t\to+\infty}} \langle\Phi_{\boldsymbol{k}'}|\mathbb{1}|\Phi_{\boldsymbol{k}}\rangle - i \lim_{\substack{t_0\to-\infty\\ t\to+\infty}} \int_{t_0}^{t} dt' \ \left\langle \Phi_{\boldsymbol{k}'}\middle|\hat{V}_I(t')\middle|\Phi_{\boldsymbol{k}}\right\rangle \tag{14.21}$$

$$+ i^2 \lim_{\substack{t_0\to-\infty\\ t\to+\infty}} \int_{t_0}^{t} dt' \int_{t_0}^{t'} dt'' \ \left\langle \Phi_{\boldsymbol{k}'}\middle|\hat{V}_I(t')\hat{V}_I(t'')\middle|\Phi_{\boldsymbol{k}}\right\rangle + \dots \tag{14.22}$$

We can see that the resulting expression starts with a term of zeroth order in the interaction-picture potential $\hat{V}_I$, followed by a term of first order, followed by a term of second order, and so on. The zeroth-order term is simply equal to a delta function since the states $|\Phi_{\boldsymbol{k}}\rangle$ form an orthonormal set,

$$S^{(0)}_{\boldsymbol{k}'\boldsymbol{k}} = \delta^{(3)}(\boldsymbol{k}' - \boldsymbol{k}) \ . \tag{14.23}$$

Then, by applying the definition of the interaction-picture operator, Eq. (14.9), to $\hat{V}_I(t)$, the first-order term can be rewritten as

$$S^{(1)}_{\boldsymbol{k}'\boldsymbol{k}} = -i \lim_{\substack{t_0\to-\infty\\ t\to+\infty}} \int_{t_0}^{t} dt' \ \left\langle \Phi_{\boldsymbol{k}'}\middle|e^{i\hat{H}_0 t'}\hat{V}e^{-i\hat{H}_0 t'}\middle|\Phi_{\boldsymbol{k}}\right\rangle \tag{14.24}$$

$$= -i \lim_{\substack{t_0\to-\infty\\ t\to+\infty}} \int_{t_0}^{t} dt' \ \left\langle \Phi_{\boldsymbol{k}'}\middle|e^{iE_{k'} t'}\hat{V}e^{-iE_k t'}\middle|\Phi_{\boldsymbol{k}}\right\rangle \tag{14.25}$$

$$= -i \ V_{\boldsymbol{k}'\boldsymbol{k}} \int_{-\infty}^{+\infty} dt' \ e^{i(E_{k'}-E_k)t'} \ , \tag{14.26}$$

where in the second line we applied the operators $e^{i\hat{H}_0 t}$ and $e^{-i\hat{H}_0 t}$ to the states $\langle\Phi_{\boldsymbol{k}'}|$ and $|\Phi_{\boldsymbol{k}}\rangle$, respectively, while in the third line we identified $\left\langle \Phi_{\boldsymbol{k}'}\middle|\hat{V}\middle|\Phi_{\boldsymbol{k}}\right\rangle$ as the matrix element of $\hat{V}$ and we took the limits. We know that[2]

$$\int_{-\infty}^{+\infty} dt' \ e^{i(E_{k'}-E_k)t'} = 2\pi\delta(E_{k'} - E_k) \ . \tag{14.27}$$

[2] This can be seen as follows: The integral $\int_{-\infty}^{+\infty} d\tau \ e^{i(E_{k'}-E_k)\tau}$ does not converge in an ordinary sense since the integrand oscillates throughout the entire domain without ever decaying. However, we can calculate the integral in the weak limit, *i.e.*, if we consider the integrated expression as *acting on some other expression* – we have already encountered this strategy when discussing the inverse operators $\hat{G}_0$ and $\hat{G}$ in Lecture 11. To this end, let us consider an integrand $e^{i\omega t}e^{-\epsilon|t|}$, where $\epsilon > 0$ is a small parameter which damps the oscillations at $t \to \pm\infty$. We can split the integral into two domains at $t = 0$, which allows us to write

$$I(\omega,\epsilon) = \int_{-\infty}^{+\infty} dt \ e^{i\omega t}e^{-\epsilon|t|} = \int_{-\infty}^{0} dt \ e^{(i\omega+\epsilon)t} + \int_{0}^{+\infty} dt \ e^{(i\omega-\epsilon)t} \ .$$

These two integrals converge, yielding

$$I(\omega,\epsilon) = \left[\frac{e^{i\omega t}e^{\epsilon t}}{i\omega+\epsilon}\right]_{-\infty}^{0} + \left[\frac{e^{i\omega t}e^{-\epsilon t}}{i\omega-\epsilon}\right]_{0}^{\infty} = \frac{1}{i\omega+\epsilon} - \frac{1}{i\omega-\epsilon} = \frac{2\epsilon}{\omega^2+\epsilon^2} \ .$$

Based on the integral we considered in Footnote 5 of Lecture 11, we then see that

$$\lim_{\epsilon\to0}\int_{-\infty}^{+\infty} dt \ e^{i\omega t}e^{-\epsilon|t|} = \lim_{\epsilon\to0}\frac{2\epsilon}{\omega^2+\epsilon^2} = 2\pi\delta(\omega) \ .$$

Consequently, the first-order term becomes

$$S^{(1)}_{\boldsymbol{k'k}} = -2\pi i \; V_{\boldsymbol{k'k}} \; \delta(E_{k'} - E_k) \; . \tag{14.28}$$

Next, we deal with the second-order term,

$$S^{(2)}_{\boldsymbol{k'k}} = i^2 \lim_{\substack{t_0\to-\infty \\ t\to+\infty}} \int_{t_0}^{t} dt' \int_{t_0}^{t'} dt'' \int d^3q \; \left\langle \Phi_{\boldsymbol{k'}} \middle| e^{i\hat{H}_0 t'} \hat{V} e^{-i\hat{H}_0 t'} \left|\Phi_{\boldsymbol{q}}\right\rangle \left\langle \Phi_{\boldsymbol{q}}\right| e^{i\hat{H}_0 t''} \hat{V} e^{-i\hat{H}_0 t''} \middle| \Phi_{\boldsymbol{k}} \right\rangle \tag{14.29}$$

$$= i^2 \lim_{\substack{t_0\to-\infty \\ t\to+\infty}} \int d^3q \int_{t_0}^{t} dt' \int_{t_0}^{t'} dt'' \; e^{iE_{k'}t'} e^{-iE_q t'} e^{iE_q t''} e^{-iE_k t''} \left\langle \Phi_{\boldsymbol{k'}} \middle| \hat{V} \middle| \Phi_{\boldsymbol{q}} \right\rangle \left\langle \Phi_{\boldsymbol{q}} \middle| \hat{V} \middle| \Phi_{\boldsymbol{k}} \right\rangle \tag{14.30}$$

$$= i^2 \int d^3q \; V_{\boldsymbol{k'q}} \int_{-\infty}^{+\infty} dt' \; e^{i(E_{k'}-E_q)t'} \int_{-\infty}^{t'} dt'' \; e^{i(E_q-E_k)t''} \; V_{\boldsymbol{qk}} \; , \tag{14.31}$$

where in the first line we applied the definition of the interaction-picture operator, Eq. (14.9), to $\hat{V}_I(t')$ and $\hat{V}_I(t'')$ as well as inserted the resolution of identity, in the second line we applied the $\hat{H}_0$ operators to the various bras and kets that they happened to be next to, and in the third line we identified the matrix elements of the two $\hat{V}$ operators and took the limits. The inner integral is equal[3]

$$\int_{-\infty}^{t'} dt'' \; e^{i(E_q-E_k)t''} = \lim_{\eta\to 0} \frac{e^{i(E_q-E_k)t'}}{i(E_q - E_k - i\eta)} \; . \tag{14.34}$$

so that altogether

$$S^{(2)}_{\boldsymbol{k'k}} = i^2 \lim_{\eta\to 0} \int d^3q \; V_{\boldsymbol{k'q}} \int_{-\infty}^{+\infty} dt' \; e^{i(E_{k'}-E_q)t'} \frac{e^{i(E_q-E_k)t'}}{i(E_q - E_k - i\eta)} \; V_{\boldsymbol{qk}} \tag{14.35}$$

$$= i \lim_{\eta\to 0} \int d^3q \; V_{\boldsymbol{k'q}} \int_{-\infty}^{+\infty} dt' \; \frac{e^{i(E_{k'}-E_k)t'}}{E_q - E_k - i\eta} \; V_{\boldsymbol{qk}} \tag{14.36}$$

$$= -2\pi i \; \delta(E_{k'} - E_k) \lim_{\eta\to 0} \int d^3q \; V_{\boldsymbol{k'q}} \frac{1}{E_k - E_q + i\eta} \; V_{\boldsymbol{qk}} \; , \tag{14.37}$$

where in the second line we noticed that the exponents with E_q simply cancel out, while in the third line we performed the integral over t' – which had the same form as already encountered in the first-order term, Eq. (14.27) – and introduced an overall minus sign while also switching the signs of terms in the denominator. With this, one cannot help but notice that

$$\lim_{\eta\to 0} \frac{1}{E_k - E_q + i\eta} \tag{14.38}$$

[3] In this integral, the integrand oscillates indefinitely at the lower limit. To deal with this, we add a small regulator term $e^{\eta(t''-t')}$ (where we also introduce a dependence on t' because it will nicely get rid of the regulator at the upper limit of the integral) and consider

$$I(\omega,\eta) = \int_{-\infty}^{t'} dt'' \; e^{i\omega t''} e^{\eta(t''-t')} = \int_{-\infty}^{t'} dt'' \; e^{i(\omega-i\eta)t''} \; e^{-\eta t'} \; , \tag{14.32}$$

where we used $\omega = (E_q - E_k)$. This integral can now be easily evaluated to be

$$I(\omega,\eta) = \left[\frac{e^{i\omega t''} e^{\eta t''}}{i(\omega - i\eta)} \right]_{-\infty}^{t'} e^{-\eta t'} = \frac{e^{i\omega t'}}{i(\omega - i\eta)} \; , \tag{14.33}$$

where, as we wanted, the regulator term fulfilled its duty at $t'' = -\infty$ by suppressing the integrand as well as disappeared at the upper limit. The original integral is obtained from the above result by applying the limit $\eta \to 0$.

is the free Green's function for the outgoing solution, Eq. (12.1). Since we understand the meaning of taking the $\eta \to 0$ limit in this context (see Section 11.4), we will suppress it from now on. Gathering the computed terms together, up to the second order the S-matrix element is given by

$$S_{\boldsymbol{k}'\boldsymbol{k}} = S^{(0)}_{\boldsymbol{k}'\boldsymbol{k}} + S^{(1)}_{\boldsymbol{k}'\boldsymbol{k}} + S^{(2)}_{\boldsymbol{k}'\boldsymbol{k}} + \dots \tag{14.39}$$

$$= \delta^{(3)}(\boldsymbol{k}' - \boldsymbol{k}) - 2\pi i\ \delta(E_{k'} - E_k) \left[V_{\boldsymbol{k}'\boldsymbol{k}} + \int d^3q\ V_{\boldsymbol{k}'\boldsymbol{q}} \frac{1}{E_k - E_q + i\eta} V_{\boldsymbol{q}\boldsymbol{k}} \right] + \dots \tag{14.40}$$

14.2.2 Relation between the T-matrix and the S-matrix

In Eq. (14.40), the term in the square bracket is exactly what we would have gotten from the matrix-element representation of the Lippmann–Schwinger equation for the T-matrix, Eq. (13.12), if we iteratively substituted the Lippmann–Schwinger equation for $T_{\boldsymbol{q}\boldsymbol{k}}$ in place of $T_{\boldsymbol{q}\boldsymbol{k}}$ on the right-hand side and only considered the first two terms. Indeed, one can show that all higher order terms in the $S_{\boldsymbol{k}'\boldsymbol{k}}$ expansion conspire to produce a T-matrix element, so that finally we can write[4]

$$S_{\boldsymbol{k}'\boldsymbol{k}} = \delta^{(3)}(\boldsymbol{k}' - \boldsymbol{k}) - 2\pi i\ \delta(E_{k'} - E_k)\ T_{\boldsymbol{k}'\boldsymbol{k}}\ . \tag{14.41}$$

Thus, we now explicitly see that the S-matrix encapsulates both the situation where nothing has happened, described by the diagonal term $\delta^{(3)}(\boldsymbol{k}' - \boldsymbol{k})$, and a contribution due to the influence of the potential – as evident from the definition of the T-matrix element, Eq. (13.1) – constrained to conserve energy *via* the term $\delta(E_{k'} - E_k)$, which in turn forces $T_{\boldsymbol{k}'\boldsymbol{k}}$ to stay on-shell.

14.3 Partial wave expansion of the T- and the S-matrix

The following discussion is rather technical, although without significant subtleties so that altogether it should not be very difficult. If you are short on time, you can skip the details; make sure, however, to read Secs. 14.3.3 and 14.3.5.

There is one more thing left to do if we want to connect the S-matrix that as derived in Sec. 14.2 with the S-matrix element we introduced as part of the asymptotic solution, Eq. (8.5): partial wave expansion. This means that we need to connect the S-matrix considered in the momentum space, introduced above, with the S-matrix considered in the angular-momentum basis.

14.3.1 Partial wave decomposition of free and full states

Assuming a rotationally-invariant Hamiltonian, the energy eigenstates can be chosen to have a definite angular momentum. Such states are then labeled by energy E, the orbital angular momentum quantum number l, and the magnetic quantum number m. In this basis, the wavefunctions factorize into spherical harmonics $Y_{lm}(\hat{\boldsymbol{r}})$ and radial wavefunctions $u_l(k, r)$. These components corresponding to specific values of l are called partial waves.

First, we want to express the free $|\Phi\rangle$ and full states $|\Psi\rangle$, which solve their respective Schrödinger equations, Eqs. (11.5) and (11.6), in the angular-momentum basis. The normalization conditions of $|\Phi\rangle$ and $|\Psi\rangle$ in the angular-momentum basis can be stated as

$$\langle \Phi_{E'l'm'} | \Phi_{Elm} \rangle = \delta_{ll'}\delta_{mm'}\delta(E - E')\ , \tag{14.42}$$

$$\langle \Psi_{E'l'm'} | \Psi_{Elm} \rangle = \delta_{ll'}\delta_{mm'}\delta(E - E')\ . \tag{14.43}$$

[4] Albeit without a formal proof because we already spent some time on this subject and life is short.

The decomposition of the free states $\langle \boldsymbol{r}|\Phi_{Elm}\rangle$ into radial wavefunctions and spherical harmonics is known exactly because the radial wavefunctions must be the (Ricatti-)Bessel functions (see Sec. 7.3.1),

$$\langle \boldsymbol{r}|\Phi_{Elm}\rangle \equiv \Phi_{Elm}(\boldsymbol{r}) = A_l \frac{\hat{\jmath}_l(kr)}{kr} Y_{lm}(\hat{\boldsymbol{r}}) \ , \tag{14.44}$$

where A_l are constants to be determined. With this, we can write the normalization condition, Eq. (14.42), in the coordinate space,

$$\int d^3r \ \Phi^*_{E'l'm'}\Phi_{Elm} = \frac{|A_l|^2}{k'k}\int_0^\infty dr \ \hat{\jmath}_{l'}(k'r)\hat{\jmath}_l(kr) \int d\Omega \ Y^*_{l'm'}(\hat{\boldsymbol{r}})Y_{lm}(\hat{\boldsymbol{r}}) = \delta_{ll'}\delta_{mm'}\delta(E-E') \ . \tag{14.45}$$

Since the spherical harmonics satisfy

$$\int d\Omega \ Y^*_{l'm'}(\hat{\boldsymbol{r}})Y_{lm}(\hat{\boldsymbol{r}}) = \delta_{ll'}\delta_{mm'} \ , \tag{14.46}$$

we get this part of the normalization condition for free. Next, we use deal with the integral over r by invoking the orthogonality condition for the Ricatti-Bessel functions,

$$\int_0^\infty dr \ \hat{\jmath}_l(k'r)\hat{\jmath}_l(kr) = \frac{\pi}{2}\delta(k-k') \ . \tag{14.47}$$

Changing the variables of the delta function from momentum to energy[5] yields

$$\int_0^\infty dr \ \hat{\jmath}_{l'}(k'r)\hat{\jmath}_l(kr) = \frac{\pi}{2}\frac{k'}{\mu}\delta(E-E') \ . \tag{14.51}$$

Thus, to satisfy the normalization condition, Eq. (14.45), we need $\frac{|A_l|^2}{k'k}\frac{\pi k'}{2\mu} = 1$, or equivalently

$$A_l = i^l\sqrt{\frac{2\mu k}{\pi}} \ , \tag{14.52}$$

where we added a phase i^l which does not change the normalization but will nicely simplify some of the expressions below. Altogether, the form of the free Hamiltonian solution in the angular-momentum basis is

$$\Phi_{Elm}(\boldsymbol{r}) = i^l\sqrt{\frac{2\mu k}{\pi}}\frac{\hat{\jmath}_l(kr)}{kr}Y_{lm}(\hat{\boldsymbol{r}}) \ . \tag{14.53}$$

[5]This is done in the following way: As we saw in Footnote 5 of Lecture 11, the delta function is defined by what it does to other functions when integrated over. Thus, the meaning of $\delta(k-k')$ only comes fully into view in an expression like

$$\int_0^\infty dk' \ f(k')\delta(k'-k) = f(k) \ , \tag{14.48}$$

where $f(k')$ is an arbitrary function. With $E'_k = \frac{k'^2}{2\mu}$, we can change the variables according to $dE_{k'} = \frac{k'}{\mu}dk'$, so that

$$\int_0^\infty dk' \ f(k')\delta(k-k') = \int_0^\infty dE_{k'} \ \frac{\mu}{k'}f\big(k'(E')\big)\delta(k'-k) \ . \tag{14.49}$$

However, this should really be the same as

$$\int_0^\infty dE_{k'}f\big(E'\big)\delta(E'-E) \ . \tag{14.50}$$

For this to be the case, we need $\frac{\mu}{k'}\delta(k-k') = \delta(E-E')$.

In analogy to the free state, Eq. (14.44), the partial wave expansion of the full wavefunction $\Psi_{Elm}(\boldsymbol{r})$ can be written as

$$\Psi_{Elm}(\boldsymbol{r}) = A_l \frac{u_l(kr)}{kr} Y_{lm}(\hat{\boldsymbol{r}}) = i^l \sqrt{\frac{2\mu k}{\pi}} \frac{u_l(kr)}{kr} Y_{lm}(\hat{\boldsymbol{r}}) \ , \tag{14.54}$$

where $u_l(kr)$ is the full solution. Here, the coefficients A_l are the same as for the free wavefunction $\Phi_{Elm}(\boldsymbol{r})$ because asymptotically, the full solutions *must* look like free solutions, albeit with a phase shift (as we have seen in Lecture 7) – and a phase shift does not affect the normalization.

With the free and full states normalized to one, we now have two resolutions of identity,

$$\sum_{l=0}^{\infty} \sum_{m=-l}^{l} \int_0^{\infty} dE \ \ |\Phi_{Elm}\rangle \langle \Phi_{Elm}| = 1 \ , \tag{14.55}$$

$$\sum_{l=0}^{\infty} \sum_{m=-l}^{l} \int_0^{\infty} dE \ \ |\Psi_{Elm}\rangle \langle \Psi_{Elm}| = 1 \ . \tag{14.56}$$

14.3.2 Partial-wave expansion of momentum and scattering eigenstates

With this, we now want to express plane waves and scattered waves in terms of the free and full solutions in the angular-momentum basis, *i.e.*, perform a partial-wave expansion with $\Phi_{Elm}(\boldsymbol{r})$ and $\Psi_{Elm}(\boldsymbol{r})$ as the basis states.

Applying the resolution of identity in terms of the free states, Eq. (14.55), to a momentum eigenstate (*i.e.*, a plane wave), we can express it as a linear combination of $|\Phi_{Elm}\rangle$ states,

$$|\boldsymbol{k}\rangle = \sum_{l=0}^{\infty} \sum_{m=-l}^{l} \int_0^{\infty} dE \ \ |\Phi_{Elm}\rangle \langle \Phi_{Elm}|\boldsymbol{k}\rangle \ . \tag{14.57}$$

Here, $|\boldsymbol{k}\rangle$ and $|\Phi_{Elm}\rangle$ are eigenstates of the same Hamiltonian $\hat{H}_0$ with eigenvalues E_k and E, respectively, but simply expressed in different bases. As a result, orthogonality of eigenstates with different eigenvalues implies that the overlap $\langle \Phi_{Elm}|\boldsymbol{k}\rangle$ is proportional to some coefficient dependent on the quantum numbers l and m and a delta function in E,

$$\langle \Phi_{Elm}|\boldsymbol{k}\rangle = C_{lm}(\hat{\boldsymbol{k}})\delta(E - E_k) \ , \tag{14.58}$$

which makes the energy integral in Eq. (14.57) trivial, yielding

$$|\boldsymbol{k}\rangle = \sum_{l=0}^{\infty} \sum_{m=-l}^{l} C_{lm}(\hat{\boldsymbol{k}}) \, |\Phi_{Elm}\rangle \ . \tag{14.59}$$

We can then look at this relation in the coordinate space by applying $\langle \boldsymbol{r}|$ from the left,

$$\langle \boldsymbol{r}|\boldsymbol{k}\rangle \equiv \phi_{\boldsymbol{k}}(\boldsymbol{r}) = \frac{1}{(2\pi)^{3/2}} e^{i\boldsymbol{k}\cdot\boldsymbol{r}} = \sum_{l=0}^{\infty} \sum_{m=-l}^{l} C_{lm}(\hat{\boldsymbol{k}}) \Phi_{Elm}(\boldsymbol{r}) \ , \tag{14.60}$$

where we use $\phi_{\boldsymbol{k}}(\boldsymbol{r})$ to denote a (normalized) plane wave in the coordinate basis. Since the partial wave expansion of a plane wave, Eq. (7.54), can be written in terms of the spherical harmonics as[6]

$$e^{i\boldsymbol{k}\cdot\boldsymbol{r}} = 4\pi \sum_{l=0}^{\infty} \sum_{m=-l}^{l} i^l j_l(kr) Y_{lm}(\hat{\boldsymbol{k}}) Y^*_{lm}(\hat{\boldsymbol{k}}) \ , \tag{14.61}$$

[6] In going from Eq. (7.54), we use the standard result $\sum_{m=-l}^{l} Y^*_{lm} Y_{lm} = \frac{2l+1}{4\pi}$.

by comparing with Eq. (14.60), we see that we must have

$$\sum_{l=0}^{\infty}\sum_{m=-l}^{l} C_{lm}(\hat{\boldsymbol{k}})\Phi_{Elm}(\boldsymbol{r}) = \sqrt{\frac{2}{\pi}}\sum_{l=0}^{\infty}\sum_{m=-l}^{l} i^l j_l(kr)Y_{lm}(\hat{\boldsymbol{k}})Y^*_{lm}(\hat{\boldsymbol{k}}) \ . \tag{14.62}$$

Together with the explicit form for the free solution in the angular-momentum basis Φ_{Elm}, Eq. (14.53), this yields

$$C_{lm}(\hat{\boldsymbol{k}}) = \frac{1}{\sqrt{\mu k}}Y^*_{lm}(\hat{\boldsymbol{k}}) \ , \tag{14.63}$$

so that finally we can write the decomposition of a plane wave in terms of the free solutions $\Phi_{Elm}(\boldsymbol{r})$,

$$\phi_{\boldsymbol{k}}(\boldsymbol{r}) = \frac{1}{\sqrt{\mu k}}\sum_{l=0}^{\infty}\sum_{m=-l}^{l} Y^*_{lm}(\hat{\boldsymbol{k}})\Phi_{Elm}(\boldsymbol{r}) \ . \tag{14.64}$$

Analogously, one can now use the resolution of identity in terms of the full Hamiltonian eigenstates, Eq. (14.56), to expand the scattering wavefunction,

$$\left|\Psi^{(+)}_{\boldsymbol{k}}\right\rangle = \sum_{l=0}^{\infty}\sum_{m=-l}^{l}\int_0^{\infty} dE \ \left|\Psi_{Elm}\right\rangle\left\langle\Psi_{Elm}\middle|\Psi^{(+)}_{\boldsymbol{k}}\right\rangle \ . \tag{14.65}$$

Since the scattering wavefunction $\left|\Psi^{(+)}_{\boldsymbol{k}}\right\rangle$ is a linear combination of angular-momentum-basis eigenstates of the full Hamiltonian[7] $|\Psi_{Elm}\rangle$, the energies E and E_k must be equal for the overlap to be non-zero given that states with different energies are orthogonal. Therefore, we can write

$$\left\langle\Psi_{Elm}\middle|\Psi^{(+)}_{\boldsymbol{k}}\right\rangle = D_{lm}(\hat{\boldsymbol{k}})\delta(E-E_k) \ , \tag{14.66}$$

which collapses the expansion in Eq. (14.65) to

$$\left\langle\boldsymbol{r}\middle|\Psi^{(+)}_{\boldsymbol{k}}\right\rangle \equiv \psi^{(+)}_{\boldsymbol{k}}(\boldsymbol{r}) = \sum_{l=0}^{\infty}\sum_{m=-l}^{l} D_{lm}(\hat{\boldsymbol{k}})\left\langle\boldsymbol{r}|\Psi_{Elm}\right\rangle \ , \tag{14.67}$$

where we applied $\langle\boldsymbol{r}|$ from the left in order to look at the states in the coordinate space. We know that asymptotically, the scattering state $\psi^{(+)}_{\boldsymbol{k}}$ is a sum of an incoming plane wave and an outgoing spherical wave,

$$\psi^{(+)}_{\boldsymbol{k}} \to \frac{1}{(2\pi)^{3/2}}\left(e^{i\boldsymbol{k}\cdot\boldsymbol{r}} + f(\theta)\frac{e^{ikr}}{r}\right) \tag{14.68}$$

where we introduced an overall normalization which matches our discussion of plane waves above. Because the scattering state *contains* an incoming plane wave, its expansion in terms of the $\Psi_{Elm}(\boldsymbol{r})$ states must be such that asymptotically, the normalization of the plane wave in terms of the $\Phi_{Elm}(\boldsymbol{r})$ states that we obtained above, Eq. (14.64), is reproduced. This is the case if $D_{lm}(\hat{\boldsymbol{k}}) = C_{lm}(\hat{\boldsymbol{k}})$, and we arrive at

$$\psi^{(+)}_{\boldsymbol{k}}(\boldsymbol{r}) = \frac{1}{\sqrt{\mu k}}\sum_{l=0}^{\infty}\sum_{m=-l}^{l} Y^*_{lm}(\hat{\boldsymbol{k}})\Psi_{Elm}(\boldsymbol{r}) \ . \tag{14.69}$$

[7] We know that because the scattering wavefunction must obey the Schrödinger equation for the full Hamiltonian. We are truly discussing here expressing the same wavefunction in different bases.

Finally, we note that Eqs. (14.64) and (14.69) immediately imply

$$|\Phi_{\boldsymbol{k}}\rangle = \frac{1}{\sqrt{\mu k}} \sum_{l=0}^{\infty} \sum_{m=-l}^{l} Y_{lm}^*(\hat{\boldsymbol{k}}) \, |\Phi_{Elm}\rangle \ , \tag{14.70}$$

$$\left|\Psi_{\boldsymbol{k}}^{(+)}\right\rangle = \frac{1}{\sqrt{\mu k}} \sum_{l=0}^{\infty} \sum_{m=-l}^{l} Y_{lm}^*(\hat{\boldsymbol{k}}) \, |\Psi_{Elm}\rangle \ . \tag{14.71}$$

14.3.3 An aside on incoming, outgoing, and scattered states

If you are confused about the multitude of states that we discussed above, you are not alone.

First, note that somewhat contrary to its name, the scattering state contains not only the outgoing wave, but also the incoming wave. In other words, the name implies that the state is *a solution to a scattering problem*, but not that it singles out the *scattered wave*.

To further shine a light on this, let us consider a 1D scattering problem with a short-range potential at $x = 0$. The scattering solution $\psi_k^{(+)}(x)$ is the solution of the full Hamiltonian which at large distances behaves like

$$\psi_k^{(+)}(x) = \begin{cases} e^{ikx} + Re^{-ikx} & \text{for } x \to -\infty \\ Te^{ikx} & \text{for } x \to \infty \end{cases} \ . \tag{14.72}$$

This solution describes the fact that in the region with $x \ll 0$ we have the incoming and the reflected wave, while in the region with $x \gg 0$ we have the transmitted wave. Note that the solution in the region $x \ll 0$ contains the solution of the free Hamiltonian: the plane wave e^{ikx}. Instead of this structure, we could also write $\psi_k^{(+)}(x)$ as

$$\psi_k^{(+)}(x) = e^{ikx} + \{\text{part generated by the potential}\} \ . \tag{14.73}$$

Both forms have to be solutions of the same Hamiltonian.

What we tried to achieve in the previous section is to take the solution written in a form as in Eq. (14.73) and rewrite it in terms of the eigenstates of the full Hamiltonian, which look more like the function in Eq. (14.72). On our way to do this, we also obtained such expressions for the free Hamiltonian solutions, motivated by the fact that in this case the form of the solutions is known and that the resulting normalization can be used for normalization of the full Hamiltonian states.

14.3.4 Partial-wave expansion of the T-matrix element

Finally, we take a look at the T-matrix element, defined in Eq. (13.1). Inserting into that definition the partial-wave expansions for the $\langle\Phi_{\boldsymbol{k}'}|$ and $\left|\Psi_{\boldsymbol{k}}^{(+)}\right\rangle$ states, Eqs. (14.70) and (14.71), we obtain

$$T_{\boldsymbol{k}'\boldsymbol{k}} = \left\langle \Phi_{\boldsymbol{k}'} \middle| \hat{V} \middle| \Psi_{\boldsymbol{k}}^{(+)} \right\rangle = \frac{1}{\mu\sqrt{k'k}} \sum_{l'=0}^{\infty} \sum_{m'=-l'}^{l'} \sum_{l=0}^{\infty} \sum_{m=-l}^{l} Y_{l'm'}(\hat{\boldsymbol{k}}') Y_{lm}^*(\hat{\boldsymbol{k}}) \left\langle \Phi_{E'l'm'} \middle| \hat{V} \middle| \Psi_{Elm}^{(+)} \right\rangle \ . \tag{14.74}$$

Using two resolutions of identity in the position space, $\int d^3r \ |\boldsymbol{r}\rangle \langle \boldsymbol{r}|$, we write the matrix element as

$$\left\langle \Phi_{E'l'm'} \middle| \hat{V} \middle| \Psi_{Elm}^{(+)} \right\rangle = \int d^3r \int d^3r' \ \langle \Phi_{E'l'm'} | \boldsymbol{r}' \rangle \left\langle \boldsymbol{r}' \middle| \hat{V} \middle| \boldsymbol{r} \right\rangle \left\langle \boldsymbol{r} \middle| \Psi_{Elm}^{(+)} \right\rangle \tag{14.75}$$

$$= \int d^3r \int d^3r' \ \langle \Phi_{E'l'm'} | \boldsymbol{r}' \rangle \, V(r) \delta^3(\boldsymbol{r} - \boldsymbol{r}') \left\langle \boldsymbol{r} \middle| \Psi_{Elm}^{(+)} \right\rangle \tag{14.76}$$

$$= \int d^3r \ \langle \Phi_{E'l'm'} | \boldsymbol{r} \rangle \, V(r) \left\langle \boldsymbol{r} \middle| \Psi_{Elm}^{(+)} \right\rangle \ . \tag{14.77}$$

Inserting the coordinate-space representations of the free and full solutions in the angular-momentum basis, Eqs. (14.53) and (14.54), then yields

$$\left\langle \Phi_{E'l'm'} \middle| \hat{V} \middle| \Psi^{(+)}_{Elm} \right\rangle = (-i)^{l'} i^{l} \frac{2\mu}{\pi} \frac{1}{\sqrt{k'k}} \int dr\ \hat{\jmath}_{l'}(k'r) V(r) u_l(kr) \int d\Omega\ Y^*_{l'm'}(\hat{\boldsymbol{r}}) Y_{lm}(\hat{\boldsymbol{r}}) \ . \tag{14.78}$$

Given the normalization for the spherical harmonics, Eq. (14.46), we then immediately arrive at

$$\left\langle \Phi_{E'l'm'} \middle| \hat{V} \middle| \Psi^{(+)}_{Elm} \right\rangle = (-i)^{l'} i^{l} \frac{2\mu}{\pi} \frac{1}{\sqrt{k'k}} \int dr\ \hat{\jmath}_{l'}(k'r) V(r) u_l(kr)\ \delta_{ll'} \delta_{mm'} \ , \tag{14.79}$$

which inserted back into the partial-wave expansion of the T-matrix, Eq. (14.74) yields

$$T_{\boldsymbol{k}'\boldsymbol{k}} = \frac{2}{\pi k' k} \sum_{l=0}^{\infty} \sum_{m=-l}^{l} Y_{lm}(\hat{\boldsymbol{k}}') Y^*_{lm}(\hat{\boldsymbol{k}}) \int dr\ \hat{\jmath}_l(k'r) V(r) u_l(kr) \ . \tag{14.80}$$

If we now demand that $T_{\boldsymbol{k}'\boldsymbol{k}}$ is on-shell, then it enforces $k' = k$. This and the addition theorem for spherical harmonics, $\sum_m Y_{lm}(\hat{\boldsymbol{k}}') Y^*_{lm}(\hat{\boldsymbol{k}}) = \frac{2l+1}{4\pi} P_l(\cos\theta)$ (where θ is the angle between the unit vectors $\hat{\boldsymbol{k}}$ and $\hat{\boldsymbol{k}}'$), allows us to write

$$T_{\boldsymbol{k}'\boldsymbol{k}} = \sum_{l=0}^{\infty} (2l+1) P_l(\cos\theta) \left[\frac{1}{4\pi\mu k} T_l(E_k) \right] \ , \tag{14.81}$$

where we defined

$$T_l(E_k) \equiv \left\langle \phi_{Elm} \middle| \hat{V} \middle| \psi_{Elm} \right\rangle = \frac{2\mu}{\pi} \int dr\ \hat{\jmath}_l(kr) V(r) u_l(kr) \ . \tag{14.82}$$

14.3.5 Partial-wave expansion of the S-matrix element

One can perform a similar expansion for the S-matrix and then connect it with the results for the T-matrix, Eqs. (14.81) and (14.82). However, here we can also take a shortcut. Recalling the relationship between the scattering amplitude and the T-matrix element, Eq. (13.13), we see that

$$f(\theta) = -\frac{\pi}{k} \sum_{l=0}^{\infty} (2l+1) P_l(\cos\theta) \big[T_l(E_k) \big] \ . \tag{14.83}$$

By comparing with the expression for the scattering amplitude in terms of the S-matrix element, Eq. (8.15), we see that we must have

$$S_l(k) = 1 - 2\pi i\ T_l(E_k) \ , \tag{14.84}$$

which is exactly what we would have expected from the relation between the S-matrix and the T-matrix that we obtained in Eq. (14.41).

We have finally connected the formal scattering theory developed in Lectures 11-13 with the partial-wave description of scattering developed in Lectures 7-9. In particular, we now understand the meaning of the S-matrix element, which was completely mysterious when we introduced it in Eq. (8.5). Given the definition of the S-matrix as the transition amplitude between initial and final states, S_l clearly describes how the interaction modifies the l-th partial wave[8]. In the case of purely elastic scattering one has $S_l = e^{2i\delta_l}$, so that the S-matrix element simply encodes the phase shift acquired by that partial wave. If other elastic channels are allowed, the S-matrix becomes block-diagonal in the angular momentum representation, with each block corresponding to a particular value of l.

[8] Note that for a central potential, the different partial waves (corresponding to different values of l) do not mix, as is indeed evident from Eqs. (14.82) and (14.84).

14.4 Properties of the S-matrix

Let us highlight several key characteristics of the S-matrix. While so far it has been defined in by its matrix elements, as in Eqs. (14.20) and (14.84), it is clear that the S-matrix corresponds to a *scattering operator* $\hat{S}$ that takes the initial (incoming) state and returns the final (outgoing) state[9],

$$|\Phi_{\text{out}}\rangle = \hat{S}\,|\Phi_{\text{in}}\rangle \ . \tag{14.85}$$

Since the probability must be conserved, the norms of the initial and final state must be equal,

$$\langle\Phi_{\text{in}}|\Phi_{\text{in}}\rangle = \langle\Phi_{\text{out}}|\Phi_{\text{out}}\rangle = \left\langle \Phi_{\text{in}}\middle|\hat{S}^\dagger\hat{S}\middle|\Phi_{\text{in}}\right\rangle \ , \tag{14.86}$$

where in the second equality we used Eq. (14.85). This can only be true for any arbitrary $|\Phi_{\text{in}}\rangle$ if

$$\hat{S}^\dagger\hat{S} = \mathbb{1} \ , \tag{14.87}$$

i.e., $\hat{S}$ is *unitary*. Indeed, from Eq. (14.20) we see that $\hat{S} \equiv \lim_{\substack{t_0\to-\infty\\ t\to+\infty}} \hat{U}_I(t,t_0)$, and since $\hat{U}_I(t,t_0)$ is unitary, see Eq. (14.14), so must be its limit.

Choosing a basis of asymptotic states $|\alpha\rangle$, the matrix element $S_{\beta\alpha} \equiv \left\langle \beta\middle|\hat{S}\middle|\alpha\right\rangle$ gives the amplitude for a state prepared in channel α to emerge in channel β. Since the probability of emerging in *any* state must be equal 1, we immediately obtain

$$\sum_\beta \left|S_{\beta\alpha}\right|^2 = \sum_\beta S^*_{\beta\alpha}S_{\beta\alpha} = 1 \ . \tag{14.88}$$

The same must be true for any superposition of incoming states, *e.g.*, $\psi = c_1\,|\alpha\rangle + c_2\,|\alpha'\rangle$, so that

$$\sum_\beta \left|S_{\beta\alpha} + S_{\beta\alpha'}\right|^2 = \sum_\beta \left|c_1S_{\beta\alpha} + c_2S_{\beta\alpha'}\right|^2 \tag{14.89}$$

$$= \sum_\beta \left(|c_1|^2S^*_{\beta\alpha}S_{\beta\alpha} + c_1^*c_2S^*_{\beta\alpha}S_{\beta\alpha'} + c_1c_2^*S^*_{\beta\alpha'}S_{\beta\alpha} + |c_2|^2S^*_{\beta\alpha'}S_{\beta\alpha'}\right) \tag{14.90}$$

$$= |c_1|^2 + |c_2|^2 \ . \tag{14.91}$$

This again leads to the unitarity condition,

$$\sum_\beta S^*_{\beta\alpha'}S_{\beta\alpha} = \delta_{\alpha'\alpha} \ . \tag{14.92}$$

14.5 Final word about the S-matrix

Note that the S-matrix encapsulates *all* information about a scattering process, since all measurable quantities can be expressed in terms of its elements $S_{\boldsymbol{k}'\boldsymbol{k}}$. Indeed, from its definition, Eq. (14.20), it is an operator which evolves a state prepared in the far past into the far future, and its matrix elements evaluate the overlap (the probability amplitude) of the initial state with a proposed final state. Once these transition amplitudes are known, all observable quantities – such as scattering probabilities and cross sections – can be constructed.

That the S-matrix fully determines a scattering problem was already evident in Lectures 8-9, where the problem became tractable because we decomposed the dynamics into independent partial

[9]Here we denote $|\Phi_{\boldsymbol{k}}\rangle \equiv |\Phi_{\text{in}}\rangle$ and $|\Phi_{\boldsymbol{k}'}\rangle \equiv |\Phi_{\text{out}}\rangle$ to make the notation more transparent.

waves. However, this is only one possible representation. Equations (14.41) and (13.13) show that the S-matrix elements may be computed in any convenient basis using the machinery of formal scattering theory. Thus, the S-matrix framework extends well beyond the partial-wave approach.

The S-matrix element can in principle be calculated from the Schrödinger equation of the system. Of course, in practice, since the Hamiltonian for the whole system is a complicated many-body operator, exact solutions are feasible only in certain special cases. In other cases, one may, for example, replace the many-body interaction by a model two-body interaction. When the number of partial waves is small, one may attempt direct analysis of scattering phase shifts. Another approach is the optical model, where effects of reaction channels are described by means of a complex potential that takes into account absorption from elastic channels (see In-class Activity 6b). In the strong coupling model, a limited number of reaction channels are included explicitly, leading to coupled radial equations. We will cover some of these approaches in the coming lectures in more detail.

Lecture sources: In this lecture, sections 14.1 and 14.2 are written based on a vague memory of Prof. K. Redlich's (University of Wrocław) lecture series on the S-matrix and an extended interaction with `ChatGPT` to derive it in a similar way. Section 14.3 is based on Bertulani & Danielewicz [6].

Lecture 15

Compound nucleus reactions I

Prerequisites: Lectures 1, 7, 8, 9, 14.
Guiding question: ***Are compound nuclei the mosh pit of nuclear reactions?***

Thus far, we have discussed only elastic reactions, where the projectile and target do not change their identities: $\mathrm{a} + \mathrm{A} \to \mathrm{a} + \mathrm{A}$. In that case, the process can be described by a *single channel*, *i.e.*, a particular combination of an entrance and an exit channel[1] corresponding to a single elastic scattering amplitude or, equivalently, a single S-matrix element for each partial wave. We now begin the exploration of reactions in which the exit channel may be different from the entrance channel. In other words, we acknowledge that there is often a whole list of possible outcomes in a reaction. For example, a neutron incident on a nucleus may

- scatter elastically: $\mathrm{A(n,n)A}$
- excite the nucleus and scatter inelastically (*i.e.*, $k' \neq k$): $\mathrm{A(n,n)A^*}$
- be captured radiatively: ${}^{x}\mathrm{A} + \mathrm{n} \to {}^{\mathrm{x+1}}\mathrm{A} + \gamma$
- induce neutron emission: ${}^{x}\mathrm{A} + \mathrm{n} \to {}^{\mathrm{x-1}}\mathrm{A} + 2\mathrm{n}$
- induce fission

and so on.

If a reaction has several *open reaction channels*[2], such as elastic scattering, inelastic scattering, and radiative capture, a single-channel description cannot determine how the incoming flux is redistributed among these different outcomes. To understand the data, we must therefore generalize our description of scattering to include multiple reaction channels.

15.1 Compound nucleus reactions

15.1.1 Observed spectrum of neutron scattering

That more than just elastic scattering takes place is evident in data. Fig. 15.1 shows the total cross section for neutrons scattering of natural tungsten (which contains several isotopes with roughly equal abundances) as a function of the neutron's incident energy. We can see that for *very* low incident energies, the cross section for $n + {}^{x}\mathrm{W}$ scattering falls monotonically. At $E_n \approx 4$ eV, scattering off ${}^{182}\mathrm{W}$ produces a sharp resonance. This is closely followed by resonances in scattering off ${}^{183}\mathrm{W}$, ${}^{186}\mathrm{W}$, and then again in ${}^{182}\mathrm{W}$ and ${}^{183}\mathrm{W}$. The defining characteristic of these resonances is that they are exceedingly sharp.

[1] An overview of different channels and reaction types was given in Lecture 1.
[2] Here, "open" means that the channel is allowed given the system's energy, conserved quantum numbers, *etc.*

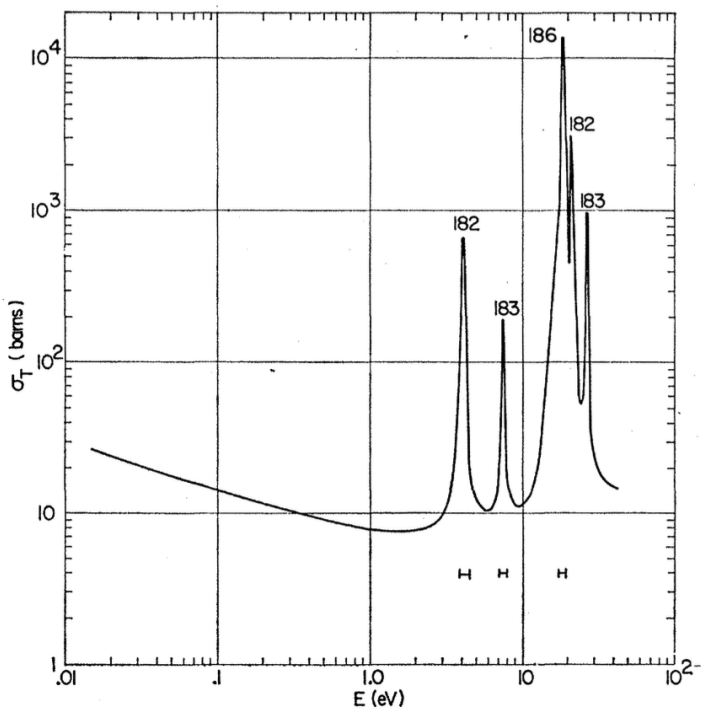

Figure 15.1: Total cross section for scattering of low energy neutrons on natural tungsten which contains several isotopes with roughly equal abundances. Resonance peaks for ^{182}W, ^{183}W, and ^{186}W are clearly visible. Figure from Ref. [19].

This behavior is more or less universal. Figure 15.2 shows the cross section for neutron capture on ^{238}U as a function of incident neutron energy. The top left panel shows a monotonically decreasing cross section as a function of energy for very low incident neutron energies. This region is often referred to as the *thermal region*[3]. The top right panel clearly shows the first few resonances at energies on the order of 10 MeV. For medium-mass nuclei, the widths of such resonances are usually on the order of eV and the spacings between the resonances are on the order of keV. In heavy nuclei, these magnitudes can be substantially reduced (as you can see in Figs. 15.1 and 15.2). This behavior persists up to about 1 MeV for heavy nuclei and up to about 10 MeV for light nuclei. The corresponding region in the dependence of the total cross section on the energy is called the *resonance region*, or sometimes also more descriptively as *resolved resonance region* for the simple reason that the resonances are well separated there. Finally, the bottom panel shows the neutron capture cross section over 9 orders of magnitude in neutron incident energy. We can see that for $n + {}^{238}$U, the resonant region extends up to about 10^4 eV. Above that energy, the spacing between the resonances becomes comparable with their widths, so that the resonances start to overlap and the *excitation function* – *i.e.*, the dependence on the energy – becomes a smooth average over the resonant behavior[4]. This energy region is called the *continuum region* or *unresolved resonance region*.

[3]The name comes from the fact that in experiments at these energies, the neutron energy is set by the condition of being in thermal equilibrium with the surrounding material (*e.g.*, a moderator or reactor material). This can be expected when neutrons scatter many times in a medium, losing or gaining energy through collisions so that their kinetic energy distribution approaches the distribution of the atoms in the material.

[4]Note that this effect can also arise from insufficient experimental resolution: even assuming that theoretically the peaks are distinct (that is, that the widths of the peaks are smaller than the spacing between them), if the detector cannot resolve energy differences on the order of the resonance spacing, their contributions will be averaged out.

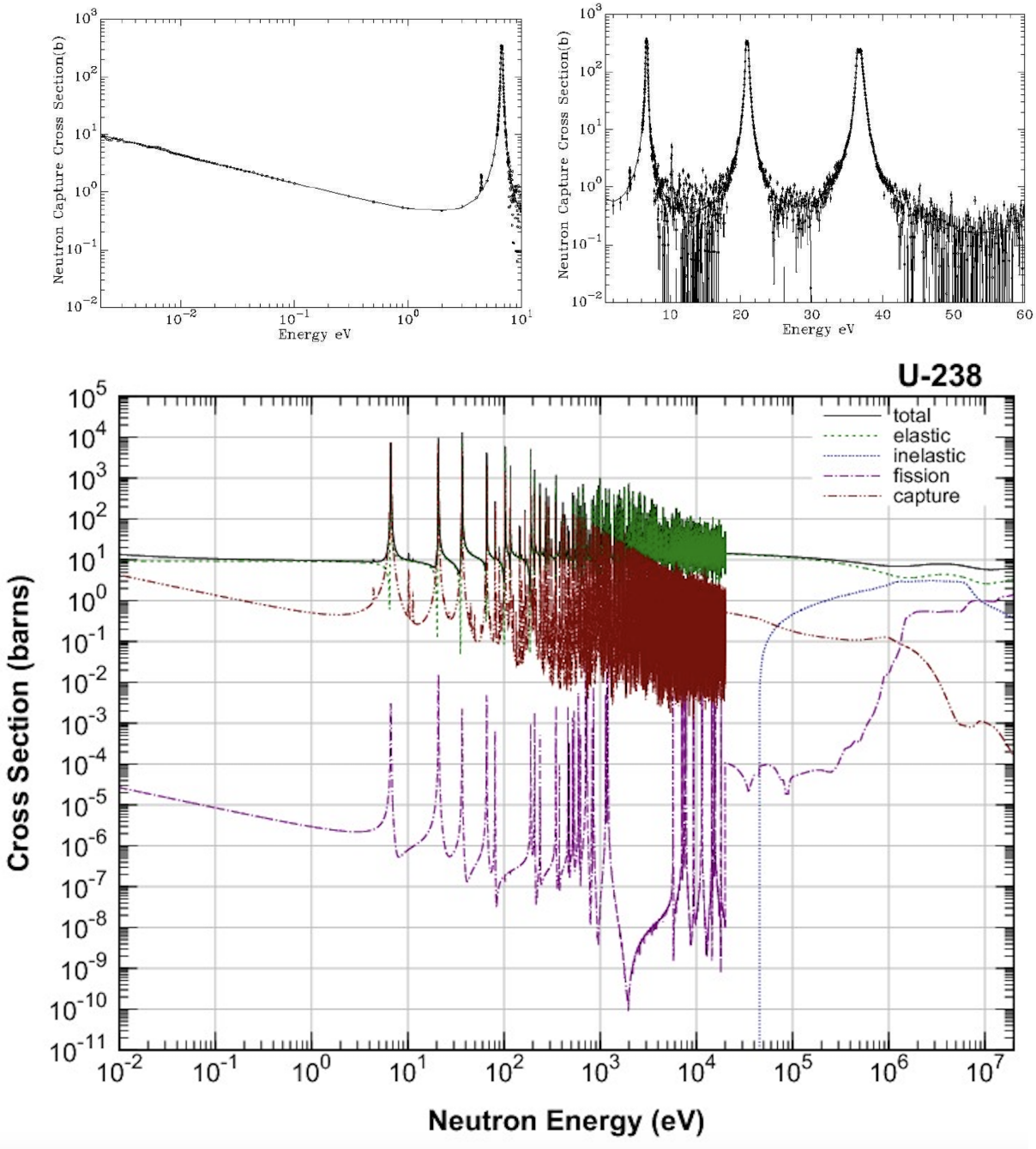

Figure 15.2: Cross section for neutron capture on ^{238}U as a function of the incident neutron energy. Top panels show experimental data as summarized in Ref. [20], while the bottom panel shows a combination of experimental measurements, modeling, and consistency constraints from Ref. [21].

15.1.2 Insights from comparison to single-particle potential scattering

Perhaps the most striking characteristic of reactions involving neutron capture on heavy nuclei becomes apparent when one tries to describe it theoretically. While scattering (including elastic scattering) off a single-particle potential can produce resonances, the properties of resonances obtained in such models do not align with what we see here. Indeed, one of the earliest mod-

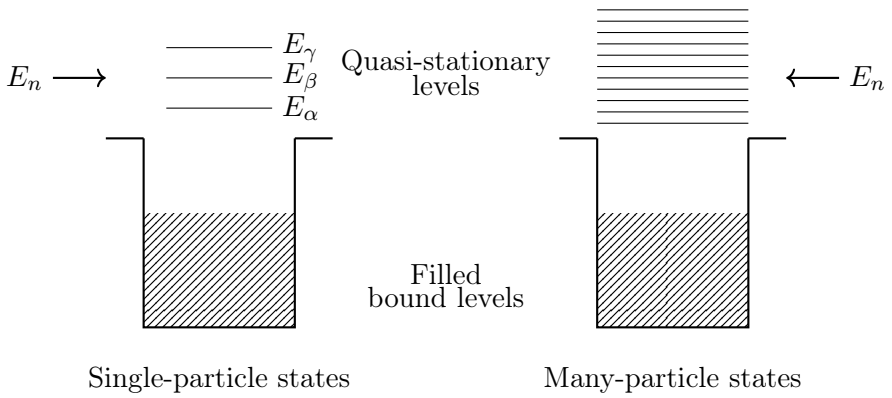

Figure 15.3: A sketch comparing the density of energy levels in a system with only a single-particle degree of freedom and in a many-body system.

els describing nuclear reactions was a single-particle potential model, developed by Hans Bethe in 1935 [22]. We have actually explored a very similar approach in Sec. 9.2: a simple square-well potential of depth V_0 and range r_0. In this model, we saw that (elastic) resonant behavior occurs when $Kr_0 = \left(n + \frac{l+1}{2}\right)\pi$, where $K^2 = 2\mu(E + V_0)$. From this, one can compute the spacing of the resonances to be[5] $\Delta E = \frac{\pi}{r_0}\sqrt{\frac{2V_0}{\mu}}$, which for $r_0 \approx 10$ fm, $V_0 \approx 50$ MeV, and $\mu \approx 940$ MeV (appropriate for a light projectile impinging on a heavy target) yields $\Delta E \approx 20$ MeV. Evidently, while potential scattering *can* produce resonances, it does not naturally describe the closely-spaced *fine resonances* in the resonance region.

There are two key insights that we get from the deep square-well potential example: 1) As discussed in Sec. 9.2, the resonance energies correspond to *quasi-stationary levels* of the system, and 2) the large spacing of the resonances can be linked to the *single-particle treatment* of scattering. Indeed, if we stop treating the nucleus as a rigid source of potential and instead consider it to be a many-body system, this many-body system can respond in a myriad ways to the incident neutron, creating exponentially more possible excited states. Schematically, the difference between the energy levels of a single-particle system and of a many-particle system is sketched in Fig. 15.3.

The intuition behind the numerous closely-spaced energy levels of a many-body system is the following: In the ground state, all lowest-lying single-particle orbitals are occupied while all higher orbitals are empty. If some energy is deposited into the system, nucleons can be promoted from the occupied orbitals to one of the empty orbitals above. Each such promotion creates a *particle-hole excitation* (*i.e.*, an excited nucleon in one of the states above the filled states and a hole left in the filled sea). Even a small excitation energy allows many possible configurations. For example, one nucleon may be excited from an occupied state to any of the (kinematically allowed) empty orbitals, or two nucleons can be excited simultaneously, and in general the excitation energy can be shared among several nucleons in numerous different ways. Moreover, there are many ways to choose which nucleons are excited and which orbitals they occupy, resulting in different total energies of the nucleus. As the excitation energy increases, the number of such configurations increases rapidly. Now let us add the fact that the nucleons interact with each other. These interactions mix the configurations and split degeneracies, producing a very dense spectrum of many-body eigenstates.

[5] With $Kr_0 = \left(n + \frac{l+1}{2}\right)\pi$, the two adjacent resonances satisfy $K^{(2)} - K^{(1)} = \pi/r_0$. Using the fact that $E \ll V_0$, which is justified for low-energy scattering discussed here, one can Taylor-expand the difference $K^{(2)} - K^{(1)} \approx \sqrt{\frac{\mu}{2V_0}}\left(E^{(2)} - E^{(1)}\right)$, which immediately yields the quoted result.

15.1.3 Phenomenology of compound nucleus reactions

Based on these insights, in 1936 Niels Bohr introduced the *compound nucleus model* [23] to explain the narrow resonances observed in scattering of low-energy neutrons[6]. In essence, the model assumed that the reactions are a two-stage process: the formation of a relatively long-lived intermediate nucleus (the compound nucleus), followed by its subsequent decay. The model further assumes that the formation of the compound nucleus occurs rapidly (on a timescale comparable to the time it takes a nucleon to traverse the nucleus) while – consistent with the narrow resonance peaks[7] – the subsequent decay is comparatively slow. Because the compound nucleus lives relatively long, several important consequences follow:

- The incident neutron interacts with many target nucleons, sharing its kinetic energy among them.
- Emission of a nucleon requires that sufficient energy be concentrated in a single nucleon to overcome the nuclear binding and escape the nuclear potential. Since the excitation energy of the compound nucleus is distributed among many nucleons and many internal degrees of freedom, such a fluctuation is comparatively unlikely and therefore occurs on a relatively long timescale. This explains the long lifetime of compound-nucleus states.
- Since a relatively long time passes between the formation of the compound nucleus and its eventual decay, during which the nucleons continue to interact and exchange energy and momentum, the system effectively equilibrates. As a result, the mode of decay is largely independent of the mode of formation. This is known as the *independence hypothesis*.

In this picture, the compound nucleus can decay through several possible channels (neutron emission, γ emission, fission, *etc.*), with probabilities determined only by the corresponding partial decay widths. In particular, it does not matter *from what direction* the incident neutron approached the target nucleus, and consequently decay cross sections of the compound nucleus are largely isotropic. Evidently, being captured in a compound-nucleus reaction is somewhat like entering a mosh pit: once you do, you can no longer tell when or where you will be pushed out.

Let us then consider the neutron capture reaction as a two-stage process,

$$\mathrm{A} + \mathrm{a} \rightarrow \mathrm{C}^* \rightarrow \mathrm{b} + \mathrm{B} \ , \tag{15.1}$$

where C is the compound nucleus and, following the independence hypothesis, the decay of C^* is independent of the nature of the projectile a and target A. This can be checked experimentally by comparing the decays of the same compound nucleus formed in different primary reactions. As an example, $^{64}\mathrm{Zn}^*$ can be produced *via* the following two entrance channels,

$$^{60}\mathrm{Ni} + \alpha \rightarrow {}^{64}\mathrm{Zn}^* \quad \text{and} \quad {}^{63}\mathrm{Cu} + \mathrm{p} \rightarrow {}^{64}\mathrm{Zn}^* \ , \tag{15.2}$$

and the excited zinc nucleus can then decay along three alternative exit channels,

$$^{64}\mathrm{Zn}^* \rightarrow \mathrm{n} + {}^{63}\mathrm{Zn} \ , \quad {}^{64}\mathrm{Zn}^* \rightarrow \mathrm{n} + \mathrm{n} + {}^{63}\mathrm{Zn} \ , \quad \text{and} \quad {}^{64}\mathrm{Zn}^* \rightarrow \mathrm{n} + \mathrm{p} + {}^{62}\mathrm{Cu} \ . \tag{15.3}$$

Cross sections for each of these options are compared with each other in Fig. 15.4, where the axes for the proton incident energy (upper horizontal axis) and the α-particle incident energy (lower horizontal axis) have been aligned to correspond to the same excitation energy of the compound nucleus [24]. Within 10–20%, the two entrance channels lead to the same yields in the decay channels, essentially confirming the independence hypothesis

[6] We note here that these experiments involve specifically neutrons due to the fact that low-energy protons cannot easily reach the nuclear interior because of the Coulomb barrier.

[7] Remember that the decay width is inversely proportional to the lifetime of the resonance.

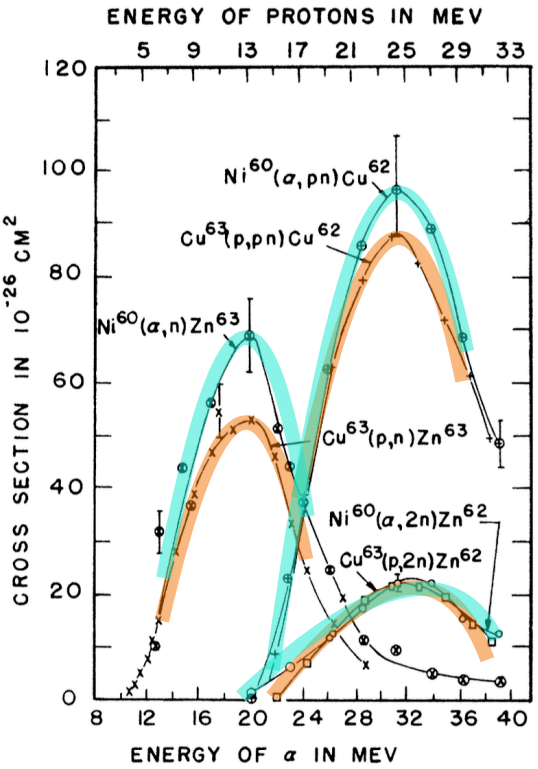

Figure 15.4: Comparison of cross sections for decay channels of the intermediate compound nucleus ^{64}Zn formed via two distinct entrance channels: in scattering of α particles on ^{60}Ni (highlighted in teal) and in scattering of protons on ^{63}Cu (highlighted in orange). Within 10–20%, the two entrance channels lead to the same yields in the decay channels. Figure modified from Ref. [24].

In-class Activity 15a: Compound nucleus lifetime

Based on data shown in Figs. 15.1 and 15.2, how does the lifetime of a compound nucleus compare to the nuclear transit time?

Solution

As we have discussed in Lecture 9, the width of a resonance is inversely proportional to its lifetime, see Eq. (9.17). Restoring $\hbar$ (the Particle Data Group [15] gives $\hbar \approx 6.582 \times 10^{-22}$ MeV s), the lifetime of resonances with widths of $\sim$ 1eV is

$$\tau \approx \frac{6.582 \times 10^{-22}\ \text{MeV s}}{10^{-6}\ \text{MeV}} \approx 10^{-15}\ \text{s} . \tag{15.4}$$

In comparison, the nuclear crossing time is on the order of[a] $t_0 = 2R/v$, where $R \approx 10$ fm is the nuclear radius. With $E_n = 10$ eV, which corresponds to $v = \sqrt{2E/m} \approx 4.38 \times 10^6$ m/s, we get

$$t_0 \approx 10^{-21}\ \text{s} . \tag{15.5}$$

Evidently, compound nucleus reactions last 6 million times longer than the time it takes to cross a nucleus, where the latter is a good proxy for the duration of direct reactions.

[a] Note that if one wants to compute the same at relativistic speeds, one needs to take into account that the nucleus is contracted in the lab frame. In that case, the crossing length is $2R/\gamma$, and thus $t_0 = 2R/\gamma v$.

The difference in duration between compound and direct reactions has profound consequences for how they present in experimental data. One consequence is the independence hypothesis. Another, closely related, is that cross sections for compound-nucleus reactions are typically nearly isotropic, reflecting the fact that the compound nucleus lives long enough to equilibrate (*i.e.*, lose the memory of the entrance direction). In contrast, cross sections for direct reactions are usually forward-peaked since the process occurs on a short time scale and retains information about the incident projectile momentum.

15.2 Multi-channel scattering

15.2.1 Loss of flux

For elastic scattering in a central potential, the partial wave expansion (see Lectures 7–9) provides a complete solution of the scattering problem. In this approach, the asymptotic effect of the potential on each angular momentum component is encoded in a phase shift δ_l, derived in Eq. (7.50), or equivalently in the partial-wave S-matrix element, which we defined in Eq. (8.5) as $S_l(E) = e^{2i\delta_l(E)}$ and which we have shown in Sec. 14.3 to be related to the scattering operator $\hat{S}$. As discussed in Sec. 14.4, since $\hat{S}$ evolves an incoming state into an outgoing state, it must conserve total probability (or, equivalently, the norm of the incident wave function), which means that $\hat{S}$ is unitary, Eq. (14.87). Since a central potential does not mix different angular momentum components[8], probability must be conserved within each angular momentum channel l. Consequently, we must have $|S_l| = 1$, which follows from the unitarity property of the S-matrix (see Sec. 14.4).

This simple picture stops being universally applicable if we admit that some of the incoming flux may "disappear" into other processes (for example, an incident neutron may be absorbed as in a compound-nucleus reaction). Of course, the full quantum-mechanical evolution of the system still conserves total probability, but some of the probability flux must be removed from the elastic channel. As a result, if we describe only the elastic channel, the "effective elastic S-matrix" is no longer unitary. One can easily incorporate this change into the existing formalism by writing

$$S_l(E) = \eta_l(E) e^{2i\delta_l(E)} \ , \tag{15.6}$$

where $0 \leq \eta_l(E) \leq 1$ is known as the *inelasticity parameter*. If $\eta_l(E) = 1$, the scattering is purely elastic. If $\eta_l(E) < 1$, then some of the incident flux has been transferred into other reaction channels.

Often, problems in which the incident flux is redirected into other channels are modeled by using an *optical potential*[9] with an imaginary component, where the latter describes the loss of flux in the system (see In-class Activity 6b). Let us stress again that it does not mean probability is truly lost; rather, the approach acknowledges that some of the flux has left the elastic channel and gone into channels which one does not attempt to describe explicitly.

This strategy is appropriate if we are only interested in elastic observables. However, if we want to know how the flux is distributed among reaction channels, we must treat those channels explicitly.

15.2.2 Reaction channels

Formally, a reaction channel is a complete asymptotic specification of the system which includes the particle content and the internal state of the fragments. Reaction channels may serve either as entrance channels or exit channels. As an example, for neutron-induced reactions on tungsten

[8] Which means that for purely elastic scattering, the scattering matrix in the angular momentum basis is diagonal.

[9] The name comes from an analogy with optics: a complex refractive index both changes the phase of a light wave and attenuates its amplitude.

(see Fig. (15.1)), we can have the elastic channel (neutron + tungsten nucleus in its ground state), inelastic channel (neutron + tungsten nucleus in an excited state), or radiative capture channel (compound nucleus + γ rays), among others.

Once we admit multiple channels as possible outcomes of a reaction, this shifts our entire viewpoint: now, to describe scattering, we must be able to include transitions between channels, for example, from the initial state of a neutron and a ^{182}W to a final state of a ^{183}W and a γ ray.

15.2.3 Multichannel S-matrix

When several channels are possible, the scattering problem must be formulated in *channel space*. In particular, the outcome for a given partial wave l can no longer be described by a single number, $S_l = e^{2i\delta_l}$. Instead, there are now multiple outcomes for each set of conserved quantum numbers, corresponding to a *block* in the S-matrix whose entries connect one channel to another. In general, the conserved quantum numbers are the total angular momentum and parity, written together as J^π. The S-matrix therefore becomes block-diagonal in J^π.

At first sight this may seem surprising. For a purely central two-body potential the orbital angular momentum l is conserved, and one might therefore expect the S-matrix to be block-diagonal in l. In (non-elastic) nuclear reactions, however, the interaction couples the projectile to the internal degrees of freedom of the target, and the orbital angular momentum of the entrance channel is not generally conserved. It is straightforward to see why on a simple example: l characterizes the relative motion of the projectile and target in the entrance channel, but if the system forms a compound nucleus, it makes no sense to assign a value of l to the intermediate state. Crucially, no conservation laws are broken in the process. What must be conserved is *total* angular momentum J, where $\boldsymbol{J} = \boldsymbol{l} + \boldsymbol{S}$ and $\boldsymbol{S}$ is the total intrinsic spin of the system, and the system's parity $\pi = \pi_{\text{proj}}\pi_{\text{targ}}(-1)^l$. As an example, consider a neutron scattering on a spin-zero nucleus, in which case the channel spin is $S = \frac{1}{2}$. Consequently, for $l = 0$ we have $J = \frac{1}{2}$, for $l = 1$ we can have $J = \frac{1}{2}$ or $J = \frac{3}{2}$, for $l = 2$ we can have $J = \frac{3}{2}$ or $J = \frac{5}{2}$, and so on. Evidently, two different values of the entrance-channel orbital angular momenta correspond to compound-nucleus states with the same J.

As a result, the diagonal blocks in the S-matrix corresponding to each possible value of J^π mix states in the channel space. Explicitly, such blocks have the following structure

$$S^{J^\pi} = \begin{pmatrix} S_{11}^{J^\pi} & S_{12}^{J^\pi} & \cdots \\ S_{21}^{J^\pi} & S_{22}^{J^\pi} & \cdots \\ \vdots & \vdots & \ddots \end{pmatrix}, \tag{15.7}$$

where the channel indices 1, 2, ... label different reaction channels, for example n+A, n+A*, γ+B, *etc.* The diagonal elements $S_{aa}^{J^\pi}$ correspond to processes in which the system begins and ends in the same channel. In an experiment where the incoming state is prepared in channel a, $S_{aa}^{J^\pi}$ describes elastic scattering while the off-diagonal elements describe reactions into other channels. Unitarity then requires that each block is also unitary, $S^{J^\pi\dagger}S^{J^\pi} = \mathbb{1}$. This expresses the fact that total probability is conserved even though flux may be transferred between different reaction channels. From this perspective, what appears as "absorption" in an optical-model description corresponds to probability flowing from the elastic channel into other explicitly included channels.

Lecture sources: This lecture is based mostly on Jackson [4].

Lecture 16

Compound nucleus reactions II

Prerequisites: Lectures 7, 8, 9, 15.
Guiding question: ***If you don't even ask where the flux goes, can you still see the effect?***

16.1 Compound nucleus reaction cross section

A compound nucleus reaction proceeds in two stages: first, particles in a given entrance channel α form a compound nucleus, and then the compound nucleus decays into a given exit channel β. As we saw in the last lecture, the entrance channel can be, *e.g.*, a neutron scattering on a heavy nucleus, $\mathrm{n} + {}^{238}\mathrm{U}$, forming a compound nucleus ${}^{239}\mathrm{U}^*$, and the exit channel can then be, for example, a de-excited ${}^{239}\mathrm{U}$ and a γ ray. But not only neutron scattering leads to compound nuclei. For example, the reaction

$$\mathrm{d} + {}^{10}\mathrm{B} \rightarrow {}^{11}\mathrm{B}^* + \mathrm{p} \quad \text{followed by} \quad {}^{11}\mathrm{B}^* \rightarrow 2\alpha + \mathrm{t} \tag{16.1}$$

is also a compound nucleus reaction.

The cross section for a given entrance channel α and exit channel β can be written as

$$\sigma_{\beta\alpha} = \sigma_{\mathrm{CN}}(\alpha) P_{\mathrm{CN}}(\beta) \ , \tag{16.2}$$

where $\sigma_{\mathrm{CN}}(\alpha)$ is the cross section for forming a compound nucleus in the channel α and $P_{\mathrm{CN}}(\beta)$ is the probability for that compound nucleus to decay into a particular exit channel β. Evidently, we treat the first part of the reaction dynamically – by considering itcross section $\sigma_{\mathrm{CN}}(\alpha)$ – while the treatment of the second part is purely statistical.

The probability $P_{\mathrm{CN}}(\beta)$ for a decay along a particular channel β is related to the *partial width* Γ_β associated with that channel. The partial widths satisfy

$$\sum_\beta \Gamma_\beta = \Gamma \ , \tag{16.3}$$

where Γ is the total width of the compound nucleus such that $\tau = 1/\Gamma$ is the lifetime of the compound nucleus. Thus the *branching probability* or *branching ratio* for decay through channel β is

$$P_{\mathrm{CN}}(\beta) = \frac{\Gamma_\beta}{\Gamma} \ , \tag{16.4}$$

and the cross section becomes

$$\sigma_{\beta\alpha} = \sigma_{\rm CN}(\alpha)\frac{\Gamma_\beta}{\Gamma} \ . \tag{16.5}$$

This relation is intuitive: the width Γ_β is proportional to the decay rate into channel β. A larger partial width therefore corresponds to a higher probability that the compound nucleus will decay through that channel rather than through another channel with a smaller width.

16.2 Elastic and absorption cross sections

As we saw in Lecture 7, once can express the asymptotic radial wavefunction as a sine wave with a phase shift, Eq. (7.49), which in turn one can also write in terms of the S-matrix element S_l as in Eq. (8.4), repeated here for convenience,

$$u_l^{\rm II}(k,r) \to \alpha_l''\Big[S_l(k)e^{ikr} - (-1)^l e^{-ikr}\Big] \ . \tag{16.6}$$

The above can be further rewritten as

$$u_l^{\rm II}(k,r) \to \alpha_l''\Big[\Big(S_l(k)-1\Big)e^{ikr} + \Big(e^{ikr} - (-1)^l e^{-ikr}\Big)\Big] \ , \tag{16.7}$$

where we see, using the partial wave expansion of a plane wave, Eq. (7.54), together with the asymptotic form of the Bessel function, Eq. (8.8), that the second term in the above equation is proportional to the incident wave $e^{i\boldsymbol{k}\cdot\boldsymbol{r}}$. Then, from the definition, $\Big(S_l(k)-1\Big) \sim f_l(\theta,\phi)$, and the total elastic cross section is given as in Eq. (8.20), repeated here for convenience,

$$\sigma_{\rm el} = \frac{\pi}{k^2}\sum_l (2l+1)\big|S_l - 1\big|^2 \ . \tag{16.8}$$

On the other hand, the form we see in Eq. (16.6) is also very useful, since we see that the solution is divided into the *incoming* (e^{-ikr}) and *outgoing* (e^{ikr}) wave, which allows us to compare the magnitudes of their amplitudes. Evidently, the incoming wave has an amplitude of magnitude equal 1, while the outgoing wave has an amplitude of magnitude equal $|S_l(k)|$. If we now allow the S-matrix element to carry some inelasticity through the inelasticity parameter η, Eq. (15.6), then the incident flux will not be equal to the outgoing flux, or in other words, $|S_l| \neq 1$. We can then use the magnitude of the missing probability flux, which is proportional to $1 - \big|S_l(k)\big|^2$, to define the *absorption cross section*,

$$\sigma_{\rm abs} = \frac{\pi}{k^2}\sum_l (2l+1)\Big(1 - \big|S_l(k)\big|^2\Big) \ , \tag{16.9}$$

which is also sometimes called a *reaction cross section*[1].

16.3 Resonances in elastic and absorption cross sections

We have already discussed resonances in Sec. 9.1, where we derived the Breit-Wigner form of the cross section near a resonance, Eq. (9.14). There, the derivation was based on an assumption that the logarithmic derivative $\mathcal{L}^{\rm I}$ is real which – as already noted there – is only true for purely elastic processes. In particular, $\mathcal{L}^{\rm I}$ becomes complex in the presence of complex potentials which lead to a loss of probability flux and thus describe absorption (see Sec. 15.2.1). Thus, to describe resonances in the presence of absorption, we need to generalize the derivation, which we will do below.

[1]The idea being that if the scattering is elastic, it's *not* a reaction, while any non-elastic process *is* a reaction.

16.3.1 Obtaining S_l from the matching condition

With $u_l^{\mathrm{II}}(k,r)$ given by Eq. (16.6), we can assume that for a given channel the interaction ceases to matter at separation distances greater than the *channel radius* R, and then we can explicitly calculate the logarithmic derivative[2] at that R,

$$\mathcal{L}^{\mathrm{II}} = ikR\frac{S_l e^{ikR} + (-1)^l e^{-ikR}}{S_l e^{ikR} - (-1)^l e^{-ikR}} \ . \tag{16.10}$$

Since the matching condition requires that $\mathcal{L}^{\mathrm{I}} = \mathcal{L}^{\mathrm{II}}$, we can solve the above equation for S_l,

$$S_l = \frac{\mathcal{L}^{\mathrm{I}} + ikR}{\mathcal{L}^{\mathrm{I}} - ikR}(-1)^l e^{-2ikR} \ . \tag{16.11}$$

Note that if $\mathcal{L}^{\mathrm{I}}$ is real, then $|S_l| = 1$, *i.e.*, the reaction is purely elastic. Conversely, we see that if $\mathrm{Im}\big[\mathcal{L}^{\mathrm{I}}\big] < 0$, then $|S_l| < 1$, *i.e.*, there is some redirection of the elastic flux[3].

With this, the elastic cross section, Eq. (16.8), becomes

$$\sigma_{\mathrm{el}} = \frac{\pi}{k^2}\sum_l (2l+1)\big|1 - S_l\big|^2 = \frac{\pi}{k^2}\sum_l (2l+1)\left|e^{2ikR} - (-1)^l\frac{\mathcal{L}^{\mathrm{I}} + ikR}{\mathcal{L}^{\mathrm{I}} - ikR}\right|^2 \tag{16.12}$$

$$= \frac{\pi}{k^2}\sum_l (2l+1)\left|e^{2ikR} - (-1)^l\left(1 + \frac{2ikR}{\mathcal{L}^{\mathrm{I}} - ikR}\right)\right|^2 , \tag{16.13}$$

while the absorption cross section, Eq. (16.9), becomes

$$\sigma_{\mathrm{abs}} = \frac{\pi}{k^2}\sum_l (2l+1)\Big(1 - \big|S_l(k)\big|^2\Big) = \frac{\pi}{k^2}\sum_l (2l+1)\left(1 - \left|\frac{\mathcal{L}^{\mathrm{I}} + ikR}{\mathcal{L}^{\mathrm{I}} - ikR}\right|^2\right) \tag{16.14}$$

$$= \frac{\pi}{k^2}\sum_l (2l+1)\frac{-4\mathrm{Im}\big[\mathcal{L}^{\mathrm{I}}\big]kR}{\Big(\mathrm{Re}\big[\mathcal{L}^{\mathrm{I}}\big]\Big)^2 + \Big(\mathrm{Im}\big[\mathcal{L}^{\mathrm{I}}\big] - kR\Big)^2} \ . \tag{16.15}$$

16.3.2 Identifying resonant behavior

It is evident that the absorption cross section, Eq. (16.15), is maximum when $\mathrm{Re}\big[\mathcal{L}^{\mathrm{I}}\big] = 0$. We can get an intuition as to why that is by considering purely elastic scattering[4]. In that case, the radial solution u_l^{I} is real. Consequently, the logarithmic derivative at the boundary is also real, and the condition $\mathrm{Re}\big[\mathcal{L}^{\mathrm{I}}\big] = 0$ is equivalent to $\mathcal{L}^{\mathrm{I}} = 0$. This, in turn, is nothing else than demanding that $du_l^{\mathrm{I}}/dr = 0$, *i.e.*, that the wave has an extremum at the boundary, which is a condition for a standing wave. As we have already seen when discussing the deep square well potential in Sec. 9.2, satisfying this condition is equivalent to an occurrence of a resonance. With this insight, we use

[2] Similarly as in Sec. 9.1, in principle we should put a subscript l on $\mathcal{L}^{\mathrm{II}}$ and other following quantities to stress their relation to a particular partial wave l. However, we choose not to do that so as to not overwhelm the notation.

[3] Note that $\mathrm{Im}\big[\mathcal{L}^{\mathrm{I}}\big]$ cannot be positive, as that would lead to $|S_l| > 1$, which violates conservation of probability.

[4] You may think it makes no sense to explain a feature of non-elastic scattering by considering elastic scattering. The reason we can do that is because the resonant part of the elastic cross section (which we will isolate below) is *also* maximal when $\mathrm{Re}\big[\mathcal{L}^{\mathrm{I}}\big] = 0$. However, because the elastic cross section in addition contains a non-resonant contribution, this feature is less obvious, which is why we first pointed it out by looking at the absorption cross section, Eq. (16.15).

Taylor expansion around the resonance energy E_R to write $\mathcal{L}^{\rm I}$ as a sum of the first leading real contribution and a complex contribution,

$$\mathcal{L}^{\rm I} \approx -a(E-E_R) - ib + \dots \ , \tag{16.16}$$

where $a = \left(d({\rm Re}\mathcal{L}^{\rm I})/dE\right)_{E=E_R}$ and $b = {\rm Im}\mathcal{L}^{\rm I}$.

Using the above expansion, in the vicinity of a resonance the elastic cross section, Eq. (16.13), becomes

$$\sigma_{\rm el}\big|_{E\sim E_R} = \frac{\pi}{k^2}\sum_l (2l+1)\left| e^{2ikR} - (-1)^l\left(1 - \frac{2i\frac{kR}{a}}{(E-E_R) + i\left(\frac{b+kR}{a}\right)}\right)\right|^2 \ , \tag{16.17}$$

where we can identify the non-resonant contribution to the cross section, also referred to as the *potential or shape-elastic scattering*, which away from the resonance will be given by

$$\sigma_{\rm el}^{\rm (NR)} = \frac{\pi}{k^2}\sum_l (2l+1)\left| e^{2ikR} - (-1)^l\right|^2 \ , \tag{16.18}$$

and the resonant contribution which will dominate near the resonance,

$$\sigma_{\rm el}^{\rm (R)} = \frac{\pi}{k^2}\sum_l (2l+1)\frac{\left(\frac{2kR}{a}\right)^2}{(E-E_R)^2 + \left(\frac{b+kR}{a}\right)^2} \ , \tag{16.19}$$

and which represents the scattering arising from re-emission of the absorbed neutron by the compound nucleus, or *compound-elastic scattering*. Note that the latter describes a very specific situation: we interpret it as the projectile and target first forming an intermediate state (a compound nucleus) and then disintegrating *into the original participants with their exact original energies*, so that the final energy of the projectile particle equals the incident energy. Of course, since each elementary particle of a given species is exactly the same as any other particle from the same species, there is no way of telling whether, *e.g.*, the outgoing neutron is exactly the same as the incident one[5]. However, since it has the same energy as the projectile, we can call the process "elastic."

Similarly, again using the Taylor expansion of the logarithmic derivative, Eq. (16.16), the absorption cross section, Eq. (16.15), becomes

$$\sigma_{\rm abs}\big|_{E\sim E_R} = \frac{\pi}{k^2}\sum_l (2l+1)\frac{4\frac{bkR}{a^2}}{\left(E-E_R\right)^2 + \left(\frac{b+kR}{a}\right)^2} \ . \tag{16.20}$$

Let us appreciate the fact that we obtained a fully practical expression for the absorption cross section, Eq. (16.20), including the possibility of resonant behavior, without having to specify the detailed mechanism by which the missing flux is redistributed. All we had to do in order to arrive at this result was to acknowledge the possibility that some of the initial flux may leave the elastic channel, or equivalently that $|S_l| < 1$, and the rest automatically followed from the definition of the absorption cross section given in Eq. (16.9). Note also that while the magnitude of the absorption cross section is determined by $b = {\rm Im}[\mathcal{L}^{\rm I}]$, for both the resonant-elastic and the absorption cross section it is the distance from a (common!) resonance energy E_R that drives the resonant behavior. This reflects the fact that, although the final decay channels may be very different – for example emission of a neutron in the elastic channel *versus* emission of a γ-ray in neutron capture – both processes originate from the existence of the same quasi-bound state in the positive-energy spectrum of the system. The formation of this intermediate state corresponds to the creation of a compound nucleus, and it is the enhanced probability for forming this state that amplifies the subsequent processes.

[5]Strictly speaking, the question doesn't even make sense. They are all indistinguishable.

16.3.3 Partial widths

Looking at Eqs. (16.20) and (16.19), with insight from Sec. 9.1, we can now identify the *partial width Γ_α for re-emission of the incident neutron through channel α*,

$$\Gamma_\alpha \equiv \frac{2kR}{a} \ , \tag{16.21}$$

the total width

$$\Gamma \equiv \frac{2(b+kR)}{a} \ , \tag{16.22}$$

and the *absorption width* (often also referred to as the *reaction width*) as

$$\Gamma_r \equiv \sum_{\beta\neq\alpha} \Gamma_\beta = \Gamma - \Gamma_\alpha = \frac{2b}{a} \ . \tag{16.23}$$

Note that, in agreement with our intuition, the resonance width is inversely proportional to a, which is the slope of $\mathrm{Re}\left[\mathcal{L}^{\mathrm{I}}\right]$ as a function of energy, while the absorption width is proportional to b, which is the imaginary part of $\mathcal{L}^{\mathrm{I}}$. Along with these definitions, we also restore the subscript l on all derived quantities (see Footnote 2) and write the compound-elastic and absorption cross sections, Eqs. (16.19) and (16.20), as

$$\sigma_{\mathrm{el}}^{(\mathrm{R})}(E) = \frac{\pi}{k^2}\sum_l (2l+1)\frac{\Gamma_{l,\alpha}^2}{(E-E_{l,R})^2 + \left(\frac{\Gamma_l}{2}\right)^2} \ , \tag{16.24}$$

where we omitted the shape-elastic contribution because the resonant part will dominate near the resonance, and

$$\sigma_{\mathrm{abs}}(E) = \frac{\pi}{k^2}\sum_l (2l+1)\frac{\Gamma_{l,r}\Gamma_{l,\alpha}}{\left(E-E_{l,R}\right)^2 + \left(\frac{\Gamma_l}{2}\right)^2} \ , \tag{16.25}$$

respectively. The total cross-section for compound-nucleus formation through channel α is then obtained by adding these two contributions, which yields

$$\sigma_{\mathrm{CN}}(\alpha) = \sigma_{\mathrm{el}}^{(\mathrm{R})} + \sigma_{\mathrm{abs}} = \frac{\pi}{k^2}\sum_l (2l+1)\frac{\Gamma_l\Gamma_{l,\alpha}}{\left(E-E_{l,R}\right)^2 + \left(\frac{\Gamma_l}{2}\right)^2} \ , \tag{16.26}$$

and with this the cross section for the process $\alpha \to \beta$, Eq. (16.5), is given by

$$\sigma_{\beta\alpha} = \frac{\pi}{k^2}\sum_l (2l+1)\frac{\Gamma_{l,\beta}\Gamma_{l,\alpha}}{\left(E-E_{l,R}\right)^2 + \left(\frac{\Gamma_l}{2}\right)^2} \ . \tag{16.27}$$

Finally, we stress that while this derivation treated l as a good quantum number, it is the *total angular momentum and parity J^π* that are strictly conserved, as discussed in Sec. 15.2.3. That is, in realistic nuclear reactions the projectile spin $\boldsymbol{s}_a$, the target spin $\boldsymbol{s}_A$, and the orbital angular momentum of the system $\boldsymbol{L}$ couple to give the conserved total angular momentum $\boldsymbol{J} = \boldsymbol{L} + \boldsymbol{s}_a + \boldsymbol{s}_A$, and parity $\pi = \pi_a\pi_A(-1)^l$ is conserved as well. Including the spin degrees of freedom then leads to a more elaborate but conceptually straightforward extension of the formalism, in which the cross sections are expressed as sums over channels with definite J^π. At this moment, we choose to omit the description of spin to focus on the essential features of the covered topics such as, for example, the

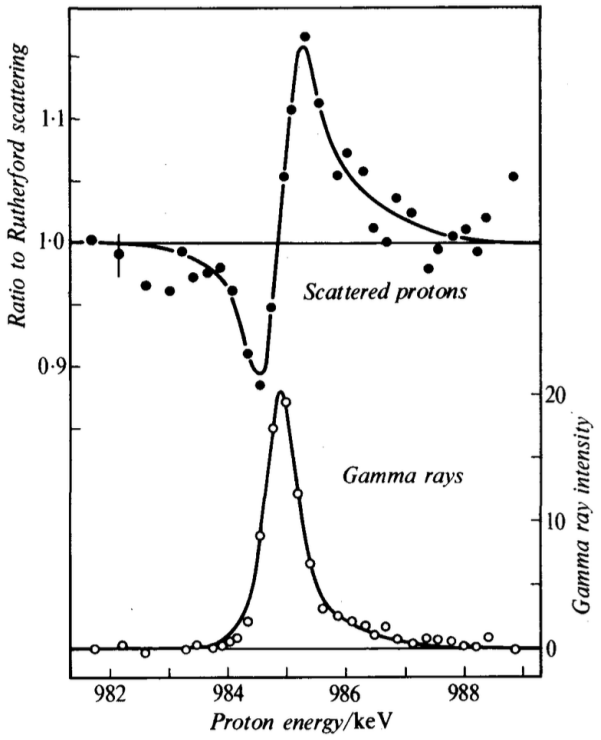

Figure 16.1: Scattering and absorption of protons at the 985-keV resonance in the reaction $\mathrm{p} + {}^{27}\mathrm{Al}$. The top panel shows the yield of scattered protons, while the bottom panel shows the yield of capture radiation. Figure from Ref. [17].

emergence of the resonant behavior from the vanishing of the real part of $\mathcal{L}^{\mathrm{I}}$, signaling maximum amplitude at the matching radius, or the relation of the resonance width to the imaginary part of $\mathcal{L}^{\mathrm{I}}$. If and when we need to consider spin, we will be able to do that without bigger problems. For example, the compound-nucleus cross section in this case becomes

$$\sigma_{\beta\alpha} = \frac{\pi}{k^2} \sum_J \frac{2J+1}{(2s_a+1)(2s_A+1)} \frac{\Gamma_{\beta J}\Gamma_{\alpha J}}{(E-E_{RJ})^2 + (\Gamma_J/2)^2} \ . \tag{16.28}$$

In the above formula, although the total angular momentum and the spin clearly affect the overall magnitude of the cross section, it is also clear that the essential physics remains unchanged.

In-class Activity 16a: Resonant behavior in scattering of charged particles

How can you explain the behavior plotted in the upper panel of Fig. 16.1?

Solution

What we see is a modification of a resonant peak due to the interference of the non-resonant Coulomb scattering amplitude and the resonant part of the nuclear scattering amplitude. To show this is the case, let us consider the S-matrix in the partial-wave expansion. For proton (or any other charged particle) scattering, it's given by

$$S_l(E) = e^{2i\sigma_l} e^{2i\delta_l(E)} \ , \tag{16.29}$$

where σ_l is the Coulomb phase shift and $\delta_l(E)$ is the nuclear phase shift. Near the resonance,

the nuclear phase shift can be decomposed into a slowly varying background part and a resonant part,

$$\delta_l(E) = \delta_l^{\rm bg}(E) + \delta_l^{\rm res}(E) \ , \tag{16.30}$$

where the resonant piece behaves like

$$\delta_l^{\rm res}(E) \approx \begin{cases} 0 & E \ll E_R \\ \pi/2 & E \approx E_R \\ \pi & E \gg E_R \end{cases} \tag{16.31}$$

Near the resonance, we can neglect the nuclear background contribution so that the full scattering amplitude may be written as

$$f(\theta, E) \approx f_C(\theta, E) + f_{\rm res}(\theta, E) \ . \tag{16.32}$$

Over the small energy interval relevant for the resonance, $f_C(\theta, E)$ varies only slightly, while $f_{\rm res}(\theta, E)$ changes rapidly. Consequently, for a fixed angle θ, we can treat f_C as a complex constant A, and write the resonant piece as[a]

$$f_{\rm res}(E) = \frac{B}{(E - E_R) + i\Gamma/2} \ , \tag{16.33}$$

where B is another slowly varying complex number. Then the cross section is given by

$$\frac{d\sigma}{d\Omega} = \left|f(E)\right|^2 = |A|^2 + \frac{|B^2|}{(E - E_R)^2 + \Gamma^2/4} + 2{\rm Re}\left[A^* \frac{B}{(E - E_R) + i\Gamma/2}\right] \ . \tag{16.34}$$

Here, the first term is the Rutherford-like background, the second is a symmetric Breit-Wigner bump, and the third is an interference term which we will show to produce the asymmetric dip-peak shape in the p + ^{27}Al resonance shown in Fig. 16.1.
Let's denote

$$A^* B = C e^{i\phi} \ , \tag{16.35}$$

with $C > 0$. In that case

$$2{\rm Re}\left[A^* \frac{B}{(E - E_R) + i\Gamma/2}\right] = 2C{\rm Re}\left[\frac{e^{i\phi}}{(E - E_R) + i\Gamma/2}\right] \ . \tag{16.36}$$

Defining $\Delta E = E - E_R$, we can write multiply both the numerator and the denominator in the bracket by $\Delta E - i\Gamma/2$, so that now the interference term is equal

$$\frac{2C}{(\Delta E)^2 + \Gamma^2/4} {\rm Re}\Big[e^{i\phi}(\Delta E - i\Gamma/2)\Big] \ . \tag{16.37}$$

Expanding the exponent and taking the real part leads to

$$\frac{2C}{(\Delta E)^2 + \Gamma^2/4} {\rm Re}\Big[\Delta E \cos\phi + \Gamma/2 \sin\phi\Big] \ . \tag{16.38}$$

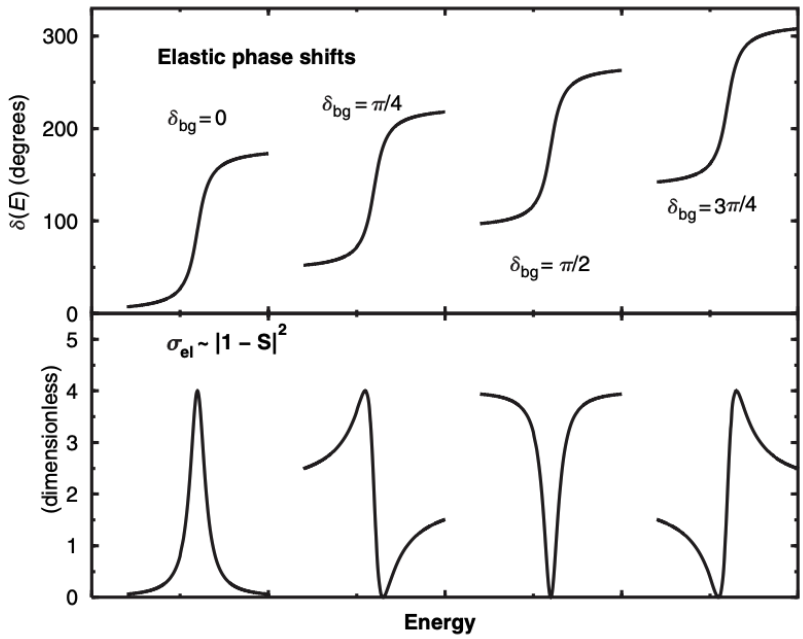

Figure 16.2: Possible modifications of the Breit-Wigner resonance shape due to a slowly-varying background phase. The upper panel shows resonant phase shifts with background phase shifts equal 0, $\pi/4$, $\pi/2$, and $3\pi/4$, and the lower panel shows the corresponding contribution to the total elastic scattering cross section. Figure from Ref. [5].

The first term is odd in ΔE: it's negative below the resonance and positive above. Assuming that $\cos\phi > 0$, then the interference is destructive for $E < E_R$ and constructive for $E > E_R$. If $\cos\phi < 0$, we will instead have positive interference below the resonance and destructive interference above, *i.e.*, a peak followed by a dip. The influence of the even term, proportional to $\sin\phi$, is also important: whenever $\sin\phi > 0$, it will contribute positively on both sides of the resonance, and negatively if $\sin\phi < 0$. This results in a variety of different possible modifications to the resonant cross section, see Fig. 16.2.

What is ϕ? From the definition, Eq. (16.35), it is a relative phase between the smooth background contribution and the resonant contribution. It is different for every specific collision system, energy, *etc.*, but in principle it can be calculated[b] and, of course, one can extract it from fits to measurements. Importantly, the background does not have to be due to the Coulomb force: the nuclear background scattering amplitude can also produce interference. Nevertheless, the Coulomb contribution to the scattering amplitude is often stronger than the nuclear background contribution, so that it dominates the interference term.

[a] That the scattering amplitude has this form can be inferred from combining Eqs. (8.21) and (9.14).
[b] As long as the interaction is well-known, which is naturally the central problem of nuclear physics.

Lecture sources: This lecture is based mostly on Jackson [4].

Lecture 17

Compound nucleus reactions III

Prerequisites: Lectures 6, 11, 12, 13, 15, 16.
Guiding question: ***How does coupling to a continuum of scattering states transform a discrete configuration into a quasi-bound state, and how does it change its properties?***

In Sec. 16.3, we used the partial wave expansion and the matching condition at the channel radius R (understood as the boundary beyond which the short-range interaction is negligible and the wave function can be matched to its asymptotic form) to identify resonant contributions to the elastic and absorption cross sections, Eqs. (16.19) and (16.20), and then we used them to obtain the resonant cross section for the process $\alpha \to \beta$, Eq. (16.27). The cross section for a given reaction channel $\alpha \to \beta$ can also be obtained using the T-matrix formalism developed in Sec. 13.1. In this formulation, the matrix elements $T_{\beta\alpha}$ connect an initial channel α with a final channel β, naturally accommodating multichannel scattering which we started discussing in Sec. 15.2.

17.1 The background and resonant contributions of the T-matrix

We start from the full Lippmann–Schwinger equation for the T operator, Eq. (13.8), repeated here for convenience,

$$\hat{T}(E) = \hat{V} + \hat{V}\hat{G}^{(+)}(E)\hat{V} \ , \tag{17.1}$$

where $\hat{G}^{(+)}(E) = \lim_{\epsilon\to 0}(E - \hat{H} + i\epsilon)^{-1}$, as defined in Eq. (11.13), and $\hat{H}$ is the full Hamiltonian. To proceed, we must use a number of insights from complex analysis. This is because the behavior of the Green's operator $\hat{G}^{(+)}(E)$ is governed by its complex poles. The key property is that in the vicinity of such a complex pole, we can decompose $\hat{G}^{(+)}(E)$ into its singular (divergent) and regular contributions,

$$\hat{G}^{(+)}(E) = \frac{\hat{\mathcal{R}}_R}{E - z_R} + \hat{G}^{(+)}_{\rm reg}(E) \ , \tag{17.2}$$

where $\hat{\mathcal{R}}_R$ is the *residue operator* of the pole, z_R is an isolated complex pole, and $\hat{G}^{(+)}_{\rm reg}(E)$ is the regular part which varies smoothly with energy[1]. In scattering theory, poles of the Green's

[1]To develop an intuition how such a division can be done, let us consider a function $f(z) = e^z/(z-1)$, where z is a complex number. It is evident that the function is singular for $z = 1$, which is a simple pole (which means that a term of the form $(z - z_0)^{-1}$ is the *most singular term* there is). We can divide this function into a singular and regular contribution based on a realization that if the numerator can be written as a power series in $(z - 1)$, then

operator in the complex energy plane correspond to resonances. If such a pole lies close to the real energy axis, the propagator becomes strongly enhanced for real energies $E \approx \mathrm{Re}[z_R]$, producing the characteristic resonant behavior of the cross section.

To investigate the behavior of the system near the pole, we can substitute the decomposition from Eq. (17.2) into the equation for the T-matrix, Eq. (17.1), which yields

$$\hat{T}(E) = \left(\hat{V} + \lim_{\epsilon\to 0}\ \hat{V}\hat{G}^{(+)}_{\mathrm{reg}}(E)\hat{V}\right) + \hat{V}\frac{\hat{\mathcal{R}}_R}{E - z_R}\hat{V} \tag{17.3}$$

$$= \hat{T}^{(\mathrm{bg})}(E) + \hat{V}\frac{\hat{\mathcal{R}}_R}{E - z_R}\hat{V}\ , \tag{17.4}$$

where we organized the terms into a background (*i.e.*, smoothly varying) and resonant contribution. To understand the structure of the pole in the $\hat{G}^{(+)}_{\mathrm{reg}}(E)$ operator and determine the form of the residue operator $\hat{\mathcal{R}}_R$, let us now consider a simple model of the compound nucleus Hamiltonian.

17.2 A simple model of the compound nucleus reaction

A minimal Hamiltonian which describes formation of a compound nucleus can be written in terms of a discrete[2] configuration $|R\rangle$, describing the resonant compound nucleus state, and continuum states $|c, E'\rangle$, where c labels open channels (*e.g.*, states with specific values of the total angular momentum and parity). We note that these states are *not* eigenstates of the Hamiltonian[3], but

only a few terms in that series will be singular, while all others will behave well for any z. Using the definition of the exponential function, we have

$$f(z) = \frac{e\ e^{z-1}}{z-1} = \frac{e}{z-1}\left(1 + (z-1) + \frac{(z-1)^2}{2} + \frac{(z-1)^3}{6} + \dots\right) = \frac{e}{z-1} + e\left(1 + \frac{(z-1)}{2} + \frac{(z-1)^2}{6} + \dots\right)\ .$$

This form isolates the "truly singular" term in $f(z)$ and at the same time identifies the "remaining regular" part. One may, naturally, consider more complicated functions, such as $g(z) = e^z/(z-1)^2$, which has a second-order pole at $z = 1$ and can be similarly rewritten as

$$g(z) = \frac{e}{(z-1)^2} + \frac{e}{z-1} + e\left(\frac{1}{2} + \frac{(z-1)}{6} + \dots\right)\ .$$

In general, one may form a *Laurent series* of any complex function,

$$h(z) = \sum_{n=-\infty}^{\infty} a_n \big(z - z_0\big)^n\ ,$$

where for functions with simple poles the sum starts at $n = -1$ (that is, $a_n = 0$ for all $n < -1$), for functions with second-order poles the sum starts at $n = -2$, *etc.* We define the *residue* of the pole as the coefficient of the $(z - z_0)^{-1}$ term, *i.e.*, $\mathrm{Res}_{z=z_0} f(z) \equiv a_{-1}$. As you might remember, residues are key for the *Cauchy residue theorem*, which states that if a function has isolated poles inside a closed contour C, then $\oint_C dz\ f(z) = 2\pi i \sum_k \mathrm{Res}_{z=z_k} f(z)$, where the sum runs over all poles z_k inside the contour. This is exactly what we used in Sec. 11.4 to compute the explicit expression for $\hat{G}_0$ in the coordinate representation.

The key point about the Laurent series is that it isolates the few singular terms (all non-zero terms with $n < 0$), which naturally dominate in the vicinity of the pole, and separates them from the regular contributions which carry the most significance everywhere else. This crisp division allows us to draw conclusions that would otherwise be obscured. Crucially, the concept of dividing into a regular and singular contributions can be directly extended from complex functions to operators, which we used in Eq. (17.2).

[2]Here, "discrete" simply means that a given category of states can be labeled with an integer index, leading to a *discrete set* of states (in this case only one state), as opposed to the "continuum" states which are labeled by a real number, for example by values of the energy E.

[3]This is because the state $|R\rangle$ is not stationary (*i.e.*, it decays), which means that the associated probability density changes in time and so it cannot be a true eigenstate of the Hamiltonian.

simply states which form a convenient basis for the *model-space*, *i.e.*, which span the minimal subspace of the Hilbert space relevant for describing the formation and decay of the compound nucleus[4]. We take states $|R\rangle$ and $|c, E'\rangle$ to satisfy the orthogonality conditions

$$\langle R|R\rangle = 1 \ , \quad \langle c, E'|c', E''\rangle = \delta_{cc'}\delta(E' - E'') \ , \quad \langle R|c, E'\rangle = 0 \ . \tag{17.5}$$

The Hamiltonian can then be schematically written as

$$\begin{aligned}\hat{H} = E_R^{(0)} \, |R\rangle \, \langle R| + \sum_c \int dE' \ E' \, |c, E'\rangle \, \langle c, E'| \\ + \sum_c \int dE' \, \Big(V_c(E') \, |R\rangle \, \langle c, E'| + V_c^*(E') \, |c, E'\rangle \, \langle R| \Big) \ ,\end{aligned} \tag{17.6}$$

where $E_R^{(0)}$ is the energy the compound state would have in the absence of coupling to the continuum[5], E' are energies of the continuum states, and $V_c(E')$ is the coupling of the resonance to the channel c at energy E'.

Writing a Hamiltonian as in Eq. (17.6) may seem weird. In a more formal approach, such a Hamiltonian can arise when the full many-body Hamiltonian of the reaction system is projected onto a reduced model space containing only a few relevant configurations. In the present case, we choose a model space consisting of a single internal compound configuration $|R\rangle$ and the continuum scattering states $|c, E'\rangle$ describing the open reaction channels. The first two terms in Eq. (17.6) then describe the energies that these configurations would have if they did not interact with each other[6], while the terms proportional to $V_c(E')$ couple the discrete configuration $|R\rangle$ and the continuum channels. These off-diagonal terms express the fact that the system may transition from a continuum channel into the compound configuration or *vice versa*.

Moreover, although this representation may look unusual, similar constructions appear in many areas of physics. For example, in neutrino physics the neutrino mass eigenstates diagonalize the Hamiltonian, while the neutrino flavor states are linear combinations of those mass eigenstates. Therefore, if the Hamiltonian is written in the flavor basis, it is not diagonal and contains terms that mix the flavor states. The time evolution generated by this non-diagonal Hamiltonian leads directly to the phenomenon of neutrino oscillations, in which a neutrino created in one flavor state (for example an electron neutrino) over time develops a finite probability to be detected in another flavor state (such as a muon neutrino).

Using the assumed basis states $|R\rangle$ and $|c, E'\rangle$, we can decompose any state with energy E as

$$|\Psi_E\rangle = a(E) \, |R\rangle + \sum_{c'} \int dE'' \ b_{c'}(E; E'') \, |c', E''\rangle \ , \tag{17.7}$$

where the amplitudes $a(E)$ and $b_{c'}(E; E'')$ keep track of the magnitudes of contributions from the discrete states $|R\rangle$ and the continuum of states $\{ |c', E''\rangle \}$ to the state $|\Psi_E\rangle$. Because the Hamiltonian mixes the discrete state $|R\rangle$ and the continuum channels, a state with a definite energy generally contains components of both types. In particular, even if initially we prepare the system in one state, say $|R\rangle$, it will evolve into a mixture of the form shown above. Formally, we can write this as

$$|\Psi_E\rangle = \hat{G}^+(E) \, |R\rangle \ , \tag{17.8}$$

[4] As such, the model space does *not* include, for example, the full spectrum of internal nuclear states of the isolated nucleus.

[5] The meaning of this will become clear in the following.

[6] See above.

where $\hat{G}^+(E)$ is the full Green's function, Eq. (11.13), associated with the Hamiltonian $\hat{H}$, Eq. (17.6). Given the decomposition of $|\Psi_E\rangle$, Eq. (17.7), we can immediately see that

$$a(E) = \langle R|\Psi_E\rangle = \left\langle R\middle|\hat{G}^+(E)\middle|R\right\rangle \ . \tag{17.9}$$

In other words, if we extract the amplitude $a(E)$, we will obtain the matrix element of the Green's function between the states $|R\rangle$, *i.e.*, the amplitude for the system of energy E to evolve from the configuration $|R\rangle$, through whichever continuum states the operator $\hat{G}^+(E)$ takes it to, and back to the same configuration.

As evident from the definition of $\hat{G}^+(E)$ as an inverse operator, Eq. (11.13), the relation in Eq. (17.8) can be equivalently written as

$$\left(E - \hat{H} + i\epsilon\right)|\Psi_E\rangle = |R\rangle \ . \tag{17.10}$$

Since the action of the Hamiltonian on the eigenstates $|R\rangle$ and $|c, E'\rangle$ is

$$\hat{H}\,|R\rangle = E_R^{(0)}\,|R\rangle + \sum_c \int dE'\ V_c^*(E')\,\left|c, E'\right\rangle \tag{17.11}$$

and

$$\hat{H}\left|c', E'\right\rangle = E'\left|c', E'\right\rangle + V_{c'}(E')\,|R\rangle \ , \tag{17.12}$$

respectively, we can immediately see that applying $\hat{H}$ to Ψ_E yields

$$\begin{aligned}\hat{H}\,|\Psi_E\rangle &= a(E)\left(E_R^{(0)}\,|R\rangle + \sum_c \int dE'\ V_c^*(E')\left|c, E'\right\rangle\right) \\ &\quad + \sum_{c'} \int dE''\ b_{c'}(E; E'')\left(E''\left|c', E''\right\rangle + V_{c'}(E'')\,|R\rangle\right) \qquad (17.13)\\ &= \left(a(E)E_R^{(0)} + \sum_c \int dE'\ b_c(E; E')V_c(E')\right)|R\rangle \\ &\quad + \sum_c \int dE'\ \left(a(E)V_c^*(E') + E'b_c(E; E')\right)\left|c, E'\right\rangle \ , \qquad (17.14)\end{aligned}$$

where in the second equality we gathered terms multiplying the same basis vectors and renamed some dummy indices. With this and Eq. (17.7), we can rewrite the left-hand side of Eq. (17.10) as

$$\begin{aligned}\left(E - \hat{H} + i\epsilon\right)|\Psi_E\rangle &= \left(E + i\epsilon\right)|\Psi_E\rangle - \hat{H}\,|\Psi_E\rangle \qquad (17.15)\\ &= \left[\left(E - E_R^{(0)} + i\epsilon\right)a(E) - \sum_c \int dE'\ b_c(E; E')V_c(E')\right]|R\rangle \qquad (17.16)\\ &\quad + \sum_c \int dE'\ \left[\left(E - E' + i\epsilon\right)b_c(E; E') - a(E)V_c^*(E')\right]\left|c', E'\right\rangle \ . \qquad (17.17)\end{aligned}$$

Since the above needs to be equal to the right-hand side of Eq. (17.10), the coefficient of $|c', E'\rangle$ must vanish while the coefficient of $|R\rangle$ must be equal 1. The first condition yields

$$b_c(E; E') = \frac{a(E)V_c^*(E')}{\left(E - E' + i\epsilon\right)} \ , \tag{17.18}$$

which, after inserting it into the second condition, allows us to arrive at

$$\left[E - E_R^{(0)} + i\epsilon - \sum_c \int dE' \, \frac{|V_c(E')|^2}{\left(E - E' + i\epsilon\right)}\right] a(E) = 1 \ , \tag{17.19}$$

from which we immediately obtain

$$a(E) = \left\langle R \middle| \hat{G}^+(E) \middle| R \right\rangle = \frac{1}{E - E_R^{(0)} - \sum_c \int dE' \, \frac{|V_c(E')|^2}{\left(E - E' + i\epsilon\right)} + i\epsilon} \ . \tag{17.20}$$

17.2.1 Self-energy

Looking at the above equation, we are inspired to define

$$\Sigma(E) \equiv \sum_c \int dE' \, \frac{|V_c(E')|^2}{\left(E - E' + i\epsilon\right)} \ . \tag{17.21}$$

The quantity $\Sigma(E)$ describes contributions arising from processes in which the system leaves the configuration $|R\rangle$, propagates in a continuum state $|c, E'\rangle$, and then returns to $|R\rangle$ again[7]. With this, we can now write the amplitude $a(R)$, Eq. (17.20), as

$$a(E) = \left\langle R \middle| \hat{G}^+(E) \middle| R \right\rangle = \frac{1}{E - E_R^{(0)} - \Sigma(E) + i\epsilon} \ . \tag{17.22}$$

In the above expression, it is evident that $\Sigma(E)$ modifies the propagator between states $|R\rangle$. Since this modification is quantified by a shift of the propagator pole in the complex energy plane and given that it corresponds to a process in which the state $|R\rangle$ evolves, through intermediate excursions into the continuum states, *back to self*, the quantity $\Sigma(E)$ is called the *self-energy* of the resonance, and we take the energy of the resonance to be

$$E_R = E_R^{(0)} + \Sigma(E) \ . \tag{17.23}$$

This may seem odd: why are we allowed to modify what we consider as energy? The reason is straightforward but requires some getting used to: we do this for the simple reason that the combined quantity E_R plays the role usually taken by the state's energy E'. Indeed, Eq. (17.22) has the same structure as $(E - E' + i\epsilon)^{-1}$, and so clearly the combination $E_R^{(0)} + \Sigma(E)$ behaves like energy[8].

Overall, what have we achieved here? We have identified Eq. (17.22) as the matrix element of the propagator, *i.e.*, an object that evolves the state kets for a given Hamiltonian (see Sec. 12.2.1). Evidently, that matrix element is modified by the presence of the interaction, whose effect is folded into the self-energy $\Sigma(E)$, Eq. (17.21). This modification reflects the fact that propagation from $|R\rangle$ to $|R\rangle$ can involve intermediate excursions into continuum channels, $|R\rangle \to |c, E'\rangle \to |R\rangle$. Thus, the self-energy represents the correction to the propagator arising from coupling to the continuum, *i.e.*, from the interaction of the resonant state $|R\rangle$ with the continuum states.

[7] Intuitively, this follows from the structure of the Hamiltonian, Eq. (17.6): transitions from $|R\rangle$ to $|c, E'\rangle$ occur with amplitude $V_c^*(E')$, while transitions back occur with amplitude $V_c(E')$, whose product yields $|V_c(E')|^2$. Consequently, $\Sigma(E)$ must correspond to a process involving both of these transitions.

[8] In other words, if it looks like a duck and quacks like a duck...

17.2.2 Bare and dressed particles

In the language of quantum field theory (QFT), we call a propagator modified by the interaction a *dressed propagator*. The idea is simple: a *bare particle* – *i.e.*, a particle which does not interact – corresponds to the propagator[9]

$$\frac{1}{p^2 - m_0^2} \ , \tag{17.24}$$

while the propagator for an interacting particle changes due to the interactions, becoming

$$\frac{1}{p^2 - m_0^2 - \Sigma(p^2)} \ . \tag{17.25}$$

Note that the mathematical structure of the propagator is the same, but now it looks like it propagates a particle with a modified mass equal

$$m = \sqrt{m_0^2 + \Sigma(p^2)} \ . \tag{17.26}$$

We say that the interaction "dresses the particle," which invokes an image of changing its appearance and that is the correct intuition: the interaction makes the particle whose bare mass is m_0 look like a particle with an *effective mass* given by Eq. (17.26).

This concept is ubiquitous in physics, including nuclear physics. Almost any decent model of the nuclear interaction will lead to a description in which the nucleons acquire effective masses. This is where a lot of the fun starts: for example, given that particles with positive isospin respond slightly differently[10] to the nuclear medium than particles with negative isospin, the effective masses of protons and neutrons will also be slightly different, which is known as the *effective mass splitting*. Furthermore, if protons and neutrons have slightly different effective masses, they will respond slightly differently to external forces, leading to slightly different dynamics, which one may hope to see in the final observables. In particular, different effective masses of protons and neutrons lead to different thresholds for pion production.

This is used in heavy-ion collision experiments aimed at extracting the symmetry energy[11] based on subthreshold pion production in the dense region created in the collisions. Since $\mathrm{p}+\mathrm{p}$ scattering leads preferentially to π^+ production while $\mathrm{n}+\mathrm{n}$ tends to produce π^-, the ratio of π^- and π^+ yields, $R_\pi = N_{\pi^-}/N_{\pi^+}$, tells us something about the isospin composition of the dense region where the pions are produced: if there are relatively many neutrons in that region, signified by a relatively large R_π, it means that the potential associated with excess isospin is not very strong; conversely, if the dense region appears more isospin-equilibrated, that would indicate a high repulsion for excess isospin, suggesting a substantial symmetry energy.

The concept of the effective mass extends far beyond properties of nucleons. For example, the bare quark mass is on the order of 1 MeV (for light quarks), while a proton or a neutron, both composed of three quarks, have masses on the order of 1 GeV. Most of this mass originates not from the quark masses themselves, but from the dynamics of QCD[12]. In many effective descriptions of hadron structure this complicated dynamics is captured by introducing constituent quarks, which are quasiparticles with effective masses of about $m_q \approx 350$ MeV. These masses can be viewed as "dressed" masses that include the effects of interactions with the QCD vacuum.

[9] To emphasize that the mass corresponds to a bare particle, one usually adds a "0" subscript.

[10] The fact that it's not a huge difference, at least around the saturation density of nuclear matter, is established experimentally.

[11] That is, the isospin-dependence of the nuclear equation of state or, equivalently, of the nuclear interaction.

[12] Namely, the energy stored in gluon fields and the effects of spontaneous chiral symmetry breaking.

17.3 The residue operator $\hat{\mathcal{R}}_R$

We now use the structure of our model space to infer the form of the residue operator $\hat{\mathcal{R}}_R$. Since our model Hamiltonian, Eq. (17.6), contains only one discrete configuration $|R\rangle$, the resonant sector is a one-dimensional subspace. Any operator acting within that subspace must be proportional to

$$|R\rangle\langle R| \ . \tag{17.27}$$

Given that the singular part of the propagator, Eq. (17.2), comes entirely from propagation through that resonant sector, the residue operator must then have the form

$$\hat{\mathcal{R}}_R = Z_R\,|R\rangle\langle R| \ , \tag{17.28}$$

where Z_R is a scalar. We can then consider the matrix element of $\hat{G}^{(+)}(E)$, Eq. (17.2), between the states $|R\rangle$,

$$\left\langle R\middle|\hat{G}^{(+)}(E)\middle|R\right\rangle = \frac{\left\langle R\middle|\hat{\mathcal{R}}_R\middle|R\right\rangle}{E-z_R} + \left\langle R\middle|\hat{G}^{(+)}_{\rm reg}(E)\middle|R\right\rangle \ . \tag{17.29}$$

However, using the form of the residue operator, Eq. (17.28), and the normalization of the state $|R\rangle$, Eq. (17.5), the above immediately becomes

$$\left\langle R\middle|\hat{G}^{(+)}(E)\middle|R\right\rangle = \frac{Z_R}{E-z_R} + \left\langle R\middle|\hat{G}^{(+)}_{\rm reg}(E)\middle|R\right\rangle \ . \tag{17.30}$$

Given the computed matrix element of $\hat{G}^{(+)}(E)$, Eq. (17.22), it is evident that $Z_R = 1$ and $z_R = E_R^{(0)} + \Sigma(E) - i\epsilon$. With this, the T-matrix near a resonance, Eq. (17.4), can be written as

$$\hat{T}(E) = \hat{T}^{(\rm bg)}(E) + \hat{V}\frac{|R\rangle\langle R|}{E - E_R^{(0)} - \Sigma(E) + i\epsilon}\hat{V} \ . \tag{17.31}$$

17.4 Emergence of the decay width

Since we already admitted that the state $|R\rangle$ is not stable, we should not be surprised that it has a finite width. Often, one would just write $\mathrm{Re}\Sigma(\mathrm{E}) = \Delta\mathrm{E}$ and $\mathrm{Im}\Sigma(\mathrm{E}) = -\Gamma/2$ and be done with it. However, the connection can be shown in a more explicit way. Note that we can always write

$$\frac{1}{x+i\epsilon} = \frac{x-i\epsilon}{x^2+\epsilon^2} = \frac{x}{x^2+\epsilon^2} - i\frac{\epsilon}{x^2+\epsilon^2} \ . \tag{17.32}$$

Consequently, the self-energy, Eq. (17.21), can be written as

$$\Sigma(E) = \sum_c \int dE' \ |V_c(E')|^2 \frac{(E-E')}{\left(E-E'\right)^2+\epsilon^2} - i\sum_c \int dE' \ |V_c(E')|^2 \frac{\epsilon}{\left(E-E'\right)^2+\epsilon^2} \ . \tag{17.33}$$

If we now consider the $\epsilon \to 0$ limit, then the fraction under the integrand in the second term looks, up to a factor of π, like a delta function (see Footnote 5 in Lecture 11). Thus we can write

$$\lim_{\epsilon\to 0} \mathrm{Im}\ \Sigma(\mathrm{E}) = -\lim_{\epsilon\to 0}\sum_c \int dE' \ |V_c(E')|^2 \frac{\epsilon}{\left(E-E'\right)^2+\epsilon^2} \tag{17.34}$$

$$= -\pi \sum_c \int dE' \ |V_c(E')|^2 \delta(E-E') \tag{17.35}$$

$$= -\pi \sum_c |V_c(E)|^2 \equiv -\frac{\Gamma(E)}{2} \ . \tag{17.36}$$

Thus, the imaginary part is driven by the on-shell condition $E' = E$, and represents the decay of the unstable state into open channels.

For evaluating the real part of $\Sigma(E)$, which is the first term in Eq. (17.33), it is useful to change the variables according to $x = E' - E$, with which we get

$$\lim_{\epsilon\to 0} \mathrm{Re}\ \Sigma(\mathrm{E}) = \lim_{\epsilon\to 0} \sum_c \int dx\ |V_c(x+E)|^2 \frac{-x}{x^2+\epsilon^2}\ . \tag{17.37}$$

This lets us clearly see that the integrand is odd in x while the divergence is even in x, which means that we may get some mileage from appropriately dividing the integration range. Denoting $|V_c(x+E)|^2 = f(x+E)$ for clarity and generality[13] and considering a generic integration region from minus to plus infinity[14], we can divide the integral into three parts, including one that is symmetric around the divergence at $x = 0$,

$$\int_{-\infty}^{\infty} dx = \int_{-\infty}^{-\delta} dx + \int_{-\delta}^{\delta} dx + \int_{\delta}^{\infty} dx\ . \tag{17.38}$$

Let us consider that diverging "central" part first. in the vicinity of $x = 0$ we can expand

$$f(x+E) \approx f(E) + x f'(E) + \dots\ , \tag{17.39}$$

so that the integral is

$$\mathcal{I}_{-\delta}^{\delta} = \int_{-\delta}^{\delta} dx \left(f(E) + x f'(E) + \dots \right) \frac{-x}{x^2+\epsilon^2}\ . \tag{17.40}$$

The first term is odd and therefore it integrates to zero. The second term behaves like $x^2/(x^2+\epsilon^2)$, which in the limit $\epsilon \to 0$ approaches 1 and therefore the integral gives a finite contribution. All higher-order terms in the expansion of $f(x+E)$ are higher order in x and therefore remove the divergence. Consequently, we see that considering an even interval around the pole removes the divergence because the factor $-x/(x^2+\epsilon^2)$ is antisymmetric. The remaining contribution from the central region is finite and, moreover, it vanishes as $\delta \to 0$. For the remaining parts of the integral, we have $|x| > \delta$, so that in the limit $\epsilon \to 0$ one obtains a well-defined integrand $(-1/x)\, f(x+E)$. Putting everything together, we see that

$$\lim_{\epsilon\to 0} \mathrm{Re}\ \Sigma(\mathrm{E}) = \lim_{\delta\to 0} \sum_c \left[\int_{E_{\mathrm{th}}^{(c)}-E}^{-\delta} dx\ |V_c(x+E)|^2 \frac{-1}{x} + \int_{\delta}^{\infty} dx\ |V_c(x+E)|^2 \frac{-1}{x} \right] \equiv \Delta E\ , \tag{17.41}$$

where we acknowledged that the lower limit of the integral is constrained by the energy threshold for channel c, $E_{\mathrm{th}}^{(c)}$, and where we denote the (finite and well-defined) outcome of the integration as ΔE. The effect of ΔE is shifting the resonance position: now, for an incident beam of E, it will occur if $E \approx E_R^{(0)} + \Delta E$. The finite width $\Gamma(E)$ encapsulates the fact that the state $|R\rangle$ is not stable and thus can decay. Altogether, the matrix element of the Green's function becomes then

$$a(E) = \left\langle R \middle| \hat{G}^+(E) \middle| R \right\rangle = \frac{1}{E - E_R + i\Gamma(E)/2}\ , \tag{17.42}$$

where $E_R = E_R^{(0)} + \Delta E$ is the shifted resonance energy.

[13] This trick will apply to any sufficiently smooth function $f(x)$.

[14] One can always restrict it to a smaller range provided that the range includes the singularity.

The tricks involved in the evaluation of the self-energy are so common that they are given their own abstract notation. That is, we often write

$$\lim_{\epsilon\to 0}\int dx\ \frac{f(x)}{x-a+i\epsilon} = \mathcal{P}\int dx\ \frac{f(x)}{x-a} - i\pi f(a)\ . \tag{17.43}$$

The symbol $\mathcal{P}$ marks a *principal-value integral*, and it literally instructs us to evaluate the integral by excluding a symmetric region around the pole and then taking the limit of that region shrinks to zero. The integral over x does not need to extend from minus to plus infinity, which is of importance for calculations where there is a threshold value of the integrated variable[15]. Note that while the notation using $\mathcal{P}$ may *look* funny, and the instruction to evaluate the integral by excluding a symmetric region around the pole and then taking the limit of the region becoming zero may *seem* random, they correspond to several very well-defined mathematical steps, as shown above, which prove that we can indeed do this and obtain the correct result. The identity

$$\frac{1}{x-a+i\epsilon} = \mathcal{P}\frac{1}{x-a} - i\pi\delta(x-a) \tag{17.44}$$

is known as the Sokhotski–Plemelj formula[16]. This identity is equivalent to Eq. (17.43), as it is supposed to be understood in a *distribution sense*, which is another way of saying that, like the delta function, one needs to apply it to a test function and integrate to obtain a meaningful result.

17.5 T-matrix in the channel space

We can now come back to our expression for the T-matrix, Eq. (17.31). Using the expressions for the real and imaginary part of the self-energy, Eq. (17.41) and (17.36), and taking the element of the matrix between an initial channel α and final channel β leads to

$$T_{\beta\alpha}(E) = T^{(\mathrm{bg})}_{\beta\alpha}(E) + \frac{\left\langle\beta\middle|\hat{V}\middle|R\right\rangle\left\langle R\middle|\hat{V}\middle|\alpha\right\rangle}{E-E_R+i\Gamma(E)/2}\ . \tag{17.45}$$

With this, we can immediately obtain the scattering amplitude for the $\alpha\to\beta$ process using Eq. (13.13),

$$f_{\beta\alpha}(\theta,\phi) = -4\mu\pi^2\ T_{\beta\alpha}(E)\Big|_{\mathrm{on-shell}}\ , \tag{17.46}$$

where the subscript "on-shell" indicates that the energy argument of the T-matrix is taken to correspond to the physical energy of the asymptotic scattering states, and from this we immediately get the differential cross section, Eq. (6.68),

$$\frac{d\sigma_{\beta\alpha}}{d\Omega} = \left(4\mu\pi^2\right)^2\left|T_{\beta\alpha}(E)\right|^2\ . \tag{17.47}$$

If we assume that the cross section is dominated by the resonant contribution, we then get

$$\frac{d\sigma^{(\mathrm{R})}_{\beta\alpha}}{d\Omega} \approx \left(4\mu\pi^2\right)^2\frac{\left|\left\langle\beta\middle|\hat{V}\middle|R\right\rangle\right|^2\left|\left\langle R\middle|\hat{V}\middle|\alpha\right\rangle\right|^2}{\left(E-E_R\right)^2+\left(\Gamma(E)/2\right)^2}\ . \tag{17.48}$$

[15] For example, integral over energy have well-defined thresholds.
[16] In physics, sometimes just "Plemelj formula."

The quantities $\left|\left\langle \beta\middle|\hat{V}\middle|R\right\rangle\right|^2$ and $\left|\left\langle R\middle|\hat{V}\middle|\alpha\right\rangle\right|^2$ measure the strength of the coupling of the resonant configuration $|R\rangle$ to the exit and entrance channels, respectively. Noting that $\left\langle B\middle|\hat{V}\middle|A\right\rangle$ can be understood as the overlap of the state $|B\rangle$ with the state $|A'\rangle = \hat{V}\,|A\rangle$, which is directly proportional to the probability density of transitioning from $|A'\rangle$ to $|B\rangle$, we can infer that these matrix elements are related to the partial widths Γ_α and Γ_β (see Secs. 16.1 and 16.3.3) *via* $2\pi\left|\left\langle \beta\middle|\hat{V}\middle|R\right\rangle\right|^2 \sim \Gamma_\beta$ and $2\pi\left|\left\langle \alpha\middle|\hat{V}\middle|R\right\rangle\right|^2 \sim \Gamma_\alpha$; here, the relationship is a proportionality and not an equality because of remaining unknown phase space factors. Suppressing the detailed angular dependence, the resonant cross section for the reaction channel then takes the familiar Breit-Wigner form,

$$\sigma_{\beta\alpha}^{(\mathrm{R})} \propto \frac{\Gamma_\beta \Gamma_\alpha}{\left(E - E_R\right)^2 + \left(\Gamma(E)/2\right)^2} \ . \tag{17.49}$$

Lecture sources: This lecture is mainly based on my memories of certain treatments of neutrino oscillations and an extended interaction with `ChatGPT` to adjust that treatment to describe changes between semi-bound and continuum states.

Lecture 18

Compound nucleus reactions IV

Prerequisites: Lectures 3, 4, 6, 13, 15, 16, 17.
Guiding question: ***When things get very complicated, can they actually become easier?***

The compound nucleus model predicts the occurrence of fine resonances as a consequence of the multitude of possible quasi-bound states of the many-body system. However, if the resulting cross sections, Eqs. (16.17)–(16.20), are averaged over energy, then the rapid fluctuations associated with the narrow resonances are smoothed out, leaving a slowly varying "envelope" that decreases with energy (roughly as $1/k^2$). We can see this by considering the outline of the resonance region cross section shown in the bottom panel of Fig. 15.2. However, at higher energies (and over larger energy scales), corresponding to the continuum region where the spacing and widths of the resonances are comparable and the cross section is effectively averaged, the data exhibit qualitatively different behavior. The average cross section develops non-monotonic energy dependence, with broad maxima often referred to as *intermediate structure*[1], as can be seen in Fig. 18.1. Moreover, the position of these broad maxima as a function of energy varies slowly with the mass number A, see Fig. 18.2.

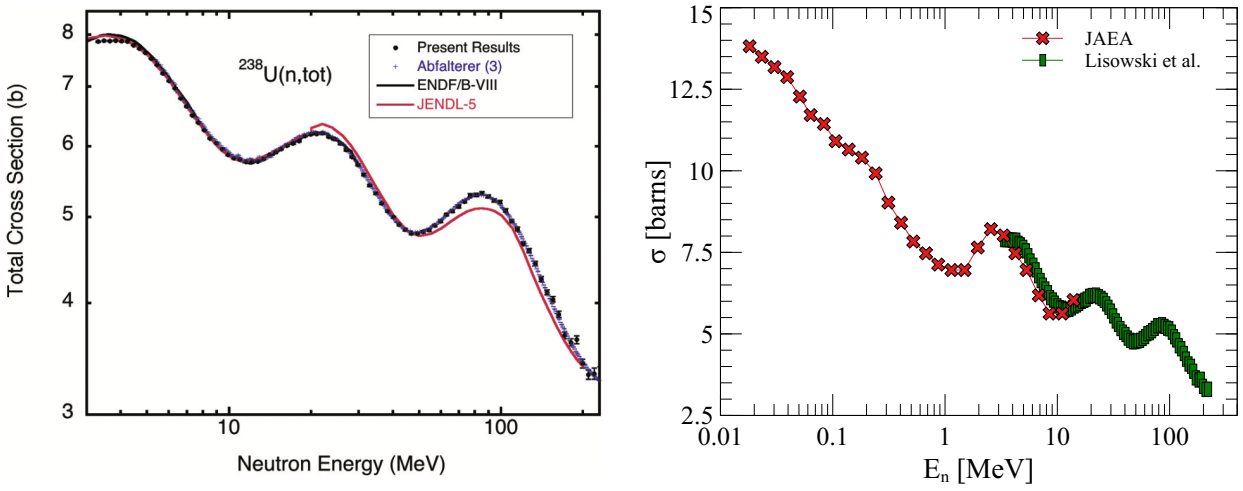

Figure 18.1: The excitation function of the total cross section for the n + ^{238}U reaction. The left panel shows results from Ref. [25], while the right panel shows those measurements ("Lisowski et al.") and measurements from Ref. [21] ("JAEA"). Figure in the left panel from Ref. [25].

[1]In older literature, such as Ref. [4], one can also encounter the term "giant resonances." However, that term has since acquired another meaning, and therefore should not be used in this context.

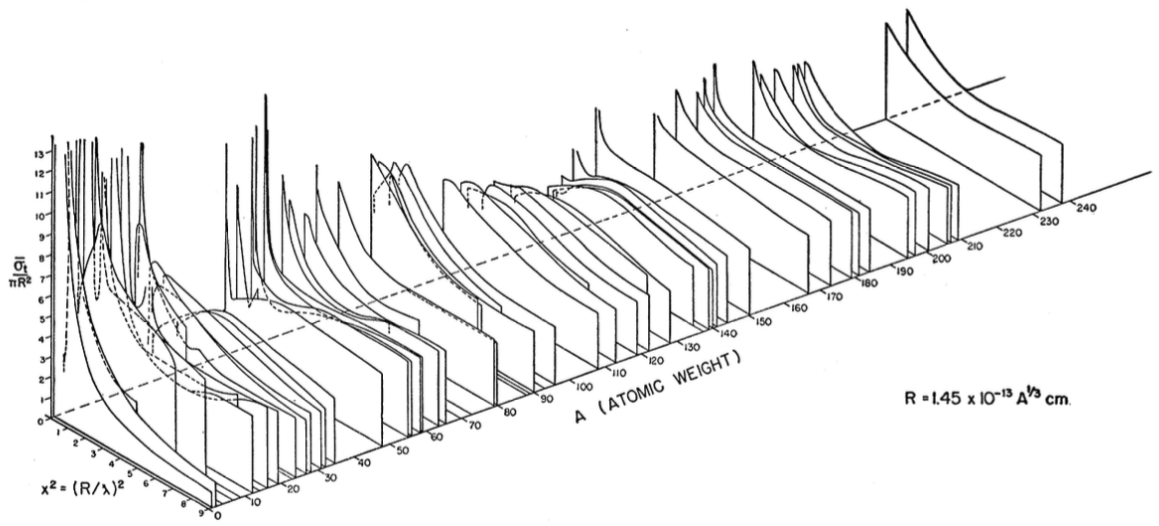

Figure 18.2: Observed neutron total cross sections averaged over the resonances as a function of energy and mass number. The energy is represented with the variable $x^2 \equiv \alpha E_{\rm kin}$, where $\alpha = A^{2/3}A/[10(A+1)]$ and $E_{\rm kin}$ is given in MeV; thus, for example, $\alpha(A=90) \approx 1.99$, while $\alpha(A=165) \approx 2.99$. Figure from Ref. [26].

The compound nucleus model by itself cannot explain the existence of these broad structures: not only is the average non-monotonic dependence on the energy not captured by this model, but also the properties of the resonances it gives rise to are dramatically different. Indeed, we can easily calculate that for a resonance whose width is on the order of 10 MeV, the corresponding lifetime is $\tau = \hbar/\Gamma \sim 10^{-21}$ s, which is entirely incompatible with long-lived compound nucleus states. Such short timescales indicate reaction mechanisms in which the incident neutron interacts with the nucleus without forming a fully equilibrated compound nucleus. This points to a description in terms of single-particle motion in an average nuclear potential, supplemented by coupling to more complex configurations, rather than a purely compound nucleus picture.

18.1 What happens if we average the cross section?

In Eqs. (16.8) and (16.9), we defined the cross sections for elastic and absorption (understood as everything that is not elastic) processes. To gain more intuition as to what is happening in the continuum region, let us consider energy averages of these cross sections. For the elastic cross section, we have

$$\langle \sigma_{\rm el} \rangle = \frac{\pi}{k^2} \sum_l (2l+1) \left\langle \left| 1 - S_l \right|^2 \right\rangle \tag{18.1}$$

$$= \frac{\pi}{k^2} \sum_l (2l+1) \left[1 - \langle S_l^* \rangle - \langle S_l \rangle + \langle |S_l|^2 \rangle \right] \tag{18.2}$$

$$= \frac{\pi}{k^2} \sum_l (2l+1) \left[\left(1 - \langle S_l^* \rangle - \langle S_l \rangle + \langle |S_l|^2 \rangle \right) + \left| \langle S_l \rangle \right|^2 - \left| \langle S_l \rangle \right|^2 \right] \tag{18.3}$$

$$= \frac{\pi}{k^2} \sum_l (2l+1) \left| 1 - \langle S_l \rangle \right|^2 + \frac{\pi}{k^2} \sum_l (2l+1) \left[\langle |S_l|^2 \rangle - \left| \langle S_l \rangle \right|^2 \right] \tag{18.4}$$

where in the third line we added and subtracted the same term, and in the fourth line we regrouped the terms. The energy average of the absorption cross section is

$$\langle \sigma_{\rm abs} \rangle = \frac{\pi}{k^2} \sum_l (2l+1) \left\langle \left(1 - \left|S_l\right|^2\right) \right\rangle \tag{18.5}$$

$$= \frac{\pi}{k^2} \sum_l (2l+1) \left[1 - \left\langle \left|S_l\right|^2 \right\rangle \right] \tag{18.6}$$

$$= \frac{\pi}{k^2} \sum_l (2l+1) \left[1 - \left(\left\langle \left|S_l\right|^2 \right\rangle + \left| \langle S_l \rangle \right|^2 - \left| \langle S_l \rangle \right|^2 \right) \right] \tag{18.7}$$

$$= \frac{\pi}{k^2} \sum_l (2l+1) \left[1 - \left|\langle S_l \rangle\right|^2 \right] - \frac{\pi}{k^2} \sum_l (2l+1) \left[\langle |S_l|^2 \rangle - \left| \langle S_l \rangle \right|^2 \right] , \tag{18.8}$$

where in the third line we again added and subtracted the same term, and in the fourth line we regrouped the terms. At this point, we note that if we define a fluctuation in the S-matrix element as a function of energy, $\delta S_l \equiv S_l - \langle S_l \rangle$, then the second terms in both above expressions are sums over

$$\langle |S_l|^2 \rangle - \left| \langle S_l \rangle \right|^2 = \left\langle |\delta S_l|^2 \right\rangle \ . \tag{18.9}$$

What do the fluctuations in the S-matrix element correspond to? In Lecture 16, we have shown that the elastic cross section, Eq. (16.8), is a sum of the non-resonant and resonant contributions, Eqs. (16.18) and (16.19). At the same time, from Eq. (16.26) we can see that the absorption cross section, Eq. (16.9), can be written as a difference between the compound nucleus formation cross section and the elastic resonant cross section. By comparing with Eqs. (18.4) and (18.8), we conclude that the second terms in both equations are proportional to averages of the elastic resonant, or compound-elastic, contribution, Eq. (16.19).

These averages of the elastic resonant contributions, corresponding to S-matrix fluctuations *via* Eq. (18.9), are expected to average to zero. This is what we see in the continuum region, where the cross section varies smoothly with energy. Consequently, we expect that the average elastic and absorption cross section can be approximated as

$$\langle \sigma_{\rm el} \rangle \approx \frac{\pi}{k^2} \sum_l (2l+1) \left|1 - \langle S_l \rangle\right|^2 \tag{18.10}$$

and

$$\langle \sigma_{\rm abs} \rangle \approx \frac{\pi}{k^2} \sum_l (2l+1) \left[1 - \left|\langle S_l \rangle\right|^2 \right] , \tag{18.11}$$

respectively – forms that can be well described by potential scattering! These averages are valid for relatively high scattering energies of about 10 MeV for nucleon scattering off medium and heavy nuclei, and of about 20–30 MeV for scattering off light nuclei.

Note that the smoothness of the cross section in the continuum region is a function of the resolution. If we were able to measure the cross section with increasing precision (*i.e.*, over ever smaller and smaller energy intervals), we would see that the smooth curve in the continuum region is actually a collection of seemingly random dips and peaks. These dips and peaks are known as *Ericson fluctuations*, and they come from interference between amplitudes associated with many

nearby resonances[2]. In the average, these fluctuations vanish because the interference terms cancel due to the lack of phase correlations between nearby resonances[3].

As we already discussed in Sec. 15.1.2, potential scattering naturally leads to resonances whose widths are on the order of 10 MeV. Given that the average elastic and absorption cross sections show such a smooth behavior, we can expect that perhaps we can describe them with purely potential scattering including imaginary (absorption) terms. With this insight, we will pursue a potential-based model to describe the observed properties of the average cross sections. A potential that achieves this goal has both real and imaginary contributions, and it is known as the *optical potential* due to its similarity to descriptions of phenomena from optics.

18.2 Note about the formal theory of optical potential

The treatment we have pursued in Lecture 17 is similar in spirit to the formal theory of optical potential, developed in large part by Herman Feshbach [27, 28], which you can review in Ref. [4] or [6], among others[4]. In the framework established by Feshbach, one begins with the full many-body Hamiltonian describing the projectile, the target, and their interaction, and partitions the Hilbert space into two sectors: the open reaction channels and the internal configurations of the compound system[5]. By eliminating the latter, one obtains an effective Hamiltonian acting only in the space of open channels. The resulting interaction is the optical potential, which can be shown to be complex and energy-dependent, and its imaginary component represents the loss of flux from the elastic channel into all other reaction channels.

While we will not go *via* the formal route, we can still motivate the form of the optical potential. Eq. (17.45) states the matrix element for the process $\alpha \to \beta$ through a resonant compound state R. Let us take the particular case $\beta = \alpha$, where α is the elastic channel. Then, let us consider the average of the matrix element $T_{\alpha\alpha}$ by summing over the many resonant states[6], in which case we are working with

$$\langle T_{\alpha\alpha}(E)\rangle \sim \langle T^{(\mathrm{bg})}_{\alpha\alpha}(E)\rangle + \sum_R \frac{\left|\left\langle R\middle|\hat{V}\middle|\alpha\right\rangle\right|^2}{(E-E_R)+i\Gamma_R/2}\,. \tag{18.12}$$

We then denote the squared matrix element by $\gamma^2(E_R) = \left|\left\langle R\middle|\hat{V}\middle|\alpha\right\rangle\right|^2$, which we generally think of as the coupling between the resonant and elastic channels. Because the resonance spectrum is dense[7], we can exchange the sum over discrete resonant states for an integral over the resonant

[2] This can be intuitively understood by recalling what a simple background shift can do to a cross section near a resonance, see Fig. 16.2. Similarly, constructive and destructive interference of amplitudes associated with overlapping resonances produce dips and peaks as a function of energy.

[3] This is also intuitive: there is no reason for any "cooperation" between the phases of nearby resonances.

[4] Since Ref. [4] can only be found in used bookstores, it is really fortunate that Ref. [6] repeats the presentation given there word for word, albeit without some of the discussion and intuition provided in the original text.

[5] For completeness, let us stress that the simplified model developed in Lecture 17 relies on the same mechanism, but applied *in the opposite direction*: instead of eliminating internal configurations to obtain an effective interaction in the continuum, we eliminated the continuum channels to obtain a self-energy $\Sigma(E)$ acting in the discrete sector. The effect is, however, similar: elimination of a subspace of the full Hilbert space leads to a complex shift of the resonance energy, whose real part corresponds to a shift along the real energy axis while the imaginary part produces the decay width associated with coupling to open channels.

[6] We skip establishing the normalization for this average, which is why from now on we stop using the equal sign.

[7] For the same reason as before: a nucleus is a complex many-body system which corresponding to many closely-spaced energy levels.

energy weighted by the *density of states* $\rho(E_R)$, so that

$$\langle T_{\alpha\alpha}(E)\rangle \sim \langle T^{(\mathrm{bg})}_{\alpha\alpha}(E)\rangle + \int dE_R\ \rho(E_R)\ \frac{\gamma^2(E_R)}{(E-E_R)+i\Gamma(E_R)/2}\ . \tag{18.13}$$

As in Sec. 17.4, the above integral can be evaluated by rewriting the complex denominator as a sum of a real and a complex term, where the integral in the real term becomes a principal value integral (*i.e.*, an integral in which we exclude an infinitesimal region around the pole, see Sec. 17.4) while the denominator in the complex term can be identified as[8] a delta function $\delta(E-E_R)$, yielding[9]

$$\langle T_{\alpha\alpha}(E)\rangle \sim \langle T^{(\mathrm{bg})}_{\alpha\alpha}(E)\rangle + \mathcal{P}\int dE\ \frac{\rho(E)\gamma^2(E_R)}{E-E_R} - i\pi\rho(E)\gamma^2(E)\ . \tag{18.14}$$

We see that the average matrix element for elastic scattering has the same structure it would have if, instead of summing over resonances, we considered single-particle scattering from a potential with a real and imaginary part. This is the motivation for considering an optical potential, introduced in the next section. Notably, this is a particular case of a more general principle that often applies in physics: when things get very complicated (*e.g.*, there are numerous resonances which additionally overlap), the combined effect of all the contributing parts (*e.g.*, the average cross section) can begin to show certain simplicity (*e.g.*, a form which is equivalent to a single-particle potential problem).

18.3 Phenomenological treatment of the optical potential

The formal theory of the optical potential is elegant and can provide a well-needed intuition (see, e.g., Ref. [4]), but using it to obtain practical results is difficult. Instead, one often *postulates* a well-motivated phenomenological form of the potential and *parametrizes* it to reproduce the behavior of nuclear matter. A commonly used form is

$$V(r) = V_R(r) + V_I(r) + V_D(r) + V_S(r) + V_C(r)\ , \tag{18.15}$$

which decomposes the relevant contributions into several terms.

18.3.1 Central term

The first term describes the interaction with the central potential, which can be represented as

$$V_R(r) = -V_0 f(r,R,a)\ , \tag{18.16}$$

with $V_0 > 0$, leading to an attractive potential, and

$$f(r,R,a) = \frac{1}{1+e^{(r-R)/a}} \tag{18.17}$$

is the Woods–Saxon distribution, describing the distribution of nucleons in the nucleus, where R denotes the radius of the nucleus and a is the diffuseness of the nuclear surface, *i.e.*, the width of the region where the distribution is significantly different from 0 or 1 (see Fig. 18.3). The form of the Woods-Saxon distribution is motivated by the approximately constant interior density and diffuse surface of medium and heavy nuclei. As a result, it tends to work well for $A \geq 40$, while it is less

[8] Here, we make an implicit assumption that while perhaps Γ is not infinitesimal, like the usual regulator ϵ, it is small enough to justify approximating the resulting expression with a delta function.

[9] We note that the complex contribution corresponds to the *Fermi golden rule*.

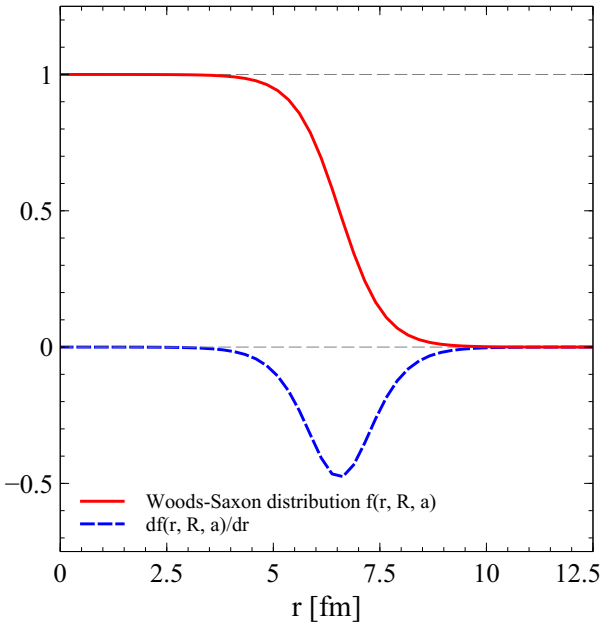

Figure 18.3: The Woods–Saxon distribution (solid red line) and its derivative with respect to the radius r (dashed blue line) as a function of r for the values of parameters corresponding to the gold nucleus, $R = 6.55$ fm and $a = 0.625$ fm [29].

well-justified for light nuclei which do not exhibit a clear saturation region. The reason to use this distribution when defining the form of the potential is that, by definition, it is proportional to the nuclear density. In a many-body problem, the potential due to interactions with many particles can be often approximated in a *mean-field* treatment, which frames the overall effect of the interaction in terms of the local density[10]. In case of the potential assumed in Eq. (18.16), we thus simply assume a linear relationship between the nucleon density in the nucleus and the potential felt by an incident nucleon. Looking at an example of a Woods-Saxon distribution for the gold nucleus, shown in Fig. 18.3, we can convince ourselves that such radial potential will improve on the basic square-well potential by basically producing a well with round walls.

18.3.2 Absorption terms

The absorption of particles is treated by both $V_I(r)$ and $V_D(r)$, given by

$$V_I(r) = -iW f(r, R_I, a_I) \tag{18.18}$$

and

$$V_D(r) = 4ia_I W_D \frac{df(r, R_I, a_I)}{dr} \ , \tag{18.19}$$

respectively, where the constants R_I and a_I may differ from those used in the radial potential $V_R(r)$; this is because, in general, the absorption region is not identical to the density distribution. The

[10] In very broad terms, a "mean-field" interaction is an effective one-body potential obtained by averaging over the many-body dynamics of the system. It captures the smooth, average behavior of the interaction while neglecting explicit correlations and fluctuations, which are instead encoded in other parts of the description (*e.g.*, the imaginary part of the optical potential). Such smooth, average behavior is often parametrized with quantities naturally defined as averages, such as the local density of nucleons.

term $V_I(r)$ describes absorption in the whole volume of the nucleus and thus can be well-described by a form proportional to the Woods–Saxon distribution $f(r, R_I, a_I)$, while $V_D(r)$ focuses on absorption at the surface, explaining why it is proportional to the derivative of $f(r, R_I, a_I)$ which is only appreciably different from zero for $r \approx R$, see Fig. 18.3. The reason behind having these complementary descriptions is that the dominant mode of absorption changes with energy. At low energies, the limited energy transfer and Pauli blocking constrain the available phase space, restricting allowed transitions to states just above the Fermi surface. As a result, excitations of nucleons in the dense interior are strongly suppressed, and reactions occur predominantly in the surface region, where the lower density corresponds to a smaller Fermi momentum and thus weaker Pauli blocking. At higher energies, a much larger phase space becomes accessible, allowing excitations throughout the nuclear interior.

18.3.3 Spin-orbit interaction

In electromagnetism, moving charges – *i.e.*, a non-static charge distribution – give rise to a magnetic field (as described by Ampère's law). A simple example is the circular magnetic field around a current-carrying wire[11]. Crucially, even if a charge distribution is static in one reference frame, it is *not* static in any other reference frame, so that electric and magnetic fields are frame-dependent: a configuration that appears purely electric in one reference frame will, in general, appear as a combination of electric and magnetic fields in another.

An analogous mechanism applies in nuclear interactions. A static nuclear mean-field potential in the lab frame generates an electric-like interaction, while in a moving frame this interaction acquires a magnetic-like component. In scattering processes, the projectile generally moves relative to the target nucleus, so that in the projectile rest frame or in the center-of-mass frame the interaction includes such magnetic-like contributions. Consequently, any description of dynamic nuclear processes needs to include the contribution due to the magnetic-like nuclear interaction, known as the *spin-orbit interaction* as it depends on both the spin and the orbital angular momentum of the system. Let us see explicitly how the form of this interaction arises.

We consider a charge distribution that is static in the lab frame, so that[12] $\boldsymbol{B} = 0$. If the primed frame moves with speed v along the x axis, then in general the electric and magnetic fields transform in the following way under the Lorentz transformation[13],

$$E'_x = E_x \ , \quad E'_y = \gamma\big(E_y - vB_z\big) \ , \quad E'_z = \gamma\big(E_z + vB_y\big) \ , \tag{18.20}$$

$$B'_x = B_x \ , \quad B'_y = \gamma\big(B_y + vE_z\big) \ , \quad B'_z = \gamma\big(B_z - vE_y\big) \ . \tag{18.21}$$

[11] Note that, as often in this case, the charge density and current may be constant in time, yet a magnetic field is still produced. It is the *motion* of charges that matters, not whether the system evolves in time.

[12] Here, we use the usual E_i and B_i symbols for the electric-like and magnetic-like fields, and you should bear in mind that at all times they refer to the nuclear, not electromagnetic force.

[13] In special relativity (see Lectures 3 and 4), the electric and magnetic fields together form the *field tensor* $F^{\mu\nu}$, which in the matrix representation is written as

$$F^{\mu\nu} = \begin{pmatrix} 0 & -E_x & -E_y & -E_z \\ E_x & 0 & -B_z & B_y \\ E_y & B_z & 0 & -B_x \\ E_z & -B_y & B_x & 0 \end{pmatrix} .$$

Then, a Lorentz-boosted field tensor is given by $F'^{\mu\nu} = \Lambda^{\mu}{}_{\alpha}\Lambda^{\nu}{}_{\beta}F^{\alpha\beta}$, where $\Lambda^{\mu}{}_{\nu}$ is the Lorentz transformation in the matrix representation, Eq. (4.18). With $\beta = v$ (since we use natural units), explicit expressions for transforming the $\boldsymbol{E}$ and $\boldsymbol{B}$ fields follow.

With $B_x = B_y = B_z = 0$, this gives

$$\boldsymbol{B}' = \Big(0, \gamma v E_z, -\gamma v E_y\Big) = -\gamma \boldsymbol{v} \times \boldsymbol{E} = \gamma \boldsymbol{v} \times \boldsymbol{\nabla} V \ , \tag{18.22}$$

where $\boldsymbol{E}$ is the electric-like field in the lab frame and in the third equality we used $\boldsymbol{E} = -\boldsymbol{\nabla} V$. For a central potential, $V = V(r)$, we have $\boldsymbol{\nabla} V = (dV/dr)\,\hat{\boldsymbol{r}}$, and using $\hat{\boldsymbol{r}} = \boldsymbol{r}/r$ we get

$$\boldsymbol{B}' = \gamma \frac{dV}{dr}\ \boldsymbol{v} \times \hat{\boldsymbol{r}} = -\frac{\gamma}{r}\frac{dV}{dr}\ \boldsymbol{r} \times \boldsymbol{v} \ . \tag{18.23}$$

In the non-relativistic limit, we have $\gamma \approx 1$ and $\boldsymbol{v} = \boldsymbol{p}/m$, yielding

$$\boldsymbol{B}' \approx -\frac{1}{mr}\frac{dV}{dr}\ \boldsymbol{r} \times \boldsymbol{p} = -\frac{1}{mr}\frac{dV}{dr}\ \boldsymbol{L} \ , \tag{18.24}$$

where we used the fact that $\boldsymbol{L} \equiv \boldsymbol{r} \times \boldsymbol{p}$. Thus we obtain the result that a central potential which is purely electric-like in the lab frame gives rise, in a moving frame, to a magnetic-like field proportional to the orbital angular momentum $\boldsymbol{L}$.

Since we now established that in a general frame the interaction includes not only an electric-like component but also a magnetic-like contribution, we need to ask what property of the nucleon couples to the latter. In analogy with electromagnetism, where magnetic fields couple to magnetic moments, we are reminded that the intrinsic magnetic moment of the nucleon is associated with its spin. For an ordinary magnetic field, if a magnetic dipole is put in the field, then the system has the lowest energy when the dipole is aligned with the field, while it has the highest energy when it is anti-aligned. Thus, the energy – and, by extension, the interaction – depends on how the spin is oriented relative to the field. This can be captured by the scalar product, and as a result the interaction energy is proportional to $\boldsymbol{s} \cdot \boldsymbol{B}'$, which in the spin-orbit case leads to a term of the form $\boldsymbol{s} \cdot \boldsymbol{L}$.

Finally, now we can write the spin-orbit contribution to the optical potential,

$$V_S(r) = \hat{\boldsymbol{s}} \cdot \hat{\boldsymbol{L}}\ \frac{V_s}{m_\pi^2}\frac{1}{r}\frac{df(r, R_S, a_S)}{dr} \ , \tag{18.25}$$

where $\hat{\boldsymbol{s}}$ is the spin of the projectile, $\hat{\boldsymbol{L}}$ is the orbital angular momentum of the projectile relative to the target nucleus, and the pion mass m_π sets a convenient normalization scale. The parameters V_S, R_S, and a_S are determined from fits to experimental data. As argued above, the radial dependence of the spin-orbit interaction is proportional to the derivative of the Woods–Saxon form, and therefore the effects due to the spin-orbit interaction are localized at the nuclear surface. This simply reflects the fact that the electric field is strongest where the potential changes most rapidly.

The spin-orbit interaction is essential for describing effects due to polarization, *i.e.*, the dependence of scattering observables on the orientation of the projectile spin relative to its motion.

18.3.4 Coulomb interaction

Lastly, Coulomb interaction is described by a term of the form

$$V_C(r) = \begin{cases} \frac{Z_1 Z_2 e^2}{2R_c}\left(3 - \frac{r^3}{R_c^2}\right) & r \le R_c \\ \frac{Z_1 Z_2 e^2}{r} & r > R_c \end{cases} \ , \tag{18.26}$$

where R_c is the *Coulomb barrier radius*, used to mark the boundary between regions where either the nuclear of Coulomb force prevails.

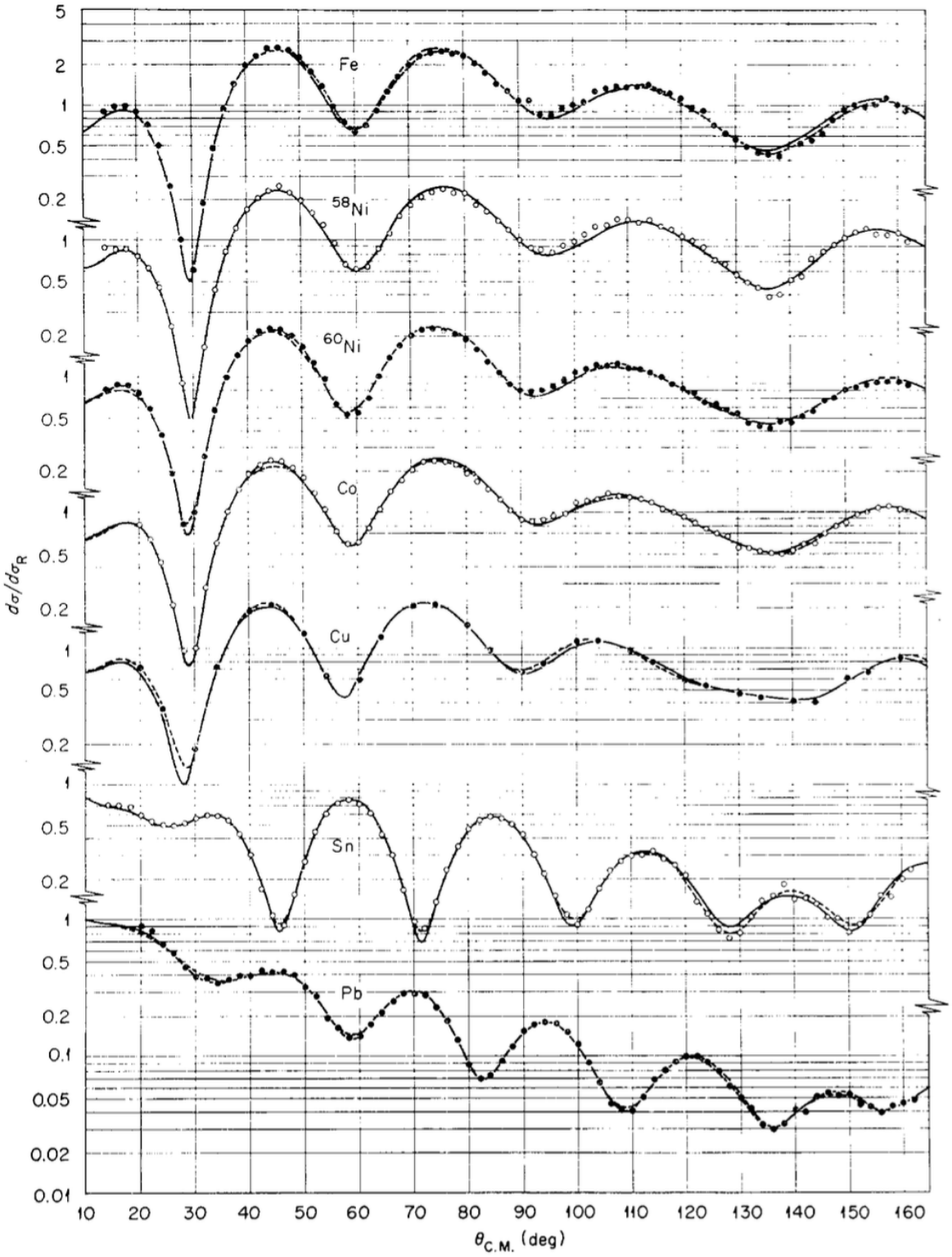

Figure 18.4: The differential cross section for 30.3-MeV protons scattering from several nuclear species. The curves through the points are optical model fits to the data. Figure from Ref. [30].

TABLE 2

Optimum optical potential parameters with the constraints $r_s = r_0$, $a_s = a$.

Target	V (MeV)	r (fm)	a (fm)	W (MeV)	W_D (MeV)	r_0' (fm)	a' (fm)	V_s (MeV)	σ_A (mb)	χ_σ^2	χ_p^2	Notes
^{28}Si	50.4	1.108	0.705	5.49	2.03	1.407	0.521	5.92	720 (729)	19 (48)	660	a, b)
	64.9	0.977	0.755	1.07	6.50	1.274	0.599	7.92	758 (766)	87 (131)	378	b, c)
^{40}Ca	47.2	1.172	0.703	1.78	4.83	1.288	0.653	5.59	904 (912)	28	640	a)
	51.1	1.125	0.764	0.08	6.55	1.289	0.593	5.81	881 (885)	120	416	c, d)
^{56}Fe	56.2	1.086	0.782	3.91	4.95	1.339	0.556	6.22	1107	411		e)
^{58}Ni	56.6	1.072	0.801	4.11	4.20	1.382	0.497	6.36	1082 (1086)	404	307	a, c)
^{60}Ni	54.8	1.101	0.776	3.47	5.00	1.328	0.589	6.19	1147 (1151)	208	630	a)
	55.0	1.101	0.775	3.15	5.37	1.323	0.589	6.26	1149 (1152)	248	597	c)
^{59}Co	55.5	1.099	0.764	3.34	5.21	1.311	0.602	6.35	1141 (1144)	213	414	a)
	55.7	1.098	0.762	3.23	5.35	1.306	0.606	6.41	1141 (1145)	216	411	c)
^{63,5}Cu	53.8	1.116	0.760	1.993	6.03	1.277	0.676	5.94	1210	111		e)
^{120}Sn	51.4	1.168	0.725	2.59	7.49	1.314	0.647	6.12	1636 (1622)	442	450	a)
	52.0	1.162	0.703	3.00	7.23	1.328	0.643	6.19	1636 (1623)	573	375	c)
^{208}Pb	55.4	1.158	0.713	2.01	8.40	1.314	0.761	5.13	2040 (1997)	169	130	a)
	54.8	1.157	0.696	2.62	7.74	1.340	0.756	4.82	2070 (2028)	252	140	c)

The χ^2 given were evaluated using 29 MeV and experimental errors for the polarizations, 30.3 MeV and 3 % errors for the cross sections, except that 10 % errors were assumed for the Ca and Si cross sections. The reaction cross sections σ_A are given for 30.3 MeV, and (in parentheses) for 29 MeV.

a) Minimizes χ_σ^2 alone.

b) Value of χ_σ^2 in parentheses is for 29 MeV cross-section data.

c) Minimizes $\chi_\sigma^2+\chi_p^2$, with χ_p^2 evaluated using the theoretical predictions at 30.3 MeV.

d) 50 % errors were assigned to the 20 cross sections at angles greater than 122°.

e) Polarization data not available.

OPTICAL MODEL

Figure 18.5: Values of the optical model parameters as obtained from fits to experimental data. Table from Ref. [30].

18.3.5 Using the optical potential

Even though it's only a phenomenological model, the optical potential, Eq. (18.15), turns out to be remarkably successful. It can be used as part of a number of different methods, including numerically solving the Schrödinger equation with the optical potential where, to make the problem tractable, one employs the method of partial waves (see Lectures 7–9).

The results of such an approach are shown in Fig. 18.4, where optical potential calculations are compared with experimentally-measured differential cross sections for 30.3-MeV protons scattering off various nuclei. Table 18.5 shows the values of the 10 varied parameters that were found to reproduce the data best in a *chi-square analysis*, also known as the *chi-square minimization* or the *weighted least squares method*, within which one searches for a parameter set that minimizes the expression

$$\chi^2 = \sum_i \frac{(\text{data}_i - \text{model}_i)^2}{\sigma_i^2} \ , \tag{18.27}$$

where the sum runs over all data points and σ_i are experimental uncertainties[14].

Such parameter fits, while successful, can at the same time reveal the main limitation of phenomenological approaches: issues with interpretability. What does a given parameter value, given all the other parameter values, actually represent? What does it mean that these parameters take different values for different nuclei? Is there any regularity to these values? While systematic trends can often be identified, the answers are not always unique or straightforward. Moreover, the need to fit parameters for each nuclear species means that the model is *not predictive*.

[14]Note that weighing each square difference by $1/\sigma_i^2$ ensures that points with smaller uncertainties are *more* important to the fit than points with large uncertainties, as it should be.

Some of these worries can be alleviated by the use of *global optical potentials*, as in Ref. [31], where the parameters are not constants, but functions of energy, nuclear shape, *etc.* Recently, efforts have also been made to motivate the phenomenological optical potentials with microscopic or *ab initio* methods, see, *e.g.*, Ref. [32].

Lecture sources: This lecture is based on Jackson [4] and Bertulani & Danielewicz [6].

Lecture 19

Compound nucleus reactions V

Prerequisites: Lectures 7, 13, 14, 15, 16, 18.
Guiding question: ***Where is nuclear structure in compound-nucleus reactions?***

19.1 The reciprocity theorem

In terms of the S-matrix, the angle-averaged cross section for the reaction $\alpha \to \beta$ is given by[1]

$$\sigma_{\beta\alpha} = \frac{\pi^2}{k_\alpha^2} \sum_l (2l+1) \left| \delta_{\beta\alpha} - S_l^{\beta\alpha} \right|^2 . \tag{19.1}$$

To obtain this expression, following the steps taken in Lecture 6, one needs to define the incoming and outgoing states (where, in particular, there exist outgoing spherical waves in all open channels, but an incoming plane wave exists only in the channel α), consider the asymptotic behavior of the corresponding wavefunctions, and take the product of outgoing and incoming fluxes. We are not going to repeat this procedure here (for those interested, it is described in Ref. [4]), but you can convince yourself that this expression makes sense by comparing with Eq. (8.20), which, while derived in the context of elastic scattering, displays a strikingly similar form. In particular, note that the expression above reduces to Eq. (8.20) in the case of the elastic channel, $\sigma_{\alpha\alpha}$. Recalling the relationship between the T-matrix and the S-matrix, see Sec. 14.2.2, we can also write

$$\sigma_{\beta\alpha} = \frac{\pi^2}{k_\alpha^2} \sum_l (2l+1) \left| T_l^{\beta\alpha} \right|^2 . \tag{19.2}$$

Now, if the reaction is *time-reversal invariant*, which means that for a process $\alpha \to \beta$ the reverse process $\beta \to \alpha$ occurs with the same amplitude (up to phase conventions), then the partial-wave S-matrix is symmetric,

$$S_l^{\beta\alpha} = S_l^{\alpha\beta} , \tag{19.3}$$

which is known as the *reciprocity theorem* or *reciprocity relation*. Given Eq. (19.1), this immediately leads to

$$k_\alpha^2 \sigma_{\beta\alpha} = k_\beta^2 \sigma_{\alpha\beta} , \tag{19.4}$$

[1] Note that we are using a convention in which the subscript in the cross section needs to be read from right to left to reflect the "direction" of the reaction.

which is known as the *principle of detailed balance*. If one considers scattering of particles with spin, the cross sections include additional factors due to spin degeneracy of channels α and β, and the principle of detailed balance becomes

$$g_\alpha k_\alpha^2 \sigma_{\beta\alpha} = g_\beta k_\beta^2 \sigma_{\alpha\beta} \ , \tag{19.5}$$

where g_α and g_β are the total numbers of spin states in channels α and β, respectively; explicitly, we have $g_i = (2I_a + 1)(2I_A + 1)$. Although stated here for the total cross section, the principle of detailed balance applies differentially, so that we also have

$$g_\alpha k_\alpha^2 \left(\frac{d\sigma}{d\Omega}\right)_{\beta\alpha} = g_\beta k_\beta^2 \left(\frac{d\sigma}{d\Omega}\right)_{\alpha\beta} \ . \tag{19.6}$$

19.2 Weisskopf–Ewing theory

As discussed in Sec. 16.1, the cross section for the compound nucleus reaction $\alpha \to \beta$ can be written as a product of the cross section for compound nucleus formation in the entrance channel α, $\sigma_{\rm CN}(\alpha)$, and the relative decay rate or branching ratio into the channel β. This results in Eq. (16.5), repeated here for convenience,

$$\sigma_{\beta\alpha} = \sigma_{\rm CN}(\alpha)\frac{\Gamma_\beta}{\Gamma} \ , \tag{19.7}$$

where Γ_β is the partial decay width into channel β, and $\Gamma = \sum_\beta \Gamma_\beta$ is the total decay width. Using the principle of detailed balance (*i.e.*, assuming time reversal invariance), Eq. (19.5), we can then write

$$g_\alpha k_\alpha^2 \sigma_{\rm CN}(\alpha)\Gamma_\beta = g_\beta k_\beta^2 \sigma_{\rm CN}(\beta)\Gamma_\alpha \ . \tag{19.8}$$

Since the channels α and β can be chosen arbitrarily[2], this implies that

$$\Gamma_\beta \sim g_\beta k_\beta^2 \sigma_{\rm CN}(\beta) \ , \tag{19.9}$$

i.e., the partial width for decay through the channel β is proportional to the cross section for forming the same compound nucleus formation with β as the entrance channel. In other words, channels that are more easily formed are also more likely to be populated in the decay. Since the total decay width is a sum over the partial widths, Eq. (16.3), we can then rewrite the cross section for the process $\alpha \to \beta$, Eq. (19.7), as

$$\sigma_{\beta\alpha} = \sigma_{\rm CN}(\alpha)\frac{g_\beta k_\beta^2 \sigma_{\rm CN}(\beta)}{\sum_\beta g_\beta k_\beta^2 \sigma_{\rm CN}(\beta)} \ . \tag{19.10}$$

The above expression assumes discrete channels β. In practice, however, specifying channel β does not uniquely determine the final state. Indeed, the emitted particle carries a kinetic energy E_β with a *continuum* of allowed values, and similarly the residual nucleus can be characterized by a continuum of excitation energies U_β[3]. Thus, the final states form a continuum, and the cross section

[2] Which means that quantities referring strictly to channel α should not depend on channel β and *vice versa*.

[3] Naturally, while E_β and U_β can take continuum values, they are not independent as they are constrained by energy conservation.

should reflect that. On the left-hand side of the cross section for the process $\alpha \to \beta$, Eq. (19.10), such a generalization gives rise to a differential cross section,

$$\sigma_{\beta\alpha} \to \frac{d\sigma_{\beta\alpha}}{dE_\beta} dE_\beta \equiv \sigma_{\beta\alpha}(E_\beta) dE_\beta \ , \tag{19.11}$$

where in the second equality we abused the notation a little bit to write the differential cross section simply as $\sigma_{\beta\alpha}(E_\beta)$[4]. With this change, the partial decay width into channel β on the right-hand side of Eq. (19.10), Γ_β, must be now weighted by the *density of accessible residual nucleus states* $\omega(U_\beta)$, also referred to as the *nuclear level density*, corresponding to the interval dE_β. For a fixed ejectile energy E_β, the energy conservation for the decay of the compound nucleus gives

$$E_{\rm CN} - B_\beta = E_\beta + U_\beta \ , \tag{19.12}$$

where $E_{\rm CN}$ is the compound nucleus energy, B_β is the separation energy needed for the ejectile to leave the compound nucleus, E_β is the kinetic energy of the emitted ejectile, and U_β is the excitation energy of the residual nucleus. Since $E_{\rm CN}$ and B_β are fixed for the decay under consideration, variation of the above equation gives

$$dU_\beta = -dE_\beta \ , \tag{19.13}$$

so that an ejectile energy interval dE_β corresponds one-to-one to a residual excitation interval dU_β of equal magnitude[5]. The number of accessible residual states corresponding to the interval dE_β therefore satisfies

$$\omega(U_\beta) dE_\beta \sim \omega(U_\beta) dU_\beta \ , \tag{19.14}$$

and we can write

$$\Gamma_\beta = g_\beta k_\beta^2 \sigma_{\rm CN}(\beta) \to g_\beta k_\beta^2 \sigma_{\rm CN}(\beta) \omega(U_\beta) dE_\beta \ . \tag{19.15}$$

This is fairly intuitive: the more states are available in the channel β (now including considerations of energy), the likelier it is that the compound nucleus is going to decay along that pathway. Applying the same substitution in the denominator of the total cross section, Eq. (19.11), where the total decay width is obtained by summing over all emitted-particle channels and integrating over their allowed energies, we obtain

$$\sigma_{\beta\alpha}(E_\beta) dE_\beta = \sigma_{\rm CN}(\alpha) \frac{g_\beta k_\beta^2 \sigma_{\rm CN}(\beta) \omega(U_\beta) dU_\beta}{\sum_\beta \int dU_\beta \ g_\beta k_\beta^2 \sigma_{\rm CN}(\beta) \omega(U_\beta)} \ . \tag{19.16}$$

Finally, using the fact that $k_\beta^2 = 2\mu_\beta E_\beta$, where μ_β is the reduced mass of the ejectile, and inserting explicit expressions for the spin degeneracies, we arrive at the *Weisskopf–Ewing*[6] *formula* for the angle-integrated cross section,

$$\sigma_{\beta\alpha}(E_\beta) dE_\beta = \sigma_{\rm CN}(\alpha) \frac{(2I_\beta + 1) \mu_\beta E_\beta \sigma_{\rm CN}(\beta) \omega(U_\beta) dU_\beta}{\sum_\beta \int dU_\beta \ (2I_\beta + 1) \mu_\beta E_\beta \sigma_{\rm CN}(\beta) \omega(U_\beta)} \ . \tag{19.17}$$

This is a very interesting result, linking the cross section for the compound nucleus process $\alpha \to \beta$ to the number of states available in the residual nucleus at energy U_β. However, naturally it leaves

[4] We choose this way because otherwise, the notation would quickly become too cluttered.
[5] The minus sign is irrelevant for the purpose of counting states.
[6] Pronounced "YOO-ing."

us with an additional task of determining the level density $\omega(U_\beta)$. While a detailed description can, naturally, be arbitrarily complicated, it turns out that to a good approximation, one can model the level density with an exponential form,

$$\omega(U) \propto e^{U/T} \ . \tag{19.18}$$

Here, T is an *effective nuclear temperature*. In contrast to the ordinary thermodynamic temperature, which reflects equilibrium with a heat bath, the effective nuclear temperature characterizes how rapidly the number of available nuclear states grows with excitation energy. More precisely, one may define it through the logarithmic slope of the level density,

$$\frac{1}{T} = \frac{d}{dU} \ln \omega(U) \ . \tag{19.19}$$

Thus, Eq. (19.18) amounts to assuming that this slope is approximately constant over the excitation-energy interval of interest.

With this approximation, the energy spectrum of emitted particles becomes especially transparent. Since energy has to be conserved, see Eq. (19.12), we have

$$U_\beta = E_{\rm CN} - B_\beta - E_\beta \tag{19.20}$$

and the level density, Eq. (19.18), becomes

$$\omega(U_\beta) \propto \exp\left(\frac{E_{\rm CN} - B_\beta - E_\beta}{T}\right) \propto \exp\left(-\frac{E_\beta}{T}\right) \ . \tag{19.21}$$

As a result, apart from the formation factor $\sigma_{\rm CN}(\beta)$ and the phase-space factor E_β, the emitted-particle spectrum, described by the Weisskopf-Ewing cross section, Eq. (19.17), also assumes an approximately Maxwellian form in this approximation.

In general, computation of the Weisskopf–Ewing cross section, Eq. (19.17), requires two separate models as input: 1) the compound nucleus formation cross section $\sigma_{\rm CN}$, which is nothing else than the absorption cross section discussed in Lecture 16, often computed using optical potentials that we discussed in discussed in Lecture 17, and 2) the density of energy levels $\omega(U)$, which can be computed within a number of approaches.

Moreover, while it is convenient to consider only a single process $\alpha \to \beta$, in reality the compound nucleus can undergo several sequential decays. For example, the compound nucleus may first emit an α-particle, after which the residual nucleus emits a neutron. Conversely, the compound nucleus may first emit a neutron and only later an α-particle. Since the final residual nucleus is usually not measured, the observed yield of a given ejectile may include primary, secondary, and higher-generation emissions. Each step is then treated with the same statistical decay formalism, but with the excitation energy, separation energies, and available decay channels updated after each emission.

Note that the assumption of statistical decay into the β channel implies that the compound nucleus has reached approximate equilibration, so that its decay can be described in terms of level densities and branching ratios. As a result, we expect the Weisskopf–Ewing theory to break down at sufficiently high incident energies, where pre-equilibrium emission and other direct or early-stage processes can contribute significantly. This can be seen in Fig. 19.1, showing a comparison of Weisskopf–Ewing calculations with experimental data.

19.3 Hauser–Feshbach theory

The Hauser–Feshbach approach improves on the Weisskopf–Ewing theory by considering the cross section for the compound-nucleus process $\alpha \to \beta$ while explicitly enforcing conservation of total

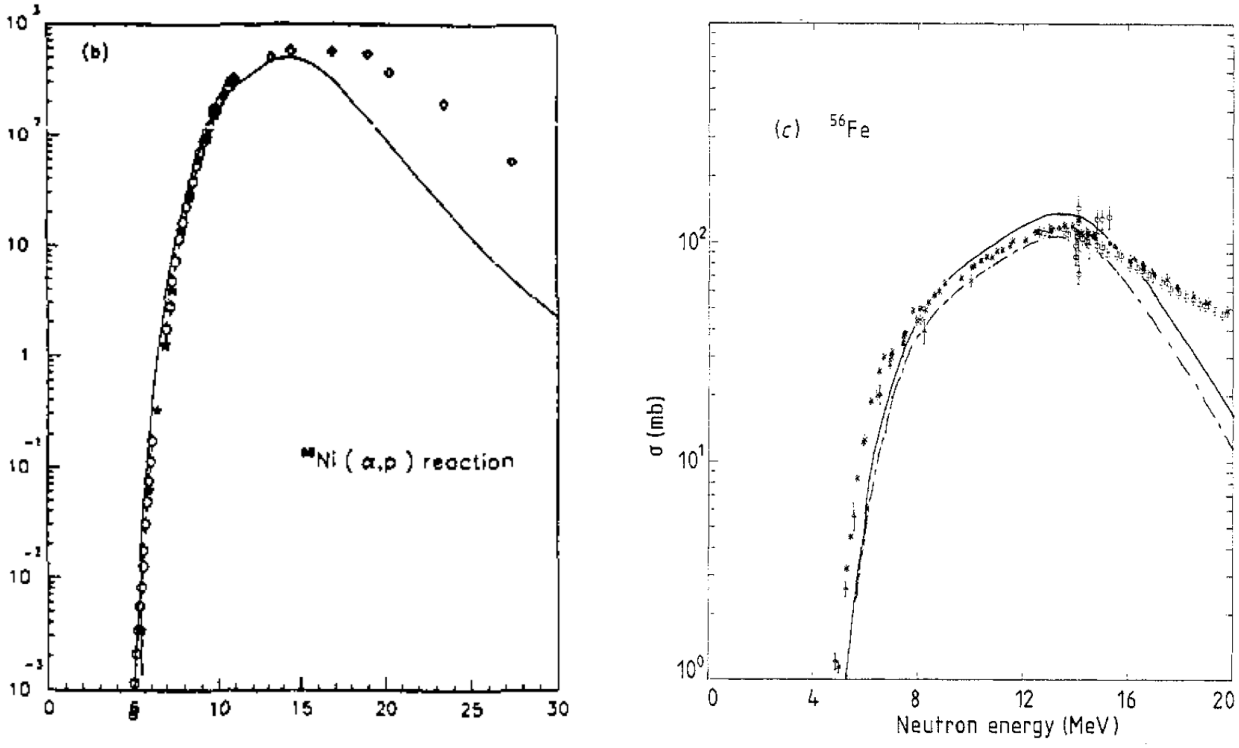

Figure 19.1: Comparison of Weisskopf–Ewing calculations (lines) with experimental data (data points with error bars) for the ^{58}Ni+α (*left*, with the incident α energy in MeV and cross section in milibarns) and ^{56}Fe+n (*right*, with two theoretical curves corresponding to two parametrizations of density levels). Figures from Refs. [33] and [34].

angular momentum and parity. The total angular momentum $\boldsymbol{J}$ of the compound nucleus is

$$\boldsymbol{J} = \boldsymbol{l} + \boldsymbol{s} \ , \tag{19.22}$$

where $\boldsymbol{l}$ is the orbital angular momentum and $\boldsymbol{s} = \boldsymbol{s}_a + \boldsymbol{I}_A$ is the channel spin[7]. Then

$$J = |l - s|, |l - s| + 1, \ldots, l + s \tag{19.23}$$

are all allowed values of J.

The cross section[8] for the $\alpha \to \beta$ process is now obtained by summing over all compound-nucleus states characterized by angular momentum J and parity π,

$$\sigma_{\beta\alpha} = \sum_{J,\pi} \sigma_{\beta\alpha}^{J\pi} = \sum_{J,\pi} \sigma_{\rm CN}^{J\pi}(\alpha) \frac{\Gamma_\beta^{J\pi}}{\sum_\beta \Gamma_\beta^{J\pi}} \ . \tag{19.24}$$

As in the case of the Weisskopf–Ewing theory, the detailed balance principle gives

$$\Gamma_\beta^{J\pi} \propto g_\beta k_\beta^2 \sigma_{\rm CN}^{J\pi}(\beta) \ , \tag{19.25}$$

[7]Here, s_a and $\boldsymbol{I}_A$ denote the intrinsic spin of the projectile and target, respectively. For a nucleus, the word "spin" refers to its total intrinsic angular momentum.

[8]Note that, again, we are abusing the notation a bit since $\sigma_{\beta\alpha}$ really refers here to an energy-differential cross section, $d\sigma_{\beta\alpha}/dE$.

where

$$g_\beta = (2I_B + 1)(2s_b + 1) \ , \tag{19.26}$$

with I_B and s_b denoting the spins of the residual nucleus and the emitted particle in channel β, respectively. Thus the cross section becomes

$$\sigma_{\beta\alpha} = \sum_{J,\pi} \sigma_{\rm CN}^{J\pi}(\alpha) \frac{g_\beta k_\beta^2 \sigma_{\rm CN}^{J\pi}(\beta)}{\sum_\beta g_\beta k_\beta^2 \sigma_{\rm CN}^{J\pi}(\beta)} \ . \tag{19.27}$$

The compound nucleus cross section $\sigma_{\rm CN}^{J\pi}$ can be related to the reaction (absorption) cross section, Eq. (16.9),

$$\sigma_{\rm abs} = \frac{\pi}{k^2} \sum_l (2l+1) \Big[1 - \big| \langle S_l \rangle \big|^2 \Big] \tag{19.28}$$

$$= \frac{\pi}{k^2} \sum_l (2l+1) T_l \ , \tag{19.29}$$

where we introduced the *transmission coefficient* T_l,

$$T_l \equiv \Big[1 - \big| \langle S_l \rangle \big|^2 \Big] \ . \tag{19.30}$$

To connect this partial-wave expression with the J-resolved formulation, one assumes that the transmission coefficients depend primarily on the orbital angular momentum l and are independent of how l and s are coupled to a given total J. As a result, the coupling to J is treated statistically. One may then write the J^π-resolved compound nucleus formation cross section as

$$\sigma_{\rm CN}^{J\pi}(\alpha) = \frac{\pi}{k_\alpha^2} \frac{2J+1}{(2I_A+1)(2s_a+1)} \sum_{s,l}^{J\pi} T_l(\alpha) \ , \tag{19.31}$$

where the sum runs over all (s, l) combinations that couple to the given J^π. We can apply the same reasoning to $\sigma_{\rm CN}^{J\pi}(\beta)$, so that

$$g_\beta k_\beta^2 \sigma_{\rm CN}^{J\pi}(\beta) = \pi(2J+1) \sum_{s,l}^{J\pi} T_l(\beta) \ , \tag{19.32}$$

and with this Eq. (19.27) becomes the *Hauser–Feshbach formula*,

$$\sigma_{\beta\alpha} = \frac{\pi}{k_\alpha^2} \sum_{J,\pi} \frac{2J+1}{(2I_A+1)(2s_a+1)} \frac{\Big(\sum_{s,l}^{J\pi} T_l(\alpha) \Big) \Big(\sum_{s',l'}^{J\pi} T_{l'}(\beta) \Big)}{\sum_\beta \sum_{s,l}^{J\pi} T_l(\beta)} \ . \tag{19.33}$$

The transmission coefficients, $T_l(\alpha)$ and $T_l(\beta)$, can be calculated using, *e.g.*, the optical model.

Crucially, identifying the *channel transmission coefficients*,

$$T_\alpha^{J\pi} \equiv \sum_{s,l}^{J\pi} T_l(\alpha) \ , \tag{19.34}$$

(and similarly for the channel β) not only allows us to write the Hauser–Feshbach cross section in a more compact form,

$$\sigma_{\beta\alpha} = \frac{\pi}{k_\alpha^2} \sum_{J,\pi} \frac{2J+1}{(2I_A+1)(2s_a+1)} \frac{T_\alpha^{J\pi} T_\beta^{J\pi}}{\sum_\beta T_\beta^{J\pi}} \ , \tag{19.35}$$

but also allows for a key reformulation of the approach. If there are numerous terms contributing to Eq. (19.34), the sum may be substituted by an integral over *level density*. In this case, the channel transmission coefficient can be written schematically as

$$T_\beta^{J\pi} \sim \sum_{s,l}^{J\pi} \int dU \ T_l(E_\beta) \ \rho(U, J_f, \pi_f) \ , \tag{19.36}$$

where $\rho(U, J_f, \pi_f)$ is the density of states of the residual nucleus at excitation energy U and with quantum numbers compatible with the decay. Thus, the channel transmission coefficient incorporates both the probability to penetrate the interaction region, described by the optical-model transmission coefficients T_l, and the number of available final states, described by the level density.

The "exact" Hauser–Feshbach formula, Eq. (19.33), is only used in limited cases where the sum can be restricted to known excitation levels; this is the case at low excitation energies, where the level scheme is known[9]. However, in almost all practical calculations, such as those performed with the code `TALYS`, the quantities entering Eq. (19.35) are constructed as follows. The optical model is used to compute the partial-wave transmission coefficients T_l for each open particle channel. These are then combined, according to Eq. (19.34), into channel transmission coefficients $T_\beta^{J\pi}$. For decay into discrete final states of the residual nucleus, the sum over final states is carried out explicitly. At higher excitation energies, where the density of states becomes sufficiently large that individual levels are no longer resolved, or for unstable nuclei where the nuclear levels are often unknown, the spectrum is treated as a *continuum*. In this regime, the sum over final states is replaced by an integration weighted by a model for the nuclear level density, while electromagnetic decay channels are described using gamma-strength functions. Thus, the Hauser–Feshbach cross section is obtained by combining three main ingredients: optical-model transmission coefficients, nuclear level densities, and gamma-strength functions. All of these depend on energy, so that the energy dependence of the cross section emerges naturally once these inputs are specified. An example of such a result is shown in Fig. 19.2.

19.4 Everything everywhere all at once: compound nucleus, optical potential, Weisskopf-Ewing, and Hauser-Feshbach

In this lecture, we have obtained more equations for calculating a cross section for a compound nucleus reaction: the Weisskopf–Ewing cross section, Eq. (19.17), and the Hauser–Fehsbach formula, Eq. (19.35). Since this further adds to several such formulae derived recently, it would be surprising if you were not confused. Let us then review what happened.

In Lecture 16, we derived the non-resonant (shape) elastic, resonant elastic or compound-elastic, and absorption cross sections, Eqs. (16.18), (16.19), and (16.20), respectively. These equations can meaningfully describe the experimental data assuming that the resonance peaks are well-separated. We know that this is not true in the continuum region. There, one can argue that rapid fluctuations in the cross section, caused by interference between amplitudes of overlapping resonances, average

[9] In fact, codes such as `TALYS` do exactly that for low-lying states.

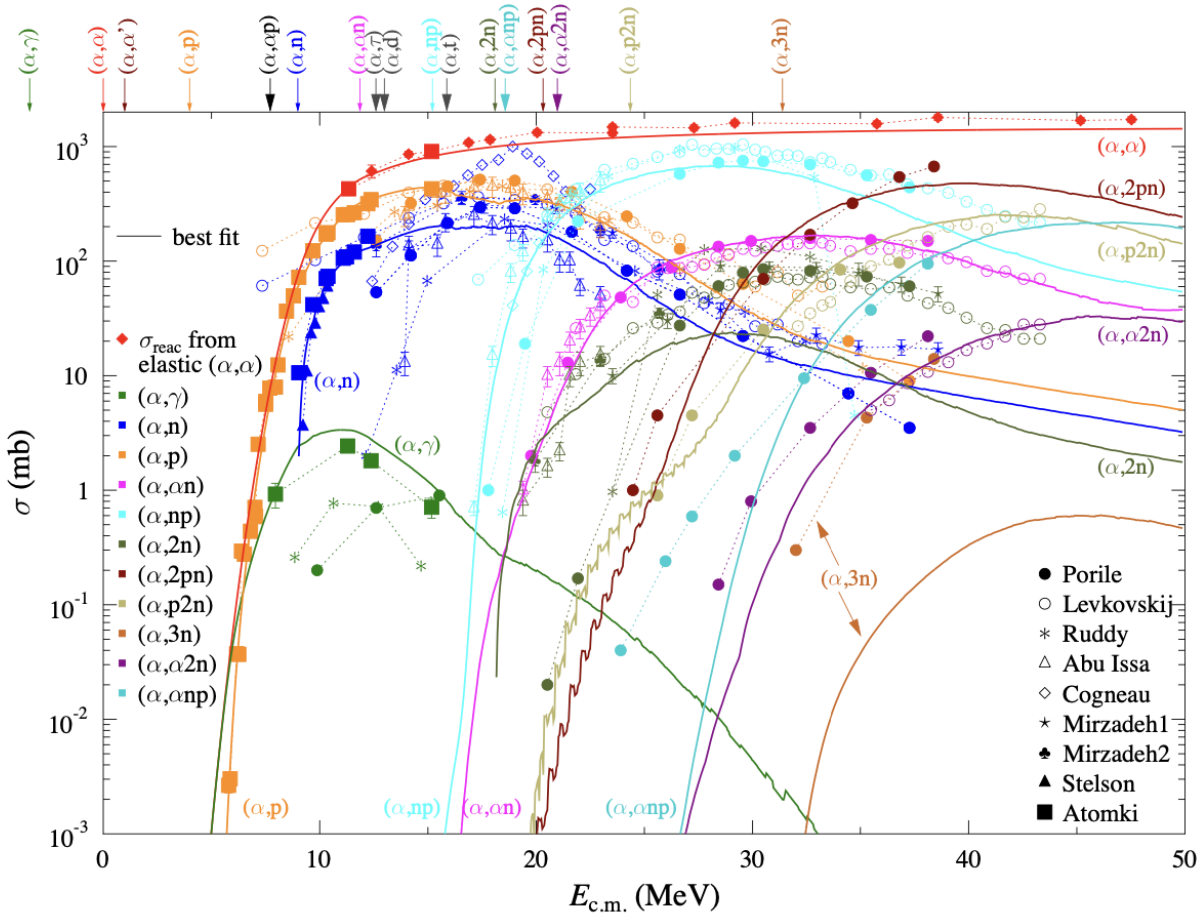

Figure 19.2: Comparison of experimentally-measured cross sections of α-induced reactions on ^{64}Zn, where data labeled σ_{reac} are total reaction cross sections derived from elastic scattering angular distributions and all data sets are connected by thin dotted lines to guide the eye, to best-fit Hauser–Feshbach calculations from `TALYS` (solid lines). Figure from Ref. [35].

to a smooth energy dependence over any reasonable energy interval (as we noted, if one considers very small energy intervals, one discovers Ericson fluctuations). This smooth dependence can be described using an optical model with a complex potential, whose imaginary part accounts for the loss of flux from the elastic channel into all other reaction channels (see Sec. 18.3). This can quite successfully describe experimental measurements such as shown in Fig. 18.2. However, this still leaves some of the story out, as the optical model does not provide a description of how the absorbed flux is distributed among the many possible exit channels.

This is where the Weisskopf–Ewing theory enters: following the independence hypothesis (see Sec. 15.1.3), it factorizes the reaction $\alpha \to \beta$ into a compound-nucleus formation and decay. Within this approach, it combines the cross section for the formation of a compound nucleus in the entrance channel α, $\sigma_{\text{CN}}(\alpha)$ – which can be obtained from the reaction cross section calculated with an optical potential[10] – with statistical information about the available final states, as described by the level

[10]This identification assumes that the dominant contribution to the reaction cross section arises from compound-nucleus formation.

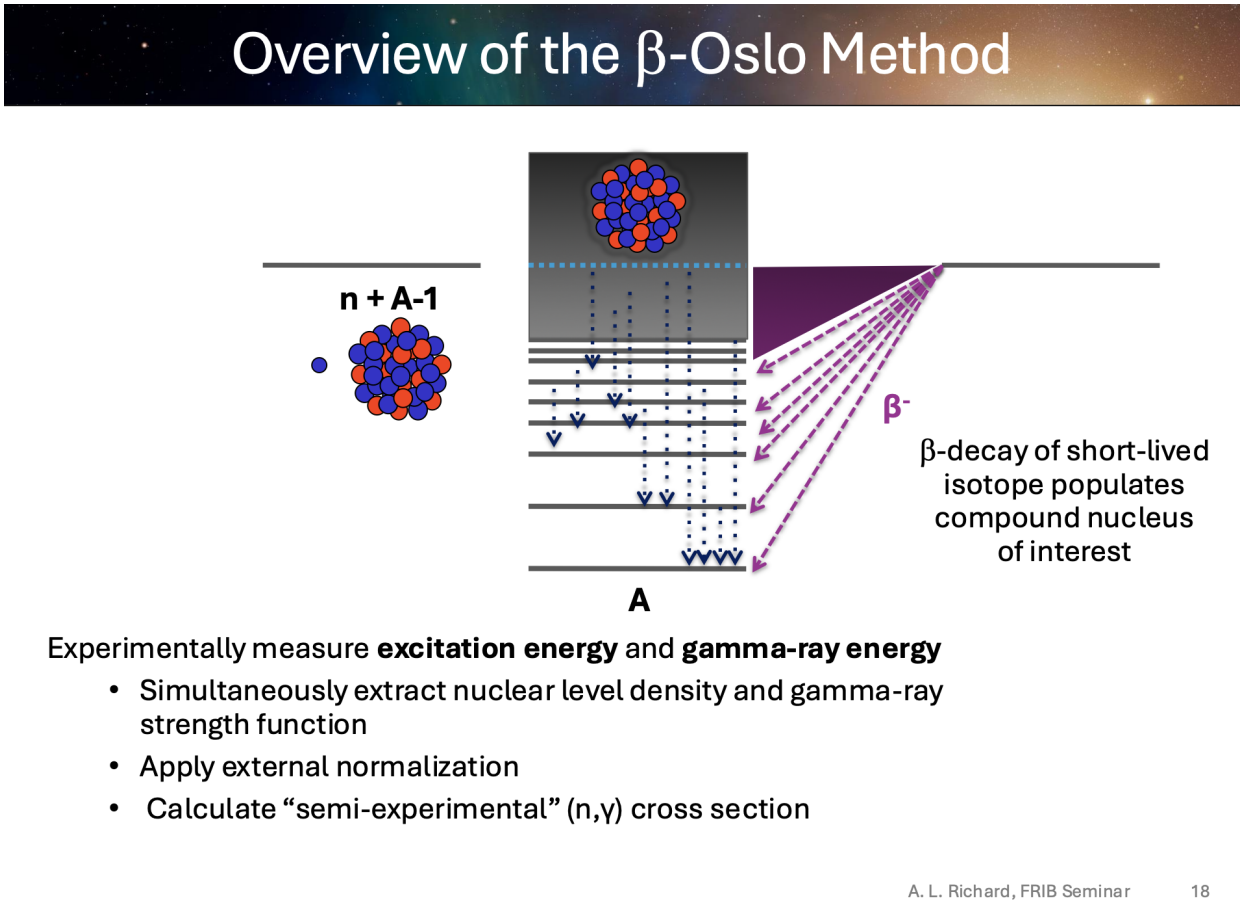

Figure 19.3: A slide from a recent seminar by Prof. Andrea Richard from Ohio University. The video of the presentation can be accessed under Ref. [36].

density of the residual nucleus, $\omega(U_\beta)$. This level density determines the number of accessible final states and thus the relative probability for decay into a given exit channel β. Together, this yields the cross section for the process $\alpha \to \beta$.

The Hauser–Feshbach theory refines this picture. Rather than expressing the decay probability in terms of the level density explicitly, it introduces transmission coefficients $T_\beta^{J\pi}$, which represent the average coupling strength of the compound nucleus to the exit channel β in a given J^π sector. These transmission coefficients can be obtained from the optical model, and it has the advantage that it accounts for the different dynamical couplings of each channel, including effects such as barrier penetration and angular-momentum constraints.

Crucially, both Weisskopf–Ewing theory and Hauser–Feshbach approach allow for an explicit test of *structure* calculations, which is why one sees these methods everywhere. Conversely, experimental measurements of level densities and γ strength functions can provide crucial input to Hauser–Feshbach calculations for processes which cannot be easily measured in the laboratory.

In-class Activity 19a: Nuclear level density measurements

In a recent Nuclear Science Seminar, Prof. Andrea Richard from Ohio University discussed the importance of neutron capture, *i.e.*, (n,γ) reactions for nucleosynthesis and nuclear physics applications. Because a neutron target cannot be prepared, it is not possible to directly measure these cross sections for short-lived nuclei[a]. Figure 19.3 shows one slide from Prof. Richard's presentation. Can you explain what is the proposed way to obtain neutron capture cross sections?

Solution

The slide shows a general picture for a particular method of extracting a cross section for a process of the type $n + A - 1 \rightarrow A + \gamma$. In the *$\beta$-Oslo method*, one studies the β-decay of a short-lived nucleus that populates a wide range of excited states in the nucleus of interest A. The nucleus A then de-excites by γ-emission, and the method centers on measuring the resulting γ-ray cascades to extract the nuclear level density and the *γ-strength function*, *i.e.*, a function that reflects the average probability for γ-ray emission (or absorption) as a function of energy. The "Oslo" in the name refers to an analysis technique that factorizes the γ-ray spectra into the nuclear level density and the γ-strength function, while "β" refers to measuring the β-decay electrons *in coincidence*, *i.e.*, simultaneously with the γ emission to enable a clean identification of the decay channel and an event-by-event reconstruction of the initial excitation energy from the γ-ray cascade. This allows one to reconstruct the γ strength function as well as the excitation energy E_x (which is a sum of energies of all emitted γ's) of the compound nucleus from the total γ-ray cascade energy. From these data, one can obtain the distribution of primary (first-generation) γ rays for each excitation energy. Under the assumption that the decay probability factorizes, this distribution can be written as

$$P(E_x, E_\gamma) \propto \rho(E_x - E_\gamma) T_\gamma(E_\gamma) \ , \tag{19.37}$$

where ρ is the nuclear level density and T_l is the γ-ray transmission coefficient, related to the γ-strength function. By fitting this factorized form to the measured primary γ-ray spectra over a range of excitation energies, one can simultaneously extract the functional forms of the level density $\rho(U)$ and the γ-strength function. With these two inputs and transmission coefficients for the neutron channel obtained from an optical model, one can compute the neutron-capture cross section using the Hauser–Feshbach formula, Eq. (19.35). In this way, the β-Oslo method provides the key statistical ingredients – level density and the γ-strength function – needed to predict (n,γ) cross sections for nuclei that cannot be studied directly.

[a] The latter of which, necessarily, must be the projectiles in such experiments.

Lecture sources: This lecture is based on Jackson [4] and Bertulani & Danielewicz [6].

Lecture 20

Fusion and fission

Prerequisites: Lectures 5, 6, 16, 18.
Guiding question: ***Why don't heavy nuclei simply fly apart?***

20.1 Reactions with heavy nuclei

Reactions that involve heavy nuclei[1], both as a projectile and a target, exhibit certain features which make them stand out. Since heavy nuclei carry a large electric charge, the projectile experiences a large Coulomb repulsion from the target nucleus. Given that the interaction is dominated by Coulomb forces at large distances while nuclear forces only start to matter at short distances, for heavy nuclei one needs to first ask whether a nuclear interaction takes place at all, *i.e.*, whether the projectile can overcome the *Coulomb barrier*. This can be estimated by evaluating the Coulomb potential at the *touching radius* (also referred to as *contact distance*), which can be computed by adding the nuclear radii estimated with $R_i = r_0 A_i^{1/3}$, where $r_0 = 1.2$ fm and A_i is the mass number. Consequently, the Coulomb barrier is given by

$$V_C^{(\mathrm{B})} = \frac{Z_1 Z_2 e^2}{r_0\left(A_1^{1/3} + A_2^{1/3}\right)} \,. \tag{20.1}$$

For example, overcoming the Coulomb barrier in the reaction $^{249}\mathrm{Cf} + {}^{50}\mathrm{Ti}$ (see Sec. 1.4.2) requires about 5.2 MeV per nucleon. This leads to a substantial *total* energy that can be deposited in the target. Reactions involving heavy projectiles can also carry a lot of angular momentum, which can be transferred to the target. This allows one to study, *e.g.*, high-spin states and rotational bands.

Since due to the Coulomb barrier, the nuclear force may not even be involved in a reaction, it is useful to estimate the distance of closest approach D for a given impact parameter b (see Sec. 5.1), which for a classical projectile of energy E can be calculated to be[2]

$$D = \frac{Z_1 Z_2 e^2}{2E} + \sqrt{\left(\frac{Z_1 Z_2 e^2}{2E}\right)^2 + b^2} \,. \tag{20.2}$$

[1] In this context, "heavy" can mean any nucleus with a mass number $A > 4$, but of course it also includes nuclei with hundreds of nucleons.

[2] At the distance of closest approach D, the radial component of velocity vanishes. Thus, the kinetic energy is purely tangential and can be expressed in terms of the angular momentum L, so that the total energy is $E = \frac{L^2}{2\mu D^2} + \frac{Z_1 Z_2 e^2}{D}$. For a projectile incoming at an impact parameter b we have $L = \mu v b$ (see Lecture 5), so that $L^2 = 2\mu E b^2$. Substituted into the energy conservation equation, this yields $D^2 - \frac{Z_1 Z_2 e^2}{E} D - b^2 = 0$, which is solved by Eq. (20.2).

Naturally, in experiment one can only control the incident energy of the projectile E. In particular, for d to be sufficiently small that the nuclear force is at play, we also need a sufficiently small impact parameter b which, however, we can only control indirectly. This can be done, *e.g.*, by classifying events according to observables that correlate with the impact parameter of the reaction. For example, in reactions which can be treated classically, the impact parameter can be related to the scattering angle through the deflection function $\theta(b)$ (see Lecture 5).

If we consider the projectile as a whole, then at energies which just overcome the Coulomb barrier its momentum per nucleon is on the order of $p \sim 100$ MeV/nucleon[3], and the de Broglie wavelength is (using natural units where $p = k$)

$$\lambda_{\mathrm{dB}} = \frac{2\pi}{Ap} \sim \frac{12}{A} \text{ fm} , \tag{20.3}$$

which easily satisfies $\lambda_{\mathrm{dB}} \ll R$, where we take R to be in the range 4–7 fm, already for medium mass nuclei. Because the projectile wavefunction has such a small wavelength, we can say it probes the potential *locally*. We also note that for an impact parameter b the angular momentum of the projectile is $L = (Ap)b$. Assuming that the largest impact parameter corresponds to R, we get

$$L_{\max} \sim (Ap)R \sim \frac{R}{\lambda_{\mathrm{dB}}} \gg 1 , \tag{20.4}$$

which, given $L = \sqrt{l(l+1)}$, immediately yields $l_{\max} \gg 1$. This tells us that many partial waves contribute to the scattering process, so that l behaves almost like a continuous variable and can be related semi-classically to the impact parameter. As a result, we are able to map partial waves onto impact parameters and replace sums by integrals.

Treating the reaction semi-classically allows us to use the geometric interpretation of the cross section: assuming that there is always a reaction[4] for impact parameters satisfying $b \leq b_0$, we have

$$\sigma_r = \pi b_0^2 . \tag{20.5}$$

Because one can establish σ_r experimentally, it is possible to then extract b_0 and, consequently, the corresponding smallest distance[5] D_0 using Eq. (20.2). By plotting this distance against $A_1^{1/3} + A_2^{1/3}$, we can verify whether an assumption that a reaction takes place for radii smaller than the touching radius is justified. As can be seen in Fig. 20.1, a best-fit line actually gives $D_0 \sim 1.36(A_1^{1/3} + A_2^{1/3})$, implying that *grazing collisions* (*i.e.*, collisions at the largest impact parameters that still lead to a reaction) occur at distances somewhat larger than the naive touching-spheres estimate based on $r_0 \simeq 1.2$ fm, as 1.36 fm $> r_0$.

The type of the reaction that occurs provided $b < b_0$ depends both on b and on the energy E. For *peripheral collisions*, characterized by $b \lesssim b_0$, only a small part of each nucleus participates and the interaction time is short. One therefore predominantly expects processes such as elastic or inelastic scattering and transfer reactions, rather than compound-nucleus formation. For small values of b and sufficiently large impact energies, one expects more violent reactions in which the projectile penetrates the target. As a result, the reaction may lead to

- *fusion*, *i.e.*, merging of the colliding nuclei,
- *fission*, *i.e.*, splitting of a nucleus into two (or more) fragments, or

[3] Assuming $E_{\mathrm{kin}} \sim 5$ MeV/nucleon, we can immediately calculate the momentum of a single nucleon using Eqs. (4.36) and (4.38), $p = \sqrt{E^2 - m_N^2} = \sqrt{(m_N + E_{\mathrm{kin}})^2 - m_N^2} = \sqrt{E_{\mathrm{kin}}(2m_N + E_{\mathrm{kin}})} \sim 97$ MeV.

[4] Note that in this context, we only call a scattering event a "reaction" if it involves the nuclear force.

[5] We note that here, the meaning of the smallest distance is somewhat different than when we used it in Lecture 5: there, it referred to the minimal distance achieved in a head-on collision.

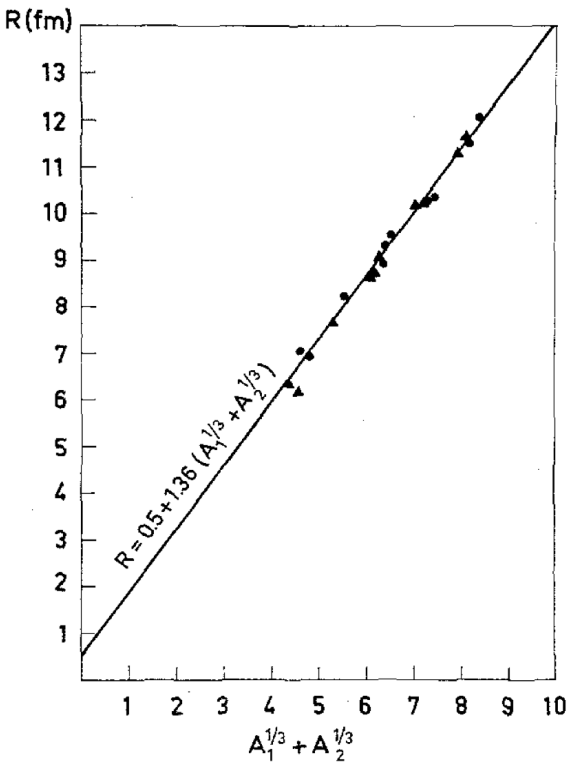

Figure 20.1: Smallest distance between two nuclei in a grazing collision. Figure from Ref. [37].

- *deep inelastic collision*, *i.e.*, an extended interaction between projectile and target involving nucleon exchange and substantial conversion of kinetic energy into internal excitation, but without forming a compound nucleus[6].

20.2 Fusion reactions

Fusion is preferred for lighter systems and at low energies, where it is more likely that a compound nucleus is formed; this compound system subsequently de-excites either by γ-ray or particle emission. Because of large angular momentum transfer, fusion reactions are one of the best ways to produce and study high-spin states in nuclei. Indeed, states with angular momenta on the order of $30\hbar$ can be populated in reactions such as, *e.g.*, (^{16}O, xn), where a heavy projectile is absorbed by the target nucleus and part of the excitation energy is carried away by evaporation of x neutrons. At very low energies, nuclear fusion also drives stellar energy production, as first suggested by Hans Bethe [38]. When measured below the Coulomb barrier, fusion reactions additionally provide a way to study nuclear structure, given that the fusion cross section depends exponentially on the barrier penetration probability and is therefore strongly influenced by details of the nuclear potential and couplings to internal degrees of freedom.

A simple picture of fusion models it as tunneling through a local potential barrier that arises in

[6]Note that this name will mean something *very* different in high-energy physics, where *deep inelastic scattering* refers to a high-energy process in which a projectile (typically an electron, muon, or neutrino) probes the internal structure of a hadron (such as a proton).

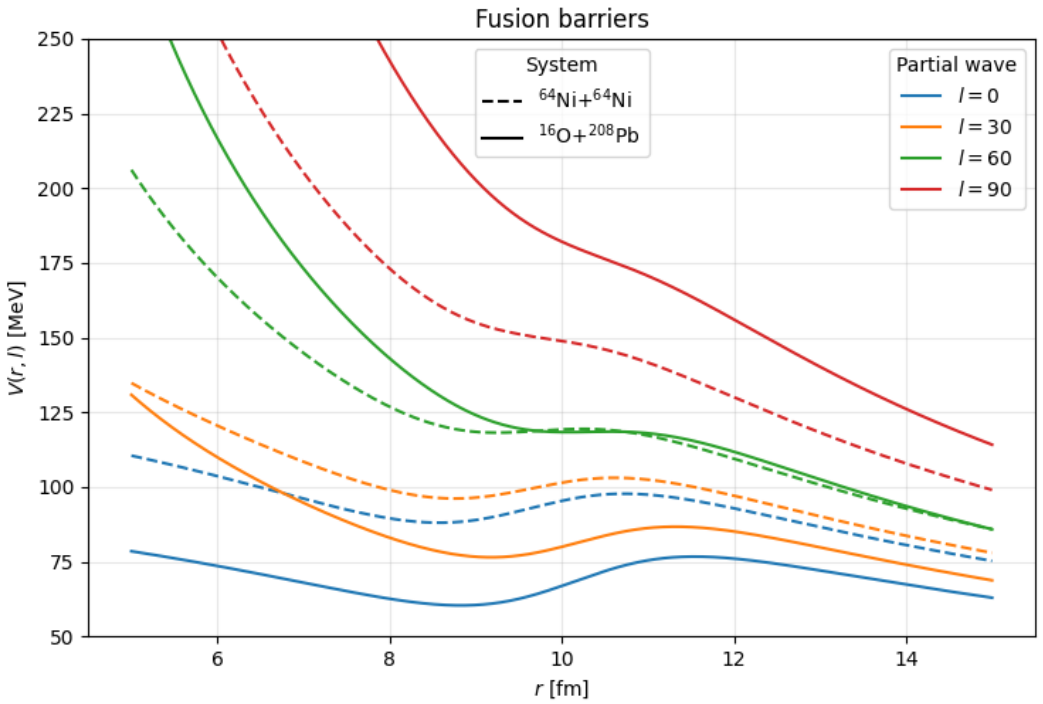

Figure 20.2: Comparison of fusion barriers, calculated according to Eq. (20.6), for different systems and at different angular momenta.

a potential with nuclear, Coulomb, and (effective) centrifugal terms,

$$V(r,l) = V_N(r) + V_C(r) + \frac{l(l+1)}{2\mu r^2} \ . \tag{20.6}$$

Here, $V_N(r)$ can be well modeled with an attractive potential of a Woods–Saxon type, Eq. (18.16), while the Coulomb contribution is that of a uniformly charged sphere, Eq. (18.26). As a function of r, this potential displays a characteristic peak of height V_B, *i.e.*, the *fusion barrier* whose location and magnitude varies depending on the system at hand, see Fig. 20.2. Fusion (capture) occurs when the system penetrates this barrier, since a local pocket in the potential corresponds to a classically trapped configuration and facilitates compound-nucleus formation. For sufficiently large l, the centrifugal term can remove this pocket, so that the system is no longer trapped and such partial waves do not contribute to fusion; this behavior is evident in Fig. 20.2.

20.3 The 3D Wentzel–Kramers–Brillouin approximation

In Sec. 6.3, we used a 1-dimensional treatment of the Wentzel–Kramers–Brillouin (WKB) approximation to examine the *ansatz* for the asymptotic behavior of a wavefunction solving a scattering problem, Eq. (6.16). We now return to WKB to describe barrier penetration in fusion. Because it's been a while since we discussed WKB, let us quickly re-derive the key formulas while also updating the discussion to 3 dimensions[7].

[7]The latter, as you will see, is only useful to a limited extent.

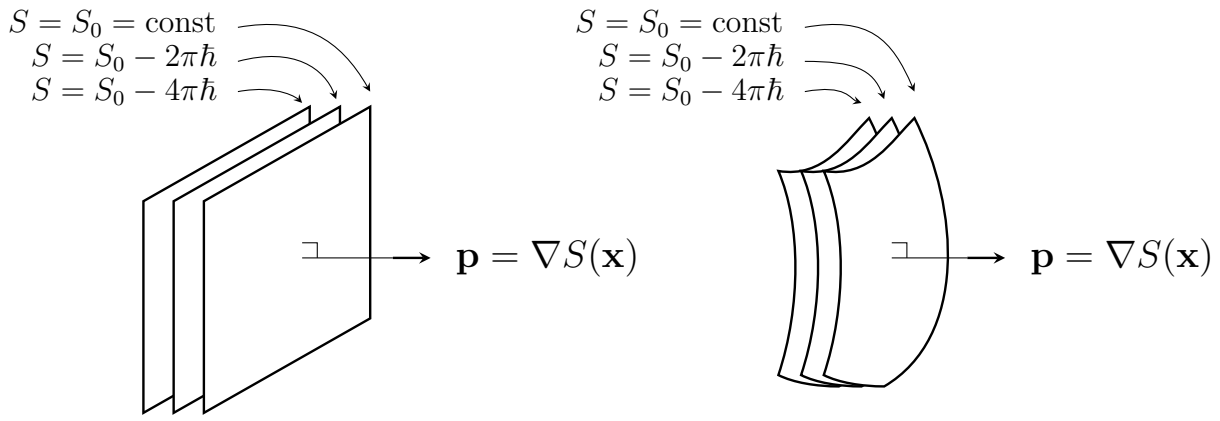

Figure 20.3: Surfaces of constant phase for a plane wave (*left*) and for a wave propagating through a slowly varying potential (*right*). The surfaces shown differ by either one (2π) or two (4π) full oscillations. The local momentum is perpendicular to the wavefronts and is given by $\mathbf{p} = \nabla S(\mathbf{x})$. Copied from a figure in Ref. [39].

20.3.1 General considerations

The three-dimensional Schrödinger equation is[8],

$$\left[-\frac{\hbar^2}{2\mu}\hat{\boldsymbol{\nabla}}^2 + \hat{V}(\boldsymbol{r})\right]\psi(\boldsymbol{r}) = E\psi(\boldsymbol{r}) \ . \tag{20.7}$$

If $\hat{V}(\boldsymbol{r}) = 0$, the solution is a plane wave,

$$\phi(\boldsymbol{r}) = Ae^{iS(\boldsymbol{r})/\hbar} \ , \tag{20.8}$$

where

$$S(\boldsymbol{x}) = \boldsymbol{p}\cdot\boldsymbol{r} \ . \tag{20.9}$$

Note that $\boldsymbol{p} = \boldsymbol{\nabla}S(\boldsymbol{r})$, *i.e.*, the momentum is the gradient of the phase of the wavefunction. This make sense: the gradient explicitly encodes the fact that the momentum is perpendicular to the wavefront (*i.e.*, a surface of constant phase), see the left panel in Fig. 20.3, and shows that the momentum measures how quickly the phase changes over an infinitesimal distance $d\boldsymbol{r}$ (so that larger momentum means faster oscillations). For a plane wave, $\boldsymbol{\nabla}S(\boldsymbol{r}) = \boldsymbol{p}$ is independent of position, and the wavefronts are parallel planes.

Now let us consider a slowly-varying potential $V(\boldsymbol{r})$. It is natural to expect that the wavefronts respond to the changes in the potential as they propagate in space. Since the potential varies slowly, these wavefront deformations are also slowly-varying functions of the position. In particular, locally such slow variations correspond to only slight deviations from a plane wavefront, see the right panel in Fig. 20.3.

More precisely, if the characteristic length scale over which the potential varies is L, we say that V varies slowly if the local wavelength $\lambda(\boldsymbol{r})$ is much smaller than L, $\lambda(\boldsymbol{r}) \ll L$. Since the de Broglie wavelength is given by $\lambda_{\text{dB}} \equiv 2\pi\hbar/|\boldsymbol{\nabla}S(\boldsymbol{r})| = 2\pi\hbar/|\boldsymbol{p}|$, this condition is equivalent to

$$\frac{2\pi\hbar}{|\boldsymbol{p}|L} \ll 1 \ . \tag{20.10}$$

[8] As in Sec. 6.3, in this derivation we keep explicit factors of $\hbar$ because WKB is obtained from an expansion in $\hbar$, the latter of which is valid if $\hbar$ is small compared to the characteristic classical action of the problem.

Note that the quantity $|\boldsymbol{p}|L$, which is the typical momentum multiplied by the distance over which it changes appreciably, has the dimension of action (see Footnote 8 in Lecture 6). Thus, the WKB approximation corresponds to the regime in which the quantum of action $\hbar$ is small compared to the characteristic classical action of the motion.

It is then reasonable to assume that for a slowly-varying potential the solution to the Schroödinger equation will locally resemble a plane wave, but with slowly-varying amplitude and slowly-vary local wavevector (*i.e.*, slowly-varying gradient of the phase),

$$\psi_{\mathrm{WKB}}(\boldsymbol{r}) = A(\boldsymbol{r}) e^{\frac{iS(\boldsymbol{r})}{\hbar}} = e^{\frac{i}{\hbar}\left[S(\boldsymbol{r}) - i\hbar \ln A(\boldsymbol{r})\right]} \ . \tag{20.11}$$

This is the *WKB approximation*, also called the *semiclassical or quasiclassical approximation*. The form following the second equality allows us to interpret the term $-i\hbar \ln A(\boldsymbol{r})$ as the first order correction to the phase $S(\boldsymbol{r})$, and motivates the more general *ansatz*

$$\psi(\boldsymbol{r}) = e^{\frac{i}{\hbar}W(\boldsymbol{r})} \ , \tag{20.12}$$

where

$$W(\boldsymbol{r}) = W_0(\boldsymbol{r}) + \hbar W_1(\boldsymbol{r}) + \hbar^2 W_2(\boldsymbol{r}) + \ldots \tag{20.13}$$

and, comparing with Eq. (20.11), we can immediately identify

$$W_0(\boldsymbol{r}) = S(\boldsymbol{r}) \quad \text{and} \quad W_1(\boldsymbol{r}) = -i \ln A(\boldsymbol{r}) \ . \tag{20.14}$$

Thus, the WKB ansatz corresponds to keeping the first two terms in an expansion of the phase function $W(\boldsymbol{r})$ in powers of $\hbar$, separating the leading classical contribution from quantum corrections.

Substituting the postulated wavefunction, Eq. (20.12), into the Schrödinger equation leads to

$$\frac{1}{2\mu}\Big(\boldsymbol{\nabla} W(\boldsymbol{r})\Big)^2 - \frac{i\hbar}{2\mu}\boldsymbol{\nabla}^2 W(\boldsymbol{r}) + V(\boldsymbol{r}) = E \ . \tag{20.15}$$

Using the expansion of $W(\boldsymbol{r})$, Eq. (20.13), we obtain

$$\frac{1}{2\mu}\Big(\boldsymbol{\nabla} W_0(\boldsymbol{r}) + \hbar\boldsymbol{\nabla} W_1(\boldsymbol{r}) + \ldots\Big)^2 - \frac{i\hbar}{2\mu}\Big(\boldsymbol{\nabla}^2 W_0(\boldsymbol{r}) + \hbar\boldsymbol{\nabla}^2 W_1(\boldsymbol{r}) + \ldots\Big) + V(\boldsymbol{r}) = E \ , \tag{20.16}$$

where we can now consider terms by order in $\hbar$. Thus, at zeroth order in $\hbar$, we have

$$\frac{1}{2\mu}\Big(\boldsymbol{\nabla} W_0(\boldsymbol{r})\Big)^2 + V(\boldsymbol{r}) = E \ , \tag{20.17}$$

while at first order in $\hbar$ we obtain

$$\boldsymbol{\nabla} W_0(\boldsymbol{r}) \cdot \boldsymbol{\nabla} W_1(\boldsymbol{r}) - \frac{i}{2}\boldsymbol{\nabla}^2 W_0(\boldsymbol{r}) = 0 \ . \tag{20.18}$$

By Eq. (20.14), the zeroth-order equation, Eq. (20.17), can be also written as

$$\big(\boldsymbol{\nabla} S(\boldsymbol{r})\big)^2 = 2\mu\big(E - V(\boldsymbol{r})\big) \ , \tag{20.19}$$

which with the identification

$$\boldsymbol{p}(\boldsymbol{r}) = \boldsymbol{\nabla} S(\boldsymbol{r}) \tag{20.20}$$

can be recognized as the *time-independent Hamilton-Jacobi equation* (see Footnote 8 in Lecture 6), equivalent to the classical energy conservation condition,

$$\frac{\boldsymbol{p}^2(\boldsymbol{r})}{2\mu} + V(\boldsymbol{r}) = E \ , \tag{20.21}$$

written in terms of the action $S(\boldsymbol{r})$. Thus, the leading WKB phase is the classical action, and may be written as a formal solution of the differential equation in Eq. (20.19),

$$S(\boldsymbol{r}) = S(\boldsymbol{r_0}) + \int_{\boldsymbol{r}_0}^{\boldsymbol{r}} d\boldsymbol{r}' \ \sqrt{2\mu\big(E - V(\boldsymbol{r})\big)} \ , \tag{20.22}$$

where the integral is taken along a classical trajectory connecting $\boldsymbol{r}_0$ and $\boldsymbol{r}$.

Then, using Eq. (20.14) again, the first order equation, Eq. (20.18), becomes

$$\Big(\boldsymbol{\nabla} S(\boldsymbol{r})\Big) \cdot \Big(\boldsymbol{\nabla} \ln A(\boldsymbol{r})\Big) + \frac{1}{2}\boldsymbol{\nabla}^2 S(\boldsymbol{r}) = 0 \tag{20.23}$$

or, equivalently,

$$\boldsymbol{\nabla} \cdot \Big(A^2(\boldsymbol{r})\boldsymbol{\nabla} S(\boldsymbol{r})\Big) = 0 \ , \tag{20.24}$$

which is known as the *amplitude transport equation*. Carrying out the gradient operation then yields

$$\boldsymbol{\nabla} \cdot \Big(A^2(\boldsymbol{r})\boldsymbol{\nabla} S(\boldsymbol{r})\Big) = 2A(\boldsymbol{r})\big[\boldsymbol{\nabla} A(\boldsymbol{r})\big] \cdot \boldsymbol{\nabla} S(\boldsymbol{r}) + A^2(\boldsymbol{r})\boldsymbol{\nabla} \cdot \big[\boldsymbol{\nabla} S(\boldsymbol{r})\big] \tag{20.25}$$

$$= 2\big[\boldsymbol{\nabla} A(\boldsymbol{r})\big] \cdot \boldsymbol{p}(\boldsymbol{r}) + A(\boldsymbol{r})\boldsymbol{\nabla} \cdot \boldsymbol{p}(\boldsymbol{r}) = 0 \ , \tag{20.26}$$

where in the second equality we used the fact that momentum is the gradient of the phase, Eq. (20.20).

In contrast to the 1D case (see Sec. 6.3), the above equation does not yield a general expression for the amplitude $A(\boldsymbol{r})$ in terms of $\boldsymbol{p}(\boldsymbol{r})$ alone. However, gaining some insight is still possible. Indeed, using Eq. (20.20) the amplitude transport equation, Eq. (20.24), can also be rewritten as

$$\boldsymbol{\nabla} \cdot \Big(A^2(\boldsymbol{r})\boldsymbol{v}(\boldsymbol{r})\Big) = 0 \ , \tag{20.27}$$

which constrains how the amplitude varies along the integral curves of the vector field $\boldsymbol{v}(\boldsymbol{r}) \propto \boldsymbol{\nabla} S(\boldsymbol{r})$. In particular, if the amplitude A and action S are real, as they are in classically allowed regions, a handy interpretation arises. In that case one can compute that the probability current, given by Eq. (6.50), is

$$\boldsymbol{j}_{\text{WKB}} = \frac{1}{\mu} A^2(\boldsymbol{r})\boldsymbol{\nabla} S(\boldsymbol{r}) = A^2(\boldsymbol{r})\boldsymbol{v}(\boldsymbol{r}) \ . \tag{20.28}$$

Thus, Eq. (20.27) shows that the WKB approximation corresponds to classical trajectories carrying conserved probability flux. To an extent, this is the main takeaway of the 3D derivation.

20.3.2 Formal WKB applicability condition

Following the form of the WKB *ansatz* in Eq. (20.11) and the expansion by orders of $\hbar$ postulated in Eq. (20.13), we can surmise that the WKB approximation holds if $S(\boldsymbol{r})$ is the leading term, *i.e.*, if the magnitude of the first order correction $-i\hbar \ln A(\boldsymbol{r})$ is small compared to the magnitude of $S(\boldsymbol{r})$.

More precisely, we demand that this holds for variations *along a classical trajectory*, *i.e.*, under the directional derivative $\hat{\boldsymbol{p}} \cdot \boldsymbol{\nabla} = (\boldsymbol{p} \cdot \boldsymbol{\nabla})/|\boldsymbol{p}|$. This condition yields

$$\left|\hat{\boldsymbol{p}} \cdot \boldsymbol{\nabla} S(\boldsymbol{r})\right| \gg \left|\hbar \hat{\boldsymbol{p}} \cdot \boldsymbol{\nabla} \ln A(\boldsymbol{r})\right| . \tag{20.29}$$

Given Eq. (20.20), the left-hand side immediately simplifies to $|\boldsymbol{p}(\boldsymbol{r})|$, while the right-hand side can be rewritten as

$$\left|\hbar \frac{\hat{\boldsymbol{p}} \cdot \boldsymbol{\nabla} A(\boldsymbol{r})}{A(\boldsymbol{r})}\right| = \left|\hbar \frac{\boldsymbol{p} \cdot \boldsymbol{\nabla} A(\boldsymbol{r})}{|\boldsymbol{p}(\boldsymbol{r})| A(\boldsymbol{r})}\right| = \left|\frac{\hbar}{2} \frac{\boldsymbol{\nabla} \cdot \boldsymbol{p}}{|\boldsymbol{p}(\boldsymbol{r})|}\right| \tag{20.30}$$

where in the second equality we used Eq. (20.26). Altogether, Eq. (20.29) then becomes

$$|\boldsymbol{p}(\boldsymbol{r})| \gg \left|\frac{\hbar}{2} \frac{\boldsymbol{\nabla} \cdot \boldsymbol{p}(\boldsymbol{r})}{|\boldsymbol{p}(\boldsymbol{r})|}\right| , \tag{20.31}$$

which is equivalent to

$$\left|\hbar \frac{\boldsymbol{\nabla} \cdot \boldsymbol{p}(\boldsymbol{r})}{p(\boldsymbol{r})^2}\right| \ll 1 , \tag{20.32}$$

where $p(\boldsymbol{r}) = |\boldsymbol{p}(\boldsymbol{r})|$. Finally, using $\boldsymbol{p} = \hbar \boldsymbol{k}$, we then arrive at the *WKB applicability condition*,

$$\left|\frac{\boldsymbol{\nabla} \cdot \boldsymbol{k}(\boldsymbol{r})}{k^2(\boldsymbol{r})}\right| \ll 1 , \tag{20.33}$$

20.3.3 1D WKB solutions with turning points

In Sec. 6.3, we have only considered a 1D WKB solution corresponding to an outgoing wave, Eq. (6.29). However, in general the WKB wavefunction can be either incoming or outgoing,

$$\psi^{(\pm)}_{\mathrm{WKB}}(x) = \frac{A}{\sqrt{p(x)}} \exp\Big(\pm \frac{i}{\hbar} \int^x dx'\, p(x') \Big) , \tag{20.34}$$

where the local momentum is defined as

$$p(x) = \sqrt{2\mu\big(E - V(x)\big)} , \tag{20.35}$$

and a general solution is a superposition of these two possibilities.

Furthermore, previously we have discussed the behavior of the WKB *ansatz* far away from the region where the potential dominates. However, now we want to apply it directly in the interaction region. For this, we may need to consider a number of possibilities. In particular, Fig. 20.4 shows a situation in which the potential is larger than the particle's energy E in region I and smaller than E in region II. Classically, "Region I" is forbidden, while "Region II" is allowed. In the classically allowed region, $E > V(x)$ and the momentum, Eq. (20.35), is real and so the general solution is oscillatory,

$$\psi^{\mathrm{II}}_{\mathrm{WKB}}(x) = \frac{1}{\sqrt{p(x)}} \left[A_+ \exp\Big(\frac{i}{\hbar} \int_a^x dx'\, p(x') \Big) + A_- \exp\Big(-\frac{i}{\hbar} \int_a^x dx'\, p(x') \Big) \right] . \tag{20.36}$$

Conversely, in the classically forbidden region, $E < V(x)$ and the momentum becomes imaginary. We can always define

$$\kappa = \sqrt{2\mu\big(V(x) - E\big)} , \tag{20.37}$$

with which one can write $p(x) = i\kappa(x)$, so that the wavefunction becomes exponential,

$$\psi^{\mathrm{I}}_{\mathrm{WKB}}(x) = \frac{1}{\sqrt{\kappa(x)}}\left[B_+ \exp\left(\frac{1}{\hbar}\int_a^x dx'\ \kappa(x')\right) + B_- \exp\left(-\frac{1}{\hbar}\int_a^x dx'\ \kappa(x')\right)\right] , \tag{20.38}$$

where $x < a$ so that the integral limits will enforce a sign change. To obtain a physically acceptable (square-integrable) solution as $x \to -\infty$, we set $B_- = 0$, so that finally

$$\psi^{\mathrm{I}}_{\mathrm{WKB}}(x) = \frac{C}{\sqrt{\kappa(x)}} \exp\left(\frac{1}{\hbar}\int_a^x dx'\ \kappa(x')\right) . \tag{20.39}$$

Notably, the boundary between the two regions, $x = a$ (see Fig. 20.4), is defined by the condition

$$E = V(a) , \tag{20.40}$$

for which $p(a) = 0$. The WKB approximation fails in the vicinity of $x = a$ – known as the *turning point* since this is where a classical particle literally turns around – because the WKB amplitude, $1/\sqrt{p(x)}$, diverges; however, we know this is not a physical behavior. The solution to this conundrum is to locally replace the WKB approximation with another function[9]. This means that we need to find *another* approximate solution near the turning point. We can do this by expanding the potential near $x = a$,

$$V(x) \approx V(a) + V'(a)(x - a) . \tag{20.41}$$

Taking $E = V(a)$, the Schrödinger equation then reduces to

$$-\frac{\hbar^2}{2\mu}\frac{d^2\psi_{\mathrm{TP}}}{dx^2} + V'(a)(x - a)\psi_{\mathrm{TP}} = 0 , \tag{20.42}$$

where the subscript "TP" reminds us that we are solving for the wavefunction near the turning point. Since $V'(a) < 0$ (see Fig. 20.4), we write

$$V'(a)(x - a) = |V'(a)|(a - x) . \tag{20.43}$$

Then defining

$$z = \frac{a - x}{l} , \tag{20.44}$$

[9] Yes, we are literally going to "patch" the problem – and it's going to work!

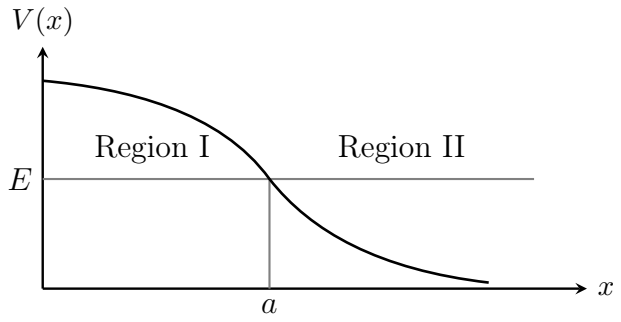

Figure 20.4: Classically forbidden ("Region I", where $V(x) > E$) and allowed ("Region II", where $V(x) < E$) regions for a particle of energy E; the turning point $x = a$ is defined by $V(a) = E$.

we have

$$\frac{d^2}{dx^2} = \frac{d}{dx}\frac{d}{dx} = \frac{\partial z}{\partial x}\frac{d}{dz}\left(\frac{\partial z}{\partial x}\frac{d}{dz}\right) = \frac{1}{l^2}\frac{d^2}{dz^2} \ , \tag{20.45}$$

so that Eq. (20.42) becomes

$$-\frac{\hbar^2}{2\mu l^2}\frac{d^2\psi_{\rm TP}}{dz^2} + |V'(a)|lz\psi_{\rm TP} = 0 \ . \tag{20.46}$$

Taking

$$l = \left(\frac{\hbar^2}{2\mu|V'(a)|}\right)^{1/3} \ , \tag{20.47}$$

we immediately arrive at the *Airy equation*,

$$\frac{d^2\psi_{\rm TP}}{dz^2} - z\psi_{\rm TP} = 0 \ , \tag{20.48}$$

for which the solution is composed out of *Airy functions*,

$$\psi_{\rm TP}(z) = C_1{\rm Ai}(z) + C_2{\rm Bi}(z) = C_1{\rm Ai}\Big(\frac{a-x}{l}\Big) + C_2{\rm Bi}\Big(\frac{a-x}{l}\Big) \ . \tag{20.49}$$

The Airy functions do not have a closed form. Nevertheless, they provide a smooth interpolation between the oscillatory behavior of the WKB approximation in the allowed region and its exponential behavior in the forbidden region while removing the WKB divergence at turning points.

20.3.4 Matching conditions at the turning point

To use the result that we have just obtained, we need to now match the WKB solutions on both sides of the turning point to Airy functions. First, note that the matching needs to be carried out some distance *away* from the turning point, where *both* the WKB approximation and the Airy functions provide valid representations of the wavefunction. Exactly at the turning point, the argument of $\psi_{\rm TP}(z)$ is zero, see Eq. (20.44). We assume that regions sufficiently far from the turning point should correspond to either $z \ll -1$ or $z \gg 1$, so that we can use the asymptotic (and analytic!) forms of the Airy functions that can be directly compared to the WKB solutions.

Let us consider the forbidden region first. There, $z \gg 1$ and we can write

$${\rm Ai}(z)\big|_{z\gg 1} \sim \frac{1}{2\sqrt{\pi}z^{1/4}}\exp\Big(-\frac{2}{3}z^{3/2}\Big) \ . \tag{20.50}$$

Using the Taylor expansion of the potential, Eq. (20.41), the magnitude of the imaginary momentum, Eq. (20.37), can be approximated as

$$\kappa(x) = \sqrt{2\mu\big(V(x)-E\big)} \approx \sqrt{2\mu|V'(a)|(a-x)} \ . \tag{20.51}$$

With this, we can compute

$$\frac{1}{\hbar}\int_x^a dx'\ \kappa(x') \approx \frac{\sqrt{2\mu|V'(a)|}}{\hbar}\int_x^a dx'\ \sqrt{a-x'} = \frac{\sqrt{2\mu|V'(a)|}}{\hbar}\frac{2}{3}(a-x)^{3/2} = \frac{2}{3}z^{3/2} \ . \tag{20.52}$$

By comparing with Eq. (20.50), we can immediately see that

$$\mathrm{Ai}(z)\big|_{z\gg 1} \sim \frac{1}{2\sqrt{\pi}z^{1/4}} \exp\Big(-\frac{1}{\hbar}\int_x^a dx'\ \kappa(x')\Big)\ . \tag{20.53}$$

Since, moreover, $\kappa^{-1/2} \propto z^{-1/4}$, we arrive at a conclusion that the Airy function at large positive z behaves exactly like the exponentially decaying WKB solution, Eq. (20.39).

$$\psi^{\mathrm{I}}_{\mathrm{WKB}}(x) = \frac{C}{\sqrt{\kappa(x)}} \exp\Big(\frac{1}{\hbar}\int_a^x dx'\ \kappa(x')\Big)\ . \tag{20.54}$$

Now, let us consider the allowed region, which corresponds to $z \ll -1$. In this limit, denoting $z = -s$ with $s > 0$, we have

$$\mathrm{Ai}(z)\big|_{z\ll -1} \sim \frac{1}{\sqrt{\pi}s^{1/4}} \sin\Big(\frac{2}{3}s^{3/2} + \frac{\pi}{4}\Big)\ . \tag{20.55}$$

We can again use the Taylor expansion of the potential, Eq. (20.41), to expand the momentum, Eq. (20.35),

$$p(x) \approx \sqrt{2\mu|V'(a)|(x-a)}\ , \tag{20.56}$$

where we used the fact that $V'(a) < 0$. With this, we can compute

$$\frac{1}{\hbar}\int_a^x dx'\ p(x') \approx \frac{\sqrt{2\mu|V'(a)|}}{\hbar}\int_a^x dx'\ \sqrt{x-a} = \frac{\sqrt{2\mu|V'(a)|}}{\hbar}\frac{2}{3}(x-a)^{3/2} = \frac{2}{3}s^{3/2}\ , \tag{20.57}$$

so that comparing with Eq. (20.55) immediately yields

$$\mathrm{Ai}(z)\big|_{z\ll -1} \sim \frac{1}{\sqrt{p(x)}} \sin\Big(\frac{1}{\hbar}\int_a^x dx'\ p(x') + \frac{\pi}{4}\Big)\ . \tag{20.58}$$

This, naturally, can be rewritten as

$$\mathrm{Ai}(z)\big|_{z\ll -1} \sim \frac{1}{\sqrt{p(x)}}\left[\exp\left[i\Big(\frac{1}{\hbar}\int_a^x dx'\ p(x') + \frac{\pi}{4}\Big)\right] - \exp\left[-i\Big(\frac{1}{\hbar}\int_a^x dx'\ p(x') + \frac{\pi}{4}\Big)\right]\right]\ , \tag{20.59}$$

which is a well-defined combination of an outgoing and incoming WKB solution in the allowed region. With this, we see that matching to the Airy function from the classically allowed side forces us to assume an "additional" phase shift of $\pi/4$.

To conclude, we stress again that while the Airy functions match the diverging behavior of the WKB approximation at $z \gg 1$ and $z \ll -1$, they *do not* diverge at $z = 0$, *i.e.*, at the turning point. This is why we use them.

20.4 The radial WKB approximation

Scattering is, naturally, inherently a 3D problem. However, if the potential is spherically symmetric, we can use the partial wave expansion to take advantage of the 1D WKB formalism derived above.

As discussed in Lecture 7, for a spherically-symmetric potential the wavefunction factorizes as

$$\psi_{klm}(\boldsymbol{r}) = \frac{u_l(k,r)}{r} Y_{lm}(\theta,\phi)\ , \tag{20.60}$$

where $Y_{lm}(\theta,\phi)$ are the spherical harmonics and $ul(k,r)$ solves the radial equation, Eq. (7.22) , repeated here in a slightly different but equivalent notation,

$$\frac{\hbar^2}{2\mu}\frac{\partial^2}{\partial r^2}u_l(k,r)+\left[E-V(r)-\frac{\hbar^2 l(l+1)}{2\mu r^2}\right]u_l(k,r)=0\ . \tag{20.61}$$

As discussed in Lecture 5 in the context of classical scattering, one can define an effective potential that includes the centrifugal term,

$$V_{\rm eff}(r)=V(r)+\frac{\hbar^2 l(l+1)}{2\mu r^2}\ . \tag{20.62}$$

With this, the radial equation, Eq. (20.61), becomes

$$\frac{\partial^2}{\partial r^2}u_l(k,r)+\frac{2\mu}{\hbar^2}\Big[E-V_{\rm eff}(r)\Big]u_l(k,r)=0\ . \tag{20.63}$$

As usual, we can define

$$k_{\rm eff}=\sqrt{\frac{2\mu}{\hbar^2}\Big[E-V_{\rm eff}(r)\Big]} \tag{20.64}$$

and call it a day, since we have already derived everything in Secs. 20.3.3 and 20.3.4... or, *can we?*

It turns out that life is not so simple. This is because the treatment in Secs. 20.3.3 and 20.3.4 differs by two important points: 1) the variable x can assume values from $-\infty$ to $+\infty$, while r is restricted to the real positive axis, and 2) we did not take into account the angular momentum, which happens to introduce a singularity near $r=0$. These two features complicate the situation. In particular, the WKB approximation does not reproduce the correct divergent behavior introduced by the centrifugal term $\hbar^2 l(l+1)/(2\mu r^2)$ as $r\to 0$. To see that, consider Eq. (20.61). As discussed in Sec. 7.3.1, near the origin the $\hbar^2 l(l+1)/(2\mu r^2)$ term dominates and, as a result, the regular solutions to the radial equation behave like r^{l+1}, while the irregular solutions diverge with r^{-l}. However, if one applies a naive WKB scheme, one obtains Eq. (20.64) with the effective potential given by Eq. (20.62), which near $r=0$ can be well approximated with

$$k_{\rm eff}\big|_{r\approx 0}\sim\frac{i\hbar\sqrt{l(l+1)}}{r}\equiv i\kappa_{\rm eff}\ . \tag{20.65}$$

This in turn leads to[10]

$$u_{\rm WKB}(r)\sim\frac{1}{\sqrt{\kappa_{\rm eff}(r)}}e^{\pm\int dr'\ \kappa_{\rm eff}(r')}\sim\sqrt{r}e^{\pm\int dr'\ \frac{\hbar\sqrt{l(l+1)}}{r}}\sim\sqrt{r}e^{\pm\sqrt{l(l+1)}\ln r}\sim r^{\frac{1}{2}\pm\sqrt{l(l+1)}}\ , \tag{20.66}$$

which does *not* reproduce the correct behavior near $r=0$.

Luckily, this can be dealt with by means of a relatively simple trick: a change of variables which takes the singular point $r=0$ to $-\infty$. Indeed, let us consider $r=e^x$. Then $dr=e^x\,dx$, so that

$$\frac{d^2}{dr^2}=e^{-x}\frac{d}{dx}\left(e^{-x}\frac{d}{dx}\right)=-e^{-2x}\frac{d}{dx}+e^{-2x}\frac{d^2}{dx^2} \tag{20.67}$$

and the radial equation, Eq. (20.61), becomes

$$-\frac{1}{2\mu}\frac{d}{dx}u_l(k,e^x)+\frac{1}{2\mu}\frac{d^2}{dx^2}u_l(k,e^x)+e^{2x}\left[E-V(e^x)-\frac{l(l+1)}{2\mu}e^{-2x}\right]u_l(k,e^x)=0\ . \tag{20.68}$$

[10]Note that we assume here that near $r=0$ we are in the forbidden region.

To deal with the first derivative, we then introduce a new wavefunction,

$$u_l(e^x) = g(x)e^{x/2} \ , \tag{20.69}$$

in terms of which we obtain

$$\frac{1}{2\mu}\frac{d^2g(x)}{dx^2} + e^{2x}\left[E - V(e^x) - \frac{l(l+1)+\frac{1}{4}}{2\mu}e^{-2x}\right]g(x) = 0 \tag{20.70}$$

or, noticing that $l(l+1)+\frac{1}{4} = (l+\frac{1}{2})^2$,

$$\frac{1}{2\mu}\frac{d^2g(x)}{dx^2} + e^{2x}\left[E - V(e^x) - \frac{\left(l+\frac{1}{2}\right)^2}{2\mu}e^{-2x}\right]g(x) = 0 \ . \tag{20.71}$$

Let us note that the above equation is still an exact Schrödinger equation, equivalent to Eq. (20.61), just written in a different way. However, the "extra term" which has been merged with the contribution due to the angular momentum, known as the *Langer modification* or *Langer correction*, now allows us to reproduce the correct singular behavior near $r = 0$ in the WKB approximation.

With this, we denote

$$\omega(x) = e^x\sqrt{2\mu\Big[E - V(e^x)\Big] - \left(l+\frac{1}{2}\right)^2 e^{-2x}} \ , \tag{20.72}$$

so that the WKB solution is given by

$$g_l^{\mathrm{WKB}}(x) = \frac{1}{\sqrt{\omega(x)}}\exp\left[\pm i\int dx\ \omega(x)\right] \ . \tag{20.73}$$

We can now also reintroduce $e^x = r$ and $g_l = u_l r^{-1/2}$, which finally yields

$$u_l^{\mathrm{WKB}}(r) = \frac{1}{\sqrt{p_{l,\mathrm{eff}}^{(\mathrm{L})}(r)}}\exp\left[\pm i\int dr\ \sqrt{2\mu\Big[E - V(r)\Big] - \frac{\left(l+\frac{1}{2}\right)^2}{r^2}}\right] \ , \tag{20.74}$$

where

$$p_{l,\mathrm{eff}}^{(\mathrm{L})}(r) = \sqrt{2\mu\left[E - V(r) - \frac{\left(l+\frac{1}{2}\right)^2}{r^2}\right]} \ . \tag{20.75}$$

Let us see that this works. Applying the same steps as in Eq. (20.66) to Eq. (20.74) yields

$$u_{\mathrm{WKB}} \sim r^{\frac{1}{2}\pm\left(l+\frac{1}{2}\right)} \sim \begin{cases} r^{l+1} \ , & + \\ r^{-l} \ , & - \end{cases} \ , \tag{20.76}$$

which indeed reproduces the behavior of the exact solutions for $r \to 0$.

20.4.1 What has just happened?

Let us recap what this section has been about. In Secs. 20.3.3 and 20.3.4, we introduced Airy-function matching as a way of handling the breakdown of the WKB approximation, Eq. (20.34), near turning points where $p = 0$.

In a problem with a central potential, we additionally need to deal with the divergent behavior of the wavefunction near $r = 0$, which is incorrect in the naive WKB treatment. This leads us to the Langer modification, which ensures that the WKB solution has the correct behavior near the origin. With the correct behavior ensured at $r = 0$, the standard WKB-Airy matching can now be applied at the true turning points of the effective potential.

20.5 Tunneling probability

In Fig. 20.2, we see that the fusion barrier is relatively slowly over distances on the order of 1 fm. This suggests that the WKB approximation can be used to describe barrier penetration in fusion and derive the fusion cross section. Because tunneling occurs when two classically allowed regions are separated by a forbidden region, the problem is characterized by *two* turning points.

Within the partial wave expansion, we consider a Langer-corrected effective potential with both nuclear and Coulomb contributions[11],

$$V_l^{\text{eff}}(r) = V_l^{(N)}(r) + V_l^{(C)} + \frac{\left(l+\frac{1}{2}\right)^2}{2\mu r^2} \ . \tag{20.77}$$

We assume that the particle energy lies below the l-dependent fusion barrier, $E < V_{B,l}$, which leads to the existence of two turning points, $r_1(l)$ and $r_2(l)$, defined by

$$V_l^{\text{eff}}(r_1) = E \ , \quad V_l^{\text{eff}}(r_2) = E \ , \quad r_1 < r_2 \ . \tag{20.78}$$

In the classically allowed regions we have $V_l^{\text{eff}}(r) < E$, so that the radial momentum is real,

$$p_l(r) = \sqrt{2\mu\left[E - V_l^{\text{eff}}\right]} \ , \tag{20.79}$$

while in the classically forbidden region, $r_1 < r < r_2$, we have $V_l^{\text{eff}}(r) > E$, so that the momentum is imaginary, $p_l = i\kappa_l$, where

$$\kappa_l(r) = \sqrt{2\mu\left[V_l^{\text{eff}} - E\right]} \ . \tag{20.80}$$

Thus, inside the barrier the WKB solution has the exponentially damped form[12],

$$u_l^{WKB}(r) \propto \frac{1}{\sqrt{\kappa_l}} e^{-\int_{r_1}^{r} dr' \ \kappa_l(r')} \ . \tag{20.81}$$

As we know, the above expression should not be evaluated exactly at r_1 or r_2, since $\kappa_l(r_i) = 0$ and the WKB prefactor diverges. Instead, the WKB solutions near the turning points r_1, r_2 must be connected using the Airy matching formulas derived above. Those formulas remove the spurious divergence of the WKB prefactor and replace it by finite matching coefficients. The important point is that these coefficients are not exponentially large or small; in other, words, the exponential attenuation across the barrier is predominantly controlled by the integral of $\kappa_l(r)$.

We therefore define the *WKB barrier action*,

$$S_l(E) \equiv \int_{r_1}^{r_2} dr \ \kappa_l(r) = \int_{r_1}^{r_2} dr \ \sqrt{2\mu\left[V_l^{\text{eff}} - E\right]} \ , \tag{20.82}$$

whose meaning is simple: $S_l(E)$ is the total exponential attenuation accumulated across the classically forbidden region. Since the wave amplitude is suppressed by a factor of order $e^{-S_l(E)}$ as it crosses the barrier, the transmission probability, which is proportional to the squared amplitude, is

$$P_l(E) \sim e^{-2S_l(E)} \ . \tag{20.83}$$

[11] Note that since we're done deriving formulae, we enter again the wonderful world of natural units, *i.e.*, $\hbar = 1$.
[12] Here, we assume that the wavefunction "enters" the barrier at $r = r_1$.

As discussed in Lecture 16, the absorption (*i.e.*, non-elastic) cross section is proportional to $1 - |S_l(k)|^2$, Eq. (16.9), where $S_l(k)$ is the S-matrix element in the partial wave expansion. Given the unitarity of the S-matrix (see Sec. 14.4), this term can be simply interpreted as *the probability that scattering is not elastic*. In the fusion reaction context, one typically assumes that once the system penetrates the barrier and reaches the internal region, it is fully absorbed (this assumption is known as the *incoming-wave boundary condition*, simply because full absorption requires that the wavefunction inside the barrier have no outgoing component). Under this assumption, the probability of non-elastic scattering can be identified with the barrier penetration probability, $1 - |S_l(k)|^2 = P_l(E)$. With this, we can write the total cross section for a fusion reaction as

$$\sigma(E) = \frac{\pi}{k^2} \sum_{l=0}^{\infty} (2l+1) P_l(E) = \frac{\pi}{k^2} \sum_{l=0}^{\infty} (2l+1) e^{-2S_l(E)} \ , \tag{20.84}$$

where $S_l(E)$ is given by Eq. (20.82). The above result is known as the *deep sub-barrier limit*, meaning it applies when E substantially differs from $V_{B,l}$. This regime of validity comes from the assumption that the wave decays strongly inside the barrier, so that one can neglect the reflection of the wave generated at the outer turning point or, equivalently, neglect multiple reflections between the two turning points.

For energies close to the barrier maximum, the wave is not strongly attenuated and thus it can undergo repeated reflections between the two turning points r_1 and r_2. Moreover, since r_1 and r_2 are not well separated, it is no longer sufficient to perform separate Airy matching at each turning point. Instead, one must treat the two turning points as a single barrier problem. This, of course, is not trivial and therefore calls for approximations. One of such uniform treatments approximates the barrier as an inverted parabola[13], which leads to the *Hill–Wheeler penetrability*, *i.e.*, transmission probability,

$$P_l(E) = \frac{1}{1 + e^{2S_l(E)}} \ . \tag{20.85}$$

Note that for $S_l(E) \gg 1$ (*i.e.*, large attenuation), the above formula reduces to the WKB result, Eq. (20.83).

20.6 Fission

Fission becomes important when the compound nucleus is sufficiently heavy. In the liquid-drop picture[14], Coulomb repulsion increasingly competes with surface tension, and for heavy nuclei the system may lower its energy by splitting into two fragments.

For fission to be energetically allowed, the mass of the initial nucleus must exceed that of the final fragments,

$$m(Z, A) > m_1(Z_1, A_1) + m_2(Z_2, A_2) > 0 \ , \tag{20.86}$$

or ,equivalently, the Q-value for fission must be positive. Using the liquid-drop model, one can estimate the binding energies and show that the competition between the Coulomb term (which favors separation) and the surface term (which favors compact shapes) leads to the approximate

[13] Note that this should be an excellent approximation near the barrier maximum.

[14] In which the nucleus is modeled as a charged, incompressible fluid drop, where bulk (volume), surface, and Coulomb energies determine its properties and deformation.

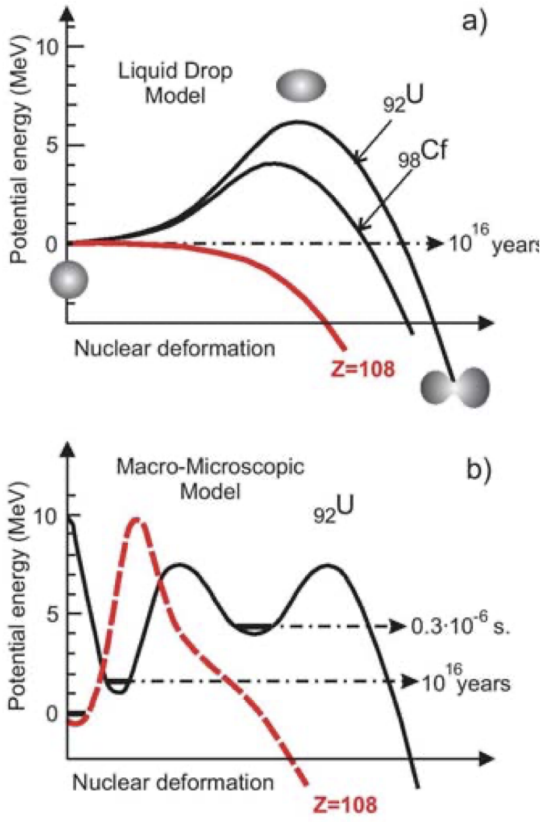

Figure 20.5: Fission barriers in the liquid-drop model (*top*) and in the liquid-drop model with shell corrections (*bottom*). Figure from Ref. [40].

condition that spontaneous fission becomes energetically favorable only for sufficiently heavy nuclei, roughly $A \gtrsim 90$.

However, energetic allowance alone does not imply immediate fission: the system must still overcome or tunnel through the *fission barrier*, *i.e.*, the energy barrier in the nuclear potential energy as a function of *deformation*, which separates the compact (approximately spherical) configuration of the compound nucleus from configurations corresponding to separated fragments. In other words, the fission barrier is the maximum in the potential energy that must be overcome (or tunneled through) for the nucleus to fission. This answers the guiding question of this lecture: heavy nuclei do not simply disintegrate because although a lower-energy configuration often exists, reaching it requires large deformations that are energetically disfavored.

You can see examples of fission barriers in Fig. 20.5, where the top panel shows the simple barriers obtained from a liquid-drop model, while the bottom panel illustrates that the situation becomes more complex once nuclear shell structure is taken into account. In particular, shell corrections can generate additional structure in the deformation-dependent potential, including secondary minima which correspond to *shape isomers*, *i.e.*, metastable states at large deformation which are separated from the ground state by a barrier. Such states can have measurable lifetimes because decay requires tunneling either back to the ground-state configuration or toward fission In fact, the observation of fission from these isomeric states provided early evidence that nuclear structure remains important even in strongly deformed nuclei [40].

At any time, fission competes with γ-ray and particle emission (such as neutron evaporation).

At low excitation energies, de-excitation typically proceeds through a sequence of particle emissions and γ decay. At higher excitation energies, the probability of reaching large deformations increases, and fission becomes more likely. In this sense, fission is not necessarily an immediate process, but rather one that can occur at some stage during the de-excitation of the compound nucleus.

Moreover, the fission barrier also depends on the angular momentum. As angular momentum increases, the rotational energy favors elongated shapes, effectively lowering the barrier. Furthermore, as the rotational energy increases, the compact configuration becomes less stable relative to deformed configurations, and beyond a critical value l_{crit} the barrier disappears altogether, leading to prompt (fast) fission without the need for tunneling.

Lecture sources: In this lecture, Sections 20.1, 20.2, 20.4, 20.5, and 20.6 are based on Bertulani & Danielewicz [6], while Section 20.3 is based on lecture notes by R. G. Littlejohn [39].

Lecture 21

Direct reactions I

Prerequisites: Lecture 5.
Guiding question: ***How can reactions probe angular momentum and parity of nuclei?***

21.1 Introduction to direct reactions

Let us consider the scales "resolved" in a given reaction. To this end, let us note that the de Broglie wavelength of a projectile is inversely proportional to its momentum, $\lambda_{\rm dB} \sim 1/k$. As an example, at the incident energy of $E_n \approx 1$ MeV a nucleon has de Broglie wavelength of about 4 fm. A wavefunction with such a spread does not resolve individual nucleons, and it is more likely to interact through a compound-nucleus reaction[1]. On the other hand, a 20-MeV nucleus has a de Broglie wavelength of about 1 fm, which allows it to "see" individual nucleons rather than the whole nucleus at once. Thus, more energetic particles are more likely to participate in direct reactions (see Lecture 1), that is processes in which the incident particle interacts primarily at the surface of the target and the reaction involves at most a few *valence nucleons* (*i.e.*, nucleons at the surface of the target nucleus.)

Of course, for given entrance and exit channels it is always possible that multiple types of reactions can take place. How can we know then whether a given process, for example the *deuteron stripping reaction*[2],

$$\mathrm{d} + {}^{\mathrm{X}}\mathrm{A} \rightarrow \mathrm{n} + {}^{\mathrm{X+1}}\mathrm{A'} \quad \text{or} \quad (\mathrm{d},\mathrm{n})\ , \tag{21.1}$$

was a direct or compound nucleus reaction? As discussed in Lecture 15, one of the distinguishing features is the angular dependence of the cross section: For compound nucleus reactions, where the reaction mechanism involves forming an intermediate compound state which lives long enough for its components to fully equilibrate, the measured cross sections are isotropic, reflecting an erasure of the "memory" of the entrance channel. Conversely, transfer reactions take place fast and involve only a few nucleons, so that such "memory loss" is simply impossible; one of the consequences of this fact is that the direct reaction cross sections are significantly forward-peaked. Some transfer reactions are also simply more likely to proceed through a direct reaction. As an example, the process

$$\mathrm{d} + {}^{\mathrm{X}}\mathrm{A} = \mathrm{p} + {}^{\mathrm{X+1}}\mathrm{A} \quad \text{or} \quad (\mathrm{d},\mathrm{p}) \tag{21.2}$$

[1] In a cartoon-like simplification, you can think that at these energies the projectile must interact with the nucleus as a whole, which can be hand-waved to be more likely to result in absorption.
[2] Which is an example of a transfer reaction, see Lecture 1.

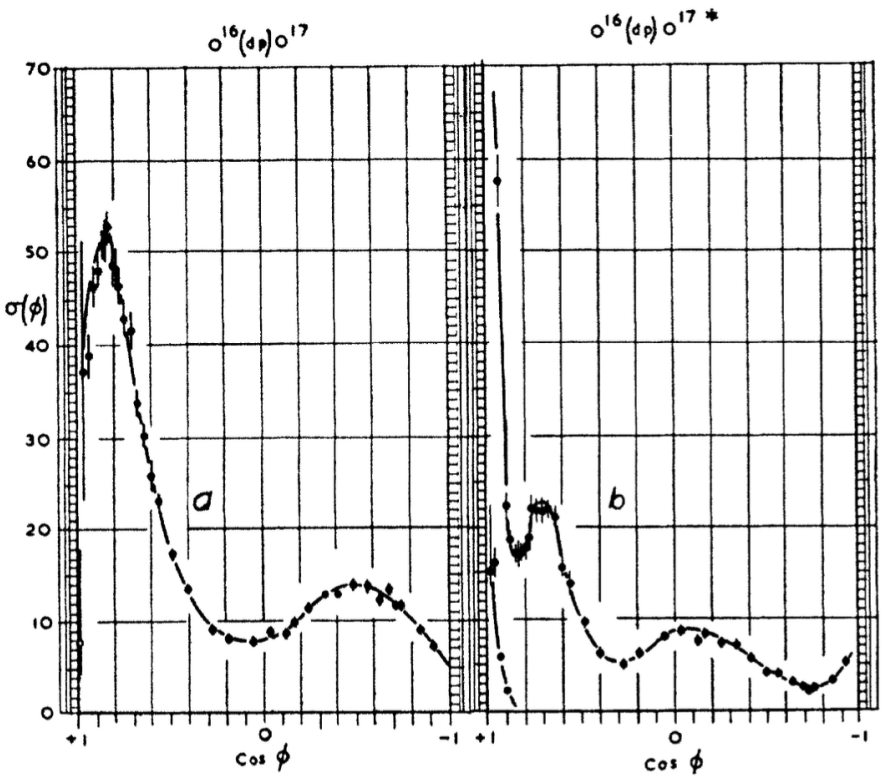

Figure 21.1: Angular distributions for two stripping reactions with an 8-MeV deuteron beam: $^{16}\mathrm{O}(\mathrm{d},\mathrm{p})^{17}\mathrm{O}$ (*left*) and $^{16}\mathrm{O}(\mathrm{d},\mathrm{p})^{17}\mathrm{O}^{*}$ (*right*). The angular distribution is plotted as a function of $\cos\theta$, and the cross section is given in arbitrary units. Figure from Ref. [41].

is less likely to occur through a compound nucleus reaction (in which the target nucleus absorbs the incident deuteron) because the subsequent emission of a proton is inhibited by the Coulomb barrier.

Single-transfer reactions such as (d,n) and (d,p) are particularly important for studies of the low-lying shell-model excited states. In a given reaction, several such states can be plausibly populated. The energy of the outgoing nucleon fixes the excited state, while the angular distribution of the emitted particles can reveal the spin and parity of the state that is populated in a particular reaction. This applies not only to stripping reactions like the ones highlighted above, but also, *e.g.*, to pickup reactions such as (p,d).

21.2 Experimental emergence of direct reactions

Direct reactions were born in the late 1940s, when Robert Serber (among others) argued that stripping reactions like (d,p) occure *via* a fast, one-step mechanism [42]. However, a particularly endearing exposition of direct reactions was given by two companion contributions to Physical Review Letters in 1950. The first letter, by Hannah Burrows[3] and collaborators, discussed the experimental results for two reactions, $^{16}\mathrm{O}(\mathrm{d},\mathrm{p})^{17}\mathrm{O}$ and $^{16}\mathrm{O}(\mathrm{d},\mathrm{p})^{17}\mathrm{O}^{*}$, which leave the target nucleus in the ground and first excited state, respectively. The differential cross sections for the reactions are shown in Fig. 21.1. The authors highlighted the strikingly different angular behavior of the two

[3]Who most likely was a student at the time.

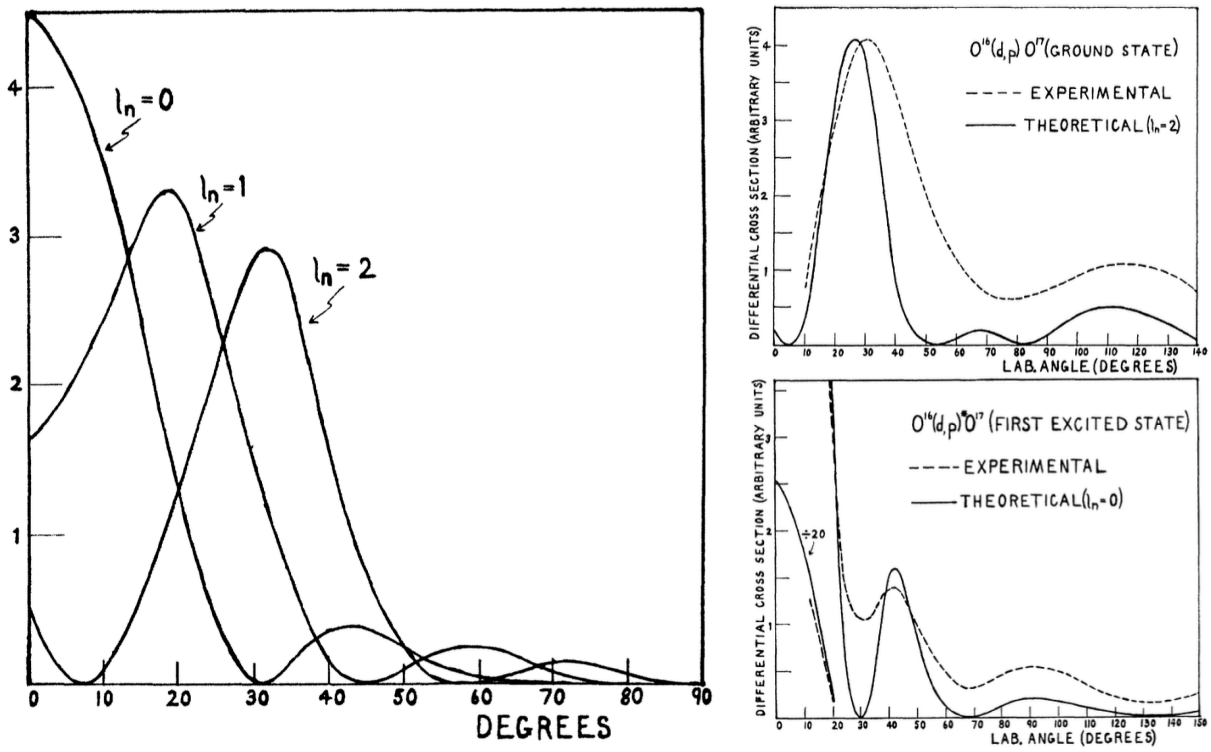

Figure 21.2: *Left:* Theoretical angular distributions for different angular momentum transfers to the nucleus. *Right:* Comparison of the theoretical predictions with experimental measurements of Ref. [41]. Figures from Ref. [43].

results: while $^{16}\mathrm{O}(\mathrm{d},\mathrm{p})^{17}\mathrm{O}$ has a peak around $\theta \approx 34°$, $^{16}\mathrm{O}(\mathrm{d},\mathrm{p})^{17}\mathrm{O}^*$ seems to instead exhibit a dip in that region; moreover, it experiences a peak at $\theta \approx 45°$ and also, seemingly[4], at $\theta \approx 0$.

The companion letter, authored by Stuart Butler[5], showed that such an angular distribution could be obtained in a reaction which does *not* lead to a formation of a compound nucleus, but in a process involving high incident angular momenta of classical impact parameters on the order of the nuclear radius. With this, he showed that the position of the maxima is determined by the spins[6] and parities of the nuclear states involved. Indeed, since in a semi-classical treatment one can assume a 1-to-1 relation between the scattering angle and the impact parameter (see Lecture 5), one can identify the angular momentum transferred to the nucleus and, therefore, determine the spin and parity of the final nucleus. This is our first hint that direct reactions can yield useful information about the internal structure of the participating nuclei.

In-class Activity 21a: Inferring the spin and parity of ^{17}O and ^{17}O*

Let us follow the example of Butler and infer the spin and parity of the ground and first excited state of ^{17}O. The ground state of ^{16}O has zero spin and even parity, and a nucleon has spin 1/2 and even parity. Use the fact that the parity of the final state is $\pi_f = \pi_{\mathrm{core}}\pi_{\mathrm{p}}(-1)^l$.

[4] In the paper, the authors carefully note that while the results *indicate* a peak at $\theta \approx 0$, this couldn't be stated with certainty as the apparatus did not measure results below $\theta \sim 5°$.

[5] Who was a Ph.D. student at the time and who built his career on describing stripping reactions.

[6] Note that what one means by "spin" in this context is really "total orbital angular momentum" of the nucleus. In fact, since the strong interaction mixes L and S, only J is a good quantum number.

Solution

Before the reaction, the "core" is the ^{16}O nucleus which has zero spin and even parity. The stripping reaction adds a neutron to this core. We know the neutron's spin is 1/2, but what is its angular momentum l? Here we use the fact that the neutron arrives as part of the incident deuteron, which also contains the measured proton. Since the proton and neutron arrive at the surface of the nucleus at the same time, they better are characterized by the same l. Given that the differential cross section for the $^{16}\mathrm{O}(\mathrm{d},\mathrm{p})^{17}\mathrm{O}$ reaction is well-described by $l = 2$, the total angular momentum of ^{17}O must then be $J = l \pm \frac{1}{2}$, *i.e.* either 3/2 or 5/2. The parity of the residual nucleus is given by $\pi = \pi_{\mathrm{core}}\pi_{\mathrm{n}}(-1)^l$, so that it's even.
The differential cross section for the $^{16}\mathrm{O}(\mathrm{d},\mathrm{p})^{17}\mathrm{O}^*$ reaction, on the other hand, is well-described by $l = 0$. As a result, we must have $J = 1/2$. As before, we arrive at an even parity.

21.3 A simple model of angular momentum transfer

Some features of direct reactions can be gleaned from a simple, semi-classical treatment. Let us consider in more detail the angular momentum transfer in a direct reaction. To this end, we assume that the projectile interacts with the target nucleus strictly at the surface, which is motivated by the *strong absorption* picture, in which partial waves that penetrate into the nuclear interior are strongly attenuated, while those that remain outside are largely unaffected. Let us take the nuclear surface to be characterized by a radius R. We also know the magnitude and directions of both the incident momentum k_α and the outgoing momentum k_β.

In general, the total angular momentum of the nucleus – which, for reasons unknown to mankind, is also referred to as the nucleus' "spin" – I_A will change in the course of the reaction. Denoting this change by $\Delta\boldsymbol{L}$, we can write

$$\Delta\boldsymbol{L} = \boldsymbol{I}_B - \boldsymbol{I}_A \ , \tag{21.3}$$

where A and B denote the initial and final nuclei, respectively. If, for simplicity, we consider a spinless projectile, then conservation of total angular momentum dictates that this change must correspond to a change in the relative orbital angular momentum of the colliding pair,

$$\Delta\boldsymbol{L} = \boldsymbol{R} \times (\boldsymbol{k}_\beta - \boldsymbol{k}_\alpha) = \boldsymbol{q} \times \boldsymbol{R} \ , \tag{21.4}$$

where $\boldsymbol{q} \equiv \boldsymbol{k}_\alpha - \boldsymbol{k}_\beta$ is the momentum transfer.

If we consider an excitation of a particular definite state in the final nucleus, this fixes the magnitude of $\boldsymbol{k}_\beta$. The direction of $\boldsymbol{k}_\beta$ determines the scattering angle, and a given scattering angle corresponds to a fixed $\boldsymbol{q}$. Given that we have to satisfy Eq. (21.4), we see that particles scattered into a particular angle θ correspond to points on the surface of the target nucleus which satisfy $\boldsymbol{q}(\theta) \times \boldsymbol{R} = \text{const}$, which further implies $R\sin\sphericalangle(\boldsymbol{q},\boldsymbol{R}) = \text{const}$. This condition is satisfied by two rings on the surface of the nucleus, as we can see in Fig. 21.3, where it is evident that $R\sin\alpha = \Delta L/q$ is the distance from the point defined by $\boldsymbol{R}$ to a line which passes through the origin and is parallel to the direction of $\boldsymbol{q}$. Consequently, the emission into the angle θ proceeds from a ring of radius $\Delta L/q$; moreover, since $\sin\alpha = \sin(\pi - \alpha)$, there exists two such rings.

With this, we can already get some insight. In order to stay on the surface, the ring radius must be smaller than R, or

$$\frac{\Delta L}{q} \leq R \ , \tag{21.5}$$

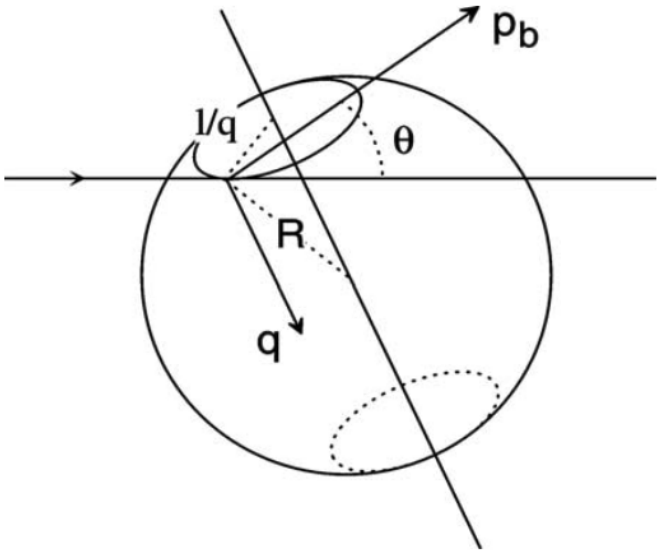

Figure 21.3: A sketch of the relations between the scattering angle θ and the location on the surface of the nucleus where the reaction must have taken place. Figure from Ref. [6].

which may put a meaningful limit on the angle of observation. For example, if the energy transfer is small such that $k_\alpha \approx k_\beta$, then one can approximate

$$q \approx k \sin\theta \approx k\theta \ , \tag{21.6}$$

where $k = (k_\alpha + k_\beta)/2$, which plugged into the constraint in Eq. (21.5) yields

$$\theta \geq \frac{\Delta L}{kR} \ . \tag{21.7}$$

In other words, for transfers with $\Delta L \neq 0$ to occur, one needs to observe scattering through an angle of at least $\theta \approx (kR)^{-1}$. Conversely, considering a maximum momentum transfer where $\boldsymbol{q} = \boldsymbol{k}_\alpha - (-\boldsymbol{k}_\alpha) = 2k_\alpha$, we can also see that the angular momentum transfer is limited by

$$\Delta L \leq 2k_\alpha R \ . \tag{21.8}$$

In-class Activity 21b: Interference pattern in direct reactions

Since for any given scattering angle the particles may originate from either of the two "scattering rings" on the nucleus, we can expect interference between the reaction products from those two opposite ends. Assuming that the scattering angle is small (or, equivalently, that the ring radius is small, which corresponds to either a small angular momentum transfer ΔL or a large momentum transfer q), derive the average phase difference between waves emitted from the two opposite rings on the nucleus. Discuss the resulting interference pattern.
Hint: Assume that the emitted waves are plane waves.

Solution

For a plane wave, $e^{i\boldsymbol{k}\cdot\boldsymbol{r}}$, the phase is $\phi \equiv \boldsymbol{k}\cdot\boldsymbol{r}$. For a small scattering angle we can again take $\boldsymbol{k}_1 \approx \boldsymbol{k}_2$ and define $\boldsymbol{k} = (\boldsymbol{k}_1 + \boldsymbol{k}_2)/2$. Then, for two waves originating at points $\boldsymbol{r}_1$ and $\boldsymbol{r}_2$,

the phase difference is

$$\Delta\phi \approx \boldsymbol{k} \cdot (\boldsymbol{r}_1 - \boldsymbol{r}_2) \ . \tag{21.9}$$

As discussed above, the ring radius is $\rho = R\sin\alpha = L/q$. If we have a small scattering angle, that radius is small, $\rho \ll R$, and the reaction points are concentrated near the poles. In that case we can approximate $\boldsymbol{r}_1 \approx +R\hat{\boldsymbol{q}}$ and $\boldsymbol{r}_2 \approx +R\hat{\boldsymbol{q}}$, so that $\Delta\boldsymbol{r} \approx 2R\hat{\boldsymbol{q}}$ and the phase difference becomes

$$\Delta\phi \approx \boldsymbol{k} \cdot 2R\hat{\boldsymbol{q}} = 2kR\cos\beta \ , \tag{21.10}$$

where $\beta = \sphericalangle(\boldsymbol{k}, \hat{\boldsymbol{q}})$. From the geometry we can see that $\cos\beta = \sin\theta \approx \theta$, and we arrive at

$$\Delta\phi \approx 2kR\theta \ . \tag{21.11}$$

If this difference equals $2n\pi$ or $(2n+1)\pi$, we'll have constructive or destructive interference, respectively. In other words, we expect the differential cross section to show a diffraction pattern with maxima at angles $\theta = n\pi/(kR)$, *i.e.*, with peaks separated in angle roughly by

$$\Delta\theta = \frac{\pi}{(kR)} \ . \tag{21.12}$$

Moreover, given the minimum angle corresponding to the angular momentum transfer ΔL, Eq. (21.7), the first peak will occur at an angle of order

$$\theta \sim \frac{\Delta L}{kR} \ . \tag{21.13}$$

Note that we have derived quite general features from a single assumption of strong absorption, which constrains direct reactions to occur only at the surface of the nucleus. In particular, we did not even specify the type of the reaction (inelastic, stripping, pick-up, ...). For this reason, the features highlighted above will appear in a wide range of reactions.

Lecture sources: This lecture is based on Satchler [7] and Krane [8].

Lecture 22

Direct reactions II

Prerequisites: Lectures 11, 11, 13.
Guiding question: ***How to formally describe reaction calculations?***

22.1 Reaction Hamiltonian

In deriving results in scattering theory (see Lectures 11–13), we have worked with a single-particle Hamiltonian that one can write as $\hat{H} = \hat{H}_0 + \hat{V}$, where $\hat{H}_0$ is the free Hamiltonian. We strayed from this simple form in Sec. 13.2, where we separated the potential into two parts, $\hat{V} \to \hat{\mathcal{V}} = \hat{V} + \hat{U}$, to derive the two-potential formulae, Eqs. (13.37) and (13.38), and the distorted wave Born approximation (DWBA), Eq. (13.44).

However, if we genuinely consider describing *reactions*, we need to expand beyond this simple picture. In general, for a reaction a+A → b+B, the system is described by a *many-body Hamiltonian*

$$\hat{H} = \hat{H}_a + \hat{H}_A + \hat{T}_{aA} + \hat{V}_{aA} \ , \tag{22.1}$$

where $\hat{H}_a$ describes the internal states of the projectile, $\hat{H}_A$ describes internal states of the target, $\hat{T}_{aA}$ describes their relative kinetic energy, and $\hat{V}_{aA}$ is the interaction between the projectile and the target. However, we can just as well write the Hamiltonian in terms of the reaction products,

$$\hat{H} = \hat{H}_b + \hat{H}_B + \hat{T}_{bB} + \hat{V}_{bB} \ . \tag{22.2}$$

The two forms are equivalent: they are the same Hamiltonian $\hat{H}$ in different *channel decompositions*, corresponding to different asymptotic clusterings of the same many-body system[1]. We say that the Hamiltonian in Eq. (22.1) is the Hamiltonian in the entrance channel, while the one in Eq. (22.2) is the Hamiltonian in the exit channel.

As before, to proceed it is convenient to divide the potential into two parts,

$$\hat{V} \to \hat{\mathcal{V}} = \hat{V} + \hat{U} \ . \tag{22.3}$$

We assume that the (new) potential $\hat{V}$ depends only on the channel coordinates (and possibly also on the channel spin) and does *not* act on the internal coordinates of the projectile and target. This means that it does not change the internal states of the projectile and target, *i.e.*, it describes elastic

[1]Loosely speaking, one can say that the Hamiltonian $\hat{H}$ has to describe both the possibility of the system being a combination of a and A as well as being a combination of b and B.

processes within a given channel. The potential $\hat{U}$, on the other hand, does depend on both the channel coordinates and some (not necessarily all) of the internal coordinates, making it responsible for transitions between different internal states – *i.e.*, for reactions. Altogether, we can then write

$$\hat{H} = \hat{H}_a + \hat{H}_A + \hat{T}_{aA} + \hat{V}_{aA} + \hat{U}_{aA} \tag{22.4}$$

$$= \hat{H}_b + \hat{H}_B + \hat{T}_{bB} + \hat{V}_{bB} + \hat{U}_{bB} \ . \tag{22.5}$$

Note that, in general, the potentials $\hat{V}$ and $\hat{U}$ are not the same for the entrance and exit channels[2].

22.2 Scattering theory for reactions

The more rich structure of the Hamiltonian demands that we update some of the elements of our treatment of formal scattering. In the end, we will arrive at formulas which are rather intuitive generalizations of the T-matrix formalism we developed in Lecture 13. The following, therefore, is more likely to provide a reminder than an epiphany.

We have defined the T-matrix in Eq. (13.1), repeated here for convenience[3],

$$T_{\boldsymbol{k}'\boldsymbol{k}} = \left\langle \Phi_{\boldsymbol{k}'} \middle| \hat{\mathcal{V}} \middle| \Psi^{(+)}_{\boldsymbol{k}} \right\rangle \ ; \tag{22.6}$$

and then, using a separated form of the potential, we obtained the two-potential formulae, Eqs. (13.37) and (13.38), also repeated here

$$T_{\boldsymbol{k}'\boldsymbol{k}} = \left\langle \chi^{(-)}_{\boldsymbol{k}'} \middle| \hat{V} \middle| \Phi_{\boldsymbol{k}} \right\rangle + \left\langle \chi^{(-)}_{\boldsymbol{k}'} \middle| \hat{U} \middle| \Psi^{(+)}_{\boldsymbol{k}} \right\rangle \tag{22.7}$$

$$= \left\langle \Phi_{\boldsymbol{k}'} \middle| \hat{V} \middle| \chi^{(+)}_{\boldsymbol{k}} \right\rangle + \left\langle \chi^{(-)}_{\boldsymbol{k}'} \middle| \hat{U} \middle| \Psi^{(+)}_{\boldsymbol{k}} \right\rangle \ . \tag{22.8}$$

Changing the space in which we consider the process from the momentum to the channel space – where we denote the entrance and the exit channel by α and β, respectively – and assuming $\alpha \neq \beta$ leads to the vanishing of the first terms in both of the expressions above[4], so that we obtain

$$T_{\beta\alpha} = \left\langle \chi^{(-)}_{\beta} \middle| \hat{U} \middle| \Psi^{(+)}_{\alpha} \right\rangle \ . \tag{22.9}$$

We will see below that this result, here pulled out of thin air[5], is in fact quite well-motivated.

22.2.1 Channel Hamiltonians

To truly discuss reactions, let us now consider a full Hamiltonian $\hat{H}$ for the reaction $\alpha \to \beta$. This Hamiltonian can be partitioned in two ways,

$$\hat{H} = \hat{H}_\alpha + \hat{U}_\alpha = \hat{H}_\beta + \hat{U}_\beta \ , \tag{22.10}$$

where $\hat{H}_\alpha$ and $\hat{H}_\beta$ are *channel Hamiltonians* whose eigenstates describe motion restricted to the entrance and exit channels, respectively. For example, in the notation of Eq. (22.4), we would

[2] In the same way, we don't expect the Hamiltonians $\hat{H}_a$, $\hat{H}_A$ and $\hat{H}_b$, $\hat{H}_B$ to be the same – they simply correspond to different systems.

[3] Note that the potential entering this definition is the total potential $\hat{\mathcal{V}}$, Eq. (22.3).

[4] This is because $\hat{V}$ describes only elastic scattering and thus does not connect different internal states, *i.e.*, channels: since we consider $\alpha \neq \beta$, the corresponding matrix element is zero.

[5] Questions one could be asking include: What are channel states Ψ_α and χ_β? In which channel should one express the operator $\hat{U}$? Does this expression lead to a Lippmann–Schwinger-like relation for $T_{\beta\alpha}$? *etc.*

write $\hat{H}_\alpha = \hat{H}_a + \hat{H}_A + \hat{T}_{aA} + \hat{V}_{aA}$ and $U_\alpha = U_{aA}$, and similarly for $\hat{H}_\beta$. The channel Hamiltonians admit *distorted scattering states* satisfying

$$\left(\hat{H}_\alpha - E\right)\left|\xi_\alpha \Phi_\alpha \chi_\alpha^{(+)}\right\rangle = 0 \,, \tag{22.11}$$

$$\left(\hat{H}_\beta - E\right)\left|\xi_\beta \Phi_\beta \chi_\beta^{(+)}\right\rangle = 0 \,, \tag{22.12}$$

where ξ_α is a wavefunction for the internal state of the projectile, Φ_α is a wavefunction for the internal state of the target, and $\chi_\alpha^{(+)}$ is the distorted wave describing their relative motion in the presence of the potential $\hat{V}_{aA}$; analogous definitions apply for ξ_β, Φ_β, and $\chi_\beta^{(+)}$. The two decompositions, Eq. (22.10), correspond to different choices of asymptotic boundary conditions, and will lead to the *prior* and *post* forms of the T-matrix element.

Let us stop here for a moment. At the level of channel labels, the T-matrix element, Eq. (22.9), already suggests a matrix element of the transition interaction between an entrance-channel state and an exit-channel state. However, in a genuine reaction problem the same exact many-body Hamiltonian may be partitioned according to either the entrance or the exit channel, Eq. (22.10). We therefore need a general result that relates T-matrix elements constructed from two different Hamiltonian partitions of the same system. This is the purpose of the two-Hamiltonian identity which we derive below; once established, it yields the prior and post forms of the reaction T-matrix as special cases.

22.2.2 Two-Hamiltonian identity

Let us consider two Hamiltonians defined with respect to the same reference Hamiltonian $\hat{H}_0$, $\hat{H}_1 = H_0 + \hat{\mathcal{V}}_1$ and $\hat{H}_2 = \hat{H}_0 + \hat{\mathcal{V}}_2$, so that they can be treated within a common scattering framework (*i.e.*, a common Green's function $\hat{G}_0$[6]). Let us also consider free channel states labeled $|i\rangle$ ("initial") and $|f\rangle$ ("final"); these states define the asymptotic boundary conditions, where the corresponding scattering solutions describe waves that behave like $|i\rangle$ in the incoming region and like $|f\rangle$ in the outgoing region. We know that the eigenvectors of $\hat{H}_1$ and $\hat{H}_2$ must obey the free Lippmann–Schwinger equation, Eq. (12.3), so that we have

$$\left|\Psi_1^{(+)}\right\rangle = |i\rangle + \hat{G}_0^{(+)}\hat{\mathcal{V}}_1\left|\Psi_1^{(+)}\right\rangle \tag{22.13}$$

as well as

$$\left\langle\Psi_2^{(-)}\right| = \langle f| + \left\langle\Psi_2^{(-)}\right|\hat{\mathcal{V}}_2\hat{G}_0^{(+)}. \tag{22.14}$$

Here, $\left|\Psi_1^{(+)}\right\rangle$ is the scattering solution of $\hat{H}_1$ with incoming boundary condition in channel i, while $\left\langle\Psi_2^{(-)}\right|$ is the corresponding bra solution of $\hat{H}_2$ with outgoing boundary condition in channel f. With this, we can consider two T-matrix elements between the free entrance and exit channels, which from the definition are given by

$$\left\langle f\middle|\hat{T}_1\middle|i\right\rangle = \left\langle f\middle|\hat{\mathcal{V}}_1\middle|\Psi_1^{(+)}\right\rangle \tag{22.15}$$

and

$$\left\langle f\middle|\hat{T}_2\middle|i\right\rangle = \left\langle f\middle|\hat{\mathcal{V}}_2\middle|\Psi_2^{(+)}\right\rangle = \left\langle\Psi_2^{(-)}\middle|\hat{\mathcal{V}}_2\middle|i\right\rangle \,, \tag{22.16}$$

[6]Note that as defined here, $\hat{H}_0$ need not be a free particle Hamiltonian and therefore $\hat{G}_0$ need not be a free Green's function.

where the last equality follows from the corresponding representation of the T-matrix in terms of the outgoing scattering state.

To make contact between the two expressions, we now consider

$$\left\langle \Psi_2^{(-)} \middle| \left(\hat{\mathcal{V}}_1 - \hat{\mathcal{V}}_2\right) \middle| \Psi_1^{(+)} \right\rangle = \left\langle \Psi_2^{(-)} \middle| \hat{\mathcal{V}}_1 \middle| \Psi_1^{(+)} \right\rangle - \left\langle \Psi_2^{(-)} \middle| \hat{\mathcal{V}}_2 \middle| \Psi_1^{(+)} \right\rangle \ . \tag{22.17}$$

Let us start with the first term. Using the Lippmann–Schwinger equation for $\left\langle \Psi_2^{(-)} \right|$, Eq. (22.14), we can rewrite

$$\left\langle \Psi_2^{(-)} \middle| \hat{\mathcal{V}}_1 \middle| \Psi_1^{(+)} \right\rangle = \left\langle f \middle| \hat{\mathcal{V}}_1 \middle| \Psi_1^{(+)} \right\rangle + \left\langle \Psi_2^{(-)} \middle| \hat{\mathcal{V}}_2 \hat{G}_0^{(+)} \hat{\mathcal{V}}_1 \middle| \Psi_1^{(+)} \right\rangle \tag{22.18}$$

$$= \left\langle f \middle| \hat{T}_1 \middle| i \right\rangle + \left\langle \Psi_2^{(-)} \middle| \hat{\mathcal{V}}_2 \hat{G}_0^{(+)} \hat{\mathcal{V}}_1 \middle| \Psi_1^{(+)} \right\rangle \ , \tag{22.19}$$

where in the second equation we used the definition of $\left\langle f \middle| \hat{T}_1 \middle| i \right\rangle$, Eq. (22.15). Similarly, we can use the Lippmann–Schwinger equation for $\left| \Psi_1^{(+)} \right\rangle$, Eq. (22.13), to rewrite the second term in Eq. (22.17) as

$$\left\langle \Psi_2^{(-)} \middle| \hat{\mathcal{V}}_2 \middle| \Psi_1^{(+)} \right\rangle = \left\langle \Psi_2^{(-)} \middle| \hat{\mathcal{V}}_2 \middle| i \right\rangle + \left\langle \Psi_2^{(-)} \middle| \hat{\mathcal{V}}_2 \hat{G}_0^{(+)} \hat{\mathcal{V}}_1 \middle| \Psi_1^{(+)} \right\rangle \tag{22.20}$$

$$= \left\langle f \middle| \hat{T}_2 \middle| i \right\rangle + \left\langle \Psi_2^{(-)} \middle| \hat{\mathcal{V}}_2 \hat{G}_0^{(+)} \hat{\mathcal{V}}_1 \middle| \Psi_1^{(+)} \right\rangle \ , \tag{22.21}$$

where in the second equality we used the definition of $\left\langle f \middle| \hat{T}_2 \middle| i \right\rangle$, Eq. (22.16). The second terms in Eqs. (22.19) and (22.21) are the same, which allows us to rewrite the matrix element considered in Eq. (22.17) as

$$\left\langle \Psi_2^{(-)} \middle| \left(\hat{\mathcal{V}}_1 - \hat{\mathcal{V}}_2\right) \middle| \Psi_1^{(+)} \right\rangle = \left\langle f \middle| \hat{T}_1 \middle| i \right\rangle - \left\langle f \middle| \hat{T}_2 \middle| i \right\rangle \ , \tag{22.22}$$

which, using the fact that $\hat{\mathcal{V}}_1 - \hat{\mathcal{V}}_2 = \hat{H}_1 - \hat{H}_2$, can be immediately rewritten as

$$\left\langle f \middle| \hat{T}_1 \middle| i \right\rangle = \left\langle f \middle| \hat{T}_2 \middle| i \right\rangle + \left\langle \Psi_2^{(-)} \middle| \left(\hat{H}_1 - \hat{H}_2\right) \middle| \Psi_1^{(+)} \right\rangle \ . \tag{22.23}$$

The above equation is known as the *two-Hamiltonian identity*.

22.2.3 Application of the two-Hamiltonian identity to reactions

Let us apply the two-Hamiltonian identity, Eq. (22.23), to a *reaction* problem in which the system can be described in terms of two different channel decompositions, corresponding to the entrance channel $\alpha = \{\mathrm{a}, \mathrm{A}, \boldsymbol{k}_a\}$ and the exit channel $\beta = \{\mathrm{b}, \mathrm{B}, \boldsymbol{k}_b\}$, respectively. As shown in Eq. (22.10), the full Hamiltonian can be partitioned in two equivalent ways. Here, we take

$$\hat{H}_\alpha = \hat{H}_a + \hat{H}_A + \hat{T}_{aA} + \hat{V}_{aA} \ , \qquad \hat{U}_\alpha = \hat{U}_{aA} \tag{22.24}$$

and

$$\hat{H}_\beta = \hat{H}_b + \hat{H}_B + \hat{T}_{bB} + \hat{V}_{bB} \ , \qquad \hat{U}_\beta = \hat{U}_{bB} \ . \tag{22.25}$$

The Hamiltonians $\hat{H}_\alpha$ and $\hat{H}_\beta$ describe motion restricted to the entrance and exit channels, respectively, while $\hat{U}_{aA}$ and $\hat{U}_{bB}$ are responsible for transitions between channels.

To obtain the T-matrix element, we make use of the two-Hamiltonian identity, setting $\hat{H}_1 = \hat{H}_\alpha$ and $\hat{H}_2 = \hat{H}$. Since $\hat{H}_\alpha$ contains only the elastic interaction within the entrance channel, it cannot connect distinct initial and final channels, so that $\left\langle f\middle|\hat{T}_1\middle|i\right\rangle = 0$. The two-Hamiltonian identity then gives

$$\left\langle f\middle|\hat{T}_2\middle|i\right\rangle = \left\langle \Psi_{2f}^{(-)}\middle|\hat{U}_\alpha\middle|\Psi_{1i}^{(+)}\right\rangle \ . \tag{22.26}$$

At this point, we introduce the standard approximation that the eigenfunction of the Hamiltonian $\hat{H}_\alpha$ ("initial" wavefunction) can be written as a product of the internal projectile state ξ_a, the internal target state Φ_A, and the relative motion (distorted) wavefunction of a and A as a system,

$$\Psi_{1i}^{(+)} = \xi_a \Phi_A \chi_a^{(+)} \ . \tag{22.27}$$

Similarly connecting the "final" wavefunction to the exit channel (even if only acknowledging it with the subscripts), we get

$$\left\langle f\middle|\hat{T}_2\middle|i\right\rangle = \left\langle \Psi_{bB}^{(-)}\middle|\hat{U}_{aA}\middle|\xi_a\Phi_A\chi_a^{(+)}\right\rangle \ . \tag{22.28}$$

Alternatively, we can apply the two-Hamiltonian identity using the partition

$$\hat{H}_1 = \hat{H}_\beta \ , \qquad \hat{H}_2 = \hat{H} \ . \tag{22.29}$$

Proceeding in the same way, we then obtain

$$\left\langle f\middle|\hat{T}_2\middle|i\right\rangle = \left\langle \chi_b^{(-)}\xi_b\Phi_B\middle|\hat{U}_{bB}\middle|\Psi_{aA}^{(+)}\right\rangle \ . \tag{22.30}$$

The two expressions in Eqs. (22.28) and (22.30) are formally equivalent and are known as the *prior* and *post forms of the T-matrix element*, respectively. In a way, they can be thought of as generalizations of the two-potential formula, Eq. (13.38), to the description of reactions. Because a reaction is, by definition, not elastic[7], in contrast to the two potential formula, Eq. (13.38), the prior and post forms do *not* contain an "elastic term," *i.e.*, a term with respect to $\hat{V}$.

In an exact treatment, the prior and post forms of the T-matrix element, Eqs. (22.28) and (22.30) , yield identical results; however, in practical calculations (such as DWBA), one of the wavefunctions is typically approximated, and the equivalence is no longer guaranteed. As a result, the choice between prior and post forms is guided by convenience: one uses the form in which the *interaction operator* $\hat{U}$ acts on the more accurately described channel wavefunction. In particular, the prior form is often preferred when the entrance-channel distorted wave is well controlled, while the post form is advantageous when the exit-channel description is more reliable. As such, these forms play a central role in approximate reaction theories, such as the DWBA, where they provide alternative starting points for constructing the transition amplitude.

22.3 Alternative derivation of the two-Hamiltonian identity

This section derives Eq. (22.23) in a different, longer, and altogether not terribly enlightening way, even though it's nice to see that one can get the same result using mostly only wave calculus. Learn

[7]Which is a property we explicitly used to set $\left\langle f\middle|\hat{T}_1\middle|i\right\rangle = \left\langle f\middle|\hat{T}_2\middle|i\right\rangle = 0$ above, leading to the final form of Eqs. (22.28) and (22.30).

from my mistakes and skip this section. I leave it here for completeness and for those who are not happy with the derivation in Sec. 22.2.2 – I predict you will find new appreciation for it soon...

Let $\hat{H}_1$ and $\hat{H}_2$ be two possible Hamiltonians for a given quantum system such that $\hat{H}_1$ and $\hat{H}_2$ have the same kinetic energy, but their potential energies may be different[8], and consequently the spectrum of asymptotic channels (and their thresholds) need not coincide[9]. Let us denote stationary solutions of $\hat{H}_1$ and $\hat{H}_2$ at some energy E as Ψ_1 and Ψ_2, respectively. Crucially, certain channels may be open to collisions governed by $\hat{H}_1$ and closed to collisions governed by $\hat{H}_2$, and *vice versa*[10].

When considering multi-channel scattering, each set of initial conditions a can be associated with a free channel state Φ_a (in the simplest case, a plane wave so that $\Phi_a = e^{i\boldsymbol{k}_a\cdot\boldsymbol{r}_\alpha}$) and two stationary scattering solutions, $\Psi_a^{(+)}$ and $\Psi_a^{(-)}$; here, the choice of Φ_a together with the outgoing (+), or incoming (-) boundary condition uniquely determines the corresponding solution $\Psi_a^{(\pm)}$. Assuming the simplest form for Φ_a, $\Psi_a^{(+)}$ is a solution having an ($e^{i\boldsymbol{k}_a\cdot\boldsymbol{r}_a}$ + outgoing wave) asymptotic behavior in the entrance channel and a purely outgoing behavior in all other open channels[11], while $\Psi_a^{(-)}$ is a solution having an ($e^{i\boldsymbol{k}_a\cdot\boldsymbol{r}_a}$ + incoming wave) asymptotic behavior in the entrance channel and a purely incoming behavior in all other open channels[12]. That is, for a given boundary condition $a = (\alpha, \boldsymbol{k}_a)$[13], we are dealing with

$$\hat{H}\Psi_a^{(\pm)} = E\Psi_a^{(\pm)} \ , \tag{22.31}$$

and for any open channel γ we have

$$\Psi_a^{(\pm)} \sim \begin{cases} e^{i\boldsymbol{k}_a\cdot\boldsymbol{r}_\alpha} + f_{\alpha a}^{(\pm)}(\Omega_\alpha)\frac{e^{\pm ik_a r_\alpha}}{r_\alpha} & r_{\alpha\to\infty} \ , \quad \gamma = \alpha \\ f_{\gamma a}^{(\pm)}(\Omega_\gamma)\frac{e^{\pm ik_c r_\gamma}}{r_\gamma} & r_{\gamma\to\infty} \ , \quad \gamma \neq \alpha \end{cases} . \tag{22.32}$$

Let us assume that channel β is open to collisions governed by $\hat{H}_2$. If this is the case, then there exists an incoming wave solution $\Psi_{2b}^{(-)}$[14], corresponding to the initial conditions $b \equiv (\beta, \boldsymbol{k}_b)$, which satisfies

$$\hat{H}_2\Psi_{2b}^{(-)} = E\Psi_{2b}^{(-)} \ . \tag{22.33}$$

For any open channel γ we then have

$$\Psi_{2b}^{(-)} \sim \begin{cases} e^{i\boldsymbol{k}_b\cdot\boldsymbol{r}_\beta} + f_{2\beta b}^{(-)}(\Omega_\beta)\frac{e^{-ik_b r_\beta}}{r_\beta} & r_\beta \to \infty, \quad \gamma = \beta \\ f_{2\gamma b}^{(-)}(\Omega_\gamma)\frac{e^{-ik_c r_\gamma}}{r_\gamma} & r_\gamma \to \infty, \quad \gamma \neq \beta \end{cases} . \tag{22.34}$$

[8] We assume that any difference between the potentials goes asymptotically to zero faster than $1/r$.

[9] This can happen if, *e.g.*, the two Hamiltonians correspond to different internal structures.

[10] This can happen if, *e.g.*, different internal structures of $\hat{H}_1$ and $\hat{H}_2$ solutions lead to different threshold energies relative to E.

[11] If the exit channel is different than the entrance channel, $b \neq a$, the boundary condition forbids incoming flux in channel b, so tgat only outgoing waves may appear.

[12] An incoming solution is the *time-reversed* counterpart of a scattered wave: while $\Psi_a^{(+)}$ describes a beam coming in and the scattering producing outgoing spherical waves, which is what experiments realize, $\Psi_a^{(-)}$ describes spherical waves converging from infinity and producing an outgoing plane wave. Physically, the second option never takes place because it would require arranging sources at infinity in all directions in just the right way, but *mathematically* it is a valid solution and, moreover, it is essential for formulating reaction amplitudes.

[13] Note that the boundary condition a includes the symbol denoting the entrance channel α *and* the incoming wave vector labeled by a, $\boldsymbol{k}_a$; this may initially feel like an unnecessary use of multiple labels for the same thing, however, note that a given channel α may correspond to various values of $\boldsymbol{k}_a$, with each of these values corresponding to a different initial state (*i.e.*, boundary condition) in the same entrance channel. Following this logic, we will use Greek letters to describe channels and the "corresponding" Roman letters to describe states, *e.g.*, $b = (\beta, \boldsymbol{k}_b)$.

[14] Note that now we put an additional label on states, denoting whether they are solutions of $\hat{H}_1$ or $\hat{H}_2$.

i.e., $\Psi_{2b}^{(-)}$ is the incoming wave solution of the scattering problem governed by $\hat{H}_2$, describing either elastic scattering (top) or a transition to the open channel δ (bottom).

Let us now consider the Hamiltonian eigenvalue equation, Eq. (22.31), for $\hat{H} = \hat{H}_1$ and the case of outgoing waves with initial conditions $a = (\alpha, \boldsymbol{k}_a)$, corresponding to the solution $\Psi_{1a}^{(+)}$, *i.e.*,

$$\hat{H}_1 \Psi_{1a}^{(+)} = E \Psi_{1a}^{(+)} \ . \tag{22.35}$$

We can multiply both sides of this eigenvalue equation by $\Psi_{2b}^{(-)*}$ from the left,

$$\Psi_{2b}^{(-)*} \left(\hat{H}_1 \Psi_{1a}^{(+)} \right) = E \Psi_{2b}^{(-)*} \Psi_{1a}^{(+)} \ . \tag{22.36}$$

We can also consider the complex conjugate of the eigenvalue equation for $\hat{H}_2$ with an incoming boundary condition, Eq. (22.33), which explicitly is $\left(\hat{H}_2 \Psi_{2b}^{(-)} \right)^* = E \Psi_{2b}^{(-)*}$. Multiplying this equation by $\Psi_{1a}^{(+)}$ from the right yields

$$\left(\hat{H}_2 \Psi_{2b}^{(-)} \right)^* \Psi_{1a}^{(+)} = E \Psi_{2b}^{(-)*} \Psi_{1a}^{(+)} \ . \tag{22.37}$$

Subtracting the latter from the former leads to

$$\Psi_{2b}^{(-)*} \left(\hat{H}_1 \Psi_{1a}^{(+)} \right) - \left(\hat{H}_2 \Psi_{2b}^{(-)} \right)^* \Psi_{1a}^{(+)} = 0 \ . \tag{22.38}$$

Now, we have assumed that the kinetic parts of the two Hamiltonians $\hat{H}_1$ and $\hat{H}_2$ are equal, *i.e.*, that we have $\hat{H}_1 = \hat{H}_0 + \hat{V}_1$ and $\hat{H}_2 = \hat{H}_0 + \hat{V}_2$ with the same kinetic operator $\hat{H}_0$. We can therefore rewrite Eq. (22.38) as[15]

$$\left[\Psi_{2b}^{(-)*} \left(\hat{H}_0 \Psi_{1a}^{(+)} \right) - \left(\hat{H}_0 \Psi_{2b}^{(-)} \right)^* \Psi_{1a}^{(+)} \right] + \Psi_{2b}^{(-)*} \left(\hat{V}_1 - \hat{V}_2 \right) \Psi_{1a}^{(+)} = 0 \ . \tag{22.39}$$

We can always perform an integration over all coordinates, which we jointly denote by $\int d\tau$; here, $\int d\tau$ goes over relative coordinates as well as over all internal coordinates (spins, intrinsic wavefunctions) *in each channel*[16]. This yields

$$\int d\tau \ \left[\Psi_{2b}^{(-)*} \left(\hat{H}_0 \Psi_{1a}^{(+)} \right) - \left(\hat{H}_0 \Psi_{2b}^{(-)} \right)^* \Psi_{1a}^{(+)} \right] + \int d\tau \ \Psi_{2b}^{(-)*} \left(\hat{V}_1 - \hat{V}_2 \right) \Psi_{1a}^{(+)} = 0 \ . \tag{22.40}$$

From the definition, we have

$$\int d\tau \ \Phi^*(\tau) \Psi(\tau) \equiv \langle \Phi | \Psi \rangle \ , \tag{22.41}$$

which implies

$$\int d\tau \ \Phi^*(\tau) \left(\hat{H} \Psi(\tau) \right) \equiv \left\langle \Phi \middle| \hat{H} \Psi \right\rangle \equiv \left\langle \Phi \middle| \hat{H} \middle| \Psi \right\rangle \ , \tag{22.42}$$

allowing us to rewrite the second term in Eq. (22.40),

$$\int d\tau \ \left[\Psi_{2b}^{(-)*} \left(\hat{H}_0 \Psi_{1a}^{(+)} \right) - \left(\hat{H}_0 \Psi_{2b}^{(-)} \right)^* \Psi_{1a}^{(+)} \right] + \left\langle \Psi_{2b}^{(-)} \middle| \hat{V}_1 - \hat{V}_2 \middle| \Psi_{1a}^{(+)} \right\rangle = 0 \ . \tag{22.43}$$

[15] Here we explicitly assume that $\hat{V}_1$ and $\hat{V}_2$ are real.

[16] In other words, $\int d\tau$ is not a single integral but a sum of integrals, $\sum_\gamma \int d\tau_\gamma$.

In the first term, we can invoke the explicit form of $\hat{H}_0$ in each channel γ, yielding[17]

$$-\sum_\gamma \frac{1}{2\mu_\gamma}\int d^3r_\gamma \left[\Psi_{2b}^{(-)*}\left(\nabla_\gamma^2\Psi_{1a}^{(+)}\right) - \left(\nabla_\gamma^2\Psi_{2b}^{(-)}\right)^*\Psi_{1a}^{(+)}\right] + \left\langle \Psi_{2b}^{(-)}\middle|\hat{V}_1 - \hat{V}_2\middle|\Psi_{1a}^{(+)}\right\rangle = 0\ . \tag{22.44}$$

It follows from the Green's theorem that

$$\int d^3r\ \left(\phi^*\nabla^2\psi - \psi\nabla^2\phi^*\right) = \oint d\boldsymbol{S}\cdot\left(\phi^*\boldsymbol{\nabla}\psi - \psi\boldsymbol{\nabla}\phi^*\right)\ , \tag{22.45}$$

which allows us to covert the volume integral involving the kinetic-energy operator into a surface integral, yielding

$$\left\langle \Psi_{2b}^{(-)}\middle|\hat{V}_1 - \hat{V}_2\middle|\Psi_{1a}^{(+)}\right\rangle = \sum_\gamma \frac{1}{2\mu_\gamma}\lim_{r_\gamma\to\infty}\oint d\boldsymbol{S}_\gamma\ \cdot\left[\Psi_{2b}^{(-)*}\boldsymbol{\nabla}_\gamma\Psi_{1a}^{(+)} - \Psi_{1a}^{(+)}\boldsymbol{\nabla}_\gamma\Psi_{2b}^{(-)*}\right]\ . \tag{22.46}$$

Here, the limit $r_\gamma\to\infty$ appears because the scattering problem is defined in all space, so the boundary of the integration volume is taken to infinity in each open channel. Again using the fact that the kinetic parts of the Hamiltonians are identical, we can rewrite the above equation as

$$\left\langle \Psi_{2b}^{(-)}\middle|\hat{H}_1 - \hat{H}_2\middle|\Psi_{1a}^{(+)}\right\rangle = \sum_\gamma \frac{1}{2\mu_\gamma}\lim_{r_\gamma\to\infty}\oint d\boldsymbol{S}_\gamma\ \cdot\left[\Psi_{2b}^{(-)*}\boldsymbol{\nabla}_\gamma\Psi_{1a}^{(+)} - \Psi_{1a}^{(+)}\boldsymbol{\nabla}_\gamma\Psi_{2b}^{(-)*}\right]\ . \tag{22.47}$$

For a sphere (which we can always take as the surface of choice) with radius r_γ, we have $d\boldsymbol{S}_\gamma = \hat{\boldsymbol{r}}_\gamma r_\gamma^2 d\Omega_\gamma$, which means that the divergence reduces to

$$d\boldsymbol{S}_\gamma\cdot\boldsymbol{\nabla}_\gamma = r_\gamma^2 d\Omega_\gamma\ \hat{\boldsymbol{r}}_\gamma\cdot\boldsymbol{\nabla} = r_\gamma^2 d\Omega_\gamma\frac{\partial}{\partial r}\ , \tag{22.48}$$

leaving us with

$$\left\langle \Psi_{2b}^{(-)}\middle|\hat{H}_1 - \hat{H}_2\middle|\Psi_{1a}^{(+)}\right\rangle = \sum_\gamma \frac{1}{2\mu_\gamma}\lim_{r_\gamma\to\infty}\oint d\Omega_\gamma\ r_\gamma^2\left[\Psi_{2b}^{(-)*}\frac{\partial}{\partial r_\gamma}\Psi_{1a}^{(+)} - \Psi_{1a}^{(+)}\frac{\partial}{\partial r_\gamma}\Psi_{2b}^{(-)*}\right]\ . \tag{22.49}$$

[17] Explicitly, because we have multiple (distinct) channels, the wavefunction decomposes as

$$\Psi(\tau) = \sum_\gamma \phi_\gamma(\xi)\chi_\gamma(\boldsymbol{r}_\gamma)\ ,$$

where $\phi_\gamma(\xi)$ is the wavefunction corresponding to the internal degrees of freedom, jointly denoted with ξ, while $\chi_\gamma(\boldsymbol{r}_\gamma)$ describes the center-of-mass motion of the channel γ. With this, the integration in Eq. (22.43) is really a sum of integrals; indeed, looking at the first term we see that

$$\begin{aligned}\int d\tau\ \Psi_{2b}^{(-)*}\left(\hat{H}_0\Psi_{1a}^{(+)}\right) &= \int d\tau\ \sum_\gamma \phi_\gamma^*(\xi)\chi_{2b\gamma}^{(-)^*}(\boldsymbol{r})\left(\hat{H}_0\sum_{\gamma'}\phi_{\gamma'}(\xi')\chi_{1a\gamma'}^{(+)}(\boldsymbol{r}')\right)\\ &= \int d\xi d\boldsymbol{r}\ \sum_{\gamma,\gamma'}\phi_\gamma^*(\xi)\chi_{2b\gamma}^{(-)^*}(\boldsymbol{r})\left(\phi_{\gamma'}(\xi')\hat{H}_{0,\gamma'}\chi_{1a\gamma'}^{(+)}(\boldsymbol{r}')\right)\ ,\end{aligned}$$

where in the second equality we wrote the integral measure explicitly and we used the fact that $\hat{H}_0\sim\sum_\gamma\nabla_\gamma^2\sim\sum_\gamma H_{0,\gamma}$ is diagonal in the channel space (it does not mix different γ's). Since the internal states are orthogonal, $\int d\xi\ \phi_\gamma^*(\xi)\phi_{\gamma'}(\xi') = \delta_{\gamma\gamma'}$, the double sum collapses, yielding

$$\int d\tau\ \Psi_{2b}^{(-)*}\left(\hat{H}_0\Psi_{1a}^{(+)}\right) = \sum_\gamma\int d\boldsymbol{r}\ \chi_{2b\gamma}^{(-)^*}(\boldsymbol{r})\left(\hat{H}_{0,\gamma'}\chi_{1a\gamma'}^{(+)}(\boldsymbol{r}')\right)\ .$$

The same steps can be applied to the second term in Eq. (22.43).

Because of the limit $r_\gamma \to \infty$, we can evaluate the surface terms using the asymptotic forms of the wavefunctions, which are explicitly given by Eqs. (22.32) and (22.34). The two cases of elastic and inelastic scattering, explicitly considered in Eqs. (22.32) and (22.34), can be written jointly with the help of the Kronecker delta, yielding[18]

$$\Psi^{(+)}_{1a} \sim \delta_{\gamma\alpha} e^{i\boldsymbol{k}_a\cdot\boldsymbol{r}_\alpha} + f^{(+)}_{1\gamma a}(\Omega_\gamma)\frac{e^{ik_\gamma r_\gamma}}{r_\gamma} \tag{22.50}$$

and

$$\Psi^{(-)}_{2b} \sim \delta_{\gamma\beta} e^{i\boldsymbol{k}_b\cdot\boldsymbol{r}_\beta} + f^{(-)}_{2\gamma b}(\Omega_\gamma)\frac{e^{-ik_\gamma r_\gamma}}{r_\gamma}\ . \tag{22.51}$$

With this, we can see that the terms in Eq. (22.49) will generally have the structure

$$(\text{plane}\times\nabla\text{plane})\ ,\ \ (\text{plane}\times\nabla\text{spherical})\ ,\ \ (\text{spherical}\times\nabla\text{plane})\ ,\ \ (\text{spherical}\times\nabla\text{spherical})\ . \tag{22.52}$$

Let's consider these cases one by one. For $\gamma \neq \alpha, \beta$, $\Psi^{(+)}_{1a}$ and $\Psi^{(-)*}_{2b}$ are purely spherical,

$$\Psi^{(+)}_{1a} \sim f^{(+)}_{1\gamma a}(\Omega_\gamma)\frac{e^{ik_\gamma r_\gamma}}{r_\gamma} \quad \text{and} \quad \Psi^{(-)*}_{2b} \sim f^{(-)*}_{2\gamma b}(\Omega_\gamma)\frac{e^{ik_\gamma r_\gamma}}{r_\gamma}\ . \tag{22.53}$$

Since the dependence on r_γ in these two functions is exactly the same, we can see that the term in the square bracket in Eq. (22.49) will yield zero – thus, we get no contribution from $\gamma \neq \alpha, \beta$.

Next, let us consider the plane-plane contribution, which can exist only if $\gamma = \alpha = \beta$. In that case, we have

$$\Psi^{(+)}_{1a} \sim e^{i\boldsymbol{k}_\gamma\cdot\boldsymbol{r}_\gamma} \quad \text{and} \quad \Psi^{(-)*}_{2b} \sim e^{-i\boldsymbol{k}_\gamma\cdot\boldsymbol{r}_\gamma}\ . \tag{22.54}$$

the term in the square bracket in Eq. (22.49) will look like

$$e^{-i\boldsymbol{k}_\gamma\cdot\boldsymbol{r}_\gamma}\frac{\partial}{\partial r}e^{i\boldsymbol{k}_\gamma\cdot\boldsymbol{r}_\gamma} - e^{i\boldsymbol{k}_\gamma\cdot\boldsymbol{r}_\gamma}\frac{\partial}{\partial r}e^{-i\boldsymbol{k}_\gamma\cdot\boldsymbol{r}_\gamma} = 2ik_\gamma\cos\theta\ . \tag{22.55}$$

Since $\int d\Omega\ \cos\theta = 0$, the contribution from $\gamma = \alpha = \beta$ also vanishes.

We are then left with two mixed terms, forcing $\gamma = \alpha \neq \beta$ or $\gamma = \beta \neq \alpha$. For the β channel, *i.e.*, $\gamma = \beta \neq \alpha$, Eqs. (22.50) and (22.51) make it evident that $\Psi^{(+)}_{1a}$ reduces to the spherical part, and as a consequence (as we've shown above) the only part of $\Psi^{(-)}_{2b}$ that contributes is the plane wave part. Thus the relevant contribution from Eq. (22.49) becomes[19]

$$I_\beta = \frac{1}{2\mu_\beta}\frac{1}{(2\pi)^3}\lim_{r_\beta\to\infty}\oint d\Omega_\beta\ r_\beta^2\left[e^{-i\boldsymbol{k}_b\cdot\boldsymbol{r}_\beta}\frac{\partial\left(f^{(+)}_{1\beta a}(\Omega_\beta)\frac{e^{ik_b r_\beta}}{r_\beta}\right)}{\partial r_\beta} - f^{(+)}_{1\beta a}(\Omega_\beta)\frac{e^{ik_b r_\beta}}{r_\beta}\frac{\partial e^{-i\boldsymbol{k}_b\cdot\boldsymbol{r}_\beta}}{\partial r_\beta}\right]\ . \tag{22.56}$$

Using

$$\frac{\partial}{\partial r_\beta}\frac{e^{ik_b r_\beta}}{r_\beta} = \left(ik_b - \frac{1}{r_\beta}\right)\frac{e^{ik_b r_\beta}}{r_\beta} \tag{22.57}$$

[18] Here we also adjust subscripts on Eq. (22.32) to correspond to the outgoing solution in a system governed by $\hat{H}_1$.

[19] Here, unlike in the other two cases above, we finally invoke the normalization of both the plane and scattered contribution. Indeed, the plane wave $e^{i\boldsymbol{k}\cdot\boldsymbol{r}}$ comes with a normalization factor of $(2\pi)^{-3/2}$, see Eq. (12.39), and so does the scattered wave, see Eq. (12.43).

and

$$\frac{\partial}{\partial r_\beta} e^{-i\boldsymbol{k}_b\cdot\boldsymbol{r}_\beta} = -ik_b\cos\theta e^{-i\boldsymbol{k}_b\cdot\boldsymbol{r}_\beta} \ , \tag{22.58}$$

we get

$$I_\beta = \frac{1}{2\mu_\beta}\frac{1}{(2\pi)^3}\lim_{r_\beta\to\infty}\oint d\Omega_\beta\ r_\beta^2\ f^{(+)}_{1\beta a}(\Omega_\beta)\left[ik_b(1+\cos\theta)-\frac{1}{r_\beta}\right]\frac{e^{ik_b r_\beta(1-\cos\theta)}}{r_\beta} \ , \tag{22.59}$$

where θ is the angle between $\boldsymbol{r}_\beta$ and $\boldsymbol{k}_b$. For $r_\beta\to\infty$, this term oscillates rapidly with the exception of $\theta = 0$. As a result, only a small neighborhood of the forward[20] direction contributes, so that one can approximate $f^{(+)}_{1\beta a}(\Omega_\beta)\approx f^{(+)}_{1\beta a}(\Omega_b)$ and take it outside the integral, yielding

$$I_\beta = \frac{f^{(+)}_{1\beta a}(\Omega_b)}{2\mu_\beta(2\pi)^3}\lim_{r_\beta\to\infty}\oint d\Omega_\beta\ \left[ik_b(1+\cos\theta)-\frac{1}{r_\beta}\right] r_\beta e^{ik_b r_\beta(1-\cos\theta)} \ . \tag{22.60}$$

However, since only $\theta\approx 0$ matters, we can write

$$1-\cos\theta\approx\frac{\theta^2}{2} \qquad \text{and} \qquad d\Omega\approx 2\pi\theta d\theta \ , \tag{22.61}$$

while the limit $r_\beta\to 0$ further allows us to write, to leading order.

$$ik_b(1+\cos\theta)-\frac{1}{r_\beta}\approx 2ik_b \ . \tag{22.62}$$

Putting everything together, we obtain

$$I_\beta = \frac{f^{(+)}_{1\beta a}(\Omega_b)}{2\mu_\beta(2\pi)^3}\lim_{r_\beta\to\infty} 2ik_b r_\beta\int 2\pi\theta d\theta\ e^{ik_b r_\beta\frac{\theta^2}{2}} \ . \tag{22.63}$$

Substituting

$$u=\frac{k_b r_\beta\theta^2}{2} \qquad \Rightarrow \qquad du = k_b r_\beta\theta\ d\theta \qquad \Rightarrow \qquad \theta\ d\theta = \frac{du}{k_b r_\beta} \tag{22.64}$$

immediately leads to[21]

$$I_\beta = \frac{f^{(+)}_{1\beta a}(\Omega_b)}{\mu_\beta(2\pi)^3}\lim_{r_\beta\to\infty} 2\pi i\int_0^\infty du\ e^{iu} \ . \tag{22.65}$$

Lastly, we compute the remaining integral using the old trick with a regulator[22], *i.e.*, by considering

$$\int_0^\infty du\ e^{iu} = \lim_{\epsilon\to 0^+}\int_0^\infty du\ e^{iu}e^{-\epsilon u} = \lim_{\epsilon\to 0^+}\int_0^\infty du\ e^{(i-\epsilon)u} = \lim_{\epsilon\to 0^+}\left[\frac{e^{(i-\epsilon)u}}{i-\epsilon}\right]_0^\infty = -\frac{1}{i} \ , \tag{22.66}$$

[20] With respect to $\boldsymbol{k}_b$.

[21] The limits of the integral come from the fact that at $u(\theta=0)=0$, while $u(\theta=\pi)=k_b r_\beta\pi^2/2$ becomes infinite in the limit $r_\beta\to\infty$.

[22] Which we previously used in Lectures 11 and 14.

so that finally

$$I_\beta = -\frac{2\pi f^{(+)}_{1\beta a}(\Omega_b)}{\mu_\beta (2\pi)^3} = -\frac{f^{(+)}_{1\beta a}(\Omega_b)}{4\pi^2 \mu_\beta} \ . \tag{22.67}$$

Computing the contribution due to the α channel is entirely analogous, with the difference that the highly oscillatory term is $e^{ik_a r_\alpha (1+\cos\theta)}$, so that the integral localizes at $\theta = \pi$, *i.e.*, in the direction opposite to the incident beam. As a result, we obtain

$$I_\alpha = \frac{f^{(-)*}_{2\alpha b}(-\Omega_a)}{4\pi^2 \mu_\alpha} \ . \tag{22.68}$$

With this, Eq. (22.49) becomes

$$\left\langle \Psi^{(-)}_{2b} \middle| \hat{H}_1 - \hat{H}_2 \middle| \Psi^{(+)}_{1a} \right\rangle = \frac{f^{(-)*}_{2\alpha b}(-\Omega_a)}{4\pi^2 \mu_\alpha} - \frac{2\pi f^{(+)}_{1\beta a}(\Omega_b)}{4\pi^2 \mu_\beta} \ . \tag{22.69}$$

Using Eq. (13.13), we can express the above equation in therms of T-matrix elements, obtaining

$$\left\langle b \middle| \hat{T}_1 \middle| a \right\rangle = \left\langle b \middle| \hat{T}_2 \middle| a \right\rangle + \left\langle \Psi^{(-)}_{2b} \middle| \hat{H}_1 - \hat{H}_2 \middle| \Psi^{(+)}_{1a} \right\rangle \ . \tag{22.70}$$

Lecture sources: In this lecture, Secs. 22.1 and 22.2 are based on Jackson [4], while Sec. 22.3 is based on Messiah [3].

Lecture 23

Direct reactions III

Prerequisites: Lectures 13, 21, 22.
Guiding question: ***How does structure enter direct reaction calculations?***

23.1 Distorted wave Born approximation

In the last lecture, we have obtained two exact and equivalent expressions for T-matrix elements[1] for a reaction process, Eqs. (22.28) and (22.30), repeated here for convenience,

$$\left\langle f\middle|\hat{T}\middle|i\right\rangle = \left\langle \Psi^{(-)}_{bB}\middle|\hat{U}_{aA}\middle|\xi_a\Phi_A\chi^{(+)}_a\right\rangle \tag{23.1}$$

and

$$\left\langle f\middle|\hat{T}\middle|i\right\rangle = \left\langle \chi^{(-)}_b\xi_b\Phi_B\middle|\hat{U}_{bB}\middle|\Psi^{(+)}_{aA}\right\rangle \ . \tag{23.2}$$

The exact scattering states $\Psi^{(+)}_{aA}$ and $\Psi^{(-)}_{bB}$, invoked in the expressions above, are scattering solutions of the full Hamiltonian $\hat{H}$ that includes couplings between all channels, *i.e.*, allows transitions between different configurations such as elastic scattering, inelastic excitation (A $\rightarrow$ A*), or transfer and breakup channels. As a result, the exact wavefunction contains components in many channels simultaneously and describes the full multichannel dynamics. This is not tractable in practice.

Therefore, we replace $\Psi^{(+)}_{aA}$ and $\Psi^{(-)}_{bB}$ by eigenfunctions of the corresponding channel Hamiltonians $\hat{H}_\alpha$ and $\hat{H}_\beta$, which retain only elastic interactions within a given partition and generate the distorted waves in each channel. In this approximation, each channel is treated independently: for example, an entrance-channel state a+A propagates without dynamically coupling to b+B or A* during the scattering, and such couplings are accounted for only through the potential $\hat{U}$, often also referred to as the *transition operator*.

We further assume that these channel eigenfunctions factorize according to

$$\Psi^{(+)}_{aA} \rightarrow \chi^{(+)}_a\xi_a\Phi_A \quad \text{and} \quad \Psi^{(-)}_{bB} \rightarrow \chi^{(-)}_b\xi_b\Phi_B \ , \tag{23.3}$$

where χ depends on the relative projectile-target coordinates, while ξ and Φ depend on the internal coordinates of the projectile and target, respectively. Applied to the prior and post forms, Eqs. (22.28) and (22.30), this yields

$$\left\langle f\middle|\hat{T}\middle|i\right\rangle = \left\langle \chi^{(-)}_b\xi_b\Phi_B\middle|\hat{U}_{aA}\middle|\chi^{(+)}_a\xi_a\Phi_A\right\rangle \tag{23.4}$$

[1] Which, as we know from Eq. (13.13), carry information equivalent to that contained in a scattering amplitude.

and

$$\left\langle f\middle|\hat{T}\middle|i\right\rangle = \left\langle \chi_b^{(-)}\xi_b\Phi_B\middle|\hat{U}_{bB}\middle|\chi_a^{(+)}\xi_a\Phi_A\right\rangle \ . \tag{23.5}$$

Let us stop here for a moment and evaluate what has happened. In the exact theory, the operators $\hat{U}_{aA}$ and $\hat{U}_{bB}$ represent equivalent forms of the same transition operator; as a result, the prior and post forms, Eqs. (22.28) and (22.30), are truly equivalent. However, once the scattering states are approximated by channel eigenfunctions, this equivalence is no longer guaranteed. In other words, the prior and post forms will, in general, lead to different results. Naturally, these differences should be small if approximating the full wavefunctions by the factorized expressions in Eq. (23.3) is justified.

Since now the post and prior forms are *not* equivalent, we need to choose between them. In practice, one adopts the form in which the interaction operator acts on the more accurately described channel. Denoting the chosen transition interaction with $\hat{U}$, this then finally leads to the standard *DWBA expression for the reaction T-matrix element*[2],

$$\left\langle f\middle|\hat{T}\middle|i\right\rangle = \left\langle \chi_b^{(-)}\xi_b\Phi_B\middle|\hat{U}\middle|\chi_a^{(+)}\xi_a\Phi_A\right\rangle \ . \tag{23.6}$$

We have more or less handwaved the above result, but it can also be obtained formally. Indeed, we know from Lecture 13 that the Lippmann–Schwinger equation can be written in terms of the distorted wavefunctions, Eq. (13.26). Employing a factorization of the full wavefunction as in Eq. (23.3), that Lippmann–Schwinger equation can then be written as an infinite sum of the form

$$\Psi_i^{(+)} = \left(\sum_{n=0}^{\infty}\left(\hat{G}^{(+)}\hat{U}\right)^n\right)\chi_i^{(+)}\xi_i\Phi_i \ , \tag{23.7}$$

where $\hat{G}^{(+)}$ is the Green function for the Hamiltonian $\hat{H} = \hat{T}+\hat{V}$ and the distorted waves $\chi_i^{(+)}$ take into account the influence of the potential $\hat{V}$. This leads to a series

$$T_{fi} = \left\langle \chi_f^{(-)}\xi_f\Phi_f\middle|\hat{U}\middle|\Psi_i^{(+)}\right\rangle \tag{23.8}$$

$$= \left\langle \chi_f^{(-)}\xi_f\Phi_f\middle|\hat{U}\middle|\chi_i^{(+)}\xi_i\Phi_i\right\rangle + \left\langle \chi_f^{(-)}\Phi_f\middle|\hat{U}\hat{G}^{(+)}\hat{U}\middle|\chi_i^{(+)}\xi_i\Phi_i\right\rangle + \dots \ , \tag{23.9}$$

where the first term is the DWBA contribution. The second and higher-order terms describe *multiple scattering processes* in which the potential acts more than once and the system passes through intermediate states.

23.2 Structure form factors

Equation (23.6) can still be further simplified. Let us denote the relative projectile–target coordinate by $\boldsymbol{r}$ and all internal coordinates (*e.g.*, spin degrees of freedom of the projectile and target, *etc.*) by σ. We insert two resolutions of identity in these variables, which yields

$$\left\langle f\middle|\hat{T}\middle|i\right\rangle = \left\langle \chi_b^{(-)}\xi_b\Phi_B\middle|\left[\sum_\sigma\int d^3r\,|\boldsymbol{r},\sigma\rangle\langle\boldsymbol{r},\sigma|\right]\hat{U}\left[\sum_{\sigma'}\int d^3r'\,|\boldsymbol{r}',\sigma'\rangle\langle\boldsymbol{r}',\sigma'|\right]\middle|\xi_a\Phi_A\chi_a^{(+)}\right\rangle \tag{23.10}$$

$$= \sum_{\sigma,\sigma'}\int d^3r\int d^3r'\,\left[\chi_b^{(-)}(\boldsymbol{r}_b)\xi_b(\sigma)\Phi_B(\sigma)\right]^*\,U(\boldsymbol{r},\sigma;\boldsymbol{r}',\sigma')\;\xi_a(\sigma')\Phi_A(\sigma')\chi_a^{(+)}(\boldsymbol{r}_a) \ . \tag{23.11}$$

[2] If you need a reminder on DWBA, see Sec. 13.2.2.

If we further assume that U is local, $U(\boldsymbol{r},\sigma;\boldsymbol{r}',\sigma') = U(\boldsymbol{r},\sigma)\delta^3(\boldsymbol{r}-\boldsymbol{r}')\delta_{\sigma\sigma'}$, we obtain

$$\left\langle f\middle|\hat{T}\middle|i\right\rangle = \sum_\sigma \int d^3r \, \left[\chi_b^{(-)}(\boldsymbol{r}_b)\xi_b(\sigma)\Phi_B(\sigma)\right]^* \, U(\boldsymbol{r},\sigma) \, \xi_a(\sigma)\Phi_A(\sigma)\chi_a^{(+)}(\boldsymbol{r}_a) \, . \tag{23.12}$$

Because nuclear forces are short-range, we can further make a reasonable assumption that $\boldsymbol{r}_a \approx \boldsymbol{r}_b \approx \boldsymbol{r}$. With this, we can rearrange the above equation to get

$$\left\langle f\middle|\hat{T}\middle|i\right\rangle = \int d^3r \, \chi_b^{(-)*}(\boldsymbol{r})\Big[\sum_\sigma \xi_b^*(\sigma)\Phi_B^*(\sigma) \, U(\boldsymbol{r},\sigma) \, \xi_a(\sigma)\Phi_A(\sigma)\Big]\chi_a^{(+)}(\boldsymbol{r}) \, . \tag{23.13}$$

It is then customary to define the *form factor*

$$F(\boldsymbol{r}) \equiv \sum_\sigma \xi_b^*(\sigma)\Phi_B^*(\sigma) \, U(\boldsymbol{r},\sigma) \, \xi_a(\sigma)\Phi_A(\sigma) \, , \tag{23.14}$$

so that we have

$$T^{(\mathrm{DWBA})} = \int d^3r \, \chi_b^{(-)*}(\boldsymbol{r})F(\boldsymbol{r})\chi_a^{(+)}(\boldsymbol{r}) \, . \tag{23.15}$$

In this approach, the form factor $F(\boldsymbol{r})$ contains all effects due to nuclear structure. This separation is the practical strength of the DWBA formulation: the distorted waves describe the reaction dynamics and can be constrained by elastic scattering, while the form factor contains the nuclear-structure information. In particular, by comparing the resulting non-elastic cross sections with experimental data, one can test the assumed structure model entering $F(\boldsymbol{r})$.

23.2.1 Clebsch-Gordan coefficients

As discussed before (see, *e.g.*, Sec. 13.2.2), the distorted waves can often be computed directly and tested against measurements of the corresponding *elastic* scattering cross sections. At the same time, various models of nuclear structure can be tested by constructing the corresponding form factors $F(\boldsymbol{r})$. Still, computing the T-matrix element, Eq. (23.15), is not trivial.

Often, to make the problem more tractable, one performs a partial wave expansion of the distorted waves,

$$\chi_a^{(+)}(\boldsymbol{r}) = \sum_{l_a m_a} \frac{u_{l_a}^{(+)}(r)}{r} Y_{l_a m_a}(\theta,\phi) \quad \text{and} \quad \chi_b^{(-)}(\boldsymbol{r}) = \sum_{l_b m_b} \frac{u_{l_b}^{(-)}(r)}{r} Y_{l_b m_b}(\theta,\phi) \, , \tag{23.16}$$

and a *multipole expansion* of the form factor (or, equivalently, the transition operator U, since the form factor is defined as its matrix element between internal states),

$$F(\boldsymbol{r}) = \sum_{\lambda\mu} F_{\lambda\mu}(r)Y_{\lambda\mu}(\theta,\phi) \, . \tag{23.17}$$

Crucially, the multipole rank λ determines the angular momentum transfer between initial and final states.

Indeed, inserting the above expansions into the DWBA T-matrix element, Eq. (23.15), yields

$$T^{(\mathrm{DWBA})} = \sum_{l_b m_b}\sum_{\lambda\mu}\sum_{l_a m_a} \int dr \, u_{l_b}^{(-)*}(r)F_{\lambda\mu}(r)u_{l_a}^{(+)}(r) \int d\Omega \, Y_{l_b m_b}^*(\theta,\phi)Y_{\lambda\mu}(\theta,\phi)Y_{l_a m_a}(\theta,\phi) \, . \tag{23.18}$$

To understand what this expression is telling us, we consider the product $Y_{\lambda\mu}(\theta,\phi)Y_{l_a m_a}(\theta,\phi)$, which can itself be expanded in spherical harmonics,

$$Y_{\lambda\mu}(\theta,\phi)Y_{l_a m_a}(\theta,\phi) = \sum_{LM} C_{LM} Y_{LM}(\theta,\phi) \ . \tag{23.19}$$

We obtain the expansion coefficients C_{LM} using the fact that spherical harmonics are orthogonal, $\int d\Omega \ Y^*_{L'M'} Y_{LM} = \delta_{LL'}\delta_{MM'}$, so that multiplying Eq. (23.19) by $Y^*_{l_b m_b}(\theta,\phi)$ and integrating over the solid angle yields

$$C_{l_b m_b} = \int d\Omega \ Y^*_{l_b m_b}(\theta,\phi) Y_{\lambda\mu}(\theta,\phi) Y_{l_a m_a}(\theta,\phi) \ . \tag{23.20}$$

Thus, the integral over the solid angle in the spherical harmonic expansion of the T-matrix, Eq. (23.18), is just the coefficient of the $Y_{l_b m_b}(\theta,\phi)$ harmonic in the spherical harmonic expansion of the product $Y_{\lambda\mu}(\theta,\phi)Y_{l_a m_a}(\theta,\phi)$. In other words, the coefficient $C_{l_b m_b}$ is the *overlap* of the spherical harmonic $Y_{l_b m_b}(\theta,\phi)$ with the product $Y_{\lambda\mu}(\theta,\phi)Y_{l_a m_a}(\theta,\phi)$.

The allowed values of M then follow directly from the ϕ-dependence of spherical harmonics, explicitly given by $Y_{lm}(\theta,\phi) = N_{lm} P_l^m(\cos\theta) e^{im\phi}$, where N_{lm} is a normalization constant. From this form, it is clear that under a rotation by an arbitrary angle φ, $\phi \to \phi + \varphi$, the product of spherical harmonics transforms as

$$Y_{\lambda\mu}(\theta,\phi)Y_{l_a m_a}(\theta,\phi) \to e^{i(m_a+\mu)\varphi} Y_{\lambda\mu}(\theta,\phi)Y_{l_a m_a}(\theta,\phi) \ . \tag{23.21}$$

On the other hand, in the expansion of this product in spherical harmonics, Eq. (23.19), under the same rotation each contribution $Y_{LM}(\theta,\phi)$ transforms as

$$Y_{LM}(\theta,\phi) \to e^{iM\varphi} Y_{LM}(\theta,\phi) \ . \tag{23.22}$$

Thus, for the expansion to be consistent with the behavior of the product under rotations, only terms with $M = m_a + \mu$ can be non-zero.

To determine the allowed values of L, we note that the product $Y_{\lambda\mu}(\theta,\phi)Y_{l_a m_a}(\theta,\phi)$ carries the angular structure of two angular momenta, λ and l_a. The largest possible total angular momentum arises when these are aligned, $L_{\max} = \lambda + l_a$, while the smallest possible value arises when they are anti-aligned, $L_{\min} = |\lambda - l_a|$. Quantum-mechanically, L can take each integer value between these extremes, so that $|\lambda - l_a| \le L \le \lambda + l_a$.

Therefore, the expansion coefficients $C_{l_b m_b}$ are only non-zero for m_b and l_b satisfying

$$m_b = \mu + m_a \quad \text{and} \quad |\lambda - l_a| \le l_b \le \lambda + l_a \ . \tag{23.23}$$

This statement can be expressed more formally. The solid angle integral in the expression for the T-matrix element, Eq. (23.18), which we have shown is equivalent to the expansion coefficient $C_{l_b m_b}$, Eq. (23.20), has a known closed form

$$C_{l_b m_b} = (-1)^{m_b} \sqrt{\frac{(2l_b+1)(2\lambda+1)(2l_a+1)}{4\pi}} \begin{pmatrix} l_b & \lambda & l_a \\ 0 & 0 & 0 \end{pmatrix} \begin{pmatrix} l_b & \lambda & l_a \\ -m_b & \mu & m_a \end{pmatrix} \ , \tag{23.24}$$

where the quantities in the parentheses are *Wigner $3j$-symbols*. The Wigner $3j$-symbols are, in turn, related to the *Clebsch-Gordan coefficients* through

$$\begin{pmatrix} l_1 & l_2 & l_3 \\ m_1 & m_2 & m_3 \end{pmatrix} \propto \langle l_1, m_1, l_2, m_2 | l_3, -m_3 \rangle \ , \tag{23.25}$$

where $\langle l_1, m_1, l_2, m_2 | l_3, -m_3 \rangle$ expresses the overlap between the uncoupled and coupled angular momentum bases for the same Hilbert space. As a result, we have

$$C_{l_b m_b} \propto \langle l_a, 0, \lambda, 0 | l_b, 0 \rangle \, \langle l_a, m_a, \lambda, \mu | l_b, m_b \rangle \ , \tag{23.26}$$

where the Clebsch-Gordan coefficients vanish whenever the selection rules, Eq. (23.23), are *not* satisfied.

Physically, this result means that the multipole component $F_{\lambda\mu}$ of the form factor carries angular momentum λ and angular momentum projection μ. Therefore, it can only connect an incoming partial wave characterized by (l_a, m_a) to outgoing partial waves (l_b, m_b) allowed by the angular-momentum addition, Eq. (23.23). Thus, the angular structure of the transition operator determines which partial waves are coupled in the reaction: a monopole form factor, $\lambda = 0$, can only connect $l_a = l_b$ and $m_a = m_b$, while a quadrupole form factor, $\lambda = 2$, can connect l_a to $l_b \in \{l_a - 2, l_a, l_a + 2\}$ (provided that $l_b \geq 0$). In this way, the angular dependence of $F(\boldsymbol{r})$ encodes the angular momentum transferred to the internal nuclear degrees of freedom.

Finally, while the integration over the solid angle can be performed analytically, as above, the remaining radial integrals are then often evaluated numerically.

23.3 Plane wave Born approximation

Further simplification of Eq. (23.15) can be obtained by employing plane waves

$$\chi_a^{(+)}(\boldsymbol{r}) = e^{i\boldsymbol{k}_a \cdot \boldsymbol{r}} \quad \text{and} \quad \chi_b^{(-)*} \to e^{-i\boldsymbol{k}_b \cdot \boldsymbol{r}} \ , \tag{23.27}$$

which yields the *plane wave Born approximation (PWBA)*, often simply referred to as the *Born approximation (BA)*

$$T^{(\mathrm{BA})} = \int d^3r \ e^{i\boldsymbol{q}\cdot\boldsymbol{r}}(\boldsymbol{r}) F(\boldsymbol{r}) \ , \tag{23.28}$$

where we introduced the momentum transfer $\boldsymbol{q} = \boldsymbol{k}_a - \boldsymbol{k}_b$. In this case, the partial wave expansion allows us to write

$$T^{(\mathrm{BA})} = \sum_{l=0}^{\infty} i^l \sqrt{4\pi(2l+1)} \int dr \ r^2 \ j_l(qr) \int d\Omega \ Y_{l0}(\theta, \phi) F(\boldsymbol{r}) \ . \tag{23.29}$$

As before, in general $F(\boldsymbol{r})$ is not spherically symmetric given that various internal functions entering $F(\boldsymbol{r})$, Eq. (23.14), may describe nuclei with non-zero spins. Indeed, using Eq. (23.17), we obtain

$$T^{(\mathrm{BA})} = \sum_{l=0}^{\infty} i^l \sqrt{4\pi(2l+1)} \int dr \ r^2 \ j_l(qr) \sum_{\lambda\mu} F_{\lambda\mu}(r) \int d\Omega \ Y_{l0}(\theta, \phi) Y_{\lambda\mu}(\theta, \phi) \tag{23.30}$$

$$= \sum_{l=0}^{\infty} i^l \sqrt{4\pi(2l+1)} \int dr \ r^2 \ j_l(qr) \sum_{\lambda\mu} F_{\lambda\mu}(r) \ \delta_{0\mu}\delta_{l\lambda} \tag{23.31}$$

$$= \sum_{l=0}^{\infty} i^l \sqrt{4\pi(2l+1)} \int dr \ r^2 \ j_l(qr) \ F_{l0}(r) \ . \tag{23.32}$$

where in the second equality we used the fact that $Y_{l0}^*(\theta, \phi) = Y_{l0}(\theta, \phi)$ to invoke the orthogonality relation for spherical harmonics. Usually, only one or two expansion coefficients F_{l0} are non-negligible.

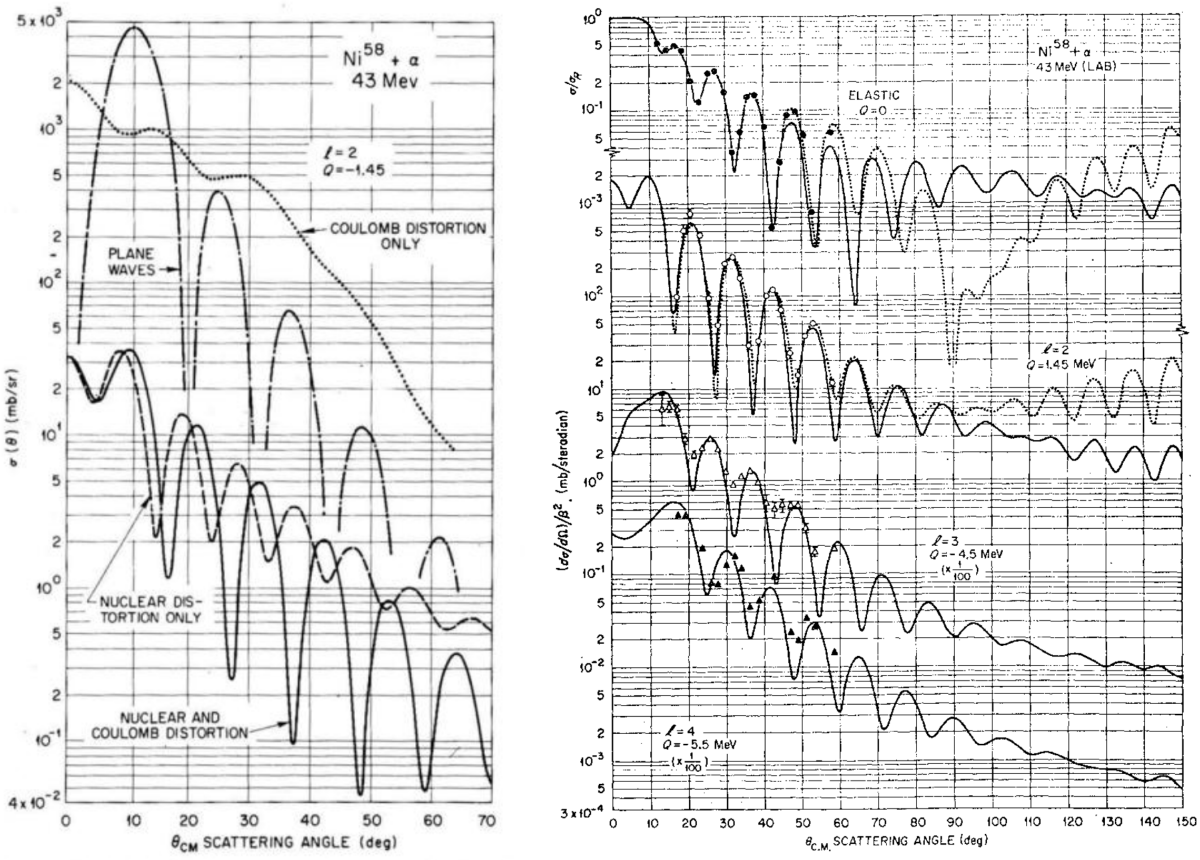

Figure 23.1: *Left:* Comparison of inelastic cross sections predicted using PWBA and DWBA with only Coulomb, only nuclear, and both Coulomb and nuclear distorted waves. Figure from Ref. [7]. *Right:* Predicted and experimentally measured angular distributions for scattering of α-particles on ^{68}Ni at $E_{\text{kin}} = 43$ MeV. Figure from Ref. [44].

For example, in inelastic α-particle scattering from even nuclei, the target, projectile, and ejectile all have zero spin, so that the momentum transfer $\Delta L = l$ is equal to the intrinsic angular momentum of the target after the collision I_B.

In Fig. 23.1, the left panel shows a comparison of inelastic cross sections predicted using PWBA and DWBA with only Coulomb, only nuclear, and both Coulomb and nuclear distorted waves. The right panel in the same figure shows a comparison of DWBA calculations and experimental data for α-particles scattering off ^{68}Ni at $E_{\text{kin}} = 43$ MeV, where the nuclear form factors have been computed using a rotational and vibrational model of the nucleus [44][3].

23.4 Diffractive behavior

One can further simplify the PWBA expression for the T-matrix element. To this end, we argue that while the use of plane waves may be justified outside the nucleus, the wavefunctions should become zero inside the nucleus (reflecting absorption). On the other hand, we can also argue that the form factor $F(\boldsymbol{r})$, which reflects the properties of the nucleus, should diminish rapidly beyond the nucleus.

[3]We note that Ref. [44] goes into considerable detail in varying the theoretical model, showing the research importance of the kind of tests that we used in solving Problem 3 of Homework 4.

As a result, we adopt the *surface approximation*, in which we assume that only contributions at the nuclear surface, $r \approx R$, contribute significantly. In that way, we can rewrite the partial-wave expansion of the T-matrix element in the Born approximation, Eq. (23.32), as

$$T^{(\mathrm{BA})} \approx \sum_l C_l j_l(qR) \ , \tag{23.33}$$

where the constants C_l determine the magnitude of contributions from different values of l. If only one partial wave contributes, then – by Eqs. (6.68) and (13.13) – the differential cross section is simply proportional to the square of the corresponding Bessel function,

$$\frac{d\sigma}{d\Omega} \propto \left[j_l(qR)\right]^2 \ . \tag{23.34}$$

In the above expression, the angular dependence enters through q, which for an inelastic collision satisfies

$$q^2 = k_\alpha^2 + k_\beta^2 - 2k_\alpha k_\beta \cos\theta \ . \tag{23.35}$$

Given the oscillatory nature of the Bessel functions, it is clear that the Born-approximation cross section, Eq. (23.34), will display an oscillatory, diffraction-like pattern, similarly to the basic classical treatment of Butler, see Figs. 21.2 and 23.1.

Lecture sources: This lecture is based on Jackson [4] and Satchler [7].

Lecture 24

Direct reactions IV

Prerequisites: Lectures 21, 23.
Guiding question: ***How do we actually compute reactions?***

24.1 Direct inelastic scattering

If we neglect the possibility of exchanging particles between the projectile and the target, the emitted particle is the same as the projectile. In that case, $\boldsymbol{r}_a = \boldsymbol{r}_b$ in the DWBA T-matrix element, Eq. (23.12), without any approximation, and the rest of the treatment presented in the previous lecture follows. Here, we discuss how the form of the potential $\hat{U}$ (or, equivalently, the underlying nuclear structure) can be inferred from the measurements.

It is known that states most strongly excited by inelastic scattering involve a collective motion, such as rotational or vibrational modes[1]. As a result, we can use a potential that treats the nucleus *collectively*, which often means a potential based on the local density of nucleons ρ. For example, if the interaction of the projectile with a single target nucleon can be well-described by a potential $u(r_{tp})$, where $r_{tp} = |\boldsymbol{r}_t - \boldsymbol{r}_p|$ is the distance between them, then the overall potential can be written in the coordinate space as

$$U(\boldsymbol{r}_p) = \int d\boldsymbol{r}_t \; \rho(\boldsymbol{r}_t) u(r_{tp}) \; . \tag{24.1}$$

This reflects the fact that the projectile interacts with the *entire nuclear density distribution*, rather than with individual nucleons.

Consequently, if the target density distribution is not spherical, then neither is the potential. This means that we can consider the potential U as composed of two parts,

$$U(\boldsymbol{r}) = U_0(\boldsymbol{r}) + \Delta U(\boldsymbol{r}) \; , \tag{24.2}$$

where U_0 is a spherically symmetric part of the potential, while ΔU is a deformed remainder.

If we restrict ourselves to surface effects, then a convenient way to obtain such a potential separated into a symmetric and deformed part is to postulate that $U(\boldsymbol{r})$ depends on a surface radius parameter R, $U(\boldsymbol{r}, R)$. A non-spherical nuclear surface can be described by

$$R(\theta, \phi) = R_0 + \sum_{lm} \delta_{lm} Y_{lm}(\theta, \phi) \; , \tag{24.3}$$

[1] Intuitively, this is because the transition amplitude is naturally dominated by coherent contributions from many nucleons as opposed to isolated single-particle motion.

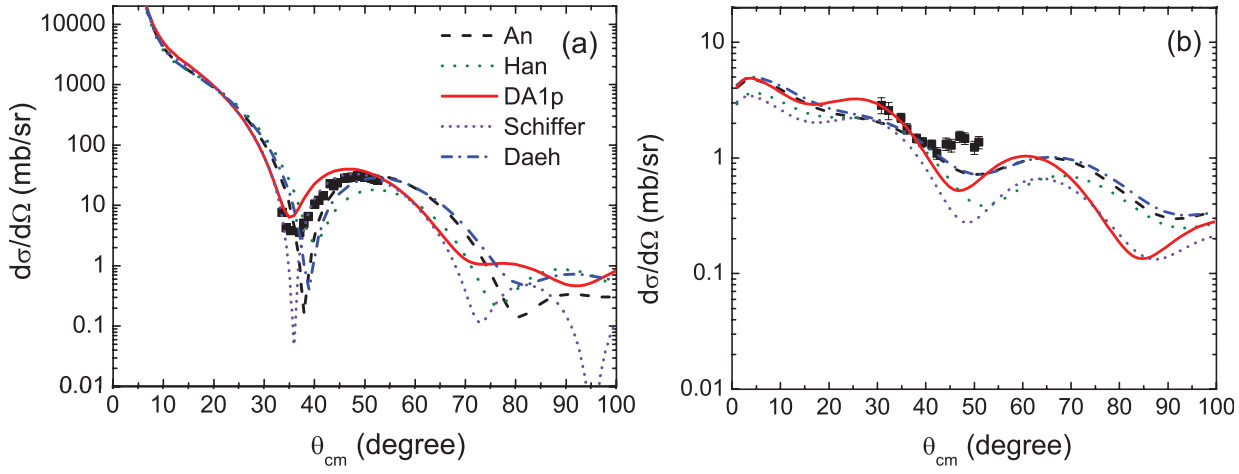

Figure 24.1: Comparison of experimental (black points) and calculated (lines) differential cross sections for the deuteron elastic scattering (*left*) and inelastic scattering to the first excited state of ^{15}C (*right*). Figure from Ref. [45].

where δ_{lm} are known as *deformation lengths* and $Y_{lm}(\theta,\phi)$ are, naturally, the spherical harmonics. Expand the potential $U(\boldsymbol{r},R)$ around R_0, we then obtain

$$U(\boldsymbol{r},R) = U(\boldsymbol{r},R_0) + \left.\frac{\partial U(\boldsymbol{r},R)}{\partial R}\right|_{R=R_0} \big(R-R_0\big) + \dots \tag{24.4}$$

$$= U(\boldsymbol{r},R_0) + \left.\frac{\partial U(\boldsymbol{r},R)}{\partial R}\right|_{R=R_0} \sum_{lm} \delta_{lm} Y_{lm}(\theta,\phi) + \dots \ , \tag{24.5}$$

where in the second equality we used the form of the nuclear deformation, Eq. (24.3). The above equation is a first-order expansion in the deformation which, compared to Eq. (24.2), naturally leads to equating

$$U_0(\boldsymbol{r}) = U(\boldsymbol{r},R_0) \quad \text{and} \quad \Delta U(\boldsymbol{r}) = \left.\frac{\partial U(\boldsymbol{r},R)}{\partial R}\right|_{R=R_0} \sum_{lm} \delta_{lm} Y_{lm}(\theta,\phi) \ . \tag{24.6}$$

Note that in the above, while be tied our reasoning to non-sphericity of the target nucleus, R_0 should be understood as the characteristic radius of the potential, not the nuclear radius.

Since U_0 is spherically symmetric, it corresponds to the $l=0$ component in the multipole expansion of $U(\boldsymbol{r})$. As is evident from our discussion of the Clebsch-Gordan coefficients[2], Sec. 23.2.1, the $l=0$ component contributes when there is no angular momentum transfer, *i.e.*, for elastic scattering. Consequently, the spherically symmetric potential U_0 governs elastic scattering[3], while ΔU drives inelastic transitions. Moreover, since the radial factor $\partial U(\boldsymbol{r},R)/\partial R\big|_{R=R_0}$ in Eq. (24.6) is the same for all (l,m), it can be constrained by elastic scattering.

The remaining unknown, δ_{lm}, characterizes the given transition and can be extracted from inelastic scattering measurements. For example, in the case of a rotational nucleus, $\delta_{lm} = R_0\beta_l$, where β_l is the 2^l-pole deformation of the potential shape. Because δ_{lm} enters as a multiplicative constant,

[2]To be precise, there we discussed the multipole expansion of the form factor rather than the potential, but the conclusions are all the same.

[3]Note that this does *not* mean that the elastic scattering cross section has no angular structure, as this can still come from interference of various partial waves in the incident and scattered wavefunctions.

it controls the *magnitude* of the measured inelastic cross-section and can be found from comparisons to results of, *e.g.*, PWBA or DWBA calculations.

This is illustrated in the study by J. Chen *et al.*, probing the quadrupole transition strength of ^{15}C with deuteron inelastic scattering [45]. In that paper, the matter deformation parameter β_d was extracted by requiring that the inelastic scattering differential cross section satisfies

$$\left(\frac{d\sigma}{d\Omega}\right)_{\rm exp} = \beta_d^2 \left(\frac{d\sigma}{d\Omega}\right)_{\rm DWBA} , \tag{24.7}$$

which in turn can be used to extract the deformation parameter *via* $\beta_d = \delta_d/(r_0 A^{1/3})$. With $r_0 = 1.2$ fm, the authors extracted the value $\beta_d = 0.29(3)$ using the optical potential marked in the left panel of Fig. 24.1 as "DA1p," corresponding to $\delta_d = 0.93(1)$ fm.

24.2 Transfer reactions

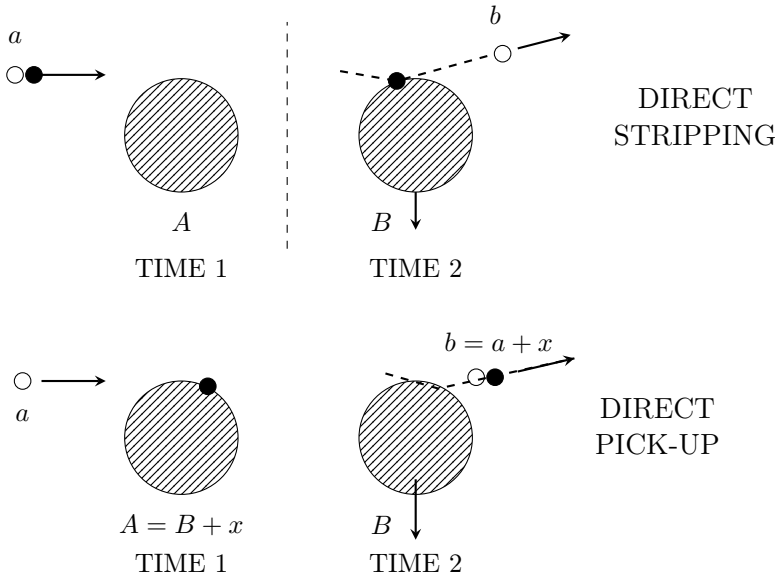

Figure 24.2: Sketch of a stripping (*top*) and a pick-up (*bottom*) reaction. Inspired by a similar figure in Ref. [7].

The canonical transfer reactions are deuteron stripping reactions, (d, p) and (d, n), and their inverse pick-up reactions, (p, d) and (n, d). A typical situation is sketched in Fig. 24.2, where in the top panel a peripheral collision between an impinging deuteron and the target leaves one of the deuteron's nucleons bound to the target, while the other nucleon proceeds in the forward direction. This picture suggests two physical features of such reactions: 1) the differential cross section is strongly forward-peaked, and 2) the angular momentum ΔL transferred to the nucleus is that carried by the captured nucleon. Similarly, a pick-up reaction, sketched in the bottom panel of the same figure, takes place when an impinging nucleon captures a proton or a neutron during a peripheral collision.

24.2.1 DWBA amplitude

Let us identify elements entering the DWBA expression for the T-matrix element, Eq. (23.11), in the case of a pick-up reaction[4]. To fix the attention, let us consider the (p, d) reaction. The interaction responsible for the transfer is the neutron-proton interaction, $U_{np}(\boldsymbol{r}_{\boldsymbol{\Delta}})$, where $\boldsymbol{r}_{\boldsymbol{\Delta}} = \boldsymbol{r}_n - \boldsymbol{r}_p$ is the relative coordinate of the neutron-proton system. The wavefunction for the projectile's internal degrees of freedom, $\xi_a(\sigma)$, simply describes the proton's spin, which we will neglect in this discussion together with the spin of the deuteron. The wavefunction for the ejectile's internal degrees of freedom describes the deuteron in its ground state,

$$\xi_b(\sigma) \to \psi_d(\boldsymbol{r}_\Delta) \ , \tag{24.8}$$

where $\boldsymbol{r}_{\boldsymbol{\Delta}}$ plays the role of the internal coordinate of the neutron-proton system, whose center-of-mass motion in turn depends on the coordinate $\boldsymbol{r}_d = (\boldsymbol{r}_p + \boldsymbol{r}_n)/2$, so that $\chi_b^{(-)} \to \chi_d^{(-)}(\boldsymbol{r}_d)$. The wavefunction of the target, $\Phi_A(\sigma)$, can in general be complicated. However, in the special case in which the target consists of a doubly-closed core plus a neutron (*i.e.*, in which the target is a special case of a *halo nucleus*), it can be argued that $\Phi_A(\sigma)$ can be well-approximated by

$$\Phi_A(\sigma) = \Phi_B(\sigma)\phi_n(\boldsymbol{r}_n) \ , \tag{24.9}$$

where $\Phi_B(\sigma)$ is the wavefunction of the residual nucleus and ϕ_n is a single-particle wavefunction of the transferred neutron. This form allows one to immediately integrate[5] over the internal degrees of freedom σ, yielding

$$\sum_{\sigma,\sigma'} \Phi_B^*(\sigma)\Phi_A(\sigma') = \sum_{\sigma,\sigma'} \Phi_B^*(\sigma)\Phi_B(\sigma')\phi_n(\boldsymbol{r}_n) = \sum_{\sigma} \delta(\sigma-\sigma')\phi_n(\boldsymbol{r}_n) \ , \tag{24.10}$$

where we used the orthogonality of the core states $\Phi_B(\sigma)$. With these identifications, the DWBA T-matrix element, Eq. (23.11), becomes[6]

$$T^{(\mathrm{DWBA})} = \int d^3r_n \int d^3r_p \ \chi_d^{(-)*}(\boldsymbol{r}_d)\psi_d^*(\boldsymbol{r}_\Delta) \ U_{np}(\boldsymbol{r}_\Delta,\sigma) \ \phi_n(\boldsymbol{r}_n)\chi_p^{(+)}(\boldsymbol{r}_p) \ . \tag{24.11}$$

24.2.2 PWBA amplitude

We can further simplify the above result by considering the Born approximation. In this limit, the transition amplitude becomes

$$T^{(\mathrm{BA})} = \int d^3r_n \int d^3r_p \ e^{-i\boldsymbol{k}_d\cdot\boldsymbol{r}_d}\psi_d^*(\boldsymbol{r}_\Delta) \ U_{np}(\boldsymbol{r}_\Delta,\sigma) \ \phi_n(\boldsymbol{r}_n)e^{i\boldsymbol{k}_p\cdot\boldsymbol{r}_p} \ . \tag{24.12}$$

Noting that $\boldsymbol{r}_p = \boldsymbol{r}_n - \boldsymbol{r}_\Delta$ and $\boldsymbol{r}_d = \boldsymbol{r}_n - \frac{1}{2}\boldsymbol{r}_\Delta$ then allows us to write

$$T^{(\mathrm{BA})} = \int d^3r_n \int d^3r_p \ e^{-i\boldsymbol{k}_d\cdot\left(\boldsymbol{r}_n-\frac{1}{2}\boldsymbol{r}_\Delta\right)}\psi_d^*(\boldsymbol{r}_\Delta) \ U_{np}(\boldsymbol{r}_\Delta,\sigma) \ \phi_n(\boldsymbol{r}_n)e^{i\boldsymbol{k}_p\cdot\left(\boldsymbol{r}_n-\boldsymbol{r}_\Delta\right)} \tag{24.13}$$

$$= \int d^3r_n \int d^3r_p \ e^{-i\boldsymbol{k}_d\cdot\boldsymbol{r}_n}e^{i\boldsymbol{k}_d\cdot\frac{1}{2}\boldsymbol{r}_\Delta}\psi_d^*(\boldsymbol{r}_\Delta) \ U_{np}(\boldsymbol{r}_\Delta,\sigma) \ \phi_n(\boldsymbol{r}_n)e^{i\boldsymbol{k}_p\cdot\boldsymbol{r}_n}e^{-i\boldsymbol{k}_p\cdot\boldsymbol{r}_\Delta} \tag{24.14}$$

$$= \int d^3r_n e^{-i\boldsymbol{q}\cdot\boldsymbol{r}_n}\phi_n(\boldsymbol{r}_n) \int d^3r_\Delta \ e^{i\boldsymbol{K}\cdot\boldsymbol{r}_\Delta}\psi_d^*(\boldsymbol{r}_\Delta) \ U_{np}(\boldsymbol{r}_\Delta,\sigma) \ , \tag{24.15}$$

[4] Because of time-reversal invariance, the reverse reactions are characterized by the same transition amplitudes.

[5] That is, sum.

[6] Note that we have implicitly chosen to work in the *prior form*: the coordinates are those of "free" proton and neutron, the potential describes the interaction between th proton and neutron, *etc.*

where $\boldsymbol{q} = \boldsymbol{k}_d - \boldsymbol{k}_p$ and $\boldsymbol{K} = \frac{1}{2}\boldsymbol{k}_d - \boldsymbol{k}_p$. This result can be understood as follows: from momentum conservation, if the deuteron is to have the momentum $\boldsymbol{k}_d$ and the incoming proton has the momentum $\boldsymbol{k}_p$, then the picked-up neutron must supply the momentum $\boldsymbol{q}$. In the outgoing deuteron, the proton and the neutron each carry the center-of-mass momentum $\frac{1}{2}\boldsymbol{k}_d$. Thus the proton momentum changes by $\Delta\boldsymbol{k}_p = \frac{1}{2}\boldsymbol{k}_d - \boldsymbol{k}_p = \boldsymbol{K}$, while the neutron momentum changes by $\Delta\boldsymbol{k}_n = \frac{1}{2}\boldsymbol{k}_d - \boldsymbol{q} = -\frac{1}{2}\boldsymbol{k}_d + \boldsymbol{k}_p = -\boldsymbol{K}$. This momentum difference is accounted for by the internal motion of the deuteron, described by $\psi_d(\boldsymbol{r}_\Delta)$, and momentum transfer between the neutron and the proton due to their mutual interaction U_{np}, both of which appear in the finite-range facto

$$\int d^3r_\Delta \; e^{i\boldsymbol{K}\cdot\boldsymbol{r}_\Delta}\psi_d^*(\boldsymbol{r}_\Delta)\; U_{np}(\boldsymbol{r}_\Delta,\sigma) \tag{24.16}$$

in Eq. (24.15). Now, for the process to be possible, one must be able to find a neutron with momentum $\boldsymbol{q}$. Given the neutron's wavefunction in the coordinate space, $\phi_n(\boldsymbol{r}_n)$, the probability to find a neutron with momentum $\boldsymbol{q}$ is given by the Fourier transform of $\phi_n(\boldsymbol{r}_n)$, *i.e.*, the first integral occurring in Eq. (24.15),

$$\int d^3r_n e^{-i\boldsymbol{q}\cdot\boldsymbol{r}_n}\phi_n(\boldsymbol{r}_n) \; . \tag{24.17}$$

Since the neutron-proton potential is short-range, one often introduces the *zero-range approximation*,

$$V_{np}(\boldsymbol{r}_p - \boldsymbol{r}_n)\psi_d^*(\boldsymbol{r}_\Delta) \approx D_0\delta^{(3)}(\boldsymbol{r}_p - \boldsymbol{r}_n) \; , \tag{24.18}$$

which reduces the finite-range factor to

$$\int d^3r_\Delta \; e^{i\boldsymbol{K}\cdot\boldsymbol{r}_\Delta} \; D_0\delta^{(3)}(\boldsymbol{r}_\Delta) = D_0 \; , \tag{24.19}$$

and the Born amplitude becomes

$$T^{(\mathrm{BA})} \approx D_0 \int d^3r_n \; e^{-i\boldsymbol{q}\cdot\boldsymbol{r}_n}\phi_n(\boldsymbol{r}_n) \; . \tag{24.20}$$

Thus, in the zero-range approximation, the neutron wavefunction plays the role of the form factor, see Eq. (23.28).

24.2.3 Angular momentum

Assuming that the neutron wavefunction $\phi_n(\boldsymbol{r}_n)$ is characterized by a definite angular momentum L, it can be always written as

$$\phi_n(\boldsymbol{r}_n) = u_{nL}(r_n)Y_{LM}(\theta_n,\phi_n) \; . \tag{24.21}$$

Then, as we have done in Sec. 23.3, we can expand the plane wave in the zero-range BA T-matrix element, Eq. (24.20), in partial waves, by means of which we immediately obtain

$$T^{(\mathrm{BA})} \approx D_0 \sum_{l=0}^{\infty}(-i)^l\sqrt{4\pi(2l+1)}\int dr_n \; r_n^2 \; j_l(qr_n)u_{nL}(r_n)\int d\Omega \; Y_{l0}(\theta,\phi)Y_{LM}(\theta_n,\phi_n) \tag{24.22}$$

$$\propto \int dr_n \; r_n^2 \; j_L(qr_n)u_{nL}(r_n) \; , \tag{24.23}$$

where we used the orthonormality of the spherical harmonics. This result highlights that the angular momentum transfer characterizing the reaction is L, *i.e.*, it is determined by the angular momentum of the orbital occupied by the neutron before the reaction. As in Sec. 23.4, making the surface approximation leads to a diffractive behavior of the same nature as seen in Eqs. (23.33) and (23.34).

24.2.4 Spectroscopic factor

Naturally, the case in which the picked-up neutron originates from a configuration that can be approximated as a closed-shell core plus a single neutron is particularly simple. More complicated situations, where the neutron is removed from the correlated many-body state of the core, can still be treated similarly as above; however, in that case one can no longer assume that the nuclear wavefunction factorizes as in Eq. (24.9). In the end, the calculated cross section is multiplied by a *spectroscopic factor* S_L, which reflects the probability of finding the target nucleus in a configuration corresponding to the observed state of the residual nucleus and the transferred nucleon. Since S_L enters multiplicatively, it can be determined by fitting calculated cross-sections to experimental measurements, which provides an excellent test of nuclear structure models that can be used to obtain S_L. Consequently, stripping and pick-up reactions are an excellent probe of nuclear structure.

24.2.5 Discussion

As expected, DWBA yields better results than PWBA, the latter of which is equivalent to the "Butler theory," discussed in Lecture 21. This is illustrated in Fig. 24.3, where results of PWBA and DWBA calculations are compared with experimentally measured differential cross section for neutron transfer in scattering of deuterons on ^{40}Ca.

Naturally, a single nucleon can be transferred in reaction involving projectiles other than the deuteron, *e.g.*, (^{3}He, d) or (α, t). Transfer processes may even involve heavier ions, as in the reaction (^{14}N, ^{13}N). It is to be noted that, in contrast to examples discussed above, in the case of such heavier projectiles it is generally not appropriate to employ the zero-range approximation.

Transfer may also involve more than one nucleon, as in reactions (d, ^{6}Li) or (^{12}C, ^{16}C) which both pick up an α-particle-like cluster. Similarly, one can consider two-nucleon transfer reactions such

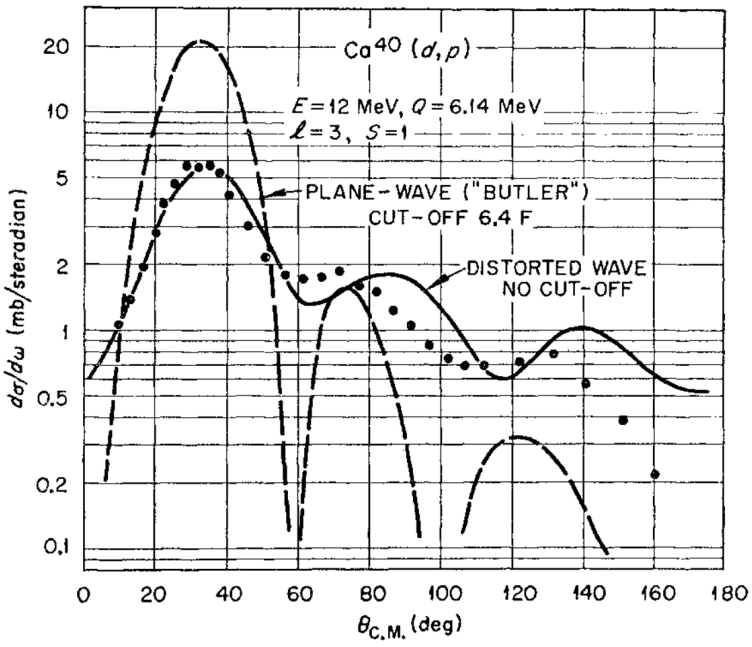

Figure 24.3: Comparison of PWBA and DWBA predictions against experimental results for a neutron-transfer reaction in scattering of deuterons on ^{40}Ca. Figure from Ref. [46].

as (t, p) or (^{16}O, ^{18}O). Since picking up a cluster of particles is directly tied to the probability of forming such a cluster inside the nucleus, these reactions probe detailed features of nuclear structure. Indeed, while single-nucleon transfers probe the probability of finding *one nucleon* in a given state, picking up two nucleons depends not only on their individual one-particle states, but also on the *correlations* between them.

Lecture sources: This lecture is heavily based on Satchler [7].

Lecture 25

High energy reactions I

Prerequisites: Lectures 13, 22, 23.
Guiding question: ***How does the physics of reactions change for fast projectiles?***

In Section 22.2, we obtained the post and prior forms of the T-matrix element for inelastic scattering of a composite projectile and target, Eqs. (22.28) and (22.30), repeated here without specifying whether we are considering the prior or post form[1],

$$T_{fi} = \left\langle \chi_f^{(-)} \xi_f \Phi_f \middle| \hat{U} \middle| \Psi_i^{(+)} \right\rangle \ . \tag{25.1}$$

This general result allows one to make several formal modifications. We have seen it already in Sec. 23.1, where we obtained the DWBA expression for reaction processes, Eq. (23.6), and in Sec. 23.3 where we further obtained the PWBA expression. Then, in Lecture 24, we discussed examples of applying DWBA and PWBA to direct reaction processes. In this lecture, we will again use the formal result in Eq. (25.1) to arrive at modifications illuminating the properties of high-energy processes, *i.e.*, reactions with fast projectiles.

To proceed, it is useful to assume that the full scattering state $\Psi_i^{(+)}$ factorizes into the product of the wavefunction describing the relative motion of the projectile-target system $\psi_i^{(+)}$, the wavefunction describing the internal state of the projectile ξ_i, and the wavefunction describing the internal state of the target Φ_i, so that we have

$$T_{fi} = \left\langle \chi_f^{(-)} \xi_f \Phi_f \middle| \hat{U} \middle| \psi_i^{(+)} \xi_i \Phi_i \right\rangle \ . \tag{25.2}$$

The difference from the treatment leading to the DWBA, Sec. 23.1, is that here we don't reduce the wavefunction $\psi_i^{(+)}$ to the distorted wave $\chi_i^{(+)}$, *i.e.*, we admit that $\psi_i^{(+)}$ can be influenced by the potential $\hat{U}$, which keeps the discussion more general.

25.1 Multiple scattering approximation

Equation (25.1) makes it apparent that the problem admits description in terms of distorted waves $\chi^{(\pm)}$, corresponding to the action of the potential $\hat{V}$, so that one considers the action of the reaction potential $\hat{U}$ "on top" of the elastic scattering generated by $\hat{V}$. In this description, the wavefunction far away from the potential naturally factorizes into the distorted wave χ and the

[1] As discussed below Eq. (23.5), which form one chooses is usually driven by which channel (entrance or exit) can be more accurately described in a given situation.

wavefunctions for the internal degrees of freedom, ξ and Φ. Since we are treating the distorted waves as our basis, one can imagine that analogously to the definition of the T-matrix element, Eq. (13.1), one can rewrite Eq. (25.1) as

$$T_{fi} = \left\langle \chi_f^{(-)} \xi_f \Phi_f \middle| \hat{t}^+ \middle| \chi_i^{(+)} \xi_i \Phi_i \right\rangle \ , \tag{25.3}$$

which defines[2] the *transition operator* $\hat{t}^+$ that satisfies the following Lippmann–Schwinger equation,

$$\hat{t}^+ = \hat{U} + \hat{U}\hat{G}^{(+)}\hat{t}^+ \ . \tag{25.4}$$

These definitions mirror the definition of the T-matrix element, Eq. (13.1), and its Lippmann-Schwinger equation, Eq. (13.8). The difference is that the $\hat{T}$-matrix elements, computed between free states, represent the effects of the *entire* Hamiltonian, while the $\hat{t}$ operator represents only the effects of the potential $\hat{U}$ and, consequently, its elements should be computed between states built out of distorted waves[3] and waves representing the internal states of the projectile and target. In some way, we can think of $\hat{t}$ as describing scattering of the projectile by $\hat{U}$ in the medium generated by the potential $\hat{V}$.

The operator $\hat{t}^+$ still considers the action of the potential $\hat{U}$ on the entire nucleus, which is naturally a non-trivial problem. We can simplify the situation if we replace the many-body interaction $\hat{U}$ by a sum of independent two-body interactions with individual nucleons,

$$\hat{U} \to \sum_{j \in A} \hat{U}_{(j)} \ , \tag{25.5}$$

where the index j labels the nucleons. Such form of the potential is justified if the interaction with the j-th nucleon happens "instantaneously," giving the rest of the nucleus no time to respond, which is valid for a highly energetic projectile. Note that by writing the potential as a sum of independent terms, we are also implicitly neglecting correlations between the target nucleons, *i.e.*, each nucleon is treated as an independent scattering center and the influence of other nucleons on the j-th nucleon's contribution to the potential is not taken into account.

This in turn suggests introducing a *two-body transition operator* $\hat{t}_{(j)}$, which describes the scattering of the projectile by the j-th nucleon in the target nucleus and satisfies the following Lippmann–Schwinger equation,

$$\hat{t}^+_{(j)} = \hat{U}_{(j)} + \hat{U}_{(j)}\hat{G}^{(+)}\hat{t}^+_{(j)} \ . \tag{25.6}$$

The operator $\hat{t}_{(j)}$ describes the full scattering amplitude for the two-body system composed of the projectile and the j-th nucleon[4]. The question then is how can one express $\hat{t}^+$ in terms of $\hat{t}_{(j)}$ so that the distorted Born series in terms of the $\hat{t}^+$-operator, Eq. (25.3), can be rewritten in terms of

[2] What you see here is another example of proposing a hypothetical operator ("Let's just assume an operator $\hat{t}^+$ exists that has the following properties") and then working with the equations until we get some additional insight ("Oh, look, we actually got something interesting!").

[3] That is, states already "dressed" by the potential $\hat{V}$.

[4] This it means that although we have reduced the problem to a two-body problem, the description of the scattering still admits multiple interactions. You can see this if you repeatedly substitute the expression for $\hat{t}^+_{(j)}$ back into itself in Eq. (25.6). This yields a Born series for the operator $\hat{t}^+_{(j)}$,

$$\hat{t}^+_{(j)} = \hat{U}_{(j)} + \hat{U}_{(j)}\hat{G}^{(+)}\hat{U}_{(j)} + \hat{U}_{(j)}\hat{G}^{(+)}\hat{U}_{(j)}\hat{G}^{(+)}\hat{U}_{(j)} + \dots \ ,$$

where the first term corresponds to a single action of the potential, the second term describes two applications of the potential separated by propagation as described by $\hat{G}^{(+)}$, and so on.

individual scatterings described by $\hat{t}^+_{(j)}$. To arrive at such an expression, let us further introduce an auxiliary wavefunction $\psi^{(+)}_{(j)}$, defined[5] through the relation

$$\hat{t}^+_{(j)}\psi^{(+)}_{(j)} = \hat{U}_{(j)}\psi^{(+)} \ . \tag{25.7}$$

This relation defines $\psi^+_{(j)}$ implicitly: it is a wavefunction such that the action of the two-body operator $\hat{t}^+_{(j)}$ on it reproduces the effect of the potential $\hat{U}_{(j)}$ on the full wavefunction $\psi^{(+)}$. The physical interpretation of $\psi^+_{(j)}$ will become clear in the following.

With these preliminary definitions, let us consider the Lippmann–Schwinger equation with distorted waves, Eq. (13.26), for $\psi^{(+)}$,

$$\psi^{(+)} = \chi^{(+)} + \hat{G}^{(+)}\hat{U}\psi^{(+)} \ . \tag{25.8}$$

Applying the $\hat{U}_{(k)}$ operator on both sides of the above equation and using Eq. (25.5) then yields

$$\hat{U}_{(k)}\psi^{(+)} = \hat{U}_{(k)}\chi^{(+)} + \hat{U}_{(k)}\hat{G}^{(+)}\sum_j \hat{U}_{(j)}\psi^{(+)} \ . \tag{25.9}$$

Next, applying Eq. (25.7) results in

$$\hat{t}_{(k)}\psi^{(+)}_{(k)} = \hat{U}_{(k)}\chi^{(+)} + \hat{U}_{(k)}\hat{G}^{(+)}\sum_j \hat{t}_{(j)}\psi^{(+)}_{(j)} \ . \tag{25.10}$$

Then, using the Lippmann–Schwinger equation for the $\hat{t}^+_{(k)}$ operator, Eq. (25.6), on the left-hand side and singling out the term $j = k$ on the right-hand side yields

$$\hat{U}_{(k)}\psi^{(+)}_{(k)} + \hat{U}_{(k)}\hat{G}^{(+)}\hat{t}^+_{(k)}\psi^{(+)}_{(k)} = \hat{U}_{(k)}\chi^{(+)} + \hat{U}_{(k)}\hat{G}^{(+)}\hat{t}_{(k)}\psi^{(+)}_{(k)} + \hat{U}_{(k)}\hat{G}^{(+)}\sum_{j\neq k}\hat{t}_{(j)}\psi^{(+)}_{(j)} \ , \tag{25.11}$$

which can be immediately reduced to

$$\psi^{(+)}_{(k)} = \chi^{(+)} + \hat{G}^{(+)}\sum_{j\neq k}\hat{t}_{(j)}\psi^{(+)}_{(j)} \tag{25.12}$$

$$= \chi^{(+)} + \hat{G}^{(+)}\sum_{j\neq k}\hat{t}_{(j)}\chi^{(+)} + \hat{G}^{(+)}\sum_{j\neq k}\hat{t}_{(j)}\hat{G}^{(+)}\sum_{i\neq j}\hat{t}_{(i)}\chi^{(+)} + \dots \ , \tag{25.13}$$

where in the second line we have turned the implicit equation for $\psi^{(+)}_{(k)}$ into an explicit series by iterating the right-hand side, *i.e.*, repeatedly substituting the expression for $\psi^{(+)}_{(j)}$ back into itself. Looking at Eq. (25.12) allows us to arrive at a physical interpretation of the wavefunction $\psi^{(+)}_{(k)}$: it is the wavefunction of the projectile as it arrives at nucleon k, having already undergone all scatterings from the other nucleons $k \neq j$. Indeed, the first term is just the distorted wave, while the second term encodes the modification of the wavefunction due to two-body interactions (to all orders, see Footnote 4) with all nucleons except the k-th one.

Now we are ready to rewrite the full matrix element, Eq. (25.2), by first applying Eq. (25.5) to express the total potential as a sum over contributions from individual nucleons $\hat{U}_{(j)}$, then using Eq. (25.7) to express the action of each $\hat{U}_{(j)}$ on the total wavefunction $\psi^{(+)}$ in terms of the action of

[5] In analogy to Eq. (13.2).

the $\hat{t}_{(j)}$ operator on the auxiliary wavefunction $\psi^{(+)}_{(j)}$, and finally using the series expansion of $\psi^{(+)}_{(k)}$, Eq. (25.13). This yields

$$T_{fi} = \left\langle \chi_f^{(-)} \xi_f \Phi_f \middle| \sum_k \hat{t}_{(k)} \middle| \chi^{(+)} \xi_i \Phi_i \right\rangle + \left\langle \chi_f^{(-)} \xi_f \Phi_f \middle| \sum_k \hat{t}_{(k)} \hat{G}^{(+)} \sum_{j \neq k} \hat{t}_{(j)} \middle| \chi^{(+)} \xi_i \Phi_i \right\rangle + \dots \ . \quad (25.14)$$

Note that the above result, known as the *multiple scattering series*, is a series in the number of nucleons that the projectile interacts with, not in the order of interaction (an example of a series in the latter is the Born series). Consequently, the first term in the series describes the interaction of the projectile with a single target nucleon; here, the sum over k is a coherent sum over possible target nucleons that could be struck, not a sum over simultaneous interactions. Then, the higher-order terms describe successive scatterings from two different nucleons, three different nucleons, and so on (see Fig. 25.1). If we can assume that the projectile interacts with the target nucleus only *via* a single scattering event off one of the nucleons, then we can terminate the above expression after the first term which yields the *multiple scattering approximation*. The name highlights the fact that the operator $\hat{t}_{(k)}$ sums to all orders the interaction of the projectile with the j-th nucleon in the presence of the potential $\hat{U}$ (see Footnote 4).

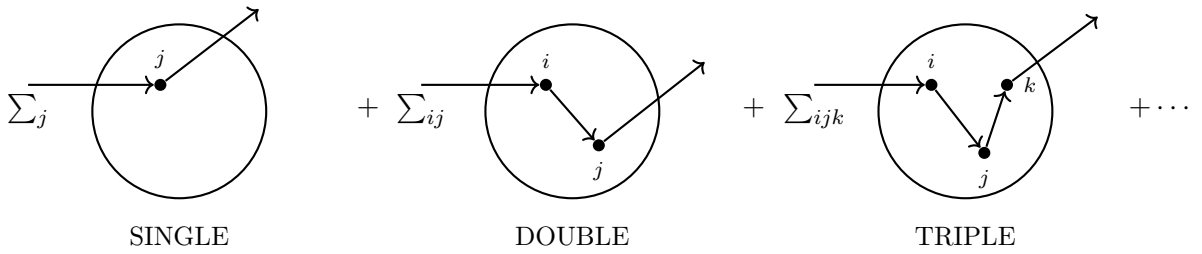

Figure 25.1: Schematic picture of the multiple scattering series, in which the projectile successively scatters from one, two, and more target nucleons. Inspired by a similar figure in Ref. [7].

Finally, we note that the above assumptions, together with neglecting the internal degrees of freedom in the projectile as well as any correlations beyond the active nucleon, imply that the T-matrix element factorizes into a reaction part and a structure part,

$$T_{fi} \approx \sum_{j \in A} \left\langle \chi_f^{(-)} \middle| \hat{t}^{+}_{(j)} \middle| \chi_i^{(+)} \right\rangle \left\langle \Phi_f \middle| \hat{\mathcal{O}}_j \middle| \Phi_i \right\rangle \ , \quad (25.15)$$

where $\chi_i^{(+)}$ and $\chi_f^{(-)}$ are distorted waves describing the relative motion of the projectile and target while $\hat{\mathcal{O}}_j$ is an operator acting on the nuclear wavefunction (facilitating, *e.g.*, removal or addition of a nucleon j). In particular, the second matrix element contains information about the nuclear structure and leads to spectroscopic factors.

This approach forms the basis of many direct reaction models, *e.g.*, for knockout reactions such as $(\mathrm{p}, 2\mathrm{p})$ or stripping reactions like (d, p) (see Lecture 18). For example, for the neutron-stripping reaction, one neutron is transferred from the projectile to the target. The transition amplitude can then be written schematically as

$$T_{fi} = \left\langle \chi_p^{(-)} \middle| \hat{t}_{nA} \middle| \chi_d^{(+)} \right\rangle \times \left\langle \Phi_B \middle| a_n^{\dagger} \middle| \Phi_A \right\rangle \ , \quad (25.16)$$

where the first matrix element describes the reaction dynamics (the neutron-target interaction that transfers momentum and embeds the neutron into the final bound state), while the second term

describes the addition of a neutron to the target and determines which states are populated and with what strength, which in turn depends on the nuclear structure.

25.2 Impulse approximation

If one can assume that the incident particle interacts with only one nucleon at a time, that the amplitude of the incident wave reaching each nucleon in the target nucleus is unaffected by the presence of the other nucleons, and that the binding energies of the target nucleons are much smaller than the incident energy, then it is appropriate to assume that the projectile effectively *propagates freely* between successive interactions with individual nucleons. Formally, this is described by a transition operator for scattering of free particles off of the j-th nucleon $\hat{\tau}^{+}_{(j)}$, which satisfies the Lippmann–Schwinger equation

$$\hat{\tau}^{+}_{(j)} = \hat{U}_{(j)} + \hat{U}_{(j)}\hat{G}_0^{(+)}\hat{\tau}^{+}_{(j)} \ , \tag{25.17}$$

where we note that the propagator is that of a free particle, $\hat{G}_0^{(+)}$. This set of assumptions is known as the *impulse approximation*, and it reflects a physical situation in which the interaction happens almost instantaneously, giving the rest of the nucleus no time to respond, which is appropriate for a highly energetic projectile.

By substituting $\hat{\tau}^{+}_{(j)}$ for $\hat{t}^{+}_{(j)}$ and keeping only the first term in Eq. (25.14), we are then naturally led to the *distorted wave impulse approximation (DWIA)*,

$$T_{fi} = \left\langle \chi_f^{(-)}\xi_f\Phi_f \middle| \sum_j \hat{\tau}^{(+)}_{(j)} \middle| \chi_i^{(+)}\xi_i\Phi_i \right\rangle \ . \tag{25.18}$$

Here, the sum over j carries the same meaning as in the multiple scattering series, Eq. (25.14): in any given event the projectile strikes one nucleon, but since the struck nucleon is not identified in the final state, one must sum coherently over all possibilities.

When the distorted waves are replaced by plane waves, which is equivalent to setting $\hat{V} = 0$, we obtain the *plane wave impulse approximation (PWIA)*,

$$T_{fi} = \left\langle \phi_f\xi_f\Phi_f \middle| \sum_j \hat{\tau}^{(+)}_{(j)} \middle| \phi_i\xi_i\Phi_i \right\rangle \ . \tag{25.19}$$

It is worth noting that in contrast to DWIA, the PWIA formula also applies to elastic scattering, *i.e.*, to the situation where $|i\rangle = |f\rangle$. This is simply because with $\hat{V} = 0$, the potential $\hat{U}$ becomes the only potential in the problem which now can also describe the possibility of elastic scattering, previously reserved for $\hat{V}$ (see Sec. 22.2.3). Note that for elastic scattering, one simply takes $\Phi_f = \Phi_i$, which means that the contribution due to the nuclear matrix element reduces to a ground-state expectation value, as we will see explicitly in the next section.

25.3 Impulse approximation for elastic scattering

Let us consider elastic scattering in the framework of PWIA. To evaluate the matrix element in Eq. (25.19), we need to translate the abstract notation used there into something directly manageable. To this end, we use a number of position-space resolutions of identity – specifically, $A + 1$ of

them[6] for both the initial and final wavefunctions, which will look somewhat like

$$\int d\boldsymbol{r}\,|\boldsymbol{r}\rangle\langle\boldsymbol{r}|\;\int d\boldsymbol{r}'\,|\boldsymbol{r}'\rangle\langle\boldsymbol{r}'|\;\left[\prod_{j=1}^{A}\int d\boldsymbol{r}_j\,|\boldsymbol{r}_j\rangle\langle\boldsymbol{r}_j|\right]\left[\prod_{j'=1}^{A}\int d\boldsymbol{r}_{j'}\,|\boldsymbol{r}_{j'}\rangle\langle\boldsymbol{r}_{j'}|\right], \tag{25.20}$$

where $\boldsymbol{r}$ and $\boldsymbol{r}'$ denote the coordinates of the initial and final wavefunction for the relative projectile-target motion, while $\boldsymbol{r}_j$ and $\boldsymbol{r}'_j$ denote the internal coordinates of the initial and final nuclear state, respectively. In the impulse approximation for the T-matrix element, Eq. (25.19), the summation over the active nucleon j can be taken in front of the expression. Then, inserting the above resolutions of identity yields[7][8]

$$T_{fi} = \sum_j \langle\phi_f|\left\langle\Phi_f\middle|\hat{\tau}_{(j)}\middle|\phi_i\right\rangle|\Phi_i\rangle \tag{25.21}$$

$$= \sum_j \int d\boldsymbol{r}' \int d\boldsymbol{r} \prod_{j'=1}^{A}\int d\boldsymbol{r}_{j'} \prod_{j=1}^{A}\int d\boldsymbol{r}_j\;\langle\phi_f|\boldsymbol{r}'\rangle\langle\Phi_f|\boldsymbol{r}_{j'}\rangle\langle\boldsymbol{r}',\boldsymbol{r}_{j'}|\hat{\tau}_{(j)}|\boldsymbol{r},\boldsymbol{r}_j\rangle\langle\boldsymbol{r}|\phi_i\rangle\langle\boldsymbol{r}_j|\Phi_i\rangle \tag{25.22}$$

$$= \sum_j \int d\boldsymbol{r}' \int d\boldsymbol{r} \prod_{j'=1}^{A}\int d\boldsymbol{r}_{j'} \prod_{j=1}^{A}\int d\boldsymbol{r}_j$$
$$\times\;\frac{e^{-i\boldsymbol{k}'\cdot\boldsymbol{r}'}}{(2\pi)^{3/2}}\Phi^*(\boldsymbol{r}_{1'},\ldots,\boldsymbol{r}_{A'})\left\langle\boldsymbol{r}',\boldsymbol{r}_{j'}\middle|\hat{\tau}_{(j)}\middle|\boldsymbol{r},\boldsymbol{r}_j\right\rangle\frac{e^{i\boldsymbol{k}\cdot\boldsymbol{r}}}{(2\pi)^{3/2}}\Phi(\boldsymbol{r}_1,\ldots,\boldsymbol{r}_A)\,. \tag{25.23}$$

Since the operator $\hat{\tau}_{(j)}$ by definition describes the interaction with only the j-th nucleon, the coordinates of all nucleons except the j-th one will be the same before and after the scattering since they are explicitly not included in the interaction. Formally, this is encoded in the $\hat{\tau}_{(j)}$ operator by taking elements between $\boldsymbol{r}_k$ and $\boldsymbol{r}_{k'}$ for $k'\neq j$ to produce delta functions of the form $\delta^{(3)}(\boldsymbol{r}_k-\boldsymbol{r}_{k'})$. Performing integration over these delta functions then yields

$$T_{fi} = \frac{1}{(2\pi)^3}\sum_j \int d\boldsymbol{r}' \int d\boldsymbol{r} \int d\boldsymbol{r}_{j'} \int d\boldsymbol{r}_j\; e^{-i\boldsymbol{k}'\cdot\boldsymbol{r}'}\left\langle\boldsymbol{r}',\boldsymbol{r}_{j'}\middle|\hat{\tau}_{(j)}\middle|\boldsymbol{r},\boldsymbol{r}_j\right\rangle e^{i\boldsymbol{k}\cdot\boldsymbol{r}}$$
$$\times\;\prod_{\substack{k=1\\k\neq j}}^{A}\int d\boldsymbol{r}_k\;\Phi^*(\boldsymbol{r}_1,\ldots,\boldsymbol{r}_{j'},\ldots,\boldsymbol{r}_A)\Phi(\boldsymbol{r}_1,\ldots,\boldsymbol{r}_j,\ldots,\boldsymbol{r}_A)\,, \tag{25.24}$$

where in the second line we integrate over all coordinates except those of the struck nucleon. Now, the nuclear wavefunction Φ is *antisymmetrized*, which means it changes sign under the exchange of any two nucleon coordinates[9]. This powerful symmetry means that all nucleon labels enter Φ on equal footing. As a result, integrating the $A-1$ coordinates of the *spectator nucleons* yields the same result regardless of which nucleon j is taken as the struck one, so that we can just as well relabel nucleon j as nucleon 1. With this, it is useful to define the *density function* or *density matrix* $\rho(\boldsymbol{r},\boldsymbol{r}')$,

$$\rho(\boldsymbol{r},\boldsymbol{r}') = \int d\boldsymbol{r}_2\ldots d\boldsymbol{r}_A\;\Phi^*(\boldsymbol{r}',\boldsymbol{r}_2,\ldots,\boldsymbol{r}_A)\Phi(\boldsymbol{r},\boldsymbol{r}_2,\ldots,\boldsymbol{r}_A)\,, \tag{25.25}$$

[6] Throughout this section, we take the projectile to be a single nucleon. The extension to composite particles can be done by including the projectile's internal structure *via* the wavefunction ξ. Nevertheless, the basic form of the results remains the same.

[7] Again, neglecting the internal degrees of freedom of the projectile.

[8] We also stop displaying the superscript "(+)" on the operator $\hat{\tau}_j$ to improve the readability.

[9] As required by the Pauli exclusion principle for identical fermions.

which sums over the $A-1$ "other nucleons" to yield a one-body property; note that with this definition, the diagonal element $\rho(\boldsymbol{r},\boldsymbol{r}) \equiv \rho(\boldsymbol{r})$ is the nuclear one-body density in the ground state. This allows us to considerably simplify our expression,

$$T_{fi} = \frac{1}{(2\pi)^3} \sum_j \int d\boldsymbol{r}' \int d\boldsymbol{r} \int d\boldsymbol{r}_{j'} \int d\boldsymbol{r}_j \; e^{-i\boldsymbol{k}'\cdot\boldsymbol{r}'} \left\langle \boldsymbol{r}', \boldsymbol{r}_{j'} \middle| \hat{\tau}_{(j)} \middle| \boldsymbol{r}, \boldsymbol{r}_j \right\rangle e^{i\boldsymbol{k}\cdot\boldsymbol{r}} \rho(\boldsymbol{r}_{j'}, \boldsymbol{r}_j) \; . \tag{25.26}$$

The matrix element $\left\langle \boldsymbol{r}', \boldsymbol{r}_{j'} \middle| \hat{\tau}_{(j)} \middle| \boldsymbol{r}, \boldsymbol{r}_j \right\rangle$ is now expressed in the coordinate space, while it is often more convenient to compute it in the momentum space. At this point it should not surprise us that we can transform the above expression to the desired from by inserting resolutions of identity, this time in momentum space, such that[10]

$$\begin{aligned} \left\langle \boldsymbol{r}' \right| \left\langle \boldsymbol{r}_{j'} \right| \hat{\tau}_{(j)} \left| \boldsymbol{r} \right\rangle \left| \boldsymbol{r}_j \right\rangle &= \int d\boldsymbol{p} \int d\boldsymbol{p}' \int d\boldsymbol{p}_j \int d\boldsymbol{p}_{j'} \\ &\quad \times \left\langle \boldsymbol{r}' \middle| \boldsymbol{p}' \right\rangle \left\langle \boldsymbol{p}' \right| \left\langle \boldsymbol{r}_{j'} \middle| \boldsymbol{p}_{j'} \right\rangle \left\langle \boldsymbol{p}_{j'} \right| \hat{\tau}_{(j)} \left| \boldsymbol{p} \right\rangle \left\langle \boldsymbol{p} \middle| \boldsymbol{r} \right\rangle \left| \boldsymbol{p}_j \right\rangle \left\langle \boldsymbol{p}_j \middle| \boldsymbol{r}_j \right\rangle \qquad (25.27) \\ &= \frac{1}{(2\pi)^6} \int d\boldsymbol{p} \int d\boldsymbol{p}' \int d\boldsymbol{p}_j \int d\boldsymbol{p}_{j'} \; e^{i\boldsymbol{p}'\cdot\boldsymbol{r}'} e^{i\boldsymbol{p}_{j'}\cdot\boldsymbol{r}_{j'}} \left\langle \boldsymbol{p}', \boldsymbol{p}_{j'} \middle| \hat{\tau}_{(j)} \middle| \boldsymbol{p}, \boldsymbol{p}_j \right\rangle e^{-i\boldsymbol{p}\cdot\boldsymbol{r}} e^{-i\boldsymbol{p}_j\cdot\boldsymbol{r}_j} \; , \qquad (25.28) \end{aligned}$$

which inserted into Eq. (25.26) yields

$$\begin{aligned} T_{fi} = \frac{1}{(2\pi)^9} \sum_j \int d\boldsymbol{r}' \int d\boldsymbol{r} \int d\boldsymbol{r}_{j'} \int d\boldsymbol{r}_j \int d\boldsymbol{p} \int d\boldsymbol{p}' \int d\boldsymbol{p}_j \int d\boldsymbol{p}_{j'} \\ \times \; e^{i(\boldsymbol{p}'-\boldsymbol{k}')\cdot\boldsymbol{r}'} e^{i\boldsymbol{p}_{j'}\cdot\boldsymbol{r}_{j'}} \left\langle \boldsymbol{p}', \boldsymbol{p}_{j'} \middle| \hat{\tau}_{(j)} \middle| \boldsymbol{p}, \boldsymbol{p}_j \right\rangle e^{-i\boldsymbol{p}_j\cdot\boldsymbol{r}_j} e^{-i(\boldsymbol{p}-\boldsymbol{k})\cdot\boldsymbol{r}} \rho(\boldsymbol{r}_{j'}, \boldsymbol{r}_j) \; . \end{aligned} \tag{25.29}$$

The integrals over the positions of the projectile-target system now become delta functions,

$$\int d\boldsymbol{r} \; e^{-i(\boldsymbol{p}-\boldsymbol{k})\cdot\boldsymbol{r}} = (2\pi)^3 \delta^{(3)}(\boldsymbol{p}-\boldsymbol{k}) \quad \text{and} \quad \int d\boldsymbol{r}' \; e^{i(\boldsymbol{p}'-\boldsymbol{k}')\cdot\boldsymbol{r}'} = (2\pi)^3 \delta^{(3)}(\boldsymbol{p}'-\boldsymbol{k}') \; , \tag{25.30}$$

so that now

$$T_{fi} = \frac{1}{(2\pi)^3} \sum_j \int d\boldsymbol{k}_j \int d\boldsymbol{k}_{j'} \int d\boldsymbol{r}_{j'} \int d\boldsymbol{r}_j \; e^{i\boldsymbol{k}_{j'}\cdot\boldsymbol{r}_{j'}} \left\langle \boldsymbol{k}', \boldsymbol{k}_{j'} \middle| \hat{\tau}_{(j)} \middle| \boldsymbol{k}, \boldsymbol{k}_j \right\rangle e^{-i\boldsymbol{k}_j\cdot\boldsymbol{r}_j} \rho(\boldsymbol{r}_{j'}, \boldsymbol{r}_j) \; , \tag{25.31}$$

where we also relabeled $\boldsymbol{p}_j \to \boldsymbol{k}_j$ and $\boldsymbol{p}_{j'} \to \boldsymbol{k}_{j'}$ for consistency of the notation.

Since $\hat{\tau}_{(j)}$ conserves the total momentum of the projectile-nucleon pair, its matrix element contains a factor $(2\pi)^3\delta^{(3)}(\boldsymbol{k}+\boldsymbol{k}_j-\boldsymbol{k}'-\boldsymbol{k}_{j'})$, which we now write out explicitly[11]

$$\begin{aligned} T_{fi} = \sum_j \int d\boldsymbol{k}_j \int d\boldsymbol{k}_{j'} \; \delta^{(3)}(\boldsymbol{k}+\boldsymbol{k}_j-\boldsymbol{k}'-\boldsymbol{k}_{j'}) \\ \times \int d\boldsymbol{r}_{j'} \int d\boldsymbol{r}_j \; e^{i\boldsymbol{k}_{j'}\cdot\boldsymbol{r}_{j'}} \left\langle \boldsymbol{k}', \boldsymbol{k}_{j'} \middle| \hat{\tau}_{(j)} \middle| \boldsymbol{k}, \boldsymbol{k}_j \right\rangle e^{-i\boldsymbol{k}_j\cdot\boldsymbol{r}_j} \rho(\boldsymbol{r}_{j'}, \boldsymbol{r}_j) \; . \end{aligned} \tag{25.32}$$

Denoting the momentum transfer as

$$\boldsymbol{q} \equiv \boldsymbol{k} - \boldsymbol{k}' \; , \tag{25.33}$$

[10] Here, since we're working in natural units, p is used as just another character that can be used to denote momentum.

[11] Note that if we were extra precise, we would now denote $\left\langle \boldsymbol{k}', \boldsymbol{k}_{j'} \middle| \hat{\tau}_{(j)} \middle| \boldsymbol{k}, \boldsymbol{k}_j \right\rangle$ slightly differently to acknowledge that the delta function has been factored out. Alas...

we can perform the integration over $\boldsymbol{k}_{j'}$, obtaining

$$T_{fi} = \sum_j \int d\boldsymbol{k}_j \int d\boldsymbol{r}_{j'} \int d\boldsymbol{r}_j \; e^{-i\boldsymbol{k}_j\cdot(\boldsymbol{r}_j-\boldsymbol{r}_{j'})} e^{i(\boldsymbol{k}-\boldsymbol{k}')\cdot\boldsymbol{r}_{j'}} \left\langle \boldsymbol{k}', \boldsymbol{q}+\boldsymbol{k}_j \middle| \hat{\tau}_{(j)} \middle| \boldsymbol{k}, \boldsymbol{k}_j \right\rangle \rho(\boldsymbol{r}_{j'}, \boldsymbol{r}_j) \; . \tag{25.34}$$

At high incident energies, on the order of 100 MeV, the kinetic energy of the target nucleon is negligible compared to that of the incident nucleon. As a result, the two-nucleon scattering amplitude should *not* depend on $\boldsymbol{k}_j$,

$$\left\langle \boldsymbol{k}', \boldsymbol{q}+\boldsymbol{k}_j \middle| \tau(j) \middle| \boldsymbol{k}, \boldsymbol{k}_j \right\rangle \quad \rightarrow \quad \left\langle \boldsymbol{k}', \boldsymbol{q} \middle| \tau(j) \middle| \boldsymbol{k}, 0 \right\rangle \; . \tag{25.35}$$

With this, in Eq. (25.34) $\boldsymbol{k}_j$ only remains in the factor $e^{-i\boldsymbol{k}_j\cdot(\boldsymbol{r}_j-\boldsymbol{r}'_j)}$, so that the integration over $d\boldsymbol{k}_j$ yields[12] $(2\pi)^3\delta^{(3)}(\boldsymbol{r}_j-\boldsymbol{r}'_j)$. Performing the integration over $\boldsymbol{r}'_j$ then results in

$$T_{fi}(\boldsymbol{k}', \boldsymbol{k}) = \sum_j (2\pi)^3 \left\langle \boldsymbol{k}', \boldsymbol{q} \middle| \tau(j) \middle| \boldsymbol{k}, 0 \right\rangle \int d\boldsymbol{r}_j \; e^{i\boldsymbol{q}\cdot\boldsymbol{r}_j} \rho(\boldsymbol{r}_j) \tag{25.36}$$

$$= \sum_j (2\pi)^3 \left\langle \boldsymbol{k}', \boldsymbol{q} \middle| \tau(j) \middle| \boldsymbol{k}, 0 \right\rangle F(q) \; , \tag{25.37}$$

where $F(q)$, defined here as

$$F(q) \equiv \int d\boldsymbol{r} \; e^{i\boldsymbol{q}\cdot\boldsymbol{r}} \rho(\boldsymbol{r}) \; , \tag{25.38}$$

is nothing else as the Fourier transform of the nuclear form factor, which we have already encountered, albeit in a different form, in Eq. (23.14). Here, $F(q)$ encodes how the spatial distribution of nuclear matter modulates the scattering amplitude, with different q values probing the density at different length scales. Overall, we see that assuming the target nucleon's momentum to be negligible factorizes the T-matrix element into a product of the matrix element for two-nucleon scattering and the form factor $F(q)$.

Since $F(q)$ encodes the effects due to nuclear structure and the matrix element $\langle \boldsymbol{k}', \boldsymbol{q}|\tau(j)|\boldsymbol{k}, 0\rangle$ has been explicitly assumed *not* to depend on the target nucleon momentum $\boldsymbol{k}_j$, it follows that each target nucleon contributes in the exactly same way. With this, the sum over j is trivial, yielding a multiplicative factor of A, so that

$$T_{fi}(\boldsymbol{k}', \boldsymbol{k}) = A(2\pi)^3 \left\langle \boldsymbol{k}', \boldsymbol{q} \middle| \tau(1) \middle| \boldsymbol{k}, 0 \right\rangle F(q) \; , \tag{25.39}$$

where we relabeled $j \rightarrow 1$ for clarity of notation.

We note that in nucleon-nucleus scattering, the relation between $|\boldsymbol{k}|$ and $|\boldsymbol{k}'|$ is determined by the kinematics of the nucleon-nucleus system. Since this is bound to differ from the kinematics of a two-nucleon system, the two-nucleon matrix element in Eq. (25.39) is *off-shell*. At the same time, at the energies in question the two-nucleon matrix element depends strongly on q^2 but not as much on the incident energy, measured by k. This is because in this energy regime the dominant contribution to the nucleon-nucleon amplitude comes from the short-range part of the nuclear force which sets the relevant scale. The momentum transfer q controls how much much of this short-range structure is probed, while varying the overall energy merely shifts the amplitude along a slowly-varying envelope[13]. To declutter the notation, we then define

$$\left\langle \boldsymbol{k}', \boldsymbol{q} \middle| \tau(1) \middle| \boldsymbol{k}, 0 \right\rangle \equiv \tau(E, q^2) \; . \tag{25.40}$$

[12] We have shown how this happens for a 1D integral in Footnote 2 of Lecture 14.

[13] This is an empirical observation that is well supported at intermediate to high energies.

It is worth noting that $\tau(E, q^2)$ is a T-matrix element in its own right. As a result, following the relationship between the T-matrix element and the scattering amplitude, Eq. (13.13), one can write the scattering amplitude for the two-nucleon process described by $\tau(E, q^2)$ as

$$M(E, q^2) \equiv f_{n,n}(\theta, \phi) = -\frac{\mu_0}{2\pi}(2\pi)^3 \tau(E, q^2) \ , \tag{25.41}$$

where $\mu_0 = m/2$ is the reduced mass for *two-nucleon* scattering and m is the nucleon mass. Here, following a standard convention, we denote the two-nucleon scattering amplitude with $M(E, q^2)$, which will also help to avoid confusion with the scattering amplitude $f(\theta, \phi)$ for the full nucleon-nucleus collision. The latter is given by

$$f(\theta, \phi) = -\frac{\mu_A}{2\pi} T_{fi}(\boldsymbol{k}', \boldsymbol{k}) \ , \tag{25.42}$$

where $\mu_A = Am/(A+1)$ is the reduced mass of the nucleon-nucleus system. Using the PWIA expression for the T-matrix element, Eq. (25.39), together with the two-nucleon scattering amplitude, Eq. (25.41), in the expression for the nucleon-nucleus scattering amplitude, Eq. (25.42), we get

$$f(\theta, \phi) = A\frac{\mu_A}{\mu_0} M(E, q^2) F(q) = \frac{2A^2}{A+1} M(E, q^2) F(q) \ . \tag{25.43}$$

25.4 Impulse approximation for inelastic scattering

In the case of inelastic scattering in the impulse approximation, the T-matrix element for a transition from the initial state i to the final state f is given by Eq. (25.18), where $\chi_f^{(\pm)}$ are the distorted wavefunctions for the projectile. To obtain an expression in terms of a two-nucleon scattering amplitude as in Sec. (25.3), we need the operator $\hat{\tau}_j$ to act on plane wave states. This can be achieved by expanding the distorted waves in the plane wave basis,

$$\chi^{(+)}(\boldsymbol{k}, \boldsymbol{r}) = \int d\boldsymbol{\kappa} \ a(\boldsymbol{\kappa}, \boldsymbol{k}) e^{i\boldsymbol{\kappa}\cdot\boldsymbol{r}} \ , \tag{25.44}$$

$$\chi^{(-)}(\boldsymbol{k}', \boldsymbol{r}) = \int d\boldsymbol{\kappa}' \ a(\boldsymbol{\kappa}', \boldsymbol{k}') e^{i\boldsymbol{\kappa}'\cdot\boldsymbol{r}} \ . \tag{25.45}$$

With this, after manipulations mirroring those in Sec. (25.3), Eq. (25.18) becomes

$$T_{fi} = \sum_j \left\langle \chi_f^{(-)} \right| \langle \Phi_f | \, \hat{\tau}_{(j)} \left| \chi_i^{(+)} \right\rangle | \Phi_i \rangle \tag{25.46}$$

$$= \sum_j \int d\boldsymbol{r}_{j'} \int d\boldsymbol{r}_j \int d\boldsymbol{\kappa}' \int d\boldsymbol{\kappa} \int d\boldsymbol{p}_j$$
$$\times \ a(\boldsymbol{\kappa}', \boldsymbol{k}') \ e^{i(\boldsymbol{\kappa} + \boldsymbol{p}_j - \boldsymbol{\kappa}')\cdot\boldsymbol{r}_{j'}} \left\langle \boldsymbol{\kappa}', \boldsymbol{\kappa} + \boldsymbol{p}_j - \boldsymbol{\kappa}' \right| \hat{\tau}_{(j)} \left| \boldsymbol{\kappa}, \boldsymbol{p}_j \right\rangle e^{-i\boldsymbol{p}_j\cdot\boldsymbol{r}_j} \ a(\boldsymbol{\kappa}, \boldsymbol{k}) \rho_{fi}(\boldsymbol{r}_{j'}, \boldsymbol{r}_j) \ , \tag{25.47}$$

where ρ_{fi} is the *transition density* which is a one-body matrix element between two different nuclear states[14]. As in the case of elastic scattering, we now make an assumption that the matrix element does not depend on $\boldsymbol{p}_j$ and rearrange the terms so that the integration over $\boldsymbol{p}_j$ becomes a delta function. Together with denoting $\boldsymbol{q} \equiv \boldsymbol{\kappa} - \boldsymbol{\kappa}'$, this yields

$$T_{fi} = \sum_j \int d\boldsymbol{r}_j \int d\boldsymbol{\kappa}' \int d\boldsymbol{\kappa} \ a(\boldsymbol{\kappa}', \boldsymbol{k}') \left\langle \boldsymbol{\kappa}', \boldsymbol{q} \right| \hat{\tau}_{(j)} \left| \boldsymbol{\kappa}, 0 \right\rangle a(\boldsymbol{\kappa}, \boldsymbol{k}) e^{i\boldsymbol{q}\cdot\boldsymbol{r}_j} \rho_{fi}(\boldsymbol{r}_j) \ . \tag{25.48}$$

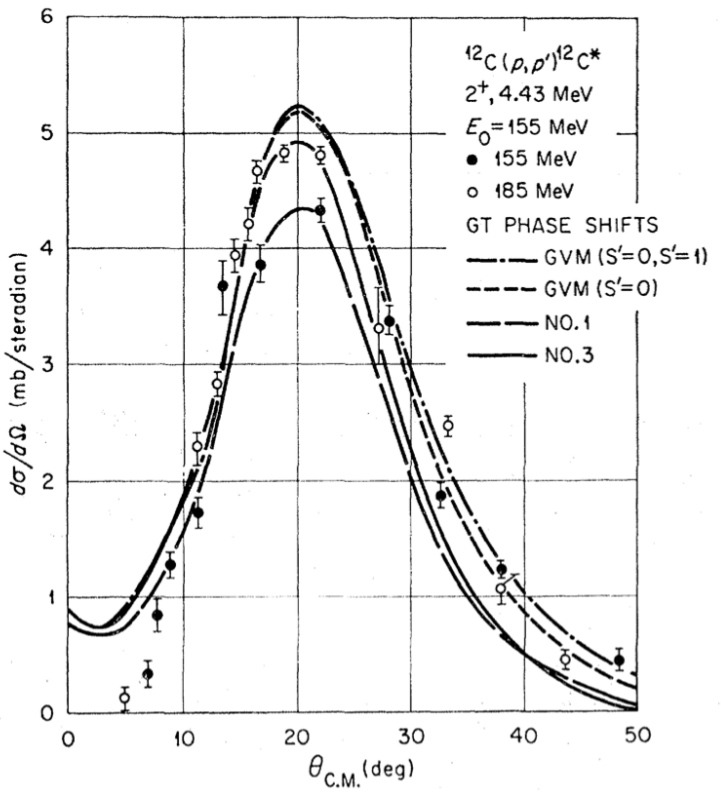

Figure 25.2: Differential cross section for the inelastic reaction ^{12}C(p, p')^{12}C*, with experimental data marked by points with error bars and theoretical calculations based on DWIA with varied nuclear structure input marked with lines. Figure from Ref. [47].

At this point we make an additional assumption[15] that the variation of the matrix element for the two-nucleon scattering with the momenta $\boldsymbol{\kappa}$ and $\boldsymbol{\kappa}'$ is small and therefore the matrix element can be replaced by a mean value. We then also assume that this mean value corresponds to the asymptotic projectile momenta $\boldsymbol{k}$ and $\boldsymbol{k}'$. With this assumption we can now recognize the remaining terms dependent on $\boldsymbol{\kappa}$ and $\boldsymbol{\kappa}'$ as the distorted waves, see Eqs. (25.44) and (25.45), so that we can write

$$T_{fi} = \sum_j \int d\boldsymbol{r}_j \; \chi_f^{(-)*}(\boldsymbol{k}', \boldsymbol{r}_j) \left\langle \boldsymbol{\kappa}', \boldsymbol{q} \middle| \hat{\tau}_{(j)} \middle| \boldsymbol{\kappa}, 0 \right\rangle \chi_i^{(+)}(\boldsymbol{k}, \boldsymbol{r}_j) \rho_{fi}(\boldsymbol{r}_j) \; . \tag{25.49}$$

Introducing the scattering amplitude for the two-nucleon process in analogy to the case of elastic scattering, Eq. (25.41),

$$M_j(E, q^2) \equiv f_{j;n,n}(\theta, \phi) = -\frac{\mu_0}{2\pi}(2\pi)^3 \hat{\tau}_j(E, q^2) \; , \tag{25.50}$$

then finally yields

$$T_{fi} = -\frac{4\pi^2}{\mu_0} \sum_j \int d\boldsymbol{r}_j \; \chi_f^{(-)*}(\boldsymbol{k}', \boldsymbol{r}_j) M_j(E, q^2) \chi_i^{(+)}(\boldsymbol{k}, \boldsymbol{r}_j) \rho_{fi}(\boldsymbol{r}_j) \; . \tag{25.51}$$

[14] Intuitively, it can be interpreted as the probability of removing a nucleon at position $\boldsymbol{r}_j$ from the initial state and placing it at position $\boldsymbol{r}_{j'}$ in the final state, with all other nucleons integrated out.

[15] As compared to the case of elastic scattering.

We note that the structure of the above equation looks exactly as if we replaced the operator $\hat{\tau}_j$ by $\hat{\tau}_j(E, q^2)\delta^{(3)}(\boldsymbol{r} - \boldsymbol{r}_j)$. For this reason this result is sometimes referred to as the *zero-range form of DWIA for inelastic scattering*. This may be slightly misleading as the q^2-dependence of the matrix element ensures that a significant part of the long-range behavior of the two-nucleon interaction is taken into account[16].

An example of using DWIA in practice is shown in Fig. 25.2. In this study, analyzing the inelastic reaction ^{12}C(p, p')^{12}C*, the transition density has been extracted from scattering of electrons on ^{12}C using two chosen fits. This density was then used in DWIA calculations, shown with lines labeled "No. 1" and "No. 3". The figure also shows results using transition densities obtained from appropriate nuclear structure models, labeled as "GVM." It is evident that the impulse approximation performs well enough to provide a way to differentiate between different nuclear structure inputs.

Lecture sources: This lecture is based on Jackson [4].

[16] As you may remember from the discussion after the In-class Activity 11a, the dependence on the momentum transfer q is the Fourier-space representation of spatial structure.

Lecture 26

High energy reactions II

Prerequisites: Lectures 8, 11, 12, 13, 22, 25.
Guiding question: ***How does the physics of reactions change for really fast projectiles?***

Let us again consider the multiple scattering series, obtained in Eq. (25.14), repeated here for convenience,

$$T_{fi} = \left\langle \chi_f^{(-)} \xi_f \Phi_f \middle| \sum_k \hat{t}_{(k)} \middle| \chi^{(+)} \xi_i \Phi_i \right\rangle + \left\langle \chi_f^{(-)} \xi_f \Phi_f \middle| \sum_k \hat{t}_{(k)} \hat{G}^{(+)} \sum_{j \neq k} \hat{t}_{(j)} \middle| \chi^{(+)} \xi_i \Phi_i \right\rangle + \dots \ . \quad (26.1)$$

This series is organized by the number of distinct nucleons the projectile interacts with. In Sec. 25.2, we assumed free-particle propagation between collisions and truncated the series by keeping only single-nucleon scatterings to obtain the impulse approximation.

Alternatively, one can attempt to sum all terms in the series. This is possible by making certain simplifying assumptions. In particular, the key assumption in the *eikonal (Glauber) approximation*[1] is that the projectile travels in a straight line through the target, with its transverse position entirely unchanged, so that

$$\boldsymbol{r} = \boldsymbol{b} + z\hat{\boldsymbol{k}} \ , \qquad \boldsymbol{b} = \text{const} \ . \quad (26.2)$$

Physically, this is the case at high collision energies where the projectile moves so fast that the additional transverse velocity due to interactions with the scattering potential can be neglected in comparison, leading to strongly forward-peaked cross sections.

The eikonal approximation also implies that the successive scatterings from different nucleons are independent of each other. Indeed, since the projectile's motion is confined to a straight line, it passes each nucleon j at a well-defined transverse separation $\boldsymbol{b} - \boldsymbol{b}_j$, independently of previous scatterings. This independence also implies that the projectile propagates freely between scatterings. From Lecture 8, we know that the effect of interaction with a scattering center can be summarized in a phase shift or, alternatively, the corresponding S-matrix element. As a result, each nucleon j at a transverse position $\boldsymbol{b}_j$ contributes a phase to the wavefunction as the projectile passes by, and these phases simply add up along the trajectory. This integrated behavior, often summarized in a function $\chi(\boldsymbol{r})$ that is sometimes referred to as *the eikonal*, determines how the phase (and thus the wavefronts) propagates.

[1] The name comes from the Greek word "eikōn," which means "image" or "representation." As everything else in scattering theory, it entered through optics, where it refers to a function that encodes the shape of wavefronts. It will become more clear in the following why this name is used here.

26.1 Formal derivation of the Glauber approximation

How do the above assumptions affect the multiple scattering series, Eq. (26.1)? First, the assumption that the projectile propagates freely between scatterings reduces the propagator to that of a free particle, $\hat{G}_0^{(+)}$, whose explicit form we derived in Eq. (12.2), repeated here for convenience,

$$G_0^{(\pm)}(E_k;\boldsymbol{r},\boldsymbol{r}') = \frac{-2\mu}{4\pi|\boldsymbol{r}-\boldsymbol{r}'|}e^{ik|\boldsymbol{r}-\boldsymbol{r}'|} \ . \tag{26.3}$$

This function literally propagates an outgoing wave generated at the point $\boldsymbol{r}'$ to the point $\boldsymbol{r}$, where it may scatter again, becoming an outgoing wave for another propagator. To separate the projectile's motion into the longitudinal and transverse directions, we write $\boldsymbol{r} = (\boldsymbol{b}, z)$ and $\boldsymbol{r}' = (\boldsymbol{b}', z')$, so that

$$|\boldsymbol{r}-\boldsymbol{r}'| = \sqrt{(\boldsymbol{b}-\boldsymbol{b}')^2+(z-z')^2} = (z-z')\sqrt{1+\frac{(\boldsymbol{b}-\boldsymbol{b}')^2}{(z-z')^2}} \approx (z-z')+\frac{(\boldsymbol{b}-\boldsymbol{b}')^2}{2(z-z')} \ , \tag{26.4}$$

where in the second equality we have taken $z-z'>0$ and in the third equality we used the fact that for strongly-forward propagation we have $z-z' \gg |\boldsymbol{b}-\boldsymbol{b}'|$. As a result,

$$e^{ik|\boldsymbol{r}-\boldsymbol{r}'|} \approx e^{ik(z-z')}e^{ik\frac{(\boldsymbol{b}-\boldsymbol{b}')^2}{2(z-z')}} = e^{ik(z-z')}\frac{2\pi i(z-z')}{k}\left(\frac{k}{2\pi i(z-z')}e^{ik\frac{(\boldsymbol{b}-\boldsymbol{b}')^2}{2(z-z')}}\right) \ , \tag{26.5}$$

where in the second equality we used the brackets to isolate a term which becomes a delta function at high energies[2]. With this, taking $|\boldsymbol{r}-\boldsymbol{r}'| \approx z-z'$, the free propagator can be approximated as

$$G_0^{(+)}(E_k;\boldsymbol{r},\boldsymbol{r}') \approx \frac{-i}{v}e^{ik(z-z')}\theta(z-z')\delta^{(2)}(\boldsymbol{b}-\boldsymbol{b}') \ . \tag{26.6}$$

---

[2] To see this, let us consider the function $K_\epsilon(\boldsymbol{b}-\boldsymbol{b}') = (2\pi i\epsilon)^{-1}e^{i\frac{(\boldsymbol{b}-\boldsymbol{b}')^2}{2\epsilon}}$, where $\epsilon = (z-z')/k$. We want to show that in the limit of $\epsilon \to 0$ we have

$$\lim_{\epsilon\to 0}\mathcal{I}_K = \lim_{\epsilon\to 0}\int d^2b' \ K_\epsilon(\boldsymbol{b}-\boldsymbol{b}')F(\boldsymbol{b}') \to F(\boldsymbol{b})$$

for any smooth function $F(\boldsymbol{b})$, *i.e.*, the *kernel* K_ϵ behaves like a delta function. This can be easily done with the help of Fourier transforms of both $K_\epsilon(\boldsymbol{b}-\boldsymbol{b}')$ and $F(\boldsymbol{b}')$. Indeed, we can always write $F(\boldsymbol{b}') = \int \frac{d^2q}{(2\pi)^2} \ e^{i\boldsymbol{q}\cdot\boldsymbol{b}'}\tilde{F}(\boldsymbol{q})$, so that

$$\mathcal{I}_K = \int d^2b' \ K_\epsilon(\boldsymbol{b}-\boldsymbol{b}')\int\frac{d^2q}{(2\pi)^2} \ e^{i\boldsymbol{q}\cdot\boldsymbol{b}'}\tilde{F}(\boldsymbol{q}) = \int\frac{d^2q}{(2\pi)^2} \ \tilde{F}(\boldsymbol{q})\int d^2b' \ K_\epsilon(\boldsymbol{b}-\boldsymbol{b}')e^{i\boldsymbol{q}\cdot\boldsymbol{b}'} \ ,$$

where in the second equality we simply changed the order of integration. Changing the variables according to $\boldsymbol{\rho} = \boldsymbol{b}-\boldsymbol{b}'$, $d^2b' = d^2\rho$ yields

$$\mathcal{I}_K = \int\frac{d^2q}{(2\pi)^2} \ \tilde{F}(\boldsymbol{q})e^{i\boldsymbol{q}\cdot\boldsymbol{b}}\int d^2\rho \ K_\epsilon(\boldsymbol{\rho})e^{-i\boldsymbol{q}\cdot\boldsymbol{\rho}} = \int\frac{d^2q}{(2\pi)^2} \ e^{i\boldsymbol{q}\cdot\boldsymbol{b}}\tilde{F}(\boldsymbol{q})\tilde{K}_\epsilon(\boldsymbol{q}) \ .$$

Here, $\tilde{K}_\epsilon(\boldsymbol{q})$ is the Fourier transform of $K_\epsilon(\boldsymbol{\rho})$, which is explicitly given by

$$\tilde{K}_\epsilon(\boldsymbol{q}) = \int d^2\rho \ e^{-i\boldsymbol{q}\cdot\boldsymbol{\rho}}\frac{1}{2\pi i\epsilon}e^{i\frac{\rho^2}{2\epsilon}} = e^{-i\frac{\epsilon q^2}{2}}\int d^2\rho \ \frac{1}{2\pi i\epsilon}e^{i\frac{(\boldsymbol{\rho}-\epsilon\boldsymbol{q})^2}{2\epsilon}} = e^{-i\frac{\epsilon q^2}{2}}\int d^2u \ \frac{1}{2\pi i\epsilon}e^{i\frac{u^2}{2\epsilon}} = e^{-i\frac{\epsilon q^2}{2}} \ ,$$

where in the second equality we have completed the square in the exponent, in the third equality we changed the integration variable according to $\boldsymbol{u} = \boldsymbol{\rho}-\epsilon\boldsymbol{q}$, $d^2u = d^2\rho$, and in the fourth equality we performed the integral (known as the *Fresnel integral*, *i.e.*, an oscillatory Gaussian-type integral), which equals 1 because we chose a convenient normalization for the kernel. We can now easily see that $\lim_{\epsilon\to 0}\tilde{K}_\epsilon(\boldsymbol{\rho}) = 1$, with which we immediately obtain

$$\lim_{\epsilon\to 0}\mathcal{I}_K = \int\frac{d^2q}{(2\pi)^2} \ e^{i\boldsymbol{q}\cdot\boldsymbol{b}}\tilde{F}(\boldsymbol{q}) \equiv F(\boldsymbol{b}) \ ,$$

which shows that $\lim_{\epsilon\to 0}K_\epsilon(\boldsymbol{b}-\boldsymbol{b}') \to \delta^{(2)}(\boldsymbol{b}-\boldsymbol{b}')$ in the sense of distributions (*i.e.*, when integrated with a test function, see Footnote 5 in Lecture 11).

where we used the fact that $k/\mu = v$ and the factor $\theta(z - z')$ expresses the outgoing boundary condition, *i.e.*, the fact that the projectile propagates forward along the beam direction from z' to z. In matrix elements between high-energy projectile states, the factor $e^{ik(z-z')}$ in the eikonal Green's function cancels the rapidly oscillating longitudinal phases of the incoming and outgoing plane waves. After this cancellation, only the slowly varying transverse phase $e^{i\boldsymbol{q}\cdot\boldsymbol{b}}$ remains[3], and the effective propagator between scatterings is

$$G^{(+)}_{\rm eik}(E_k; \boldsymbol{r}, \boldsymbol{r}') \approx \frac{-i}{v}\theta(z - z')\delta^{(2)}(\boldsymbol{b} - \boldsymbol{b}') \ . \tag{26.7}$$

With this, we can now consider the multiple scattering series. First, let us evaluate the scattering amplitude, which is given in terms of the T-matrix element in Eq. (13.13), repeated here for convenience

$$f(\boldsymbol{q}) = -4\mu\pi^2 \left\langle \boldsymbol{k}_f \middle| \hat{T} \middle| \boldsymbol{k}_i \right\rangle \ , \tag{26.8}$$

where $\boldsymbol{q} = \boldsymbol{k}_i - \boldsymbol{k}_f$. Following Eq. (12.2), the single-scattering term is $\hat{T} = \sum_j \hat{t}_j$, so that in the coordinate representation[4]

$$f^{(1)}(\boldsymbol{q}) = -4\mu\pi^2 \sum_j \int d^3r \ e^{-i\boldsymbol{k}_f\cdot\boldsymbol{r}} t_j(\boldsymbol{r} - \boldsymbol{r}_j) e^{i\boldsymbol{k}_i\cdot\boldsymbol{r}} \ . \tag{26.9}$$

As before, using the small-angle approximation allows us to write

$$e^{-i\boldsymbol{k}_f\cdot\boldsymbol{r}} e^{i\boldsymbol{k}_i\cdot\boldsymbol{r}} \approx e^{i\boldsymbol{q}\cdot\boldsymbol{b}} \ , \tag{26.10}$$

so that

$$f^{(1)}(\boldsymbol{q}) = -4\mu\pi^2 \sum_j \int d^2b \ e^{i\boldsymbol{q}\cdot\boldsymbol{b}} \int dz \ t_j(\boldsymbol{b} - \boldsymbol{b}_j, z - z_j) \ . \tag{26.11}$$

With the benefit of knowing where we're going, we now define the *profile function for scattering from nucleon j*,

$$\Gamma_j(\boldsymbol{b} - \boldsymbol{b}_j) \equiv \frac{i}{v} \int dz \ t_j(\boldsymbol{b} - \boldsymbol{b}_j, z - z_j) \ , \tag{26.12}$$

so that

$$f^{(1)}(\boldsymbol{q}) = 4ik\pi^2 \int d^2b \ e^{i\boldsymbol{q}\cdot\boldsymbol{b}} \sum_j \Gamma_j(\boldsymbol{b} - \boldsymbol{b}_j) \ . \tag{26.13}$$

[3] As as example, consider $\left\langle \boldsymbol{k}_f \middle| \hat{t}_j \hat{G}^{(+)}_0 \hat{t}_k \middle| \boldsymbol{k}_i \right\rangle$, where we suppress the target nucleon coordinates and consider a local interaction for simplicity. In the coordinate space , this matrix elements is proportional to an integral of the form

$$\left\langle \boldsymbol{k}_f \middle| \hat{t}_j \hat{G}^{(+)}_0 \hat{t}_k \middle| \boldsymbol{k}_i \right\rangle \propto \int d^3r \int d^3r' \ e^{-i\boldsymbol{k}_f\cdot\boldsymbol{r}} t_j(\boldsymbol{r}) G^{(+)}_0(\boldsymbol{r}, \boldsymbol{r}') t_k(\boldsymbol{r}') e^{i\boldsymbol{k}_i\cdot\boldsymbol{r}'} \ .$$

We take $\boldsymbol{k}_i = k\hat{\boldsymbol{z}}$ and $\boldsymbol{k}_f \approx k\hat{\boldsymbol{z}} - \boldsymbol{q}$, which is justified in the small-angle approximation. Using the Glauber limit of the free propagator, Eq. (26.6), the matrix element is the shown to contain the following exponentials,

$$e^{-i\boldsymbol{k}_f\cdot\boldsymbol{r}} e^{ik(z-z')} e^{i\boldsymbol{k}_i\cdot\boldsymbol{r}'} \approx e^{-ikz} e^{i\boldsymbol{q}\cdot\boldsymbol{r}} e^{ikz} e^{-ikz'} e^{ikz'} = e^{i\boldsymbol{q}\cdot\boldsymbol{r}} \ ,$$

i.e., $e^{ik(z-z')}$ cancels against the longitudinal plane-wave phases already present in the asymptotic states.

[4] And assuming a local form for the elementary interaction.

Next, we consider the double-scattering term, which tackles two successive scatterings from nucleons j and k,

$$\hat{T}^{(2)} = \sum_k \hat{t}_k \hat{G}^{(+)}_{\rm eik} \sum_{j\neq k} \hat{t}_j \ . \tag{26.14}$$

Using the reduced Glauber propagator, Eq. (26.7), in the coordinate space this matrix element is proportional to

$$t_k(\boldsymbol{b}, z_k)\Big[-\frac{i}{v}\theta(z_k - z_j)\delta^{(2)}(\boldsymbol{b}-\boldsymbol{b}')\Big] t_j(\boldsymbol{b}', z_j) \ . \tag{26.15}$$

The transverse plane integrations then reduce the above to

$$-\frac{i}{v}\theta(z_k - z_j) t_k(\boldsymbol{b}, z_k) t_j(\boldsymbol{b}, z_j) \ . \tag{26.16}$$

With this, the double-scattering contribution to the scattering amplitude is

$$\begin{aligned} f^{(2)}(\boldsymbol{q}) = -4\mu\pi^2 \sum_k \sum_{j\neq k} \int d^2b \ e^{i\boldsymbol{q}\cdot\boldsymbol{b}} \\ \times \int dz \int dz' \ \Big[-\frac{i}{v}\theta(z_k - z_j)\Big] t_k(\boldsymbol{b}-\boldsymbol{b}_k, z - z_k) t_j(\boldsymbol{b}-\boldsymbol{b}_j, z' - z_j) \ , \end{aligned} \tag{26.17}$$

where we identified $\theta(z-z') = \theta(z_k - z_j)$ since the scattering takes place at the positions of nucleons j and k. At this point, let us note that explicitly

$$\begin{aligned} \sum_k \sum_{j\neq k} \theta(z_k - z_j) = \theta(z_1 - z_2) + \theta(z_1 - z_3) + \ldots \theta(z_1 - z_A) \\ + \ \theta(z_2 - z_1) + \theta(z_2 - z_3) + \ldots \theta(z_2 - z_A) + \cdots + \theta(z_A - z_1) + \ldots \theta(z_A - z_{A-1}) \ . \end{aligned} \tag{26.18}$$

We can see that for every term with an argument $z_k - z_j$ there is a term with an argument $z_j - z_k$. Since

$$\theta(z_k - z_j) + \theta(z_j - z_k) = 1 \ , \tag{26.19}$$

we can equivalently write

$$\sum_k \sum_{j\neq k} \theta(z_k - z_j) t_k t_j = \sum_k \sum_{j<k} t_k t_j \ , \tag{26.20}$$

so that

$$f^{(2)}(\boldsymbol{q}) = \frac{4i\mu\pi^2}{v} \sum_k \sum_{j<k} \int d^2b \ e^{i\boldsymbol{q}\cdot\boldsymbol{b}} \Big[\int dz_k \ t_k(\boldsymbol{b}-\boldsymbol{b}_k, z - z_k)\Big] \Big[\int dz_j \ t_j(\boldsymbol{b}-\boldsymbol{b}_j, z - z_j)\Big] \tag{26.21}$$

$$= -4ik\pi^2 \int d^2b \ e^{i\boldsymbol{q}\cdot\boldsymbol{b}} \sum_k \sum_{j<k} \Gamma_k(\boldsymbol{b}-\boldsymbol{b}_k)\Gamma_j(\boldsymbol{b}-\boldsymbol{b}_j) \ . \tag{26.22}$$

where in the second equality we used the definition of the profile function, Eq. (26.12).

Repeating the same steps for higher order terms yields

$$f(\boldsymbol{q}) = 4ik\pi^2 \int d^2b \ e^{i\boldsymbol{q}\cdot\boldsymbol{b}} \Big[\sum_j \Gamma_j - \sum_k \sum_{j<k} \Gamma_k\Gamma_j + \sum_l \sum_{k<l} \sum_{j<k} \Gamma_l\Gamma_k\Gamma_j - \ldots \Big] \ , \tag{26.23}$$

where the summation in the bracket can be also written as a product of profile functions,

$$f(\boldsymbol{q}) = 4ik\pi^2 \int d^2b \; e^{i\boldsymbol{q}\cdot\boldsymbol{b}} \Big[1 - \prod_{j=1}^{A} \Big[1 - \Gamma_j(\boldsymbol{b} - \boldsymbol{b}_j) \Big] \Big] \; . \tag{26.24}$$

At this point we define the *Glauber S-matrix*,

$$S(\boldsymbol{b}; \boldsymbol{b}_1, \ldots, \boldsymbol{b}_A) \equiv \prod_{j=1}^{A} \Big[1 - \Gamma_j(\boldsymbol{b} - \boldsymbol{b}_j) \Big] \tag{26.25}$$

and with this we obtain the Glauber amplitude,

$$f(\boldsymbol{q}) = 4ik\pi^2 \int d^2b \; e^{i\boldsymbol{q}\cdot\boldsymbol{b}} \big[1 - S(\boldsymbol{b}) \big] \; . \tag{26.26}$$

The product form of $S(\boldsymbol{b})$, Eq. (26.25), makes it particularly clear that the effects of interactions with successive nucleons multiply in the S-matrix or, equivalently, that their eikonal phases add up. With this insight, it also customary to write

$$S(\boldsymbol{b}) \equiv e^{i\chi(\boldsymbol{b})} \; , \tag{26.27}$$

where the function $\chi(\boldsymbol{b})$ is the eikonal function, for obvious reasons also called the *eikonal phase*.

For small scattering angles and elastic scattering, we have

$$\boldsymbol{q} \cdot \boldsymbol{b} \approx qb \cos\phi \; , \tag{26.28}$$

where ϕ is the angle between $\boldsymbol{b}$ and the projection of $\boldsymbol{q}$ onto the transverse plane[5]. Furthermore, for elastic scattering we can use the relationship between the momentum transfer and the scattering angle, Eq. (12.51), which allows us to further approximate

$$qb \cos\phi \approx 2kb \sin\frac{\theta}{2} \cos\phi \; . \tag{26.29}$$

With this and using the representation of the Glauber S-matrix from Eq. (26.27), the Glauber scattering amplitude, Eq. (26.26), becomes

$$f(\boldsymbol{q}) = -4ik\pi^2 \int db \; b \int d\phi \; e^{2ikb \sin\frac{\theta}{2} \cos\phi} \big[e^{i\chi(\boldsymbol{b})} - 1 \big] \; . \tag{26.30}$$

If $\chi(\boldsymbol{b})$, and therefore the underlying potential, is azimuthally symmetric, then we can carry out the integration over ϕ using

$$\int_0^{2\pi} d\phi \; e^{i\lambda\cos\phi} = 2\pi J_0(\lambda) \; , \tag{26.31}$$

arriving at

$$f(\boldsymbol{q}) = -8ik\pi^3 \int db \; b \; J_0\Big(2kb \sin\frac{\theta}{2} \Big) \big[e^{i\chi(\boldsymbol{b})} - 1 \big] \; . \tag{26.32}$$

[5] In principle, what should enter this relationship is not q, but the projection of q onto the transverse plane $q_\perp$. However, for small scattering angles the momentum transfer is almost entirely transverse. Indeed, for a scattering angle θ we can write $\boldsymbol{k}_f = k\sin\theta\;\hat{\boldsymbol{x}} + k\cos\theta\;\hat{\boldsymbol{z}}$, so that $\boldsymbol{q} = k(1-\cos\theta)\;\hat{\boldsymbol{z}} - k\sin\theta\;\hat{\boldsymbol{x}}$. Since $\sin x$ is of the first order in x while $\cos x$ is of the second order, the transverse contribution to $\boldsymbol{q}$ dominates at small angles, so that $\boldsymbol{q} \approx \boldsymbol{q}_\perp$ is a good approximation.

26.2 Alternative derivation

The following is an alternative derivation of the Glauber scattering amplitude. If contrast to the treatment based on the T-matrix, presented above, the approach below uses mostly concepts from wave mechanics.

As we have shown above, the outcomes of multiple scatterings for a fast projectile which moves in a straight line and propagates freely between collisions can be reorganized by summing their cumulative effect along the trajectory of the projectile. These cumulative effects can always be expressed by means of the phase of the wavefunction. This suggest that one can write the full wavefunction as a product of a plane wave and a *modulation function*,

$$\Psi^{(+)}(\boldsymbol{r}) = e^{i\boldsymbol{k}\cdot\boldsymbol{r}}\rho(\boldsymbol{r}) \ , \tag{26.33}$$

where the plane wave describes the free propagation while $\rho(\boldsymbol{r})$ encodes the effect of the interaction. Note that the above form can be also written as

$$\Psi^{(+)}(\boldsymbol{r}) = e^{i\boldsymbol{k}\cdot\boldsymbol{r}}\rho(\boldsymbol{r}) \sim e^{i\left(\boldsymbol{k}\cdot\boldsymbol{r}+\chi(\boldsymbol{r})\right)} \ . \tag{26.34}$$

This *ansatz* for the form of the wavefunction is often what is literally meant by the *eikonal approximation*.

To see where this assumption leads formally, let us consider the coordinate-space Lippmann–Schwinger equation, Eq. (12.8), repeated here with the explicit expression for the Green function, Eq. (12.2), and explicitly writing out the plane wave $\Phi_{\boldsymbol{k}}(\boldsymbol{r})$,

$$\Psi^{(+)}_{\boldsymbol{k}}(\boldsymbol{r}) = e^{i\boldsymbol{k}\cdot\boldsymbol{r}} - \frac{\mu}{2\pi}\int d\boldsymbol{r}' \ \frac{e^{ik|\boldsymbol{r}-\boldsymbol{r}'|}}{|\boldsymbol{r}-\boldsymbol{r}'|}V(\boldsymbol{r}')\Psi^{(+)}_{\boldsymbol{k}}(\boldsymbol{r}') \ . \tag{26.35}$$

Inserting the eikonal approximation, Eq. (26.33), and multiplying by $e^{-i\boldsymbol{k}\cdot\boldsymbol{r}}$ yields an equation for the modulation function $\rho(\boldsymbol{r})$,

$$\rho(\boldsymbol{r}) = 1 - \frac{\mu}{2\pi}\int d\boldsymbol{r}' \ \frac{e^{ik|\boldsymbol{r}-\boldsymbol{r}'|}}{|\boldsymbol{r}-\boldsymbol{r}'|}e^{-i\boldsymbol{k}\cdot(\boldsymbol{r}-\boldsymbol{r}')}V(\boldsymbol{r}')\rho(\boldsymbol{r}') \ . \tag{26.36}$$

To evaluate this integral, we make the substitution

$$\boldsymbol{u} = \boldsymbol{r} - \boldsymbol{r}' \tag{26.37}$$

so that $d\boldsymbol{r}' = d\boldsymbol{u}$, yielding

$$\rho(\boldsymbol{r}) = 1 - \frac{\mu}{2\pi}\int d\boldsymbol{u} \ \frac{e^{iku}}{u}e^{-i\boldsymbol{k}\cdot\boldsymbol{u}}V(\boldsymbol{r}-\boldsymbol{u})\rho(\boldsymbol{r}-\boldsymbol{u}) \ . \tag{26.38}$$

Expressing $\boldsymbol{u}$ in spherical coordinates, remembering that the z-axis is aligned with $\boldsymbol{k}$ so that $\boldsymbol{k}\cdot\boldsymbol{u} = ku\cos\theta$, yields

$$\rho(\boldsymbol{r}) = 1 - \frac{\mu}{2\pi}\int_0^\infty du \ u^2 \int_{-1}^{+1} d(\cos\theta) \ \int_0^{2\pi} d\phi \ \frac{e^{iku(1-\cos\theta)}}{u}V(\boldsymbol{r}-\boldsymbol{u})\rho(\boldsymbol{r}-\boldsymbol{u}) \ . \tag{26.39}$$

Noting

$$\frac{e^{iku(1-\cos\theta)}}{u} = -\frac{d}{d\cos\theta}\frac{e^{iku(1-\cos\theta)}}{iku^2} \tag{26.40}$$

leads to

$$\rho(\boldsymbol{r}) = 1 + \frac{\mu}{2\pi}\int_0^\infty du\ u^2 \int_{-1}^{+1} d(\cos\theta)\ \int_0^{2\pi} d\phi\ \left[\frac{d}{d\cos\theta}\frac{e^{iku(1-\cos\theta)}}{iku^2}\right] V(\boldsymbol{r}-\boldsymbol{u})\rho(\boldsymbol{r}-\boldsymbol{u})\ , \quad (26.41)$$

which allows us to perform integration by parts with respect to $\cos\theta$,

$$\rho(\boldsymbol{r}) = 1 + \frac{\mu}{2\pi}\int_0^\infty du\ u^2\ \int_0^{2\pi} d\phi\ \left(\left[\frac{e^{iku(1-\cos\theta)}}{iku^2} V(\boldsymbol{r}-\boldsymbol{u})\rho(\boldsymbol{r}-\boldsymbol{u})\right]_{\cos\theta=-1}^{\cos\theta=+1}\right. \quad (26.42)$$

$$\left. - \int_{-1}^{+1} d\cos\theta\ \frac{e^{iku(1-\cos\theta)}}{iku^2}\frac{d}{d\cos\theta} V(\boldsymbol{r}-\boldsymbol{u})\rho(\boldsymbol{r}-\boldsymbol{u})\right)\ . \quad (26.43)$$

26.2.1 Order of magnitude considerations

At this point we discuss the relative magnitude of terms in the above equation. In the high energy limit, we can expect the product $V(\boldsymbol{r}')\rho(\boldsymbol{r}')$ to vary slowly within a distance of the order of the wavelength $1/k$[6], which allows us to claim that contributions to the integral from regions in which the exponential varies rapidly are small[7]. Conversely, contributions to the integral will be largest for $\boldsymbol{r}'$ such that $e^{iku(1-\cos\theta)}$ is almost stationary. This can be achieved, in particular, if the argument of the exponential is zero, which takes place for $\cos\theta = 1$. With this, we can safely approximate that only the boundary term corresponding to $\cos\theta = 1$ contributes substantially to the final result, while the term corresponding to $\cos\theta = -1$ oscillates rapidly with u and therefore contributes only subdominantly after the remaining u-integration, which simplifies the first term in the above equation,

$$\rho(\boldsymbol{r}) \approx 1 + \frac{\mu}{2\pi}\int_0^\infty du\ u^2\ \int_0^{2\pi} d\phi\ \left(\frac{1}{iku^2} V(\boldsymbol{r}-\boldsymbol{u})\rho(\boldsymbol{r}-\boldsymbol{u})\right. \quad (26.44)$$

$$\left. - \int_{-1}^{+1} d\cos\theta\ \frac{e^{iku(1-\cos\theta)}}{iku^2}\frac{d}{d\cos\theta} V(\boldsymbol{r}-\boldsymbol{u})\rho(\boldsymbol{r}-\boldsymbol{u})\right)\ . \quad (26.45)$$

To size up the second term, which still involves integration over $\cos\theta$, let us note that the phase of the oscillatory term, $ku(1-\cos\theta)$, is nearly stationary when

$$\frac{d}{d\theta}\big[iku(1-\cos\theta)\big] = iku\sin\theta = 0 \quad \Rightarrow \quad \sin\theta = 0 \quad \Rightarrow \quad \theta = 0 \quad \text{or} \quad \theta = \pi\ . \quad (26.46)$$

Since $\theta = \pi$ leads to e^{2iku}, which oscillates rapidly with u, we see that the integral has the largest support near $\theta = 0$. Over what region does this support extend? The phase of the exponential changes by an amount of order unity when

$$ku\Delta(\cos\theta) \sim 1\ , \quad (26.47)$$

so that the range of $\cos\theta$ over which the exponential is *not* rapidly oscillating is

$$\Delta(\cos\theta) \sim \frac{1}{ku}\ . \quad (26.48)$$

[6] Simply because that distance is short.

[7] The logic here is that if the product $V(\boldsymbol{r}')\rho(\boldsymbol{r}')$ was instead rapidly varying, it would amplify contributions at different phases of the exponential differently, therefore perhaps yielding a non-zero result. Alas, if we assume that $V(\boldsymbol{r}')\rho(\boldsymbol{r}')$ is nearly constant (*i.e.*, slowly varying over the relevant scale), then the contributions from different phases of the exponential integrate to zero.

Next, if R denotes the characteristic length over which the product $V\rho$ varies, then varying $\cos\theta$ by an order of unity changes the argument $\boldsymbol{r}-\boldsymbol{u}$ by an amount of order u, so that one can estimate

$$\frac{d}{d(\cos\theta)}\Big[V(\boldsymbol{r}-\boldsymbol{u})\rho(\boldsymbol{r}-\boldsymbol{u})\Big] \sim \frac{u}{R}V(\boldsymbol{r}-\boldsymbol{u})\rho(\boldsymbol{r}-\boldsymbol{u}) \ . \tag{26.49}$$

This allows us to estimate the relative change in the product over the narrow interval $\Delta\theta$,

$$\frac{\Delta(V\rho)}{V\rho} \sim \frac{u}{R}\Delta\theta \sim \frac{1}{kR} \ , \tag{26.50}$$

where in the second proportionality we used Eq. (26.48). As a result, in the high-energy regime – where $kR \gg 1$ – the product $V\rho$ is essentially constant over the part of the $\cos\theta$ integration which contributes appreciably. Moreover, by comparison with the remaining part of the boundary term from integration by parts, it is evident that the remaining integral is also suppressed by a factor of $1/(kR)$ with respect to that term. Therefore, we can now write

$$\rho(\boldsymbol{r}) \approx 1 + \frac{\mu}{2\pi}\int_0^\infty du\ u^2 \int_0^{2\pi} d\phi\ \frac{1}{iku^2}V(\boldsymbol{r}-\boldsymbol{u})\rho(\boldsymbol{r}-\boldsymbol{u}) \tag{26.51}$$

$$= 1 - \frac{i}{v}\int_0^\infty du\ V(\boldsymbol{r}-\boldsymbol{u})\rho(\boldsymbol{r}-\boldsymbol{u}) \ , \tag{26.52}$$

where we used $v = k/\mu$ (in natural units). Since we argued that the vector $\boldsymbol{u}$ must be close to parallel with $\boldsymbol{k}$ for non-zero contributions to the expression above, we can also rewrite it as

$$\rho(\boldsymbol{r}) = 1 - \frac{i}{v}\int_0^\infty du\ V(\boldsymbol{r}-\hat{\boldsymbol{k}}u)\rho(\boldsymbol{r}-\hat{\boldsymbol{k}}u) \ . \tag{26.53}$$

Note that the above equation means that the value of ρ at $\boldsymbol{r}$ depends only on the values of the potential along a straight line parallel to the beam direction $\hat{\boldsymbol{k}}$ and passing through $\boldsymbol{r}$. This is exactly what we want in the eikonal approximation, where we approximate the motion of the projectile throughout the scattering event with a straight line.

26.2.2 Solving for ρ

To exploit the structure of the argument in Eq. (26.53), we divide the position $\boldsymbol{r}$ into the beam-direction and transverse components,

$$\boldsymbol{r} = \boldsymbol{b} + z\hat{\boldsymbol{k}} \ . \tag{26.54}$$

With this,

$$\boldsymbol{r}-\boldsymbol{u} = \boldsymbol{b} + (z-u)\hat{\boldsymbol{k}} \ . \tag{26.55}$$

Further denoting $z' = z-u$, we can change the integration variable in Eq. (26.53), obtaining

$$\rho(\boldsymbol{b},z) = 1 - \frac{i}{v}\int_{-\infty}^{z} dz'\ V(\boldsymbol{b},z')\rho(\boldsymbol{b},z') \ . \tag{26.56}$$

Differentiating the above equation with respect to z yields

$$\frac{d\rho(\boldsymbol{b},z)}{dz} = -\frac{i}{v}V(\boldsymbol{b},z)\rho(\boldsymbol{b},z) \ , \tag{26.57}$$

which can be put into a separable form,

$$\frac{1}{\rho(\boldsymbol{b},z)}\frac{d\rho(\boldsymbol{b},z)}{dz} = -\frac{i}{v}V(\boldsymbol{b},z)\ . \tag{26.58}$$

This we can now integrate from $-\infty$ to z, which – with the boundary condition $\rho(\boldsymbol{b},-\infty)=1$, yields

$$\ln\rho(\boldsymbol{b},z) = -\frac{i}{v}\int_{-\infty}^{z} dz'\ V(\boldsymbol{b},z')\ , \tag{26.59}$$

or equivalently

$$\rho(\boldsymbol{b},z) = \exp\left[-\frac{i}{v}\int_{-\infty}^{z} dz'\ V(\boldsymbol{b},z')\right]\ . \tag{26.60}$$

With the modulation function known, the eikonal wavefunction, Eq. (26.33), can be also written as

$$\Psi^{(+)}(\boldsymbol{r}) \approx \exp\left[i\boldsymbol{k}\cdot\boldsymbol{r} - \frac{i}{v}\int_{-\infty}^{z} dz'\ V(\boldsymbol{b},z')\right]\ . \tag{26.61}$$

26.2.3 Scattering amplitude

We now use the formal expression for the scattering amplitude[8], Eq. (12.44), which we transform from braket notation to the coordinate representation by inserting two resolutions of identity,

$$f(\theta,\phi) = -4\mu\pi^2\left\langle\Phi_{\boldsymbol{k}'}\middle|\hat{V}\middle|\Psi^{(+)}_{\boldsymbol{k}}\right\rangle \tag{26.62}$$

$$= -4\mu\pi^2\int d^3r\int d^3r'\ \langle\Phi_{\boldsymbol{k}'}|\boldsymbol{r}\rangle\left\langle\boldsymbol{r}\middle|\hat{V}\middle|\boldsymbol{r}'\right\rangle\left\langle\boldsymbol{r}'\middle|\Psi^{(+)}_{\boldsymbol{k}}\right\rangle \tag{26.63}$$

$$= -4\mu\pi^2\int d^3r\ e^{-i\boldsymbol{k}'\cdot\boldsymbol{r}}V(\boldsymbol{r})\Psi^{(+)}_{\boldsymbol{k}}(\boldsymbol{r})\ , \tag{26.64}$$

where we used the fact that the potential is local, $V(\boldsymbol{r},\boldsymbol{r}')=V(\boldsymbol{r})\delta^3(\boldsymbol{r}-\boldsymbol{r}')$. The advantage of an approach such as the eikonal approximation is that it provides the form of $\Psi^{(+)}_{\boldsymbol{k}}$ to be used. With the eikonal wavefunction *ansatz*, Eq. (26.33), the scattering amplitude becomes

$$f(\theta,\phi) = -4\mu\pi^2\int d^3r\ e^{i(\boldsymbol{k}-\boldsymbol{k}')\cdot\boldsymbol{r}}V(\boldsymbol{r})\rho(\boldsymbol{r}) \tag{26.65}$$

$$= -4\mu\pi^2\int db\ b\int d\phi\int dz\ e^{i(\boldsymbol{k}-\boldsymbol{k}')\cdot(\boldsymbol{b}+\hat{\boldsymbol{k}}z)}V(\boldsymbol{b}+\hat{\boldsymbol{k}}z)\rho(\boldsymbol{b}+\hat{\boldsymbol{k}}z)\ , \tag{26.66}$$

where in the second equality we introduced the convenient division into the *longitudinal* (*i.e.*, aligned with the beam axis) and *transverse* (*i.e.*, perpendicular to the beam axis) components. For small scattering angles, we have

$$(\boldsymbol{k}-\boldsymbol{k}')\cdot\hat{\boldsymbol{k}} \approx 0\ , \tag{26.67}$$

since the momentum transfer is almost entirely transverse. Then the remaining dot product, $(\boldsymbol{k}-\boldsymbol{k}')\cdot\boldsymbol{b}$, can be approximated as in Eq. (26.29), so that the scattering amplitude, Eq. (26.66), becomes

$$f(\theta,\phi) = -4\mu\pi^2\int db\ b\int d\phi\ e^{i2kb\sin\frac{\theta}{2}\cos\phi}\int dz\ V(\boldsymbol{b}+\hat{\boldsymbol{k}}z)\rho(\boldsymbol{b}+\hat{\boldsymbol{k}}z)\ . \tag{26.68}$$

[8] Where we still have some normalization issues, to be resolved at an opportune time.

We can express the product $V\rho$ as a derivative using Eq. (26.57), leading to

$$f(\theta,\phi) = -4ik\pi^2 \int db\ b \int d\phi\ e^{i2kb\sin\frac{\theta}{2}\cos\phi} \int dz\ \frac{d\rho}{dz} \tag{26.69}$$

$$= -4ik\pi^2 \int db\ b \int d\phi\ e^{i2kb\sin\frac{\theta}{2}\cos\phi} \Big[\rho(\boldsymbol{b},z)\Big]_{-\infty}^{\infty} \tag{26.70}$$

$$= -4ik\pi^2 \int db\ b \int d\phi\ e^{i2kb\sin\frac{\theta}{2}\cos\phi} \Big[e^{i\chi(b)} - 1\Big]\ , \tag{26.71}$$

where we used the explicit form of the modulation function, Eq. (26.60), that allows us to identify an explicit expression for the eikonal function,

$$\chi(b) = -\frac{1}{v}\int_{-\infty}^{\infty} dz\ V(\boldsymbol{b} + \hat{\boldsymbol{k}}z)\ . \tag{26.72}$$

The above expression for the scattering amplitude is now identical to the one obtained in Eq. (26.30), so that assuming azimuthal symmetry again leads to the final expression for the Glauber scattering amplitude, Eq. (26.32).

Note that the expression for the eikonal function obtained above, Eq. (26.72), is directly related to the profile function, defined in Eq. (26.12), if one applies the Born approximation to the $\hat{t}$ operator, *i.e.*, if one takes $\hat{t}^{+}_{(j)} = \hat{U}_j$ in the corresponding Lippmann-Schwinger relation, Eq. (25.6). Therefore[9], the simple local expression for $\chi(b)$, Eq. (26.72), should be understood as the Born limit of the more general derivation carried out in Sec. 26.1 where he profile function is defined through the full two-body transition operator rather than directly through the potential.

26.3 Applications of the eikonal approximation

Let us now briefly illustrate how the eikonal formalism can be used in practice. In the high-energy, forward-scattering regime, the dynamics reduces to the evaluation of the eikonal phase,

$$\chi(b) = -\frac{1}{v}\int_{-\infty}^{\infty} dz\ V(\boldsymbol{b},z)\ , \tag{26.73}$$

from which observables follow directly through the Glauber scattering amplitude, Eq. (26.32).

26.3.1 Elastic proton-nucleus scattering

First, let us consider elastic scattering of a high-energy proton from a nucleus. In this case, the interaction can be described by a (spherically symmetric) optical potential $V(r)$ (see Sec. 18.3) or, at sufficiently high energies, in terms of the nuclear density folded with an effective proton-nucleon interaction. This is analogous to the PWIA, where the scattering amplitude, Eq. (25.43), becomes sensitive to the Fourier transform of the nuclear form factor. The eikonal phase becomes

$$\chi(b) = -\frac{1}{v}\int_{-\infty}^{\infty} dz\ V\big(\sqrt{b^2+z^2}\big)\ , \tag{26.74}$$

which depends only on the transverse distance b from the center of the target, and with this the scattering amplitude, Eq. (26.32), becomes a function of magnitude but not the direction of $\boldsymbol{q}$,

$$f(q) = -8ik\pi^3 \int db\ b\ J_0\left(2kb\sin\frac{\theta}{2}\right)\Big[e^{i\chi(b)} - 1\Big]\ . \tag{26.75}$$

[9] As should be expected anytime one arrives at a simple and intuitive relation.

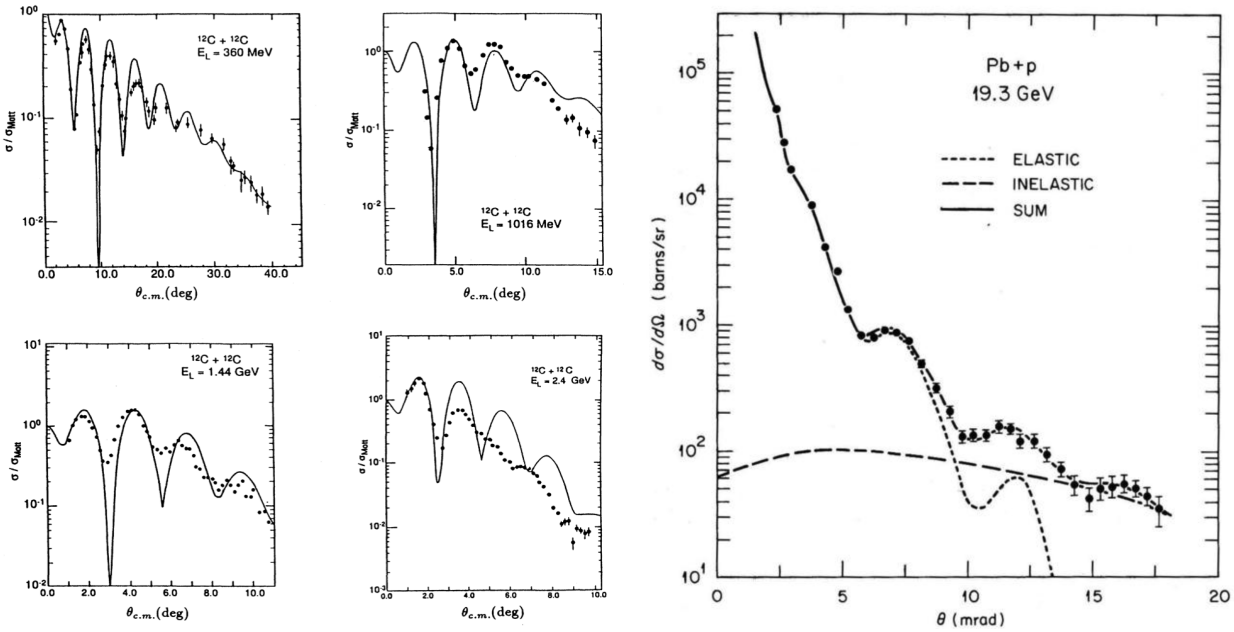

Figure 26.1: *Left:* Angular distribution for elastic scattering of ^{12}C and ^{12}C at a series of projectile energies: 360, 1016, 1440, and 2400 MeV/nucleon. The decrease in performance of the eikonal approximation beyond the very forward angles for large energies is postulated to signal the importance of in-medium cross sections in high-energy collisions. Figure from Ref. [48]. *Right:* Differential cross section for scattering of 19.3-GeV protons off ^{208}Pb. Note that the angle is measured in miniradians (mrad), where 1 mrad = 0.0573°. Figure from Ref. [7].

Let us use this occasion analyze the above formula. First of all, it is evident that the scattering amplitude is built from different impact parameters b, where each value of b corresponds to a projectile trajectory passing the nucleus at a different transverse distance from its center. The factor $J_0(qb)$ then tells us how contributions from different impact parameters interfere at a given momentum transfer q. Thus the angular distribution is sensitive to the transverse size and shape of the target. A larger nucleus has important contributions out to larger b, which shifts the diffraction minima to smaller momentum transfer. The detailed falloff of $S(b) = e^{i\chi(b)}$ near the nuclear surface controls how sharp or diffuse the edge of the target appears, and therefore affects the forward-angle slope of the cross section.

Examples of elastic reactions described within the eikonal approximation are shown in Fig. 26.1.

26.3.2 Nucleon removal reactions

A second important application is high-energy nucleon removal, where a fast projectile, consisting of a core c and a valence nucleon n, collides with a target. In the Glauber approximation, the projectile continues to move past the target on an approximately straight trajectory. During the interaction with the target, each constituent of the projectile is described by its own Glauber S-matrix,

$$S_c(\boldsymbol{b}_c) = e^{i\chi_c(\boldsymbol{b}_c)} \quad \text{and} \quad S_n(\boldsymbol{b}_n) = e^{i\chi_n(\boldsymbol{b}_n)} \ , \tag{26.76}$$

where $\boldsymbol{b}_c$ and $\boldsymbol{b}_n$ are impact parameters of the core and the valence nucleon, respectively. We can identify

$$|S_c(\boldsymbol{b}_c)|^2 \quad \text{and} \quad |S_n(\boldsymbol{b}_n)|^2 \tag{26.77}$$

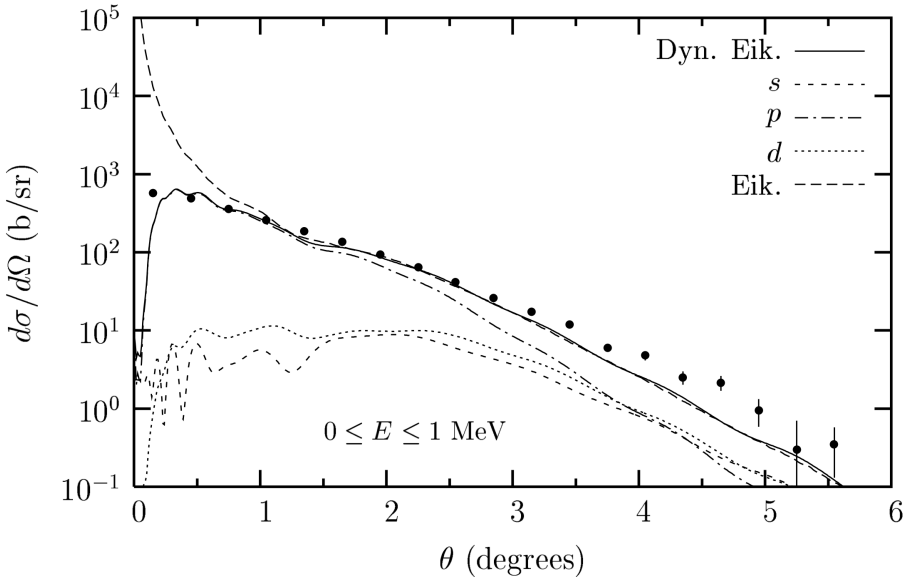

Figure 26.2: Angular distribution for the breakup reaction $^{11}\mathrm{Be} + {}^{208}\mathrm{Pb} \to {}^{10}\mathrm{Be} + n + {}^{208}\mathrm{Pb}$ at 69 MeV/nucleon. The eikonal approximation calculations are shown with a long-dashed line. The range $0 \leq E \leq 1$ MeV refers to the kinetic energy associated with the relative motion of ^{10}Be and the neutron after breakup. Figure from Ref. [50].

as *survival probabilities*, *i.e.*, probabilities that the corresponding constituent passes the target *without* being absorbed or undergoing an inelastic interaction with the target[10].

Note that stripping is an effective three-body problem: it involves the core, the valence nucleon, and the target nucleus. A general derivation of an inelastic stripping cross section, performed in Ref. [49], indeed reduces the many-body projectile-target system to an effective three-body system by using the *spectator approximation*, *i.e.*, assuming that the core of the nucleus is at most scattered elastically. In this case, it can be shown that the cross section for the stripping reaction is in general given by

$$\sigma_{\mathrm{str}} = \int d^2b \int d^3r \; |\xi_n(\boldsymbol{r})|^2 |S_c(\boldsymbol{b}_c)|^2 \left[1 - |S_n(\boldsymbol{b}_n)|^2\right] , \tag{26.78}$$

where $\xi_n(\boldsymbol{r})$ is the wavefunction of the removed nucleon relative to the core. The above formula explicitly shows that the cross section corresponds to the absorption of the valence nucleon while the core survives. The matrix elements $S_c(\boldsymbol{b}_c)$ and $S_n(\boldsymbol{b}_n)$ can be computed using the eikonal approximation, while the nucleon wavefunction is obtained from a chosen model of halo nucleus structure. Because the reaction effectively probes the spatial distribution of the nucleon inside the projectile, eikonal-based analyses are widely used to extract spectroscopic information and to study weakly-bound systems, such as halo nuclei.

A similar approach can be used for other nucleon removal reactions such as breakup. Figure 26.2 shows a comparison of two calculations, including the standard eikonal approximation to experimental data for the breakup reaction $^{11}\mathrm{Be} + {}^{208}\mathrm{Pb} \to {}^{10}\mathrm{Be} + n + {}^{208}\mathrm{Pb}$. The eikonal approximation describes the data well with the exception of very small angles at which it diverges.

[10] This can be argued on a similar basis as used in Sec. 16.2 to derive the elastic and absorption cross sections: as discussed there, $S_l(k)$ is the coefficient of the outgoing elastically-scattered (partial) wave, and so $|S_l(k)|^2$ is the probability that this partial wave remains in the elastic channel.

26.4 Comparison with DWBA and WKB

As we have just seen, the eikonal approximation replaces full three-dimensional propagation by evolution along a straight-line path at fixed transverse coordinate, reducing the problem to a two-dimensional integral over the impact parameter. It is controlled by the condition $kR \gg 1$ and is therefore appropriate for high-energy, forward scattering, where deflections are small but multiple interactions can still accumulate. In this regime, it provides a *non-perturbative resummation of multiple interactions along the trajectory*, encoded in the phase $e^{i\chi(b)}$.

Note that in contrast, the DWBA treats the interaction *perturbatively* (typically to first order), while the propagation is described by distorted waves. As a result, the eikonal approximation is more appropriate when the interaction is not weak but the kinematics is simple (high energy, forward scattering), whereas DWBA is better suited for reactions where specific transition matrix elements and angular-momentum couplings are important.

You may notice that the eikonal wavefunction *ansatz*, Eq. (26.33), bears similarities to the WKB approximation, which we discussed in Secs. 6.3, 20.3, and 20.4. Indeed, the WKB condition that the potential varies slowly can be expressed as the requirement that the de Broglie wavelength be small compared to the scale over which the potential changes, *i.e.*, $kR \gg 1$. In scattering problems, this is naturally satisfied at high energies, where the wavelength is short. The eikonal approximation can therefore be viewed as the high-energy limit of WKB in which the additional assumption of small deflections allows one to approximate the trajectories as straight lines.

Lecture sources: This lecture is based on Jackson [4] and an extended interaction with `ChatGPT` and `Claude` to derive the eikonal approximation from the multiple scattering series.

Homework 1

1.

What is the type, the Q-value, and the kinematic threshold for the following reactions?

a. ^{14}N(α,p)^{17}O (the first "nuclear transmutation" observed in the lab – Rutherford, 1919)

b. ^{11}B(d,α)^{9}Be

c. ^{7}Li(p,n)^{7}Be

d. ^{9}Be(α,n)^{12}C (reaction which led to the discovery of the neutron – Chadwick, 1932)

e. ^{9}Be(α,n)^{12}B

f. ^{238}U(n,γ)^{239}U (led to the first artificial element, ^{239}Np, *via* a subsequent β-decay – McMillan & Abelson, 1940)

g. ^{244}Pu(^{48}Ca,3n)^{289}Fl (used to produce super-heavy element ^{289}Fl, discussed in this week's Nuclear Science Seminar by Dr. Patrick Steinegger)

You may use m(p) = 1.007277 u, m(n) = 1.008665 u, m(d) = 2.013553 u, $m(\alpha)$ = 4.001506 u, $m(^{7}\text{Li})$ = 7.014907 u, $m(^{7}\text{Be})$ = 7.016930 u, $m(^{9}\text{Be})$ = 9.009987 u, $m(^{11}\text{B})$ = 11.006562 u, $m(^{12}\text{C})$ = 11.996709 u, $m(^{12}\text{B})$ = 12.01161 u, $m(^{14}\text{N})$ = 13.999234 u, $m(^{17}\text{O})$ = 16.994742 u, $m(^{48}\text{Ca})$ = 47.9416 u, $m(^{238}\text{U})$ = 238.050788 u, $m(^{239}\text{U})$ = 239.054293 u, $m(^{244}\text{Pu})$ = 244.0126 u, $m(^{289}\text{Fl})$ = 289.1279 u, along with the conversion factor 1 u = 931.494 MeV.

2.

The differential cross section $\frac{d\sigma(\Omega)}{d\Omega}$ depends on the reference frame. Assuming non-relativistic kinematics, derive an expression connecting the lab-frame cross section, $\frac{d\sigma(\Omega_{\text{lab}})}{d\Omega_{\text{lab}}}$, with the center-of-mass cross section, $\frac{d\sigma(\Omega_{\text{cm}})}{d\Omega_{\text{cm}}}$. What angular dependence should one expect to see in the lab frame for a process between two identical particles whose differential cross section in the CM frame is isotropic?

3.

Consider a reaction A(a,b)B. Assume A and B are heavy; A is at rest before the reaction takes place and B does not leave the target, so that we only measure the energy and momentum of b. How does the energy threshold for the reaction depend on the scattering angle of b?

4.

Let us revisit In-class Activity 2a, where we considered a reaction A(a,b)B in which $Q < 0$.
(a) What is the threshold laboratory frame kinetic energy of the projectile required for the reaction to take place? In your calculations, use the square of the invariant mass $M^2_{\rm inv}$, also known as the Lorentz invariant Mandelstam s variable, defined through

$$M^2_{\rm inv} \equiv s \equiv P_\mu P^\mu \ ,$$

where P^μ is the total four-momentum of the system.
(b) Now consider neutral pion production in proton-proton scattering. Check your result against the data shown in the right panel of Fig. 2.2. You will need $m_p \approx 940$ MeV and $m_\pi \approx 140$ MeV.

5.

A nucleus is unbound if its lowest-energy configuration lies above at least one particle-emission threshold so that it cannot exist as a bound state and decays promptly by particle emission. An unbound ground state of ^{28}F and an unbound excited state of ^{27}F were first observed at NSCL [1,2], where the ^{27,28}F states were populated by nucleon removal from a beam of ^{29}Ne.

a. The beam of ^{29}Ne was produced by impinging a beam of ^{48}Ca at 140 MeV/u on a ^{9}Be production target, where the products of the calcium on beryllium reaction were sent through the A1900 fragment separator. The fragment separator was optimized to the transmission of a fully ionized ^{29}Ne at $E_{\rm kin} = 62$ MeV/u. What was the corresponding magnetic rigidity $B\rho$?

b. Unbound nuclei are extremely short-lived so that only their decay products can be observed. In the case of ^{28}F, one observes the final fragments ^{27}F and n. Given the measured energies and momenta of ^{27}F and n, calculate the invariant mass $M_{\rm inv}$ of the mother nucleus. Show, assuming that only one state contributes to the measured $M_{\rm inv}$, that the difference between the invariant mass and the masses of the final decay products is equal to the excess of the state's energy E^* over the neutron separation energy, $S_n = m(^{27}\text{F}) + m(\text{n}) - m(^{28}\text{F})$.

c. Bonus question: How big of a mistake would you make if you *didn't* use relativistic formulae?

[1] G. Christian *et al.*, Phys.Rev.C 85 (2012) 034327, arXiv:1203.1369.
[2] G. Christian *et al.*, Phys.Rev.Lett. 108 (2012) 032501, arXiv:1201.1267.

6.

In the quantum-mechanical treatment of the hydrogen atom, angular momentum plays a key role. Review the derivation, explicit forms of involved operators, and eigenfunctions along with the corresponding eigenvalues. Summarize the most important features, steps, or outcomes in a short write-up (about 2 pages long).

7. (Optional)

The fundamental property of the Lorentz transformation $\Lambda^\mu_{\ \nu}$ is that it must *preserve the metric*. In other words, we demand that

$$g_{\rho\sigma} x'^\rho x'^\sigma = g_{\mu\nu} x^\mu x^\nu \ ,$$

or, equivalently and in the matrix notation, $\Lambda^{\rm T} g \Lambda = g$. Based on this property alone, consider a Lorentz boost along the x axis and derive the form of the Lorentz transformation in the Minkowski spacetime, Eq. (4.18). How can one obtain the Lorentz transformation in any direction?

Homework 2

1.

We have covered a lot of theory in the last couple of weeks. Since this foundation will be repeatedly used in the remainder of the semester, it is extremely important that you review and are (operationally) comfortable with this material. To this end, prepare a 1-page cheat sheet of key formulas, properties, and things to remember from Lectures 6-9.

2.

(a) We have talked and will talk a lot about incoming and outgoing solutions. How can you show whether a spherical wave is incoming or outgoing?
(b) The Haenkel functions, Eq. (7.32), are one of the several choices for complete sets of radial wavefunctions discussed in Sec. 7.3.1. Show that the Haenkel functions behave asymptotically as incoming and outgoing spherical waves.

3.

Let us visualize the asymptotic wavefunction in the Coulomb problem. Start from the Python code or the ROOT macro available on D2L under Homework 2. (Of course, you can also write your own code.) Each code plots the real part of the asymptotic Coulomb-distorted incoming plane wave.
(a) In the plots, which color corresponds to the crests and which to the troughs?
(b) How does the plot differ between repulsive and attractive potential? Explain the results.
(c) Modify the code to include the (asymptotic) scattered wave (skip the scattering amplitude). Comment on the results.
(d) The code uses random units. Adjust the code so that it describes Coulomb scattering of α particles on gold nuclei.
Hint: Many of the above questions benefit from modifying the wavevector, the strength of the potential, and/or both.

4.

The data in Fig. 1 shows the total cross section for $\pi^+ + \mathrm{p}$ scattering as a function of the pion incident energy. What is the mass and width of the resonant state? What is its lifetime?

[1] A. A. Carter *et al.*, Nucl.Phys.B 26 (1971) 445-460, https://doi.org/10.1016/0550-3213(71)90188-X.

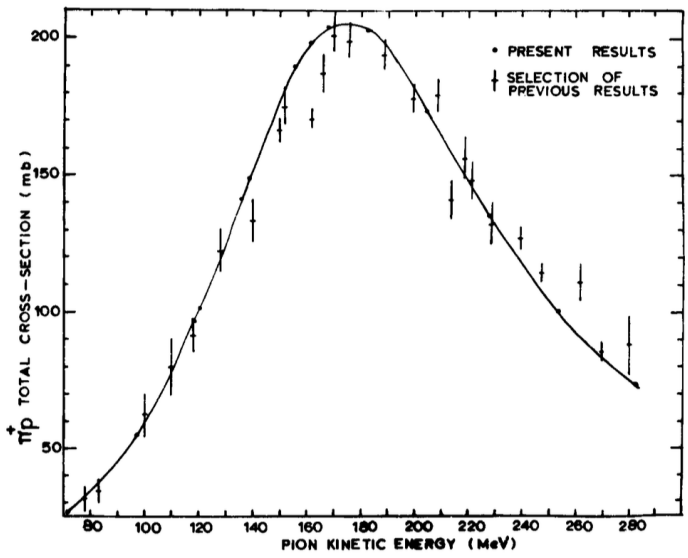

Figure 1: The π^+p total cross section. Figure from Ref. [1].

5.

Alpha particles of 8 MeV energy are scattered from a gold foil target. The back-angle cross section, $d\sigma/d\Omega(180°)$, is found to be reduced by 5% from that given by the Rutherford cross section. Assume that the reduction is caused by a short-range modification of the potential which affects only s-waves.
(a) Is the short range potential attractive or repulsive?
(b) Deduce the modification in the s-wave phase shift caused by the short range potential.
(c) What change would there be to the Rutherford result at 10%.
(d) At what angles would you expect corrections due to the atomic shielding to be important (*i.e.*, for the theory to break down)?

6. (Optional)

Show that $a = \left(d\mathcal{L}^{\mathrm{I}}/dE\right)_{E=E_\lambda}$, introduced in Eq. (9.10), is always negative.

Homework 3

1.

Assume that nucleon-nucleus elastic scattering can be described by a Gaussian potential of the form

$$V(r) = -V_0 e^{-r^2/a^2} \ .$$

(a) Use the 1st Born approximation to compute the scattering amplitude. You will need to use

$$\int_0^\infty dr\ r e^{-r^2/a^2} \sin(qr) = \frac{\sqrt{\pi}}{4} a^3 q e^{-q^2 a^2/4} \ .$$

(b) Compute and plot the differential cross section (as a function of θ).
(c) Show (analytically) that the angular distribution has width $\Gamma_\theta \sim (ka)^{-1}$. Does this agree with your plot? What does this tell you about the dependence of angular distributions on energy?

2.

How can we evaluate whether the 1st Born approximation is a reliable approach? Support your answer with analytical arguments.

3.

Consider a compound nucleus reaction.
(a) Using conservation of energy, show the relationship between the energy of the resonant state E_R, the incident neutron's energy E_n, and the neutron separation energy S_n of the compound nucleus.
(b) What prevents resonances from occurring at $E_n = 0$?

4.

(a) Consider low-energy neutron scattering. Assuming that the s-wave inside the nucleus can be approximated with e^{-iKr}, where $K = \sqrt{2\mu(E + V_0)}$ is the wavenumber inside the nucleus, show that the cross section is inversely proportional to the neutron's velocity (*the 1/v law*).
(b) Show that in the resonance region of the elastic channel, the phase shift satisfies $\tan\delta \approx \Gamma/(E - E_R)$. *Hint:* You might need to use the identity $\sin^2 x = \tan^2 x/(1 + \tan^2 x)$.
(c) Assuming 3–4 instructive values for the background phase shift $\delta_{\rm bg}$ and considering elastic scattering, plot the total phase shift, the cross section, and the "reduced" cross section, *i.e.*, a cross section divided by $4\pi/k^2$ (to remove the energy dependence).
(d) Reading off the energies and widths of several lowest resonances from Fig. 15.2, reproduce a combination of the top panels in that figure.

5.

Consider low-energy neutron scattering from a spherical nucleus described by a complex optical potential

$$U(r) = \begin{cases} -V_0 - iW_0 & r < R \ , \\ 0 & r > R \ . \end{cases}$$

Assuming $V_0 > 0$ and $W_0 > 0$, show that the scattering length is complex. What does that imply?

Homework 4

1.

Consider neutron + proton scattering in the $J = 1$ ${}^3S_1$-${}^3D_1$ *coupled channels*. Since the system can take on two angular momentum values, ${}^3S_1$ and ${}^3D_1$, it makes sense to consider the problem in terms of the angular momentum basis states, $\left|{}^3S_1\right\rangle$ and $\left|{}^3D_1\right\rangle$. In this basis, the corresponding 2×2 S-matrix block in channel space is

$$S = \begin{pmatrix} e^{2i\delta_0}\cos 2\epsilon & ie^{i(\delta_0+\delta_2)}\sin 2\epsilon \\ ie^{i(\delta_0+\delta_2)}\sin 2\epsilon & e^{2i\delta_2}\cos 2\epsilon \end{pmatrix} , \tag{1}$$

where δ_0 and δ_2 are the phase shifts for the ${}^3S_1$ and ${}^3D_1$ waves, respectively, and ϵ is a measure of mixing between the two channels[11].

(a) If the system starts in ${}^3S_1$, what is the probability to remain there and what is the probability to transition to ${}^3D_1$? Is probability conserved?

(b) What does S become in the small coupling limit, $\epsilon \to 0$?

(c) A bound state in scattering theory is associated with a strong enhancement of the scattering amplitude at a particular (negative) energy. For $\epsilon \neq 0$, can a bound state be purely ${}^3S_1$ or purely ${}^3D_1$? Why/Why not? What does this imply about the structure of the deuteron wavefunction? What are the possible experimental consequences?

2.

In the *strong absorption model*, also known as the *sharp cut-off model* or the *black-disk limit*, scattering from a strongly-absorbing nucleus is modeled by taking the S-matrix elements to be

$$S_l = \begin{cases} 0 \ , & l \leq L_0 \\ 1 \ , & l > L_0 \end{cases} .$$

Thus, partial waves with angular momentum below the cut-off value L_0 are assumed to be completely absorbed, while higher partial waves remain unaffected. In the semiclassical approximation[12], the cut-off in angular momentum corresponds to a critical impact parameter denoted as $b_c \approx R$, $L_0 + \frac{1}{2} \approx kR$, so that the model yields complete absorption for impact parameters $b \lesssim R$.

(a) Using the small angle formula, $P_l(\cos\theta) \approx J_0\left[(l+\frac{1}{2})\theta\right]$, and converting the sum over l into an integral, obtain an analytic expression for the scattering amplitude $f(\theta)$.

Hint: You will need to use the identity

$$\int_0^u du' \ u' J_0(u') = u J_1(u) \ .$$

[11] As such, it is related to the matrix element between the two partial waves.

[12] In which one identifies the quantum-mechanical angular momentum $L \approx l + \frac{1}{2}$ with the classical angular momentum $pb = kb$ (in natural units), where b is the impact parameter, so that $l + \frac{1}{2} \approx kb$.

(b) What is the differential elastic cross section? What is the total elastic cross section? Plot the differential elastic cross section as a function of the scattering angle θ.

3.

Computing the cross section within the optical model requires numerically integrating the Schrödinger equation for each considered partial wave in the region where the potential is non-zero, matching to the known asymptotic form at large r, extracting the phase shifts, and adding their contributions together.

On D2L under Homework 4, you will find a Python code for computing the differential cross section for the n + ^{56}Fe reaction. This code has been entirely generated by ChatGPT and not checked. Your task is to verify the correctness of the code.

There is no single prescription on how to do that, but you can start from a couple of "sanity checks": Check whether the formulas used are correct. Check the numerical integration procedure by feeding it a function with a known solution. Toggle several features off and on: *e.g.*, see what happens if you turn off the imaginary part of the optical potential, or if you turn off the potential altogether (what do you expect to happen?).

Only when you are convinced the code works as it should, have some fun with the optical potential parameters. How sensitive are the results to those parameters? What is the importance of the centrifugal term? How about the imaginary terms? How many partial waves contribute at a 1% level or more? How do the results change when you change the mass of the target? Produce 2-3 plots.

4. (Optional)

The form of the S-matrix in Problem 1 has not been justified, but we will do that here[13]. In the following, assume that the S-matrix is 2×2, unitary, and symmetric.

(a) Show that such a matrix depends on three real parameters.

(b) Show that it can be written in the form

$$S = O^T \begin{pmatrix} e^{2i\delta_\alpha} & 0 \\ 0 & e^{2i\delta_\beta} \end{pmatrix} O \ ,$$

where O is a real orthogonal matrix.

(c) Using

$$O = \begin{pmatrix} \cos\epsilon & \sin\epsilon \\ -\sin\epsilon & \cos\epsilon \end{pmatrix} \ ,$$

compute the matrix elements of S explicitly.

(d) Show that the result can be rewritten as

$$S = e^{i(\delta_\alpha+\delta_\beta)} \begin{pmatrix} \cos(\delta_\alpha-\delta_\beta) + i\sin(\delta_\alpha-\delta_\beta)\cos 2\epsilon & i\sin(\delta_\alpha-\delta_\beta)\sin 2\epsilon \\ i\sin(\delta_\alpha-\delta_\beta)\sin 2\epsilon & \cos(\delta_\alpha-\delta_\beta) - i\sin(\delta_\alpha-\delta_\beta)\cos 2\epsilon \end{pmatrix} \ .$$

[13] To an extent – it turned out that the connection is not as robust as orginally envisioned...

Homework 5

1.

You want to determine the spin and parity of an unknown state populated in a (d,p) reaction. Assume the target nucleus has a spin zero and positive parity.

(a) What must be measured in order to extract the angular momentum transfer ΔL? What angular range must be covered? What experimental limitations (*e.g.*, angular resolution, acceptance) most strongly affect the extraction?

(b) The measured angular distribution for an incident momentum[14] of $k \approx 1.5$ fm^{-1} shows the first peak at $\theta \approx 20^\circ$ and a peak spacing of $\Delta\theta \sim 30^\circ$. What is the nuclear radius? What is the angular momentum transfer? What are the possible J^π values of the final state?

2.

Consider elastic scattering in the potential $U(r)$. For a fixed partial wave l, define the local radial wave number

$$k_l(r) = \sqrt{2\mu\big(E - U(r)\big) - \frac{\left(l+\frac{1}{2}\right)^2}{r^2}} \ .$$

The corresponding free quantity is

$$k_l^{(0)}(r) = \sqrt{2\mu E - \frac{\left(l+\frac{1}{2}\right)^2}{r^2}} \ .$$

(a) Write the WKB expression for the elastic phase shift δ_l.
(b) State the WKB validity condition.
(c) Why is the angular momentum contribution proportional to $\left(l+\frac{1}{2}\right)^2$ instead of $l(l+1)$?
(d) Is WKB expected to work better for low l or high l? Why?
(e) What types of problems can be successfully addressed with WKB?

3.

Consider a projectile-target system at high beam energy and small scattering angle. In the eikonal (Glauber) approximation, the projectile follows a straight-line trajectory with impact parameter b.

(a) Write the eikonal phase $\chi(b)$ for an optical potential $U(r)$.
(b) Write the Glauber elastic scattering amplitude $f(q)$.
(c) State the main physical assumptions behind this approximation. How does the eikonal approximation differ from the WKB approximation?
(d) What types of problems can be successfully addressed with the Glauber approximation?

[14] Note that this quantity is a momentum in natural units; otherwise, it's a wavevector.

4.

Consider a potential

$$\mathcal{V}(\boldsymbol{r}) = V(\boldsymbol{r}) + U(\boldsymbol{r}) \ ,$$

with

$$V(r) = \begin{cases} \infty & r < a \\ 0 & r > a \end{cases} \quad \text{and} \quad U(\boldsymbol{r}) = \lambda \delta^{(3)}\big(\boldsymbol{r} - \boldsymbol{r}_0\big) \ ,$$

where $r_0 > a$. For simplicity, use the low-energy s-wave approximation for the hard-sphere distorted waves outside the sphere,

$$\chi^{(+)}_{\boldsymbol{k}}(\boldsymbol{r}) = e^{i\boldsymbol{k}\cdot\boldsymbol{r}} + f_0 \frac{e^{ikr}}{r} \quad \text{and} \quad \chi^{(-)*}_{\boldsymbol{k}}(\boldsymbol{r}) = e^{-i\boldsymbol{k}'\cdot\boldsymbol{r}} + f_0^* \frac{e^{-ik'r}}{r} \ ,$$

where

$$f_0 = -\frac{a}{1 + ika} \ .$$

Inside the sphere, the distorted waves vanish,

$$\chi^{(\pm)}_{\boldsymbol{k}}(\boldsymbol{r}) = 0 \ , \quad r < a \ .$$

(a) Write the DWBA transition amplitude as an integral.

(b) To evaluate the integral, first use the delta function, then substitute the approximate distorted waves and obtain the explicit amplitude.

(c) Check that for $V = 0$, the result reduces to the ordinary Born approximation.

(d) What types of problems can be successfully addressed with DWBA? What about PWBA?

5.

The extent to which the material covered in this class applies to your research is bound to vary, but there should be some tangible connection.

(a) Describe your research project in 1-2 paragraphs.

(b) Identify which material covered in this class applies to your research, and how.

(c) Within the general subject of nuclear reactions, identify what would be useful to know for your research, but hasn't been covered in class.

Bibliography

[1] Hans Paetz gen. Schieck. *Nuclear Reactions: An Introduction*, volume 882 of *Lecture Notes in Physics*. Springer, 2014.

[2] Charles J. Joachain. *Quantum Collision Theory*. North Holland Publishing Company, 1975.

[3] Albert Messiah. *Quantum Mechanics*. North Holland Publishing Company, 1961.

[4] Daphne F. Jackson. *Nuclear Reactions*. Methuen, London, 1970.

[5] Ian J. Thompson and Filomena M. Nunes. *Nuclear Reactions for Astrophysics: Principles, Calculation and Applications of Low-Energy Reactions*. Cambridge University Press, 2009.

[6] Carlos A. Bertulani and Paweł Danielewicz. *Introduction to Nuclear Reactions*. CRC Press, Taylor and Francis, 2021.

[7] G. R. Satchler. *Introduction to Nuclear Reactions*. The MacMillan Press Ltd., 1980.

[8] K. S. Krane. *Introductory Nuclear Physics*. John Wiley & Sons, 1988.

[9] L. D. Landau and E. M. Lifshitz. *The Classical Theory of Fields*. Pergamon Press, 1971.

[10] L. D. Landau and E. M. Lifshitz. *Quantum Mechanics, Non-relativistic Theory*. Pergamon Press, 1965.

[11] Y. Hijikata *et al.* Measurement of proton elastic scattering from ^{132}Sn at 200 MeV/nucleon. *RIKEN Accelerator Progress Report*, 57:22, 2024.

[12] G. Gamow. Zur Quantentheorie des Atomkernes. *Z. Phys.*, 51:204–212, 1928.

[13] F. Hoyle. On Nuclear Reactions Occuring in Very Hot Stars. 1. The Synthesis of Elements from Carbon to Nickel. *Astrophys. J. Suppl.*, 1:121–146, 1954.

[14] M. G. Holloway and C. P. Baker. How the barn was born. *Physics Today*, 25(7):32, 1972.

[15] Particle Data Group. Review of Particle Physics: Physical Constants. https://pdg.lbl.gov/2025/reviews/rpp2025-rev-phys-constants.pdf, 2025. Physical constants section of the Review of Particle Physics (2025 edition) by the Particle Data Group.

[16] INS Data Analysis Center. Said partial-wave analysis facility. https://gwdac.phys.gwu.edu/analysis/nn_analysis.html, 2026. Online partial-wave analysis of nucleon–nucleon and meson–nucleon scattering.

[17] W. E. Burcham. *Elements of Nuclear Physics*. Longman London and New York, 1979.

[18] Richard A. Arndt and L. David Roper. Elastic Neutron-Alpha Scattering Analyses. *Phys. Rev. C*, 1:903–922, 1970.

[19] Robert R. Spencer and Kenneth T. Faler. Neutron-Capture Gamma-Ray Studies in Isotopes of Tungsten. *Phys. Rev.*, 155:1368–1376, 1967.

[20] H. Derrien, L. C. Leal, N. M. Larson, and A. Courcelle. Neutron resonance parameters of ^{238}U and the calculated cross sections from the reich-moore analysis of experimental data in the neutron energy range from 0 kev to 20 kev. Technical Report ORNL/TM-2005/241, Oak Ridge National Laboratory, Oak Ridge, Tennessee, USA, November 2005.

[21] Japan Atomic Energy Agency Nuclear Data Center. Nuclide information: ^{238}U. https://wwwndc.jaea.go.jp/cgi-bin/nuclinfo2014?92,238, 2014. JAEA Nuclear Data Center, Chart of the Nuclides.

[22] H. A. Bethe. Theory of Disintegration of Nuclei by Neutrons. *Phys. Rev.*, 47:747–759, 1935.

[23] Niels Bohr. Neutron Capture and Nuclear Constitution. *Nature*, 137:344–348, 1936.

[24] S. N. Ghoshal. An Experimental Verification of the Theory of Compound Nucleus. *Phys. Rev.*, 80:939–942, 1950.

[25] P. W. Lisowski, M. S. Moore, and G. L. Morgan. Neutron Total Cross Sections of ^{232}Th, ^{237}Np, ^{235,238}U, and ^{239}Pu from 3 to 230 MeV. *Nucl. Sci. Eng.*, 198(10):1901–1910, 2024.

[26] H. Feshbach, C. E. Porter, and V. F. Weisskopf. Model for Nuclear Reactions with Neutrons. *Phys. Rev.*, 96:448–464, 1954.

[27] Herman Feshbach. Unified theory of nuclear reactions. *Annals Phys.*, 5:357–390, 1958.

[28] Herman Feshbach. A Unified theory of nuclear reactions. 2. *Annals Phys.*, 19:287–313, 1962.

[29] H. Schopper, editor. *Nuclear Charge Radii*, volume 20 of *Landolt-Boernstein - Group I Elementary Particles, Nuclei and Atoms*. Springer, 2004.

[30] G. R. Satchler. Optical model for 30 MeV proton scattering. *Nucl. Phys. A*, 92:273–305, 1967.

[31] A. J. Koning and J. P. Delaroche. Local and global nucleon optical models from 1 keV to 200 MeV. *Nucl. Phys. A*, 713:231–310, 2003.

[32] C. Hebborn et al. Optical potentials for the rare-isotope beam era. *J. Phys. G*, 50(6):060501, 2023.

[33] S. Ait-Tahar. Further tests of the weisskopf-ewing exciton model. *Journal of Physics G: Nuclear and Particle Physics*, 17(12):1833–1849, 1991.

[34] S. Ait-Tahar and P. E. Hodgson. Weisskopf-ewing calculations: neutron-induced reactions. *Journal of Physics G: Nuclear Physics*, 13(7):945–956, 1987.

[35] P. Mohr, Gy. Gyürky, and Zs. Fülöp. Statistical model analysis of α-induced reaction cross sections of ^{64}Zn at low energies. *Phys. Rev. C*, 95(1):015807, 2017.

[36] Andrea Richard. Exploring the intersection of astrophysics and applications through statistical nuclear physics. Nuclear Science Seminar, FRIB, 2 2026. Video recording available at: https://mediaspace.msu.edu/media/Nuclear+Science+Seminar+-+Andrea+Richard/1_8pnj2zpv.

[37] J. Wilczyński. Calculations of the critical angular momentum in the entrance reaction channel. *Nucl. Phys. A*, 216:386–394, 1973.

[38] H. A. Bethe. Energy production in stars. *Phys. Rev.*, 55:434–456, 1939.

[39] Robert G. Littlejohn. The wkb approximation. https://bohr.physics.berkeley.edu/classes/221/notes/wkb.pdf. Physics 221 lecture notes.

[40] Yuri Oganessian. Heaviest nuclei. *Nuclear Physics News*, 23(1):15–21, 2013.

[41] Hannah B. Burrows, W. M. Gibson, and J. Rotblat. Angular distributions of protons from the reaction $o^{16}(d,p)o^{17}$. *Phys. Rev.*, 80:1095–1095, Dec 1950.

[42] R. Serber. The Production of High Energy Neutrons by Stripping. *Phys. Rev.*, 72:1008–1016, 1947.

[43] S. T. Butler. On Angular Distributions from (d,p) and (d,n) Nuclear Reactions. *Phys. Rev.*, 80:1095–1096, 1950.

[44] R. H. Bassel, G. R. Satchler, R. M. Drisko, and E. Rost. Analysis of the Inelastic Scattering of Alpha Particles. I. *Phys. Rev.*, 128:2693–2707, 1962.

[45] J. Chen et al. Probing the quadrupole transition strength of ^{15}C via deuteron inelastic scattering. *Phys. Rev. C*, 106(6):064312, 2022.

[46] L. L. Lee, J. P. Schiffer, B. Zeidman, G. R. Satchler, R. M. Drisko, and R. H. Bassel. $ca^{40}(d,p)ca^{41}$, a test of the validity of the distorted-wave born approximation. *Phys. Rev.*, 136:B971–B993, Nov 1964.

[47] R. M. Haybron, M. B. Johnson, and R. J. Metzger. Inelastic Electron and Proton Scattering from Nuclei. *Phys. Rev.*, 156:1136–1145, 1967.

[48] S. M. Lenzi, Andrea Vitturi, and F. Zardi. Systematic analysis of heavy-ion reaction data in terms of an eikonal approach: Elastic and inelastic scattering. *Phys. Rev. C*, 40:2114–2123, 1989.

[49] M. S. Hussein and K. W. McVoy. Inclusive projectile fragmentation in the spectator model. *Nucl. Phys. A*, 445:124–139, 1985.

[50] G. Goldstein, D. Baye, and P. Capel. Dynamical eikonal approximation in breakup reactions of Be-11. *Phys. Rev. C*, 73:024602, 2006.